

CRANFIELD UNIVERSITY

JOANNA MARGARET DUNSTER

DEVELOPING A METHODOLOGY FOR THE NON-DESTRUCTIVE ANALYSIS OF
BRITISH SOFT-PASTE PORCELAIN

CRANFIELD DEFENCE AND SECURITY

PHD THESIS

Academic Year: 2015 - 2016

Supervisors: PROF. ANDREW SHORTLAND

DR KELLY DOMONEY

APRIL 2016

© Cranfield University 2016. All rights reserved. No part of this publication may be reproduced without the written permission of the copyright owner.

[PAGE LEFT INTENTIONALLY BLANK]

Abstract

Soft-paste porcelain was produced in Britain in great quantities between the mid-18th and early 19th centuries. Due to industrial secrecy and the complexities of creating a product that would survive high-temperature firing, a range of paste recipes was employed by dozens of factories. This has resulted in an array of porcelains which vary in their elemental composition and mineralogy. This research carries out a meta-analysis of the published data for porcelain bodies and glazes and concludes that some discrimination can be achieved using the major and minor elemental composition of the bodies, and that for the glazes intra-factory variation is often greater than inter-factory variation in composition. A pilot investigation of the trace elemental composition of British porcelain is carried out using Laser Ablation Inductively Coupled Plasma Mass Spectroscopy, which finds compositional groups corresponding to different sources of clay and silica raw materials.

In the interests of preserving intact objects, there is recognised a need for a non-destructive method for analysing British porcelain, in order to provenance and date objects. Such a method would rely on data from the surface of the object, which is typically covered by glaze and over-glaze coloured enamels, and this research demonstrates that the formulae used for the glaze and enamels are in some cases characteristic of the factory, or workshop, and period at which they were created. Hand-Held XRF analysis is used to analyse the glaze, underglaze blue and polychrome enamels on a selection of porcelain objects from different factories, and compositional traits are identified that allow some factories and periods to be distinguished. Glass standards are developed, which are representative of the glaze and enamel composition, and which could allow X-ray fluorescence (XRF) data to be calibrated for fully quantitative results.

Keywords: Porcelain, Characterisation, Provenance, Ceramic, Enamel, Glass, Standards, X-ray Fluorescence Spectroscopy, Laser Ablation Inductively Coupled Plasma Mass Spectroscopy, Colorimetry, Spectrophotometry

[PAGE LEFT INTENTIONALLY BLANK]

Acknowledgements

It has been said that it takes a village to raise a child, and I say that it certainly takes a community to produce a PhD thesis. These pages give me the opportunity to thank the community of wise and generous people who have aided me in carrying out this work, while retaining my sanity. Foremost among them, of course, are my excellent supervisors, Prof. Andrew Shortland and Dr Kelly Domoney; if I have learned anything from this process, it is thanks to them. I also owe a huge debt of gratitude to Prof. Keith Rogers and the Cranfield Forensic Institute for their generosity in allowing me to carry out this research there.

Thanks are due to the great number of people who have contributed to this work with their expertise, advice and artefacts.

They are: Dr Fiona Brock, Maggie Canning-White, Dr Debra Carr, Richard Hall, Dr Karl Harrison, Bea Kingdon, Dr David Lane, Dr Annie Maddison-Warren, Adrian Mustey, Dr John Painter and Mike Williams, all of Cranfield University; Jessica Goff, Ian McKay, Mandy Smith and colleagues, of the Barrington Library, Cranfield University; Prof. Ian Freestone, of the Institute of Archaeology, University College London; Prof. Patrick Degryse, of the KU Leuven; Gary Smith, of Scientific and Medical Products, Ltd., Dan Nesbitt and Hazel Ganiaris, of the London Archaeology Archive and Resource Centre; Jacqui Pearce, of the Museum of London Archaeology; Charles Dawson, Jonathan Grey, Patricia Macleod, Steve McManus, Nick Panes, Mary White and Peter White, of the English Ceramic Circle; Maurice Hillis and Roger Pomfrett, of the Northern Ceramic Society; George Haggerty, of the National Museum of Scotland, Edinburgh; Felicity Marno and Antonia Agnew, of Stockspring Antiques, London; Daniel Bone, Catherine Caseley and Timothy Wilson, of the Ashmolean Museum, Oxford; John Sandon, of Bonhams, London; Brian Adams, of the Bovey Tracey Pottery Museum; Dr Paul McKay, Haydn Hansell and Miles Thompson, of Juno Antiques, London; Dinah Reynolds; Rosalind Sword; and Rosalie Wise-Sharpe.

For myself, I am grateful to my family and friends, who have alternately supported, encouraged, sympathised with, cajoled and outright bullied me to the finish.

They are: my parents, Ruth Dunster and Michael Dunster; my siblings, Catherine Dunster and Paul Dunster; my family, Marnie Jack, Sean McDonald, Jenny Flood and Ray Flood; and my dear friends, Paraskevi 'Vivian' Christogianni, Kayleigh Cooper, Olivia Gale, Dr Rita Giannini, Dr Charlene Greenwood, Oznur Gulhan, Deborah Harrison, Ian Hodgson, Maarten Horn, Dr Grace Jennings, Christina Mackie, Jemma Mitchell, Raquel Murray, Dr James 'Ross' Nicoll, Tobias Shanker, and Charlotte Willis. Thank you all.

I must give special thanks to Dr Nathan Flood for his patient advice and wise guidance; he is the model of an excellent researcher.

Finally, I wish to dedicate this work to the memory of Ernest George Dunster and Ada Mary Dunster, without whose unwavering belief and support, none of this would have been possible.

Contents

Abstract	i
Acknowledgements	iii
Contents	v
Tables	ix
Figures	xiv
Equations	xxviii
List of Definitions	xxx
1 Introduction	1
<i>1.1 Context of the project</i>	2
1.1.1 Historic context	2
1.1.2 Methodological context	4
<i>1.2 Scope and structure of the project</i>	5
2 Historical and Technical Review of British Porcelain	7
<i>2.1 Scope of this chapter</i>	8
<i>2.2 The history of the porcelain industry in Britain</i>	9
2.2.1 Imported Chinese porcelain	9
2.2.2 The invention of porcelain in continental Europe	11
2.2.3 Industrial production of earthenware and glass	19
2.2.4 Industrial production of soft-paste porcelain	21
<i>2.3 Systems of classification for British soft-paste porcelain</i>	41
2.3.1 Macroscopic appearance	41
2.3.2 Elemental compositional analysis	48
2.3.3 Mineral phase compositional analysis	54
<i>2.4 Analytical techniques for porcelain and fine ceramics</i>	57
2.4.1 Elemental compositional analysis	57
2.4.2 Other compositional analysis	63
2.4.3 Qualitative techniques	64
<i>2.5 Developments in non-destructive analysis for archaeological science</i>	65
<i>2.6 Conclusions</i>	66

3 A meta-analysis of published data from the analysis of British porcelain	68
3.1 <i>Introduction</i>	68
3.2 <i>Using major and minor elements to discriminate samples by paste</i>	70
3.2.1 Magnesian	71
3.2.2 Phosphatic	73
3.2.3 Frit	78
3.2.4 Silica-alumina-calcium and hard-paste	79
3.3 <i>Using major and minor elements to discriminate samples by glaze</i>	81
3.3.1 Leaded glazes	81
3.3.2 Hybrid hard-paste glazes	84
3.4 <i>Conclusion</i>	86
3.4.1 Porcelain paste	87
3.4.2 Porcelain glazes	88
4 Materials and Methods	89
4.1 <i>Introduction</i>	89
4.2 <i>Materials</i>	90
4.2.1 Mounted samples from intact objects and archaeological sherds	91
4.2.2 Intact objects	93
4.2.3 Archaeological sherds	94
4.3 <i>Methods</i>	95
4.3.1 Building Novel Glass Standards for Calibration	96
4.3.2 Scanning Electron Microscopy with Energy Dispersive Spectroscopy	Error! Bookmark not defined.
4.3.3 X-ray Fluorescence Spectroscopy	103
4.3.4 Hand-Held XRF Instrumentation	113
4.3.5 Spectrophotometry	121
4.3.6 Laser Ablation Inductively Coupled Plasma Mass Spectroscopy	124
4.4 <i>Summary and conclusions</i>	130
5 Results I: non-invasive analytical techniques	132
5.1 <i>Introduction</i>	132
5.2 <i>Hand-Held X-ray Fluorescence Spectroscopy</i>	132
5.2.1 Methodological test	132
5.2.2 Analysis of intact objects of British porcelain	138

5.3 Spectrophotometry	183
5.3.1 Analysis of intact objects in the Ashmolean Museum, Oxford	183
5.4 Summary and conclusions	187
6 Results II: Laser Ablation Inductively Coupled Plasma Mass Spectroscopy	189
6.1 Introduction	189
6.2 Laser Ablation Inductively Coupled Plasma Mass Spectroscopy	190
6.2.1 Methodological test	190
6.2.2 Analysis of porcelain bodies	198
6.2.3 Analysis of porcelain glazes	229
6.3 Summary and conclusions	245
7 Discussion: using multiple analytical techniques to characterise British porcelain	248
7.1 Introduction	248
7.2 Characterising British porcelain using multiple analytical techniques	249
7.2.1 Evaluating SEM-EDS data from published sources	249
7.2.2 Trace elemental compositional data from LA-ICPMS analysis	252
7.2.3 HH-XRF: qualitative elemental compositional data	259
7.2.4 Spectrophotometry: hue and chroma of glazes	265
7.2.5 Testing visual connoisseurship hypotheses: inter-factory versus intra-factory variation in glaze hue and major and minor elemental composition	265
7.3 Developing a Non-Destructive Method for the Elemental Compositional Analysis of British Porcelain	266
7.3.1 X-ray Fluorescence Spectroscopy in the study of archaeological materials	267
7.3.2 Understanding XRF data	267
7.3.3 Evaluating XRF for use on British porcelain	269
7.4 Contributions to the narrative of technical and historical development of British porcelain in the 18th century	271
7.4.1 Intra-factory variation	271
7.4.2 Inter-factory variation	276
7.4.3 Re-examining the Eccles samples: the contribution of trace elements	294
7.5 Summary	300
8 Conclusions and recommendations	301
8.1 Conclusions	301

8.1.1 Characterising and distinguishing British porcelain using multiple analytical techniques	302
8.1.2 Developing a method for the fully-quantitative elemental compositional analysis of British porcelain using XRF	307
8.1.3 Contributions to the narrative of the technological and historical development of British porcelain	308
8.1.4 Summary	310
<i>8.2 Recommendations for further work</i>	<i>311</i>
8.2.1 Refine and expand the XRF method	311
8.2.2 Identify a compositional chronology for enamelling and gilding	312
8.2.3 Further LA-ICPMS analysis to include more pastes, glazes and cobalt blue	313
8.2.4 Compare trace elemental composition from porcelain pastes with geological materials and contemporary fine ceramics	314
REFERENCES	315
APPENDICES	343

Tables

<i>Table 1 - categories of ceramics, classified by firing temperature (after He Li, 2004; pp. 38 – 39)</i>	7
<i>Table 2 - modal bulk elemental compositions (wt%) of five compositional categories (Freestone, 2000)</i>	48
<i>Table 3 - mean (μ) and standard deviation (σ) bulk elemental composition (wt%) of Brownlow Hill, Liverpool (BH; Owen and Hillis, 2003) and Bonnin and Morris, Philadelphia (BM; Owen, 2001a) glazes on phosphatic samples, obtained from mounted sections using SEM with EDS</i>	53
<i>Table 4 - compositional categories for British soft-paste porcelain from the most common factories. All % data in these tables is absolute, and ratios are calculated from the absolute composition.</i>	87
Table 5 - compositional categories for British porcelain glazes from the most common factories	88
<i>Table 6 - samples of porcelain from Caughley, Liverpool, and Worcester, donated by John Sandon. The letters u/g denote an unglazed sherd.</i>	92
<i>Table 7 - samples of porcelain from several factories, donated by the British Museum Reference Library. The letters u/g denote an unglazed sherd.</i>	92
<i>Table 8 - notional and measured (SEM-EDS) composition of eight glass standards in weight percent as oxides</i>	100
<i>Table 9 - the coefficient of determination (R^2) for SEM-EDS data vs notional composition for fourteen elements, present in eight glass standards</i>	103
<i>Table 10 - common sources of interference in X-ray Fluorescence analysis, and the spectral artefacts produced by these effects</i>	106
<i>Table 11 - density (g/cm^3) and composition (wt% ox.) for three model lead glazes, used in energy transmission calculations</i>	108
<i>Table 30 - adapted from Domoney (2012; Table 6.8). Elements detected at low voltage condition, peak position and potential overlaps for characteristic lines. Voltage: 15keV; current: 45μA; filter: 500μm Al</i>	116
<i>Table 13 - adapted from Domoney (2012; Table 6.8). Elements detected at high voltage condition, peak position and potential overlaps for characteristic lines. Voltage: 45keV; current: 15μA; filter: 25μm Fe</i>	117
<i>Table 32 - analytical stability of Oxford Instruments XMET5100 hand held XRF instrument through time. Mean data and a single standard deviation from multiple analyses of the 3a2 soil standard.</i>	118
<i>Table 33 - analytical conditions of Konica Minolta CM-700d Hand-Held spectrophotometer</i>	121
<i>Table 34 - analytical settings used in the laser ablation of porcelain samples</i>	127
<i>Table 35 - analytical settings used for the ICPMS analysis of porcelain samples</i>	129
<i>Table 41 - peak area data from Hand-Held XRF analysis of eight porcelain glazes, obtained under low-voltage (15keV) and high-voltage (45keV) conditions</i>	133
<i>Table 42 - coefficient of determination (R^2) for the relationship between the Hand-Held XRF and SEM-EDS/WDS data for eight porcelain glazes</i>	136

<i>Table 43 - coefficient of determination (R^2) for the relationship between Hand-Held XRF data gathered under a low-voltage condition and a high-voltage condition</i>	137
<i>Table 44 - elements present in lead-rich soft-paste porcelain glazes</i>	139
<i>Table 45 – compositional categories based on elements present in soft-paste porcelain lead glazes, in addition to Al, Si, K, Ca, Ti, Fe, Cu and Pb</i>	140
<i>Table 46 - elements present in enamel colours on Worcester porcelain</i>	147
<i>Table 47 - compositional categories based on elements present in blue overglaze enamels, in addition to Al, Si, K, Ca, Ti, Fe, Co, Ni and Pb</i>	148
<i>Table 48 - compositional categories based on elements present in green enamel grounds and borders, in addition to Al, Si, K, Ca, Ti, Fe, Cu and Pb</i>	148
<i>Table 49 - compositional categories based on elements present in green painted enamels, in addition to Al, Si, K, Ca, Ti, Fe, Cu and Pb</i>	149
<i>Table 50 - compositional categories based on elements present in orange enamels, in addition to Al, Si, K, Ca, Ti, Fe, Cu and Pb</i>	149
<i>Table 51 - compositional categories based on elements present in pink enamels, in addition to Al, Si, K, Ca, Ti, Fe and Pb</i>	150
<i>Table 52 - compositional categories based on elements present in purple enamels, in addition to Al, Si, K, Ca, Ti, Fe and Pb</i>	150
<i>Table 53 - compositional categories based on elements present in red enamels, in addition to Al, Si, K, Ca, Ti, Fe and Pb</i>	151
<i>Table 54 - compositional categories based on elements present in turquoise enamel borders and grounds, in addition to Al, Si, K, Ca, Ti, Fe, Cu and Pb</i>	151
<i>Table 55 - compositional categories based on elements present in yellow enamels, in addition to Al, Si, K, Ca, Ti, Fe and Pb</i>	152
<i>Table 56 - elements present in underglaze blue decoration</i>	172
<i>Table 57 - compositional categories based on elements present in underglaze blue pigment, in addition to Al, Si, K, Ca, Ti, Fe, Co, Ni and Pb</i>	173
<i>Table 58 - elements present in gilded decoration</i>	178
<i>Table 59 - compositional categories based on elements present in overglaze gilding, in addition to Al, Si, K, Ca, Ti, Fe, Cu, Au and Pb</i>	179
<i>Table 60 - mean spectrophotometric data from eighteen porcelain objects</i>	183
<i>Table 61 - linear operator (m) and coefficient of determination (R^2) for the relationship between the SEM-EDS and LA-ICPMS data for ten elements in porcelain pastes</i>	192
<i>Table 62 - linear operator (m) and coefficient of determination (R^2) for the relationship between the SEM-EDS and LA-ICPMS data for nine elements present in porcelain glazes</i>	194
<i>Table 63 - expected and mean measured values (μ) for NIST 610, NIST 610 and CMG A, with the mean difference ($\mu\Delta$) that has been used in Figure 146</i>	195

<i>Table 64 - samples analysed using Laser Ablation Inductively Coupled Plasma Mass Spectroscopy</i>	198
<i>Table 65 - LA-ICPMS data for British porcelain phosphatic bodies in weight percent as oxides</i>	200
<i>Table 66 - LA-ICPMS data for British porcelain frit bodies in weight percent as oxides</i>	200
<i>Table 67 - LA-ICPMS data for British porcelain magnesian bodies in weight percent as oxides</i>	201
<i>Table 68 - LA-ICPMS data for British porcelain SAC and hybrid hard-paste bodies in weight percent as oxides</i>	201
<i>Table 69 – table of correlation between the trace elements, minus REEs, in the porcelain pastes</i>	205
<i>Table 70 - Rare Earth Elements (REE) in British porcelain pastes. All values are chondrite normalised (CN).</i>	216
<i>Table 71 - Rare Earth Elements (REE) in British porcelain pastes. All values are MUQ normalised (MUQ).</i>	223
<i>Table 72 - LA-ICPMS data for British porcelain glazes in weight percent as oxides</i>	230
<i>Table 73 - table of correlation between the trace elements, minus REEs, in the porcelain glazes</i>	233
<i>Table 74 - Rare Earth Elements (REE) in British porcelain glazes. All values are chondrite normalised (CN).</i>	240
<i>Table 75 - summary of distinguishing features from the major and minor elemental, trace elemental, and MUQ-normalised REE composition of British porcelain samples analysed by LA-ICPMS</i>	255
<i>Table 76 - compositional features that distinguish British porcelain using SEM-EDS/WDS, XRF and LA-ICPMS, sorted by factory</i>	278
<i>Table 77 - compositional features that can be used to distinguish British porcelain glazes using XRF data</i>	285
<i>Table 78 - compositional features that can be used to distinguish cobalt blue decoration on British porcelain using XRF data</i>	286
<i>Table 79 - compositional categories for British porcelain pastes using major and minor elemental compositional data. All % data in these tables is absolute, and ratios are calculated from the absolute composition.</i>	287
Table 80 - compositional categories for British porcelain glazes using major and minor elemental compositional data. All % data in these tables is absolute, and ratios are calculated from the absolute composition.	288
<i>Table 81 - compositional categories for British porcelain pastes using trace elemental compositional data. All % data in these tables is absolute, and ratios are calculated from the absolute composition.</i>	289
<i>Table 82 - model composition of porcelain raw materials, after Tite and Bimson (1991)</i>	295
<i>Table 83 - summary of formulae used in the porcelain samples analysed by Tite and Bimson (1991), according to the authors' interpretation</i>	295

<i>Appendix Table 1 - sources of interference encountered in LA-ICPMS analysis of glass and porcelain samples, and the mitigating actions taken in this research to avoid these effects.</i>	352
<i>Appendix Table 2 - spectroscopic interferences from isobaric polyatomic ions that may be formed during LA-ICPMS analysis of glass or ceramic materials (Russo et al, 2002)</i>	353
<i>Appendix Table 3 - electron configuration for sodium (Na, 11), silicon (Si, 14) and argon (Ar, 18)</i>	360
<i>Appendix Table 4 - electron shell transitions, according to Siegbahn notation.....</i>	362
<i>Appendix Table 5 - elemental compositional data of porcelain pastes, obtained from mounted sections using SEM-EDS (Tite and Bimson, Freestone, Middleton and Cowell, Ramsay) and SEM with EDS and WDS (Owen)</i>	372
<i>Appendix Table 6 - elemental composition of porcelain glazes, obtained from powdered glaze (Ramsay and Gabszewicz; Ramsay et al; Tite and Bimson) and mounted sections (Owen et al; Middleton and Cowell)</i>	387
<i>Appendix Table 20 - peak area data from XRF analysis of ten glazed porcelain sherds, used in a methodological test.....</i>	424
<i>Appendix Table 21 - peak area data from Hand-Held XRF analysis of Oxford Instruments #3a2 soil standard over five sessions of analysis</i>	437
<i>Appendix Table 22 - certified values for Oxford Instruments soil standard #3a2, analysed by XMET5100 HH-XRF under the SOIL LE condition for 240 seconds, mean of four analyses, calculated using the software's empirical calibration programme</i>	438
<i>Appendix Table 23 - contamination, silicon and rhodium peaks from analyses of a silicon disk, obtained under the low-voltage (upper) and high-voltage (lower) conditions</i>	439
<i>Appendix Table 24 - peak area data from Hand-Held XRF analysis of glazes on porcelain objects and sherds</i>	440
<i>Appendix Table 25 - peak area data from Hand-Held XRF analysis of underglaze blue on porcelain objects and sherds.....</i>	450
<i>Appendix Table 26 - peak area data from Hand-Held XRF analysis of underglaze blue subtracted from glaze data</i>	454
<i>Appendix Table 27 - peak area data from Hand-Held XRF analysis of overglaze blue enamel.....</i>	458
<i>Appendix Table 28 - peak area data from Hand-Held XRF analysis of overglaze green enamel grounds and borders.....</i>	459
<i>Appendix Table 29 - peak area data from Hand-Held XRF analysis of overglaze green painted enamels</i>	460
<i>Appendix Table 30 - peak area data from Hand-Held XRF analysis of overglaze orange enamels.....</i>	462
<i>Appendix Table 31 - peak area data from Hand-Held XRF analysis of overglaze pink enamels</i>	463
<i>Appendix Table 32 - peak area data from Hand-Held XRF analysis of overglaze purple enamels</i>	464
<i>Appendix Table 33 - peak area data from Hand-Held XRF analysis of overglaze red enamels.....</i>	464
<i>Appendix Table 34 - peak area data from Hand-Held XRF analysis of overglaze turquoise enamels</i>	465

<i>Appendix Table 35 - peak area data from Hand-Held XRF analysis of overglaze yellow enamels.....</i>	466
<i>Appendix Table 36 - peak area data from Hand-Held XRF analysis of gilding.....</i>	467
<i>Appendix Table 37 - LA-ICPMS data (parts per million) for 53 British porcelain pastes, major and minor elements</i>	542
<i>Appendix Table 38 - LA-ICPMS data (parts per million) for 53 British porcelain pastes, trace elements minus REEs (see Appendix Table 39).....</i>	544
<i>Appendix Table 39 - LA-ICPMS data (parts per million) for 53 British porcelain pastes, uncorrected REEs</i>	547
<i>Appendix Table 40 - normalisation values used for Rare Earth Elements (REEs) in British porcelain pastes.</i>	548
<i>Appendix Table 41 - LA-ICPMS data (parts per million) for 36 British porcelain glazes, major and minor elements</i>	549
<i>Appendix Table 42 - LA-ICPMS data (parts per million) for 36 British porcelain glazes, trace elements minus REEs.....</i>	551
<i>Appendix Table 43 - LA-ICPMS data (parts per million) for 36 British porcelain glazes, uncorrected REEs</i>	554

Figures

- Figure 1 - blue and white Chinese porcelain, with a typically Chinese pattern (left) and adapted European scenes (right) (museum numbers, PDF.A.611 and Franks.582 respectively, both British Museum) .10
- Figure 2 - images of early Meissen tea bowls and saucers with design incorporating Chinese (left) and European (right) decorative themes (museum numbers C.600&A-1920 and C.44&A-1954 respectively, Victoria and Albert Museum)13
- Figure 3 - white salt-glazed stoneware coffee-pot (left), and portrait bust (right) from John Dwight’s Fulham pottery (museum numbers AF.3145AN103468001 and 1887,0210.103AN415095001 respectively, British Museum)15
- Figure 4 - ‘A’-marked cup (left) with Chinese tea bowl in Kakiemon style (museum numbers C.28-1959 and C.1308-1924 respectively, Victoria and Albert museum)18
- Figure 5 - ‘A’-marked tea bowl and saucer in Meissen European-style (left, museum number C.143&A-1984; Victoria and Albert Museum), with comparable Meissen tea bowl and saucer (right, museum number Franks.88; British Museum)18
- Figure 6 - image of Bow second patent saucer in Kakiemon style (left) and tea bowl and saucer in Chinese style (right) (museum numbers C.68-1964 and C.219&A-1940 respectively, Victoria and Albert Museum).....22
- Figure 7 - Limehouse underglaze blue sauceboat (left; museum number 1965,1002.1, British Museum) and pickle dish (right; museum number C.923-1924, Victoria and Albert Museum)23
- Figure 8 - Lund’s Bristol polychrome enamelled sauceboat (left) and figure of a Chinese Taoist Immortal, with underglaze manganese purple decoration (right) (museum numbers C.1297-1924 and C.97-1938 respectively, Victoria and Albert Museum)24
- Figure 9 - Chelsea red-anchor period polychrome sugar bowl (left) and Chinese-style musicians, modelled by Joseph Willems (right) (museum numbers C.3&A-1966 and C.40-1974 respectively, Victoria and Albert Museum)25
- Figure 10 - Chelsea gold-anchor period rose-ground teapot (left) and polychrome figure of a musician, modelled by Joseph Willems (right) (museum numbers 517&A-1902 and C.32-1973 respectively, Victoria and Albert Museum)25
- Figure 11 - Isleworth underglaze blue saucer (left; museum number 1928,0213.3.CR, British Museum, 2015) and coffee cup, part of a set (right; museum number C.82&A-1956, Victoria and Albert Museum).....26
- Figure 12 - Vauxhall underglaze blue and white mug (left), and polychrome enamelled ewer (right) (museum numbers 414:110-1885 and C.1336-1924 respectively, Victoria and Albert Museum)27
- Figure 13 - map of the British Isles showing the locations of the major porcelain factories active in the 17th and early 18th centuries. The symbols used for the factories on this map are used throughout the thesis in graphs and plots to refer to their respective factories.28

Figure 14 - map of London showing the location of the major porcelain factories that were active in the 18th and early 19th centuries. Isleworth is considered a London factory, but it is not included on this map, as it is to the west of the map area, see Figure 13. Map data ©2013 Google.....	29
Figure 15 - maps of Worcester (left) and Liverpool (right) showing the locations of the major porcelain factories operating during the 18th and early 19th centuries. Map data ©2013 Google.	30
Figure 16 - Derby polychrome enamelled sauceboat (left) and figure of a dancing man (right) (museum numbers C.277-1976 and C.540-1921 respectively, Victoria and Albert Museum)	31
Figure 17 - Worcester underglaze blue tea-bowl and saucer with Meissen-style Indianische Blumen (left) and Sèvres-style blue-ground tea-pot with gilding (right) (museum numbers CIRC.338&A-1916 and 414:602/&A-1885 respectively, Victoria and Albert Museum).....	33
Figure 18 - Liverpool (John Pennington) tea bowl and saucer and tea canister (Seth Pennington) with Chinese design in underglaze blue (museum numbers C.847&A-1924 and C.420-1924 respectively, Victoria and Albert Museum)	35
Figure 19 - Caughley underglaze blue jug (left) and tea-bowl and saucer (right) (museum numbers C.197B-1921 and C.197G-1921 respectively, Victoria and Albert Museum)	36
Figure 20 - Coalport polychrome vase and cover (left) and rose-ground plate (right) (museum numbers C.1205&A-1917 and 3381-1901 respectively, Victoria and Albert Museum).....	36
Figure 21 - Nantgarw blue-ground plate (left) and green-ground pen tray (right) (museum numbers 414:806-1885 and C.171-2003 respectively, Victoria and Albert Museum).....	37
Figure 22 - Swansea polychrome enamelled and printed plate (left) and rose taper stand (right) (museum numbers C.590-1935 and C.31-1944 respectively, Victoria and Albert Museum)	38
Figure 23 - Plymouth figure of Europe (upper right), Bristol figure of a boy (upper left), and Bovey Tracey fuddling cup (lower) (museum numbers 3088-1901, 414:737-1885 and C.130-1926 respectively, Victoria and Albert Museum)	40
Figure 24 - crossed-swords marks used by the Meissen porcelain factory from 1763 - 1774. Image © Old and Sold Antiques Auction and Marketplace, accessed online at http://www.oldandsold.com/pottery/germany5.shtml	42
Figure 25 - double L marks used by the Vincennes-Sevres factory from 1745 - 1753. Image © Old and Sold Antiques Auction and Marketplace, accessed online at http://www.oldandsold.com/pottery/france1.shtml	42
Figure 26 - hunting horn marks used by the Chantilly factory through the 18th century. Image © Old and Sold Antiques Auction and Marketplace, accessed online at http://www.oldandsold.com/pottery/france2.shtml	42
Figure 27 - anchor marks used by the Chelsea factory from 1750 - 1770. Image © Old and Sold Antiques Auction and Marketplace, accessed online at http://www.oldandsold.com/pottery/greatbritain5.shtml	42

Figure 28 - crescent moon marks used by the Worcester factory from 1751 - 1783. Image © Old and Sold Antiques Auction and Marketplace, accessed online at http://www.oldandsold.com/pottery/greatbritain21.shtml	42
Figure 29 - marks used by the Caughley factory: an imitation Meissen mark (left; occasional); pseudo-Chinese symbols (middle three, between 1772 - 1799); and the Worcester crescent moon (three right; between 1772 - 1799). Image © Old and Sold Antiques Auction and Marketplace, accessed online at http://www.oldandsold.com/pottery/greatbritain4.shtml	43
Figure 30 - Lowestoft porcelain decorated with local scenes in Chinese style (museum number 1887,0307,XI.1; British Museum)	44
Figure 31 - a Worcester tea bowl and saucer in Kakiemon design (left) and Bow octagonal plate with Chinese figure in landscape (right) (museum numbers 414:641-1885 and C.595-1924 respectively, Victoria and Albert Museum)	44
Figure 32 - blue ground and gilding with animal or bird-painting in the reserves, on table-ware by Meissen (left) and a later imitation by Chelsea (right) (museum numbers C.350&A-1918 and 524-1902 respectively, Victoria and Albert Museum)	45
Figure 33 - examples of the two-quail pattern on Japanese (upper left; museum number FB.2.a, British Museum), Meissen (upper right) and Bow (lower) table-wares (museum numbers C.46-2006 and C.185-1935 respectively, Victoria and Albert Museum).....	45
Figure 34 - a cup and saucer from the Worcester factory (left; museum number C.338&A-1940), and a cup and saucer made in Jingdezhen, China (right; museum number C.59I-1957), both decorated in the workshop of James Giles, with a monochrome figured landscape and gilded border, Victoria and Albert Museum	46
Figure 35 - ternary plots to distinguish glazes on Bow soft-paste (left $\text{SiO}_2 - \text{PbO} - \text{K}_2\text{O} \times 10$) (right $\text{SiO}_2 - \text{CaO} - \text{K}_2\text{O} \times 10$), the data were obtained from mounted glaze using SEM-EDS (Ramsay et al, 2003)	53
Figure 36 - SiO_2 vs MgO vs $\text{Al}_2\text{O}_3 + \text{CaO}$ for magnesian soft-paste porcelain pastes	72
Figure 37 - MgO vs CaO in magnesian porcelain pastes	73
Figure 38 - SiO_2 vs Al_2O_3 vs $\text{CaO} + \text{P}_2\text{O}_5$ in phosphatic soft-paste porcelain pastes.....	74
Figure 39 - P_2O_5 vs CaO in phosphatic porcelain pastes.....	75
Figure 40 - K_2O vs Al_2O_3 in phosphatic soft-paste porcelain and bone-china pastes from the 18th and 19th centuries	76
Figure 41 - K_2O vs Al_2O_3 for phosphatic soft-paste porcelain and bone china from the 18th and 19th centuries by factory	77
Figure 42 - $(\text{SiO}_2 + \text{PbO})$ vs Al_2O_3 vs CaO in frit porcelain pastes	78
Figure 43 - ternary plot showing SiO_2 vs Al_2O_3 vs CaO for hard-paste and hybrid hard-paste porcelain pastes	80
Figure 44 – ternary plot showing SiO_2 vs PbO vs $\text{Al}_2\text{O}_3 + \text{K}_2\text{O} + \text{CaO}$ in leaded glazes.....	82

Figure 45 - SiO ₂ vs PbO in high-lead glazes	83
Figure 46 - SiO ₂ vs PbO in low-lead glazes	84
Figure 47 - SiO ₂ vs Al ₂ O ₃ vs (CaO + K ₂ O) in hard-paste and hybrid hard-paste glazes	85
Figure 48 - phase-contrast view of the surface of glass standards 4 (left) and 8 (right).....	99
Figure 49 - phase-contrast view of the surface of glass standards 6 (left) and 7 (right).....	99
Figure 50 - SEM-EDS data plotted against the notional composition (both % as oxides) of eight glass standards	101
Figure 51 - plots of the proportion of energy (eV) transmitted through nine model lead glazes	109
Figure 75 - diagram of Hand-Held XRF system, illustrating the path of the incident X-ray, and scattered and fluorescent radiation.....	114
Figure 76 - illustration of the Region of Interest selection function in ARTAX software, used in this instance to resolve Fe K β and Co K α peak overlap (left), and Pb L β and As K β peak overlap (right)	120
Figure 77 - subtraction of glaze data from underglaze blue decorated areas using Microsoft Excel for Mac 2011 ©2010 Microsoft Corporation	120
Figure 78 - diagram of the Konica Minolta CM-700d Hand-Held spectrophotometer, and its optical system	122
Figure 79 - Commission Internationale de l'Eclairage (CIE) L*a*b colour space, showing the axes upon which measured colour values are plotted	123
Figure 80 - diagram of the laser ablation sampling system used in this research, showing the path of the carrier gas (He) and ablated material.	125
Figure 81 - diagram of an Inductively Coupled Plasma torch, illustrating the path of the ablated sample material and carrier gas (Ar).....	125
Figure 82 - diagram of an Inductively Coupled Plasma Quadrupole Mass Spectrometer, illustrating the path of the ionised sample from the torch to the detector.	126
Figure 85 - plots of the Hand-Held XRF data (peak area) against the SEM-EDS/WDS data (in weight percent as oxides) for eight of the ten porcelain glazes for which fully quantitative data were available	134
Figure 86 - plot of the detector saturation effect in spectroscopic analysis. Up to the point of saturation, the detector response (A) increases proportionally with the amount of the element in the sample (B) . Beyond the point of saturation, as B increases, A remains static.	135
Figure 87 - plots of SEM-EDS/WDS data (in % as oxides) against the Hand-Held XRF data (peak area) for Pb in the low PbO group	136
Figure 88 - plots of hand held XRF data collected under a low-voltage condition (15keV) against data from the same spot collected under a high-voltage condition (45keV) for ten porcelain glazes....	137
Figure 89 - example spectrum for glaze type 3 from LH sherd 1, showing the presence of Mn, and Bi...	141
Figure 90 - example spectrum for glaze type 9 from BTr sb1, showing the presence of Zn, Ba, and Sn ..	141

<i>Figure 91 - example spectra for glaze types 1 (red trace) and 5 (green trace), showing the presence of Mn, Co, Ni, Cu, Zn, and elevated Fe in glaze 5</i>	142
<i>Figure 92 - lead versus tin peak areas from HH-XRF analysis of leaded porcelain glazes</i>	143
<i>Figure 93 - example spectra for glaze types 1 (green trace) and 6 (red trace), showing the presence of P and elevated Ca in glaze 1, and Sn in glaze 6.....</i>	143
<i>Figure 94 - phosphorus versus calcium peak areas from HH-XRF analysis of leaded porcelain glazes</i>	144
<i>Figure 95 - example spectra for glaze types 1 (green trace) and 7 (red trace), showing the presence of Mn, and elevated Fe and Cu, in glaze 7</i>	144
<i>Figure 96 - iron versus manganese peak areas from HH-XRF analysis of leaded porcelain glazes.....</i>	145
<i>Figure 97 - iron versus silicon peak areas from HH-XRF analysis of leaded porcelain glazes</i>	145
<i>Figure 98 - enamel colours on British porcelain with blue, turquoise, green and yellow grounds or borders</i>	146
<i>Figure 99 - example spectra for blue enamel type 2 (red trace) and glaze (green trace), showing that the blue enamel contributes Cr, Mn, Fe, Co, Ni, Cu, and Zn</i>	154
<i>Figure 100 - cobalt versus nickel peak areas from HH-XRF analysis of overglaze blue enamels</i>	153
<i>Figure 101 - cobalt versus arsenic peak areas from HH-XRF analysis of overglaze blue enamels</i>	154
<i>Figure 102 - example spectra for green border/ground type 1 (red trace) and glaze (green trace), showing that the green enamel contributes Cu and Sn</i>	155
<i>Figure 103 - example spectra for green border/ground type 2 (red trace) and glaze (green trace), showing that the green enamel contributes Cr, Zn, and increased Fe</i>	156
<i>Figure 104 - chromium versus copper peak areas from HH-XRF analysis of overglaze green borders and grounds.....</i>	156
<i>Figure 105 - chromium versus copper peak areas from HH-XRF analysis of overglaze green enamels ...</i>	157
<i>Figure 106 - example spectra for orange enamel type 1 (red trace) with glaze (green trace), showing that the orange enamel contributes Fe.....</i>	158
<i>Figure 107 - iron versus manganese peak areas from HH-XRF analysis of overglaze orange enamels ...</i>	158
<i>Figure 108 - iron versus copper peak areas from HH-XRF analysis of overglaze orange enamels.....</i>	159
<i>Figure 109 - example spectra for pink enamel type 1 (red trace) and glaze (green trace), showing that the pink enamel contributes Fe and Cu</i>	160
<i>Figure 110 - example spectra for pink enamel (red trace) and glaze (green trace) on 480, showing that the pink enamel contributes Zn and Ba, possibly Co</i>	160
<i>Figure 111 - example spectra for pink enamel type 2 (red trace) and glaze (green trace), showing that the pink enamel contributes Au</i>	161
<i>Figure 112 - object number 696, a plate, showing overgilding on pink ground, with flower painting in reserves. The tested pink area is in the centre.</i>	161
<i>Figure 113 - example spectra for purple enamel (red trace) and glaze (green trace) on WJG8, showing that the purple enamel contributes Co and Ni</i>	162

<i>Figure 114 - object number WJG8, a dish with flower painting in purple, pink, red, green, blue and yellow. The tested purple area is in the upper left-hand corner.</i>	163
<i>Figure 115 - example spectra for purple enamel (red trace) and glaze (green trace) on WJG3, showing that the purple enamel contributes Fe, Co, Ni and possibly Mn.</i>	163
<i>Figure 116 - object number WJG3, a plate with purple monochromatic flower painting. The analysed area is in the upper left-hand corner.</i>	164
<i>Figure 117 - example spectra for purple enamel (red trace) and glaze (green trace) on WJG9, showing that the purple enamel contributes Mn and possibly additional Fe</i>	164
<i>Figure 118 - object number WJG9, a large armorial plate with vines on border. The analysed area is the purple pegasus form at the upper centre of the plate.</i>	165
<i>Figure 119 - examples spectra for the purple enamel (red trace) and glaze (green trace) on WWR3, showing that the purple enamel contributes Mn, Fe, Cu and possibly Co.</i>	165
<i>Figure 120 - example spectra for red enamel type 1 (red trace) and glaze (green trace), showing that the red enamel contributes Fe and Cu</i>	166
<i>Figure 121 - example spectra for red enamel type 3 (red trace) and glaze (green trace), showing that the red enamel contributes Fe, Zn, and Ba</i>	166
<i>Figure 122 - example spectra for turquoise enamel type 1 (red trace) and glaze (green trace), showing that the turquoise enamel contributes Cu</i>	167
<i>Figure 123 - example spectra for turquoise enamel type 4 (red trace) and glaze (green trace), showing that the turquoise enamel contributes Cu, As, and Sn.....</i>	168
<i>Figure 124 - example spectra for turquoise enamel type 7 (red trace) and glaze (green trace), showing that the turquoise enamel contributes Cr, Co, Zn, Au, and As.....</i>	168
<i>Figure 125 - copper versus arsenic peak areas from HH-XRF analysis of turquoise overglaze enamels ..</i>	169
<i>Figure 126 - copper versus tin peak areas from HH-XRF analysis of turquoise overglaze enamels</i>	169
<i>Figure 127 - turquoise border with overgilding, and gilded edge, on object number 702</i>	170
<i>Figure 128 - example spectra for yellow enamel 3 (red trace) and glaze (green trace), showing that the yellow enamel contributes Mn, Ni, Cu, and Sn</i>	170
<i>Figure 129 - example spectra for yellow enamel 4 (red trace) and glaze (green trace), showing that the yellow enamel contributes Cr, Mn, Fe, Zn, and Sn.....</i>	171
<i>Figure 130 - saucer with turquoise borders and bird painting, attributed to James Giles, on object number 705 . The analysed area of yellow enamel is on the bird's throat, which has adjacent gilding, at the upper centre of the image.</i>	171
<i>Figure 131 - example spectra for underglaze blue type 1 (red trace) and glaze (green trace), showing that the blue pigment contributes Fe, Co, and Ni</i>	174
<i>Figure 132 - cobalt versus nickel peak areas from HH-XRF analysis of underglaze blue</i>	174
<i>Figure 133 - example spectra for underglaze blue type 6 (red trace) and glaze (green trace), showing that the blue pigment contributes Mn, Co, and Ni</i>	175

Figure 134 - cobalt versus copper peak areas from HH-XRF analysis of underglaze blue	175
Figure 135 - cobalt versus arsenic peak areas from HH-XRF analysis of underglaze blue.....	176
Figure 136 - example spectra for underglaze blue type 9 (red trace) and glaze (green trace) on WP sherd 1, showing that the blue pigment contributes Co, Ni, Zn, and As, and possibly additional Mn, Fe and Cu.	177
Figure 137 - cobalt versus zinc peak areas from HH-XRF analysis of underglaze blue.....	177
Figure 138 - example spectrum of gilding type 1 (red trace) and glaze (green trace) on object number 480, showing that the gilding contributes Au. Obtained under low-voltage condition.	180
Figure 139 - example spectra of gilding type 2 (green trace) and glaze (red trace) on object number 1010, showing that the gilding contributes Au and Ag. Obtained under the high-voltage condition.	181
Figure 140 - gold versus silver peak areas from HH-XRF analysis of gilding	181
Figure 141 - example spectra for gilding type 4 (red trace) and glaze (green trace) on object number 804, showing that the gilding contributes Cu and Au. Obtained under low voltage condition.....	182
Figure 142 - gold versus copper peak areas from HH-XRF analysis of gilding	182
Figure 143 – lightness (left), and hue and chroma (right) of British soft-paste porcelain lead glazes.....	185
Figure 144 - plots of the SEM-EDS data against the LA-ICPMS data (both in weight percent as oxides) for 42 of the 62 porcelain pastes for which fully quantitative data were available.....	190
Figure 145 - plots of the SEM-EDS data against the LA-ICPMS data (both in weight percent as oxides) for 27 of the 61 porcelain glazes for which fully quantitative data were available, and which are securely uncontaminated by the underlying ceramic body.....	193
Figure 146 - mean difference (Δ) between calibrated LA-ICPMS data and reference data for 49 elements in three glass standards. Error bars represent a single standard deviation.	197
Figure 147 - elements measured during analysis of British porcelain pastes and glazes using LA-ICPMS	204
Figure 148 - illustrating the variability in each of the trace elements, minus REEs, in the porcelain pastes. To more clearly demonstrate the overall variability, a log scale has been used on the x axis (ppm).	204
Figure 149 - cobalt vs bismuth in British porcelain pastes, by factory	206
Figure 150 - cobalt vs bismuth in British porcelain pastes, by factory	207
Figure 151 - copper vs manganese in British porcelain pastes, by factory.....	208
Figure 152 - copper vs zinc in British porcelain pastes, by factory.....	208
Figure 153 - magnesium vs zinc in British porcelain pastes, by factory	209
Figure 154 - aluminium vs niobium in British porcelain pastes, by factory	210
Figure 155 - aluminium vs titanium in British porcelain pastes, by factory	210
Figure 156 - titanium vs zirconium in British porcelain pastes, by factory	211
Figure 157 - titanium vs hafnium in British porcelain pastes, by factory	212
Figure 158 - zirconium vs hafnium in British porcelain pastes, by factory	212

Figure 159 - lead vs tin in British porcelain pastes, by factory. In order to more clearly illustrate compositional groups with different levels of tin, a logarithmic (base 10) scale has been used on the y axis.	213
Figure 160 - thorium vs uranium in British porcelain pastes, by factory.	214
Figure 161 - Pr_{CN} vs Yb_{CN} in British porcelain pastes, by factory.	218
Figure 162 - Ce/Ce^* vs Eu/Eu^* in British porcelain pastes, by factory.	219
Figure 163 - REE_{CN} profiles for porcelain pastes from Worcester, Bow, Limehouse, and Chelsea.	220
Figure 164 - Al (ppm) vs ΣREE_{CN} in British porcelain pastes.	222
Figure 165 - REE_{MUQ} profiles for magnesian porcelain pastes from Caughley, Chaffers, Liverpool (Ball), Pomona, and Worcester. In order to more clearly illustrate the significant differences, a logarithmic (base 10) scale has been used on the y axis.	225
Figure 166 - REE_{MUQ} profiles for phosphatic porcelain pastes from Bow, Chelsea, Coalport, Derby, Lowestoft, Nantgarw, Pinxton and Swansea. In order to more clearly illustrate the significant differences, a logarithmic (base 10) scale has been used on the y axis.	226
Figure 167 - REE_{MUQ} profiles for frit porcelain pastes from Chelsea and Longton Hall, plus SAC porcelain from Limehouse. In order to more clearly illustrate the significant differences, a logarithmic (base 10) scale has been used on the y axis.	226
Figure 168 - REE_{MUQ} profiles for outliers from Bow and Limehouse, which were omitted from the calculations of mean values used in previous profiles. In order to more clearly illustrate the significant differences, a logarithmic (base 10) scale has been used on the y axis.	227
Figure 169 - REE_{MUQ} profiles for hybrid hard-paste porcelain pastes from the 'A'-marked group, New Hall, Plymouth, and Swansea. In order to more clearly illustrate the significant differences, a logarithmic (base 10) scale has been used on the y axis.	228
Figure 170 - boxplot illustrating the distribution of each of trace elements, minus REEs, in the porcelain glazes. To more clearly demonstrate the overall variability, a log scale has been used on the x axis (ppm).	232
Figure 171 - strontium vs manganese in British porcelain glazes, by factory.....	235
Figure 172 - strontium vs cesium in British porcelain glazes, by factory.....	236
Figure 173 - zirconium vs hafnium in British porcelain glazes, by factory.....	237
Figure 174 - lead vs tin in British porcelain glazes, by factory.....	237
Figure 175 - thorium vs uranium in British porcelain glazes, by factory.	238
Figure 176 - Pr_{CN} vs Yb_{CN} in British porcelain glazes, by factory.....	239
Figure 177 - Ce/Ce^*_{CN} vs Eu/Eu^*_{CN} in British porcelain glazes, by factory.	242
Figure 178 - REE_{CN} profiles for porcelain glazes from Bow, Chelsea, Limehouse, and Worcester.	243
Figure 179 - REE_{CN} profile for low-lead and leadless porcelain glazes from Coalport, Nantgarw, New Hall, Plymouth, and Swansea.....	244
Figure 180 - cobalt versus nickel peak areas from HH-XRF analysis of underglaze blue.....	263

Figure 181 - cobalt versus manganese peak areas from HH-XRF analysis of underglaze blue on Crisp and Littler's soft-paste porcelains	264
Figure 182 - cobalt versus arsenic peak areas from HH-XRF analysis of underglaze blue on Crisp and Littler's soft-paste porcelain	264
Figure 184 - silicon versus potassium peak areas from HH-XRF analysis of Worcester porcelain glazes .	273
Figure 185 - silicon versus calcium peak areas from HH-XRF analysis of Worcester porcelain glazes	273
Appendix Figure 1 - diagram of a Scanning Electron Microscope, illustrating the path of the incident electron beam from the thermionic gun to the sample surface	344
Appendix Figure 2 - illustration of the types of interaction that occur when a beam of electrons impact a sample surface under vacuum conditions	345
Appendix Figure 3 - diagram of the sections of the Laser Ablation Inductively Coupled Plasma Mass Spectroscopy technique	347
Appendix Figure 4 - diagram of a plasma torch, showing the main gas inlet tubes. The flow of gas and sample aerosol is from right to left.	349
Appendix Figure 5 - diagram of an inductively coupled plasma quadrupole ion source, which interfaces through a series of ion lenses with a quadrupole mass spectrometer. In this image, the direction of travel for the sample (represented by a red line) is from right to left.	350
Appendix Figure 6 - elements of interest, and the isoptes used, in LA-ICPMS analysis of British porcelain pastes and bodies	354
Appendix Figure 7 - periodic table of the elements, illustrating how groups of elements are formed horizontally as similar electron shell configurations cause similar material properties	359
Appendix Figure 8 - structure of an atom, illustrating the electron shells	359
Appendix Figure 9 - interaction between an atom and an incident photon from X-radiation. Where: $E =$ energy $\phi =$ binding energy of the electron in transit $h =$ Planck's constant $\nu =$ frequency $p_{pe} =$ photoelectron	361
Appendix Figure 10 - photoelectric effect (3. a) and Auger effect (3. b) within the atom illustrated in Appendix Figure 9. Where: $E =$ energy $\phi =$ binding energy of the electron in transit $a_e =$ auger electron $\kappa =$ k shell $L =$ L shell $M =$ M shell	361
Appendix Figure 11 - diagram of the Oxford Instruments X-MET5100 Hand-Held XRF instrument	364
Appendix Figure 13 - diagram of an X-ray tube, specifically the tube used by the SEA6000X benchtop XRF	365
Appendix Figure 14 - an XRF spectrum, produced using Bruker Artax software (version 7.2)	367
Appendix Figure 15 - an XRF spectrum with tags to identify the peaks as elements, produced using Bruker ARTAX software (version 7.2)	368

Appendix Figure 16 - the spectral sensitivity of the human eye, based on the four types of photo-sensitive structures; rods, β cones, γ cones, and σ cones.....	370
Appendix Figure 17 - Commission Internationale de l'Eclairage (CIE) L^*a^*b colour space, showing the axes upon which measured colour values are plotted.....	371
Appendix Figure 30 - example spectra for the glaze of sherd CY4, obtained under the low-voltage (upper) and high-voltage (lower) conditions.....	426
Appendix Figure 31 - example spectra for the glaze of sherd CY5, obtained under the low-voltage (upper) and high-voltage (lower) conditions.....	427
Appendix Figure 32 - example spectra from the glaze of sherd CY6, obtained under the low-voltage (upper) and high-voltage (lower) conditions.....	428
Appendix Figure 33 - example spectra from the glaze of sherd CY8, obtained under low-voltage (upper) and high-voltage (lower) conditions.....	429
Appendix Figure 34 - example spectra from the glaze of sherd CY9, obtained under low-voltage (upper) and high-voltage (lower) conditions.....	430
Appendix Figure 35 - example spectra from the glaze of sherd CY11, obtained under low-voltage (upper) and high-voltage (lower) conditions.....	431
Appendix Figure 36 - example spectra from the glaze of sherd CY12, obtained under low-voltage (upper) and high-voltage (lower) conditions.....	432
Appendix Figure 37 - example spectra from the glaze of sherd CY20, obtained under low-voltage condition (upper) and high-voltage (lower) conditions	433
Appendix Figure 38 - example spectra from the glaze of sherd LP3, obtained under low voltage (upper) and high-voltage (lower) conditions.....	434
Appendix Figure 39 - example spectra from the glaze of sherd W12, obtained under low-voltage (upper) and high-voltage (lower) conditions.....	435
Appendix Figure 40 - example spectra from the glaze of sherd W15, obtained under low-voltage (upper) and high-voltage (lower) conditions.....	436
Appendix Figure 41 - example spectra from analyses of Oxford Instrument soil standard #3a2, obtained under low-voltage (upper) and high-voltage (lower) conditions.....	438
Appendix Figure 42 - example spectra from analyses of a silicon disk, obtained under the low-voltage (upper) and high-voltage (lower) conditions.....	439
Appendix Figure 43 - example spectrum for glaze type 1 from HNB sherd 1, obtained under low voltage condition (upper), and high voltage condition (lower)	469
Appendix Figure 44 - example spectrum for glaze type 2 from Bow mg1, obtained under low voltage condition (upper), and high voltage condition (lower)	470
Appendix Figure 45 - example spectrum for glaze type 3 from LH 1, obtained under low voltage condition (upper), and high voltage condition (lower)	471

<i>Appendix Figure 46 - example spectrum for glaze type 4 from EMB frag 4, obtained under low voltage condition (upper), and high voltage condition (lower)</i>	472
<i>Appendix Figure 47 - example spectrum for glaze type 5 from Cy tc1, obtained under low voltage condition (upper), and high voltage condition (lower)</i>	473
<i>Appendix Figure 48 - example spectrum for glaze type 6 from LLK sherd 1, obtained under low voltage condition (upper), and low voltage condition (lower)</i>	474
<i>Appendix Figure 49 - example spectrum for glaze type 7 from Worcs sb1, obtained under low voltage condition (upper), and high voltage condition (lower)</i>	475
<i>Appendix Figure 50 - example spectrum for glaze type 8 from Cha tb1, obtained under low voltage condition (upper), and high voltage condition (lower)</i>	476
<i>Appendix Figure 51 - example spectrum for glaze type 9 from BTr sb1, obtained under low voltage condition (upper), and high voltage condition (lower)</i>	477
<i>Appendix Figure 52 - example spectrum for glaze type 10 from Cha sb1, obtained under low voltage condition (upper), and high voltage condition (lower)</i>	478
<i>Appendix Figure 53 - example spectrum for glaze type 11 from EMB sherd 1, obtained under low voltage condition (upper), and high voltage condition (lower)</i>	479
<i>Appendix Figure 54 - example spectrum for blue enamel type 1 from 377, obtained under low voltage condition (upper), and high voltage condition (lower)</i>	480
<i>Appendix Figure 55 - example spectrum for blue enamel type 2 from 292, obtained using low voltage condition (upper), and high voltage condition (lower)</i>	481
<i>Appendix Figure 56 - example spectrum for blue enamel type 3 from 111, obtained using low voltage condition (upper), and high voltage condition (lower)</i>	482
<i>Appendix Figure 57 - example spectrum for blue enamel type 4 from 65, obtained using low voltage condition (upper), and high voltage condition (lower)</i>	483
<i>Appendix Figure 58 - example spectrum for blue enamel type 5 from 804, obtained under low voltage condition (upper), and high voltage condition (lower)</i>	484
<i>Appendix Figure 59 - example spectrum for green ground/border type 1 from 1005, obtained under low voltage condition (upper), and high voltage condition (lower)</i>	485
<i>Appendix Figure 60 - example spectrum for green ground/border type 2 from 932, obtained under low voltage condition (upper), and high voltage condition (lower)</i>	486
<i>Appendix Figure 61 - example spectrum for green painted enamel type 1 from 620, obtained under low voltage condition (upper), and high voltage condition (lower)</i>	487
<i>Appendix Figure 62 - example spectrum for green painted enamel type 2 from 65, obtained under low voltage condition (upper), and high voltage condition (lower)</i>	488
<i>Appendix Figure 63 - example spectrum for green painted enamel type 3 from 697, obtained under low voltage condition (upper), and high voltage condition (lower)</i>	489

<i>Appendix Figure 64 - example spectrum for green painted enamel type 4 from 292, obtained under low voltage condition (upper), and high voltage condition (lower)</i>	490
<i>Appendix Figure 65 - example spectrum for green painted enamel type 5 from 699, obtained under low voltage condition (upper), and high voltage condition (lower)</i>	491
<i>Appendix Figure 66 - example spectrum for orange enamel type 1 from WJG4, obtained under low voltage condition (upper), and high voltage condition (lower)</i>	492
<i>Appendix Figure 67 - example spectrum for orange enamel type 2 from WJG1, obtained under low voltage condition (upper), and high voltage condition (lower)</i>	493
<i>Appendix Figure 68 - example spectrum for orange enamel type 3 from 111, obtained under low voltage condition (upper), and high voltage condition (lower)</i>	494
<i>Appendix Figure 69 - example spectrum for orange enamel type 4 from 826, obtained under low voltage condition (upper), and high voltage condition (lower)</i>	495
<i>Appendix Figure 70 - example spectrum for pink enamel type 1 from 698, obtained under low voltage condition (upper), and high voltage condition (lower)</i>	496
<i>Appendix Figure 71 - example spectrum for pink enamel type 2 from 65, obtained under low voltage condition (upper), and high voltage condition (lower)</i>	497
<i>Appendix Figure 72 - example spectrum for pink enamel type 3 from 574, obtained under low voltage condition (upper), and high voltage condition (lower)</i>	498
<i>Appendix Figure 73 - example spectrum for pink enamel type 4 from 617, obtained under low voltage condition (upper), and high voltage condition (lower)</i>	499
<i>Appendix Figure 74 - example spectrum for pink enamel type 5 from 480, obtained under low voltage condition (upper), and high voltage condition (lower)</i>	500
<i>Appendix Figure 75 - example spectrum for pink enamel type 6 from 696, obtained under low voltage condition (upper), and high voltage condition (lower)</i>	501
<i>Appendix Figure 76 - example spectrum for pink enamel type 7 from 697, obtained under low voltage condition (upper), and high voltage condition (lower)</i>	502
<i>Appendix Figure 77 - example spectrum for purple enamel type 1 from WJG8, obtained under low voltage condition (upper), and high voltage condition (lower)</i>	503
<i>Appendix Figure 78 - example spectrum for purple enamel type 2 from WJG9, obtained under low voltage condition (upper), and high voltage condition (lower)</i>	504
<i>Appendix Figure 79 - example spectrum for purple enamel type 3 from WJG3, obtained under low voltage condition (upper) and high voltage condition (lower)</i>	505
<i>Appendix Figure 80 - example spectrum for purple enamel type 4 from WWR3, obtained under low voltage condition (upper) and high voltage condition (lower)</i>	506
<i>Appendix Figure 81 - example spectrum for red enamel type 1 from 65, obtained under low voltage condition (upper), and high voltage condition (lower)</i>	507

<i>Appendix Figure 82 - example spectrum for red enamel type 2 from 620, obtained under low voltage condition (upper), and high voltage condition (lower)</i>	508
<i>Appendix Figure 83 - example spectrum for red enamel type 3 from 705, obtained under low voltage condition (upper), and high voltage condition (lower)</i>	509
<i>Appendix Figure 84 - example spectrum for turquoise enamel type 1 from 577, obtained under low voltage condition (upper), and high voltage condition (lower)</i>	510
<i>Appendix Figure 85 - example spectrum for turquoise enamel type 2 from 698, obtained under low voltage condition (upper), and high voltage condition (lower)</i>	511
<i>Appendix Figure 86 - example spectrum for turquoise enamel type 3 from 700, obtained under low voltage condition (upper), and high voltage condition (lower)</i>	512
<i>Appendix Figure 87 - example spectrum for turquoise enamel type 4 from 705, obtained under low voltage condition (upper), and high voltage condition (lower)</i>	513
<i>Appendix Figure 88 - example spectrum for turquoise enamel type 5 from 702, obtained under low voltage condition (upper), and high voltage condition (lower)</i>	514
<i>Appendix Figure 89 - example spectrum for turquoise enamel type 6 from 65, obtained under low voltage condition (upper), and high voltage condition (lower)</i>	515
<i>Appendix Figure 90 - example spectrum for turquoise enamel type 7 from 914, obtained under low voltage condition (upper), and high voltage condition (lower)</i>	516
<i>Appendix Figure 91 - example spectrum for yellow enamel type 1 from 65, obtained under low voltage condition (upper), and high voltage condition (lower)</i>	517
<i>Appendix Figure 92 - example spectrum for yellow enamel type 2 from 480, obtained under low voltage condition (upper), and high voltage condition (lower)</i>	518
<i>Appendix Figure 93 - example spectrum for yellow enamel type 3 from WWR5, obtained under low voltage condition (upper), and high voltage condition (lower)</i>	519
<i>Appendix Figure 94 - example spectrum for yellow enamel type 4 from 696, obtained under low voltage condition (upper), and high voltage condition (lower)</i>	520
<i>Appendix Figure 95 - example spectrum for yellow enamel type 5 from 292, obtained under low voltage condition (upper), and high voltage condition (lower)</i>	521
<i>Appendix Figure 96 - example spectrum for yellow enamel type 6 from 705, obtained under low voltage condition (upper), and high voltage condition (lower)</i>	522
<i>Appendix Figure 97 - example spectrum for underglaze blue type 1 from Bow pl3, obtained under low voltage condition (upper), and high voltage condition (lower)</i>	523
<i>Appendix Figure 98 - example spectrum for underglaze blue type 2 from GAH sherd1, obtained under low voltage condition (upper), and high voltage condition (lower)</i>	524
<i>Appendix Figure 99 - example spectrum for underglaze blue type 3 from dby vase1, obtained under low voltage condition (upper), and high voltage condition (lower)</i>	525

<i>Appendix Figure 100 - example spectrum for underglaze blue type 4 from dby bskt, obtained under low voltage condition (upper), and high voltage condition (lower)</i>	526
<i>Appendix Figure 101 - example spectrum for underglaze blue type 5 from LH sb1, obtained under low voltage condition (upper), and high voltage condition (lower)</i>	527
<i>Appendix Figure 102 - example spectrum for underglaze blue type 6 from Vx sb1, obtained under low voltage condition (upper), and high voltage condition (lower)</i>	528
<i>Appendix Figure 103 - example spectrum for underglaze blue type 7 from Cha sb1, obtained under low voltage condition (upper), and high voltage condition (lower)</i>	529
<i>Appendix Figure 104 - example spectrum for underglaze blue type 8 from LLK sherd 4, obtained under low voltage condition (upper), and high voltage condition (lower).....</i>	530
<i>Appendix Figure 105 - example spectrum for underglaze blue type 9 from BTr sb1, obtained under low voltage condition (upper), and high voltage condition (lower)</i>	531
<i>Appendix Figure 106 - example spectrum for underglaze blue type 10 from WP sherd 1, obtained under low voltage condition (upper), and high voltage condition (lower).....</i>	532
<i>Appendix Figure 107 - example spectrum for underglaze blue type 11 from NH sc1, obtained under low voltage condition (upper), and high voltage condition (lower)</i>	533
<i>Appendix Figure 108 - example spectrum for gilding type 1 from object number 480, obtained under low voltage condition (upper), and high voltage condition (lower)</i>	534
<i>Appendix Figure 109 - example spectrum for gilding type 2 from object number 703, obtained under low voltage condition (upper) and high voltage condition (lower)</i>	535
<i>Appendix Figure 110 - example spectrum for gilding type 3 from object number 699, obtained under low voltage condition (upper), and high voltage condition (lower)</i>	536
<i>Appendix Figure 111 - example spectrum for gilding type 4 from object number 914, obtained under low voltage condition (upper), and high voltage condition (lower)</i>	537
<i>Appendix Figure 112 - example spectrum for gilding type 5 from object 804, obtained under low voltage condition (upper), and high voltage condition (lower)</i>	538

Equations

- Equation 1 - calculation to relate observed and expected values for standards in an external calibration by linear regression. Where: y = expected value for analyte i m = the linear operator, equal to the slope of the line x = the measured value for analyte i c = sensitivity, equal to the intercept of the line with the y axis **113**
- Appendix Equation 1 - calculation to relate observed and expected values for standards in an external calibration by linear regression. Where: y = expected value for analyte i m = the linear operator, equal to the slope of the line x = the measured value for analyte i c = sensitivity, equal to the intercept of the line with the y axis **355**
- Appendix Equation 2 - process to correct the raw signal intensity in counts per second (cps) for each constituent oxide (1 to n). Where: I_i = raw signal intensity for oxide i in the sample $I_{i=IS}$ = raw intensity for the internal standard (Si) $c_{i=IS}$ = known concentration of oxide i in the internal standard **356**
- Appendix Equation 3 - process to correct the raw signal intensity in cps for each constituent oxide (1 to n) in the glass standards. Where: $I_{i,j}(\text{corr})$ = corrected signal intensity for oxide i in the glass standards j $I_{i,j}$ = raw signal intensity for oxide i in the glass standards j $I_{i=IS,j}$ = raw intensity of the internal standard in the glass standards j $c_{i=IS,j}$ = known concentration of the internal standard in the glass standards j **356**
- Appendix Equation 4 - process to calculate the response factor (F_i) for each element present in the sample. Where: F_i = response factor for i $\sum_{j=1}^m$ = sum of the points for each of the glass standards j $c_{i,j}$ = known concentration of oxide i in the glass standards j $I_{i,j}(\text{corr})$ = corrected signal intensity of oxide i in glass standard j **356**
- Appendix Equation 5 - process to calculate the elemental oxide concentration in the sample using the response factor. Where: c_i = concentration of element i as oxide in the sample $I_i(\text{corr})$ = corrected intensity for element i F_i = response factor for element i **357**
- Appendix Equation 6 - process of sum normalisation for the elemental oxide concentration in the sample. Where: $c_{i,norm}$ = normalised concentration of element i c_i = concentration of element i $\sum_{i=1}^n$ = the sum of the elemental oxides measured in the sample **357**
- Appendix Equation 7 - Moseley's law, defining the relationship between the frequency of a fluorescent photon and the atomic number and transition of the element of origin. Where: ν = frequency k_1 = a constant unique to the K transition Z = the atomic number of the element of origin k_2 = a constant unique to the K transition **366**

Appendix Equation 8 - the Planck-Einstein relation, describing the relationship between the wavelength and the energy of a photon. Where: E = energy h = Planck's constant c = speed of light λ = wavelength367

List of Definitions

- alkali glaze a vitreous coating applied to ceramic paste, which uses alkali elements (sodium, magnesium, potassium, calcium) as the principal fluxing component
- ball clay a generic term used in Britain during the 18th and 19th centuries, and by ceramic historians thereafter, to describe a type of titanium-rich kaolinitic clay typically mined in Dorset. The name is thought to refer to the ball-shaped batches in which the clay was shipped.
- BCE Before the Common Era, synonymous with BC, or Before Christ.
- bone china a clay-rich, soft-paste porcelain which used calcium phosphate, from bone ash, as the flux.
- calcined adjective to describe a material that has undergone the process of calcination. Calcination may be understood in two senses. The original sense of the word was the roasting of limestone (CaCO_3) to produce lime (CaO), releasing carbon dioxide (CO_2). The term has now come to mean the roasting of any material, in either an oxidising or reducing atmosphere, below its melting or fusing point, typically to remove a volatile component. The examples used in this research are calcined bone ash (to remove water and organic phases of the bone), and flint (to remove organic contaminants and convert some of the mineral structure to the more brittle cristobalite, so that it can be more easily ground).
- CE Common Era, synonymous with AD, or Anno Domini.

- China clay a generic term used in Britain during the 18th and 19th centuries, and by ceramic historians thereafter, to describe a low-iron and low-titanium kaolinitic clay. One large source is known in Cornwall, and other smaller sources around the country were also in use for ceramics during this period. The name is thought to refer to its suitability, and therefore widespread use, for fine ceramics in imitation of Chinese porcelain.
- China stone historical term used to describe a kaolinised granite rock, which was discovered in Cornwall during the 18th century, and used as a substitute for porcelain stone (petuntse) in the production of British hybrid hard-paste porcelain
- clay-rich frit porcelain a clay-rich, soft-paste porcelain that used lead-rich flint glass, or alkali-rich crown glass, or a combination of these glasses, as the principal fluxing component. It is distinguished from frit porcelain (also known as glassy porcelain) by the presence of much more clay in the formula, which gives this type of porcelain a distinct elemental composition.
- Crown glass a generic name for a type of glass which used alkali elements (typically sodium, potassium or calcium) as the main fluxing component. The name is thought to refer to its use in windows, which were formed using a spinning technique, resulting in a round central “crown” in the pane.
- Cullet a generic term referring to broken glass and/or ceramic pieces that were ground into a powder and used to create new ceramics or glass.
- Earthenware a class of ceramics that have been fired at a relatively low temperature (<1000°C). They are characterised by a softer, less brittle ceramic matrix, with no vitrification, and often pores.

EDS	Energy Dispersive Spectroscopy, an analytical technique, similar to WDS but quicker and less accurate, which uses x-ray excitation of electrons to detect the elemental composition of a sample.
feldspathic glaze	the name given to a glaze formulation for British porcelain, which was designed by John Rose & Co., Coalport, to replace the lead-rich glazes that were harmful to ceramic workers' health. At the time of writing, no examples have been analysed and the formula is not known. However, from the name, it may be reasonably assumed that the composition involves feldspar, and so the fluxing agent may be aluminium.
flint	a hard, sedimentary form of quartz, which was used in Britain in the 18 th century as a source of silica in some soft-paste porcelains.
flint glass	a generic name for a type of glass which used lead as the main fluxing component. The name is thought to refer to the use of flint as the source of silica and lead in its formulation.
flux	a substance added to a batch of ingredients, typically in ceramic, glass or metal-working, to reduce the melting temperature of the mixture, in order to make it easier to work or produce a ceramic or vitreous matrix.
frit porcelain / glassy porcelain	a soft-paste porcelain that used lead-rich flint glass, or alkali-rich crown glass, or a combination of these glasses, as the principal fluxing component. It is distinguished from clay-rich frit porcelain (also known as glassy porcelain) by the presence of much less clay in the formula, which gives this type of porcelain a distinct elemental composition.
gypsum	a soft sulphate mineral, which generally has the formula $\text{CaSO}_4 \cdot 2\text{H}_2\text{O}$. It was used in Meissen porcelain as a flux, and also appears to have been incorporated in a few British soft-paste porcelains.

hard-paste
porcelain

This term is contentious, because different terminologies have been used in different languages (particularly in Britain, Europe and the Far East) from the 17th century to the present. Many of these terms remain in use by different groups of specialists who study porcelain, and the choice of the specific term may be made according to the object's provenance, appearance, design, or material characteristics such as hardness and elemental or mineralogical composition. In this work, it is used following the convention of British ceramic historians, archaeologists and archaeomaterials scientists, to refer to a class of ceramics that were fired at a relatively high temperature ($\geq 1200^{\circ}\text{C}$), are white in colour, and were typically produced using just two ingredients: a pure, kaolinitic clay, and a decomposed granite stone (porcelain stone, or *petuntse*), and in a single firing cycle that produced the ceramic and fired on the alkali glaze. This is distinct from soft-paste porcelain, which used multiple raw materials and was often fired at a lower temperature in at least two firing cycles, and from hybrid hard-paste porcelain, which uses similar raw materials to hard-paste porcelain, and therefore has a comparable elemental composition, but was fired in two distinct cycles (i.e. one to form the ceramic matrix and one to fire on the glaze, which may be fluxed with lead).

HH-XRF

a Hand-Held instrumentation of the X-ray Fluorescence technique.

hybrid hard-
paste
porcelain

the name used by British ceramic historians, archaeologists and archaeomaterials scientists, to refer to a class of ceramics that were fired at a relatively high temperature ($\geq 1000^{\circ}\text{C}$), are white in colour, and were typically produced using just two ingredients: a pure, kaolinitic clay, and a decomposed granite stone (porcelain stone, or *petuntse*), and in at least two firing cycles (i.e. one to form the ceramic matrix and one to fire on the glaze, which may be fluxed with lead).

kaolinitic clays	a term given to clays that consist of, or contain large proportions of, the mineral kaolinite ($\text{Al}_2\text{Si}_2\text{O}_5(\text{OH})_4$). China clays are very pure forms of kaolinitic clays, containing very low impurities such as iron and titanium.
LA-ICPMS	Laser Ablation Inductively Coupled Plasma Mass Spectroscopy, a tandem technique which uses a powerful laser to burn a small amount of sample, this is then removed with a stream of helium gas and ionised in a plasma torch. The ionised sample is carried into a mass-spectrometer, which separates the ions by their mass to charge (M/Q) ratio. The results take the form of a spectrum, with the M/Q ratio on the x-axis, and relative intensity on the y-axis
lead glaze	a vitreous coating applied to ceramic paste, which uses lead as the principal fluxing component. During the 18 th century in Britain, it was extensively in use on tin-glaze earthenware (also known as delftware or faience), and on stonewares including soft-paste porcelain.
limestone	a sedimentary rock, composed of calcium carbonate (CaCO_3)
magnesian porcelain	a soft-paste porcelain that used magnesium, typically from steatite, as the principal fluxing component. During the early years of this ceramic's manufacture, lead was also used to further lower the melting point of the ceramic matrix.
phosphatic porcelain	a soft-paste porcelain that used calcium phosphate, typically from bone ash, as the principal fluxing component.
porcelain stone (petuntse)	a historical term used to describe a variety of micaceous or feldspathic rocks used in the production of Chinese porcelain.

SEM	Scanning Electron Microscopy, a technique for high-magnification imaging, in which a stream of electrons is pointed at the sample, and the energy of the reflected electrons gives a phase-contrast view that is representative of the elemental composition of the surface. Often used with energy dispersive spectroscopy (EDS) or wavelength dispersive spectroscopy (WDS).
Smalt	a term used in Europe during the 18 th and 19 th centuries to refer to any roasted cobalt ore that was destined for use in producing cobalt blue pigment. In porcelain, it was used as the colourant in underglaze blue decoration, and in overglaze blue, or sometimes turquoise or purple, vitreous enamels.
Soft-paste porcelain	a class of white ceramics that were produced in Europe during the mid-17 th to mid-19 th centuries, initially in imitation of Chinese porcelain. A wide variety of formulae were used to varying degrees of success, but typically included a white-firing clay, an additional source of silica (sand or flint pebbles), and a flux. Once a viable formula for hard-paste porcelain, and the innovation of bone china, had been discovered, soft-paste porcelain became obsolete, and ceased production.
Steatite (soapstone)	in geology, a talc-schist that is rich in magnesium. In Britain during the 18 th and 19 th centuries, it was used to refer to a wide range of soft, white rocks used in the production of magnesian porcelain. From the composition of this porcelain, the principal rock appears to have been steatite in the geological sense, but gypsum or calcite may also have been included in some cases.
Stoneware	a class of ceramics, including porcelain, that have been fired at $\geq 1000^{\circ}\text{C}$. They are characterised by a hard, brittle ceramic matrix, which is often vitrified, and with few pores.

WDS	Wavelength Dispersive Spectroscopy, an analytical technique, similar to EDS but with greater accuracy and precision, which uses x-ray excitation of electrons to detect the elemental composition of a sample.
white-firing clays	a generic term used to refer to clays, including ball clays and china clays, which contain sufficiently few impurities that the ceramics they produce are white in colour.
XRD	X-ray Diffraction Spectroscopy, an analytical technique that measures the angles and intensity of a reflected X-ray beam to identify the crystal phases present in the sample.
XRF	X-ray Fluorescence Spectroscopy, an analytical technique which uses an X-ray beam to excite the electrons on the surface of a sample, and measures the energy which they release to calculate the relative abundance of major and minor elements present.
Z	A value meaning the atomic number of an element, equal to the number of protons in the nucleus of a single atom.

1 Introduction

This research seeks to develop an analytical methodology to characterise and distinguish the products of different porcelain factories operating in Britain during the mid- to late-18th and early-19th century. To make the method applicable to rare and valuable ceramic objects and fragments, all techniques involved must be as minimally invasive as possible, so the emphasis must be on non-destructive and surface analyses.

The project is being carried out in response to the difficulty faced by ceramic-historians and fine art specialists in distinguishing between porcelain objects from different factories and periods, and in identifying later-decorated pieces and fakes (Sandon, 2009; p. 62; Marno, 2008; Pearce, 2008; Elliot, 2006, pp. 98-102; Manners, 2005). Visual standards have traditionally been used by connoisseurs, who rely on a consensus of forms, features and decorative motifs to provenance and date individual objects by comparison with others (Rackham, 1937; Watney, 1973; pp. xix - xxi; Sandon, 1980, pp. 87 - 88; Sandon, 1997). In this work, dates are provided by documentary sources and inscribed and armorial objects, which have allowed a stylistic chronology to be created for each factory.

The aim of this project is to develop a method from existing scientific analytical techniques that will allow the composition of British porcelain objects to be characterised, preferably quantitatively, in order to compare pieces from different factories using objective criteria. The start of this work involves reviewing and collecting existing data (Chapter 3), in order to determine what it is possible to say about British porcelain using published quantitative data. Statistical techniques for discriminative analysis will be used to establish the extent of inter-factory and intra-factory variation.

Secondly, a selection of minimally-destructive analytical techniques will be tested, both on items of intact porcelain, and on fragmentary archaeological samples, to evaluate the effectiveness of the available techniques for porcelain in different context (Chapters 4, 5, and 6).

A technique, or set of techniques, having been selected, a set of representative, matrix-matched standards and an optimised set of analytical conditions will be developed. Finally, the results of the techniques used will be critically evaluated, by comparison with the data from the invasive analytical techniques that are currently used. The novel data thus obtained will be discussed, both with regard to the suitability of the analytical techniques to the material for the purpose of distinguishing between the products of different factories, and in terms of the contribution that the results will have made to the historical and archaeological narrative of British porcelain production.

1.1 Context of the project

1.1.1 Historic context

Ceramics are an important aspect of human material culture, made using a wide variety of techniques and raw materials throughout most of the world, in almost all later periods of history and pre-history. This allows them to be used as indicators for the presence of a particular culture, and that culture's technological accomplishments. Ceramic objects occur in many contexts, from utilitarian domestic equipment, to prestige tableware and works of art. They give archaeologists and historians an insight into the social structure and patterns of production, trade and consumption. Ceramics survive the passage of time better than organic materials, because all but the most low-fired earthenwares are resilient to most taphonomic processes and they are more commonly found than metal and glass, because a clay pot cannot be melted down and reformed.

This research concerns fine ceramics of the late-eighteenth and early nineteenth centuries, set in the historical context of the Industrial Revolution. The production was driven by the increasing demand for material finery by the emerging middle class and existing wealthy upper classes (Young, 1999b; pp. 179 - 181). During this period, imported Chinese and continental European ceramics were the models for fashionable table-wares, tea-wares and decorative objects.

Introduction

British fine ceramics strove to imitate these types, in order to undercut the trade in these highly-priced wares (Godden, 2004, pp. 27 - 30). Porcelain was produced in Britain from the 1740s onwards, initially around London, where as now the majority of expenditure on luxury goods occurred (Adams, 1991; pp. 39 - 40; Young, 1999b; p. 162; Adams, 2001). Production was then increasingly moved to the North and Midlands of England, where coal and clay could be obtained conveniently (Watney, 1997, pp. 7 - 8; Sandon, 2009; p. 7; Hillis, 2011; pp. 1 - 2), and to the South West, near the soapstone quarries and china-clay sources in Cornwall (MacKenna, 1946; MacKenna, 1947; Massey, 2001; Spero, 2006; pp. 21 - 23). Multiple factories operated in competition with one another, and due to the technical difficulties of producing a paste that would survive firing at relatively high temperatures, this high-risk business ruined many proprietors within a few years, (Mallet, 1974; Barker and Cole, 1998; Owen et al, 2000; Owen and Barkla, 1997). This has resulted in an array of porcelain objects that vary in their forms and designs and also in the degree of technical accomplishment and skill with which they were made. Connoisseurs and art historians have long been able to distinguish factories and periods by the visual characteristics of groups of objects (Rackham, 1937; Watney, 1973, pp. xix - xxi; Sandon, 1980; p. 167). Scientific research has begun to demonstrate the extent to which the products of different factories and periods vary from one another in their elemental composition and mineralogy, as a consequence of using unique and changing recipes for the paste and glaze (Bimson, 1991; Freestone, 1996; Freestone, 2001; Owen, 2007).

These factories and their products will be discussed in Chapter 2, which covers their visual and material characteristics, and the insight that this provides into the available materials and technical abilities of their respective creators.

1.1.2 Methodological context

Analysis of porcelain has formerly relied upon Scanning Electron Microscopy (SEM) with attached elemental compositional analysis, such as Energy Dispersive Spectroscopy (EDS) or Wavelength Dispersive Spectroscopy (WDS) (Watney et al, 1993; Freestone, 1996; Owen et al, 1998; Owen, 2002) and upon mineralogical analysis by X-ray Diffraction Spectroscopy (Bimson, 1969; Tite and Bimson, 1991). Both of these techniques are excellent, producing reliable, accurate analyses; however, they require that a sample of material be taken to perform the analysis, and for this reason, they have been unpopular with museum curators and conservators, and dealers and private collectors of ceramics. The analytical techniques used to obtain data from ceramics and glazes will be surveyed in Chapter 2, with respect to their advantages and disadvantages, and this discussion will inform the selection of a suitable technique on which to base the new analytical methodology.

Non-destructive and micro-destructive research has previously been carried out to develop analytical methodologies and comparative data-banks for porcelain, including Chinese (Leung et al, 2000; Leung and Luo, 2000; Li et al, 2005), and continental European factories; Meissen, Du Paquier and Vincennes-Sèvres, among others (Miliani et al, 2009; Casadio et al, 2012; Domoney, 2012; Bezur and Casadio, 2013). These studies have found that the porcelain paste, glaze and decorative enamel pigments change through time, and that the major and minor elemental composition of the porcelain can be used to provenance and date pieces. Certain non-destructive analytical techniques have therefore been demonstrated to be effective for materials that are compositionally similar to British porcelain. The detailed compositional data that can be obtained without invasive sampling have been well-received by conservators, private owners of objects, and those involved in the trade of fine ceramics, who require the information that these data and their interpretation can produce without compromising the condition of the object (Shugar and Mass, 2013; pp. 20 - 21).

1.2 Scope and structure of the project

The specific research questions have been formulated in response to problems that exist within British porcelain connoisseurship, whereby a given class of objects from a certain period or factory or decorator, are frequently confused with objects not of that class, but with a similar appearance. Since a precise attribution can drastically affect the value of a piece of porcelain, it is desirable to be able to distinguish the genuine pieces from the simulacra. Some of the specific research questions addressed here are:

- 1) To what extent can different factories be distinguished using non-destructive techniques, based on characteristics of their glaze and the underglaze blue pigment used in their decoration?
- 2) Can original (18th century) enamels on Worcester porcelain be distinguished from later (19th century) enamels using non-destructive techniques?
- 3) Are there distinctive features about the trace elemental composition of porcelain pastes and glazes that can be linked with the formulae and sources of raw materials used by different factories?

This thesis will provide a survey of the historical and scientific research on porcelain in Chapter 2, beginning with a summarised history of the import and manufacture of porcelain in Europe, and, to a greater extent, in Britain. The motives of the consumers who obtained imported porcelain at huge cost will be examined, as well as those of the British factory proprietors who similarly faced financial ruin in pursuit of unsuccessful formulae for high-fired ceramics. There follows a survey of the analytical techniques that have traditionally been used to obtain data from porcelain and other ceramic and vitreous objects, and general conclusions which can be derived from these data are given.

In Chapter 3, British porcelain will be characterised using published SEM-EDS/WDS data. These published data will be collected and critically assessed, with the aim of determining the extent to which the paste and the glaze may be used to distinguish different factories and periods.

Introduction

Bipolots and ternary plots will be used to demonstrate visually the groups that correspond to different formulae for porcelain pastes, and the extent of inter-factory similarity in glaze composition.

Chapter 4 contains a description of the sample groups that will be used in the analytical studies that follow, including the reasons for selection of intact objects and archaeological sherds from a range of factories and periods. The second half of the chapter will provide details of the instruments and conditions, and the analytical methodology used in each study.

The results of the non-invasive techniques follow in Chapter 5, incorporating results from the glaze, enamels, and underglaze blue pigments of the porcelain samples analysed. The results of novel micro-destructive analysis, which includes trace elemental compositional data from porcelain pastes, are described separately in Chapter 6.

The final chapter will bring together the findings from all of the techniques and samples. They will be discussed individually with regard to the usefulness of that technique for the samples. The results will then be assessed collectively in order to determine what contributions this research has made to British porcelain studies, particularly the specific research questions listed at the beginning of this section.

2 Historical and Technical Review of British Porcelain

Porcelain is a high-fired ceramic, see Table 1, typically made from white, kaolinitic clays, a flux, and an additional source of silica. *Hard-paste* porcelain, also known as *true* porcelain, was first produced in China during the 10th century CE, having been developed from existing stonewares (see 2.2.1) (He Li, 2004; pp. 335 – 338). To make porcelain, the object is formed from a clay and silica mixture, and then fired at high temperatures (1200 – 1350°C), causing the clay and silica constituents to melt and then vitrify (Tite et al, 2012), see 2.2.1. The resulting product is therefore translucent when very thin, and produces a ringing sound when tapped. The mineral structure consists of mullite ($3\text{Al}_2\text{O}_3 \cdot 2\text{SiO}_2$) in a siliceous matrix. As the name suggests, it is very hard with a brittle fracture.

Soft-paste porcelain, also known as *artificial* porcelain, is a diverse group of white ceramics, made in Europe from the late 17th century onwards in imitation of the Chinese product, see 2.2.2. Soft-paste porcelain is generally fired at a lower temperature than hard-paste porcelain, between 1000°C to 1100°C (Godden, 2004; p. xviii), and as a result, the body is much less vitrified. This means that the resulting objects are more opaque, and softer. To achieve a melt, fluxing ingredients are added, and soft-paste porcelains may be categorised by the principal flux used. The compositional and mineralogical differences between hard-paste porcelain and the various soft-paste porcelains will be addressed below.

Table 1 - categories of ceramics, classified by firing temperature (after He Li, 2004; pp. 38 – 39)

Class of ceramics	Firing temperature (°C)	Other properties
Earthenwares	<1000°C	typically porous, absorb liquids
Stoneware	≥1000°C	harder than earthenware, low porosity, less absorbent
Porcelaneous ware	≥1000°C	low trace impurities (Fe_2O_3 1 – 3%; TiO_2 0.5 – 1%)
True porcelain	≥1200°C	white in colour, very low trace impurities (Fe_2O_3 <1%; TiO_2 < 0.5%)

Hard- and soft-paste porcelain glazes are most often clear, giving the finished object a pure, white colour, essentially the colour of the underlying ceramic seen through the glaze. This is an effective backdrop for coloured enamel, paint, prints and gilding. The history of development of these decorative pigments is important for understanding how elemental compositional analysis of porcelain objects' surfaces can provenance and date the piece.

In this chapter, the development of the porcelain industry in Britain during the 18th and early 19th centuries will be described, using historical and other sources. Primary historical documents have been used as sources wherever these are available. Where mineralogical formulae are shown, these are the values provided by Deer et al (1992), unless another reference is given.

2.1 Scope of this chapter

This chapter presents the historical and methodological context of this research. First, the context of porcelain as a product of China and then continental Europe will be provided, to demonstrate how porcelain came to be in Britain as an imported commodity. British porcelain will be introduced, first as an historic event in the development of British industrial manufacture, and then as a material that is the object of archaeological study. Then the methods that have been used to investigate and categorise porcelain will be assessed, particularly with regard to the comparability of their results and their objectivity. The scientific analytical techniques employed for porcelain characterisation will be surveyed, and the types of results that they are capable of providing will be critically assessed. Of particular interest will be the material requirements of each technique, in terms of the processes of sampling that may be used, and their effect on the porcelain object. These considerations will be important for informing the decision of analytical techniques to be used in developing the optimised methodology.

The resulting discussion of the research questions that surround British porcelain, and the methods which are being developed to answer them, will provide the basis for assessing the methodology that results from this research.

2.2 The history of the porcelain industry in Britain

2.2.1 Imported Chinese porcelain

The development of porcelain in China is a complex matter, which has been debated in historical and archaeological literature for over a century (He Li, 2004, p. 335; Kerr and Wood, 2004, pp.143-146; Harrison-Hall, 1997, pp. 182 – 184). Much of the controversy hinges on the precise definition of porcelain, distinct from white glazed earthenware and high-fired grey stoneware. Chinese *porcelain* is generally defined by the firing temperature, which must be sufficient to cause vitrification, and the white colour, caused by the lower concentration of colouring trace oxides, such as iron (Fe, 26) (Wood, 1999; p. 47).

Proto-porcelaneous stonewares, grey-white in colour and fired at high temperatures, are found from the 6th century BCE (Chen et al, 1999), and some have been found at the site of Anyang, dating to the late 12th century BCE. These have an alkali glaze, fluxed with potassium (Beurdeley and Beurdeley, 1974). Porcelain as defined above was being produced from the 10th century CE, and the recipe inferred from their composition is 70-80% petuntse (porcelain stone), and 20-30% clays of varying purity and grain-size, glazed with a porcelain stone and wood ash vitreous glaze (Wood, 1999; pp. 48 – 49; Yin et al, 2011).

There is evidence for the use of underglaze cobalt blue decoration from the early 14th century CE, during the Yuan dynasty (Carswell, 2000; p. 11). These designs used cobalt ore imported from Persia, and designs probably in imitation of Persian blue-decorated earthenwares (Carswell, 2000; pp. 11 – 12). Early forms included table-wares and tea-wares, and also sometimes imitated the forms of Persian bronzes, such as ewers and incense-burners (Du Boulay, 1984; p. 104).

The factories that produced the finest wares were placed under a mandate to supply the imperial household, while numerous private factories sold to noblemen and overseas trading companies (Du Boulay, 1984; pp. 251 - 252).

By the 15th century CE, Portuguese explorers were bringing this product to Europe; a short-lived trading relationship between China and Portugal was established by Jorge Alvares in 1513 – 14 (Carswell, 2000; pp. 128 – 129). Early in the 17th century, the influence of the Dutch United East India Company increased the volume of Chinese imports to Europe, using the heavy ceramics as ballast for huge ‘supercargo’ ships full of tea (Howard and Wallis, 1986; pp. 10 – 11; Jörg, 1982; pp. 128 - 129). It has been estimated that from the beginning of the 17th century to the end of the 18th, at least 43 million pieces of Chinese porcelain were successfully transported to Europe, although many ships were wrecked during the sea crossing (Howard and Wallis, 1986, p. 12). Blue and white was particularly favoured: Chinese styles of decoration were viewed as a fashionable novelty, see Figure 1 (left), while the Chinese factories responded to the Western appetite for their products by producing European-style scenes and armorial pieces, see Figure 1 (right) (Young, 1999b; pp. 88 - 89).



Figure 1 - blue and white Chinese porcelain, with a typically Chinese pattern (left) and adapted European scenes (right) (museum numbers, PDF.A.611 and Franks.582 respectively, both British Museum)

Knowledge of porcelain production was also acquired by Europeans visiting China. In spite of the secrecy that was built into the supply and manufacturing systems, production was observed and recorded by the French Jesuit missionary, Père Francois Xavier d’Entrecolles, in 1712 and 1722 (Tichane, 1983; p. 49). His account includes details of the materials and processes involved in porcelain manufacture, although the names used for these materials are corruptions of the Chinese terms, making it clear that d’Entrecolles was not familiar with ceramic raw materials, and he was unable to provide details about the firing cycle and temperatures.

2.2.2 The invention of porcelain in continental Europe

The value of imported porcelain drove an industry of imitation across Europe, particularly in the political and economic centres of Venice (Lane, 1954), Paris (Godden, 1993), Dresden (Menzhausen, 1990; pp. 12 - 14), London (Godden, 2004; pp. 50 - 51) and Lisbon (Dias et al, 2013). Contemporary accounts praise the elegance of the Chinese aesthetic, in contrast to the conspicuous consumption of European fine table wares of the time (Gallagher, 1953). It has been argued persuasively that a significant factor in the European attraction to Chinese porcelain was the mystery of its composition and manufacture (Gerritsen and McDowall, 2012). Even with the widely-circulated account of Pere d'Entrecolles, the terms used for the raw materials (*petuntse* for porcelain stone, *kaolin* for the clay) had no European equivalent that was known at the time, and the writer was unable to write in detail on the firing conditions, as he lacked the necessary knowledge to identify and record these important factors.

Hard-paste porcelain at Meissen

Johann Friedrich Böttger and Ehrenfried Walther von Tschirnhaus are together credited with the creation of the first European hard-paste porcelain from 1710 (Pauls-Eisenbeiss, 1972; pp. 14 - 15). The work was carried out under the patronage of the Prince Elector of Saxony, Friedrich Augustus II, in order to supply the Royal court. The formula comprised a white-firing clay mixed with a gypsum flux (Pauls-Eisenbeiss, 1972; p. 15)).

Using Augustus' financial backing, their experimental formula was taken up on a large scale to found a factory at Meissen for the purpose of supplying the King with porcelain and profit (Pietsch, 2010; pp. 15 - 16). The problem of imitating porcelain was addressed using the most advanced scientific knowledge of the period (Pauls-Eisenbeiss, 1972; p. 24), and this continued to be the case when production was attempted in other parts of Europe, including Britain.

A breakthrough occurred when kaolinitic clay was discovered nearby at Aue, which allowed the Chinese petuntse and kaolin formula to be replicated, while royal financial backing permitted experimental formulae to be produced and extensive kiln failures endured without ruination (Pauls-Eisenbeiss, 1972, p. 24). Böttger's ambition was to improve on the Chinese aesthetic, making it in keeping with the European fashions, and to replace completely both Chinese imports and European metal tablewares (Menzhausen, 1990, p. 11). Decoration of Meissen porcelain began with overglaze lacquers - organic pigments which are applied in many layers, and set by evaporation rather than firing - as Böttger had no knowledge of vitreous enamels (Pietsch, 2010; p. 16). Gilding was occasionally added by craftsmen working outside the factory, such as Johann George Funcke and Johann Jacob Gäbel, and this pair was also responsible for developing the first enamel colours for Meissen porcelain (Pietsch, 2010; pp. 16 - 18). The palette and technique were further developed by Johann Gregorius Höroldt from 1723 (Pietsch, 2010; pp. 18 - 22).

The cobalt blue pigment *smalt* was used to create the underglaze blue designs on white porcelain objects, in imitation of Chinese blue and white (see Figure 2). The source of the pigment was local; Saxony had controlled a virtual monopoly of the supply of cobalt ore in Europe since the late 15th century (Delamere, 2013; pp. 56 - 57).

Illustrated below (Figure 2), the translucent white Meissen paste, with the new European decorative style fusing Chinese and Japanese motifs with the Baroque aesthetic, made Meissen the model for European fashion in fine ceramics throughout British porcelain's formative years (Young, 1999b; pp. 78 - 79). Sets of porcelain were given as diplomatic gifts from the mid-18th century onwards (Chilton, 2007; p. 275). Dinner services, tea-wares, and dining paraphernalia such as ice pails, were designed to be used for entertaining, and thus seen by guests who might be enticed to purchase their own set (Weber, 2010; p. 155; Cassidy-Geiger, 2007; p. 16).



Figure 2 - images of early Meissen tea bowls and saucers with design incorporating Chinese (left) and European (right) decorative themes (museum numbers C.600&A-1920 and C.44&A-1954 respectively, Victoria and Albert Museum)

Experimental production in Britain

The role of the Royal Society

The Royal Society appears to have taken a keen interest in the development of a British porcelain industry; besides numerous mentions of the discoveries of raw materials useful to porcelain manufacture (Daniels, 2007; p. 22; p. 26), they also sought the products of successful formulae. In 1665, the Royal Society received an eyewitness account, detailing the raw materials and processes for making “China-dishes” in Milan (Phil. Trans. R. Soc., 1665; p. 127). A report of soft-paste porcelain production at the Saint Cloud factory in France was submitted in 1698, the first known account of soft-paste porcelains (Lister, 1699; pp. 138 – 140). The journals of the Royal Society later record a “fine white ware” which was compared favourably with Chinese and European porcelain, presented in February 1743, and that was said to have been made with raw materials sourced entirely from Britain (Daniels, 2007; p. 24). The presenter, Thomas Bryand (or Briand), founded a factory in Stoke-on-Trent, but this foundation was not known to have produced ceramics with any commercial success, before the death of Bryand in 1747 (Mountford, 1969).

John Dwight's patent

In 1672, John Dwight was granted a patent for the production of “transparent earthenware commonly known by the names of Porcelaine (*sic.*) or China” (Oswald et al, 1982; p. 26). His patent specifies the use of ball-clay from Dorset and sand from the Isle of Wight, resulting in a hard, white-coloured ceramic (Oswald et al, 1982; pp. 27 - 28). By employing the upright, square-shaped kiln that was commonly used for contemporary delftware production, he was capable of reaching the temperatures required to produce stoneware (Oswald et al, 1982; p. 28). Numerous samples of this work were submitted to the Royal Society through Robert Hooke over the next ten years (Daniels, 2007, pp. 13 - 14).

This shows that there were reports of successful products, but none are known to have been manufactured on an industrial scale or advertised for sale to the public (Oswald et al, 1982; p. 32). Three porcelain jars from the collections at Burghley House have been suggested as products of John Dwight's patent on the basis of their elemental composition (Ramsay et al, 2013), although research by Spataro et. al. differs (2009). A factory was established in Fulham for the production of ceramics to Dwight's recipe, and they used a white-firing clay with roasted flint as a source of silica, but the grey-bodied, salt-glazed ware is not generally classed as porcelain, see Figure 3 (Young, 1999a; p. 27).



Figure 3 - white salt-glazed stoneware coffee-pot (left), and portrait bust (right) from John Dwight's Fulham pottery (museum numbers AF.3145AN103468001 and 1887,0210.103AN415095001 respectively, British Museum)

The Bow patents

In 1744, a patent for porcelain was filed on behalf of Edward Heylyn and Thomas Frye, attempting to protect the use of a white micaceous clay named 'unaker', which they imported from America (Freestone, 1996). This document describes the recipe that they claimed to use, and the source of the raw materials, making it a very important exception to the secrecy that tends to surround contemporary and later porcelain factories.

Both the patent and the recipe have been discussed thoroughly elsewhere (Freestone, 1996; Ramsay et al, 2003; Ramsay and Ramsay, 2008), but a few points relevant to this thesis may be noted. Part of it reads:

"Take unaker, and by washing separate the sand and mica from it, which is of no use.; take pott ash, fern ash, pearl ash, kelp, or any other lixiviall salt, one part of sands, flints, pebbles, or any other stones of the vitrifying kind; one other part of these two principles form a glass in the usual manner of making glass; which when formed reduce into an impalpable powder." (Her Majesty's Stationery Office, 1865; pp. 1 - 3)

From this it can be deduced that the raw materials are kaolinitic clay with an alkali, or plant ash, glass flux, which the writers of the patent assume that the reader is familiar with producing.

“Then mix to one part of this powder two parts of the washed unaker, let them be well worked together until intimately mixed for one sort of ware; but you may vary the proportions of the unaker and the glass; videlicet, for some parts of the porcelain you may use one half unaker and the other half glass, and so in different proportions, till you come to four unaker and one glass after which knead it well together, and throw in on the wheel, cast it into moulds, or imprint it into utensils, ornaments, &c...” (Her Majesty’s Stationery Office, 1865; pp. 1 - 3)

The proportions of raw materials are subject to variation, depending on the requirements for forming. It may be expected that the elemental composition of the products would reflect this variation.

“It will then be in a situation to be put into the kiln and burned with wood, care being taken not to discolour the ware, otherwise the process will be much hurt. This first burning is called biscuiting” (Her Majesty’s Stationery Office, 1865; pp. 1 - 3)

Therefore, the process of firing was carried out in two stages, in the style of contemporary glazed earthenwares, beginning with a high-temperature biscuit firing to remove water and volatile elements, and harden the ware.

“if it comes out pure white, is ready to be painted blue, with lapis lazuli, lapis armenis, or zapher, which must be highly calcined and ground very fine. It is then to be dipt in the following glaze:- Take unaker forty pounds, of the above glass ten pounds, mix and calcine them in a reverbatory; then reduce and to each pound when reduced add two pounds of the above glass, which must be ground fine in water, left of a proper thickness for the ware to take up a sufficient quality.” (Her Majesty’s Stationery Office, 1865; pp. 1 - 3)

The process of decorating the fired biscuit in the ubiquitous underglaze blue is here described. The pigments named are: lapis lazuli ($\text{Na}_8[\text{Al}_6\text{Si}_6\text{O}_{24}]\text{Cl}_2$), lapis armenis

(azurite, $\text{Cu}_3(\text{OH})_2(\text{CO}_3)_2$), and zapher, the contemporary name for zaffre, the cobalt-blue pigment most commonly used in Chinese underglaze blue porcelain, which was extracted from smaltite ($(\text{Co}, \text{Ni})\text{As}_{3-x}$), skutterudite ($(\text{Co}, \text{Ni})\text{As}_3$), or cobaltite ($(\text{Co}, \text{Ni}, \text{Fe})\text{AsS}$) (Delamere, 2013; p. 41). The glaze was made from the same materials as the paste, but with a higher proportion of glass (i.e. silica) to increase transparency and hardness. This glaze mixture was applied in solution and then allowed to dry.

“When the vessels, ornaments, &c. are dry, put them in a kiln in cases, burn them with a clean wood fire, and when the glaze runs true let out the fire, and it is done” (Her Majesty’s Stationery Office, 1865; pp. 1 - 3)

This refers to the second firing, known as the glaze firing, which was carried out at lower temperature, sufficient to melt the glaze so that it bonded to the biscuit, while excess ran off.

This recipe in the Bow patents therefore describes a hard-paste body with a lead-free glaze, which is practically unique for British porcelain until the late-18th century. Freestone observed its similarity to the 'A'-marked group of porcelains (Freestone, 1996), first recognised thirty years previously (Charleston and Mallet, 1971). This group of porcelains, called 'A' mark because they commonly have an 'A' on their base, had no known production source. Freestone proposes, therefore, that the Bow patent represents the first commercially viable porcelain to have been produced in Britain. The purpose of Bow's wares, to undercut expensive imports, is evident in their design, which mimics both the Chinese forms and patterns (Figure 4) and also the European style of Meissen (Figure 5).



Figure 4 - 'A'-marked cup (left) with Chinese tea bowl in Kakiemon style (museum numbers C.28-1959 and C.1308-1924 respectively, Victoria and Albert museum)



Figure 5 - 'A'-marked tea bowl and saucer in Meissen European-style (left, museum number C.143&A-1984; Victoria and Albert Museum), with comparable Meissen tea bowl and saucer (right, museum number Franks.88; British Museum)

2.2.3 Industrial production of earthenware and glass

While porcelain was being developed experimentally in Britain, there existed the foundations of other large-scale high-temperature industries. The recipes and processes for porcelain shared requirements in terms of raw materials and technology with the existing industries of glass and ceramics.

Glass-making had been in a state of expansion since the early 16th century; factories catered to prestige table-wares in 'façon de venise' soda glass and later lead crystal, with coarser potassic "forest" glass for windows and bottles (Godfrey, 1975; pp. 225 - 226).

The manufacture of ceramics had experienced major imported innovations in the form of the stoneware formula, and tin-glaze, which allowed inexpensive imitations of porcelain to be produced in blue and white. In these ceramics, the fabric was both thinner and stronger than traditional earthenware, which permitted more sophisticated shapes to be formed and fired successfully (Edwards and Hampson, 2005; pp. 30 - 32).

Raw materials

Porcelain and glass-making both required a source of silica, typically in the form of sand or flint, the purity of which was paramount both for the transparent table- and window-glass and for achieving the prized whiteness of porcelain.

Stonewares, including the Dwight patent white wares, required very pure clays in order to fire white, with a small grain-size creating the plasticity to allow detailed modelling and complex forms. They therefore relied on ball-clay of the sort used to create tobacco pipes (Edwards and Hampson, 2005; pp. 64 - 66). There is evidence for the use of ball-clay in some British soft-paste porcelains which have an elevated level of TiO₂, see for instance Bow second patent wares (Ramsay and Ramsay, 2007), Limehouse wares (Freestone, 1993) and Swansea phosphatic porcelain (Owen et al, 1998).

The cobalt blue underglaze pigment, which gave Chinese porcelain its distinctive blue and white designs, was imported to Britain from Saxony (Delamere, 2013; pp. 67). During the mid-18th century, the Society for the Encouragement of the Arts, Manufactures and Commerce of London offered a prize for the manufacture of its products: *zaffre* (a powder produced by roasting cobalt ore and fritting it with sand) and *smalt* (a glass produced by fusing zaffre with potassium carbonate [K_2CO_3]) (Delamere, 2013; p. 68). The prize was won by Nicholas Crisp, a member of the Society who had produced soft-paste porcelain at factories in Vauxhall and Bovey Tracey, (Turnbull, 1997). William Cookworthy, founder of the Plymouth hard-paste porcelain factory, also made progress in perfecting cobalt production using a source in Cornwall (Watney, 1973, p. 3). It is unknown from what date, or by which factories, this British source of cobalt was used in preference to imported pigment; however, a similar prize was offered by the Royal Society in 1812, citing the inadequacy of the Cornwall source as its reason (Delamere, 2013; p. 69).

Kiln technology

Another significant factor in the development of porcelain in Britain was the technology to create a sufficiently high-firing kiln - soft-paste porcelains requiring a temperature of between 1100—1300°C (Young, 1999a). Furnaces capable of reaching this temperature had been brought into the country by itinerant glass-makers during the early 16th century, and had been subsequently improved to adapt to the enforced use of coal as a fuel during the final years of the 16th century and the beginning of the 17th century (Godfrey, 1975; pp. 143 - 146). However, these furnaces were small in size, prohibiting large-scale firings of multiple ceramic objects. A patent for a high-temperature kiln designed to fire stonewares and bricks had been filed in 1636 and was certainly in use by John Dwight's Fulham factory and the Staffordshire stoneware producers, by the time of the 1744 first porcelain patent (Edwards and Hampson, 2005; p. 115). These kilns were capable of reaching high temperatures, but the range was difficult to control, leading to financially devastating kiln failures during the first half-century of porcelain production (Owen and Morrison, 1999).

Crucially, the ceramic and glass-making industries had created a skilled work-force, capable of adapting its skills to porcelain manufacture, as well as the transport infrastructure, in the form of roads and navigable rivers and canals, to allow the import of raw materials and fuel, and export of the finished product (Edwards and Hampson, 2005; pp. 66 - 67, p. 245).

2.2.4 Industrial production of soft-paste porcelain

The following history of porcelain manufacture in Britain is intended to introduce the major factories and individuals that are relevant to this thesis, and to describe the course of the industry over the century between the first Bow patent in 1744 and the widespread adoption of a single bone-china formula for porcelaneous ceramics in the mid 19th century. The scale of the industry, and the complexity of its relationship to contemporary British and continental European fine ceramic and glass manufacture, prohibits an exhaustive survey in this research, but the factories and relationships that are of greatest relevance are described in context, and the references herein can be consulted for further information.

London and the first factories

As discussed above (Section 2.2.2), the first factory producing commercially-viable porcelain is now thought to have been the first Bow factory, beginning in 1744; the earliest products of which are the 'A'-marked group (Freestone, 1996).

It is not known exactly for how long the first Bow factory was active; a second Bow factory certainly existed from 1750, under the management of one of the former proprietors of the first factory, Thomas Frye. A second patent for the production of porcelain was filed in 1749, using an entirely different recipe (Hurlbutt, 1926). This formula uses as its flux a wide bracket of substances known as "virgin earth", which the patent says may be extracted, to a greater or lesser extent, from "all animal substances, all fossils of the calcareous kind, such as chalk, limestone, &c.", and has therefore been interpreted as calcium phosphate.

Once calcined, ground and washed, the “virgin earth” is mixed with a source of silica, either sand or ground quartz pebbles or flint, and fired to make a type of alkali glass. Two parts of this glass were then combined with one part of pipe-clay, as discussed above, and then cast or thrown, and fired in the biscuit kiln.

The glaze recipe is also different from the first patent, with a high proportion of lead to silica, which would allow the glaze kiln - the kiln in which the biscuit items were fired for a second time to apply the glaze - to be operated at much lower temperatures.



Figure 6 - image of Bow second patent saucer in Kakiemon style (left) and tea bowl and saucer in Chinese style (right) (museum numbers C.68-1964 and C.219&A-1940 respectively, Victoria and Albert Museum)

The products of this recipe survive, and are among the earliest examples of British soft-paste porcelain. They have a slightly phosphatic composition and lead-rich glaze. There is good correspondence between the design features of these wares and the ‘A’-marked wares, the majority of products being table-wares (particularly tea-sets, of Chinese- and Japanese-style design), see Figure 6 (Godden, 2004; pp. 51 - 52).

At the time of the failure of the first Bow factory, a short-lived business was set up by Joseph Wilson & Co. at nearby Limehouse (Watney, 1993; pp. 1 - 2). The early products of this factory have been analysed, and the composition is very similar to the late Bow first patent products, consisting of mostly SiO_2 with 5-10wt% Al_2O_3 and 3-5wt% K_2O and CaO (Freestone, 1993; pp. 72 - 73). The recipe, though, employed a cheaper ball clay, rather than the imported unaker (Freestone, 1993; p. 72).



Figure 7 - Limehouse underglaze blue sauceboat (left; museum number 1965,1002.1, British Museum) and pickle dish (right; museum number C.923-1924, Victoria and Albert Museum)

The glaze was initially silica with alkali, as in the Bow first patent products, but quickly changed to a lead-rich formula after the majority of the early glazed wares spoiled in the kiln (Ramsay et al, 2013). Within a year, the paste recipe also changed to a soft-paste with 40-50wt% SiO₂ and 2-3% MgO and P₂O₅. For this formula, the inferred ingredients are a source of silica, such as sand or pebbles, steatite (Mg₆[Si₈O₂₀]OH)₄, Deer et al, 1996), bone ash, possibly in a form resembling the Bow second patent “virgin earth”, and an alkali glass frit (Freestone, 1993).

After the failure of the Limehouse business, there is evidence that one of the principal manufacturers may have been involved in the inception of a new factory at Bristol (the name of the man is not known; Barrett, 1966). This company, founded by a Quaker glass-maker named Benjamin Lund, obtained a mining license for Cornish steatite in early 1749, allegedly the first such license awarded for the purpose of making ceramics (Morton Nance, 1935). The Bristol products, therefore, could be a second attempt by a Limehouse proprietor to create a workable magnesian formula. There are aesthetic features common to the wares of both factories, see for example the sauceboats in Figure 7 and Figure 8, which both possess an unusual fluted rim and elaborate thumb-rest made in two parts. The use of underglaze manganese purple pigment was peculiar to the Bristol factory (Figure 8), and may represent a transfer of technology from glass-working, the industry originally carried out at this factory (Toppin, 1954).



Figure 8 - Lund's Bristol polychrome enamelled sauceboat (left) and figure of a Chinese Taoist Immortal, with underglaze manganese purple decoration (right) (museum numbers C.1297-1924 and C.97-1938 respectively, Victoria and Albert Museum)

Long believed to have been the first British porcelain factory, Chelsea was certainly among the earliest. There is a newspaper column advertising “China made at Chelsea” for sale in early 1745 (Valpy, 1984), by which time the business must have been operating for long enough to have developed a workable paste and produced a stock of objects for sale. There are no surviving documentary recipes for Chelsea’s paste, but securely provenanced samples have been analysed, and have been found to have a glassy siliceous paste with a consistently high level of CaO (15-20wt%) and low levels of other alkalis (Na₂O 0.5-1.0wt%, K₂O 2-5%) and PbO (2-5wt%) (Tite and Bimson, 1991). The inferred recipe is quartz sand and clay, with lime, lead oxide and alkali from fritted crown glass, with a lead-rich glaze which may have been made from the same materials but a higher proportion of glass cullet, contributing a much higher level of lead (PbO 40-45wt%) (Tite and Bimson, 1991). Chelsea porcelain was marketed with emphasis on novelty of shape and decoration, initially of Far Eastern, and particularly Japanese, inspiration, but from the Red Anchor period onwards (ca. 1752-58, see Figure 9) increasingly conscious of Meissen and the French factories (Figure 9; Adams, 2001; pp. 30 - 31). Figures and other decorative forms developed as a speciality under the artistic direction of the modeller Joseph Willems in the 1750s (Adams, 2001; pp. 122 - 124).



Figure 9 - Chelsea red-anchor period polychrome sugar bowl (left) and Chinese-style musicians, modelled by Joseph Willems (right) (museum numbers C.3&A-1966 and C.40-1974 respectively, Victoria and Albert Museum)

With a change of creative direction in 1756, (the Gold Anchor period, see Figure 10; Sandon, 1997), a new paste appeared at Chelsea, with no PbO and significantly lower K₂O (1-2wt%), but new high levels of Al₂O₃ (~10wt%), CaO (~20wt%) and P₂O₅ (~17wt%) (Tite and Bimson, 1991). This suggests that the recipe favoured more inexpensive ingredients (Honey, 1933), with the omission of crown glass, and addition of bone ash as the flux.



Figure 10 - Chelsea gold-anchor period rose-ground teapot (left) and polychrome figure of a musician, modelled by Joseph Willems (right) (museum numbers 517&A-1902 and C.32-1973 respectively, Victoria and Albert Museum)

The factory at Isleworth, Middlesex, was forgotten by ceramic historians, and unrecognised by most collectors, from the end of the 19th century until the mid-1990s, its products being attributed to the other phosphatic-producing factories Bow, Derby, Lowestoft or Liverpool (Howard, 1998). Subsequent research has discovered that the factory was founded in 1770 by a defector from Lund's Bristol, and later the Worcester factory, Joseph Shore. Porcelain was produced there until 1787, generally functional wares decorated with underglaze blue in Chinese style, see Figure 11 (Godden, 2004; p. 228).



Figure 11 - Isleworth underglaze blue saucer (left; museum number 1928,0213.3.CR, British Museum, 2015) and coffee cup, part of a set (right; museum number C.82&A-1956, Victoria and Albert Museum)

Evidence has recently been discovered of porcelain manufacture at a ceramic factory in Vauxhall, and a dated waster has placed this as early as 1754 (Freestone et al, 2003). Documentary evidence exists for this factory, including a license for the quarrying of Cornish soapstone, in the name of Nicholas Crisp, in 1751 (Massey et al, 2007; pp. 37 - 38). Sherds excavated from the river near the site of the former factory indicate that the formula used was bone ash, with some glass or frit. Comparison of archaeological sherds with intact objects has allowed some pieces previously attributed to other factories to be confirmed as Vauxhall. These include both blue-and-white and polychrome wares. Ambitious Baroque decorative forms were made, as well as functional tea-wares and table-wares, see Figure 12 (Massey et al, 2007; p. 40, p. 43, p.60).



Figure 12 - Vauxhall underglaze blue and white mug (left), and polychrome enamelled ewer (right) (museum numbers 414:110-1885 and C.1336-1924 respectively, Victoria and Albert Museum)

A number of commercially-successful formulae having been discovered, the significant factors driving the next century of technological progression were attempts to undercut the competition by reducing the cost of production. The main expenses that confronted a porcelain factory were: transport, solved by situating factories on a river or canal, or directly near the sites where fuel, clay and stone were mined or quarried (Young, 1999b; pp. 23 - 25); raw materials, with expensive imported unaker being supplanted by locally-sourced clays (Ramsay et al, 2013); and the failure of large numbers of objects in the biscuit kiln (Owen and Morrison, 1999); which could only be solved by decades of trial and error.

Accordingly, while these London parent companies closed after a few years, the focus of porcelain manufacture was shifting to the North and West, and the localities of Liverpool, Stoke on Trent, Wales and Cornwall, see Figure 13, Figure 14 and Figure 15. These are the locations where the large-scale pottery industry had been established near sources of coal, coke and clay (Young, 1999b; pp. 23 - 25), and the transport hubs created by rivers and new canals (Edwards and Hampson, 2005; pp. 66 - 67, p. 245).

Historical and Technical Review of British Porcelain

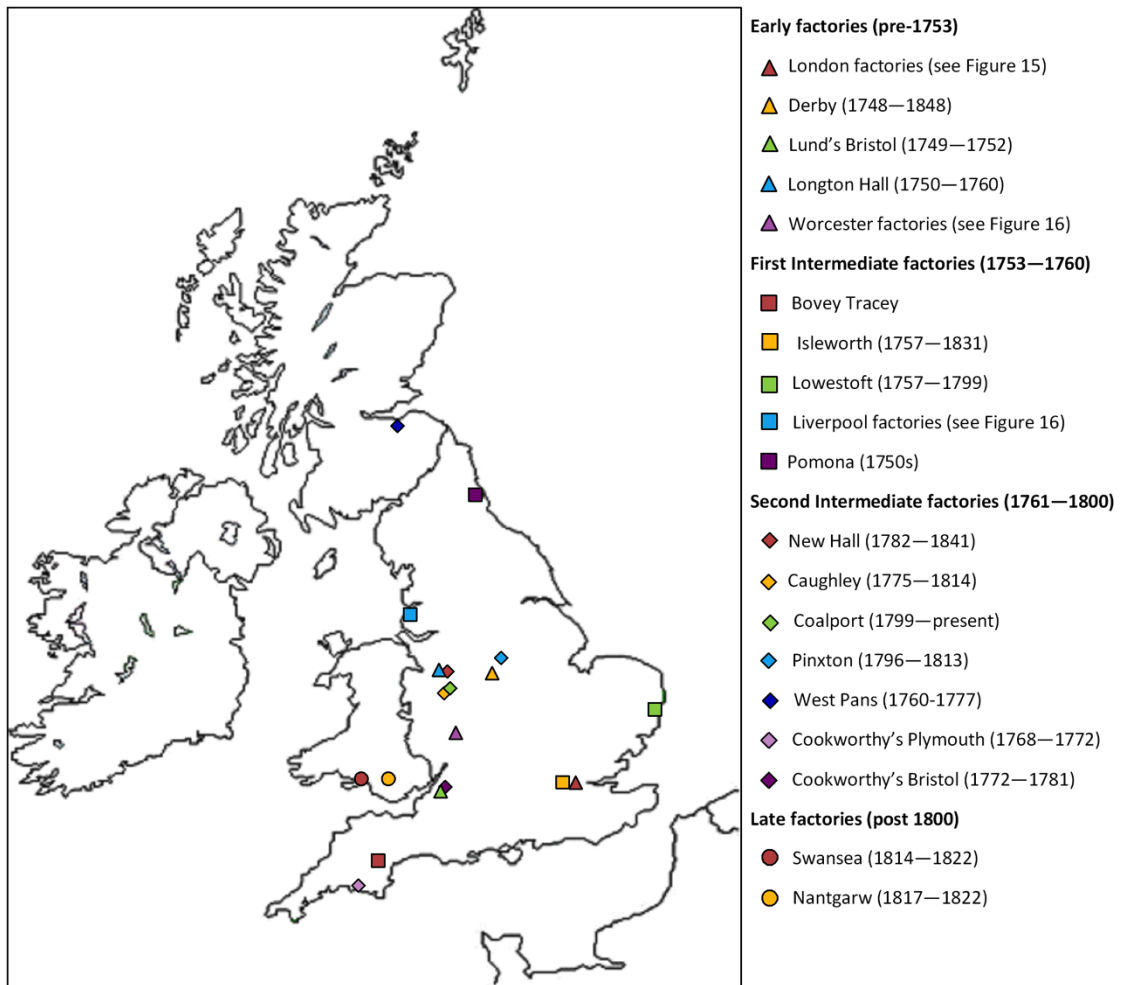


Figure 13 - map of the British Isles showing the locations of the major porcelain factories active in the 17th and early 18th centuries. The symbols used for the factories on this map are used throughout the thesis in graphs and plots to refer to their respective factories.

Historical and Technical Review of British Porcelain

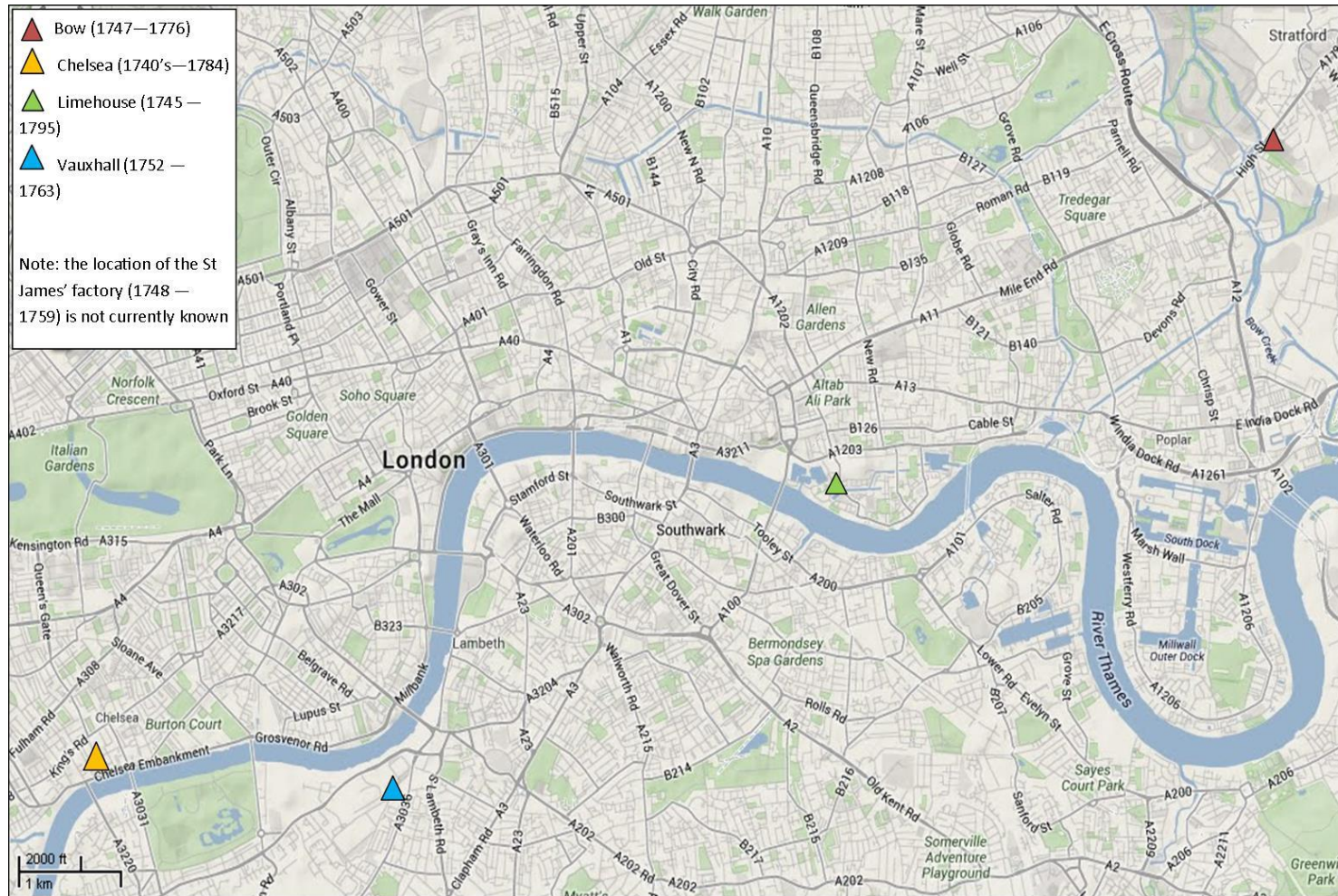


Figure 14 - map of London showing the location of the major porcelain factories that were active in the 18th and early 19th centuries. Isleworth is considered a London factory, but it is not included on this map, as it is to the west of the map area, see Figure 13. Map data ©2013 Google.

Historical and Technical Review of British Porcelain

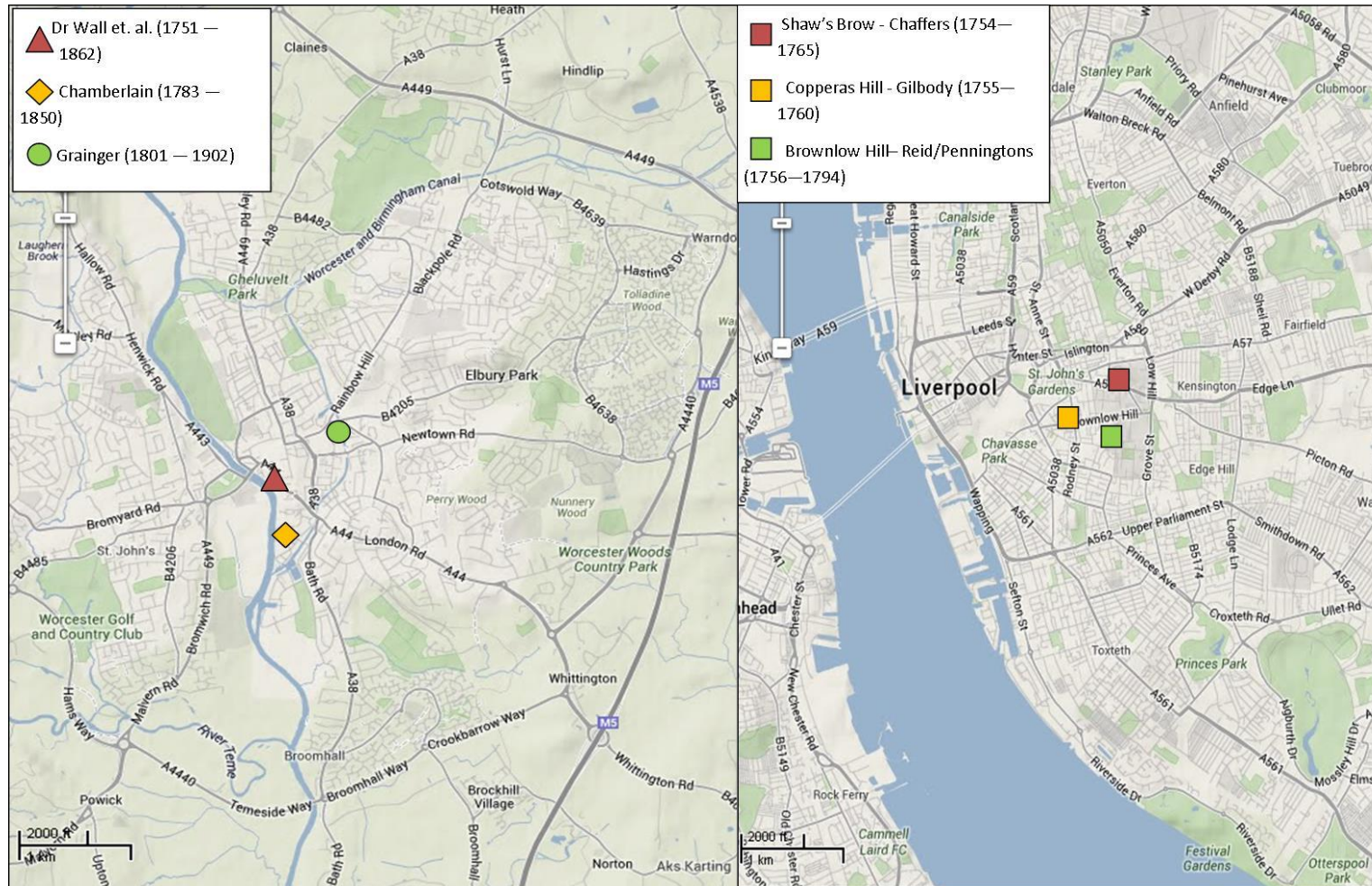


Figure 15 - maps of Worcester (left) and Liverpool (right) showing the locations of the major porcelain factories operating during the 18th and early 19th centuries.

Map data ©2013 Google.

Derbyshire, Worcestershire, Liverpool and Staffordshire

When Chelsea failed in 1769, it was bought by a newly-established porcelain factory in Derby, and the two factories were operated concurrently until 1784 (Barrett and Thorpe, 1971). From its inception in 1750, Derby had used a lead-rich flint-glass paste, with a corresponding lead-rich glaze (Owen and Barkla, 1997), producing forms that were similar to, if not in imitation of, Chelsea porcelain (Barrett and Thorpe, 1971). Upon acquiring the Chelsea factory, the composition of porcelain produced at Derby changed, with increased Al_2O_3 (~10wt%) CaO (~20wt%) and P_2O_5 (~17wt%), and virtually no PbO (<2wt%) in the paste (Owen and Barkla, 1997). As a result of the takeover, the overglaze polychrome enamels on Derby improved in appearance, and copies appeared in greater numbers of the famous Chelsea figures, see Figure 16 (Adams, 2001; pp. 182 - 183).



Figure 16 - Derby polychrome enamelled sauceboat (left) and figure of a dancing man (right) (museum numbers C.277-1976 and C.540-1921 respectively, Victoria and Albert Museum)

The inferred recipe for Derby wares post-1770 includes a source of quartz, kaolinitic clay and bone-ash (Owen and Barkla, 1997), virtually identical to the recipe that was employed at Chelsea from the beginning of the Gold Anchor period in 1756 until closure in 1769 (Adams, 2001). This bone-ash paste was used successfully at Derby, with the lead-rich glassy formula reserved for figures, until the adoption of a single bone china formula in 1810 (Barrett and Thorpe, 1971).

While many of the early porcelain factories were established by craftsmen in related materials, such as glass-makers (for example, Bow's Edward Heylin (Hurlbutt, 1926) and Bristol's Joseph Lund (Owen, 1873)), or metalworkers, (such as Chelsea's Nicholas Sprimont and Derby's William Planché (Barrett and Thorpe, 1971)), the tradition of the Royal Society's chemical experiments in porcelain continued. Especially important were John Wall, a doctor of medicine, and William Davis, an apothecary, who established a factory in Worcester, in 1751 (Binns, 1865). This partnership has been credited with establishing the most long-running and successful British porcelain business still in existence.

The products of the earliest formulae used at Worcester, which exist only in the archaeological record, are composed of predominantly SiO_2 (~80%) and contain CaO (20-30wt%) and P_2O_5 (17-25%), suggesting a recipe involving bone ash (Owen, 1998). There are a few sherds which have elevated levels of MgO (3-5wt%) and Na_2O 0.6-0.8wt%), and far lower P_2O_5 (3-5wt%) and CaO (4-6wt%), and which date to immediately before Worcester's takeover of Bristol's formula and assets (Owen, 1998). This suggests that experimentation was being carried out with a steatitic paste, and that these experiments were sufficient to convince Wall and Davis that the failing Bristol works would pay off their investment. Although the town of Worcester was then small, it was linked with the large trading hub of Bristol by the River Severn (Spero, 2005; pp. 18 – 20), from which coal and timber were shipped from Wales and china clay and steatite from Cornwall.

At the original Warmstry House premises of Worcester porcelain factory, the steatite recipe was retained (albeit with extensive compositional variation caused by experimentation) from the takeover of Lund's Bristol in 1752 until the late 1790s, when the rise of bone china made soft-paste formulae obsolete (Owen, 2003; Owen 1997). The earliest Worcester porcelain, like that of Bow, mimicked Chinese forms and designs in order to pass as imported porcelain. However, as Bow became more skilled at this, Worcester diversified into polychrome enamelled pieces in European styles (Sandon, 1993; pp. 231 - 232).

Initially, they copied and produced designs in the style of Meissen, but from the 1760s onwards, porcelain from the French factory Sèvres ascended in fashion, and Worcester, along with Chelsea, began to imitate them with increased use of coloured grounds, see Figure 17 (Marshall, 1954, pp. 68 - 69).



Figure 17 - Worcester underglaze blue tea-bowl and saucer with Meissen-style Indianische Blumen (left) and Sèvres-style blue-ground tea-pot with gilding (right) (museum numbers CIRC.338&A-1916 and 414:602/&A-1885 respectively, Victoria and Albert Museum)

Rival porcelain factories were established in Worcester by Robert Chamberlain at Diglis in 1783, and by Thomas Grainger at St Martin's Gate in 1801 (Godden, 2004; pp. 519 - 523). Both men were trained and previously employed at Worcester and in terms of their elemental composition their first products closely resemble Worcester wares of the period (Owen, 2003). Later both developed high SiO₂ (75-80wt%) and Al₂O₃ (16-20wt%) pastes which resemble hard-paste porcelain, but which were created in two firing cycles, in the style of soft-paste porcelain (Owen, 2003).

Former employees of Worcester also defected to Liverpool, with Richard Podmore bringing the magnesian formula to Chaffers in 1754 (Boney, 1957); to Caughley, Shropshire, with Thomas Turner in 1772 (Godden, 1970; pp. 435 - 436); and to Swansea and Nantgarw later in the 1770's (Owen et al, 1998). The three competing Worcester factories were united in 1862, under the name of Royal Worcester, and their products consisted of both bone china and true porcelain formulae (Owen, 2003).

In Liverpool, at least seven porcelain factories were operating in the half a century between 1753 and 1803, during the decline of the local delftware industry (Hillis, 2011; p. 2, pp. 5 - 6). The porcelain products were not generally marked according to their factory of origin and, as workers routinely moved from one factory to another, and members of a single family – the Penningtons – were involved in the management of five separate businesses, the products are difficult to distinguish, and therefore provenance, conclusively (Watney, 1997; pp. 80 - 81).

From the analysis of archaeological sherds excavated from three of the longest-lived factories, the extent of compositional similarity between the products of each factory is apparent (Owen and Sandon, 1998). The pastes employed by Gilbody at Shaw's Brow, and by John Pennington at Folly Lane, have universally high Al_2O_3 (7-10wt%), CaO (15-20wt%) and P_2O_5 (10-15wt%), with a trace of SO_3 (0.1-0.3wt%). The slightly higher mean K_2O (2.0-2.5wt%, as opposed to 1.0-1.5wt%) at Folly Lane is the only noticeable distinction (Owen and Sandon, 1998). At the Chaffers and Shaw's Brow, a MgO- and PbO-rich formula was used (MgO 7-10wt%, PbO ~7wt%), which was derived from that used at Worcester, as discussed above. The mineralogy, though, indicates that a subtly different source of steatite may have been used by Chaffers, which, unlike the Worcester Cornish steatite, contained calcite (CaCO_3). In terms of their forms, there is evident imitation of Worcester table-wares and tea-wares, using blue-and-white Chinese decorative motifs (Boney, 1957), see Figure 18.



Figure 18 - Liverpool (John Pennington) tea bowl and saucer and tea canister (Seth Pennington) with Chinese design in underglaze blue (museum numbers C.847&A-1924 and C.420-1924 respectively, Victoria and Albert Museum)

In 1772, a porcelain factory was established in the premises of a Shropshire pottery works in Caughley by Thomas Turner, a former Worcester employee (Godden, 1970; pp. 435 - 436). The first products had high SiO_2 (75-80wt%) and MgO (8-10wt%), with a varying but generally low level of PbO (1-6wt%), similar to those produced at contemporary Worcester (Owen and Sandon, 2003). This compositional similarity is matched by the forms and decorative schemes used by the two factories, making them difficult to distinguish. Most Caughley porcelain is in blue and white in imitation of Chinese imported ware, or Worcester adaptations of the same, see Figure 19 (Godden, 2004; pp. 435 – 437). The mineralogy of Caughley magnesian wares more closely resembles Chaffers' products; the presence of diopside ($\text{Ca}(\text{Mg,Fe})[\text{Si}_2\text{O}_6]$) indicating the use of a source of steatite which contained calcite (CaCO_3) (Owen and Sandon, 2003). From 1796, Caughley produced hybrid hard-paste porcelain using the two-stage soft-paste firing cycle, with a lead-rich glaze (Owen and Sandon, 2003).



Figure 19 - Caughley underglaze blue jug (left) and tea-bowl and saucer (right) (museum numbers C.197B-1921 and C.197G-1921 respectively, Victoria and Albert Museum)

At the same time, a rival porcelain factory was established, initially as two ventures which were quickly combined, less than five miles along the River Severn from Caughley at Coalport (Barker and Horton, 1999). The proprietors, John and Thomas Rose, are thought to have been employees at Caughley (Godden, 1970; p. 478), and they produced two types of porcelain, a phosphatic paste, and a hybrid hard-paste that is compositionally indistinguishable from Caughley's hard-paste formula (Owen and Sandon, 2003). The Coalport porcelains expanded on the ambition of Caughley, creating European-style objects with Regency decoration in polychrome overglaze enamels, see Figure 20 (Godden, 1970; pp. 486 - 488).



Figure 20 - Coalport polychrome vase and cover (left) and rose-ground plate (right) (museum numbers C.1205&A-1917 and 3381-1901 respectively, Victoria and Albert Museum)

From 1820, the new Coalport factory produced porcelain with high levels of CaO and P₂O₅, consistent with the use of bone ash, under the guidance of William Billingsley and Samuel Walker, formerly proprietors of another factory producing porcelain of a similar composition in Nantgarw, Wales (Owen and Sandon, 2003). In 1820, John Rose and Co. were the first factory to patent a lead-free *feldspathic* glaze for porcelain, which, it was hoped, would solve some of the serious health problems that afflicted workers who came into contact with the liquid or molten glaze (Godden, 1970; p. 14).

Wales

In 1813, William Billingsley and Samuel Walker left the Worcester porcelain factory in order to manufacture a new type of body with which they had been experimenting (Williams, 1931). Billingsley and Walker worked briefly at nearby Nantgarw with the proprietor William Weston Young and made a hybrid hard-paste ware with high CaO (20-25wt%) and P₂O₅ (15-20wt%) (Owen et al, 1998). The majority of these porcelains failed in the kiln, leading to the closure of the factory in 1814. Surviving examples are esteemed for their craftsmanship and the accomplished painting in polychrome overglaze enamels and gilding, see Figure 21 (Williams, 1931).



Figure 21 - Nantgarw blue-ground plate (left) and green-ground pen tray (right) (museum numbers 414:806-1885 and C.171-2003 respectively, Victoria and Albert Museum)

Their next attempts, at the premises of Lewis Weston Dillwyn in Swansea, produced a modified formula with much higher Al_2O_3 (20-23wt% as opposed to 12-13wt%), indicating a greater amount of kaolinitic clay (Owen et al, 1998). Dillwyn himself developed a high SiO_2 (70-73wt%) and Na_2O (0.5-1.0wt%) hybrid hard-paste, which has been inferred to contain mostly clay and quartz (Owen et al, 1998). In appearance, Swansea porcelain is unique; the forms and decorative schemes do not mimic any factory in particular, but make imaginative use of polychrome enamels and gilding in Regency style (Fairclough, 2005).



Figure 22 - Swansea polychrome enamelled and printed plate (left) and rose taper stand (right) (museum numbers C.590-1935 and C.31-1944 respectively, Victoria and Albert Museum)

Bovey Tracey, Bristol and Plymouth

In Plymouth, William Cookworthy developed a hard-paste formula, which he based on the letters of Francois Xavier D'Entrecolles describing Chinese manufacture, (see Section 2.2.2, which describes the Chinese process and materials for making hard-paste porcelain) (Tichane, 1983; p. 49). The patent that Cookworthy enrolled in 1768 specifies the use of identifiable raw materials, namely "moorstone", or "growan" (a weathered granite rock; Hitchins and Drew, 1824) and "growan clay" (a kaolinitic clay associated with the growan), which were sourced from nearby Cornwall, (Owen, 1873; pp.vi-vii). Both factories produced tea-wares and table-wares with underglaze blue decoration, but are best known for their figures, and animal and bird models, see Figure 23.

Porcelain was also produced nearby at Bovey Tracey in Devon, where a locally-sourced white-firing clay was already in use for making bricks and earthenware pottery (Stretton, 1970). Nicholas Crisp, the proprietor of a failed porcelain factory in Vauxhall, London, set up there in 1766 what was said to be a large factory for the production of delftware (a tin-glazed earthenware, typically with a blue and white decoration), and experimental soft-paste and hard-paste porcelain (Massey, 2002). Crisp worked in co-operation with William Cookworthy, carrying out experimental firings using the local sources of clay (Massey, 2002). A great deal of detail about these experiments is still known due to the surviving records of extensive correspondence between Cookworthy and Thomas Pitt (Adams and Thomas, 1996; pp. 31 - 35). The porcelain produced at Bovey Tracey was subject to a high rate of failure. Crisp appears to have given up porcelain production after having been imprisoned for bankruptcy in 1768, although the manufacture of earthenware and delftware continued until 1774 (Massey, 2002). As a result, the number of surviving pieces of Bovey Tracey porcelain is small. They include several unusual shapes, such as two examples of fuddling cups (White, 2007), see Figure 23. A further set of correspondence, which took place from 1761 - 1764 between Nicholas Crisp and Sir Charles Erskine, the owner of a newly-discovered cobalt mine at Alva, Fife, details the interest of Crisp in discovering a British source of cobalt blue pigment (Turnbull, 1997).

Although the mines did not ultimately yield sufficient ore to become a reliable source for the country's industries, it was tested on pieces produced at the Bovey Tracey factory (Turnbull, 1997).

The elemental compositions of samples of some hard-paste porcelains manufactured by William Cookworthy at Plymouth and Bristol and by Nicholas Crisp at Bovey Tracey are consistent with the use of a kaolinitic clay and a substance like porcelain stone (Owen et al, 2000). The mineralogy and composition of both Bristol and Plymouth hard-paste porcelain closely resembles Chinese and Meissen hard-paste porcelain (Owen et al, 2000).



Figure 23 - Plymouth figure of Europe (upper right), Bristol figure of a boy (upper left), and Bovey Tracey fuddling cup (lower) (museum numbers 3088-1901, 414:737-1885 and C.130-1926 respectively, Victoria and Albert Museum)



2.3 Systems of classification for British soft-paste porcelain

The aim of characterising a porcelain object is to measure aspects of its composition that are distinctive, and that can be compared with other characterised wares. By comparison, it may be possible to determine its provenance, that is, to match it to a factory and approximate date of origin. From this provenance can follow deductions about the raw materials and techniques, even individuals, employed in its manufacture.

Characterisation begins with observations about the appearance of the object, its factory marks, its form and decorative features, which may be matched with well-provenanced examples from known factories, or with archaeological material or pattern books that are associated with a factory. More recently, data have been gathered from porcelain objects and sherds to characterise them by their composition, both in terms of elements and mineral phases. These observations are matched with existing data from well-provenanced objects, raw materials extracted from their source, and experimental pieces created under controlled conditions. Systems of classification are therefore important in material studies to determine which features of the object are significant in terms of its place within the scheme of all possible objects of its type.

2.3.1 Macroscopic appearance

Factory Marks

Factory marks are applied, engraved, or painted designs, added to a porcelain object in order to identify it with a factory, maker, period, or decorating studio of origin. The most highly-esteemed European factories used marks that were recognisable in Britain, for example, Meissen's crossed swords, (Figure 24), Vincennes-Sevres' double 'L', (Figure 25), and Chantilly's hunting horn, (Figure 26). Marks are found on many British porcelain objects; these often vary through time, such as the progression of anchor marks at Chelsea, (Figure 27), or the many iterations of the crescent moon at Worcester, (Figure 28).

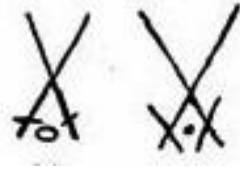


Figure 24 - crossed-swords marks used by the Meissen porcelain factory from 1763 - 1774.
Image © Old and Sold Antiques Auction and Marketplace, accessed online at <http://www.oldandsold.com/pottery/germany5.shtml>



Figure 25 - double L marks used by the Vincennes-Sevres factory from 1745 - 1753.
Image © Old and Sold Antiques Auction and Marketplace, accessed online at <http://www.oldandsold.com/pottery/france1.shtml>

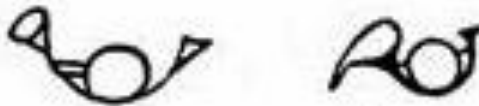


Figure 26 - hunting horn marks used by the Chantilly factory through the 18th century.
Image © Old and Sold Antiques Auction and Marketplace, accessed online at <http://www.oldandsold.com/pottery/france2.shtml>

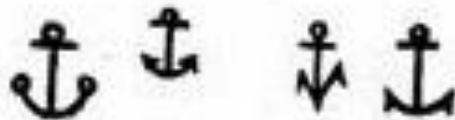


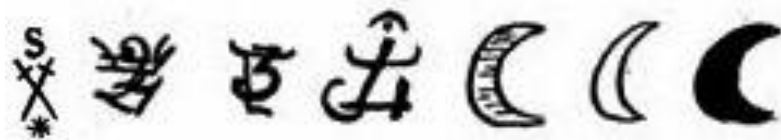
Figure 27 - anchor marks used by the Chelsea factory from 1750 - 1770.
Image © Old and Sold Antiques Auction and Marketplace, accessed online at <http://www.oldandsold.com/pottery/greatbritain5.shtml>



Figure 28 - crescent moon marks used by the Worcester factory from 1751 - 1783.
Image © Old and Sold Antiques Auction and Marketplace, accessed online at <http://www.oldandsold.com/pottery/greatbritain21.shtml>

There are many catalogues in existence that describe the significance of a mark, and the factory and period from which the object bearing the mark may originate (for those specialising in British pottery and porcelain, for example, Fisher, 1970; Poche, 1975; Godden, 1990; Cushion and Honey, 1996; Perrott, 1997; Lang, 2007).

However, these cannot be relied upon to correctly identify the factory of origin in all cases, because factories such as Caughley copied the marks that appeared on Chinese, European and other British porcelains, see Figure 29. Furthermore, in the 19th century, marks belonging to factories that produced high-quality (and therefore valuable) porcelain were frequently added to existing less valuable objects from other factories (Elliot, 1939; Charleston and Mallett, 1970).



*Figure 29 - marks used by the Caughley factory: an imitation Meissen mark (left; occasional); pseudo-Chinese symbols (middle three, between 1772 - 1799); and the Worcester crescent moon (three right; between 1772 - 1799).
Image © Old and Sold Antiques Auction and Marketplace, accessed online at <http://www.oldandsold.com/pottery/greatbritain4.shtml>*

Form and features

The most basic method for categorising an unknown item of porcelain has been to describe the colour of the surface, the patterns of underglaze pigments and the overglaze enamels, printing and gilding. By visual comparison with already provenanced wares, auction catalogues and factory records, patterns can be identified which were most common, or even unique, to a particular factory. The wares produced at Lowestoft, for example, often carried images of local scenes, such as the 'Good Cross Chapel' pattern illustrated below in Figure 30, which were visually translated into the fashionable Chinese style (Books, 2001). Chinese or Japanese wares were also directly copied, with pagodas, willow trees, dragons and figures used in the brightly coloured Kakiemon palette, and underglaze blue, see Figure 31.



Figure 30 - Lowestoft porcelain decorated with local scenes in Chinese style (museum number 1887,0307,XI.1; British Museum)



Figure 31 - a Worcester tea bowl and saucer in Kakiemon design (left) and Bow octagonal plate with Chinese figure in landscape (right) (museum numbers 414:641-1885 and C.595-1924 respectively, Victoria and Albert Museum)

Continental European wares, particularly from the French factories at Chantilly and St Cloud and from Meissen, were stylistically adapted or often copied directly, see Figure 32 (Manners, 2005). Their designs included abstract forms, often used as borders on reserves and rims; floral and fruit patterns; fauna, such as insects and birds; landscapes; and figural scenes, generally depicting a scene from a narrative, such as a fable. For a few patterns, a tradition of imitation can be discerned which descends from the original oriental ware to a Meissen adaptation which was then copied by a British factory. Ramsay and Ramsay (2007) give an example of a Kakiemon two-quail pattern which comprises two red birds in the original Japanese dish, altered to one red and one blue bird in the Meissen version, and appearing as one red and one blue bird in a Bow plate, suggesting that the designer of the Bow plate was copying the Meissen rather than the original Japanese piece, see Figure 33.



Figure 32 - blue ground and gilding with animal or bird-painting in the reserves, on table-ware by Meissen (left) and a later imitation by Chelsea (right) (museum numbers C.350&A-1918 and 524-1902 respectively, Victoria and Albert Museum)



Figure 33 - examples of the two-quail pattern on Japanese (upper left; museum number FB.2.a, British Museum), Meissen (upper right) and Bow (lower) table-wares (museum numbers C.46-2006 and C.185-1935 respectively, Victoria and Albert Museum)



However, the difference between similar designs from different factories is not always apparent, as Ramsay and Ramsay continue to discuss, citing an example of an unmarked tea-canister which carries the Chinese 'Island House' motif, and which has been variously attributed on stylistic grounds to a Chinese, Continental, or Bow second patent origin (Ramsay and Ramsay, 2007).

A further complicating factor is the presence of porcelain objects from several factories that were decorated in external workshops. The most well-known of these was run by James Giles, resident in London between 1763 and 1776. His workshop purchased blank, glazed porcelain in bulk and added enamel and gilding, before reselling the porcelain (Hanscombe, 2005; pp. 11 - 15). The result is a class of porcelain objects, the form of which may be unique to the factory of origin, but which have enamel decoration that is similar to pieces from other factories, having been decorated by the same workshop or painter (Figure 34).



Figure 34 - a cup and saucer from the Worcester factory (left; museum number C.338&A-1940), and a cup and saucer made in Jingdezhen, China (right; museum number C.59I-1957), both decorated in the workshop of James Giles, with a monochrome figured landscape and gilded border, Victoria and Albert Museum

The form of an object may be unique to a particular factory, in spite of the extensive practice of imitating successful pieces or even entire sets. However, attributions can be often be made based on the differences in morphology of features, even between designs which at first appear identical. Sauceboats are a common utilitarian and decorative shape, adapted from European metal examples. They all have an elongated bowl-shaped body with a handle at one end, a shallow, open spout at the other, and a foot rim underneath. Within this class of objects, there is a great deal of variation in the shape and relative size of all of these features, which can assist in attribution (Panes, 2009; p. 259). When identical copies by one factory of a shape produced by another are found, these may sometimes be due to the former buying the latter out, and acquiring their moulds and pattern books and even their staff (Clifford, 1969; Stevenson, 1989).

Colour and texture

Perhaps more subjective than these deliberate, decorative patterns are descriptions of hue, which have also been relied upon as a means of distinguishing between similar wares, such as Caughley and Worcester. In a direct comparison, Caughley porcelain is said to have a more “creamy” glaze hue than contemporary Worcester (Sandon, 1997; p. 138). Terms that have been applied to the appearance of porcelain surfaces include: “drab” and “mushroom-grey” (Gabszewicz and Freeman, 1982); “soft” and “tactile” (Spero, 2006; p. 69); and “buff”, “grey”, “greenish”, and “bluish” (Hillis, 2011; p. 23, p. 150).

The problems with using such terms in order to support an attribution to one factory, or period, are manifold. They are inconsistent, in that wares produced by one factory, such as Caughley, which may typically have a “creamy” glaze, also include pieces which do not, while some wares from other factories, such as Bow, have also been described in this way (Mallet, 1984). Furthermore, the visual categories are not supported by scientific analytical data; although composition can have an impact on the hue of a glaze, the hue of pieces can vary significantly between wares from the same factory and even the same kiln firing without the trace elemental composition changing significantly. Particularly importantly, the terms are subjective, relying on the viewer having experienced a wide range of wares in order for a comparison to be made and dependent on a consensus which may not exist. For example, in the case of the Watney teapot (Ramsay et al, 2011), it has been demonstrated that one man’s “clear glaze” (Begg, 2000) is another man’s “mushroom” or “drab-coloured glaze” (Gabszewicz, 2000).

“Texture” is the characteristic feature of the paste type, and described where an area of unglazed ceramic may be accessed, for instance on the base of tea-wares, table-wares and figures (Panes, 2009; pp. 253 - 254). Frit pastes are said to have the feel of a glass, soapstone can feel “slippery” to the touch, and bone ash paste suffers more than others from discolouration, although stain removal and cleaning can often mislead in this case.

2.3.2 Elemental compositional analysis

Compositional categories of porcelain pastes

The first scientific studies of British porcelain linked the major and minor elemental composition of the paste to raw materials that were thought to have been used in its production. Four compositional categories were devised based on the type of ingredients which were added as a flux to the basic clay former, namely: *glassy* or *frit*, which incorporated crushed scrap glass or a specifically-designed frit; *soapstone*, which contained steatite; *bone-ash*, which used calcined animal bones; and *hybrid hard-paste*, including modern bone-china, see Table 2 (Eccles and Rackham, 1922; Tite and Bimson, 1991).

To these have been added *clay-rich wares*, a subset of frit porcelains with higher clay and correspondingly lower frit, represented by wares from Limehouse and early Bow (Freestone, 2000; Ramsay et al, 2003).

Table 2 - modal bulk elemental compositions (wt%) of five compositional categories (Freestone, 2000)

Type	SiO ₂	TiO ₂	Al ₂ O ₃	FeO	MgO	CaO	Na ₂ O	K ₂ O	P ₂ O ₅	PbO	SO ₂
glassy/frit	62.8	0.2	4.9	0.2	0.3	20.1	0.8	5.3	0.3	4.4	0.3
magnesian	72.3	<0.2	3.4	0.4	11.0	1.9	1.4	3.3	0.3	5.7	0.3
phosphatic	51.2	0.3	5.6	0.3	0.6	23.2	0.6	0.6	15.3	0.4	1.9
bone china	43.0	<0.2	13.6	<0.2	0.5	17.4	1.6	1.6	21.2	<0.3	<0.2
clay-rich	72.4	0.8	10.7	0.5	0.7	7.1	2.8	3.0	<0.2	1.0	<0.2

Recent work criticizes the three or four recipe-based category system as inadequate to describe the range of British and American soft-paste porcelains (Owen, 2002; Ramsay and Ramsay, 2007), stating that there are simply too many exceptions for the system to be effective. Data have been gathered, for example, from the early products of the short-lived Longton Hall factory, Stoke on Trent, which were made from glass cullet, bone ash and limestone or gypsum, making them frit-phosphatic-calcic wares (Watney et al, 1993). Some porcelain was also made using both steatite and bone ash in the same paste, such as the magnesian-phosphatic wares attributed to Limehouse (Owen and Day, 1998a; Ramsay et al, 2013).

The discrete compositional categories are further complicated by the use of “grog” – powdered sherds of porcelain from China or from other European factories – by some British works in creating their own paste (Owen et al, 1998). The grog was mixed with a fluxing agent and re-formed into new objects possessing an anachronistic composition made up of possibly several types of porcelain pastes, which could change in each batch, depending on what material was available to use (Ramsay and Ramsay, 2007).

Similarly, in cases where ground glass was incorporated in a frit paste, the type of glass and therefore its composition is likely to have varied according to what was available (Owen and Barkla, 1997). The unpredictable availability of a single source of glass cullet contributed to high levels of kiln wastage, as wares from different paste batches would have been fired together in one kiln firing, and a set of temperature, time, and kiln atmospheric conditions that might have been perfect for some of the wares could have meant the failure of others simply due to differences in their composition particularly with regard to the fluxing elements (K_2O , Na_2O , PbO , MgO , P_2O_5) of the glass component. For this reason, frit-based pastes were abandoned, or efforts were made to homogenise the glass that was used.

The anomalous composition of frit porcelains from Limehouse, Pomona and Brownlow Hill suggests that the glass that was used in the paste did not originate from recycled window or vessel glass, but was manufactured specifically for the porcelain factory (Owen and Hillis, 2003). There is evidence for this process in the 1744 first Bow patent, which gives details of the raw materials and their quantities which were to be combined to make the glass frit for their porcelain (Ramsay and Ramsay, 2008).

Other ingredients were subject to seemingly arbitrary variation. For example, at Bow, a small amount of gypsum appears to have been added to some batches and omitted, or possibly added in quantities small enough to be undetectable, in others, although the composition remains otherwise unchanged (Owen and Day, 1998a).

There is also evidence that some factories used more than one formula concurrently, employing them for certain types of object. For example, Derby changed from a frit to phosphatic recipe for most of its wares in 1770 after incorporating the Chelsea factory, but when in 1796 the bone china formulation was employed for utilitarian, i.e. table-ware, a slightly phosphatic frit paste continued to be used exclusively for figures for a further twenty-five years (Owen and Barkla, 1997). These examples reinforce the importance of analysing as many sherds and objects as possible from each factory in order to build up a large data-bank before the products can be said to have been characterised.

Characterising factories by elemental composition

It has been demonstrated that the corpus of British soft-paste porcelain cannot be easily sorted into a few compositional categories, however, the method of characterising the paste of an individual object, or group of objects, by their elemental composition has been used successfully to investigate the chronology of long-standing factories, such as Limehouse (Freestone, 1993), Derby (Owen and Barkla, 1997), Worcester (Owen, 1997; Owen, 1998; Owen, 2003) Isleworth (Freestone et al, 2003), and Bow (Ramsay and Gabszewicz, 2003; Ramsay and Ramsay, 2007). The methodology of these studies is to analyse sherds or samples from intact objects which date to different points in the chronology in order to demonstrate the technological progression of their production. Comparative studies have examined the relationship between factories that operated contemporaneously, such as the Shaw's Brow and Copperas Hill premises in Liverpool (Owen and Sandon, 1998), to discuss the similarities and differences between their products.

Studies have been made of pairs or groups of factories, one of which incorporated another (such as Worcester's takeover of Bristol (Owen, 1998)), or which were amalgamated (such as Caughley and Coalport (Owen and Sandon, 2003), or Nantgarw and Swansea (Owen, 1997; Owen et al, 1998)). Sherds from these factories have been analysed, dating to before and after these events, in order to investigate the effect that a takeover could have on the technology and raw materials of manufacture.

Once a chronology has been developed using dated and securely provenanced sherds, as at Worcester, comparison can also be used to suggest a date range for wares of known provenance (Owen, 1997). Where unprovenanced sherds are recovered from other contexts, most commonly domestic floor-layers and rubbish tips, analysis of their elemental composition has been matched with data from securely provenanced samples in order to suggest where they might have been manufactured (Owen, 2001b).

The chemical data often complement conclusions made on the basis of the objects' form and pattern, such as the underglaze blue "cannonball" design on two phosphatic sherds from the Fortress of Louisbourg, Nova Scotia, which matches designs found on securely provenanced Bow sherds, while the phosphatic composition of the paste is consistent with other Bow porcelain data (Owen, 2001b).

Glaze and enamel composition

There are no published studies that examine specifically British porcelain glazes, although analyses in cross-section are usually included alongside most published studies of the paste. However, much of this research relies on archaeological sherds from factory sites, the majority of which are unglazed wasters, or which may have had their elemental and mineral composition altered through taphonomic processes (Owen, 2001a).

Traditionally, categorisation of glazes has been founded upon subjective criteria of appearance in terms of hue and texture, as described in section 2.3.1. Aspects of perceived colour and texture need not be related to elemental composition (Ramsay et al, 2011), meaning that this system of classification cannot be used to date or provenance unknown objects by comparison with securely provenance examples. Furthermore, it is unhelpful for archaeological samples, whose colour may be obscured or stained by substances present in the burial environment, or sherds may be too small to accurately perceive their colour and texture.

Lead glazes

Lead glazes on soft-paste porcelain have been classified by the lead composition as high- (>50% PbO), medium- (30-50% PbO) and low-lead (<20% PbO) (Tite and Bimson, 1991; Owen, 1998). On this basis, Tite and Bimson (1991) demonstrated that they could distinguish between triangle-period Chelsea and Longton Hall glassy porcelains.

Owen (2002) observes from analytical data that the glazes of some soft-paste porcelain may show similarities to their paste and may have been made of similar materials in different proportions. He uses the example of glazes on some steatitic porcelains, which contain significantly higher levels of Mg than glazes found on other types of porcelain.

Furthermore, evidence has been found that a new, experimental body formula was often accompanied by a novel glaze recipe (Owen and Morrison, 1999), as at Worcester, where a decrease in lead and corresponding increase in silica in the body of the wares is accompanied by a similar pattern in the composition of the glaze (Owen, 1997).

In some cases, the glazes of early, experimental phosphatic wares manufactured at Worcester are found to vary through time, even when the paste composition remains essentially unchanged (Owen, 2003). A single sherd was found with the older phosphatic composition, upon which an experimental leadless alkali glaze was trialled, before it was applied to the new hard-paste porcelain.

In many cases, the composition of the glaze has been found to be unhelpful for provenancing archaeological or uncertain porcelain objects, as the variation within the groups, for example porcelains produced at Brownlow Hill, Liverpool, and Bonnin and Morris, Philadelphia, may be greater than the variation between groups where a similar paste type was used, see Table 3 (Owen et al, 2011).

Table 3 - mean (μ) and standard deviation (σ) bulk elemental composition (wt%) of Brownlow Hill, Liverpool (BH; Owen and Hillis, 2003) and Bonnin and Morris, Philadelphia (BM; Owen, 2001a) glazes on phosphatic samples, obtained from mounted sections using SEM with EDS

		SiO ₂	Al ₂ O ₃	FeO	MgO	CaO	PbO	Na ₂ O	K ₂ O	SO ₃
BH	μ	50.29	2.86	0.63	0.90	4.50	36.35	0.88	2.53	0.58
	σ	3.98	1.86	0.67	0.59	1.48	6.49	0.46	0.70	0.12
BM	μ	46.91	1.52	0.47	0.99	2.68	43.43	0.66	2.60	1.39
	σ	4.26	1.08	0.06	0.67	1.76	6.45	0.22	0.74	0.36

Ramsay et al (2003) demonstrated that some discrimination could be achieved using a ternary plot of SiO₂ – PbO – Al₂O₃. Their graphic representation of some 18th century English porcelain glazes demonstrates the exceptional nature of compositional outliers such as the ‘A’-marked wares, Cookworthy’s Bristol and Plymouth products and some experimental glazes from the Limehouse factory. The resolution of these groups was greater than that demonstrated by a plot of SiO₂ – CaO – Al₂O₃, as there is greater variation in PbO than CaO, see Figure 35 (Ramsay et al, 2003).

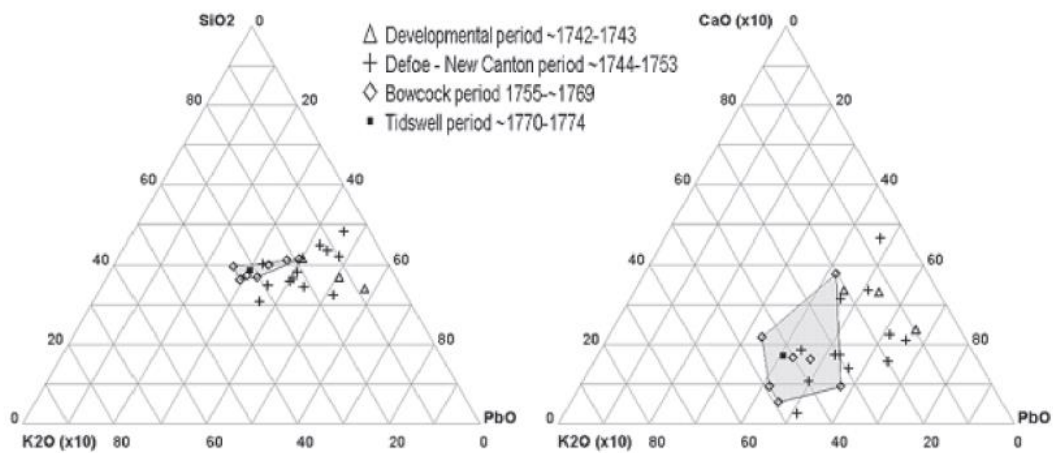


Figure 35 - ternary plots to distinguish glazes on Bow soft-paste (left SiO₂ – PbO – K₂O x 10) (right SiO₂ – CaO – K₂O x 10), the data were obtained from mounted glaze using SEM-EDS (Ramsay et al, 2003)

Alkali glazes

Glazes without lead were used on Bow first-patent porcelains (Freestone, 1996), and are a feature associated with hard-paste formulae such as those employed at Cookworthy's Bristol and Plymouth (Owen et al, 2000). The composition of these glazes is high in SiO_2 and Al_2O_3 , with K_2O and traces of Na_2O and CaO , suggesting that they were principally composed of quartz and a kaolinitic clay. A leadless *feldspathic* glaze was developed by John Rose at Coalport in 1820 (Godden, 1970, p. 14), but no analytical data have been published at this stage.

2.3.3 Mineral phase compositional analysis

Owen and Hillis (2003) identify two main senses in which the word 'composition' can apply to the scientific study of porcelain. The first, as discussed above, is the chemical composition, by which we mean the amounts of various elements, usually expressed as weight per cent oxide. A measured spot taken to be representative of the entire object, or just the glaze or body, depending on the discussion. The second is the mineralogical composition, usually known in the cited works as the "modal composition", which describes the physically distinct phases present in an area of the porcelain, which is again taken to be representative of the object, its glaze or body.

These two methods of investigating the composition of a porcelain object can complement one another, offering different types of information about the production of the paste and glaze, but often cannot be completely matched due to the limitations of the analytical equipment. For example, there may be crystallites present in the melt phase which are too small to discern using imaging techniques, although they can be detected using quantitative elemental analytical techniques, leading to some small component of the elemental composition which is not accounted for in the modal composition (Owen and Hillis, 2003). The spot-size used in elemental compositional analysis may, on the other hand, be too small to give a good bulk composition of the object, especially if it is polyphase or otherwise non-homogeneous. In this case, several spots would be required to be taken from each object, and the mean composition calculated.

Thus in most cases where the mineralogy of the porcelain paste is analysed, the chemical composition is used to calculate the proportions of materials used, as described above, while the phases are interpreted as indicators of the firing history of the object, as discussed below.

Mineralogy and paste type

The mineral structure of soft-paste porcelain consists of distinct, or partially melted, mineral phases in a silicious melt, or matrix. The type of minerals present depend on the raw materials which were employed in the porcelain paste, and might include whitlockite ($\text{Ca}_{10}(\text{PO}_4)_6(\text{OH})_2$) in phosphatic samples (Owen et al, 2011) and magnesium silicates, most commonly enstatite (MgSiO_3) in magnesian samples (Owen, 1998). In some cases, the presence or absence of a certain mineral phase, such as the calcic mineral diopside (CaMgSiO_3) in magnesian pastes, can discriminate between two compositionally similar wares (Owen and Sandon, 1998).

Firing history

The mineralogy of a sample can roughly constrain the kiln conditions in which it was biscuit-fired. The presence or absence of wollastonite (CaSiO_3), and the species of silicate polymorphs present, give a peak temperature which is higher than the temperature at which wollastonite forms, but lower than the temperature at which the silicate polymorphs lose stability (Owen and Barkla, 1997).

Very low firing temperatures can be identified by the presence of grains of relict bone ash (Owen and Hillis, 2003) or glass (Owen and Hunter, 2009) in the matrix, whereas very high temperatures are evident in highly vitrified, compositionally homogeneous wares, in which the pores have been filled by siliceous melt phase (Owen et al, 1998).

Precedents from Chinese and continental European porcelain

Analyses of porcelain from China and East Asia and from continental Europe (particularly Meissen) are more numerous than for British porcelain and more advanced in terms of the technological conclusions drawn. The elemental composition and mineralogy of Chinese porcelain and stone-wares have been linked to the raw materials of production and thereby the region where they were produced (Yu and Miao, 1996; Leung and Luo, 2000; Tite et al, 2011). Little variation has been shown in the composition of porcelain from a single region, such as the Ding kilns, Hebei province (Cui et al, 2012) and Jingdezhen, Jianxi province (Xie et al, 2009). Over a period of several hundred years, use of the same local sources of raw materials with the same recipe used to govern their proportions has ensured a consistent composition in the product.

The trace elemental composition of Chinese porcelain bodies has been used to match the wares to a source of clay and therefore group wares by provenance (Ma et al, 2012). The same technique has been applied to the Co-blue pigment used for the famous underglaze blue enamels and the results have provided a tool for dating wares to before or after a change in the geographical location from which cobalt ore was extracted (Yu and Miao, 1998; Wen et al, 2007; Figueiredo et al, 2012).

Meissen porcelain has similarly been sufficiently well-characterised to allow original early-period objects to be distinguished from later copies on the basis of elemental compositional analysis (Neelmeijer and Roscher, 2011; Domoney et al, 2012). The bodies and glazes of porcelain and stoneware objects from the first experimental wares produced at Meissen have been analysed (Colomban and Milande, 2006), and criteria suggested for the characterisation of these wares in terms of their unique raw materials. A large number of later Meissen porcelains have also been analysed, allowing the output for much of the 18th century to be characterised (Domoney et al, 2012). This showed a change in flux, which allowed wares to be dated to before or after the introduction of a potassium-rich formula (Domoney et al, 2012).

The overglaze enamels on Meissen porcelains have also been extensively studied to produce a chronology of pigment development (Casadio et al, 2012). This chronology is a highly useful tool for dating enamelled porcelain specimens by the elemental composition of their pigments, even a qualitative analysis can often provide a terminus post quem for the decoration of the object (Domoney, 2012).

2.4 Analytical techniques for porcelain and fine ceramics

The selection of which scientific analytical techniques to use when analysing porcelain depends upon the extent to which the object may be damaged in obtaining a sample and the range and limits of detection which are required. Due to the wide range of elements which may be present in any porcelain sherd, from heavy elements such as tin and lead to light elements such as sodium and silicon, it is necessary to use a technique with as good an accuracy and precision for both low and high atomic number elements. The techniques described in this section comprise those that best fit these requirements. They have been found to be effective for analysis of porcelain, or similar materials, such as fine ceramics and man-made glass.

2.4.1 Elemental compositional analysis

Quantitative elemental compositional analyses are crucial to our understanding of British porcelain's technological development, because they are the best evidence that ceramics and glass can be characterised in terms of their raw materials. The theory and instrumentation of each of the techniques used as part of this research project is described in detail in the Appendices. These are referred to throughout the following sections, which describe the methodological background with respect to the analysis of British porcelain and similar materials.

Scanning Electron Microscopy (SEM)

SEM is an important and widely-used technique in the analysis of archaeological materials (Freestone and Middleton, 1987; Olsen, 1988; Meeks et al, 2012; Calvo del Castillo and Strivay, 2012; pp. 92 - 94). For twenty-five years, it has been the most commonly-used technique for analysing British porcelain, combining high-magnification, phase-contrast, imaging with quantitative elemental compositional analysis (Tite and Bimson, 1991; Middleton and Cowell, 1993; Owen, 1994; Freestone, 1996). This technique and its capabilities are described in detail in Appendix A.1.

SEM is highly suitable for archaeological porcelain, as sherds can often be sampled relatively freely and mounted and polished to provide a smooth cross-section for analysis (Owen, 1994). Phase contrast in backscattered mode has proven helpful in identifying the mineral phases present in ceramic pastes (Freestone, 1993; Watney et al, 1993; Owen and Sandon, 1998), besides allowing the precise selection of areas for compositional analysis by spectroscopy.

Energy-Dispersive Spectroscopy (EDS) and Wavelength-Dispersive Spectroscopy (WDS) are techniques used for elemental compositional analysis alongside SEM, using the characteristic X-rays emitted by the sample. X-ray spectroscopy is described in theory and instrumentation in Appendix A.3. Both techniques can reliably detect most elements from carbon to uranium at varying limits of detection, which vary depending on the element and the analytical conditions, but can be $\leq 0.1\%$ (Goodhew et al, 2001; p. 175). Data are generated as a spectrum with peaks corresponding to the elements detected, and calibration standards may then be used to calculate the absolute composition of the sample reported in weight percent as elements or, usually by stoichiometry, as oxides. Due to the restricted size of most sample chambers, and the high vacuum required, SEM is not generally suitable for intact objects, particularly those with existing cracks and damaged areas. Furthermore, the sample must usually be coated with a conductive material, typically carbon or gold, in order to prevent an electrical charge from building on the surface during analysis. The application and removal of this coating may stain or damage surface decoration.

Laser Ablation Inductively Coupled Plasma Mass Spectroscopy (LA-ICPMS)

ICPMS is a powerful tool for elemental compositional analysis, often with greater accuracy and precision than Energy-Dispersive and Wavelength-Dispersive Spectroscopy. It has detection limits down to parts per million for most elements, and a wide range of accessible elements from lithium to uranium (Hoffman et al, 1996; p. 32). The theory and instrumentation of the instrument is described in Appendix A.2. Combined with a Laser-Ablation Inductively-Coupled Plasma sampling system, millimetre-sized areas of a sample can be targeted for analysis. This process is micro-destructive, meaning that the analysed area about 0.1mm in diameter is removed; the damage is only noticeable on very close inspection (Gratuze et al, 2001).

Since the early 1990s, these advantages have made LA-ICPMS increasingly popular for the analysis of archaeological materials (Tykot and Young, 1996; Gratuze, 1999; Gratuze et al, 2001; Speakman and Neff, 2005). Trace elemental composition has been used effectively to characterise archaeological artefacts such as obsidian (Shackley, 1998; Frahm, 2012; Freund, 2013), man-made glass (Freestone, 2006; Shortland et al, 2007; Brems and Degryse, 2013; Smirniou and Rehren, 2013), and ceramics (Maggetti, 1982; Impey et al, 1983; Jones, 1986; Neff, 2001; Neff, 2003). These studies have created trace elemental profiles for objects of a known origin, and used these profiles to link objects to raw materials. Groups have been found, corresponding to sources of raw materials and this aids in provenance studies.

This approach has proved to be effective for characterising and discriminating between groups of material from different sources of raw materials (Tykot, 1996; Mallory-Greenough et al, 1998; Freestone et al, 2002; Shortland et al, 2007; Dussubieux et al, 2009). It has been used successfully in the analysis of Chinese porcelains, where trace element ratios are employed, rather than absolute values, to compare objects with one another, and with geological samples (Bartle and Watling, 2007; Ma et al, 2012; Gianini, 2015).

X-ray Fluorescence Spectroscopy

X-ray fluorescence spectroscopy is one of the most powerful and versatile tools currently available for the elemental compositional analysis of a wide range of archaeological and historical inorganic materials. It is described in greater detail in Appendix A.3. The power of the technique comes from its wide range of detectable elements, theoretically from beryllium to uranium although in practice detection of elements lighter than sodium requires that the analysis be carried out in a vacuum (Janssens, 2013; pp.88 – 89).

Detection of all elements is simultaneous, resulting in very quick analyses; within minutes, data can be collected to relatively low limits of detection, ranging from a few percent down to occasionally tens of $\mu\text{g/g}^{-1}$ (Janssens, 2013; pp. 90 – 92). The technique is versatile because very little sample preparation is generally required. The sample chamber in benchtop systems can be used without a vacuum, and may therefore be large and easy to access; analysis is entirely non-invasive, preserving the samples.

For these reasons, XRF has been used extensively in analyses of archaeological and historical materials, and continues to grow in popularity. Shugar and Mass present data from the Art and Archaeology Technological Abstracts (AATA) database (Getty Conservation Institute), which shows a steady increase in publications that include XRF from the introduction of the technique in the 1970s to the late 1990s, and a sustained leap from 2000 onwards (Shugar and Mass, 2013; pp. 18 – 19). The potential for the technique's use for archaeological materials and research questions has been thoroughly surveyed, among the earliest is that of Hall (1960), more recently by Mantler and Schreiner (2000), and books have been devoted to specific areas, including geoarchaeology (Shackley, 2010), and portable (Potts and West, 2008) and Hand-Held instruments (Shugar and Mass eds., 2013) for *in situ* analysis.

A popular methodological approach for many samples is mapping and line scans for the acquisition of spatially-resolved elemental compositional data, which can be used to answer structural questions about objects including glazed ceramics, illuminated manuscripts, paintings, and bronze sculpture (Cheng et al, 2009; Trentelman et al, 2010; Smith, 2013). For more homogeneous samples, spot and/or bulk analysis is preferable, and in these cases it is possible to use a set of standards to produce fully-quantitative data, which can be used for statistical analysis, including Principal Component Analysis (PCA) and discriminant analysis (Hall, 2001; Papageorgiou et al, 2001; Baxter, 2001; Leung et al, 2000).

Another advantage of quantitative data is that they may be compared with the results of analyses on similar materials derived from a range of techniques. Clark (2002) envisaged the creation of a database of historical pigment data, which would enable unknown pigments to be identified quickly and easily through comparison. In such a database, quantitative elemental compositional data from XRF may be interpreted alongside data from destructive and micro-destructive techniques, such as laser-induced breakdown spectroscopy (LIBS) (Alberghina et al, 2011), particle (or proton) induced X-ray emission (PIXE) (Malmqvist, 1986; Uda, 2005) or laser-ablation inductively coupled plasma mass spectroscopy (LA-ICPMS) (Mallory-Greenough and Greenough, 2004); and mineralogical data from Raman spectroscopy (Clark, 2002; Sawczak et al, 2009; Centeno et al, 2012) and Fourier Transform Infra-red Spectroscopy (FTIR) (Centeno et al, 2012) or X-ray diffraction (Hochleitner et al, 2002; Uda, 2005; Alberghina et al, 2011).

In a museum and conservation context, material characterisation plays a part in the development of an object conservation strategy (Hochleitner et al, 2002; Alberghina et al, 2011; Fontana et al, 2014), and the added insight into the availability and selection of materials by the artist or creator contributes to art historical knowledge (Sawczak et al, 2009; Fontana et al, 2014).

For archaeologists, X-ray Fluorescence data and the associated statistical interpretation assist with provenancing studies, through comparison with securely-provenanced samples (Leung and Luo, 2000; Wu et al, 2000; Centeno et al, 2012), and raw materials at the area of production (Aloupi et al, 2000; Hall, 2004). Furthermore, compositional data can complement the role of historical sources in the interpretation of objects (Moioli and Seccaroni, 2000; Domoney et al, 2012; Turco et al, 2015).

A recent contribution to the increase in the use of XRF spectroscopy for archaeological and cultural heritage applications has been the development of portable and Hand-Held XRF (HH-XRF) systems that can be used *in situ*, allowing access to materials without the need to extract samples or remove them from context. Over the past decade, they have become more affordable, and easier to use, so that they require little technical training to operate (Bosco, 2012; Shugar and Mass, 2013). In response, the debate has been taken up in the literature as to the quality of the resulting data, and the extent to which qualitative data from uncalibrated XRF analyses may be compared between instruments and analytical methodologies, and therefore the usefulness of such data as part of scientific research (Shackley, 2010; Speakman et al, 2011; Shugar and Mass, 2013; Frahm and Doonan, 2013; Speakman and Shackley, 2013). The debate hinges on the fundamental limitation of XRF when applied to the diverse array of inorganic materials available to archaeological and cultural heritage researchers, which is the technique's susceptibility to inter-instrument variation and interference from the interaction of X-rays with different types of sample.

The variation between instruments has been surveyed thoroughly elsewhere (Craig et al, 2007; Goodale et al, 2012; Frahm and Doonan, 2013; Frahm, 2014), and the majority consensus is that, provided that the calibration procedures are rigorous, and undertaken with adequate knowledge of the sources of interference associated with the sample material, the results are reliable. Indeed, XRF results have been compared with those from instrumental neutron activation analysis (INAA) (Adan-Bayewitz et al, 1999; Xie et al, 2007; Phillips and Speakman, 2009; Speakman et al, 2013), and laboratory wavelength-dispersive XRF (Williams-Thorpe et al, 1999), and in most cases the same compositional groups were identified.

XRF has been less commonly used for the analysis of porcelain. An early scientific investigation of British porcelain from the excavation of the Longton Hall factory site employed XRF to analyse the glaze and cobalt blue of complete pieces and excavated sherds (Watney et al, 1993). They were able to distinguish Longton Hall from West Pans porcelain based on the presence of tin in the Longton Hall glazes, which was absent in West Pans glazes, and the presence of bismuth in some Longton Hall underglaze blue, and of copper in the West Pans blue decoration (Watney et al, 1993). XRF data have also been used as a check against the spectroscopic data from SEM analysis in a study of Worcester porcelain pastes (Owen, 1997). Freestone suggested that XRF may be used to quickly identify British porcelain from a specific factory where a unique compositional indicator was present, as in Bovey Tracey (White, 2007).

2.4.2 Other compositional analysis

X-Ray Diffraction Spectroscopy

X-ray diffraction spectroscopy (XRD) is not commonly used for the analysis of porcelain, however, it was the original technique used to identify phases in the various paste types of British soft-paste porcelains (Bimson, 1969; Tite and Bimson, 1991). X-rays are fired at the sample, and the diffracted energy is measured at a specific angle close to the sample surface. The diffraction patterns provide information about the number and spacing of crystal planes in the sample, which are characteristic of mineral phases. Data are reported as spectra with peaks, and the peak height provides a relative value for the proportion of the sample composed of any given mineral.

The results from XRD are most accurate when they come from homogeneous, finely ground crystalline samples. The large sample size makes XRD an unpopular choice for use with complete objects. Furthermore, the identification of crystalline phases in porcelain has largely been taken over by SEM imaging (Owen and Day, 1994), and Raman spectroscopic analysis (Ricciardi et al, 2009; Kock, 2011; Jay and Orwa, 2012).

Raman spectroscopy

Raman spectroscopy is a vibrational spectroscopic technique, which studies the interaction of radiation with molecular vibrations. The sample is exposed to a high-energy light source, and a detector measures the inelastically-scattered photons from the reaction with the sample surface. The difference between the incident energy and the inelastically-scattered energy provides a spectral “fingerprint” for the substance under analysis, which is determined by the frequency (energy), intensity (polarity) and band shape (bond environment) of the molecular vibrations (Larkin, 2011; pp.15-18).

It is possible to compare the resulting spectrum with a database, in order to establish the mineral composition of the sample, as with XRD (Colomban, 2012). This technique has been used with some success to characterise British porcelain from Worcester (Jay and Orwa, 2012), and there is potential to use it for the glaze and polychrome enamels (Kock, 2013).

2.4.3 Qualitative techniques

Ultra-violet light has long been used to test the extent of similarity or difference in the ceramic body of British porcelain objects and sherds, because the light causes certain paste types to fluoresce in different colours (Lewis, 1954). This technique has been used to characterise fake porcelain to help to distinguish them within an assemblage of disputed pieces (Elliot, 1939) and as a screening test, in order to select representative samples from among an assemblage from Liverpool, prior to chemical analysis (Watney, 1959).

Spectrophotometry is a technique that measures reflected and transmitted electromagnetic energy in the visible light range of the spectrum (i.e. wavelengths between 400 - 800 nm) to characterise an object or light-source quantitatively by its colour (Hunt and Pointer, 2011; pp. 9 - 10). This technique is described in theory in Appendix A.4. Devices to measure colour been used in object conservation for decades (Bromelle, 1955), both to assist recording of objects, and to monitor phenomena such as degradation in pigments and stone (Connors-Rowe et al, 2007; Guarneri et al, 2014).

Colorimetry in archaeological studies has been limited to some experimental recording systems for frescoes (Horgnies et al, 2014), and tomb wall-paintings (Ahmon, 2004), and also as a characterisation technique supplementing elemental compositional analysis in studies of ceramics and glazes (Yang et al, 2005; Costa et al, 2010; Polvorinos Del Rio and Castaing, 2010).

2.5 Developments in non-destructive analysis for archaeological science

Non-destructive analysis is the ideal in studies of archaeological materials, which may be rare or unique, as well as for antique porcelains and fine ceramics, where the value is significantly higher when they are intact and undamaged. Sampling methods, therefore, prioritise techniques that are minimally destructive, removing the smallest amounts of material while still ensuring that the composition of the entire object is represented (Bronk and Freestone, 2001).

From a methodological perspective, non-destructive analysis is desirable because it allows repeated analyses of the same sample area, meaning that the accuracy and precision of the technique can be tested and compared with other machines or different conditions (Shackley, 2010).

While connoisseurship based on visual standards, which is an entirely non-destructive method, may be said to be the original analytical technique for characterising archaeological and antique objects, including porcelain, the first scientific analytical techniques to be used for this purpose relied on invasive sampling. Wet chemical analysis required the destruction of a sub-sample (Eccles and Rackham, 1922), and XRD works best with a sample which has been powdered, rendering it effectively irreparable (Bimson, 1969). SEM of porcelain pastes also usually requires sub-sampling, but the chip could theoretically be reattached, and the process of analysis does not alter the sample, allowing for repeated analyses. Any ICP-MS technique is micro-destructive, but the area used may be so small that it is indistinguishable to the naked eye. Finally, XRF, Raman and spectrophotometry are surface techniques that can be performed on the object without the need for sample preparation.

2.6 Conclusions

Porcelain is a high-fired vitreous white ware, invented in China and subsequently exported across Asia and Europe. The value of porcelain caused an international industrial race to produce a comparable material, the result of which is a vast range of compositionally distinct hard- and soft-paste ceramics.

In Britain, hard-paste porcelaneous wares were produced and patented from the early 18th century, and marketed from 1744. These formulae were either too expensive or unreliable in terms of raw materials and kiln failures, to generate sufficient profit against Chinese and European imports. Consequently, they were replaced with lower-firing soft-paste wares employing relatively cheap and accessible ingredients, including Cornish steatite, bone ash and glass cullet. Scores of porcelain factories were established during the following century, but the complexity of the process and competitive nature of the market meant that relatively few achieved sustained commercial success. Those that did survive are accompanied by archaeological and documentary evidence of experimentation and development of their product, resulting in varying formulae over time. Archaeological excavation of porcelain factory sites can provide stratigraphic dating evidence to produce compositional chronologies of the ceramics produced, allowing unknown wares to be provenanced and dated by comparison.

Visual connoisseurship has been the most commonly-used method for characterising a porcelain object, based on criteria such as the factory marks, form, colour and decorative features, including enamels and gilding. Such identifications are often made by comparison with documented examples in catalogues and books.

Scientific analytical studies of porcelain and similar materials have used elemental compositional techniques, such as SEM-EDS/WDS and LA-ICPMS; and to a limited extent XRF and XRD, and qualitative techniques, including Raman spectroscopy and optical microscopy.

Such investigations of British porcelains have therefore aimed to characterise individual objects and the output of factories in terms of their major and minor elemental composition, plus their mineral phase composition. From these, the recipe and firing conditions used to produce the porcelain can be reconstructed. Studies of Chinese and continental European porcelain are further advanced in the characterisation of the ceramic paste, glazes and pigments, which can be used to provenance and date a porcelain object by comparison with similar chronologies. Furthermore, trace elemental compositional analysis of Chinese porcelain has allowed the sources of geological raw materials to be identified and samples to be matched with these sources.

Little analytical work has been dedicated to British porcelain glazes or underglaze pigments, and none to the vitreous enamels. The advantage of using the glaze and pigment, as opposed to paste and mineralogical characterisation, is that the elemental composition can be obtained from a surface analysis, removing the need to rely on broken pieces or to damage an intact object by invasive sampling.

3 A meta-analysis of published data from the analysis of British porcelain

For a method for porcelain analysis to be considered useful, it is necessary that the analytical data obtained can provide new information about the objects analysed. Since this methodology takes for its research questions the contested issues of provenance and dating, it requires that the analytical data from porcelain objects analysed show differences that correspond with factories or periods of origin. Some work has already been carried out in this direction by methods that used invasive or destructive sampling procedures.

In this chapter, the published quantitative elemental compositional data for British porcelain pastes and glazes are collected and presented using descriptive and analytical statistical methods, in order to determine the extent to which porcelain from different factories and periods may be distinguished by variations in elemental composition. This is a novel use of existing data, most of which has not been rigorously collected and compared before. It follows the method proposed by Owen (2007), whereby the major elements in the porcelain composition are plotted against one another in a diagram that is optimised to the paste type. This method is expanded to include the porcelain glazes.

Throughout this chapter, and the subsequent chapters dealing with elemental compositional data, the term “major elements” will be used to describe elements that individually comprise $\geq 8\%$ of the composition; “minor elements” are those that are $< 8\%$ but greater than 0.1% , and “trace elements” are those that are $\leq 0.1\%$. These are usually expressed as oxides.

3.1 Introduction

For almost a century, data from scientific analytical techniques have been used to characterise porcelain from numerous known factories, and to contribute to our knowledge of the ingredients and firing conditions used in its manufacture. These studies and their findings are discussed in detail in Section 2.3.2.

Factories have been individually characterised (Freestone, 1993; Watney et al, 1993; Owen, 1998; Freestone et al, 2003; Owen, 2003), or two or more factories that operated contemporaneously have been compared (Owen et al, 2000; Owen and Day, 1998a; Owen and Hillis, 2003). Once these factories have been characterised, this information can be used to contribute to the overall understanding of British porcelain manufacture in the 18th and early 19th centuries.

In the case of samples of unknown attribution, especially objects that cannot be securely provenanced based on their form or pattern, comparison with data gathered from other samples may enable them to be attributed to a factory and period of origin. The approach required is the provenance hypothesis, and it requires the following three conditions to be fulfilled:

- that the products of the place of origin have been thoroughly characterised, in terms of the attributes that are being examined
- that the products of the place of origin are unique in some of these attributes, or in the combination of attributes, relative to those of other factories
- that the unknown sample falls within the range of a single place of origin for these attributes, allowing for measurement error and within-sample variation and heterogeneity

Examining the major and minor elemental composition has been used to determine the main ingredients of porcelain production, and the proportions in which they were used, based on comparison with some of the raw materials that were available at the time (Tite and Bimson, 1991; Freestone, 2000; Owen and Barkla, 1997). Depending on the extent to which the formula used was unique to a certain factory, the major and minor composition may be used to match an unknown sample to a possible formula, and thus to a factory of origin.

In this chapter, the quantitative elemental compositional data from 325 samples of securely-provenanced porcelain that have published to date are collected and examined to compare inter-factory variation with intra-factory variation.

If the inter-factory variation is consistently greater than the intra-factory variation for two or more factories, then it can be discussed the extent to which the formulae used were unique to each factory, and what might be the reasons for similarities and differences in composition. Furthermore, compositional groups may be formed, allowing unknown samples to be placed by comparison of the elements of interest.

3.2 Using major and minor elements to discriminate samples by paste

It has been established that the raw materials determine the elemental composition of the porcelain body and that the elemental and mineralogical composition of the analysed sample can be linked to raw materials (Section 2.3.2 and references therein). With samples of unknown provenance, the degree of difference or similarity in the elemental composition of objects can suggest the extent to which different or similar recipes were used in their production and possibly whether they were produced in the same factory.

A simple method to illustrate the degree of similarity or difference between objects is by using a ternary plot, in which the elemental composition is reduced to the three greatest components, and normalised to 100%. The data are then plotted on three axes, and their proximity on the plane indicates their compositional similarity with respect to these three constituents (Rollinson, 1993; pp. 171 - 172). In this research, all available elemental compositional data for British porcelain pastes and glazes have been compiled and plotted in this way to test the extent to which factories can be distinguished. Where the normalised data are discussed, they are identified as (%norm), and where the absolute data are referred to, they are identified as (%abs). The data were obtained by SEM analysis with EDS, and in some cases WDS; the data and references are provided in Appendix A.5. The porcelain data are initially divided into the most commonly used compositional groups; although there are problems with this system, as discussed in Section 2.3.2, and see Owen (2007), there remain significant variations in the constituent elements between the compositional groups.

3.2.1 Magnesian

Magnesian soft-paste porcelains are those that were created using a flux of steatite ($\text{Mg}_6\text{Si}_8\text{O}_{20}(\text{OH})_4$), or a similar magnesian mineral (Tite and Bimson, 1991). As a result, they contain a significant amount (>5%) of MgO. The other major constituents are silica, typically from sand or flint, and in many cases lead from flint glass. Calcium may be contributed by the clay or steatite, or in some cases through the addition of crown glass.

The relationship between calcium and magnesium in magnesian porcelain is discussed in greater detail below. Aluminium, potassium, sodium and phosphorus are also present at between 1-7%abs, however these are not present in all magnesian pastes. When these key elements (SiO_2 , MgO + CaO and PbO) are plotted, they demonstrate compositional groups corresponding to different formulae and factories, see Figure 36.

To the centre and upper left of the plot area, there is a relatively high-MgO+CaO (25 – 38%norm) group, consisting of Bovey Tracey, Bristol, some early Dr Wall-period (1752–1774) Worcester and some contemporary (1751–1764) Vauxhall pastes, which contain a lower ratio of silica to flux components ($\text{SiO}_2/(\text{MgO} + \text{CaO}) = 5-6$). These may be distinguished further by the presence of BaO (~3%abs) in Bovey Tracey, which is absent in Bristol, Vauxhall and Worcester.

To the lower right of the plot area are the majority of Worcester magnesian porcelains, Caughley, Chaffers, and some Bovey Tracey and Vauxhall outliers that contain a higher ratio of silica to flux components ($\text{SiO}_2/(\text{MgO} + \text{CaO}) = 8-16$), and lower MgO overall (4-9%abs). These cannot be reliably discriminated, although Bristol, Worcester and Chaffers frequently contain >5%norm PbO in the paste, whereas Caughley and Vauxhall are generally contain <5%norm PbO.

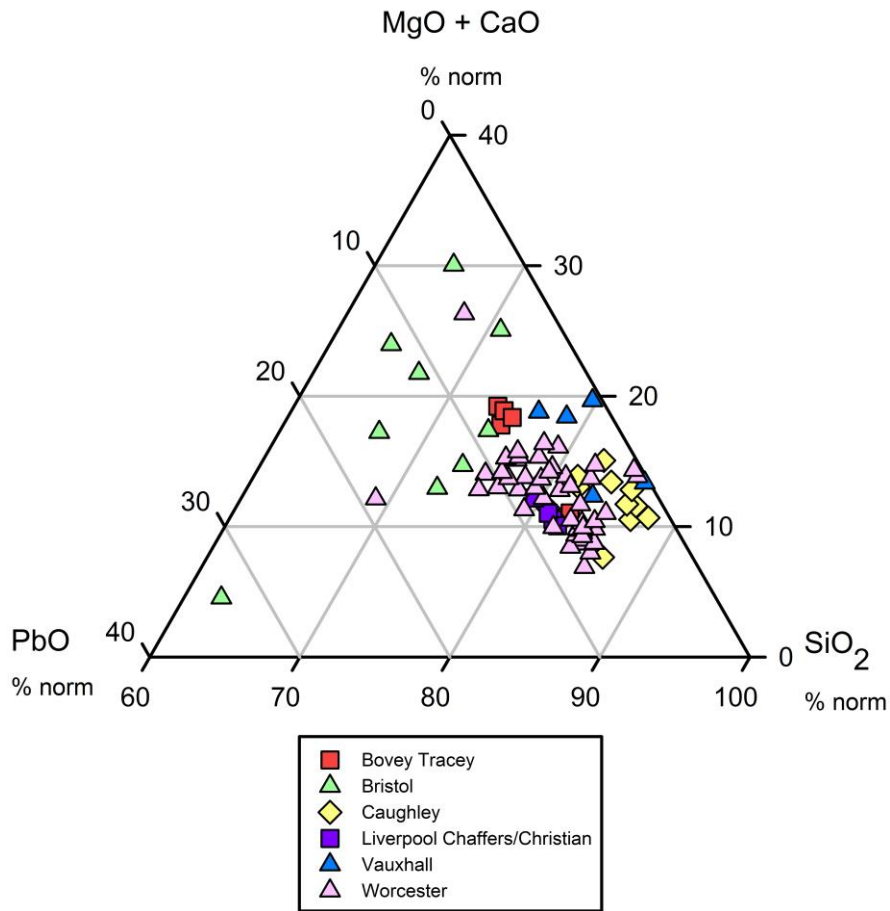


Figure 36 - SiO_2 vs MgO vs $\text{Al}_2\text{O}_3 + \text{CaO}$ for magnesian soft-paste porcelain pastes

The relationship between the calcium and magnesium present in the magnesian pastes shows two distinct groupings, see Figure 37. Worcester, Caughley, Chaffers and Vauxhall have a similar ratio of these two elements (MgO/CaO 3-5), which shows a co-increase in some cases, which suggests that these two elements have a common origin, such as the steatite flux. Bristol and early Dr Wall-period (1752-1760) Worcester form a group that is slightly depleted in calcium, relative to the main group (MgO/CaO 7-9). Bovey Tracey and outliers from Bristol, Caughley and Flight-period (1783-1792) Worcester contain significantly more calcium, relative to magnesium (MgO/CaO 11-20), suggesting that an additional source of calcium was being added to these pastes.

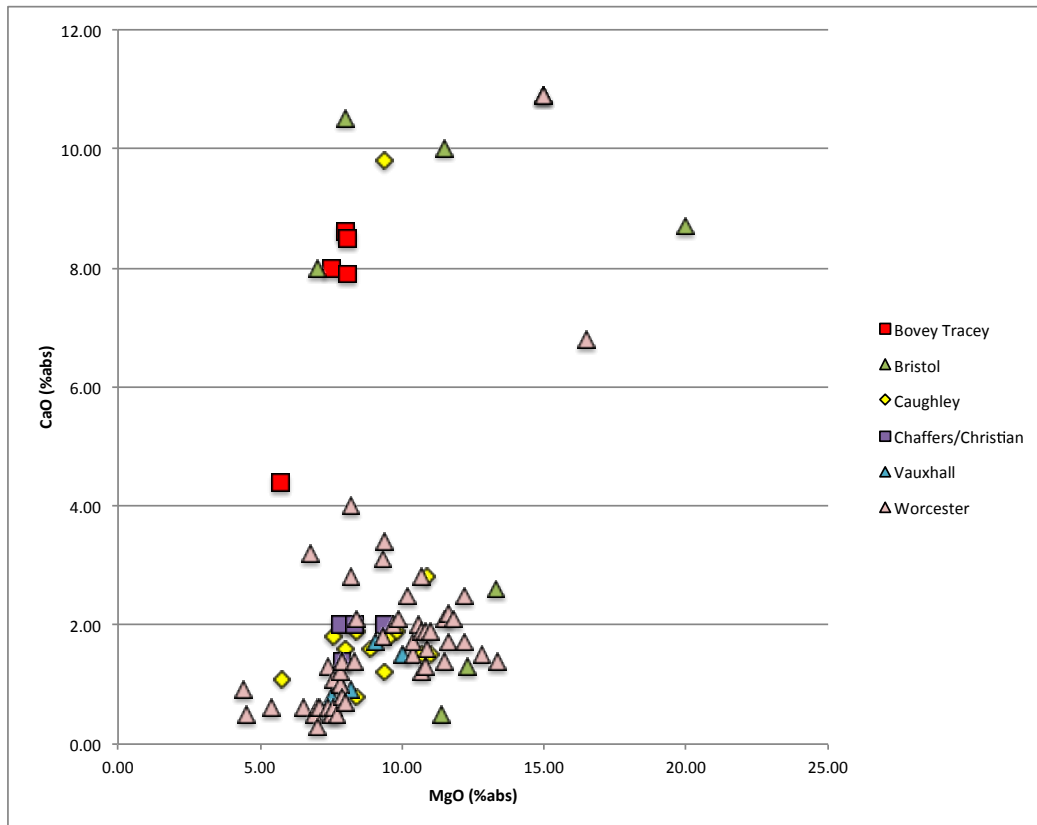


Figure 37 - MgO vs CaO in magnesian porcelain pastes

3.2.2 Phosphatic

Phosphatic soft-paste porcelain is also known as bone-ash, because it was created with a flux made of calcined animal bones. The result is a paste rich in phosphorus and calcium, with SiO₂ and Al₂O₃ as the other major constituents. When these elements are plotted on a ternary plot, see Figure 38, some compositional groups may be discerned corresponding to different formulae.

Two of the Liverpool factories (Gillbody and Pennington) show significant compositional overlap, and tend to contain more silica than flux ($\text{SiO}_2 / (\text{P}_2\text{O}_5 + \text{CaO}) = 1.2\text{-}2.5$). The early London phosphatic-producing factories, Bow and Isleworth, also overlap compositionally; their pastes are relatively low in Al₂O₃ and SiO₂ ($\text{SiO}_2 / (\text{P}_2\text{O}_5 + \text{CaO}) = 0.8\text{-}1.7$). Freestone has observed that they may be distinguished by the common presence of PbO and SO₂ in Isleworth pastes (Freestone et al, 2003). These data suggest that Isleworth porcelain contains a higher ratio of potassium to aluminium ($\text{K}_2\text{O} / \text{Al}_2\text{O}_3 = 0.2\text{-}0.5$), relative to Bow ($\text{K}_2\text{O} / \text{Al}_2\text{O}_3 = 0.1\text{-}0.2$), see Figure 41.

Lowestoft phosphatic porcelain also falls within this compositional group, and they appear to be compositionally indistinguishable from Bow.

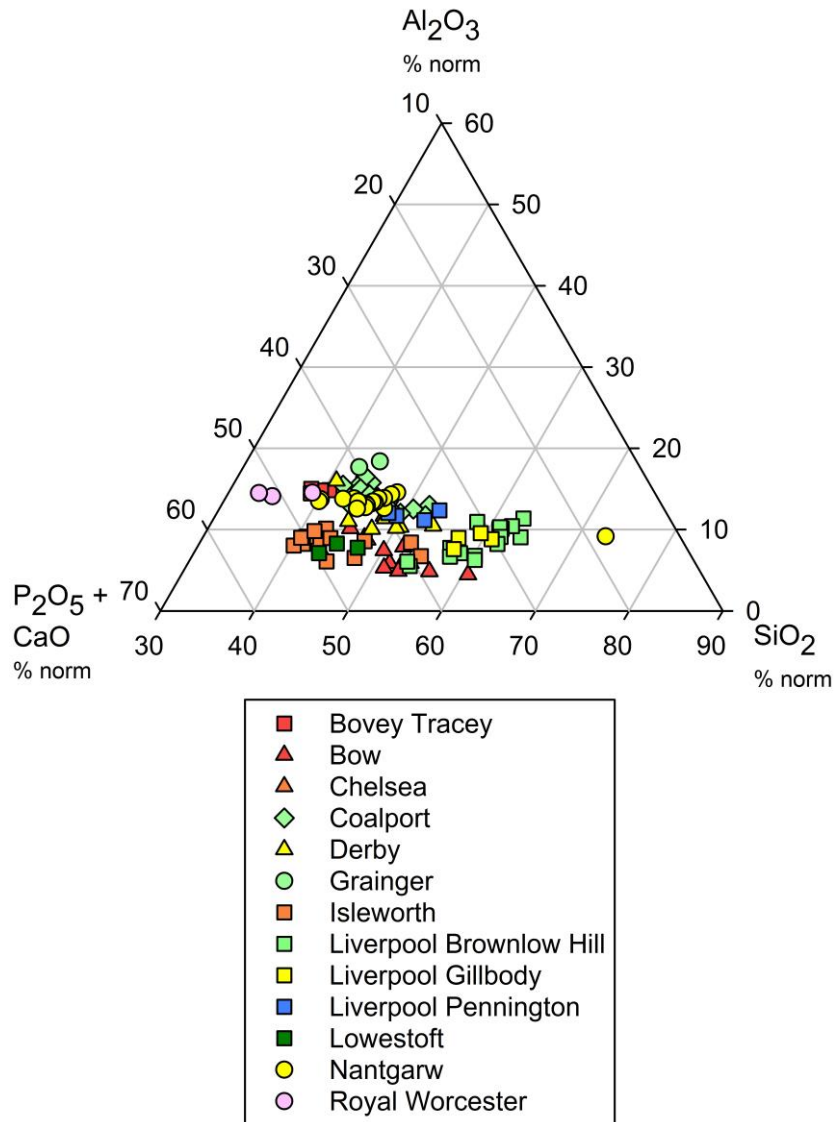


Figure 38 - SiO₂ vs Al₂O₃ vs CaO + P₂O₅ in phosphatic soft-paste porcelain pastes.

Later phosphatic-producing factories (Coalport, Grainger, Nantgarw, and Royal Worcester) form a separate compositional group, containing more alumina and less flux, relative to silica ($\text{SiO}_2/(\text{P}_2\text{O}_5 + \text{CaO}) = 0.7\text{-}1.2$). This group represents bone china and transitional wares during the development of this new formula in the late 18th and early 19th centuries.

An experimental group of phosphatic porcelain from Bovey Tracey also falls into this group, and they are compositionally indistinguishable from Royal Worcester, containing a very low ratio of silica to flux ($\text{SiO}_2 / (\text{P}_2\text{O}_5 + \text{CaO}) < 0.6$).

The relationship between the elements contributed by the flux, i.e. phosphorus and calcium, shows a strong linear trend for all factories, see Figure 39. However, pastes from Isleworth and some outliers from Bow and Liverpool Brownlow Hill are relatively enriched in calcium, which suggests that an additional source of calcium may have been added, such as crown glass. Although this is by no means a reliable way to distinguish the Liverpool phosphatic-producing factories, it is interesting to note that some different formulae were being used.

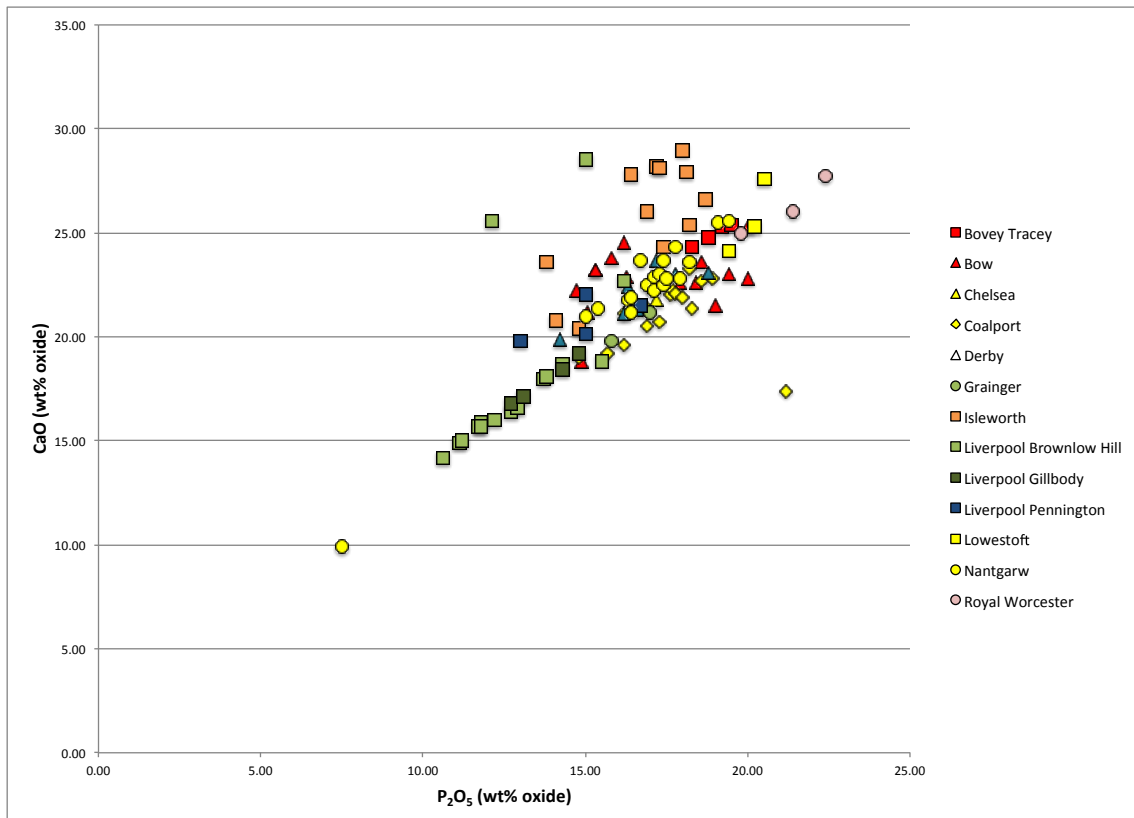


Figure 39 - P₂O₅ vs CaO in phosphatic porcelain pastes

After Freestone (2001), phosphatic soft-paste and bone china porcelains were plotted on K_2O vs Al_2O_3 , see Figure 40. The pattern that was observed – that the two elements are in proportion to one another, and that they increase through time – is loosely supported by the data gathered here, although the correlation is not strong.

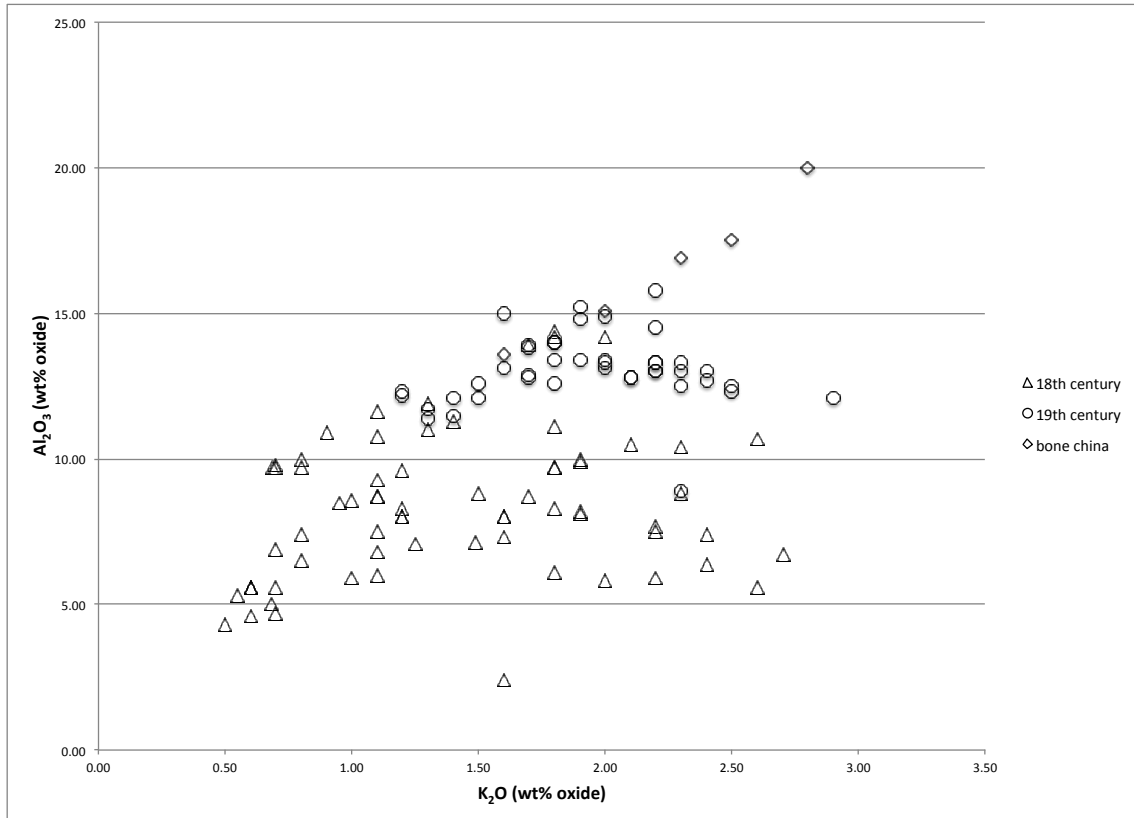


Figure 40 - K_2O vs Al_2O_3 in phosphatic soft-paste porcelain and bone-china pastes from the 18th and 19th centuries

Figure 40 adds data from 19th century soft-paste phosphatic porcelains, contemporary with the bone china, and these form a group between and overlapping with 18th century soft-paste and 19th century bone china. The data allow several distinct groups to be identified, demonstrated in Figure 41.

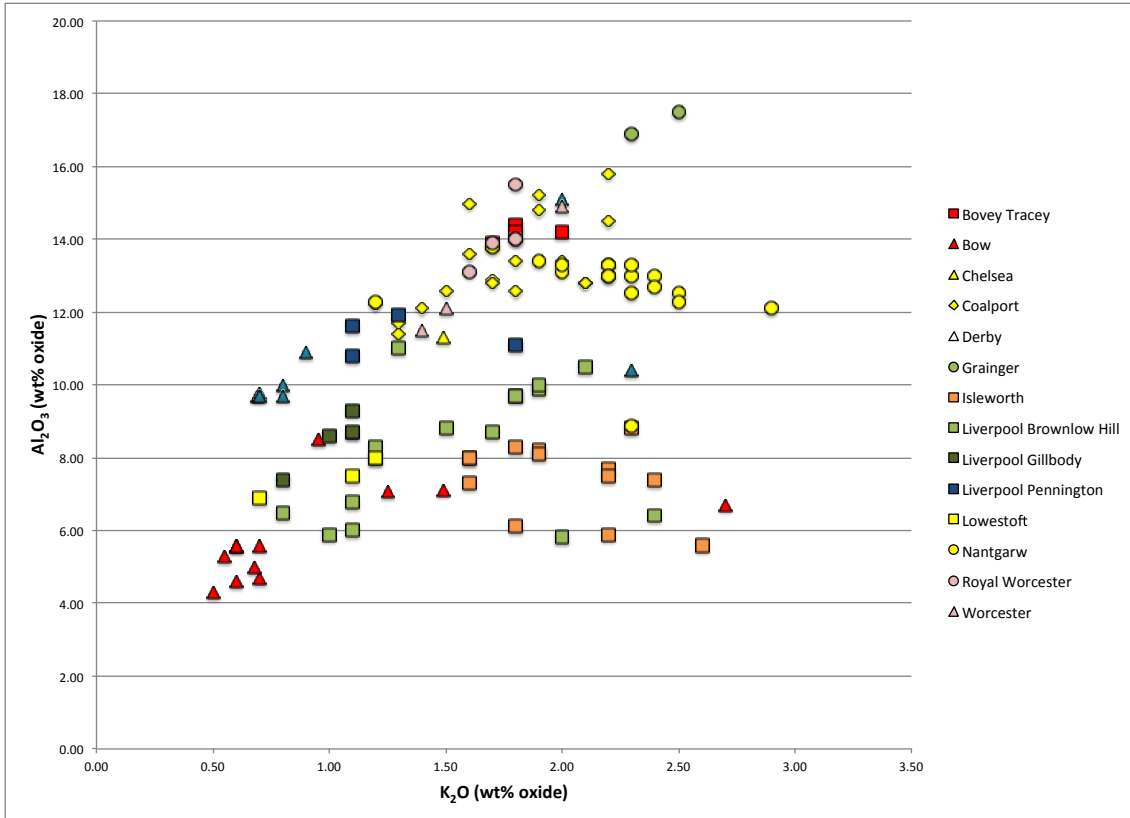


Figure 41 - K_2O vs Al_2O_3 for phosphatic soft-paste porcelain and bone china from the 18th and 19th centuries by factory

A low K_2O (0.5-1.5%abs) and low Al_2O_3 (4-10%abs) group comprises Bow, Brownlow Hill, Gilbody, Lowestoft and Vauxhall, all producing phosphatic porcelain during the mid to late 18th century. Derby porcelains from the same period form a slightly off-set group containing comparable potassium (K_2O 0.6-0.8%abs), but higher aluminium (Al_2O_3 9-11%abs). Brownlow Hill porcelains show a wide spread of data, with K_2O up to 2.5%, although the Al_2O_3 remains below 11%abs. Isleworth and Brownlow Hill porcelain represents the most significant outlying group, which has a higher ratio of potassium to aluminium (K_2O/Al_2O_3 0.2-0.5), and higher potassium in general than contemporary phosphatic pastes (K_2O 1.5-2.5%abs).

Data from bone china produced in the early 19th century is higher in K_2O (1.5-2.5%abs) and Al_2O_3 (11-17%abs). Factories include, Coalport, Grainger, late Worcester and Royal Worcester. Nantgarw phosphatic porcelains follow the pattern of Brownlow Hill, with K_2O up to 3.0% and Al_2O_3 higher at 12-14%.

3.2.3 Frit

Frit soft-paste porcelains are those which used fritted glass, or glass-making ingredients, as the flux, with silica and clay. When these components (SiO_2 , PbO and $\text{Al}_2\text{O}_3 + \text{CaO}$) are illustrated on a ternary plot, see Figure 42, two compositional groups appear. Two larger compositional groups are formed, on the basis of the silica to lead ratio, and the low-lead high-silica group forms two sub-groups, determined by the ratio of silica to alumina and calcium.

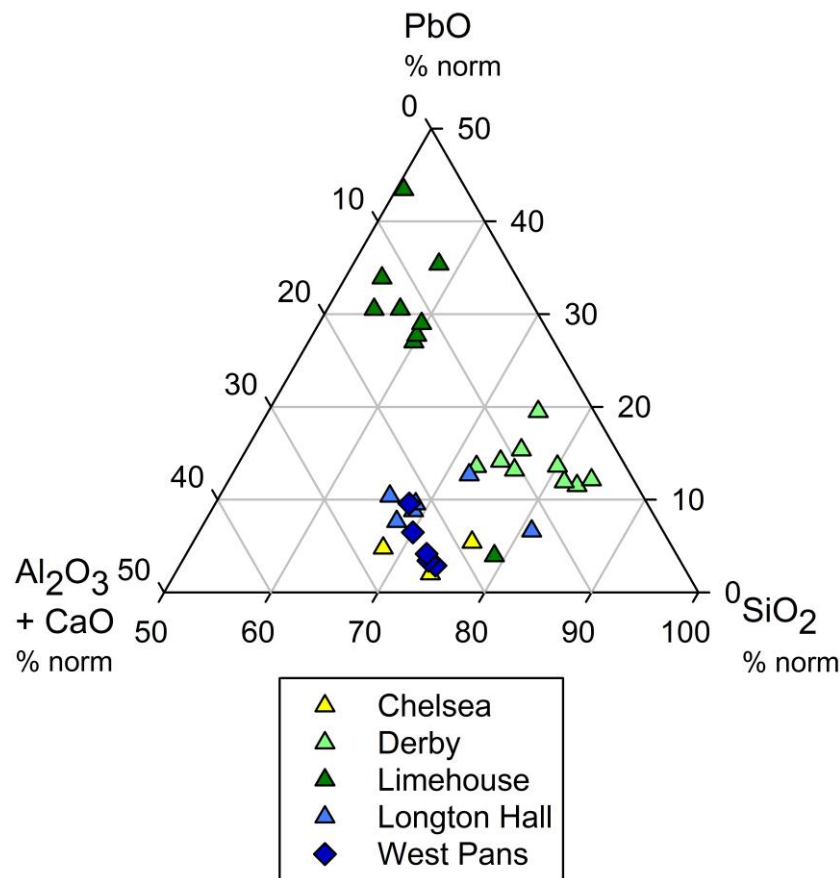


Figure 42 - ($\text{SiO}_2 + \text{PbO}$) vs Al_2O_3 vs CaO in frit porcelain pastes

The high-lead, low-silica group ($\text{PbO} > 25\% \text{norm}$, SiO_2 50-61%norm) comprises most of the Limehouse samples. These also have a relatively low amount of alumina and calcium ($\text{Al}_2\text{O}_3 + \text{CaO} < 20\% \text{norm}$), suggesting that little clay was used in their paste formulae.

In the high-silica, low-lead group (SiO_2 65-85%norm, PbO <20%norm), the three frit samples from Chelsea form a high-alumina and calcium group ($\text{Al}_2\text{O}_3 + \text{CaO}$ >16%norm) that demonstrate a wide spread, overlapping with Longton Hall, West Pans and a Limehouse outlier. A lower alumina and calcium group ($\text{Al}_2\text{O}_3 + \text{CaO}$ <16%norm) is formed by Derby frit pastes and some Longton hall outliers. These two factories may not be reliably distinguished, although many pastes from Derby contain sulphur (0.1-1.0%abs SO_2), which is not known to occur in Longton Hall pastes.

3.2.4 Silica-alumina-calcium and hard-paste

Hard-paste porcelains are defined by their firing temperature, which is higher than that for soft-paste porcelains, and by silica- and clay-rich formulae that will survive this treatment. Oriental and Meissen hard-paste porcelains were made to similar recipes, using china clay and china stone (petuntse), these ceramics and their ingredients are discussed in detail in Sections 2.2.1 and 2.2.2. Similar formulae were employed in the creation of the 'A'-marked group during the 1740s (Freestone, 1996), and at short-lived factories at Plymouth, Bovey Tracey and Bristol in the mid to late 18th century (Owen et al, 2000). Elsewhere, hybrid hard-paste wares were made to similar formulae (known as silica-alumina-calcium, or SAC, pastes), and often fired at temperatures above those used for other soft-paste porcelain formulae, but they retained the two-stage soft-paste firing cycle. These pastes are included here, because their composition is similar to that achieved by the hard-paste factories.

When displayed on a ternary plot (Figure 43), the similarity in composition among most of these wares becomes apparent. They may be divided into two main groups by the amount of calcium in the paste. The relatively high-calcium wares (CaO 5-12%norm) are the 'A'-marked group, Limehouse, Liverpool Brownlow Hill, and an outlier from Swansea, described as "glassy" in a study by Owen et al (1998).

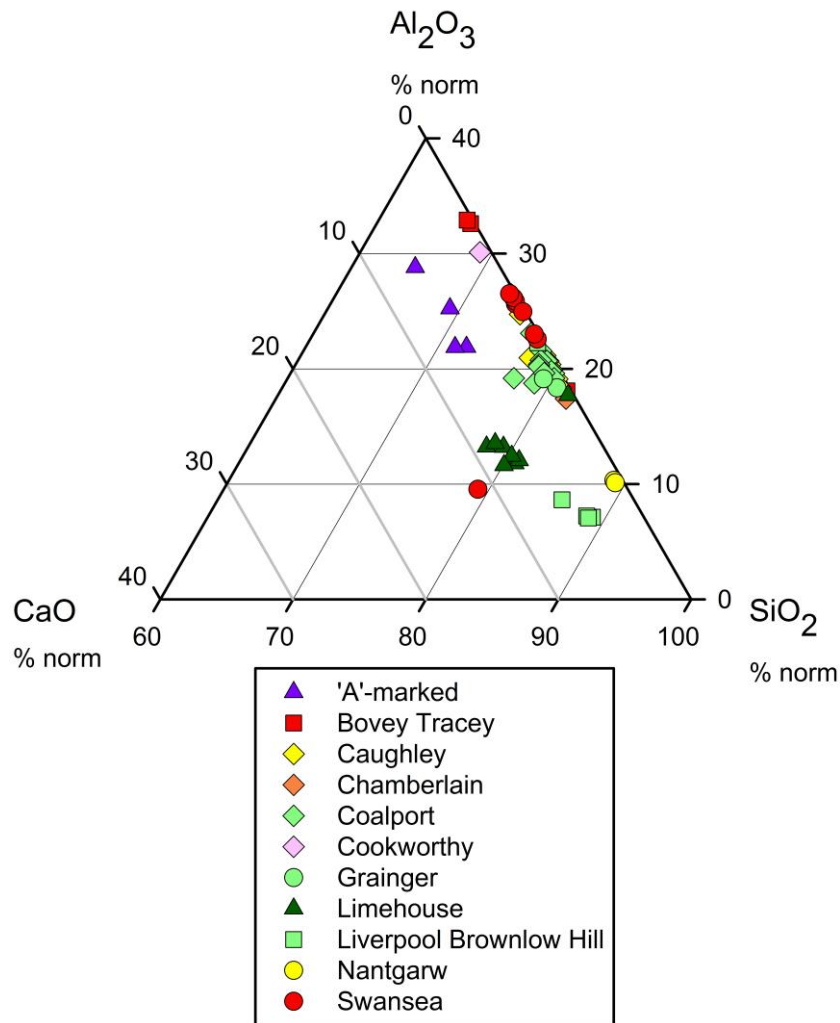


Figure 43 - ternary plot showing SiO_2 vs Al_2O_3 vs CaO for hard-paste and hybrid hard-paste porcelain pastes

The low-calcium porcelains show significant compositional overlap. Bovey Tracey can be distinguished by a lower ratio of silica to aluminium (SiO_2/Al_2O_3 2-5), and Nantgarw by a significantly higher ratio (SiO_2/Al_2O_3 9). Caughley, Chamberlain's Worcester, Coalport, Cookworthy, Grainger and Swansea occupy the range between these two (SiO_2/Al_2O_3 3-5).

3.3 Using major and minor elements to discriminate samples by glaze

The published data for glazes demonstrate variation in their elemental composition, and it may be possible to identify some factories on the basis of their glaze composition, if the extent of intra-factory and inter-factory variation can be quantified. In the following sections, the glazes are divided into two categories: leaded glazes, which comprise the vast majority of soft-paste porcelain glazes; and unleaded glazes, which are typically found on hybrid hard-paste porcelains.

3.3.1 Leaded glazes

The majority of British soft-paste porcelains were glazed with a clear, silicious glaze, fluxed with lead; this flux was effective at lowering the temperature at which the glaze mixture would melt and vitrify during the glaze firing. Since this glaze was ubiquitous in the manufacture of contemporary earthenware, including delftware, the formula used is thought to vary little between factories. The elemental compositional data of the glazes that have been analysed support this theory; where they do vary, this may be as a result of different sources of raw materials, or the glaze may be affected by the composition of the underlying porcelain paste.

When plotted by the silica former, lead flux, and other minor elements common to all (Al_2O_3 , K_2O and CaO), the extent of compositional overlap is evident, see Figure 44. The glazes on porcelain from most factories falls into the lower sector of the plot area, high in lead (PbO 30-55%norm) and silica (SiO_2 30-60%norm).

Lead and silica vary roughly in proportion to one another, depending on the amount of flux that was used, see Figure 45. Most factories for which more than a couple of samples are available show significant variation, and overlap with other factories, and there is no consistent change through time.

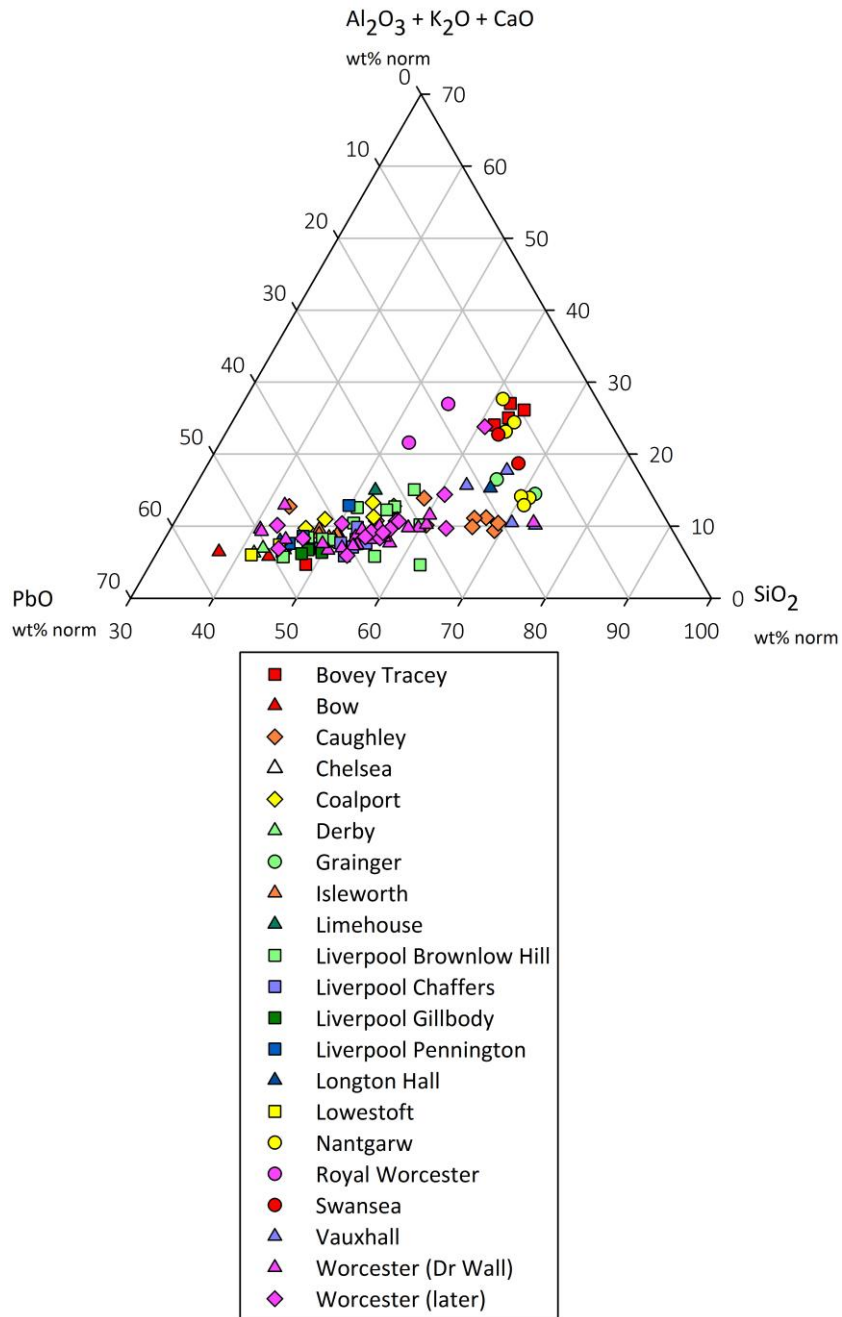


Figure 44 – ternary plot showing SiO₂ vs PbO vs Al₂O₃ + K₂O + CaO in leaded glazes

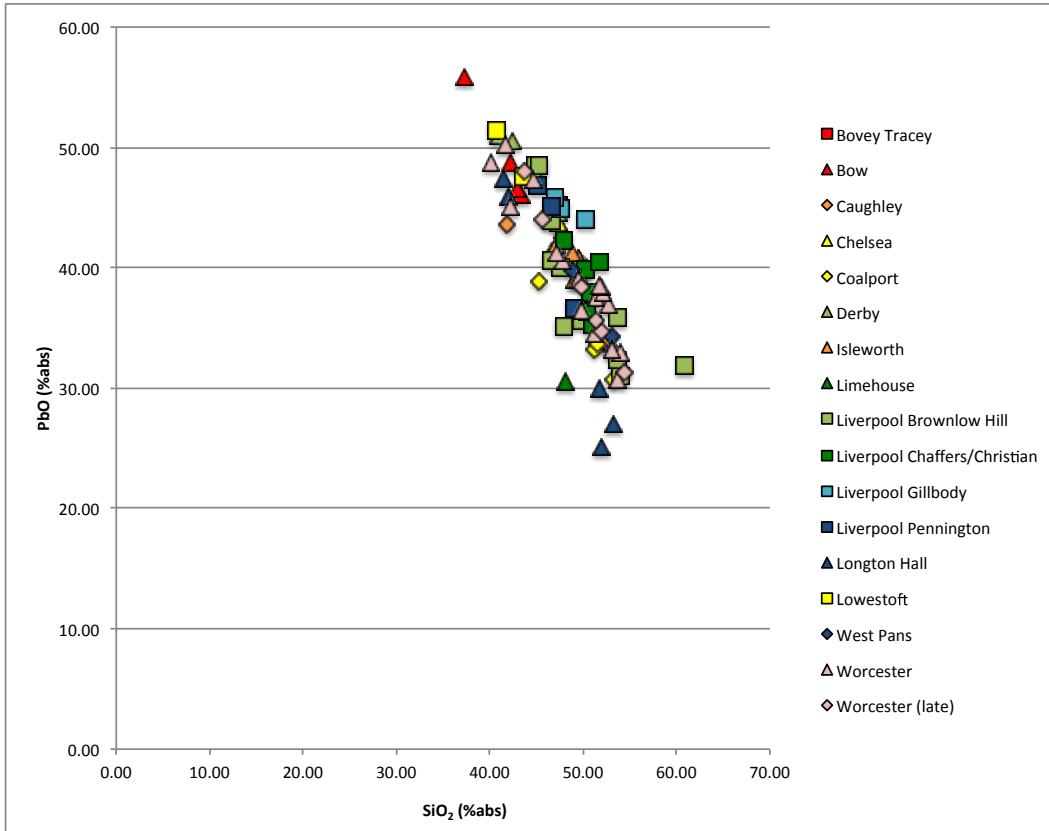


Figure 45 - SiO₂ vs PbO in high-lead glazes

Low-lead porcelain glazes are those that contain PbO 5-30%abs, and comprise early 19th-century samples from factories that mostly produced high-lead glazes (such as Worcester and Coalport), and some factories that appear to have produced exclusively low-lead glazes (such as Nantgarw and Vauxhall). As with some high-lead glazes, the presence of MgO >1%abs in the glaze distinguishes the magnesian pastes, including Bristol, Caughley, Nantgarw, Worcester and Vauxhall, although these are indistinguishable from one another.

The absolute amount of lead can further separate the low-lead glazes, in which there is no obvious trend to the relationship with silica, see Figure 46. Those with relatively low-lead (PbO <17%abs) comprise a high-calcium group (Coalport phosphatic, Bovey Tracey, Nantgarw phosphatic, Swansea, and some early phosphatic Worcester wares), and a low-calcium group of Grainger and some low-magnesium Vauxhall outliers, which can be separated by their amount of alumina, based on the limited amount of data in each category.

Those which contain slightly more lead ($\text{PbO} > 17\% \text{abs}$) comprise a low- Al_2O_3 group (Liverpool Brownlow Hill, Caughley and late Worcester), and a low-MgO Caughley outlier with $\text{Al}_2\text{O}_3 > 3\% \text{abs}$.

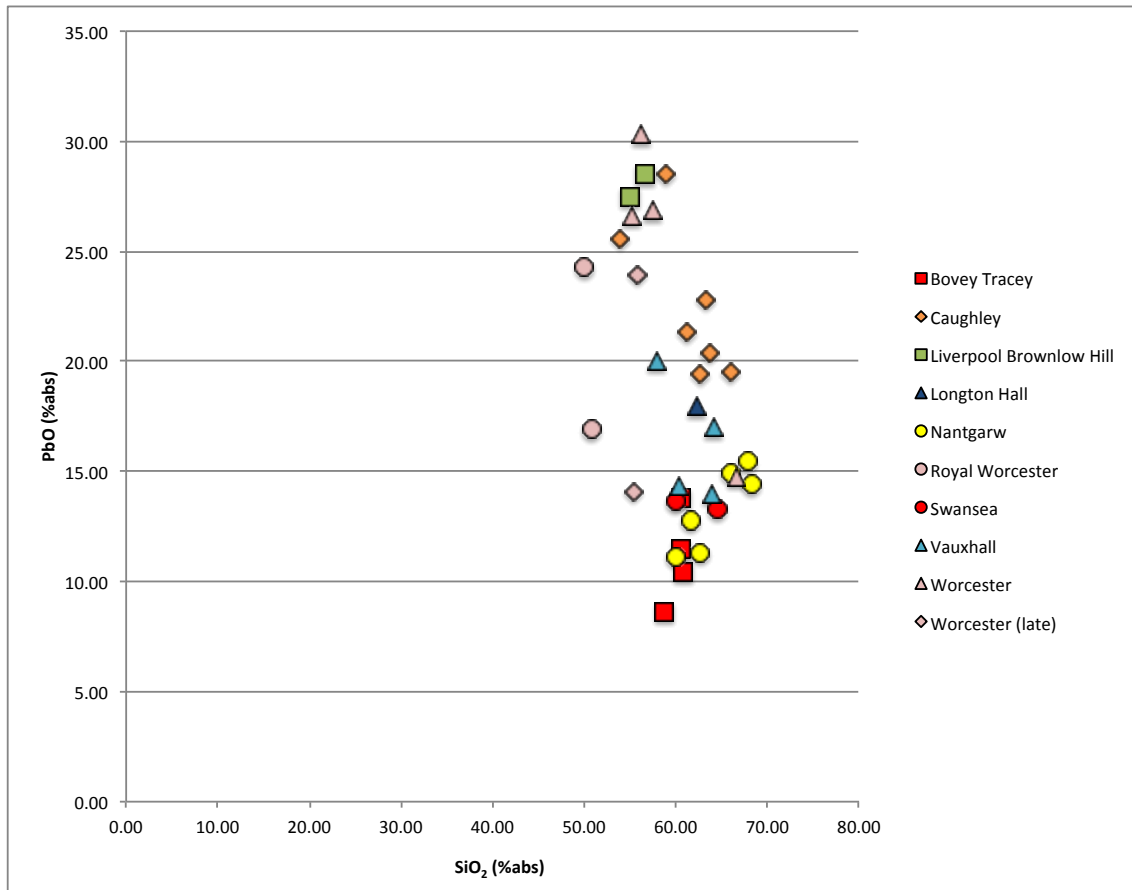


Figure 46 - SiO_2 vs PbO in low-lead glazes

3.3.2 Hybrid hard-paste glazes

Lead-free glazes are unusual in early British porcelains, even hybrid hard-paste specimens, prior to the invention of a feldspathic glaze at Coalport, which is discussed in Section 2.3.2, but for which no data have yet been obtained. Although few data are available, when they are plotted by SiO_2 vs Al_2O_3 vs ($\text{K}_2\text{O} + \text{CaO}$), there appear to be clear compositional groups, see Figure 47.

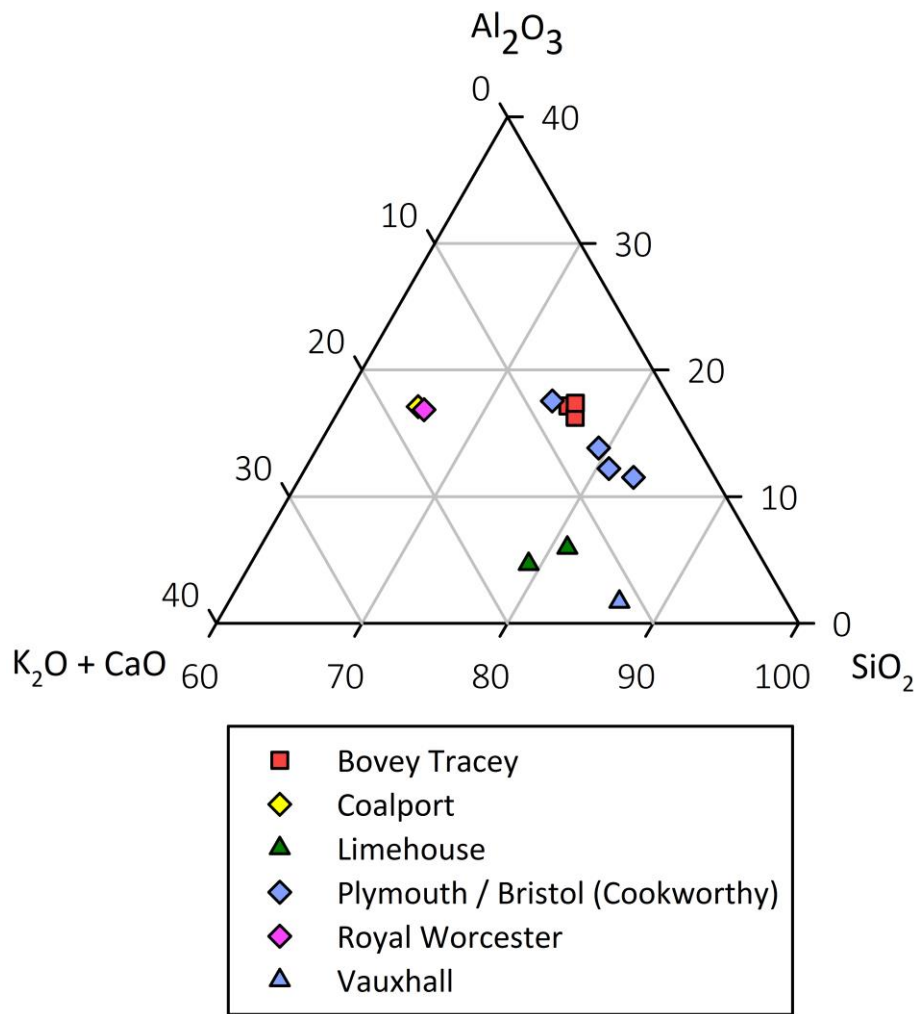


Figure 47 - SiO₂ vs Al₂O₃ vs (CaO + K₂O) (%norm) in hard-paste and hybrid hard-paste glazes

With the exceptions of Bovey Tracey and Cookworthy's Plymouth/Bristol, each factory in this group is represented by only one analysis, and this makes them less reliably distinguishable from one another, because the variation within a single factory's output is invisible, and the evidence from the leaded glazes is that such intra-factory variation can be very significant.

Cookworthy's porcelain glazes are distinctive as they contain SiO₂ >75%norm. The magnesian pastes from Bristol and Limehouse are distinguished by MgO >1%abs, and from one another by their level of Al₂O₃ (Bristol >10%abs; Limehouse <10%abs). Of the bone china porcelains, Grainger contains the least Na₂O (<1%abs), and Royal Worcester the most CaO (>5%abs).

3.4 Conclusion

Published SEM-EDS/WDS data from 325 samples of porcelain paste, and 148 samples of porcelain glaze have been collected and compared. Ternary plots have been plotted to assess the variation within paste categories, and within the categories of leaded and unleaded glazes. The presence or absence of other minor elements, or their ratios when present, were then used to assess intra-factory variation; the conclusions of these analyses are summarised in Table 4 and Table 5. Ten factories may be distinguished by their paste composition, and three by their glaze composition, based on the data available. However, some of these distinctions must be treated as preliminary, because some are based on low sample numbers.

3.4.1 Porcelain paste

Table 4 - compositional categories for British soft-paste porcelain from the most common factories.
All % data in these tables is absolute, and ratios are calculated from the absolute composition.

MgO >5wt%			
SiO ₂ /MgO+CaO 5-6		SiO ₂ /MgO+CaO 8-16	
contains BaO	does not contain BaO	PbO>5wt%	PbO<4wt%
Bovey Tracey	Dr Wall-period Worcester Lund's Bristol Vauxhall	Liverpool Chaffers Dr Wall-period Worcester	Caughley later Worcester Vauxhall

CaO + P ₂ O ₅ > 20wt%				
SiO ₂ / CaO + P ₂ O ₅ > 1.2	SiO ₂ / CaO + P ₂ O ₅ < 1.2			
Liverpool Brownlow Hill	K ₂ O + Al ₂ O ₃ < 11 wt%		K ₂ O + Al ₂ O ₃ > 13wt%	
Liverpool Gillbody	K ₂ O / Al ₂ O ₃ 0.2 - 0.5	K ₂ O / Al ₂ O ₃ 0.1 - 0.2	SiO ₂ > 41%	SiO ₂ < 40wt%
Liverpool Pennington	Isleworth	Bow	Coalport Grainger Nantgarw	Bovey Tracey Royal Worcester

PbO > 5wt%			
SiO ₂ / CaO < 6		SiO ₂ / CaO > 7	
Al ₂ O ₃ >4wt%	Al ₂ O ₃ ≤3.5wt%	PbO>20wt%	PbO<20wt%
Chelsea	Longton Hall West Pans	Limehouse	Derby

SiO ₂ + Al ₂ O ₃ + CaO > 80wt%					
SiO ₂ / CaO < 20		SiO ₂ / CaO > 20			
SiO ₂ / Al ₂ O ₃ < 3	SiO ₂ / Al ₂ O ₃ > 5	SiO ₂ / Al ₂ O ₃ < 7		SiO ₂ / Al ₂ O ₃ > 8	
'A'-marked	Limehouse	SiO ₂ > 70wt%	SiO ₂ < 70wt%	TiO ₂ >0.3wt%	TiO ₂ <0.1wt%
		Cookworthy	Caughley Chamberlain's Worcester Coalport Grainger Royal Worcester Swansea	Liverpool Brownlow Hill	Nantgarw

3.4.2 Porcelain glazes

Table 5 - compositional categories for British porcelain glazes from the most common factories

PbO < 5 wt%				
Al ₂ O ₃ < 6wt%		Al ₂ O ₃ 8 - 13wt%		Al ₂ O ₃ > 15wt%
contains SnO ₂	contains no detectable SnO ₂	CaO < 3%	CaO >3%	Bovey Tracey Bristol
Vauxhall	Limehouse	Plymouth	Grainger Royal Worcester	

PbO 5 - 30wt%		PbO > 30wt%		
Al ₂ O ₃ + K ₂ O + CaO > 15wt%		Al ₂ O ₃ + K ₂ O + CaO < 15wt%	PbO 30 - 45wt%	PbO > 45wt%
Na ₂ O > 1wt%	Na ₂ O < 1wt%			
Bovey Tracey Royal Worcester	Nantgarw (phosphatic) Swansea	Caughley Grainger Liverpool Brownlow Hill Longton Hall Nantgarw (SAC paste) Vauxhall Worcester	Caughley Coalport Isleworth Limehouse Liverpool Brownlow Hill Liverpool Chaffers Liverpool Gillbody Liverpool Pennington Worcester	Bow Bovey Tracey Caughley Chelsea Coalport Derby Liverpool Brownlow Hill Liverpool Gillbody Liverpool Pennington Longton Hall Lowestoft Worcester

4 Materials and Methods

4.1 Introduction

In seeking to develop a methodology that is optimised for the analysis of British porcelain, this research relies on numerous groups of material and employs a range of analytical techniques. Wherever possible, the same sample set has been used for all techniques, in order to compare the results with one another directly. However, in some cases, a sample set could only be accessed by a single technique; for instance, a large museum collection of intact porcelain could not be removed from the building for laboratory analysis, nor would the bigger objects have fit in the sample chamber of the SEM, or the Laser Ablation system. Furthermore, a collection of porcelain fragments, mounted in cross-section, could not be analysed by XRF, because the thickness of the glaze was much smaller than the spot size of the X-ray. In such cases, the data acquired from these samples is considered individually.

The first half of this chapter describes the material selected for analysis, and the rationale behind their selection, including any specific research questions to which their analysis would be relevant. The second half presents the analytical techniques employed; these are divided into techniques that are completely non-invasive (Hand-Held XRF, and spectrophotometry), and techniques that require invasive sampling (SEM), or are classed as micro-destructive (LA-ICPMS).

The aims of this chapter are to establish the parameters of the methodology, by illustrating the group of objects analysed, within the much larger class of material known as British porcelain, and the analytical techniques and systems that have been evaluated for their applicability to the characterisation of British porcelain.

4.2 Materials

Of the huge volumes of soft-paste porcelain produced by dozens of factories throughout the late 18th and early 19th century, a great deal survives intact or with minimal damage. Large collections exist in the British Museum, the Ashmolean Museum, the Victoria and Albert Museum, and other public collections. However, it is private collectors who curate much of the surviving British soft-paste porcelain, and their study and connoisseurship of the material has resulted in a wide array of books and periodicals, which have been invaluable in informing this research. Collectors are catered to by sellers at auction, or through antiques trade shops and dealerships, the owners of which are frequently themselves collectors or connoisseurs.

British porcelain is also commonly found at archaeological sites dating from the mid 18th century onwards; broken household ceramics are found in domestic contexts (Pearce, 2008), and large collections of spoiled wares are found among kiln furniture and refuse at factory sites (Barker and Cole, 1998). It is known that this material is subject to taphonomic processes in the soil, and that this weathering can affect the composition of the paste and glaze (Owen, 1998). These effects will be assessed using the data gathered from archaeological sherds, and comparing it with data from intact objects from the same factory, to determine the extent to which weathering can be detected in analytical data.

In seeking samples for this research, the decision was made to analyse material from all of these potential sources, in order to make the methodology applicable to as wide a range of analytical contexts as possible.

4.2.1 Mounted samples from intact objects and archaeological sherds

For the purposes of characterising the material and evaluating the analytical techniques that require invasive or micro-destructive sampling, ideally material that has already been sub-sampled from intact objects or archaeological sherds was required. Samples of this type were kindly donated for this project by John Sandon, International Director of European Ceramics and Glass with Bonhams, London. These comprise porcelain sherds from archaeological excavations at three sites in Liverpool (John and Jane Pennington's factory at Copperas Hill, and Samuel Gillbody's factory, and the factory owned by Richard Chaffers and Phillip Christian, followed by Seth Pennington, both at Shaw's Brow), and at the Caughley and Worcester factory sites, see Table 6. Technical studies of these samples using SEM-EDS and SEM-WDS have already been published (the data are provided in Appendix A.5, and the full studies are Owen, 1998; Owen and Sandon, 1998; Owen and Sandon, 2003). The existence of comparative data from this commonly-used analytical technique will allow the alternative techniques used in this study to be evaluated on the accuracy of the data that they produce.

A further fifty-four mounted samples, most of which also have published SEM-EDS data for comparison (Eccles and Rackham, 1922; Tite and Bimson, 1991; Freestone, 1993), were loaned from the British Museum Reference Library, Department of Conservation and Scientific Research, courtesy of Prof. Ian Freestone, University College London, and David Saunders, British Museum. These comprise porcelain sherds, mounted in cross-section using a clear resin, from numerous factories, see Table 7.

Materials and Methods

Table 6 - samples of porcelain from Caughley, Liverpool, and Worcester, donated by John Sandon.
The letters u/g denote an unglazed sherd.

Samples	Factory
CY2 (u/g), CY3, CY4, CY5, CY6, CY8, CY9, CY11, CY12, CY13 (u/g), CY14 (u/g), CY15 (u/g), CY16 (u/g), CY17 (u/g), CY18 (u/g), CY19, CY20, CY21	Caughley
G1 (u/g)	Grainger
LC/P1 (u/g), LC/P2 (u/g), LC/P3 (u/g), LC/P4 (u/g), LC/P5 (u/g), LC/P6 (u/g), LC/P7 (u/g), LC/P8 (u/g), LC/P9 (u/g), LC/P10 (u/g), LC/P11 (u/g), LC/P12 (u/g), LC/P14 (u/g)	Liverpool Christian, or Seth Pennington
LG1 (u/g), LG2 (u/g), LG3 (u/g), LG4 (u/g)	Gillbody (Liverpool)
LP1 (u/g), LP2 (u/g), LP3, LP4 (u/g)	John or James Pennington (Liverpool)
W11 (u/g), W12, W13 (u/g), W14 (u/g), W15	Worcester

Table 7 - samples of porcelain from several factories, donated by the British Museum Reference Library.
The letters u/g denote an unglazed sherd.

Samples	Factory
47122 R (u/g)	'A'-marked
32703 X, 29105 Q, 29100 P, 29104 S	Bow
29102 W	Bristol
1069	Caughley
32699 W, 29106 Z, 29103 U, 1055, 1076	Chelsea
1072	Coalport
1056, 1057	Crown Derby
40149 P, 40012 W, 40011 Y, 40010 P, 40009 X, 40008 Z, 40007 Q, 40006 S, 40004 W, 40003 Y, 40002 P, 40000 S	Limehouse
32704 V	Chaffers (Liverpool)
32705 T, 32706 R	Ball (Liverpool)
29098 V	Longton hall
32707 P, 29101 Y	Lowestoft
1059	Nantgarw
1053, 1054	New Hall
1058	Pinxton
32701 Q	Plymouth
32702 Z	Pomona (Newcastle)
36554 Q, 1060, 1070, 1071	Swansea
32700 S, 29099 T, 29263 P, 1062, 1063, 1064, 1065, 1066, 1067, 1068	Worcester

4.2.2 Intact objects

One-hundred and forty intact porcelain objects, all with a relatively secure provenance, have been selected for analysis using HH-XRF. In order to assess the usefulness of the data gathered, this material was selected for its relevance to questions of authenticity and attribution, which would be of interest to curators, collectors and ceramic experts. They are listed in the main sample catalogue in Appendix A.6.

The largest part of the sample set is a group from the Marshall collection of Early Coloured Worcester porcelain, which consists of 1,085 pieces (Spero, 1986). Access to the collection was granted by the Department of Western Art at the Ashmolean Museum, Oxford, where it is displayed in its entirety, according to the design of its original owner, Henry Rissik Marshall (Spero, 1986). The collection was formed in the early 20th century, and comprises Worcester porcelain of the 'First Period', also known as the 'Dr Wall Period', ca. 1751 – 1783, with coloured enamels, borders and grounds. A few of the pieces were subsequently thought to have been later decorated, mainly in the 19th century, or to have had their original decoration altered or entirely removed. Twelve suspected pieces was chosen for analysis by Rosalind Sword, who was then in the process of researching a new catalogue of the collection. For comparison, fifty-nine enamelled pieces thought to be genuine early coloured Worcester were also analysed, alongside those attributed to the contemporary decorating studio of James Giles.

These data form the bulk of the material analysed, because they provide the opportunity to characterise the Worcester factory thoroughly in terms of the glazes used during one period (Dr Wall period), and the pigments used in 18th- and 19th-century polychrome enamels. However, their intact condition meant that they could not be sampled for analysis by SEM or LA-ICPMS, and it was only possible to analyse them within the buildings in which they are stored. This provided an opportunity to employ the non-destructive, field-portable techniques that form part of the new methodology developed by this research.

In order to assess the extent of inter-factory variation, against the intra-factory variation present in Worcester porcelain, eighty-five objects from fifteen contemporary factories were analysed using the same technique. These were kindly made available by Juno Antiques, Notting Hill, London; Stockspring Antiques, Kensington, London; and the private collections of George Haggerty, Nick Panes, Roger Pomfrett, Peter Burke, and Rosalie Wise-Sharp. These are also listed in the main sample catalogue, see Appendix A.6.

4.2.3 Archaeological sherds

Archaeological porcelain recovered from former factory sites was assessed, because a relatively secure provenance could be established, based on the assumption that the sherds are wasted or broken objects that have been discarded during production. Four factory sites located in or around London have been excavated, and large quantities of ceramic material recovered. Samples were available from Bow (n = 4), Isleworth (n = 7), Limehouse (n = 7) and Vauxhall (n = 7).

Access to this material, which is now stored at the London Archaeological Archive and Resource Centre, and the Museum of London Archaeology archive, was facilitated by Jacqui Pearce and Helen Ganiaris (Museum of London Archaeology) and Dan Nesbitt, (London Archaeological Archive and Resource Centre). Sherds from the factory sites at Longton Hall, Staffordshire (n = 6), and West Pans, Lothian (n=6), were made available by George Haggerty, courtesy of the National Museum of Scotland, Edinburgh.

As with the intact sample set described in section 4.2.2, it was not possible to remove these sherds from the building in which they are stored, or to sample them for destructive analysis in the laboratory.

4.3 Methods

The analytical techniques employed in developing this methodology were selected as a result of the historical and technical review of British porcelain (section 2.4), to favour the techniques most commonly used in the analysis of British porcelain and similar material. In selecting analytical techniques for this research, the defining parameters will be:

- sensitivity, that is, the range and limits of detection;
- versatility, in terms of the type and condition of material which may be usefully analysed;
- accessibility, both of the analyst to the equipment, and the equipment to the samples (emphasised by Craddock, 2009; p. 40);
- usefulness of the resulting data, which must be comparable with the existing highly useful elemental compositional data.

XRF has proven reliability and accuracy, and it is able to detect a wide range of elements at relatively low limits of detection (Janssens, 2013; pp. 89 – 92). In this section, a set of novel glass standards are developed for use as calibration standards in a future quantitative XRF method.

Hand-Held X-ray Fluorescence spectroscopy (HH-XRF) and spectrophotometry are field-portable, and both quick and easy to use with adequate training and experience. Neither technique requires that a sample be taken from the object, and analysis does not alter the surface of the material. These techniques therefore fulfil most of the above criteria, and will be used as the foundation of the sample characterisation research.

A micro-destructive technique, Laser Ablation Inductively Coupled Plasma Mass-Spectroscopy (LA-ICPMS), will be trialled on sampled material for which Scanning Electron Microscopy data are available. This will produce trace elemental compositional data at a very high degree of precision, in order to assess the usefulness of this technique for characterising and provenance studies of British porcelain as part of this methodology.

The methods of techniques that rely on non-invasive analysis and do not require destructive sampling are described first, namely; X-ray Fluorescence Spectroscopy using a Hand-Held instrument, and spectrophotometry. The results of these analyses are presented in Chapter 5. Laser ablation inductively coupled plasma mass spectroscopy (LA-ICPMS) follows, and its results are in Chapter 6, because the analysis relies on pre-sampled material, which is a largely separate sample set from the intact objects analysed by the non-invasive methods.

4.3.1 Building Novel Glass Standards for Calibration

While there are few published studies that examine specifically porcelain glazes, much less lead-rich British porcelain glazes, some data obtained from analysis of such glazes is often included in reports of the characteristics of porcelain bodies (Tite and Bimson, 1991; Middleton and Cowell, 1993; Freestone et al, 2003; Owen and Hillis, 2003; Owen and Sandon, 2003). These data demonstrate that the glazes show intra- and inter-factory variation in composition, which is discussed in Chapter 3.

The most abundant and commonly-found minor (<8%) and trace elements ($\leq 0.1\%$) are alkalis (potassium, calcium), likely to have been added deliberately to assist in the formation of a glass network (Moretti and Hreglich, 2013) and transition metals (iron, copper), which occur as contaminants in other ingredients, particularly the sands and pebbles used for the source of silica.

Cobalt and tin are sometimes found, and these may have been added deliberately to improve the colour of the finished object, the former by adding a blue hue, which would cancel out any warm tones present, and the latter by creating an opaque white glaze, which would mask any tints or blemishes in the body. In glazes that contain cobalt, nickel and manganese are often found, as these are components of the smalt pigment used in cobalt blue decoration (Delamere, 2013; p. 41). Rarely, arsenic, barium and bismuth are also present in the glaze, for reasons that are not yet clear. Arsenic and barium have historically been used as white pigments, and so may have been added deliberately to improve the whiteness of the finished object (Eastaugh et al, 2008; pp. 29 - 30; pp. 53 - 55). Bismuth can be present as an accessory in certain lead ores (Arabinda et al, 2006).

Using these data, Domoney has designed standards that are analogous to porcelain glazes and enamels, as part of her research for the purpose of characterising porcelain glazes and enamels on Meissen porcelain (Domoney, 2012; pp. 134-135). The main constituents are silica and lead oxide, but they also contain varying levels of other elements that are present in some glazes as trace elements, and in enamels as colourants. Metal oxide pigments were obtained from CTM Potters Supplies, and mixed at Cranfield University, in accordance with the necessary Control of Substances Hazardous to Health (COSHH) and Standard Operating Procedure (SOP) protocols. Mixed batches of pigment were sent to the Roman Glassmakers company, where they were mixed with lead and silica and fired in a ceramic crucible for three hours at 1410 °C (Domoney, 2012; pp. 134 - 135).

One fragment from each batch, which appeared to show the least variation across the surface composition, was selected to be the standard. A large, flat surface of each fragment was ground using silicon carbide paper, and polished using a cloth lap and micro-crystal suspension, in order to create a smooth, flat surface. This surface was coated in carbon using a vacuum sputter coater, prior to analysis by SEM, which is described in the following section.

It has been established that SEM-EDS and SEM-WDS have been used successfully for the analysis of British porcelain (Literature Review section 2.3.2, Meta-analysis section 3.2). In this research, SEM-EDS is used only to characterize novel glass standards, which are designed to calibrate XRF data, a process described in detail in Section 4.3.1. The Hitachi SU3500 SEM, with an AMTEK Octane Plus EDS at Cranfield University was used; the analytical settings for imaging and elemental compositional analysis were as follows: 20keV accelerating voltage, 200 μ A current, 200x magnification. The glass certified reference material Corning C was used to monitor analytical drift, and for calibration alongside Corning A and NIST 610 and 612. Further information about SEM-EDS in theory and instrumentation is provided in Appendix A.1.

The surface of each standard was viewed using back-scattered electron (BSE) imaging at 15 keV, whereby the brightness of the returning electron signal indicates the average atomic number of the elements present in the surface, which demonstrates the extent of the sample homogeneity. In addition, seven analyses of large areas and small spots were taken. These analyses were ultimately used to determine the mean elemental composition of the standard for this purpose, in order to mitigate the effect of compositional variation across the surface of the samples.

Of the ten standards analysed, eight had low standard deviation around the mean value for all elements analysed, and appeared homogeneous in composition when viewed in the phase-contrast view using backscattered electrons, see Figure 48. However, two (numbers 6 and 7) were found to be inhomogeneous in composition, with silicon-enriched crystalline phases in a lead-rich glassy matrix, see Figure 49.

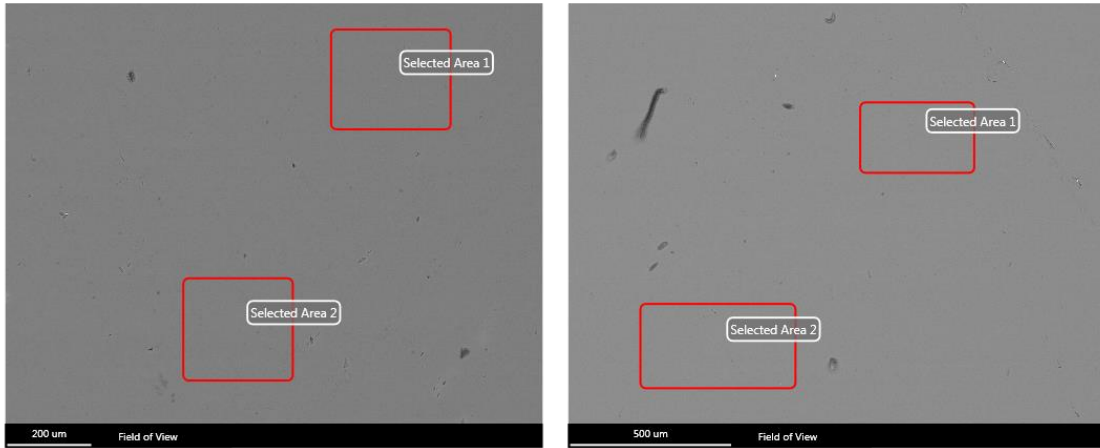


Figure 48 - phase-contrast view of the surface of glass standards 4 (left) and 8 (right)

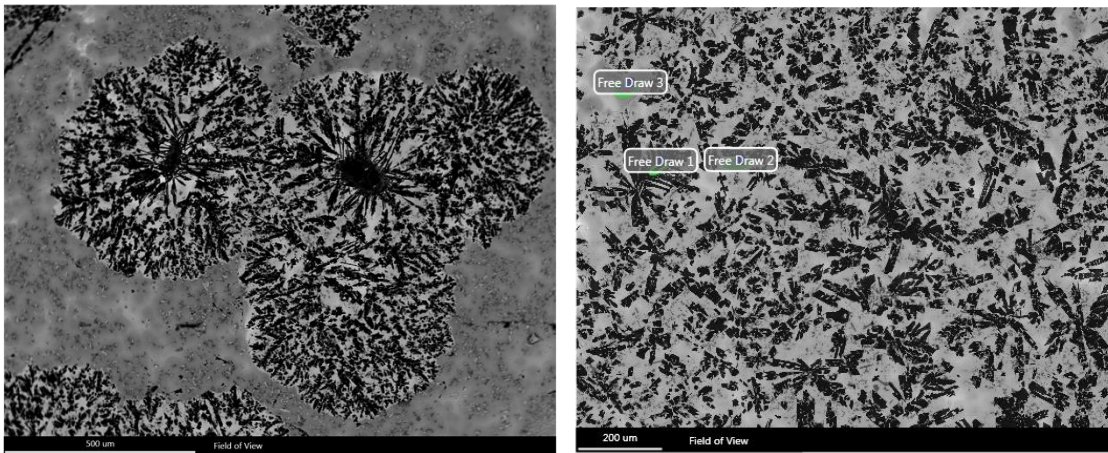


Figure 49 - phase-contrast view of the surface of glass standards 6 (left) and 7 (right)

For the eight glass standards that were successfully characterised, there is a good relationship between the notional and mean elemental compositional data, see Table 8 and Figure 50, which demonstrates that the actual composition is close to the intended composition, and represents a good spread of the elements of interest in porcelain leaded glazes and enamels. Some alumina has been contributed, which is thought to be an impurity in the source of silica. The relationship is demonstrated by plotting the notional and measured values for the elements of interest, see Figure 50 and observing the correlation through the coefficient of determination, R^2 , is used, see Table 9. The correlation coefficient (R) describes the strength of the relationship from 0 to 1 or -1, where 1 or -1 = a perfect positive or negative correspondence respectively (Harris, 2010; pp. 100 – 102).

Materials and Methods

Table 8 - notional and measured (SEM-EDS) composition of eight glass standards in weight percent as oxides

	Data	Al ₂ O ₃	SiO ₂	K ₂ O	CaO	TiO ₂	Cr ₂ O ₃	MnO	Fe ₂ O ₃	CoO	NiO	CuO	ZnO	SnO ₂	Sb ₂ O ₃	BaO	PbO	BiO
1	notional	0.00	40.00	1.00	0.00	0.00	2.00	0.00	5.00	0.00	3.00	2.00	0.00	7.00	7.00	3.00	30.00	0.00
	measured (μ)	2.10	44.60	0.60	0.00	0.00	1.90	0.00	3.50	0.00	2.80	1.90	0.00	4.60	5.60	2.60	28.10	0.00
	measured σ	0.60	0.80	0.10	-	-	0.10	-	0.10	-	-	0.10	-	1.10	0.20	0.20	0.60	-
2	notional	0.00	40.00	2.00	0.00	0.00	5.00	0.00	13.00	0.00	1.00	5.00	0.00	2.00	2.00	1.00	30.00	0.00
	measured (μ)	1.20	48.80	1.30	0.00	0.00	2.70	0.00	8.30	0.00	0.60	4.20	0.00	1.60	1.60	0.90	28.70	0.00
	measured σ	0.20	4.20	0.10	-	-	0.90	-	1.80	-	0.10	0.30	-	0.30	0.20	0.30	1.90	-
3	notional	0.00	40.00	0.00	3.00	1.00	0.00	14.00	0.00	8.00	0.00	0.00	1.00	0.00	0.00	0.00	30.00	3.00
	measured (μ)	4.10	44.60	0.00	2.80	1.00	0.00	7.60	0.00	6.90	0.00	0.00	1.10	0.00	0.00	0.00	26.00	4.70
	measured σ	0.40	2.50	0.00	0.10	0.10	-	0.30	-	0.20	-	-	0.20	-	-	-	1.30	0.80
4	notional	0.00	40.00	0.00	15.00	4.00	0.00	3.00	0.00	2.00	0.00	0.00	6.00	0.00	0.00	0.00	30.00	2.00
	measured (μ)	3.10	41.30	0.00	13.30	3.80	0.00	1.10	0.00	1.90	0.00	0.00	5.80	0.00	0.00	0.00	27.20	2.60
	measured σ	0.10	0.40	-	0.10	0.00	-	0.00	-	0.10	-	-	0.10	-	-	-	0.10	0.20
5	notional	0.00	40.00	0.00	0.00	0.00	3.00	0.00	8.00	0.00	2.50	3.00	0.00	5.00	5.00	2.50	30.00	0.00
	measured (μ)	0.88	46.80	0.00	0.00	0.00	2.53	0.00	7.35	0.00	2.50	2.45	0.00	3.25	4.43	2.45	26.45	0.00
	measured σ	0.17	1.13	0.26	-	-	0.39	-	0.13	-	0.23	0.26	-	0.54	0.26	0.37	0.60	-
8	notional	0.00	40.00	0.00	6.00	2.00	0.00	11.30	0.00	6.00	0.00	0.00	2.00	0.00	0.00	0.00	30.00	2.70
	measured (μ)	3.48	45.03	0.00	6.98	2.55		8.03	0.00	6.45	0.00	0.00	2.05	0.00	0.00	0.00	25.08	0.60
	measured σ	0.22	0.79	-	0.19	0.41		0.33	-	0.10	-	-	0.21	-	-	-	0.46	0.33
9	notional	0.00	40.00	0.00	12.00	3.00	0.00	5.70	0.00	3.00	0.00	0.00	5.00	0.00	0.00	0.00	30.00	1.30
	measured (μ)	3.00	44.53	0.00	13.43	3.38	0.00	3.20	0.00	3.40	0.00	0.00	4.73	0.00	0.00	0.00	24.25	0.60
	measured σ	0.54	0.36	-	0.10	0.41	-	0.14	-	0.12	-	-	0.15	-	-	-	0.44	0.33
10	notional	0.00	40.00	0.00	9.00	2.50	0.00	8.50	0.00	4.50	0.00	0.00	3.50	0.00	0.00	0.00	30.00	2.00
	measured (μ)	5.50	52.25	0.00	8.68	2.35	0.00	4.40	0.00	4.03	0.00	0.00	2.80	0.00	0.00	0.00	19.48	0.60
	measured σ	0.62	1.34	-	0.21	0.61	-	0.22	-	0.21	-	-	0.14	-	-	-	0.26	0.70

Materials and Methods

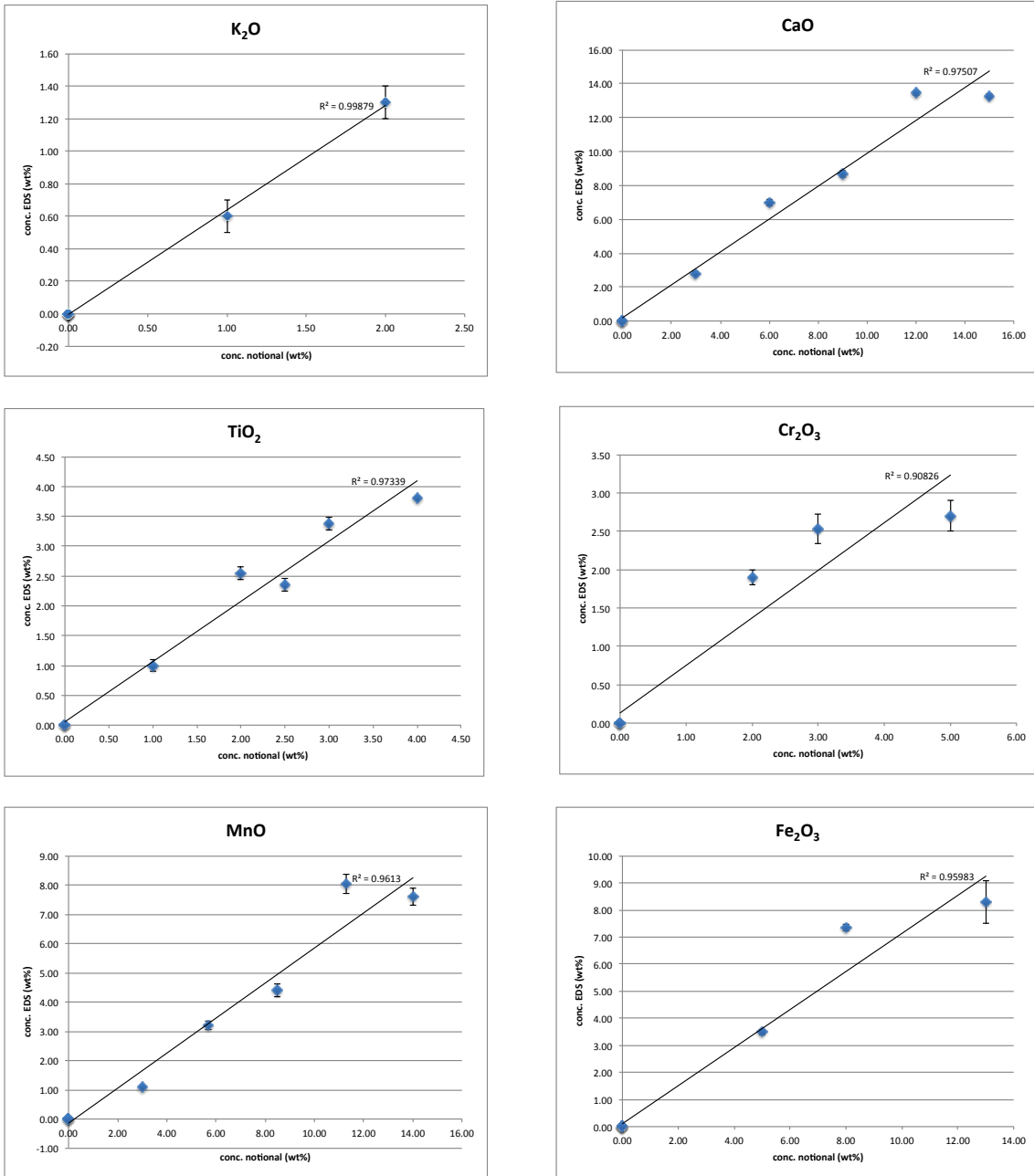


Figure 50 - concentration measured by EDS (conc. EDS) plotted against the notional composition (con. not.) (both wt% as oxides) of eight glass standards

Materials and Methods

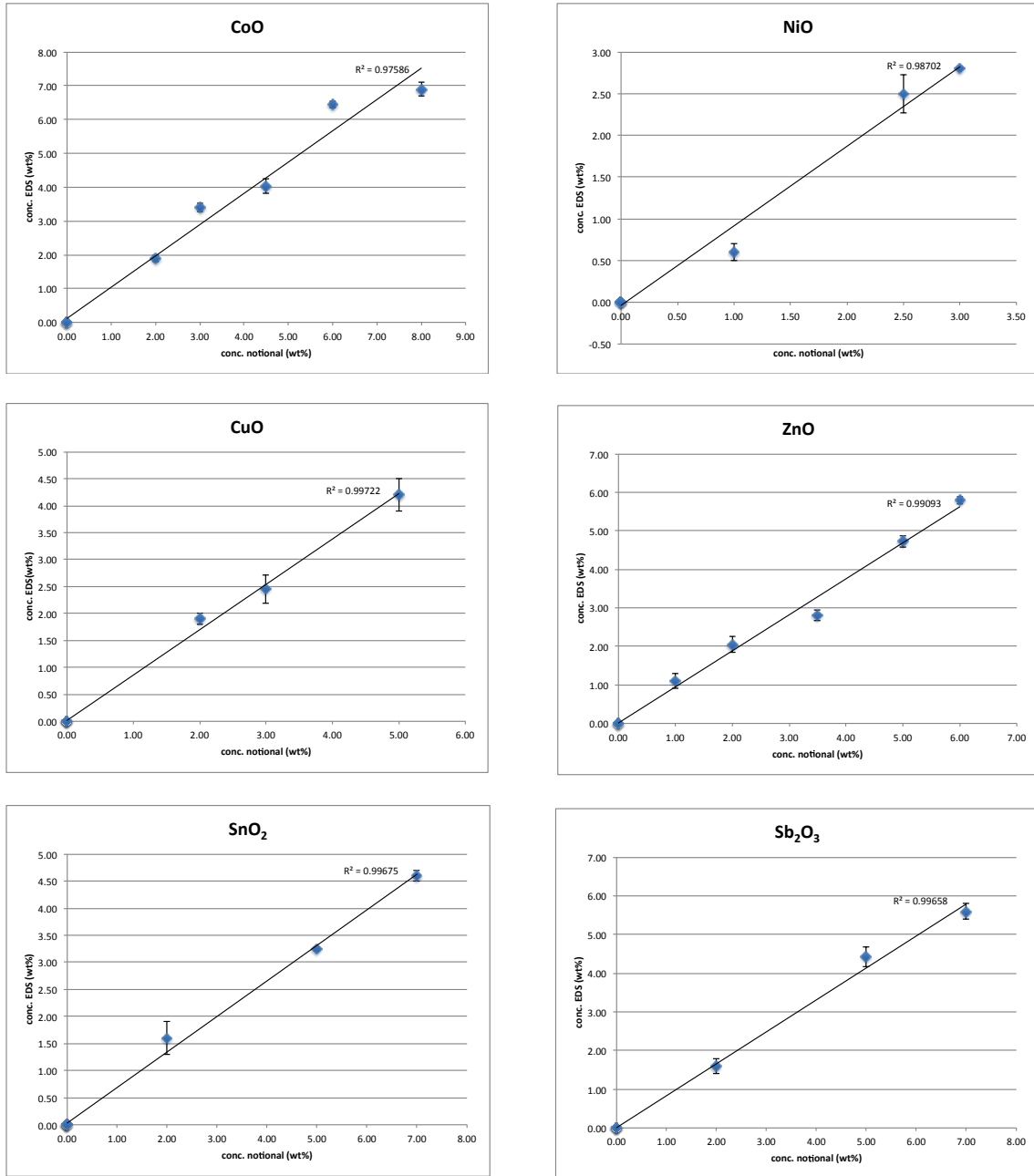


Figure 50 - concentration measured by EDS (conc. EDS) plotted against the notional composition (con. not.) (both wt% as oxides) of eight glass standards (continued)

Materials and Methods

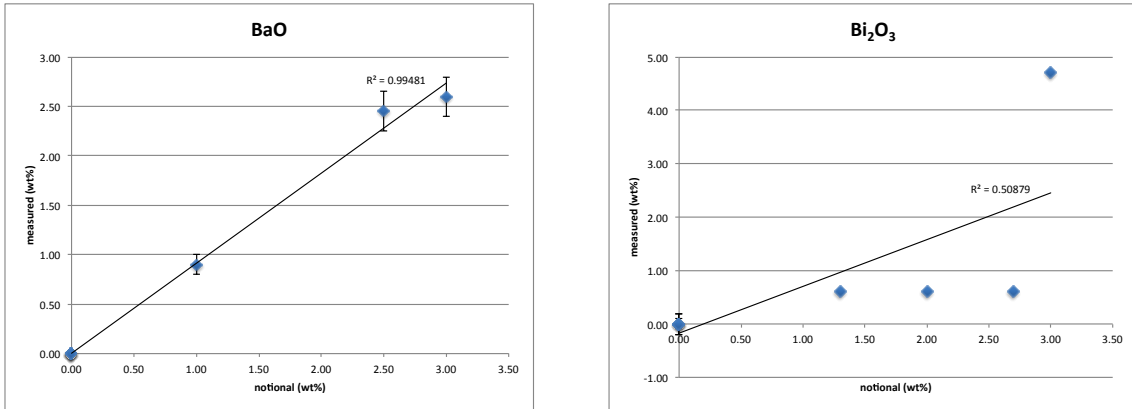


Figure 50 - concentration measured by EDS (conc. EDS) plotted against the notional composition (con. not.) (both wt% as oxides) of eight glass standards (continued)

Table 9 - the coefficient of determination (R^2) for SEM-EDS data vs notional composition for fourteen elements, present in eight glass standards

Element	K	Ca	Ti	Cr	Mn	Fe	Co	Ni	Cu	Zn	Sn	Sb	Ba	Bi
R^2	0.99	0.9	0.9	0.9	0.9	0.9	0.9	0.9	0.9	0.9	0.9	0.9	0.9	0.8
		7	7	1	6	5	7	8	9	9	9	9	9	2

To ensure that the standards would be applicable to XRF analysis, they were then analysed using the HH-XRF under the analytical conditions described in the following section. The quantitative values produced by the XMET software were then compared with the SEM-EDS data, see Table 10 and Table 11, and Figure 51.

Table 10 - composition of eight glass standards, calculated by XMET software

	wt% oxides				ppm					
	Al ₂ O ₃	SiO ₂	K ₂ O	CaO	Cr	Ni	Cu	Zn	Sb	Pb
1	1.54	15.66	0.20	0.64	24733	54200	30188	nd	490976	288919
2	1.33	15.43	0.27	0.25	56344	12652	69847	nd	45690	163064
3	2.01	15.64	0.00	0.77	nd	nd	nd	15936	nd	327374
4	1.50	10.31	0.00	1.81	nd	nd	nd	75937	nd	272602
5	1.31	16.07	0.00	0.49	46318	42845	45081	nd	27476	236787
8	2.07	18.50	0.00	1.17	nd	nd	nd	26546	nd	275083
9	1.61	10.55	0.00	1.68	nd	nd	nd	66561	nd	267042
10	1.74	11.78	0.00	1.46	nd	nd	nd	49972	nd	294639

Materials and Methods

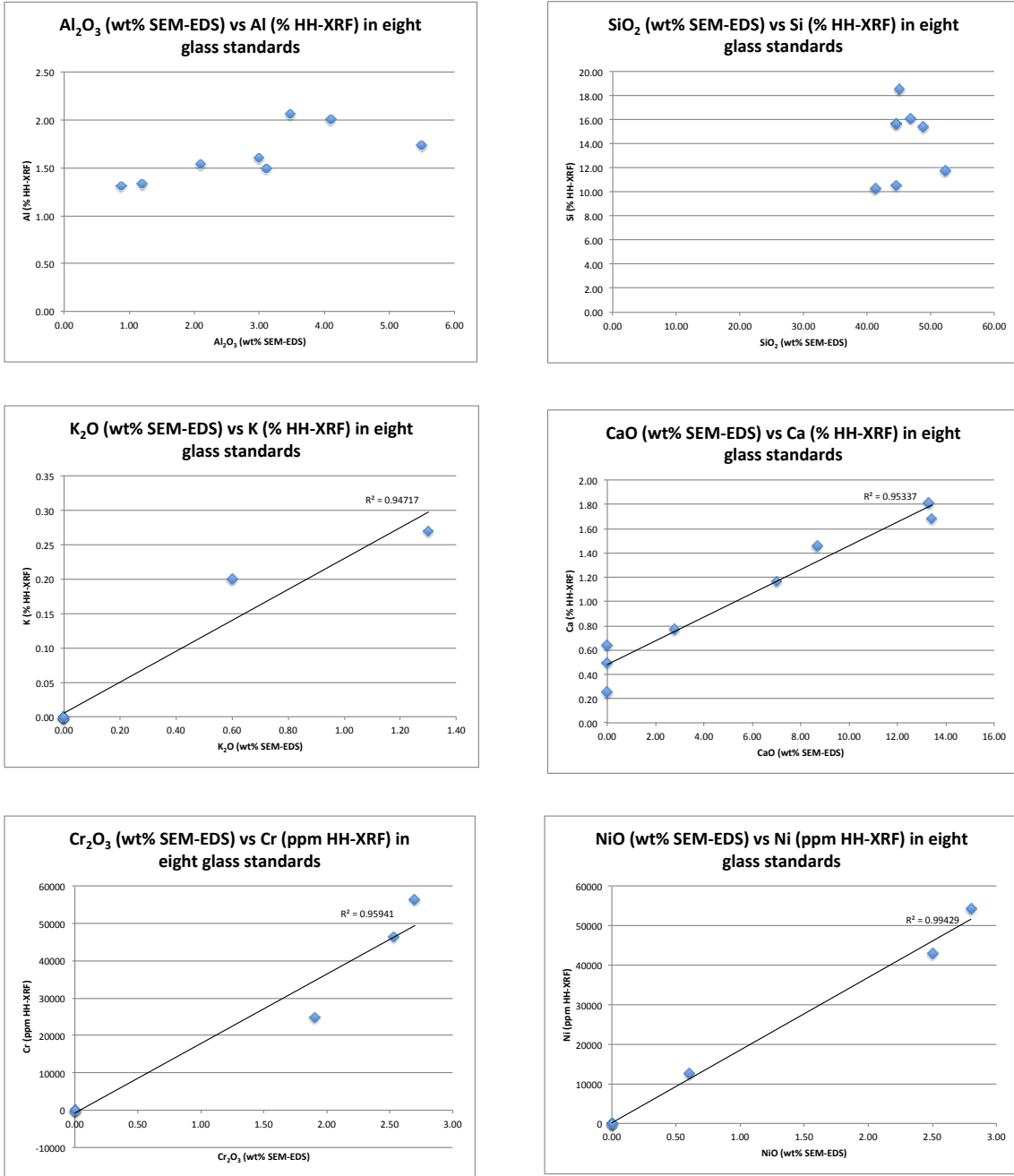


Figure 51 - SEM-EDS (wt% oxide) vs HH-XRF (wt% oxide and ppm) data for eight glass standards

Materials and Methods

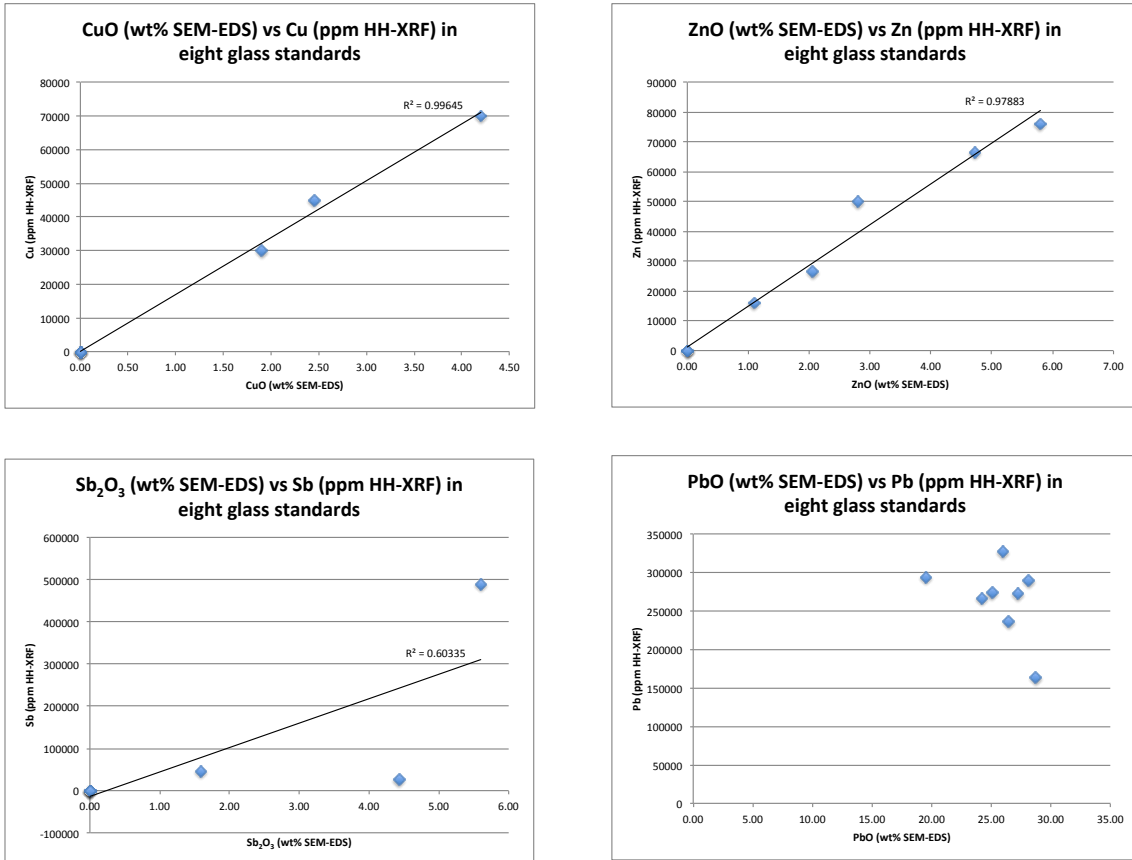


Figure 51 - SEM-EDS (wt% oxide) vs HH-XRF (wt% oxide and ppm) data for eight glass standards

Table 11 - the coefficient of determination (R²) for seven elements of interest in eight glass standards

	K ₂ O	CaO	Cr ₂ O ₃	NiO	CuO	ZnO	Sb ₂ O ₃
R ²	0.95	0.95	0.96	0.99	0.99	0.98	0.60

The relationship between the SEM-EDS data and the values generated by the XRF software is strong (R²>0.9 in most cases). However, some elements present in the glass were not identified by the software (manganese, iron, cobalt, barium, tin and bismuth), and it identified as significant constituents some elements (molybdenum, cadmium) that were not detected by the SEM-EDS. This may be a case of incorrect identification of spectral artefacts, and it demonstrates that the HH-XRF can accurately detect the elements of interest in the glass standards, but that the numbers generated by the Fundamental Parameters calibration programme should not be taken at face value.

4.3.2 X-ray Fluorescence Spectroscopy

In this section, the sources of interference in XRF analysis, and the measures that can mitigate these interferences, are described. A set of standards that are representative of, and matrix-matched to, lead porcelain glazes and enamels have been created, this has been described in Section 4.3.1 and their characterisation by SEM-EDS has been described in Section 4.3.1. The use of these standards to create a calibration procedure for XRF that is optimised for the analysis of British porcelain is beyond the parameters of this research, but it is recommended for the future.

Sources of interference in X-ray Fluorescence Analysis

During XRF analysis of any solid sample, the interaction between the sample matrix and X-rays produces varying degrees of incident beam absorption and scattering, besides the fluorescence that is used to characterise the sample (Jenkins et al, 1995; pp. 7 – 9). With the exception of absorption, all of these will be detected during analysis, and will produce effects on the spectra, known as artefacts, see Table 12.

The processes that produce characteristic peaks and interferences are described in detail, with reference to the production of a characteristic spectrum, in Appendices 3.2 and A.3.3.

Table 12 - common sources of interference in X-ray Fluorescence analysis, and the spectral artefacts produced by these effects

Source of Interference	Spectral artefact(s)
inelastically scattered incident X-ray beam	non-characteristic peaks, increasing in intensity where sample has a low atomic number
elastically scattered incident X-ray beam	peak characteristic of incident X-ray source, e.g. rhodium, which increases in intensity where sample has a low atomic number
Bremsstrahlung ('braking radiation')	continuous background below characteristic peaks

There are also characteristics of the sample that can affect the reliability of XRF data. A flat, smooth, and homogeneous surface is best, because the interaction of the incident X-radiation with the surface of the sample determines the profile of the energy that returns to the detector (Davis et al, 2010).

More problematic is peak overlap, in which two elements present in the sample produce lines that occupy the same region of interest, such as cobalt and iron (Markowicz, 2013). This is a common occurrence in samples of complex composition, or those containing many large atoms that produce many transitions, and therefore many spectral lines (Forster and Grave, 2013). It may be compensated to some extent by relying on the ratios between multiple lines to calculate the intensity of the returning signal, and also by selecting a method that maximises detector resolution (Markowicz, 2013). In modern instruments, overlapping lines are accommodated by simulating the whole spectrum during calibration, whereby peak areas are calculated using a line of best fit.

The effect of the glaze on the incident X-rays and returning fluorescent energy

The excitation of the sample by X-rays occurs on and beneath the surface of the sample, and it is important to consider the extent to which the resulting data represent the entire sample. In the case of British porcelain glazes, which are thin layers overlying a ceramic body, the density and thickness of the glaze must be known, in order to calculate the transmission of energy through the glaze, and therefore the volume of the sample that is being characterised. The calculations in this section aim to determine the proportion of returning fluorescent energy that will be transmitted, up to the greatest peak energy for the elements of interest (i.e. Sn K β = 25 keV). If there is significant transmission of this energy through the glaze, the presence of this element could be attributed either to the glaze or to the underlying ceramic. If there is no transmission of this energy through the glaze, it means that the returning fluorescent energy is attenuated by the glaze before it reaches the detector, and that the fluorescent energy that is captured by the detector represents only the composition of the glaze.

From examination of SEM micrographs, the thickness of porcelain glazes appears to vary within and between objects, depending on the object type and the flatness of the surface. Eight glazes from different porcelain objects and factories were measured using the ImageJ software (version 1.49, © Wayne Rasband, National Institute of Health, USA). The greatest glaze thickness found was 1305 μm , the least thickness was 170 μm , and the mean was found to be 389 μm ($\sigma = 35 \mu\text{m}$).

The composition of porcelain glazes is homogeneous with regard to individual objects, but varies significantly between objects, as discussed in Section 2.3.2. The amount of lead flux present is of particular concern to this section, because is a high-atomic number element, and therefore has the greatest attenuation effect on the X-rays. Therefore, nine theoretical glazes have been calculated for these experiments. They represent three compositions, a high-lead (55.8% PbO), a medium-lead glaze (33.73% PbO), and a low-lead glaze (8.66% PbO), and three thicknesses, representing the thickest (1300 μm), thinnest (170 μm), and mean glaze thickness (390 μm) measured.

The density of these model glazes was obtained from data in Newton and Davidson (1989; p. 15), see Table 13. The composition and the thickness and the density of the glaze, allowed the calculation of the energy transmission of each glaze up to 35 keV, using the online calculation tool created by Henke et al (1993) and hosted by the Lawrence Berkeley, University of California. The resulting transmission values were plotted against the energy for each glaze and thickness, see Figure 52.

Table 13 - density (g/cm^3) and composition (wt% ox.) for three model lead glazes, used in energy transmission calculations

	SiO₂	Al₂O₃	MgO	CaO	PbO	Na₂O	K₂O	SO₃	density
high-lead glaze	37.2	0.9	0.0	0.7	55.8	0.6	4.8	0.0	4.4g/cm ³
medium-lead glaze	52.3	7.0	0.0	0.8	33.7	1.0	2.6	2.1	3.3g/cm ³
low-lead glaze	58.7	11.9	0.3	8.7	8.7	3.0	3.3	0.0	2.6g/cm ³

Materials and Methods

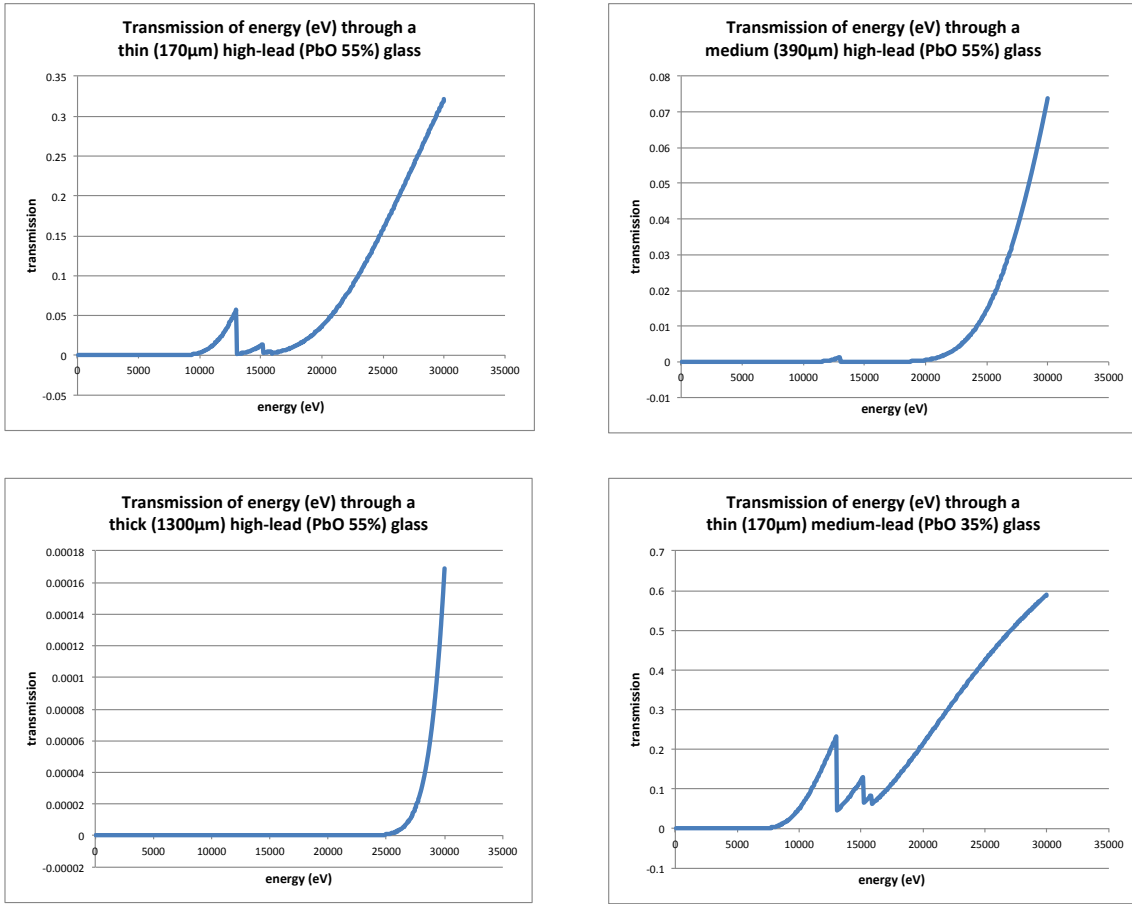
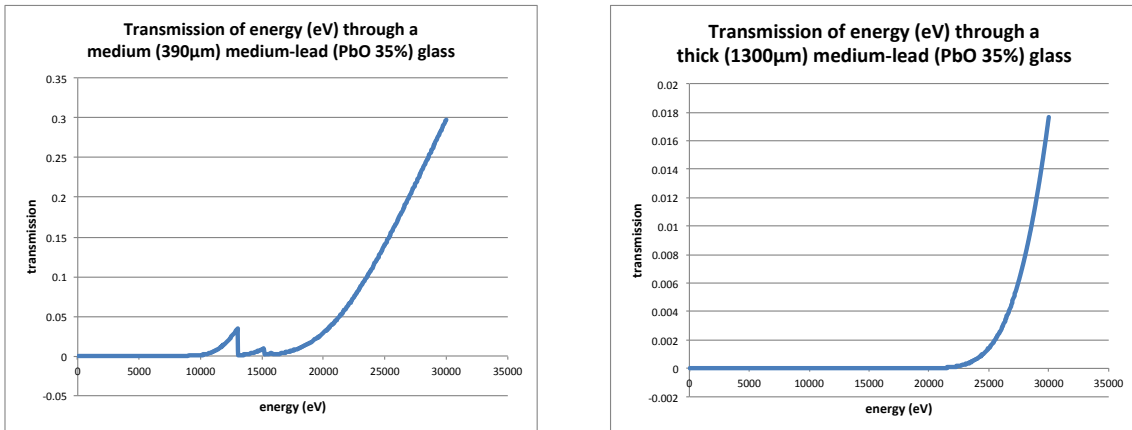


Figure 52 - plots of the proportion of energy (eV) transmitted through nine model lead glazes



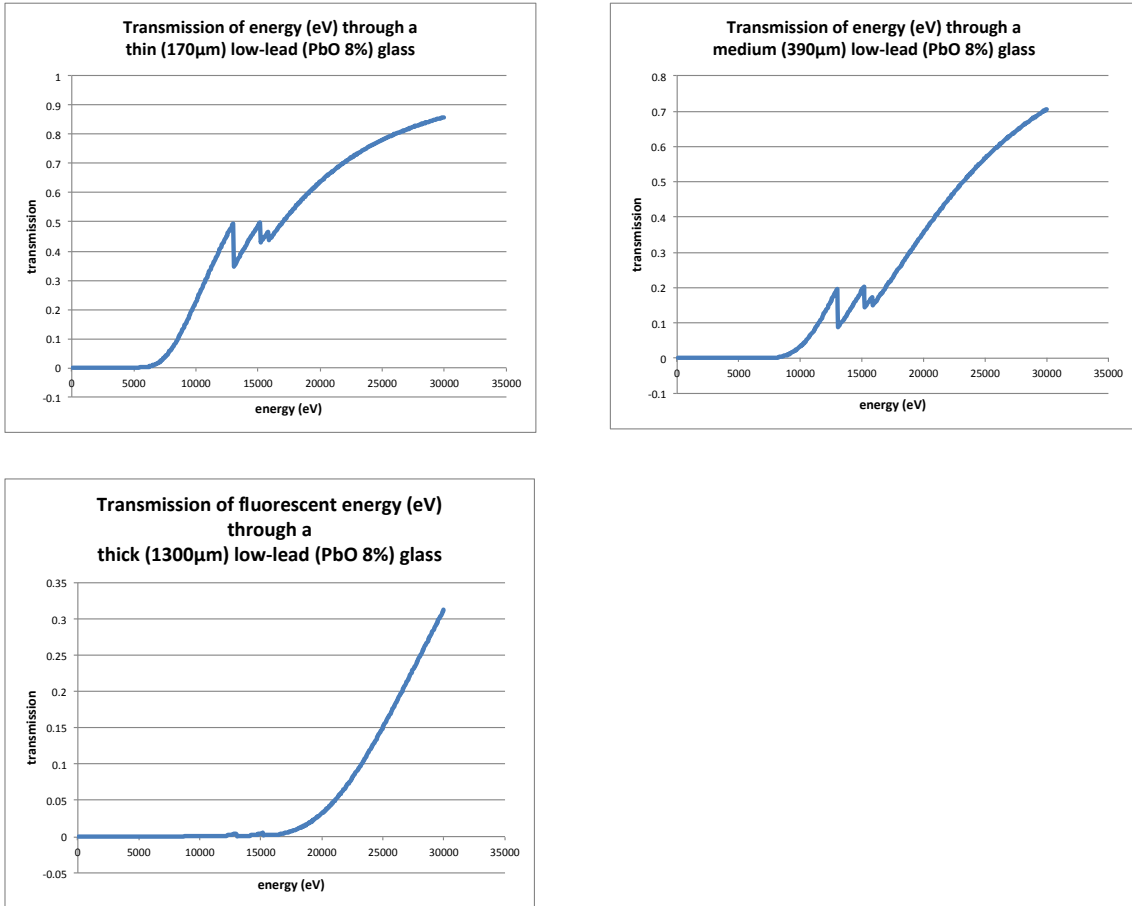


Figure 52 - plots of the proportion of energy (eV) transmitted through nine model lead glazes

It is clear from these plots that the majority of the fluorescent energy is attenuated by the thinnest high-lead (85%) and medium-lead (66%) glazes at 25 keV. The greatest proportion of transmission occurs through low-lead glazes. Through a thin, low-lead glaze, 78% of the fluorescent energy from the highest-energy peak of interest (Sn K β = 25 keV) would be transmitted.

Note the features at ~15 keV are the Pb L absorption edges. Heavy elements are not commonly found in large quantities in porcelain pastes. Lead may be found at $\leq 18\%$ in some frit pastes, but is typically $\leq 8\%$ in frit and magnesian pastes, and is rarely found in phosphatic or SAC porcelains. The majority of the ceramic composition is made up of light elements (sodium, magnesium, aluminium, phosphorus, potassium and calcium), which produce fluorescent energy ≤ 4 keV. The proportion of this energy that would be transmitted through a thin, low-lead glaze is less than 1%, meaning that they would not make a significant contribution to an XRF spectrum.

Furthermore, these calculations do not take into account the impact of attenuation of the incident energy by the lead glaze and by the air gap between the machine head and the sample surface. These effects would also be expected to decrease the proportion of incident energy that arrives at the ceramic body in order to produce excitation.

The thinnest measured porcelain glaze can be considered to be of infinite thickness with regard to the penetration of X-rays at the range of the spectrum occupied by the majority of elements found in British porcelain pastes. Therefore, what is sometimes considered to be a disadvantage in XRF analysis of cultural heritage materials, namely the shallow penetration of X-radiation into the surface of the sample (Tate, 1986), makes it ideal for the analysis of porcelain glazes, which can as a result be analysed and discussed separately from the body of the object. The composition of the glaze should still be taken into account when characterising the composition of an overglaze enamel, for which the thickness is not currently known, and of the underglaze blue pigment, which cannot be analysed separately from the overlying glaze.

Quantification techniques for elemental compositional analyses

Qualitative XRF analysis is used when the aim of the analysis is to identify the elements present, for example, in a sample of unknown composition. The spectral “finger-print” of the sample may be compared with others, in order to characterise and identify the sample; and this method requires a thorough knowledge of the interference effects and resulting spectral artefacts discussed above, in order to avoid erroneously labelling peaks. X-ray lines are labelled according to either the Seigbahn notation, or the more recent IUPAC nomenclature (Jenkins et al, 1991).

Where quantitative data are required, a relationship must be determined between the measured X-ray intensity and the element concentration. This must take into account the contribution of the instrument parameters (voltage, current, X-ray tube anode, detector performance), the heterogeneity of the sample and any interelement effects. Since the instrumental parameters will vary between instruments and analytical settings and the other two factors depend on the type and composition of sample, a new calibration equation must be calculated for each instrument and method and this should be monitored between analyses for drift or contamination (Rousseau, 2002).

The most common method of calibration for this purpose is to use a series of well-characterised standards, which are measured at the same time and under the same conditions as the unknown samples, and the measurements plotted against the known elemental concentration, in order to produce a calibration curve. This is known as the empirical method of calibration (Jenkins et al, 1995; pp. 322 – 323).

Where the impact of matrix effects is negligible, there should be a reasonable fit of the data points to a straight line, and the coefficient of determination should be close to 1 (Danzer and Currie, 1998). In that case, the equation of the line may be used to perform regression analysis, see Equation 1, in order to convert between the XRF measurements and the elemental concentration.

$$y_i = mx_i + c$$

Equation 1 - calculation to relate observed and expected values for standards in an external calibration by linear regression. Where:

y = expected value for analyte i

m = the linear operator, equal to the slope of the line

x = the measured value for analyte i

c = sensitivity, equal to the intercept of the line with the y axis

This method will be reliable only if the standard reference materials used to create the calibration curve are representative of all elements of interest within the samples and contain between an appropriate range of concentrations. Where inadequate standards are available, calculations may be made using other measurements to correct for X-ray absorption, enhancement, and sample heterogeneity (Jenkins et al, 1995). Furthermore, mathematical methods may be used to correct for matrix effects; these are surveyed by Jenkins et al (1995), and in three publications by Rousseau (Rousseau et al, 1996; Rousseau and Boivin, 1998; Rousseau, 2002).

4.3.3 Hand-Held XRF Instrumentation

Field-portable elemental compositional analyses were carried out using an Oxford Instruments X-MET 5100 Hand-Held XRF analyser with a rhodium-anode, and a Silicon Drift Detector (SDD). The analytical methodology used here follows that which was developed by Domoney (2012) for the analysis of porcelain from Meissen and Vincennes-Sèvres. The method is described below, following a brief summary of the Hand-Held XRF instrumentation. This instrument has the form of a Hand-Held gun, see Figure 53; it is controlled through a personal data assistant (PDA) mounted at the back of the body, with which the user can select analytical settings and view spectra or data during and after analysis.

The X-ray excitation energy is emitted through a circular aperture of 8mm diameter (50mm²) in the head of the instrument and controlled by a trigger mounted in the handle. The returning fluorescent and scattered energy is collected by a silicon drift detector adjacent to the X-ray aperture and processed in real-time inside the instrument to produce a spectrum.

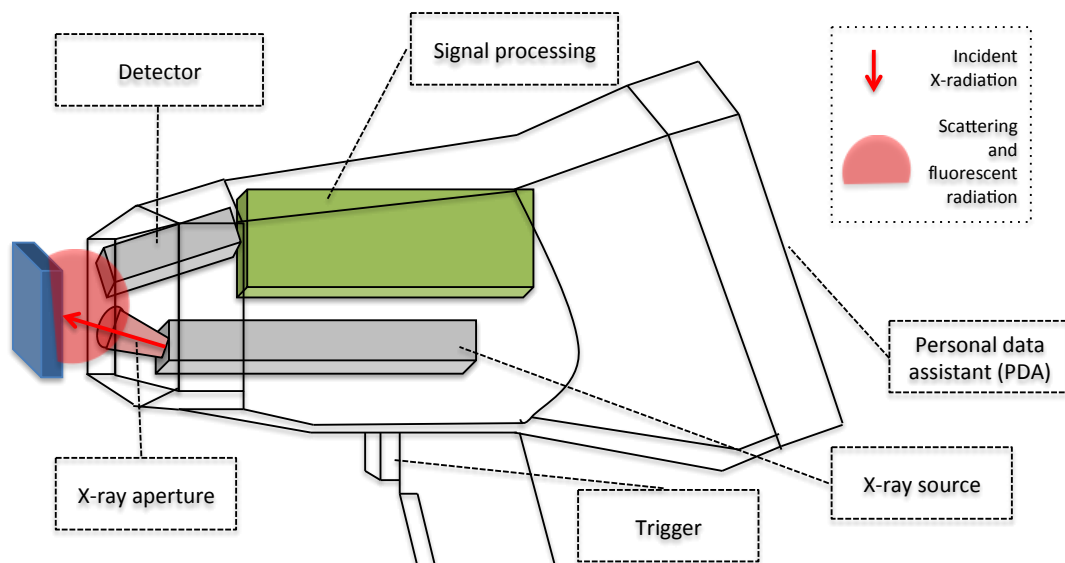


Figure 53 - diagram of Hand-Held XRF system, illustrating the path of the incident X-ray, and scattered and fluorescent radiation.

In developing her method, Domoney carried out a series of experiments on well-characterised glass or soil standards in order to determine the effect of altered conditions on the detection of the elements present in the samples. Acquisition time, aperture coverage, distance between the sample and the instrument head, angle between the sample and the instrument head, and accuracy and precision over repeated analysis were tested, and the optimum conditions were adopted as those for use in the new methodology.

It was found that the optimum acquisition time, in terms of the counts produced, was between 15 and 60 seconds, with no significant difference in mean concentration or standard deviation at 15, 30, or 60 second acquisition times (Domoney, 2012; pp. 96 - 99). It was also found that when the surface of the sample is not flat and flush with the XRF instrument head, lower detector counts, and therefore lesser peak areas in the spectra, result (Domoney, 2012; pp. 104 - 109). This she attributes to the presence of an air gap which attenuate both the incident X-ray energy, and returning fluorescent and scattered energy. The low-energy X-rays produced by low-Z elements are affected more than those of mid- and high-Z elements, resulting in a skewed spectrum.

Both accuracy and precision were found to be very good using the X-MET instrument; detection of elements present at high and low concentrations was representative of the known composition of well-characterised samples, and results were highly repeatable over ten analyses of the same sample under the same analytical conditions (Domoney, 2012; pp. 99 - 104). However, the quantified values provided by the X-MET software were found to be unreliable and the use of software other than the in-built X-MET programme was recommended (Domoney, 2012; p. 104).

Due to the wide range of elements present in Meissen (and indeed British) porcelain glazes and enamels, there was a requirement for analytical settings that would permit the optimum detection of all elements from low-Z elements, such as aluminium and silicon to high-Z elements, such as lead and tin. Domoney therefore recommends that two analyses be made of each area of interest, on every object; one at a low voltage with a higher current, to allow the detection of lighter elements (Al - Cu), see Table 14; and one at a higher voltage, with a low current, to excite heavier elements (Zn - U) (Domoney, 2012; p. 95), see Table 15. These two settings are carried out sequentially by the XRF instrument over a 30 second period; the low-voltage condition is active for 22 seconds, and high voltage condition for 8 seconds. This results in much greater total counts, and therefore peak areas, for the elements obtained under the low-voltage condition. The elements of interest in this research on British porcelain glazes and enamels, and the conditions used for their detection in this methodology are listed in Table 14 and Table 15.

Care was taken when selecting an area for analysis to ensure that the aperture of the X-ray source and detector was fully covered by the area of interest, whether glaze, gilding, or enamel, to ensure that the resulting data are representative of their composition. In analyses of archaeological fragments, dirty or obviously contaminated or weathered areas were avoided. Furthermore, on all objects, flat surfaces were selected in preference to curved or irregular surfaces whenever possible; this provides a more stable platform for the instrument to rest during analysis, and also prevents unpredictable scattering from the surface of the sample (Davis et al, 2010).

A soil standard, Oxford Instruments #3A2, was used to monitor analytical drift. The mean measured (Appendix Table 21) and expected (Appendix Table 22) values for this standard are provided in Appendix A.7, with example spectra (Appendix Figure 41). A pure silica blank was used to identify instrument artefacts, the data (Appendix Table 23) and example spectra (Appendix Figure 42) for which are also in Appendix A.7. These were both analysed at the beginning and end of every session and periodically throughout. The mean data collected from these analyses demonstrate the stability of the instrument, see Table 16.

Table 14 - adapted from Domoney (2012; Table 6.8). Elements detected at low voltage condition peak position and potential overlaps for characteristic lines. Voltage: 15keV; current: 45 μ A; filter: 500 μ m Al

Z	Element	Characteristic lines	Peak position (keV)	Potential overlaps
13	Al	K α	1.49	
		K β	1.56	
14	Si	K α	1.74	Rb L β
		K β	1.84	Sr L α
15	P	K α	1.95	
		K β	2.14	
19	K	K α	3.31	Ag L β
		K β	3.59	Sn L β
20	Ca	K α	3.69	Sn L β , Sb L β
		K β	4.01	Sn L γ
22	Ti	K α	4.51	Ba L α
		K β	4.93	Ba L β
24	Cr	K α	5.42	Ba L γ
		K β	5.95	
25	Mn	K α	5.89	
		K β	6.49	Fe K α
26	Fe	K α	6.39	Mn K β
		K β	7.06	
27	Co	K α	6.93	
		K β	7.56	Ni K α
28	Ni	K α	7.48	Co K β
		K β	8.27	
29	Cu	K α	8.05	
		K β	8.91	

Table 15 - adapted from Domoney (2012; Table 6.8). Elements detected at high voltage condition, peak position and potential overlaps for characteristic lines. Voltage: 45keV; current: 15 μ A; filter: 25 μ m Fe

Z	Element	Characteristic lines	Peak position (keV)			Potential Overlaps	
30	Zn	K α	8.64			Au L α	
		K β	9.57				
33	As	K α	10.54			Pb L α	
		K β	11.73			Au L β	
47	Ag	K α	22.16				
		K β	24.92				
		L α	2.98				
		L β	3.15				K K α
		L γ	3.52				K K β
50	Sn	K α	25.27				
		K β	25.04				
		L α	3.44				K K α
		L β	3.66				K K β
		L γ	4.13				Ca K β
51	Sb	K α	26.36				
		K β	29.73				
		L α	3.60				Sn L β
		L β	3.84				
		L γ	4.35				
56	Ba	K α	32.19				
		K β	36.83				
		L α	4.45				Ti K α
		L β	4.83				Ti K β
		L γ	5.53				
79	Au	L α	9.71	–	9.63	Zn K β	
		L β	11.44	–	12.15	As K β	
		L γ	12.97 – 13.81			Rb K α	
82	Pb	L α	10.45	–	10.55	As K α	
		L β	12.13	–	13.38	Ir L γ , Pt L γ	
		L γ	14.31 – 15.22			Sr K α	
83	Bi	L α	10.73	–	10.84		
		L β	106.43	–	17.22		
		L γ	15.25				

Materials and Methods

Table 16 - analytical stability of Oxford Instruments XMET5100 hand held XRF instrument through time.
Mean data and a single standard deviation from multiple analyses of the 3a2 soil standard.

	Al (K)	Si (K)	K (K)	Ca (K)	Ti (K)	Cr (K)	Fe (K)	Ni (K)	Cu (K)	Zn (K)	Rb (K)	Sr (K)	Zr (K)	Pb (L)
Aug 2013														
μ	336	398	26444	15938	3467	2609	61518	1845	4110	25086	1384	2124	2113	5815
σ	27	103	909	785	145	463	1361	147	157	572	90	46	413	151
%σ	8	26	3	5	4	18	2	8	4	2	7	2	20	3
Sept 2013														
μ	298	475	27196	16275	3541	2248	62805	2017	4104	24981	1405	2147	1559	6045
σ	34	78	623	516	73	490	860	163	57	465	46	45	546	112
%σ	11	16	2	3	2	22	1	8	1	2	3	2	35	2
Feb 2014														
μ	340	407	27340	16346	3496	2096	63160	1954	4237	25276	1415	2156	2051	5935
σ	92	67	628	47	61	392	642	160	51	326	13	83	641	114
%σ	27	17	2	0	2	19	1	8	1	1	1	4	31	2
May 2014														
μ	274	349	27629	16539	3617	2002	63800	1895	4150	25567	1476	2218	1891	6122
σ	54	23	326	281	125	536	1047	184	332	985	38	31	630	167
%σ	20	7	1	2	3	27	2	10	8	4	3	1	33	3
Jan 2015														
μ	350	427	28011	16473	3758	2752	65418	2166	4514	26926	1487	2216	2311	6223
σ	24	11	132	291	64	35	677	94	35	198	36	59	168	16
%σ	7	3	0	2	2	1	1	4	1	1	2	3	7	0
3a2 total														
μ	319	411	27324	16314	3576	2342	63340	1975	4223	25567	1433	2172	1985	6028
σ	32	46	582	234	116	326	1429	124	171	792	46	42	282	159
%σ	10	11	2	1	3	14	2	6	4	3	3	2	14	3

The data having been collected, the spectra are exported as .txt files, which can be viewed using Bruker ARTAX software (Version 7.2, © Bruker Systems), after having undergone conversion through a Text Converter programme created by David Wall, Cranfield University, using using Java 6 Version 1.6.032, see Appendix 3.4. The ARTAX software allows multiple spectra to be opened, and the peaks to be labelled according to the element of which they are characteristic.

Peak overlaps can also potentially cause the compositional data to be inaccurate, because one peak may be enlarged or distorted when another occupies the same region of interest. Common peak overlaps are shown in Table 14 (elements analysed under the 15 keV condition), and Table 15 (elements analysed under the 45 keV condition). Most peak areas are resolved by the ARTAX software, which calculates the accurate peak area data using the ratio between the different characteristic peaks, which is constant. However, the overlap between the iron $K\beta$ and cobalt $K\alpha$ peaks, and the arsenic $K\alpha$ peaks and lead $L\beta$ peaks must be resolved manually using the Region of Interest function in the ARTAX software, see Figure 54.

The software then strips out the background, using a line of best fit determined by the peaks selected by the user. The peak areas were then calculated and the data exported to Microsoft Excel. The peak area data for the contaminants and machine artefacts, derived from analyses of silica blanks, were subtracted from the raw sample data. Finally, to assist in interpreting underglaze blue pigment data, the glaze data from each blue and white object are subtracted from the underglaze blue, see Figure 55. The remaining elements should have been contributed by the blue pigment.

Materials and Methods



Figure 54 - illustration of the Region of Interest selection function in ARTAX software, used in this instance to resolve Fe K β and Co K α peak overlap (left), and Pb L β and As K β peak overlap (right)

The resulting peak area data represent the total counts received by the detector during the live analysis time. They are qualitative, considered in terms of the presence or absence of elements detected, and by peak area ratios where the same elements are present in different proportions.

A	B	C	D	E	F	G	H	I	J	K	L	M	N	O	P	Q	R	S	T	U	V	W	
1	Session	Sample	Factory	Date	Al	Si	P	K	Ca	Ti	Cr	Mn	Fe	Co	Ni	Cu	Zn	As	Sb	Ba	Pb	Bi	
2					119	14665		9703	7178	521			7131	11150	5829	2047		4307				189709	
3	20130919	Bow mg1 gl	Bow	1760s	102	13181		10952	5796	446			2713		1302			5025				196040	
4	20130919	Bow mg1 bl.2013	Bow	1760s	17	-496*	0	-949	1382	75*	0	0	4418*	11150*	5829*	545*	0*	-718*	0*	0	-6331*		
5																							
6		Bow mg1 bl.2011	Bow	12112345@220915_175	321	34336		1155	8179	562			2067	8195	9070	6823	3651					188247	
7	20150121	Bow mg2 gl	Bow	162	12252		6910	7954	609				1918	4795					2551			186758	
8	20150121	Bow mg1 bl.2011	Bow	00/01/00	159	2084*	0	-5755	625	-47*	0	149	3400*	9070*	6821	4*	0*	0*	-2551*	0*	0	1489*	
9																							
10		Bow pl1 bl.2013	Bow	015440@220915_174740	114	14698		15368	5158	641			3217	2991	1987	2600			5093			191703	
11	20130919	Bow pl1 gl	Bow	1760s	90	14934		17340	5392	418			2345		1479			5255				194217	
12	20130919	Bow pl1 bl.2013	Bow	1760s	24	-736*	0	-1972	-334	223*	0	0	972*	2991*	1987*	1112*	0*	0	-162*	0*	0	-2514*	
13																							
14		Bow pl3 bl.2013	Bow	0120748@220915_174740	189	15372		8832	7655	688			8664	7411	5516	1602			4437			194292	
15	20130919	Bow pl3 gl	Bow	1760s	112	16283		22899	8832	366			2076		1570			4624				197173	
16	20130919	Bow pl3 bl.2013	Bow	1760s	77	-911*	0	-14067*	-1177	322*	0	0	4788*	7411*	5516*	32*	0*	0	-187*	0*	0	-2881*	
17																							
18		Bow sb1 bl.2013	Bow	0113883@220915_174943	103	12814		1083	712	443			4013	3344	1223	1417						195907	
19	20130919	Bow sb1 gl	Bow	1750s	62	13455		9053	6515	309			2556		1486			3274				200808	
20	20130919	Bow sb1 bl.2013	Bow	1750s	41	-641*	0	-7970	-5803	134*	0	0	1457*	3344*	1223	-69*	0*	0*	-3274*	0*	0	-4901*	
21																							
22		Bow sb2 bl.2013	Bow	0114317@220915_174740	123	13613		12923	4672	886			4087	6713	5419	1827			4424			196252	
23	20130919	Bow sb2 gl	Bow	1755-57	124	11444		11474	4542	246			2059		1269			4242				190461	
24	20130919	Bow sb2 bl.2013	Bow	1755-57	-1	-2169*	0	-1469	-330	640*	0	0	2046*	6713*	5419*	558*	0*	0	-182*	0*	0	-5791*	
25																							
26		Bow sb3 bl.2013	Bow	0114848@220915_174740	116	13875		9600	5411	439			4910	7588	5755	1833			4372			187320	
27	20130919	Bow sb3 gl	Bow	1760-65	71	11137		10815	6155	633			2476		1955			5679				180539	
28	20130919	Bow sb3 bl.2013	Bow	1760-65	45	2718*	0	-1015	-744	-184*	0	0	2434*	7588*	5755*	578*	0*	0	-182*	0*	0	6820*	
29																							
30		Bow sb4 bl.2013	Bow	0122531@220915_174740	141	11656		10911	3519	491			3931	4808	3563	1335			3713			183959	
31	20130919	Bow sb4 gl	Bow	1770-75	107	10928		9756	3629	424			2032		1126			3596				178753	
32	20130919	Bow sb4 bl.2013	Bow	1770-75	34	728*	0	1155	-110	87*	0	0	1899*	4808*	3563*	209*	0*	0	117*	0*	0	5706*	
33																							
34		Bow sb5 bl.2013	Bow	0123318@220915_174740	100	13876		8421	6064	501			3907	3687	3231	1452			3853			189867	
35	20130919	Bow sb5 gl	Bow	1750-52	15	11668		11842	4343	301			1824		1405			4057				180668	
36	20130919	Bow sb5 bl.2013	Bow	1750-52	85	2208*	0	-3421	1931	200*	0	0	2085*	3687*	3231*	47*	0*	0	-204*	0*	0	9199*	
37																							
38		Bow sb6 bl.2007	Bow	015601@220915_175721	189	20970		1926	20427	8355			2009	14414	8163	2136	12108	641	7503		3805	156063	
39	20140528	BT cp gl	Bovey Tracey		113	21093		15124	20239	7034			1560	10464	8163	2136	1848	10454	8268		3803	163137	
40	20140528	BT cp bl.2013	Bovey Tracey	00/01/00	76	1877*	0	-13198	188	1121*	0	0	449	3950*	8163*	2136*	908	1654*	641	-915*	0*	-7074*	
41																							
42		BT bl.2013	Bovey Tracey	160806@220915_175721	139	23410		1759	19388	6828			2311	13256	7994	1796	1761	11099	676	6943		2593	152408
43	20130919	BT sb1 gl	Bovey Tracey		192	32865		13859	16871	6578			1866	11990				9609	7805		2573	156055	
44	20130919	BT sb1 bl.2013	Bovey Tracey	00/01/00	-53	-9459*	0	-12100	2517	250*	0	0	445	1266*	7594*	1796*	-357	-1490*	676	-862*	0*	20	-3647*
45																							
46		Bow sb7 bl.2013	Bow	0141114@220915_180317	322	19376		1045	3962	619			3126	19328	17171	9382	3837	764				178683	
47	20130919	Cha sb1 gl	Chaffers	c1758	358	20524		16078	4523	566			3021	8677				4718				178835	
48	20130919	Cha sb1 bl.2013	Chaffers	c1758	-36	-1148*	0	-9033	-561	53*	0	0	105	10651*	17171*	9382*	-881*	764*	-211*	0*	0	6828*	
49																							
50		Bow sb8 bl.2013	Bow	0140933@220915_180317	236	17311		1168	5369	566			3072	11795	23639	19946	9446	744				173361	
51	20130919	Cha sb1 gl	Chaffers	c1758	276	19093		14350	5374	542			3105	9908				7761	1113			175872	
52	20130919	Cha sb1 bl.2013	Chaffers	c1758	-40	-1782*	0	-13182	-105	24*	0	0	-33	3887*	23639*	19946*	1685	-369*	0*	0*	0*	-4511*	

Figure 55 - subtraction of glaze data from underglaze blue decorated areas using Microsoft Excel for Mac 2011 ©2010 Microsoft Corporation

4.3.4 Spectrophotometry

The colorimetric analyses were carried out using a Konica Minolta CM-700d Hand-Held spectrophotometer, which measures reflected light. Like the X-ray spectrometers, this instrument comprises an energy source, in this case, visible light (400 – 700 nm), which is filtered and directed to the sample, see Figure 56. The light source is calibrated at the beginning of each session using a white plate and a black plate, so that the intensity ranges at each wavelength, or wavelength region, of the incident light is characterised, and any contamination by the instrument or drift over time can be included in the software calculations. The reflected and scattered energy is then detected at the sample surface, producing a measurement of the difference between the initial and reflected energy.

This process is described in greater detail in Appendix A.4. Selected specifications and analytical conditions are shown in Table 17.

Table 17 - analytical conditions of Konica Minolta CM-700d Hand-Held spectrophotometer

Illumination/viewing system	di:8°, de:8° selectable SCI (specular component included) and/or SCE (specular component excluded) measurement
Detector	Silicon photodiode array (dual 36-element)
Spectral separation device	Diffraction grating
Wavelength range	400 nm – 700 nm
Wavelength pitch	10nm
Light source	Pulsed xenon lamp (with UV cut filter)
Measurement time	Approx. 1 second
Measurement cycle	10 x readings per spot, 3 x spots per object
Repeatability (quoted by manufacturer from trials using calibration plate)	Spectral reflectance $\sigma = <0.1\%$ Chromaticity value $\sigma = < \delta E^*_{ab} 0.04$
Colour space	L*a*b* (CIE1976)
Colour difference formula	δE^*_{ab} (CIE1976)

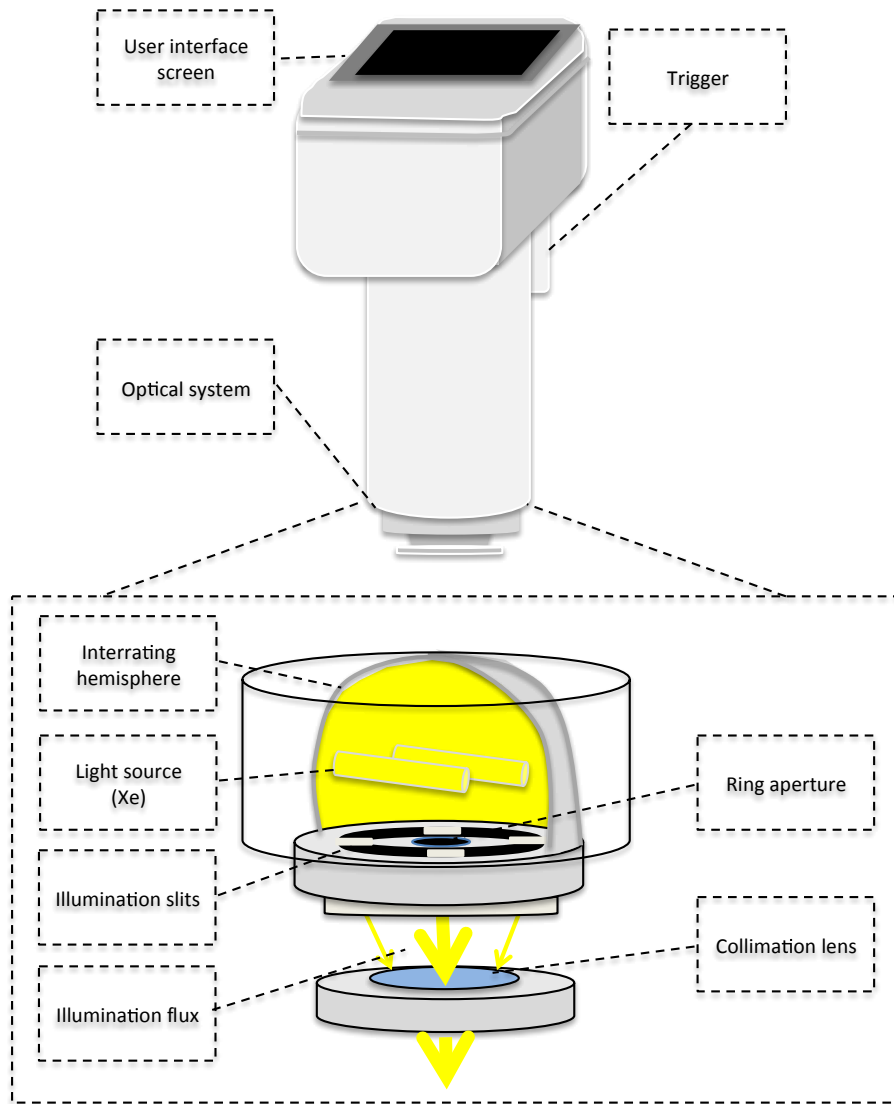


Figure 56 - diagram of the Konica Minolta CM-700d Hand-Held spectrophotometer, and its optical system

The difference between hue and brightness of the original light and the reflected light enables the software to calculate the hue and brightness of the sample. The hue and brightness of the sample are reported using the L*a*b system, see Figure 57 and Appendix A.4, and these can be plotted to demonstrate the position of the samples on the L*a*b colour-space, and also the extent of inter-sample variation.

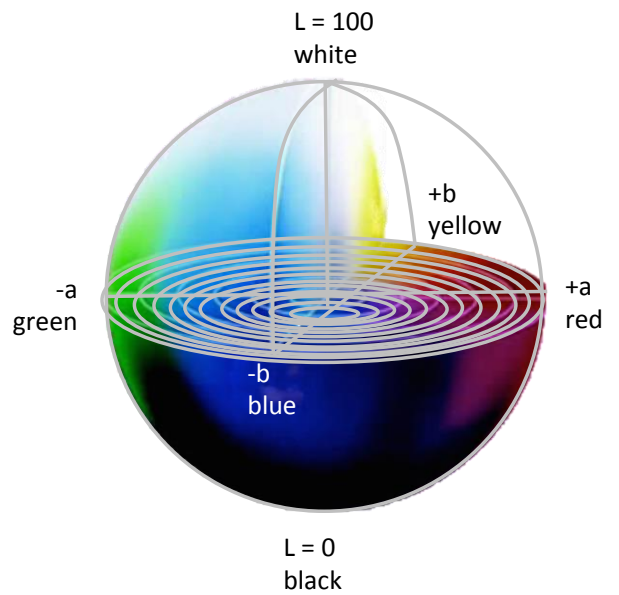


Figure 57 - Commission Internationale de l'Eclairage (CIE) $L^*a^*b^*$ colour space, showing the axes upon which measured colour values are plotted

For this research, in order to keep conditions as stable as possible between analyses, objects with large flat areas of accessible glaze, such as plates and dishes, were chosen in preference to small, highly-curved or irregularly-shaped objects, such as teabowls or figures. Such objects also tend to be thicker, and therefore less translucent, which mitigates the effect of transmitted light. Furthermore, the analytical area being a circle of 7 mm^2 , a glazed spot of at least that size, which was free of enamel and gilding, was required on each object. Three spots were analysed on glazed areas of each sample, in order to determine the variation in colour across the surface of the object. The spectrophotometer obtains ten measurements on each spot during one analytical run, and presents the result as a mean value with a standard deviation, which represents the machine error. The result for each object was determined by calculating the mean of the three analyses and the standard deviation represents both machine error, and sample heterogeneity.

4.3.5 Laser Ablation Inductively Coupled Plasma Mass Spectroscopy

Trace elemental compositional analysis was carried out using the Thermo Electron Corporation XSERIES 2 quadrupole ICP-MS with New Wave Research Q-switched Nd:YAG 213nm laser ablation sampling system, at the Cranfield Forensic Institute (Cranfield University). The principal advantages to using ICPMS are the wide range of elements that may be detected simultaneously (Li - U, with some exceptions), and the very low limits of detection at which they may be quantified accurately (better than 10ppm in most cases) (Hoffman et al, 1996; p. 32). This technique has been selected for use in developing this method, because it is micro-destructive, meaning that, although a small amount of material is removed and destroyed during analysis, the ablation crater is typically <100µm in diameter, and therefore virtually invisible to the naked eye.

The laser ablation sampling system is a relatively recent development in elemental compositional analysis, which is now used frequently in tandem with ICPMS for the analysis of archaeological samples (Gratuze, 1999; Speakman and Neff, 2005; Shortland et al, 2007; Dussubieux et al, 2009). It is chosen here in preference over solution sample introduction methods, because the amount of sample required is smaller (typically much less than 1mg, as opposed to 10-500mg that can be required to create a solution), and the laser allows a high degree of precision in selecting an area for sampling. The user having selected an area for analysis optically, the interaction between the laser and the sample surface causes a portion of material to be ablated from the sample; the particulate material is then removed using a carrier gas, see Figure 58. This gas-sample aerosol can then be introduced directly to the ICP torch.

Materials and Methods

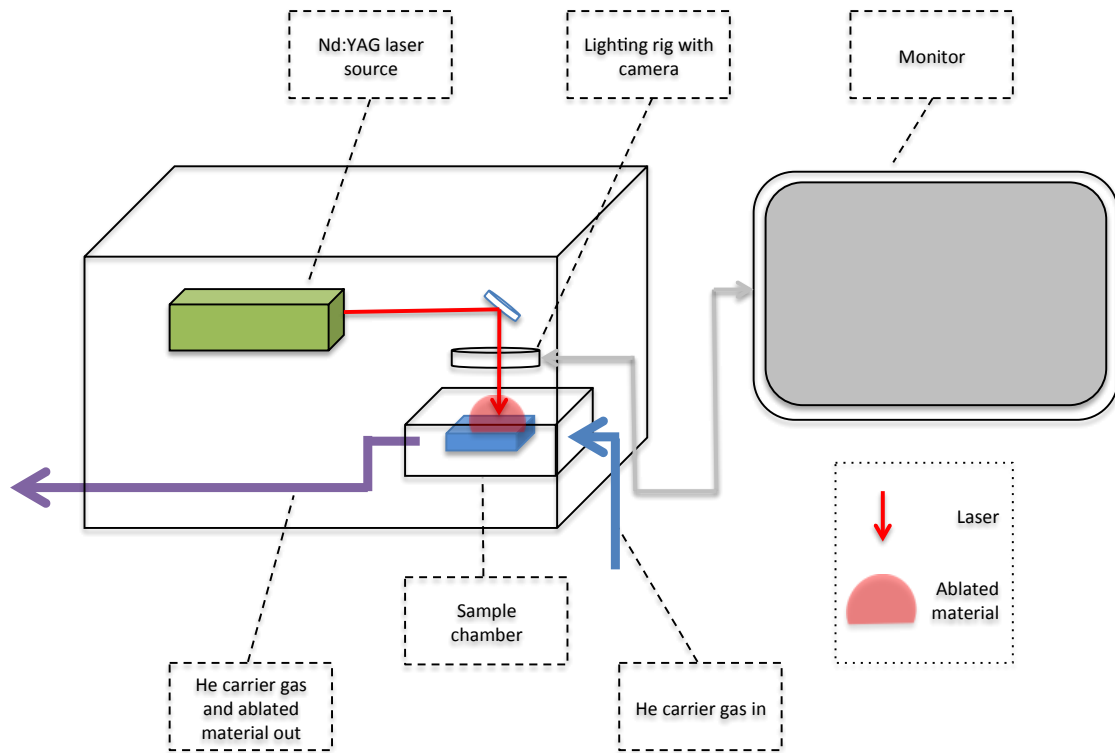


Figure 58 - diagram of the laser ablation sampling system used in this research, showing the path of the carrier gas (He) and ablated material.

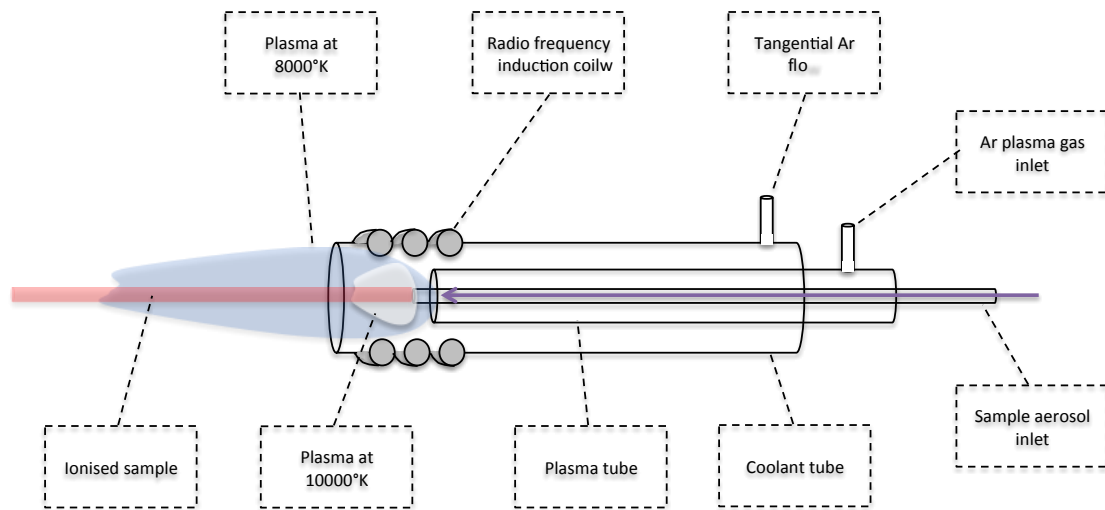


Figure 59 - diagram of an Inductively Coupled Plasma torch, illustrating the path of the ablated sample material and carrier gas (Ar).

In the ICPMS system, the sample is vaporized, atomized and ionised by a high-temperature inductively-coupled plasma torch (ICP), see Figure 59. The sample is then introduced to the mass-spectrometer, see Figure 60, where the ions are separated by their mass to charge ratio (m/Q), striking the detector at the far end of the mass spectrometer.

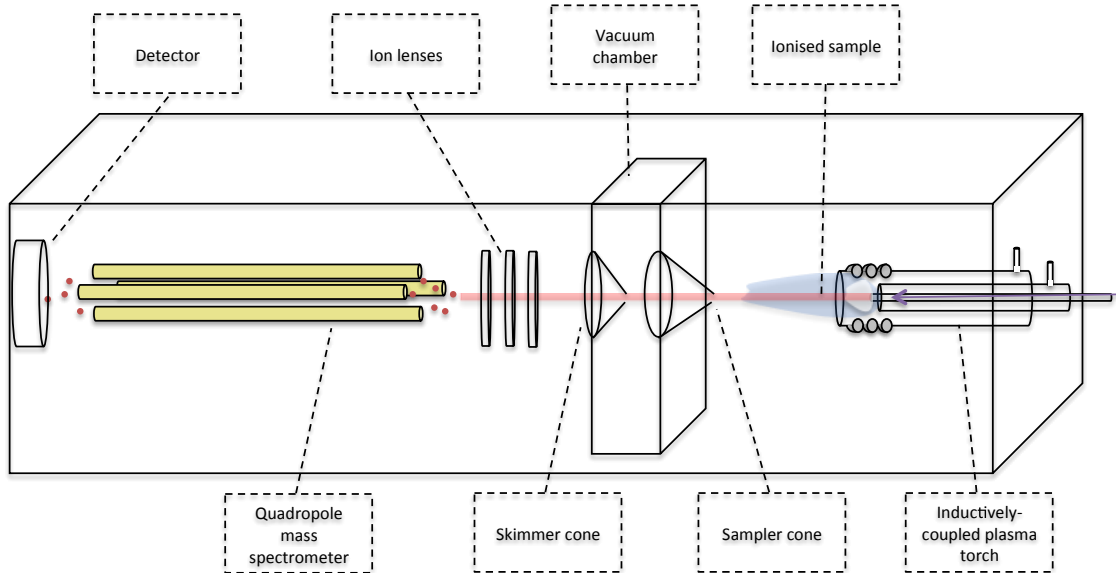


Figure 60 - diagram of an Inductively Coupled Plasma Quadrupole Mass Spectrometer, illustrating the path of the ionised sample from the torch to the detector.

Different types of mass spectrometer achieve this separation in different ways; the system that is employed in this research is a quadrupole mass spectrometer (Q-MS), which separates the ions by oscillating the energy level of the radio frequency field between the four poles, causing selected ions to become stabilised or destabilised in their flight, depending on their m/Q ratio. The result is that destabilized ions reach the detector later than ions that had a stable flight. This process is described in greater detail in Appendix A.2.3.

The detector activity is rendered as a spectrum, with the m/Q ratio on the x-axis, and the relative intensity on the y-axis. The user, with the assistance of the instrument software, can then calibrate the data using internal and external standards to relate the m/Q ratio to elements, and the relative intensity to concentration.

Analytical settings were selected with reference to the literature, and follow the methodology developed by Giannini (2015) for the analysis of Chinese porcelain. The laser ablation settings were selected to produce a representative sample of ablated material, while minimizing the amount of damage to the sample surface, see Table 18. Although the wavelength of the laser is fixed by the manufacturers (213nm), and therefore could not be experimentally altered for this research, this wavelength has been found to produce good ablation for matrices including ceramic and glass, with relatively little damage to the area surrounding the ablation crater (Jackson, 2001). Similarly, the pulsed energy output (2ns at 10Hz) is an innovation that has been found to stabilise the path of the laser beam, resulting in greater accuracy, and therefore greater sampling efficiency. Furthermore, a laser beam composed of short pulses of low-wavelength energy have been found to be the most effective combination for reducing laser-induced elemental fractionation (Russo et al, 2002). Fractionation, and other sources of interference that might be expected to be encountered in LA-ICPMS analysis of ceramic and vitreous, are described in Appendix A.2.4.

Table 18 - analytical settings used in the laser ablation of porcelain samples

Laser Ablation system New Wave Research Q-switched Nd:YAG	Analytical settings
Wavelength (nm)	213
Ablation mode	spot (80 µm)
Pulse time (ns)	2
Energy (mJ)	0.42
Energy density (J/mm)	>20
Pulse repetition rate (Hz)	10
He carrier gas flow rate (ml/ L/min ⁻²)	500

The spot ablation mode was used in order to target small areas, such as the glaze in cross-section, and multiple analyses were carried out on each sample to quantify, and to mitigate, the effect of inhomogeneity. This was expected to be particularly the case in the analysis of ceramic bodies, which are composed of mineral phases that may occupy most or all of than the analytical area (80 μ m diameter).

The ICP-MS settings were selected to allow the detection of a wide range of elements of interest and to mitigate the effects of spectral interferences and physical interferences, see Appendix A.2.4, and Table 19. The nebulizer gas flow, and the radiofrequency power of the plasma were both set to balance the effect of argon-based polyatomic interferences that occur at the high plasma temperature setting, with the formation of rare earth oxides, which can occur at low gas flow and low plasma temperatures. A tuning point was selected on the NIST 612 reference glass, and the settings tuned with reference to the analytical signal, to produce ratios of ThO⁺/Th⁺ <0.02, and CeO⁺/Ce⁺ <0.2.

An important setting of the quadrupole MS is the length of time for which any given radiofrequency/direct current ratio of the poles is held stable for the acquisition of data from that setting (called the dwell time), and the number of sweeps performed on each area of interest within the total acquisition time. Peak hopping mode allows data to be collected from only the areas in the spectrum that have been specified by the user. The acquisition time is limited by the duration of the laser ablation sampling; too long a sampling event and fractionation will be caused by the increasing depth of the ablation crater (Russo et al, 2002).

However, the integration time must be sufficiently long to characterize thoroughly the detector response at each rf/dc ratio. If this is too short, then the integration time will be insufficient to achieve acceptable peak resolution, and large errors will result (Hoffman et al, 1996; pp. 158 - 159). In this research, a longer total acquisition time was used (50 - 60 seconds), allowing between 15 - 20 sweeps of the selected peaks with 20 - 50 milliseconds dwell time at each peak, in order to obtain the greatest possible peak resolution.

The increased risk of fractionation during laser ablation was addressed by dividing the total acquisition time into three sampling events, so that a mean might be taken, and the standard deviation used to determine whether excessive fractionation had taken place, during the data processing stage.

Table 19 - analytical settings used for the ICPMS analysis of porcelain samples

Inductively Coupled Plasma Quadropole Mass Spectrometer Thermo Electron Corporation XSERIES 2	Analytical settings
RF power (W)	1430 – 1470
Ar coolant gas flow rate (L/min ⁻¹)	15
Ar auxiliary gas flow rate (L/min ⁻¹)	0.9
Ar nebulizer gas flow rate (L/min ⁻¹)	0.8 – 1.2
Extraction (V)	-720/750
Detector mode	counting and analogue mode
Acquisition mode	peak hopping
Channel per mass	1
Channel spacing	0.02
Dwell time (ms)	20 – 50
Sweeps	15 – 20
Total acquisition time (s)	50 – 60
Sampling events	3
Replicates per sample	3

The samples that were used in this study were received pre-mounted in polished SEM blocks in cross-section. Six points were analysed on each sample; three on the body, and three on the glaze, in order to minimise the impact of sample heterogeneity. Helium was used as the carrier gas, to transport the ablated material to the ICP torch, and argon was the plasma gas. During each analytical run, at fixed intervals, a measurement was carried out without the laser firing, in order to provide a “blank” signal for calibration.

Calibration of the data was carried out by sum normalization of the 49 elements measured, based on their corresponding oxides; the process follows that described by Van Elteren (2009) and used successfully by Giannini (2015) in the analysis of Chinese porcelain pastes and glazes. It is described in detail in Appendix A.2.5. This method relied on matrix-matched standards for external calibration using the empirical method. The standards used were National Institute of Standards and Technology (NIST) glass standard 612, NIST 610, and Corning Museum of Glass glass standard A, because these are matrix-matched to the porcelain glaze, and similar to the vitrified silicious matrix that comprises the greatest part of the porcelain paste. Furthermore, they contain all or most of the elements of interest in the sample at different levels, enabling an accurate calibration. The expected and measured values for these standards throughout the analysis carried out in this research are given in the LA-ICPMS results chapter, Table 42.

4.4 Summary and conclusions

The materials used in this research have been selected to represent the contexts in which British porcelain is commonly encountered and studied; intact objects in museums and private collections, and sherds or wasters in archaeological contexts associated with domestic refuse or factory sites.

In the studies of intact objects, a prolific and longstanding factory, Worcester, was selected for detailed characterisation, particularly with regard to changes that occur through time in the composition of overglaze polychrome enamels. Glazed objects with underglaze blue decoration have also been selected from fifteen contemporary factories, in order to assess the extent of inter-factory variation.

Archaeological sherds have been selected to investigate the applicability of the methodology for characterising fragmented material that may have been subject to taphonomic processes in the ground. A further collection of sherds and samples was made available for invasive sampling and micro-destructive analysis, and these have also been selected to check the comparability of results between techniques.

Analytical techniques have been chosen with reference to the literature; the aim is to evaluate a range of different types of data, each of which can illustrate a different aspect of the sample set. Priority will be given to techniques that can fulfil the requirements of non-invasive analysis, and data that can characterise and reliably distinguish objects of British porcelain. The non-invasive techniques, spectrophotometry and XRF spectroscopy have been chosen. Spectrophotometry has not been used, to date, in any published study on British porcelain, and it is hoped that this will be effective in quantifying the differences of colour that some connoisseurs describe between porcelain from different factories and periods.

A method for Hand-Held XRF analysis of porcelain has been developed by Domoney (2012), and is here tested to assess its effectiveness for use on British porcelain. To test this method, fully-quantitative elemental compositional data will be provided for comparison by SEM-EDS/WDS.

A study is to be carried out to assess the effectiveness trace elemental compositional data from LA-ICPMS, a technique that has been growing in importance in the field of archaeological science.

The result of these analyses will be a large volume of data of different types, gained through non-destructive and minimally-destructive techniques. These data will be studied alongside existing scientific data and historical information about the British porcelain industry. It will be assessed the extent to which the data contribute to the research questions selected for this study, namely quantifying inter-factory and intra-factory variation to assist in provenancing studies.

5 Results I: non-invasive analytical techniques

5.1 Introduction

In this chapter, the results of analysis by two non-invasive analytical techniques are presented. The elemental compositional technique XRF is first tested against ten well-characterised porcelain sherds. Both techniques are used to analyse a set of intact porcelain objects that have a reliable provenance and unknown composition, in order to assess the extent to which the technique can characterise the samples and inter-sample variation to further the main aims of the project.

5.2 Hand-Held X-ray Fluorescence Spectroscopy

Field-portable elemental compositional analysis was carried out by Hand-Held X-ray Fluorescence Spectroscopy (HH-XRF), in order to determine the effectiveness of this method for use on intact objects and also archaeological sherds of British porcelain that cannot be sampled or brought to the laboratory for analysis. The data considered here are qualitative; that is, they are characterised by the presence or absence of elements, and analyses are compared using the ratios between the peak areas of elements common to all. The raw data and example spectra are provided in Appendix A.7.

5.2.1 Methodological test

Ten porcelain sherds, which have been discussed in Section 4.2.3, were analysed using the analytical methodology developed by Domoney (2012). The processed data are presented, see Table 20, and then plotted against the published fully-quantitative data, see Figure 61, from SEM-EDS or SEM-WDS. The raw total counts data (Appendix Table 20) and example spectra (Appendix Figure 30 to Appendix Figure 40) are provided in Appendix A.7.

Results I: non-invasive techniques

Table 20 - peak area data from Hand-Held XRF analysis of eight porcelain glazes, obtained under low-voltage (15keV) and high-voltage (45keV) conditions

	15kev									45kev			
	Al (K) ^a	Si (K)	K (K)	Ca (K)	Ti (K)	Mn (K)	Fe (K)	Cu (K)	Zn (K)	Fe (K)	Cu (K)	Zn (K)	Pb (L)
CY11 μ	517	22734	13558	9327	977	1815	10755	1289	1548	1217	177	327	146041
σ	35	2056	975	632	123	133	727	174	84	43	26	45	5699
% σ	7	9	7	7	13	7	7	13	5	4	15	14	4
CY12 μ	700	17530	9007	4456	466	1253	4327	1945	0	435	298	0	171196
σ	99	2835	608	344	30	24	470	215	0	30	4	0	7333
% σ	14	16	7	8	7	2	11	11	-	7	1	-	4
CY5 μ	1019	25924	14709	4570	482	1317	5164	1842	0	446	268	0	178859
σ	90	401	615	332	17	63	81	102	0	24	13	0	1285
% σ	9	2	4	7	4	5	2	6	-	5	5	-	1
CY6 μ	551	19402	7041	6189	746	1887	11105	3054	1371	1038	514	507	154897
σ	102	2649	1429	679	123	234	3941	233	169	346	58	469	12418
% σ	19	14	20	11	16	12	35	8	12	33	11	92	8
CY9 μ	737	25006	13709	6178	644	1697	9191	1667	1085	981	241	177	165371
σ	62	2553	202	256	19	128	322	287	107	23	26	34	2474
% σ	8	10	1	4	3	8	4	17	10	2	11	19	1
LP3 μ	433	16024	8946	6428	495	1954	5284	1507	0	506	172	0	194033
σ	23	117	69	82	78	104	100	112	0	24	23	0	404
% σ	5	1	1	1	16	5	2	7	-	5	14	-	0
W12 μ	364	15553	10796	10181	1324	1982	7085	1273	7228	840	157	0	156264
σ	73	1084	675	927	60	70	173	61	1230	41	40	0	10691
% σ	20	7	6	9	5	4	2	5	17	5	26	-	7
W15 μ	803	16886	3658	2280	6184	11558	7809	1326	935	939	134	0	192047
σ	72	369	54	16	67	576	207	219	55	37	34	0	1254
% σ	9	2	1	1	1	5	3	17	6	4	26	-	1

^a the letter in parentheses denotes the spectral line from which the peak area was calculated, lines are generally K α except to avoid peak area overlap, and Pb L α

Results I: non-invasive techniques

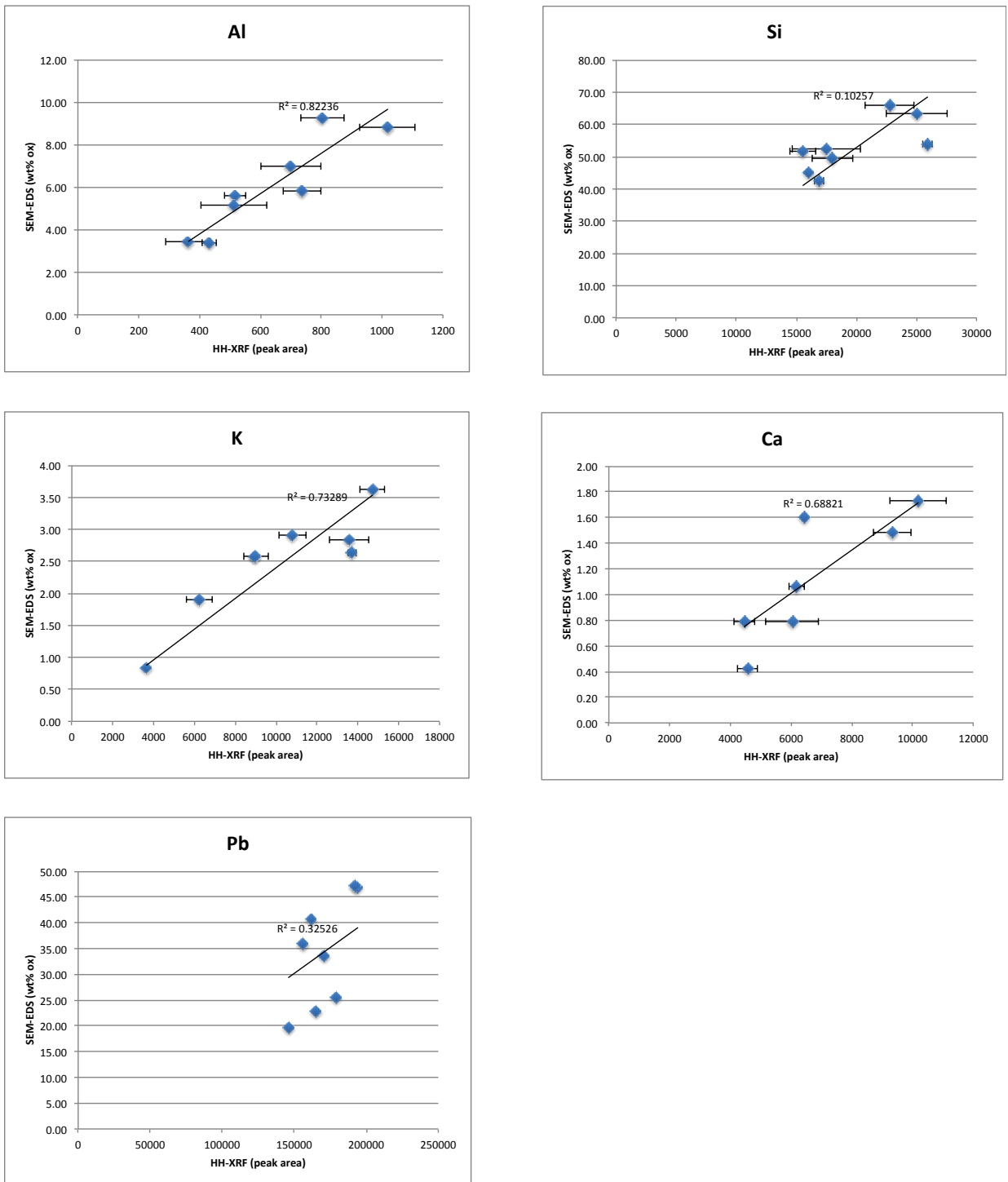


Figure 61 - plots of the Hand-Held XRF data (peak area) against the SEM-EDS/WDS data (in weight percent as oxides) for eight of the ten porcelain glazes for which fully quantitative data were available

These plots show that there is a fairly strong correlation between the HH-XRF and SEM-EDS/WDS data for aluminium and potassium, see Figure 61 and Table 21, in spite of the large standard deviation in some of these analyses. The relationship between the two data sets for silica and calcium is weaker ($R^2 < 0.5$).

The interpretation of lead is more complicated, due to the effect of detector saturation. Problems with quantifying lead in XRF data have been discussed by Domoney (2012, p. 193), when analysing high-lead glazes and enamels on European porcelains. She identifies a level of lead in her samples (~38% PbO) beyond which the instrument cannot distinguish any increase in the lead content, because the volume of returning fluorescent energy produced by the lead atoms saturate the detector. This causes the trend line to plateau, as the axis bearing the quantitative lead value continues to increase, and the counts registered by the XRF detector remain static, see Figure 62.

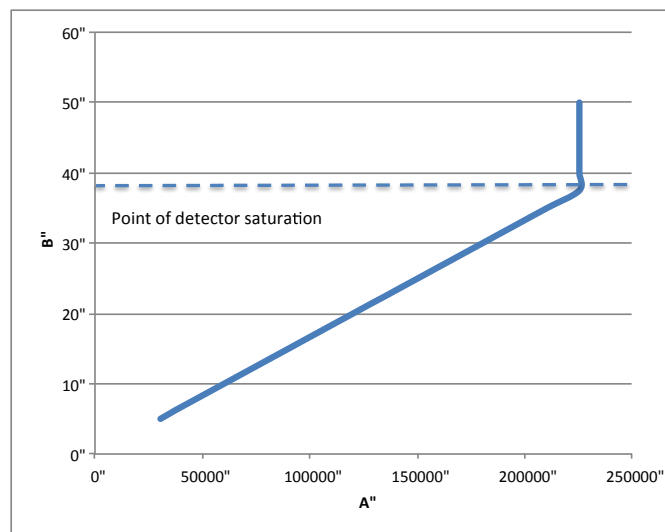


Figure 62 - plot of the detector saturation effect in spectroscopic analysis. Up to the point of saturation, the detector response (A) increases proportionally with the amount of the element in the sample (B). Beyond the point of saturation, as B increases, A remains static.

As a result, there appear to be two clusters of XRF data, which have a different relationship to the quantitative data. One group is formed by those samples, whose glaze according to the SEM-EDS/WDS data contains 19-25% PbO, and one with $\geq 33\%$ PbO.

The relatively low-lead group correlate well with the XRF data ($R^2 = 0.94$), see Figure 63 and Table 21. However, between 25% and 33% the detector reaches the point of saturation by the large volume of returning fluorescent energy, and as a result, the number of counts ceases to increase.

Table 21 - coefficient of determination (R^2) for the relationship between the Hand-Held XRF and SEM-EDS/WDS data for eight porcelain glazes

Element	Al	Si	K	Ca	Pb	Pb (low-PbO group)
R^2	0.82	0.5	0.81	0.81	0.37	0.94

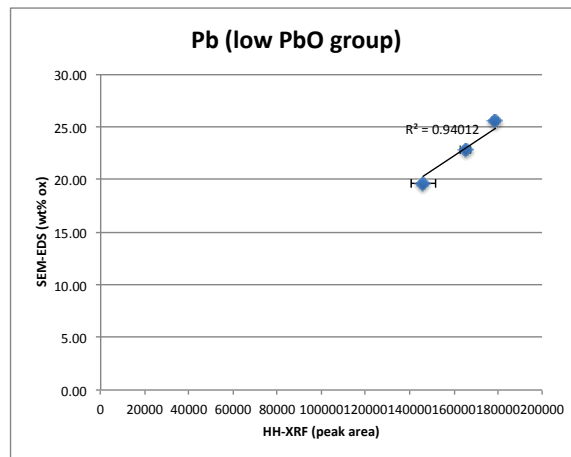


Figure 63 - plots of SEM-EDS/WDS data (in % as oxides) against the Hand-Held XRF data (peak area) for Pb in the low PbO group

The analytical methodology here developed agrees with that of Domoney (2012), in recommending the use of two sets of analytical conditions for each area of interest; a low-voltage condition to collect light elements, and a high-voltage condition to collect heavier elements. It is evident that, under the high voltage condition, the proportion of detector deadtime is much greater than under the low voltage condition, which may affect the reliability of the resulting data. To investigate the extent to which this applies to the other elements that may be quantified under the high or the low voltage condition, the elements detected under the low-voltage condition were plotted against the same elements collected from the same spot under the high-voltage condition, see Figure 64.

Results I: non-invasive techniques

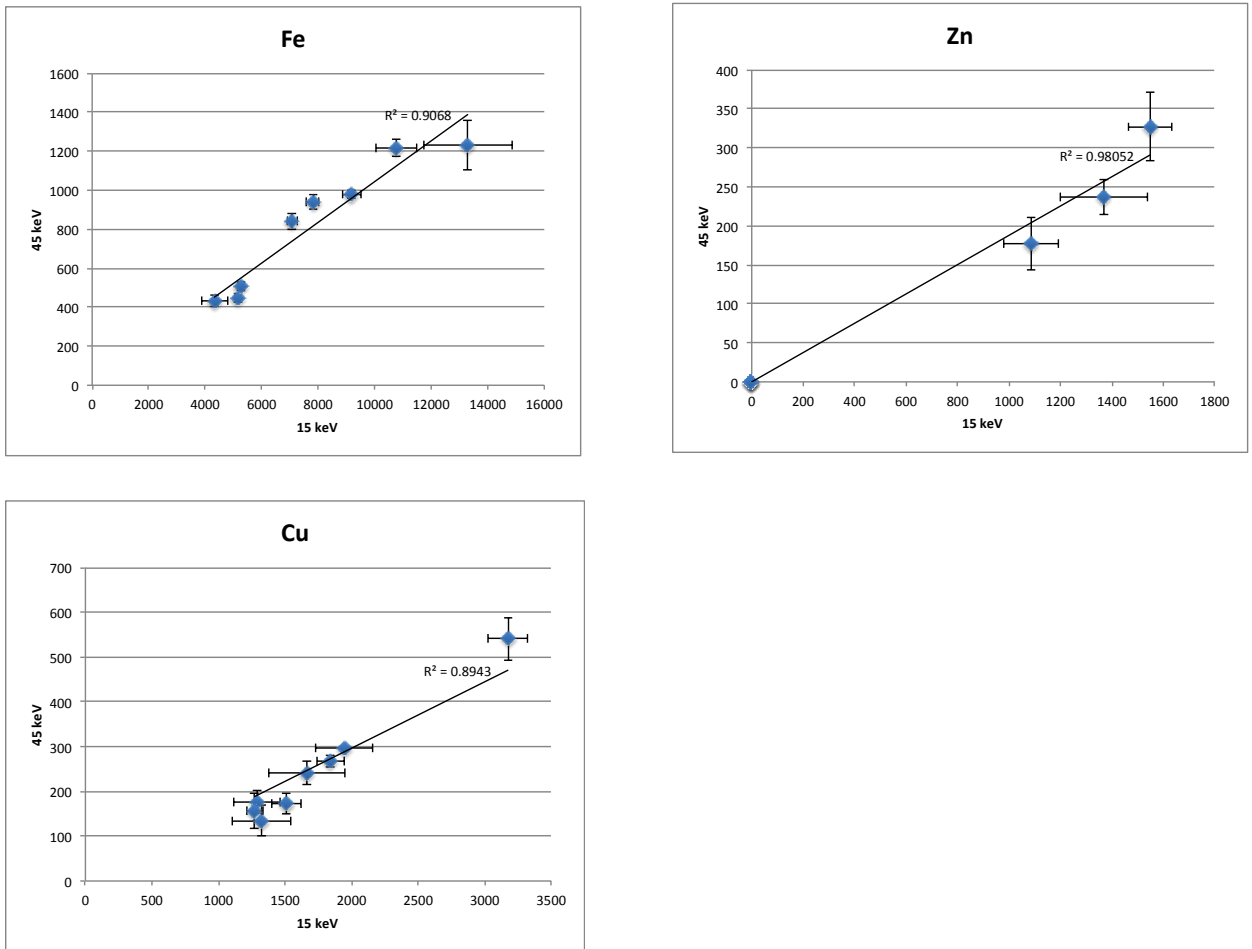


Figure 64 - plots of hand held XRF data collected under a low-voltage condition (15keV) against data from the same spot collected under a high-voltage condition (45keV) for ten porcelain glazes

Table 22 - coefficient of determination (R^2) for the relationship between Hand-Held XRF data gathered under a low-voltage condition and a high-voltage condition

Element	Fe	Cu	Zn
R^2	0.91	0.98	0.89

In general, there is a linear relationship between the two data sets for all elements, see Table 22. This is demonstrated more clearly in the elements that are present in higher concentrations, Fe and Cu, rather than Zn, because they are further from the limit of detection of the instrument, and standard deviations are generally smaller.

For the four elements shown here, the peak area collected is significantly greater under the low-voltage condition, and standard deviations are generally less, relative to the high-voltage condition. This is due to the greater analytical time (22 seconds) under the low voltage condition, relative to that of the high voltage condition (8 seconds). As a result, the limit of detection appears to be lower in the low-voltage condition, as Mn and Zn that are present in the sample at very low levels are detected under the 15keV condition, and not detected under the 45keV condition. Data from the low-voltage condition will therefore be used to determine the concentration of these mid-Z elements. For heavier elements, typically As, Sn, Sb, Ba, Pb and Bi, the high-voltage condition will be used to determine presence or absence and peak area ratios.

5.2.2 Analysis of intact objects of British porcelain

The core sample set for the analysis of intact objects was the Marshall Collection of Early Coloured Worcester Porcelain at the Ashmolean Museum, Oxford, see Section 4.2.2. Objects for comparison were also analysed at Juno Antiques, Notting Hill; Stockspring Antiques, Kensington; and the private collections of George Haggerty, Nick Panes, Roger Pomfrett, Peter Burke, and Rosalie Wise-Sharp. A catalogue of the objects analysed is provided in Appendix A.6.

In this section, Worcester porcelain from the Marshall collection is characterised in terms of the composition of its glaze, and overglaze enamels and gilding. The extent of inter-factory variation in glaze and underglaze blue pigment composition is assessed by comparison with fifteen contemporary factories (Bovey Tracey, Bow, Caughley, Chaffers, Chelsea, Derby, Isleworth, Limehouse, Liverpool (Christian, Reid, and Pennington), Longton Hall, New Hall, Vauxhall, and West Pans).

The data are presented in the form of tables, which list the elements present in each compositional category. The raw data with example spectra for each compositional category, are provided in A.7.

Characterising Worcester porcelain: glaze composition

The majority of soft-paste porcelain produced in Britain during the late 18th – early 19th centuries has a transparent lead-rich glaze and many elements (Table 23) that are similar. The compositional variation in quantitative data from British porcelain glazes is discussed as part of the meta-analysis in Section 3.3. The glazes are therefore distinguished by the presence or absence of other elements, see Table 24.

Table 23 - elements present in lead-rich soft-paste porcelain glazes

Glaze	Elements present
lead glaze	Al, Si, K, Ca, Ti, Fe, Cu, Pb

The presence of phosphorus in some glazes is associated with porcelains that have a phosphatic paste. This may represent leaching into the glaze of elements from the paste during the glaze firing, or it may be that some raw materials from the paste were used in the production of some glazes; this is discussed in Section 2.2.2. In the Hand-Held XRF data below, phosphorus is present in some glazes of porcelains attributed to factories that were known to have produced phosphatic porcelain, so it is reasonable to hypothesise that these may be phosphatic porcelains. However, the lack of phosphorus in the glaze should not be taken to mean that the porcelain is not phosphatic.

Likewise, the glazes of porcelains that have magnesian pastes sometimes contain detectable levels of magnesium, and this may be interpreted as an indication of a magnesian porcelain. However, porcelain attributed to some factories that were known to have produced magnesian porcelain may not have detectable magnesium in the glaze. For this reason, phosphorus and magnesium are not relied upon in identifying these compositional groups.

Results I: non-invasive techniques

Table 24 – compositional categories based on elements present in soft-paste porcelain lead glazes, in addition to Al, Si, K, Ca, Ti, Fe, Cu and Pb

Glaze	Distinctive Elements present	Samples	Factories
1	none	HNB1, HNB2, HNB3	Bow
2	Sn	Bow mg1, Bow pl1, Bow pl2, Bow pl3, Bow pl4, Bow sb1, Bow sb2, Bow sb3, Bow sb4, Bow sb5, Bow sb6, Bow sb7, HNB3,	Bow
3	Bi, Sn	LH 1, LH 2, LH 3, LH 4, LH 5, LH 6, LH sb1, LH mg1	Longton Hall
4	Mn, Sn	EMB4, EMB6, EMB7, EMB9, Isl sb2, Lhse sb1, Lhse sb2, Lhse sb1, LLK4, LLK5, LLK6, LLK7, Vx sb1,	Isleworth, Limehouse, Vauxhall
5	Mn, Co, Ni, As	Cy tc1, Dby sb1, Vx mg1, Vx sb2	Caughley, Derby, Vauxhall
6	Mn, Co, Ni, Sn	LLK1, LLK2, LLK3,	Limehouse
7	Mn	Cpen, GAH1, GAH2, GAH3, GAH4, GAH6, GAH7, Isl sb1, Isl sb2, JoPen mg1, JoPen sb1, Jpen pl1, JPen sb1, Lowe sc1, LRd sb1, NH sc1, NH sc2, NH sc3, NH tb1, Spen sb1, WP 1, WP 2, WP 3, WP 4, WP 5, WP 6, all Worcester	Christian, Isleworth, Lowestoft, Reid, New Hall, Pennington, West Pans, Worcester
8	Mn, Zn	Cha tb1, GAH5	Chaffers, Isleworth
9	Mn, Zn, Sn, Ba	BTr cup, BTr sb1	Bovey Tracey
10	Mn, As	Cha sb1, Dby bskt1, Dby tc1, Dby vase1, DJG1, DJG2, EMB5, Lowe sb1	Chaffers, Derby, Isleworth, Lowestoft
11	Mn, As, Sn	EMB1, EMB2, EMB3	Vauxhall

Table 24 shows the eleven compositional groups identified by the presence of distinctive elements in the one-hundred and eighty glazes analysed. Of these, Bovey Tracey and Longton Hall each occupy their own distinctive category (numbers 9 and 3 respectively), discriminated by the presence of barium and bismuth, respectively, see Figure 65 and Figure 66.

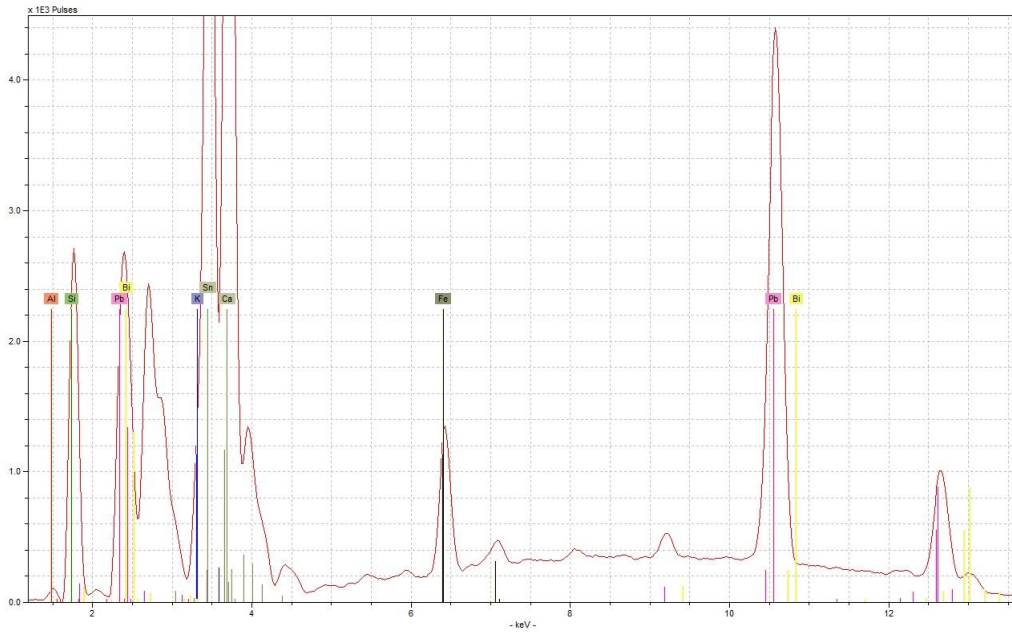


Figure 65 - example spectrum for glaze type 3 from LH sherd 1, showing the presence of Bi

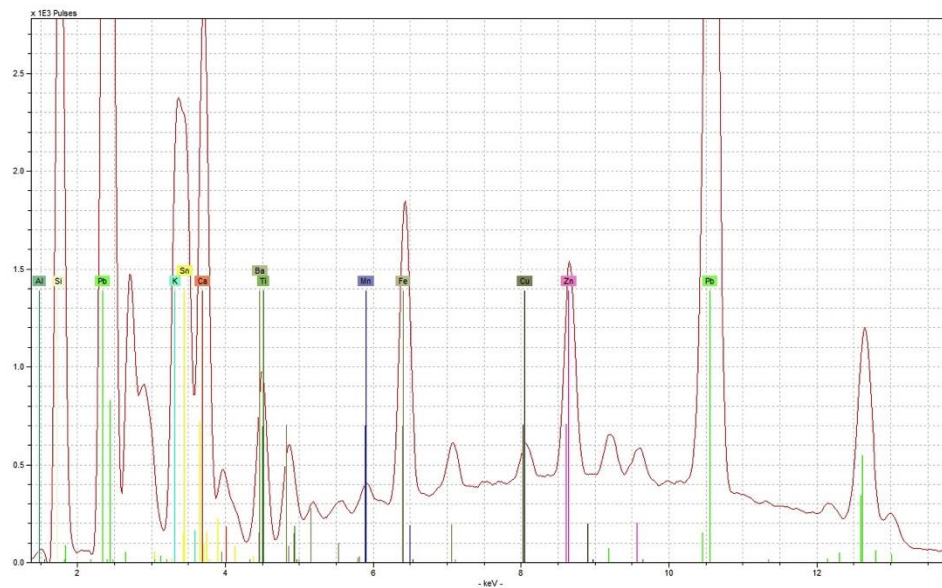


Figure 66 - example spectrum for glaze type 9 from BTr sb1, showing the presence of Zn, Ba, and Sn

Bow and Longton Hall porcelain have glazes that contain no detectable manganese, see Figure 67, and this trait is shared by some Vauxhall archaeological sherds. Tin is a common feature of glazes on porcelains attributed to, or found in contexts associated with, the London factories; Bow, Vauxhall, Isleworth and Limehouse, see Figure 69. However, not all porcelain from these factories have glazes with detectable tin. The ratio of lead to tin appears to be similar for glazes from Bovey Tracey, Limehouse and Vauxhall, see Figure 68, allowing for the detector saturation effect for a group of very tin-rich glazes from Vauxhall, which may contain more lead above the threshold that the detector is capable of distinguishing. The ratio of lead to tin appears to be slightly greater for glazes from Bow and Isleworth.

Manganese, cobalt and nickel are present in glazes from a number of pieces attributed to Caughley, Derby, Limehouse and Vauxhall, see Figure 67, but again not all porcelain from these factories contains these elements. Arsenic appears to be reliably associated with Derby porcelain, but is also present in pieces from Chaffers, Lowestoft and Isleworth. Some porcelain from Caughley and Vauxhall may also have arsenic in its glaze; however this could also be a trace element present in the cobalt pigment that is present at a low concentration throughout the glaze.

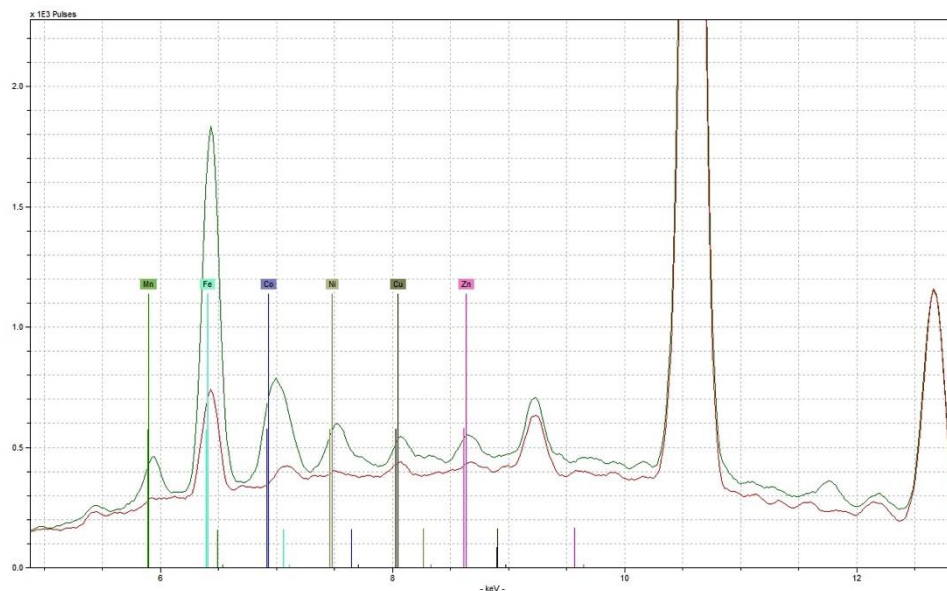


Figure 67 - example spectra for glaze types 1 (red trace) and 5 (green trace), showing the presence of Mn, Co, Ni, Cu, Zn, and elevated Fe in glaze 5

Results I: non-invasive techniques

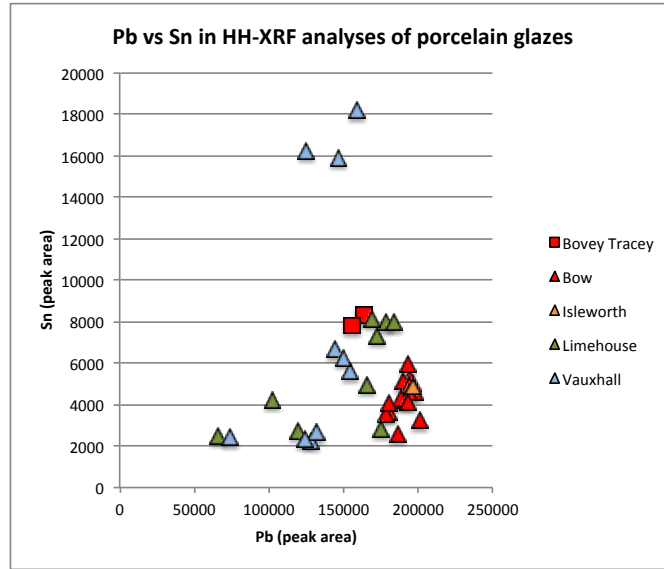


Figure 68 - lead versus tin peak areas from HH-XRF analysis of leaded porcelain glazes

As discussed above, phosphorus is found in some glazes, see Figure 69, but is not relied upon for these compositional categories, since it cannot reliably be used as an indicator of paste type. Some porcelains with phosphorus-bearing glazes contain elevated calcium, see Figure 70.

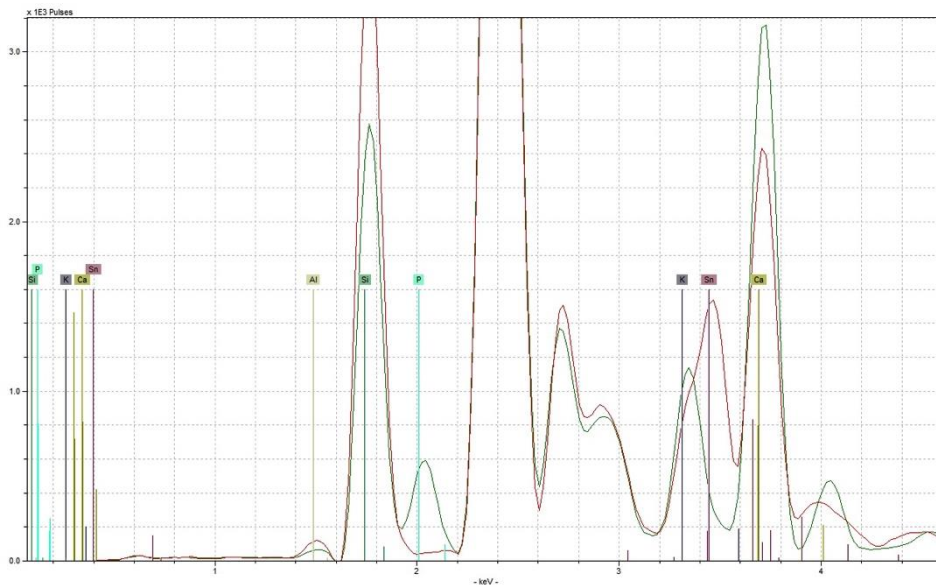


Figure 69 - example spectra for glaze types 1 (green trace) and 6 (red trace), showing the presence of P and elevated Ca in glaze 1, and Sn in glaze 6

Results I: non-invasive techniques

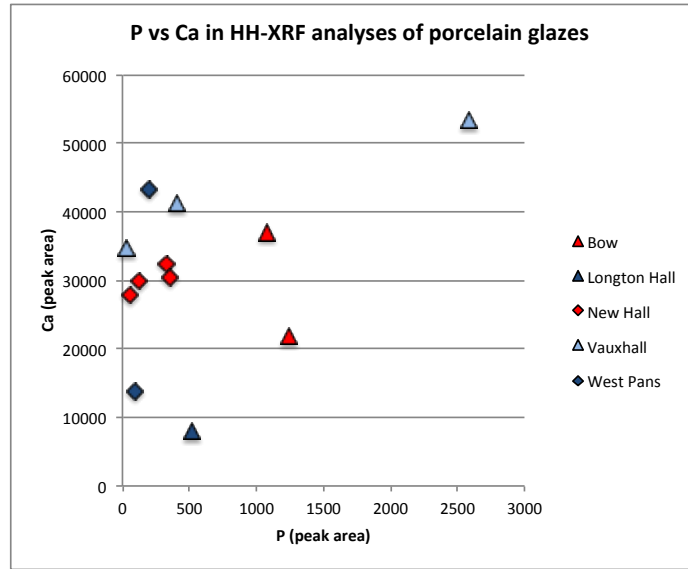


Figure 70 - phosphorus versus calcium peak areas from HH-XRF analysis of leaded porcelain glazes

While all porcelain glazes here analysed contain trace amounts of iron and copper, these elements are present in greater quantities in some glazes from Vauxhall, Bovey Tracey, and Worcester, see Figure 71. Copper shows no significant relationship to any other element. Iron is positively associated with both manganese, see Figure 72, and silicon, see Figure 73.

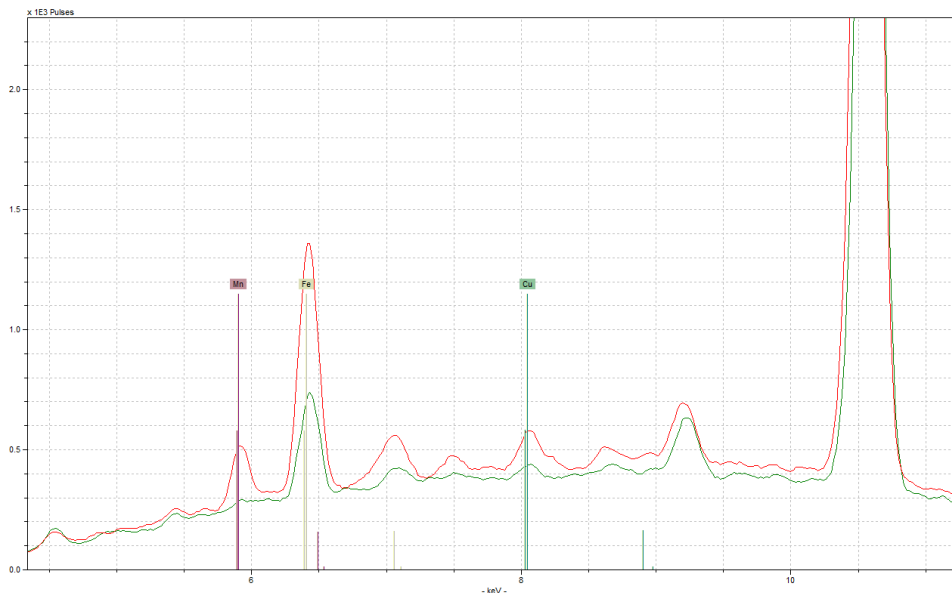


Figure 71 - example spectra for glaze types 1 (green trace) and 7 (red trace), showing the presence of Mn, and elevated Fe and Cu, in glaze 7

Results I: non-invasive techniques

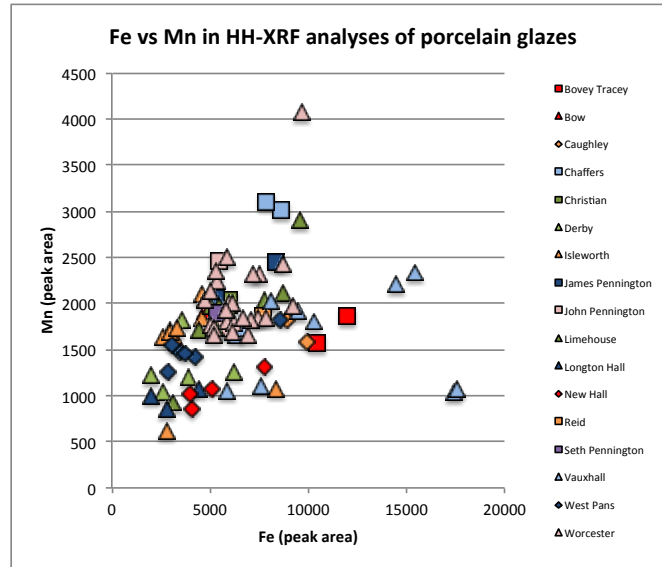


Figure 72 - iron versus manganese peak areas from HH-XRF analysis of leaded porcelain glazes

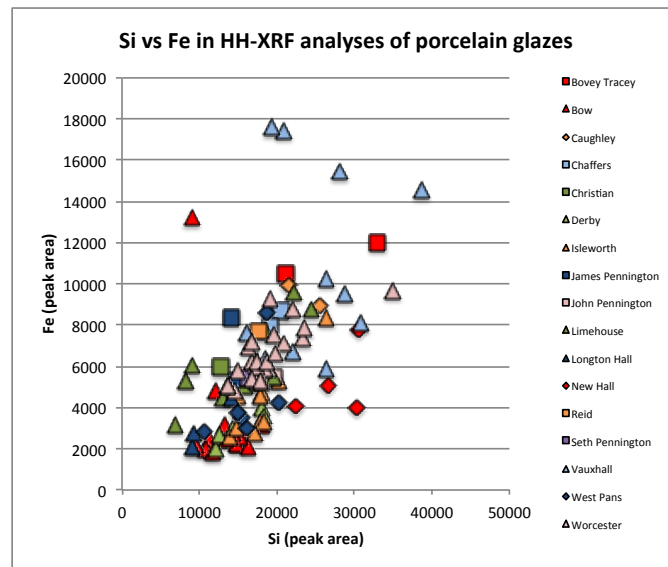


Figure 73 - iron versus silicon peak areas from HH-XRF analysis of leaded porcelain glazes

Characterising Worcester porcelain: polychrome enamels

Factory-decorated Worcester porcelain is here compared with James Giles-decorated objects from Worcester, and some porcelain that is suspected to have been re-decorated in the 19th century. Overglaze enamels were a popular form of decoration on porcelain objects, and a wide variety of hues were used. For the purposes of this research, they have been grouped by colour type (blue, green, orange, purple, red, turquoise, yellow), see Figure 74, and green enamels are subcategorised into border / ground or painted enamels. Applied gold decoration, known as gilding, is examined separately.

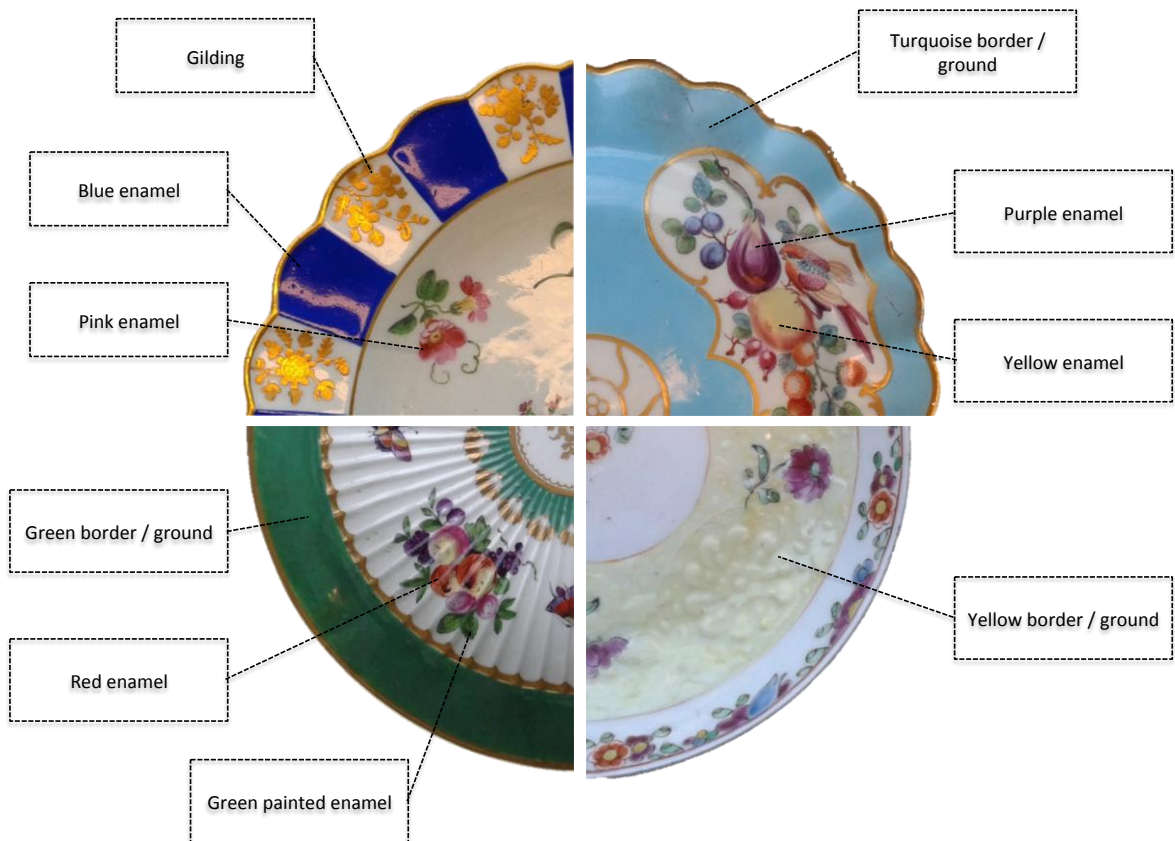


Figure 74 - enamel colours on British porcelain with blue, turquoise, green and yellow grounds or borders

The enamels have been examined separately by colour, and divided into compositional groups, based on the presence or absence of elements. The elemental composition of Worcester porcelain glazes having been demonstrated to be consistent within this period of time, see Table 24, these elements are assumed to have been contributed by the enamel.

The basic composition of each colour, as analysed, is shown in Table 25, and most often will include elements contributed by the glaze, and the enamel flux as well as the pigment. In most cases, the elemental composition of the coloured area matches the composition of the underlying glaze, with the exception of additional elements, which may then be attributed to the enamel. Compositional sub-categories are determined by the presence or absence of other minor or trace elements, and are listed in the tables that follow. The raw total counts data and example spectra for each compositional sub-category are provided in Appendix A.7 and discussed in further detail below.

Table 25 - elements present in enamel colours on Worcester porcelain

Colour	Elements present	Compositional subcategories
blue	Al, Si, K, Ca, Ti, Fe, Co, Ni, Pb	Table 26
green (border / ground, painted enamel)	Al, Si, K, Ca, Ti, Fe, Cu, Pb	Table 27, Table 28
orange	Al, Si, K, Ca, Ti, Fe, Cu, Pb	Table 29
pink	Al, Si, K, Ca, Ti, Fe, Pb	Table 30
purple	Al, Si, K, Ca, Ti, Fe, Pb	Table 31
red	Al, Si, K, Ca, Ti, Fe, Pb	Table 32
turquoise border / ground	Al, Si, K, Ca, Ti, Fe, Cu, Pb	Table 33
yellow border / ground	Al, Si, K, Ca, Ti, Fe, Pb	Table 34

Results I: non-invasive techniques

Table 26 - compositional categories based on elements present in blue overglaze enamels, in addition to Al, Si, K, Ca, Ti, Fe, Co, Ni and Pb

Blue	Distinctive Elements present	Samples	Factories
1	Cu, As	65, 377, WJG6, WJG8, WJG9, WUK1, WWR1, WWR2	Worcester, James Giles-decorated Worcester
2	Cr, Cu, Zn, Sn	292 (JG)	James Giles-decorated Worcester
3	Cu, Zn, As	111	Worcester
4	As	804	Worcester
5	Cu, As, Sn	WWR5	Worcester

Table 27 - compositional categories based on elements present in green enamel grounds and borders, in addition to Al, Si, K, Ca, Ti, Fe, Cu and Pb

Green	Distinctive Elements present	Samples	Factories
1	Sn	927 (lid grounds only), 929, 930, 934, 1005, 1010, 1012, 1014, 1016	Worcester
2	Cr, Co, Ni, Zn, Sn	927 (teapot grounds only), 932	Worcester

Results I: non-invasive techniques

Table 28 - compositional categories based on elements present in green painted enamels, in addition to Al, Si, K, Ca, Ti, Fe, Cu and Pb

Green	Distinctive Elements present	Samples	Factories
1	none	620, 704 (JG), 804, 826, 829, 929, 1016, WJG4, WJG6, WJG8, WJG9, WON1, WWR4, WWR5	Worcester, James Giles-decorated Worcester
2	Co	65, 617, 698 (JG), 703 (JG)	Worcester, James Giles-decorated Worcester
3	Co, Ni, Sn	697 (JG)	James Giles-decorated Worcester
4	Cr, Co, Ni, Zn, Sn	292 (JG), 480, 705 (JG), 914, 932, 1012, 1014	Worcester, James Giles-decorated Worcester
5	Sn	696 (JG), 699 (JG), 702 (JG), 927, 930, 934, 1010	Worcester, James Giles-decorated Worcester

Table 29 - compositional categories based on elements present in orange enamels, in addition to Al, Si, K, Ca, Ti, Fe, Cu and Pb

Orange	Distinctive Elements present	Samples	Factories
1	none	377, WJG4	Worcester, James Giles-decorated Worcester
2	Sn	WJG2	James Giles-decorated Worcester
3	Ni	111	Worcester
4	Zn	826, 829	Worcester

Results I: non-invasive techniques

Table 30 - compositional categories based on elements present in pink enamels, in addition to Al, Si, K, Ca, Ti, Fe and Pb

Pink	Distinctive Elements present	Samples	Factories
1	Cu	698 (JG), 699 (JG), 702 (JG), 703 (JG), 704 (JG), 804, WJG1, WJG2, WJG4, WJG5, WJG6, WJG8, WWR5, WWR6	Worcester, James Giles-decorated Worcester
2	Cu, Au	65	Worcester
3	Cu, As	617	Worcester
4	Cu, Zn, Sn, Ba	480	Worcester
5	Cu, Zn, Sn, Au	696 (JG)	James Giles-decorated Worcester
6	As, Au	697 (JG)	James Giles-decorated Worcester

Table 31 - compositional categories based on elements present in purple enamels, in addition to Al, Si, K, Ca, Ti, Fe and Pb

Purple	Elements present	Samples	Factories
1	Co, Ni, Cu (As?)	WJG8, WUK2	Worcester, James Giles-decorated Worcester
2	Mn	WJG9, WUK1	Worcester, James Giles-decorated Worcester
3	Fe, Co, Ni	WJG3	James Giles-decorated Worcester
4	Mn, Co, Ni, Cu, (As?)	WWR3	Worcester

Results I: non-invasive techniques

Table 32 - compositional categories based on elements present in red enamels, in addition to Al, Si, K, Ca, Ti, Fe and Pb

Red	Elements present	Samples	Factories
1	none	65, 576 (JG), WJG8, WWR1, WWR5	Worcester, James Giles-decorated Worcester
2	Au	620	Worcester
3	Cr, Zn, Sn, Ba	705 (JG)	James Giles-decorated Worcester

Table 33 - compositional categories based on elements present in turquoise enamel borders and grounds, in addition to Al, Si, K, Ca, Ti, Fe, Cu and Pb

Turquoise	Elements present	Samples	Factories
1	none	577 (JG), WJG5	James Giles-decorated Worcester
2	As	698 (JG), 699 (JG), 701 (JG), 703 (JG)	James Giles-decorated Worcester
3	Zn, Sn	700 (JG), 919 (JG)	James Giles-decorated Worcester
4	As, Sn	705 (JG)	James Giles-decorated Worcester
5	Mn	702 (JG)	James Giles-decorated Worcester
6	Co, Ni	65, 576 (JG), 704 (JG)	Worcester and James Giles-decorated Worcester
7	Cr, Zn, Au	914	Worcester

Results I: non-invasive techniques

Table 34 - compositional categories based on elements present in yellow enamels, in addition to Al, Si, K, Ca, Ti, Fe and Pb

Yellow	Elements present	Samples	Factories
1	Sn	65, 240 (JG), 697 (JG), 699 (JG), 702 (JG), 703 (JG), 704 (JG), WJG1, WJG6, WWR2	Worcester, James Giles-decorated Worcester
2	As	829	Worcester
2	Mn, Zn, Sn	480, 698 (JG)	Worcester, James Giles-decorated Worcester
3	Mn, Ni, Sn	WWR5	Worcester
4	Cr, Zn, Sn	696 (JG)	James Giles-decorated Worcester
5	Cr, Co, Ni, Zn, As	292 (JG)	James Giles-decorated Worcester
6	Cr, Zn, As, Au	705 (JG), 914	Worcester, James Giles-decorated Worcester

Blue

Blue enamels are based on cobalt, which is a strong blue colourant that is commonly used as an underglaze decoration on porcelain and other white ceramics. In these samples, it is typically accompanied by nickel, see Figure 75. Two groups are formed by the distribution of cobalt versus nickel; four samples (111, WJG9, WUK1, and WWR2) show a linear trend between these two elements, while the remaining samples contain less nickel, relative to cobalt, and there is no evident relationship. Certain blue pigments also contain copper, zinc, and arsenic. Where arsenic is present, there is evidence for a linear trend between this element and cobalt, see Figure 76. The blue enamels on one object (292) contain significant amounts of zinc, and also chromium, see Figure 77. The green and yellow enamels on this object also contain chromium and zinc.

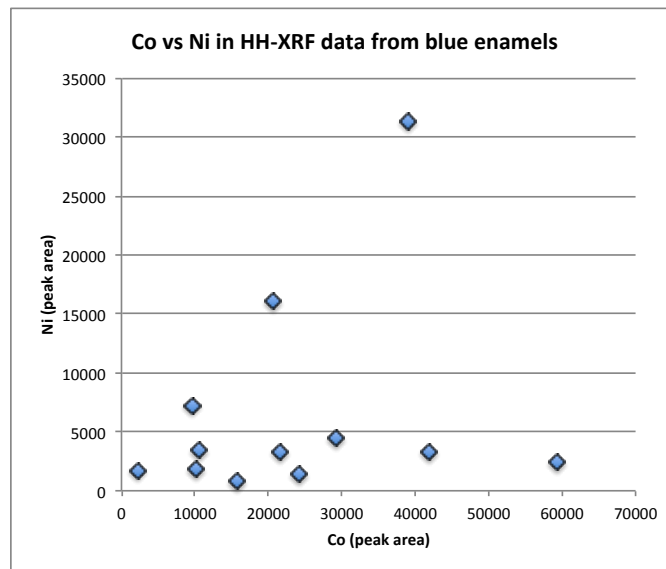


Figure 75 - cobalt versus nickel peak areas from HH-XRF analysis of overglaze blue enamels

Results I: non-invasive techniques

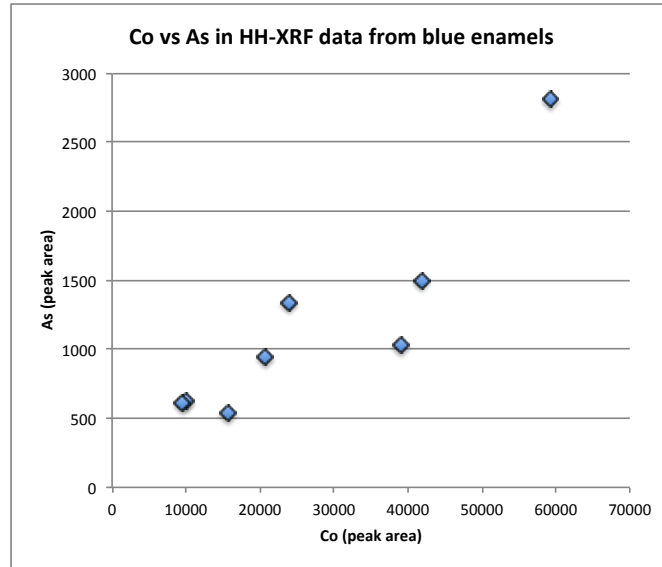


Figure 76 - cobalt versus arsenic peak areas from HH-XRF analysis of overglaze blue enamels

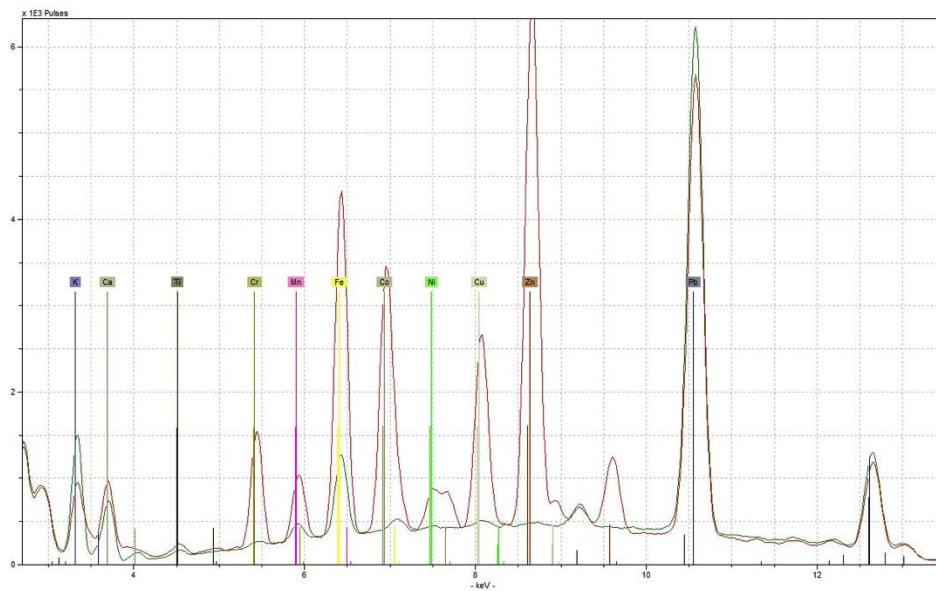


Figure 77 - example spectra for blue enamel type 2 (red trace) and glaze (green trace), showing that the blue enamel contributes Cr, Mn, Fe, Co, Ni, Cu, and Zn

Green

Although green grounds or borders and green painted enamels are treated separately in Table 24 and in Table 27 and Table 28, no significant differences were found between them, and the elements present are common to both. The colourant is copper in most cases, see Figure 78, or chromium in 932, see Figure 79. Chromium is present at low levels, relative to the chromium greens, in green enamels where copper is the main colourant on 705, 914, 1012, and 1014, see Figure 80 and Figure 81, and zinc is also found. Some copper and cobalt greens contain tin or cobalt and nickel; chromium greens typically also contain cobalt, nickel, and zinc.

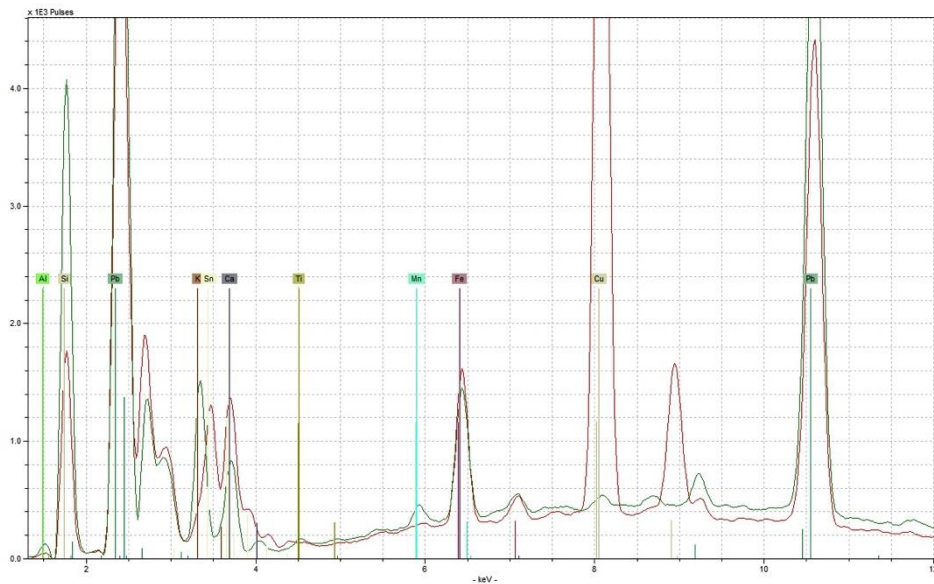


Figure 78 - example spectra for green border/ground type 1 (red trace) and glaze (green trace), showing that the green enamel contributes Cu and Sn

Results I: non-invasive techniques

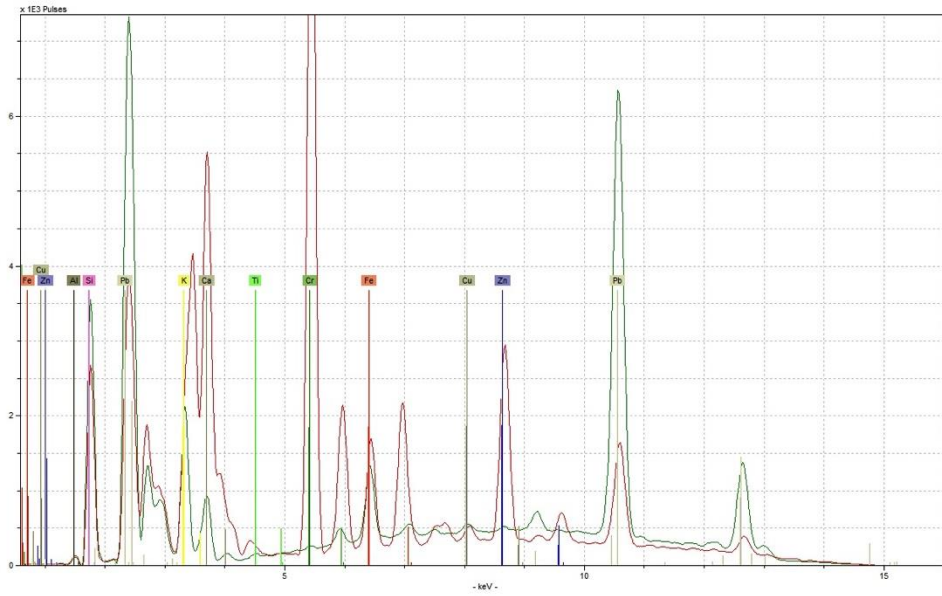


Figure 79 - example spectra for green border/ground type 2 (red trace) and glaze (green trace), showing that the green enamel contributes Cr, Zn, and increased Fe

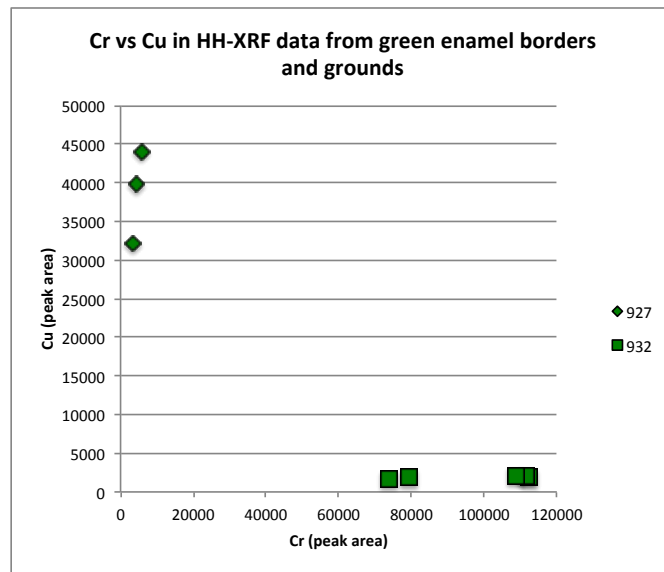


Figure 80 - chromium versus copper peak areas from HH-XRF analysis of overglaze green borders and grounds

Results I: non-invasive techniques

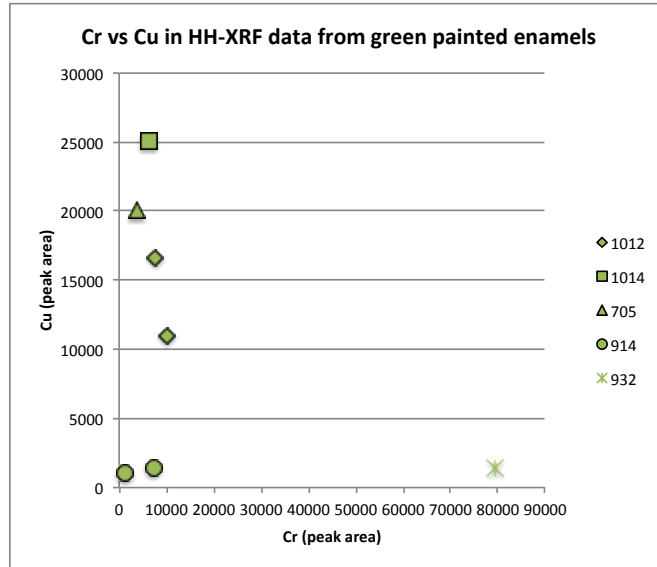


Figure 81 - chromium versus copper peak areas from HH-XRF analysis of overglaze green enamels

Orange

Orange enamels are based on iron, see Figure 82, which produces a red colour when oxidised. Manganese and copper are found in all samples at levels slightly higher than the surrounding glaze, although these elements show no strong trend with respect to the iron colourant, see Figure 83 and Figure 84. Tin and nickel are each found in just one of the samples analysed (WJG2 and 111 respectively); zinc is found in two (826 and 829).

Results I: non-invasive techniques

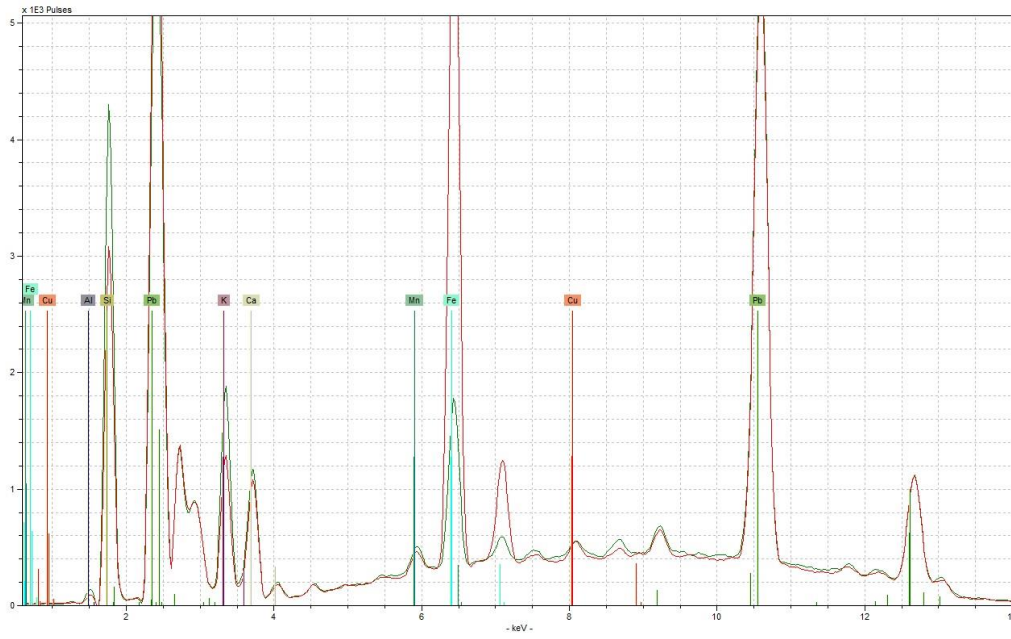


Figure 82 - example spectra for orange enamel type 1 (red trace) with glaze (green trace), showing that the orange enamel contributes Fe

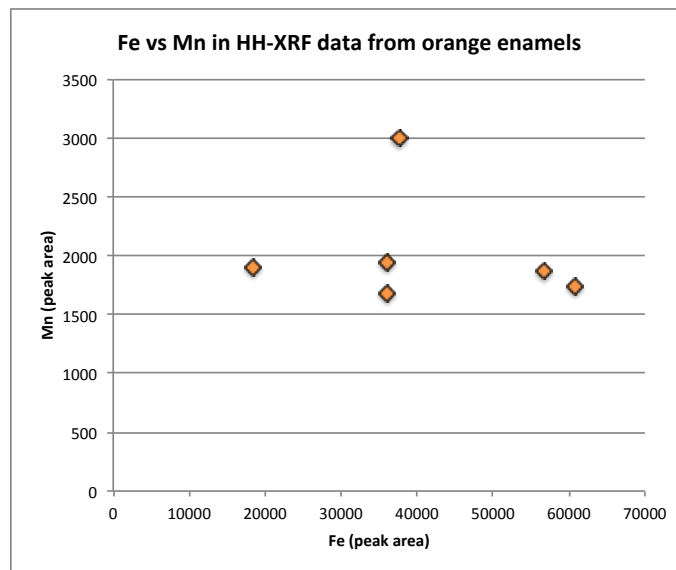


Figure 83 - iron versus manganese peak areas from HH-XRF analysis of overglaze orange enamels

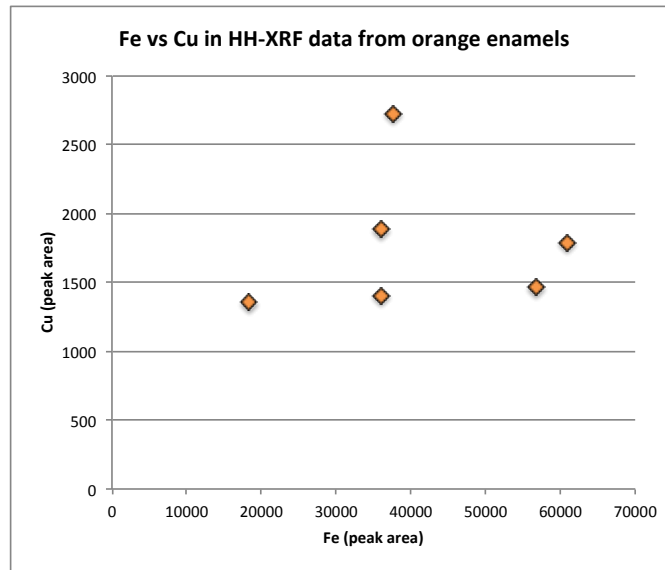


Figure 84 - iron versus copper peak areas from HH-XRF analysis of overglaze orange enamels

Pink

The pink enamels, comprising both painted enamels, and borders and grounds, may be coloured by either iron, copper, gold, or a combination of these elements, see Figure 85. Arsenic has been found in two pink enamels (617 and 697), zinc in two (480 and 696), and tin in two (480, and 696). Barium and zinc are both present in one sample (480), see Figure 86, the green enamels on which contain significant chromium and zinc. Gold has been identified in three spectra (65, 696, and 697), see Figure 87, all three of the objects of which have over-gilding on the pink grounds or borders, or a gilded edge close to the enamelled area, see Figure 88. It cannot, therefore, be stated conclusively whether the gold is present in the pink enamel pigment as a colourant, or whether it may be contamination from the surrounding gilding.

Results I: non-invasive techniques

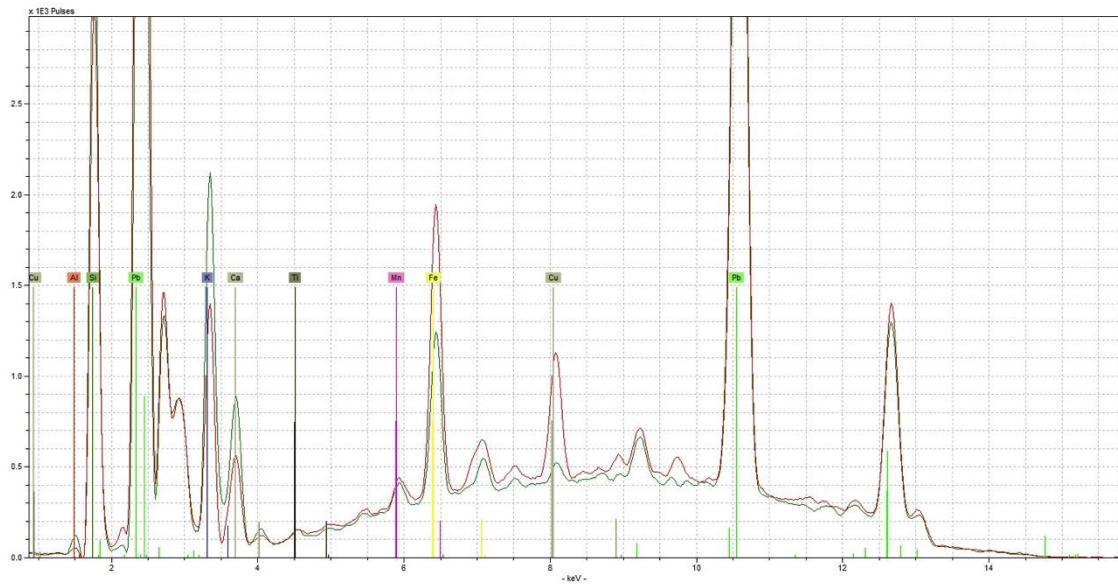


Figure 85 - example spectra for pink enamel type 1 (red trace) and glaze (green trace), showing that the pink enamel contributes Fe and Cu

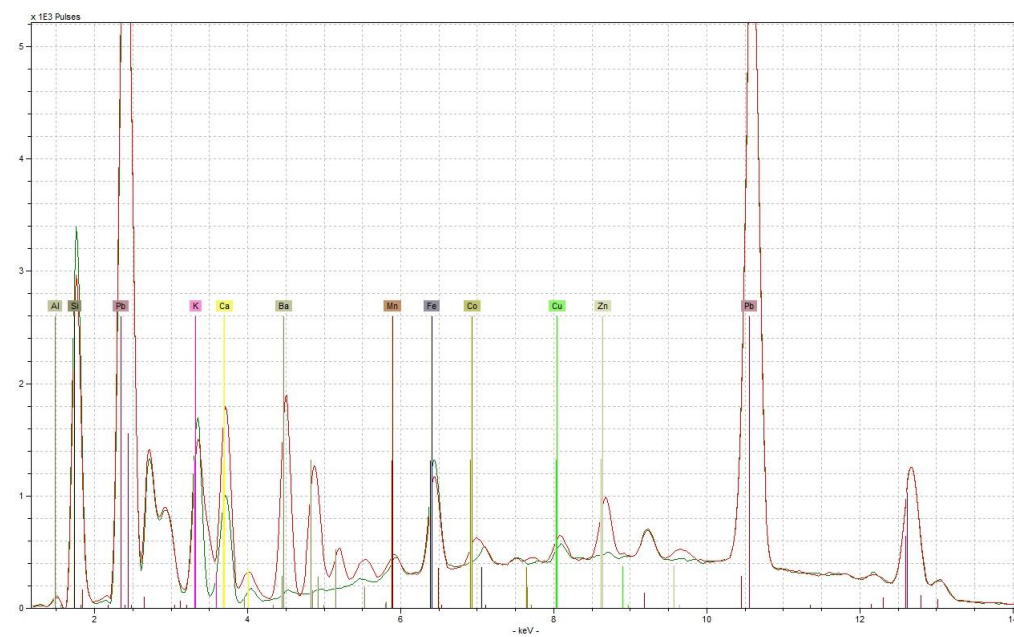


Figure 86 - example spectra for pink enamel (red trace) and glaze (green trace) on 480, showing that the pink enamel contributes Zn and Ba, possibly Co

Results I: non-invasive techniques

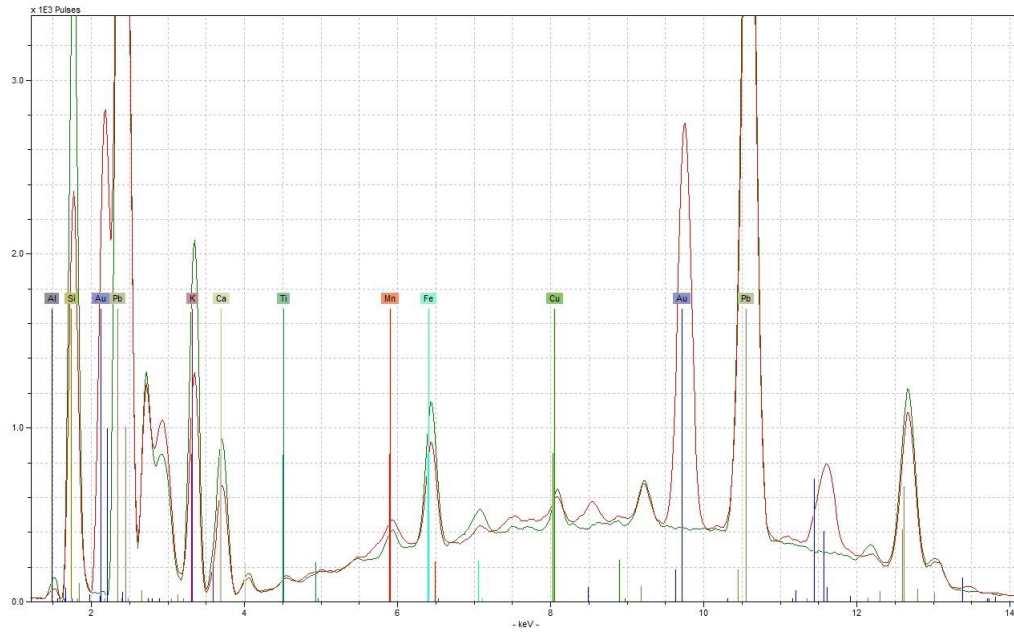


Figure 87 - example spectra for pink enamel type 2 (red trace) and glaze (green trace), showing that the pink enamel contributes Au



Figure 88 - object number 696, a plate, showing overgilding on pink ground, with flower painting in reserves. The tested pink area is in the centre.

Purple

Purple enamels are scarce among the samples analysed, and the composition of their formulae appears complex. Manganese, iron, and cobalt feature as the principal colourants, suggesting that they were used selectively as a palette to vary the purple hue. Two samples (WJG8 and WUK2) contains a great concentration of cobalt, see Figure 89, and the purple produced is dark, see Figure 90. In another sample (WJG3), iron and cobalt are present in high concentrations, see Figure 91, resulting in a brighter, pinkish purple, see Figure 92. Manganese is the colourant present at the highest level in WJG9 and WUK1, see Figure 93, and the shade of purple is similar to that produced by the iron-rich purple, see Figure 94. In addition, one sample (WWR3) contains both manganese and iron in appreciable quantities, along with copper and possibly cobalt, see Figure 95, suggesting that more than one colourant was used to modify the hue.

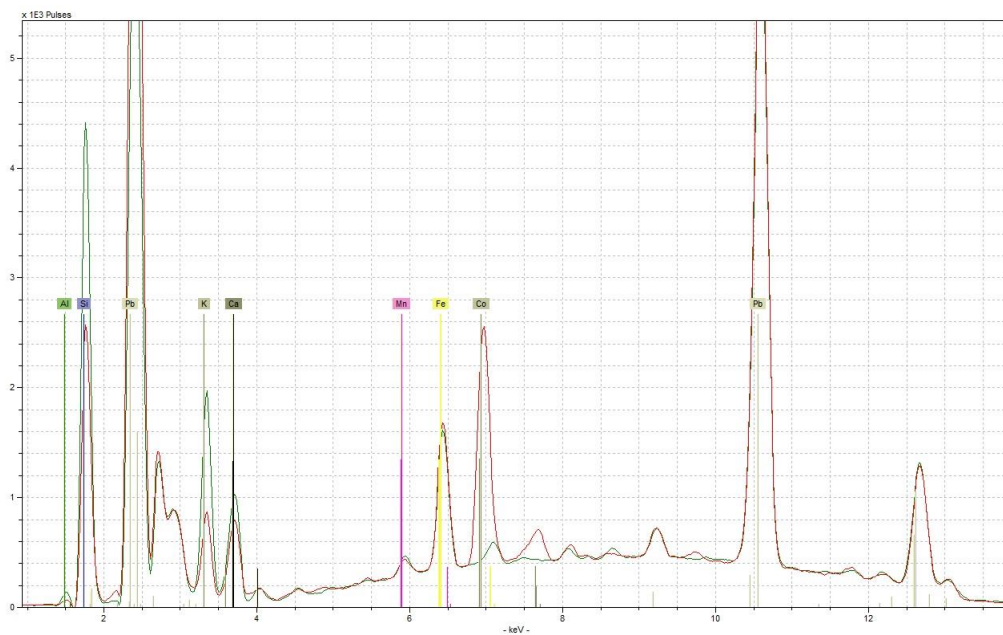


Figure 89 - example spectra for purple enamel (red trace) and glaze (green trace) on WJG8, showing that the purple enamel contributes Co

Results I: non-invasive techniques



Figure 90 - object number WJG8, a dish with flower painting in purple, pink, red, green, blue and yellow.
The tested purple area is in the upper left-hand corner.

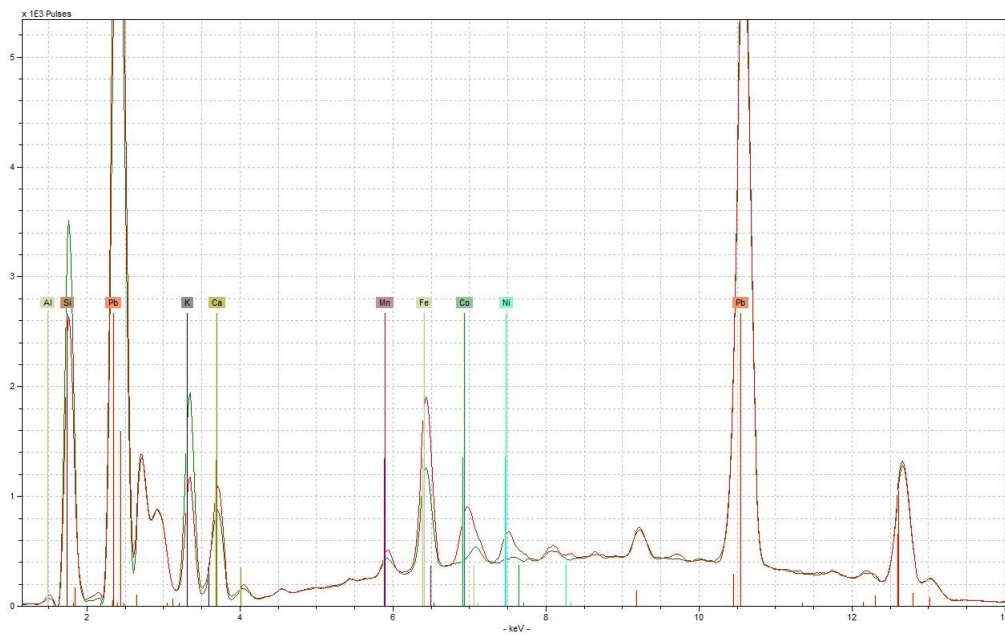


Figure 91 - example spectra for purple enamel (red trace) and glaze (green trace) on WJG3, showing that the purple enamel contributes Fe, Co, Ni and possibly Mn.

Results I: non-invasive techniques

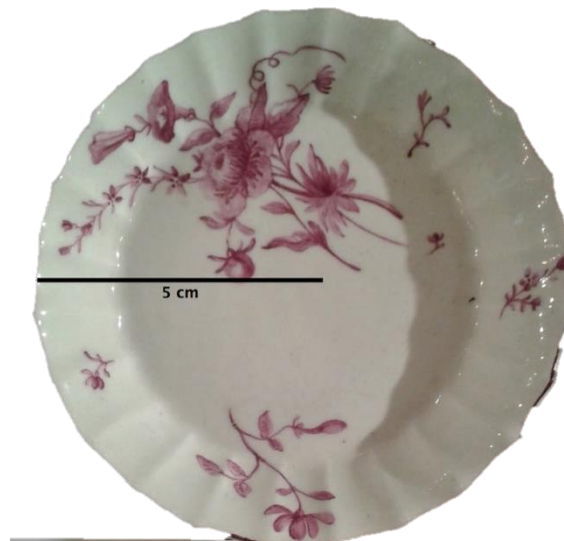


Figure 92 - object number WJG3, a plate with purple monochromatic flower painting. The analysed area is in the upper left-hand corner.

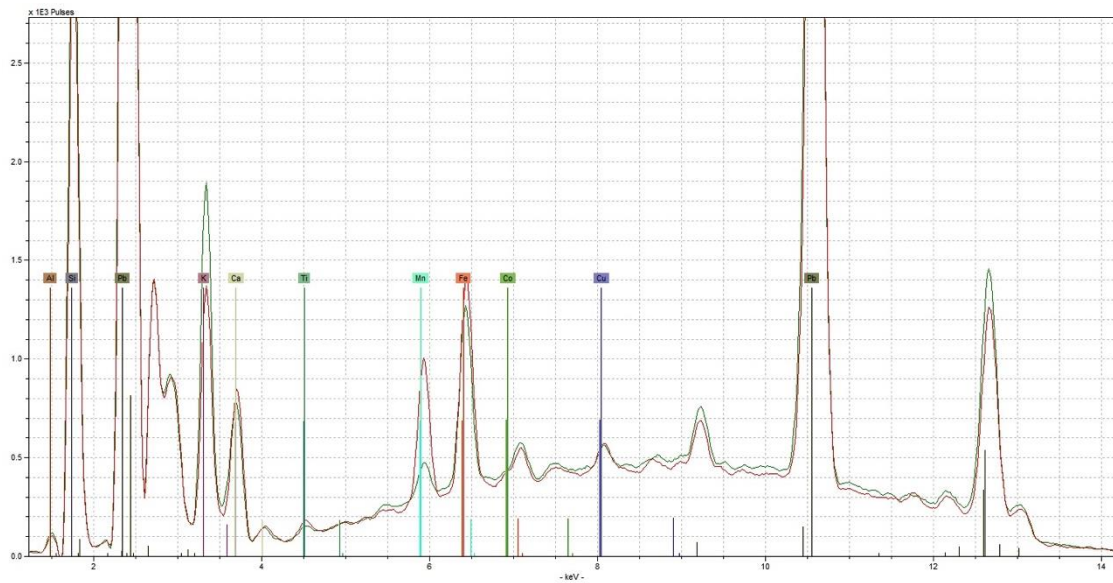


Figure 93 - example spectra for purple enamel (red trace) and glaze (green trace) on WJG9, showing that the purple enamel contributes Mn and possibly additional Fe

Results I: non-invasive techniques



Figure 94 - object number WJG9, a large armorial plate with vines on border. The analysed area is the purple pegasus form at the upper centre of the plate.

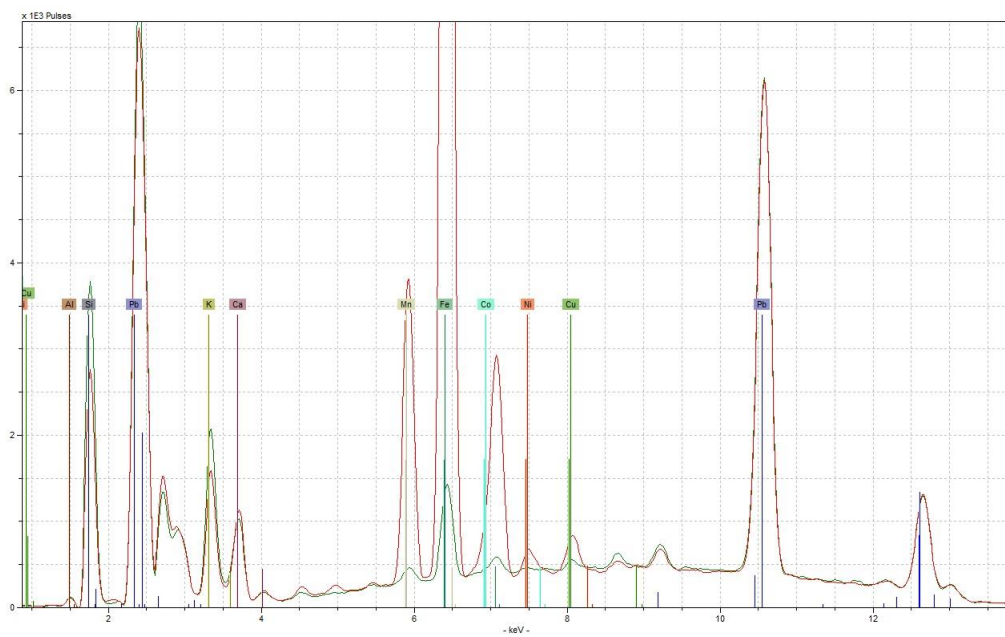


Figure 95 - examples spectra for the purple enamel (red trace) and glaze (green trace) on WWR3, showing that the purple enamel contributes Mn, Fe, Cu and possibly Co.

Red

Red enamels contain iron as the principal colourant, and most also contain copper at a slightly higher level than the surrounding glaze, see Figure 96. The red enamels on one sample (705) also contain barium, zinc and tin, see Figure 97.

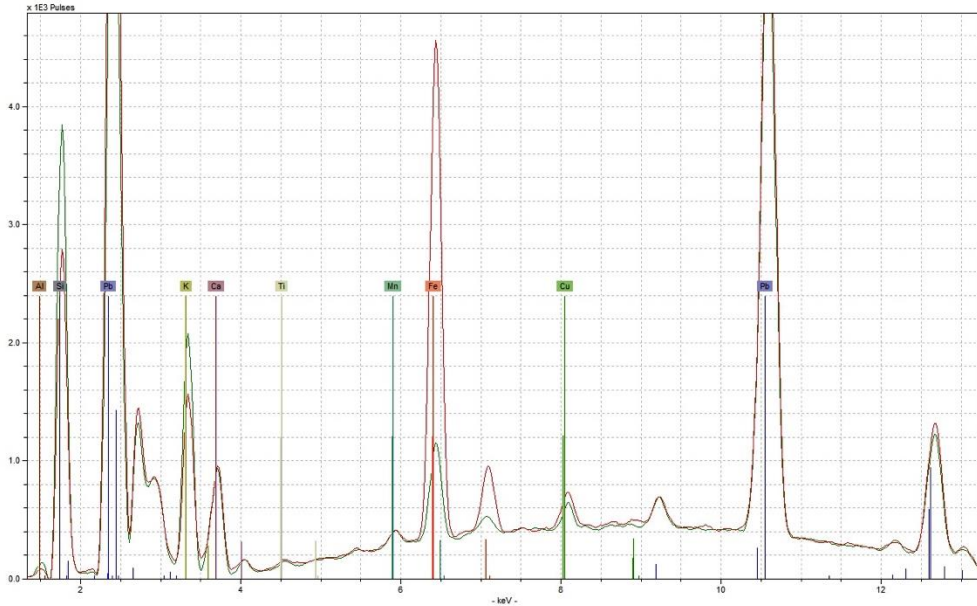


Figure 96 - example spectra for red enamel type 1 (red trace) and glaze (green trace), showing that the red enamel contributes Fe and Cu

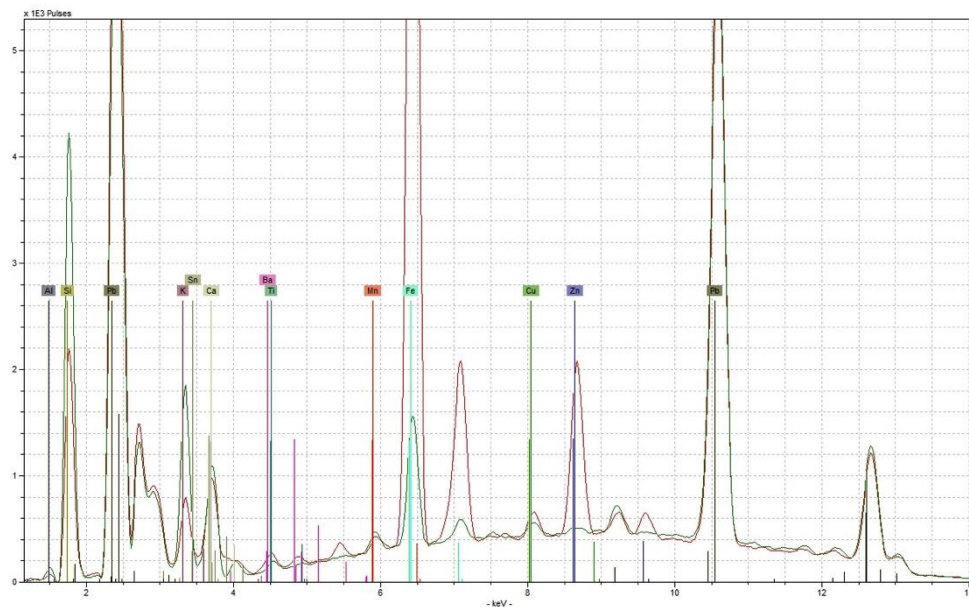


Figure 97 - example spectra for red enamel type 3 (red trace) and glaze (green trace), showing that the red enamel contributes Fe, Zn, and Ba

Turquoise

Like green overglaze enamels and grounds, the principal colourant element in most turquoise enamels is copper. All turquoise enamels contain copper at a level significantly greater than the surrounding glaze, see Figure 98 and Figure 99, with the exception of 914, on which the principal colourant appears to be chromium, see Figure 100, accompanied by zinc. Arsenic is present in eight of the fourteen enamels tested, but there is no strong trend to the relationship between this element and the colourant, see Figure 101. Tin has been included in three turquoise grounds or borders, on pieces attributed to the workshop of James Giles, but once more there is no obvious relationship between the tin and copper peak areas, see Figure 102. Cobalt and nickel are present in four turquoise enamels, one of which (702) appears to contain gold. However, it is difficult to determine whether this gold is a component of the turquoise enamel pigment, or whether it represents contamination from the surrounding gilding, due to overgilding and the proximity of the gilded edge to the narrow turquoise border, see Figure 103.

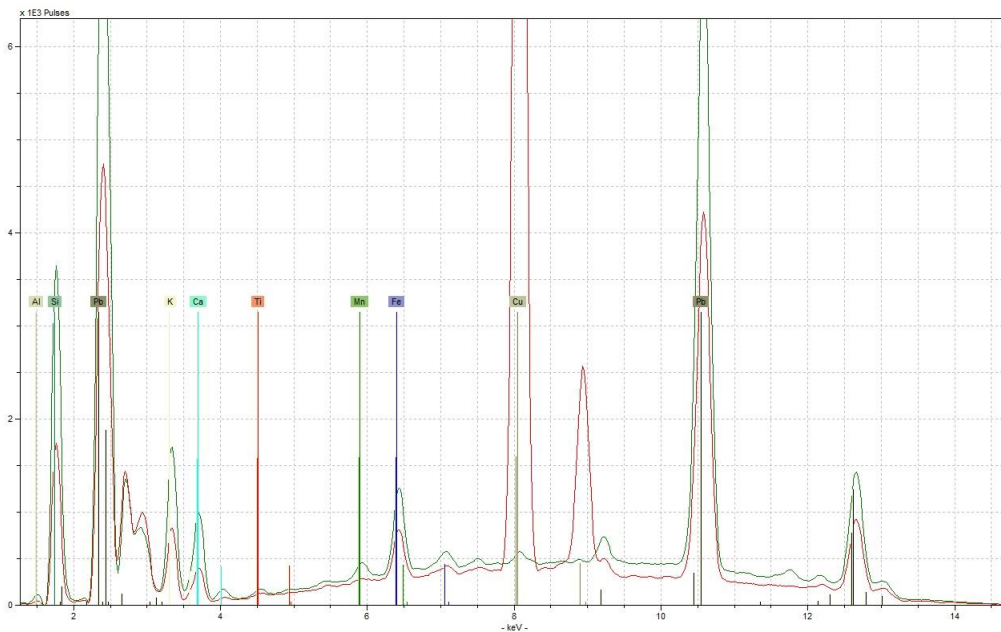


Figure 98 - example spectra for turquoise enamel type 1 (red trace) and glaze (green trace), showing that the turquoise enamel contributes Cu

Results I: non-invasive techniques

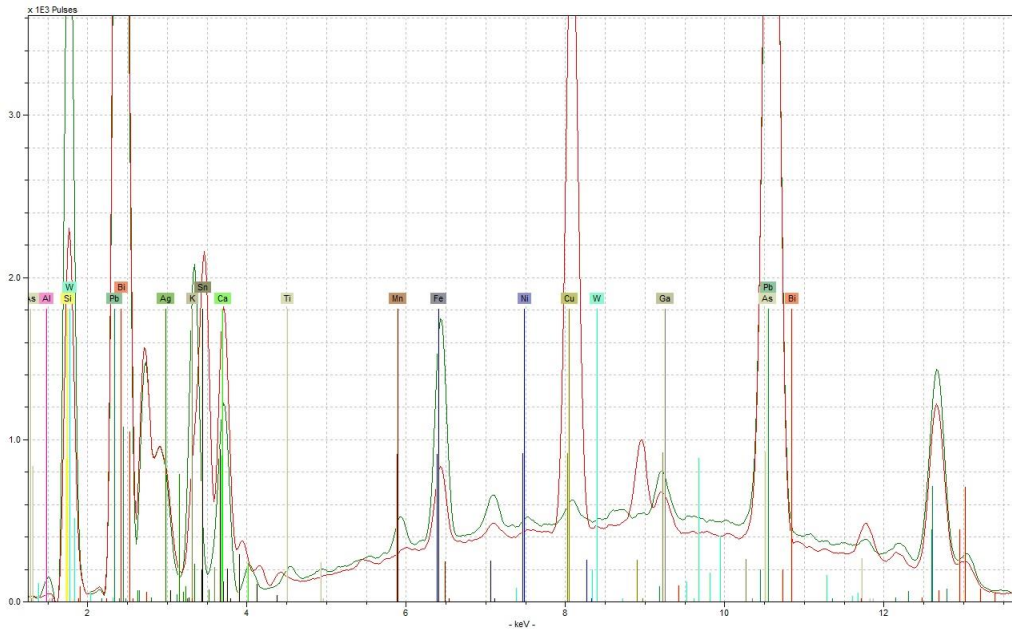


Figure 99 - example spectra for turquoise enamel type 4 (red trace) and glaze (green trace), showing that the turquoise enamel contributes Cu, As, and Sn

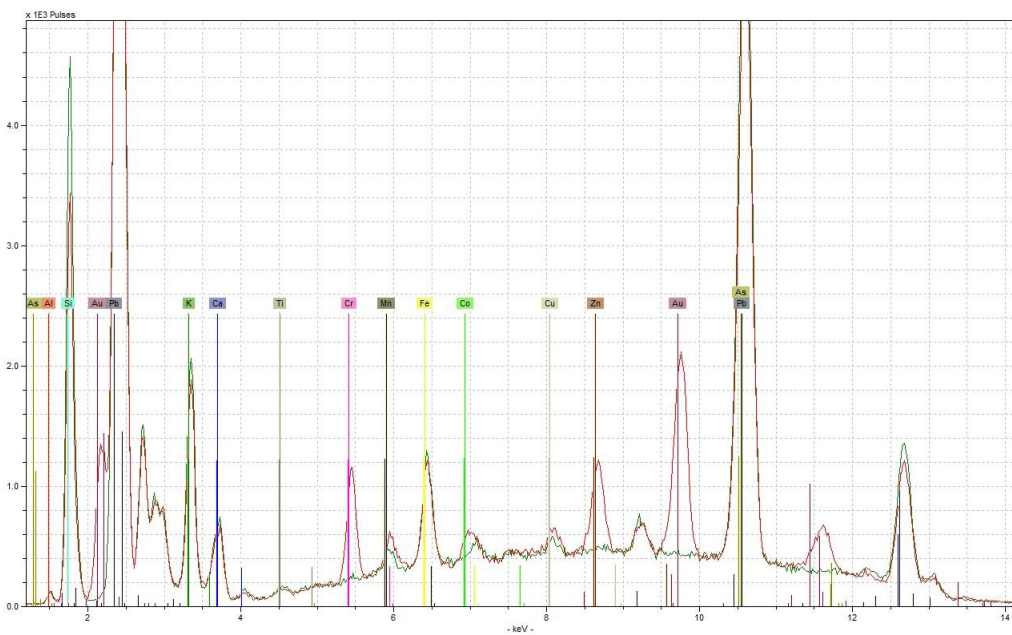


Figure 100 - example spectra for turquoise enamel type 7 (red trace) and glaze (green trace), showing that the turquoise enamel contributes Cr, Co, Zn, Au, and As

Results I: non-invasive techniques

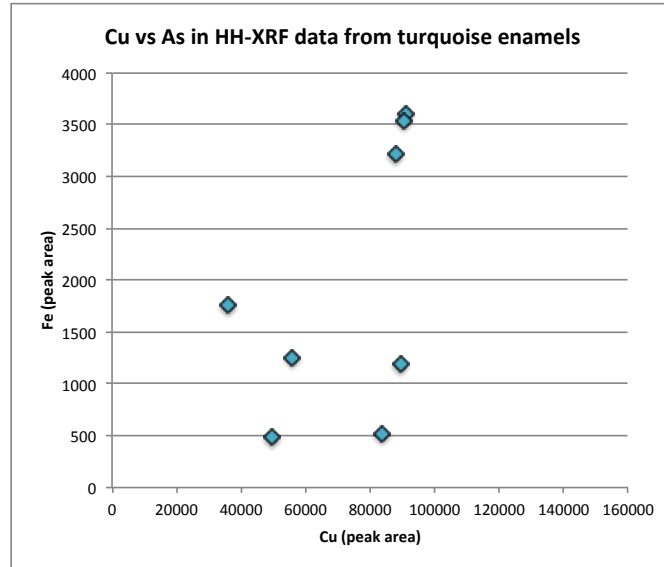


Figure 101 - copper versus arsenic peak areas from HH-XRF analysis of turquoise overglaze enamels

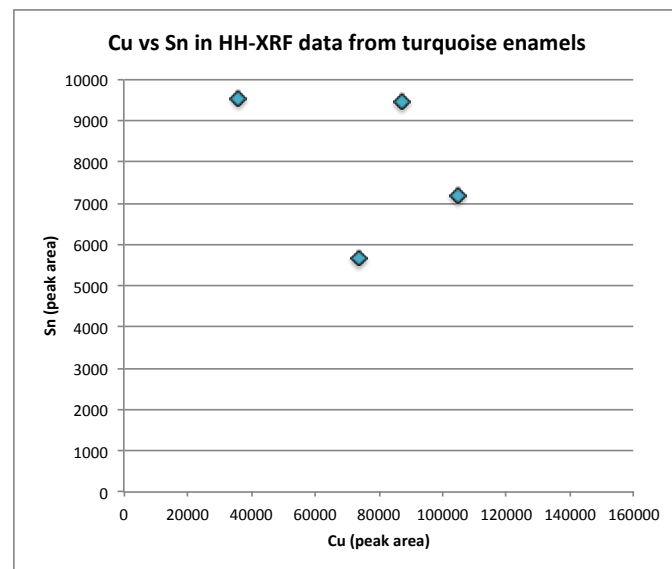


Figure 102 - copper versus tin peak areas from HH-XRF analysis of turquoise overglaze enamels



Figure 103 - turquoise border with overgilding, and gilded edge, on object number 702

Yellow

The yellow enamels are based on tin, sometimes with additional nickel, or zinc and occasionally chromium, see Figure 104 and Figure 105. Gold appears to be present in the yellow enamels of two objects (705 and 914), both of which are heavily gilded around the enamelled areas, meaning that it cannot be said conclusively that the gold in these spectra is not contamination from the gilding, see Figure 106.

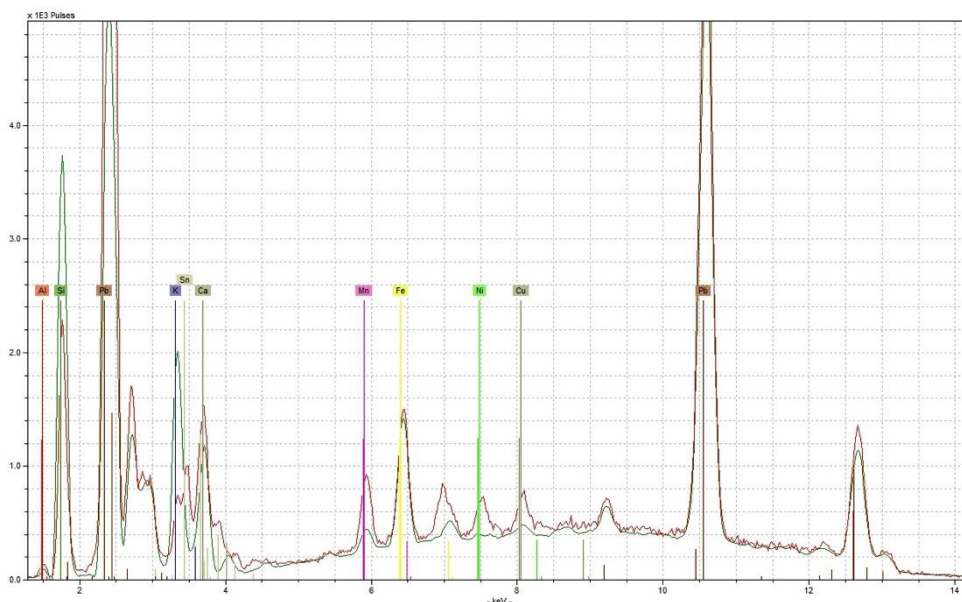


Figure 104 - example spectra for yellow enamel 3 (red trace) and glaze (green trace), showing that the yellow enamel contributes Mn, Ni, Cu, and Sn

Results I: non-invasive techniques

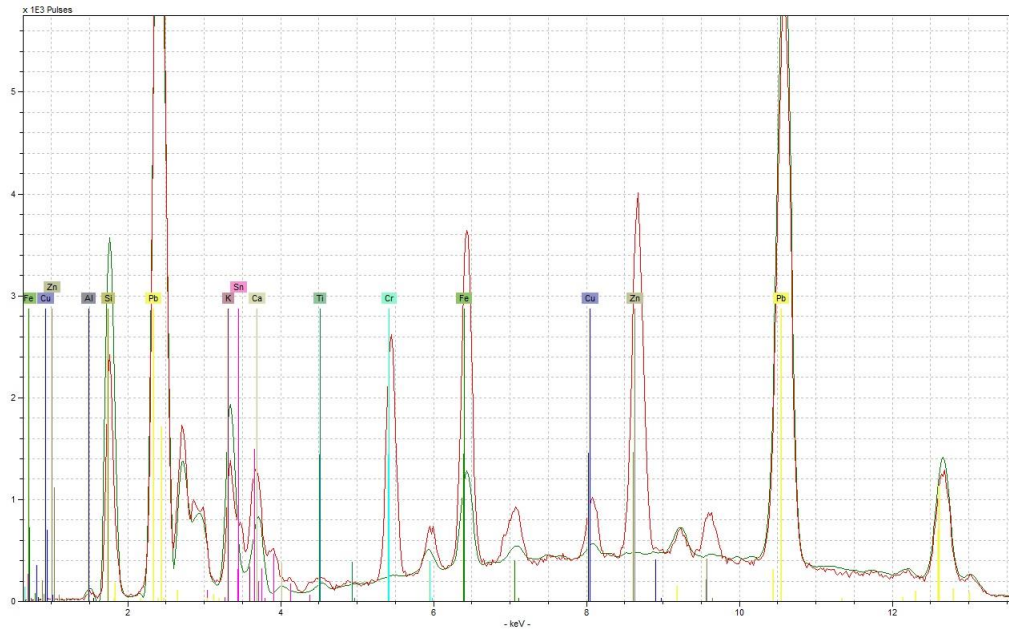


Figure 105 - example spectra for yellow enamel 4 (red trace) and glaze (green trace), showing that the yellow enamel contributes Cr, Mn, Fe, Zn, and Sn



Figure 106 - saucer with turquoise borders and bird painting, attributed to James Giles, on object number 705 . The analysed area of yellow enamel is on the bird's throat, which has adjacent gilding, at the upper centre of the image.

Underglaze blue pigment composition

Underglaze blue painted or printed designs are the form of decoration most commonly found on British porcelain, its origins and chemistry are described in Section 2.2. The pigment takes the form of a glass, known as smalt, the colourant of which is cobalt oxide, which was applied to the surface of the paste prior to the biscuit firing (Delamere, 2013; p. 41). A layer of leaded glaze separates the blue pigment from the analytical equipment, so any analysis of the blue decoration also includes the elements present in the glaze. Furthermore, lighter elements present in the underglaze blue pigment may not be detected, due to the attenuation of the returning fluorescent energy by the lead-rich glaze.

The raw peak area data and example spectra for each compositional category are provided in Appendix A.7, and the elements common to all blue data, including the composition of the overlying glaze, are listed in Table 35. In order to establish compositional categories that are based on the composition of the pigment, rather than reflecting differences in the glaze composition, the peak area data of the glaze for each object were subtracted from the blue data. The compositional categories were then formulated based on the remaining elements, see Table 36.

Table 35 - elements present in underglaze blue decoration

underglaze colour	Elements present
Co blue	Al, Si, K, Ca, Ti, Fe, Co, Ni, Pb

Results I: non-invasive techniques

Table 36 - compositional categories based on elements present in underglaze blue pigment, in addition to Al, Si, K, Ca, Ti, Fe, Co, Ni and Pb

Underglaze blue	Distinctive Elements present	Samples	Factories
1	n/a	Bow pl3, Bow sb1, Bow sb7, Cy tc1, Dby tc1, EMB2, EMB4, EMB5, EMB6, GAH2, JoPen mg1, Lhse sb2, LLK1, LLK6, LLK7, LRd sb1, SPen sb1	Bow, Caughley, Derby, Isleworth, John Pennington, Limehouse, Reid, Seth Pennington, Vauxhall
2	Cu	Bow mg1, Bow pl1, Bow pl3, Bow sb1, Bow sb2, Bow sb3, Bow sb5, Cha tb1, GAH1, GAH5, GAH6, EMB1, EMB3, EMB9, Isl tb1,	Bow, Chaffers, Isleworth, Vauxhall
3	As	Dby vase1, Lowe sb1, Worcs mg1, Worcs tb1	Derby, Lowestoft, Worcester
4	Cu, As	Dby bskt1, Dby sb1, Worcs mg1, Worcs tc1	Derby, Worcester
5	Cu, As, Sn	LH sb1, LH mg1, Vx mg1	Longton Hall, Vauxhall
6	Mn, Cu	Cha sb1, Cpen sb1, Cy tc2, EMB7, Isl sb1, Isl sb2, Jpen sb1, JoPen sb1, LH1, LH2, LH3, LH4, LH5, LH6, Lhse sb1, Lowe sc1, Vx sb1, Vx sb2	Caughley, Chaffers, Christian / Pennington, Isleworth, James Pennington, John Pennington, Limehouse, Longton Hall, Lowestoft, Vauxhall
7	Mn, Sn	LLK4, LLK5	Limehouse
8	Mn, Zn, As	BTr sb1, BTr cp	Bovey Tracey
9	Mn, Cu, Zn, As,	WP1, WP2, WP3, WP4, WP5, WP6	West Pans
10	Cu, Zn	NH sc1, NH sc2	New Hall

Iron, cobalt and nickel are present in all underglaze blue pigments, see Figure 107, at levels greater than the surrounding glaze. Cobalt and nickel show a positive trend in their relationship for all blue pigments, see Figure 108; the ratio between these two elements is perhaps slightly higher in Bovey Tracey and West Pans ($\mu=4.02$, $\sigma=0.29$ and $\mu=2.76$, $\sigma=0.64$ respectively, compared with $\mu=1.37$, $\sigma=0.51$) for the remaining factories).

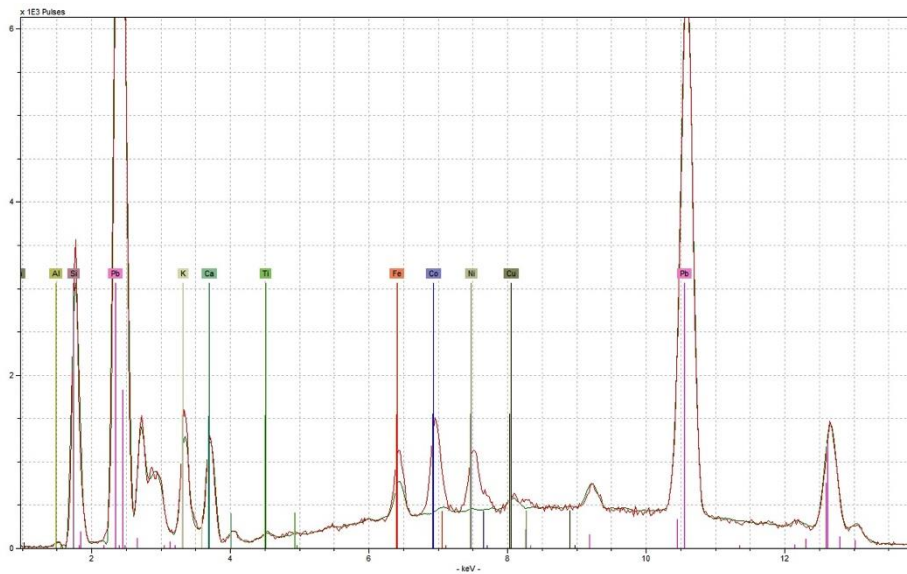


Figure 107 - example spectra for underglaze blue type 1 (red trace) and glaze (green trace), showing that the blue pigment contributes Fe, Co, and Ni

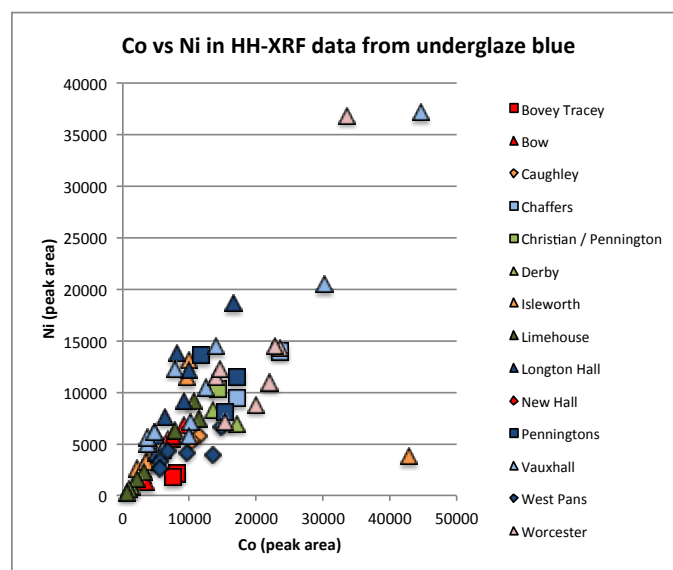


Figure 108 - cobalt versus nickel peak areas from HH-XRF analysis of underglaze blue

Results I: non-invasive techniques

Most underglaze blue pigments also contain manganese, copper, arsenic, or some combination of these elements, see Figure 109. Pigments that contain relatively little copper, relative to cobalt, may show a linear trend between these two elements, for instance, Worcester, Derby and Vauxhall, see Figure 110. Pigments that contain more copper, such as Isleworth and West Pans, show some grouping when these elements are plotted, but the ratios are more variable.

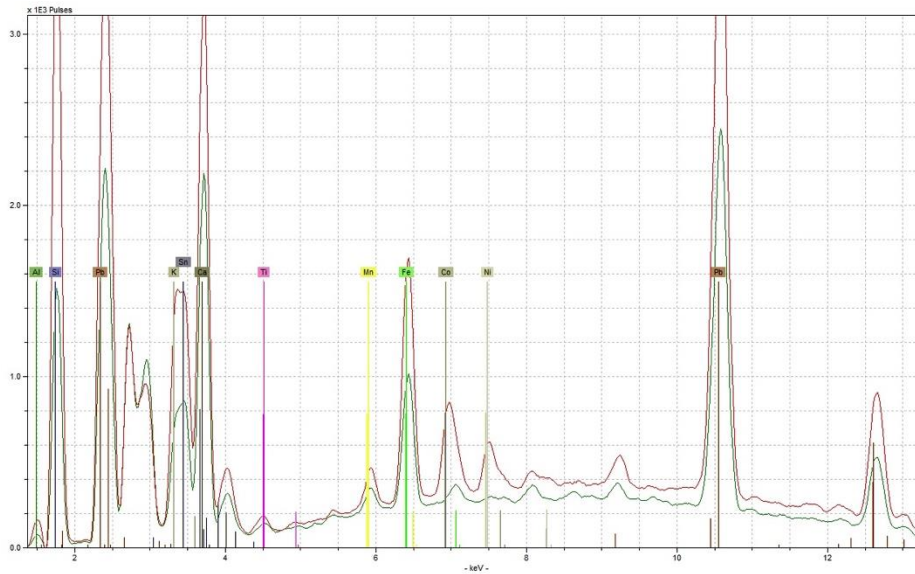


Figure 109 - example spectra for underglaze blue type 6 (red trace) and glaze (green trace), showing that the blue pigment contributes Mn, Co, and Ni

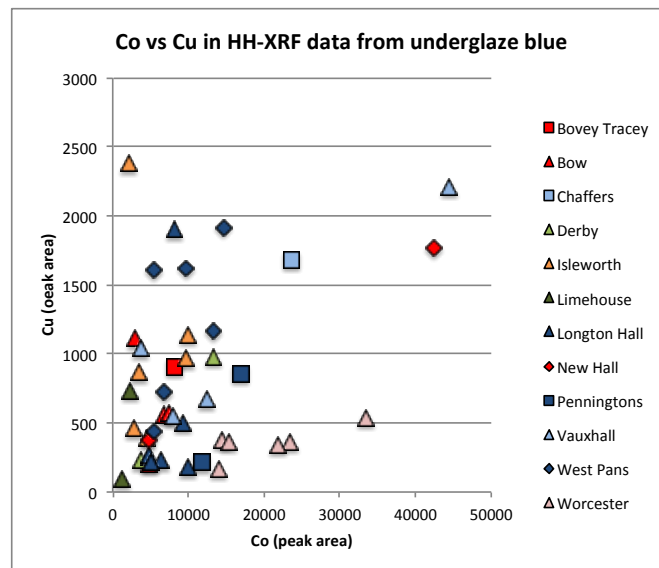


Figure 110 - cobalt versus copper peak areas from HH-XRF analysis of underglaze blue

Arsenic is associated with porcelain from West Pans, Bovey Tracey, some Derby, Limehouse, Longton Hall and Worcester. There appears to be no strong relationship between arsenic and cobalt, although groups are displayed by the Derby, Longton Hall and Bovey Tracey pigments, see Figure 111.

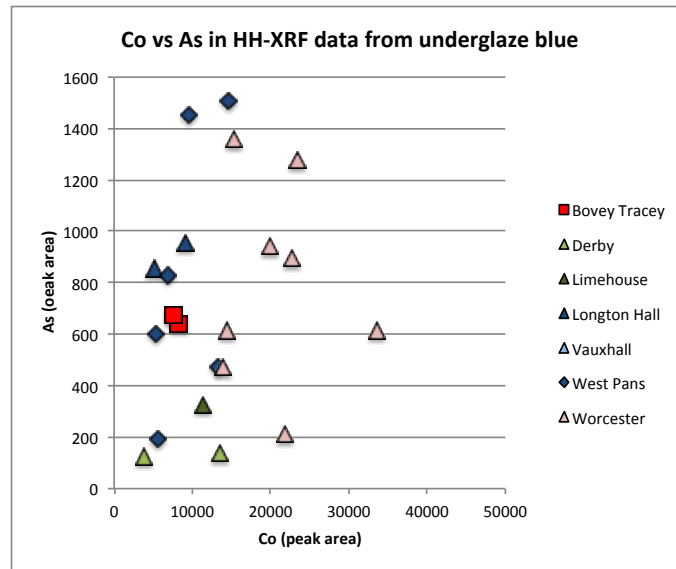


Figure 111 - cobalt versus arsenic peak areas from HH-XRF analysis of underglaze blue

In the case of Bovey Tracey porcelain, the underglaze blue is distinguished by the combination of manganese, zinc, and arsenic; this is similar to the blue pigment found on West Pans porcelain, which contains these elements, plus copper, see Figure 112. These two factories show a similar ratio of cobalt to zinc, see Figure 113, which is generally higher than that for blue pigments containing zinc from Caughley, Chaffers, and Christian/Pennington.

Results I: non-invasive techniques

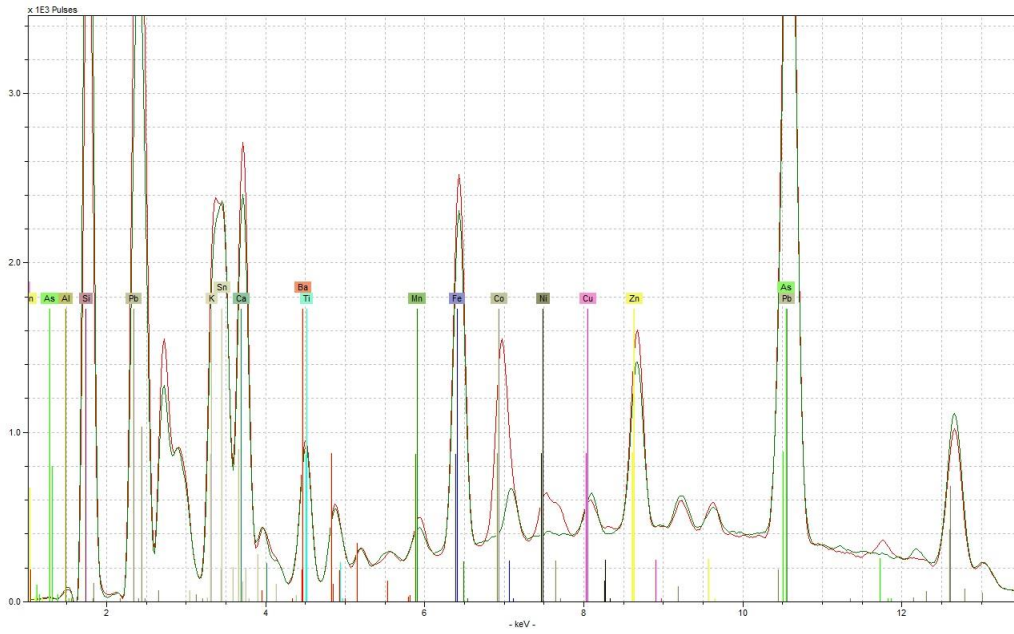


Figure 112 - example spectra for underglaze blue type 9 (red trace) and glaze (green trace) on WP sherd 1, showing that the blue pigment contributes Co, Ni, Zn, and As, and possibly additional Mn, Fe and Cu.

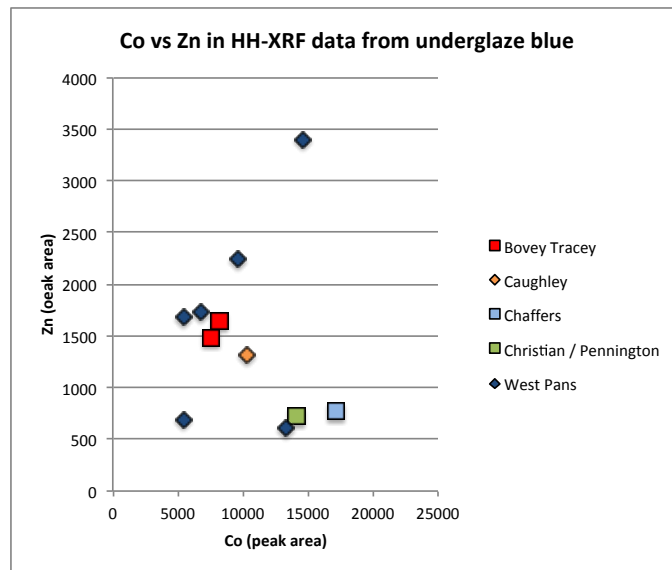


Figure 113 - cobalt versus zinc peak areas from HH-XRF analysis of underglaze blue

Gilding

Gilding is a form of decoration that consists of painted or flaked metallic gold decorations applied to the ceramic surface, and fired on at a low temperature. It often accompanies and overlies polychrome enamel decoration, and very occasionally underglaze blue. In the collection of objects analysed as part of this research, there were many examples of gilding; however, only examples with a sufficiently large areas, separated from polychrome enamels that might contaminate the data, were selected for analysis.

The XRF spectra gained from the gilding were similar to those from the surrounding glaze; probably due to the detection of elements present in the glaze through or around the gilded decoration. Spectra from both the gilding and the glaze are compared below, in order to demonstrate this similarity, and the elements that may be assumed to have been contributed by the gilded decoration because they are absent from the glaze. The elements common to all gilding are shown in Table 37. Compositional categories have been established, on the basis of the presence or absence of elements, see Table 38. Example spectra, and the complete peak area data, are provided in Appendix A.7.

Table 37 - elements present in gilded decoration

gilding	Elements present
metallic gold	Al, Si, K, Ca, Ti, Fe, Cu, Au, Pb

Results I: non-invasive techniques

Table 38 - compositional categories based on elements present in overglaze gilding, in addition to Al, Si, K, Ca, Ti, Fe, Cu, Au and Pb

Gilding	Distinctive Elements present	Samples	Factories
1	n/a	BUK1, 65, 480, 571, 574, 576 (JG), 617, 698 (JG), 704 (JG), 705 (JG), 1016, WJG7, WWR1	Bow, Worcester, James Giles-decorated Worcester
2	Ag	577 (JG), 696 (JG), 703 (JG), 934, 1006, 1010, WJG9	Worcester, James Giles-decorated Worcester
3	Fe	699 (JG), WJG5	James Giles-decorated Worcester
4	Cu, Sn	700 (JG), 914, 919 (JG)	Worcester, James Giles-decorated Worcester
5	Cu, Ag	702 (JG), 804	Worcester, James Giles-decorated Worcester

Besides the metallic gold that gives the gilding its colour and lustre, see Figure 114, the compositional categories are distinguished by the presence or absence of trace silver, copper, iron, and tin, at levels significantly greater than that of the surrounding glaze.

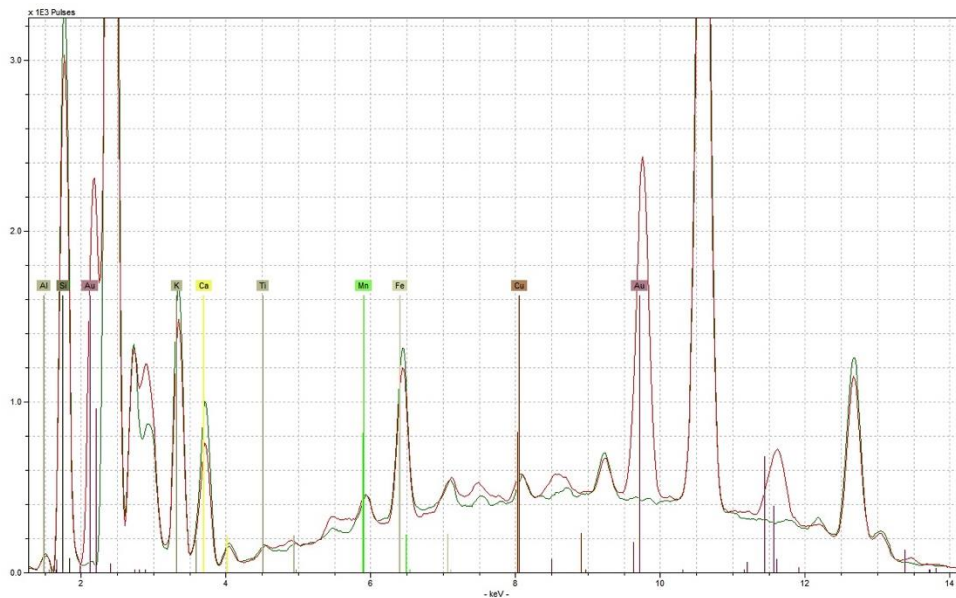


Figure 114 - example spectrum of gilding type 1 (red trace) and glaze (green trace) on object number 480, showing that the gilding contributes Au. Obtained under low-voltage condition.

Silver is found in the gilding of nine out of twenty-seven objects tested, see Figure 115. Due to the very small quantity of silver present, and extensive peak overlap of the silver L peaks at the low energy range of the spectrum, the silver $K\alpha$ and $K\beta$ peaks at the high-energy end of the spectrum was used for identification and quantification. Therefore, the spectrum obtained under the high-energy condition is used to illustrate the presence of this element. There is evidence of a positive trend in the relationship between gold and silver in the objects tested, see Figure 116, which suggests that the silver is present as a trace element in the gold metal used in this pigment.

Results I: non-invasive techniques

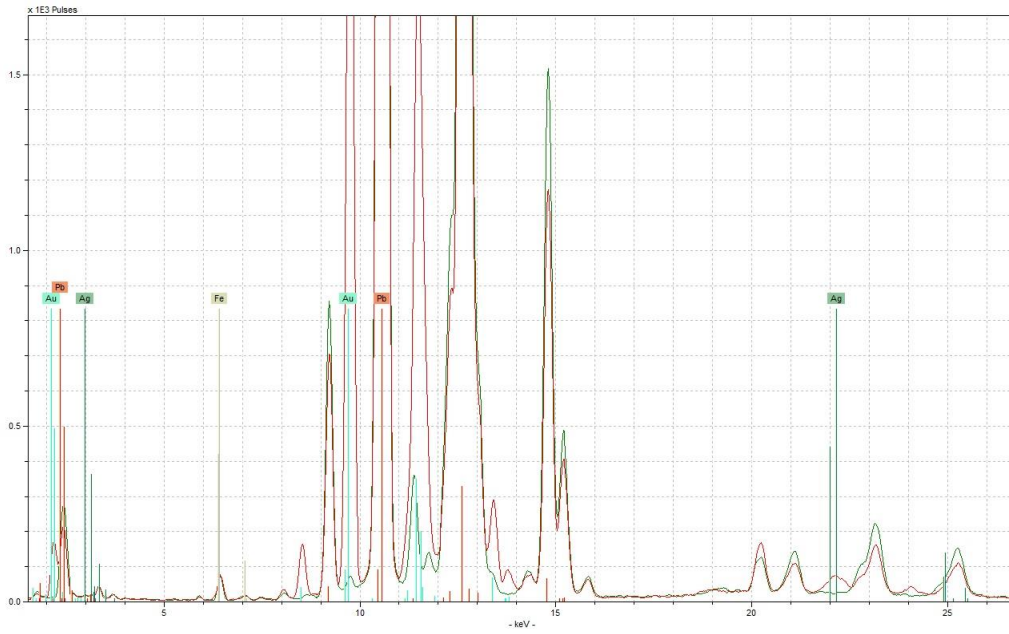


Figure 115 - example spectra of gilding type 2 (green trace) and glaze (red trace) on object number 1010, showing that the gilding contributes Au and Ag. Obtained under the high-voltage condition.

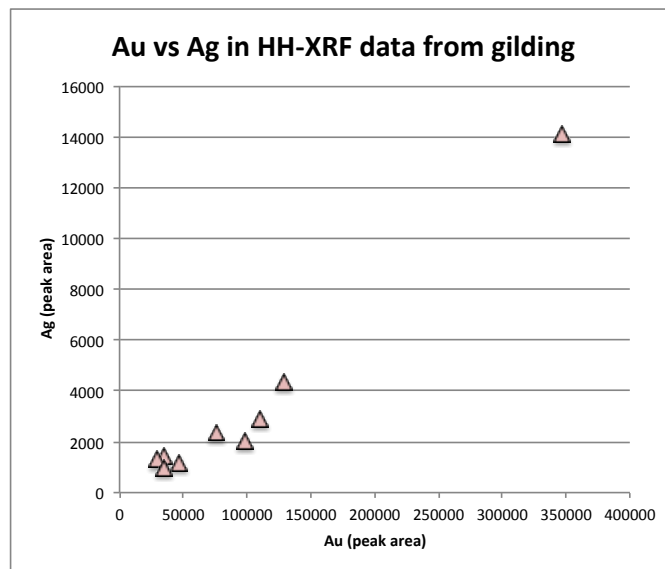


Figure 116 - gold versus silver peak areas from HH-XRF analysis of gilding

Traces of silver are accompanied in two samples by copper, and copper and tin are the distinctive trace elements in a further three samples, see Figure 117.

Results I: non-invasive techniques

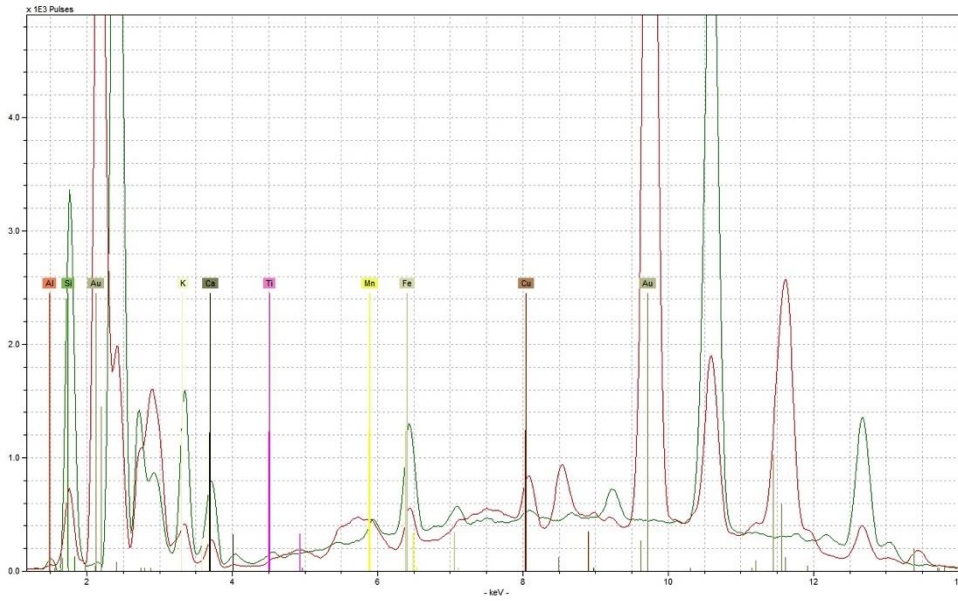


Figure 117 - example spectra for gilding type 4 (red trace) and glaze (green trace) on object number 804, showing that the gilding contributes Cu and Au. Obtained under low voltage condition.

While there is no distinct relationship between the copper and gold present in all samples, see Figure 118, when only those with elevated copper are considered, there appears to be a negative relationship between these two elements. It is therefore possible that copper was added as a secondary colourant in these cases, and that gold therefore shows a dilution effect.

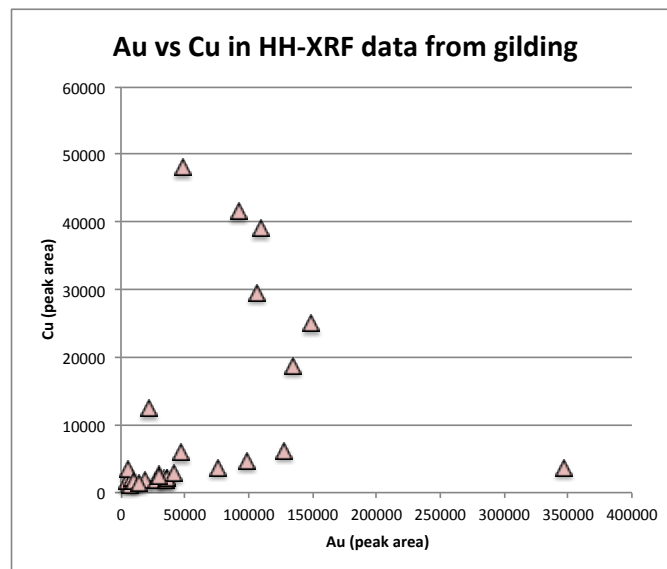


Figure 118 - gold versus copper peak areas from HH-XRF analysis of gilding

5.3 Spectrophotometry

Colorimetry by spectrophotometry was carried out in order to obtain an objective measurement of colour, testing connoisseurship hypotheses that certain factories and groups of porcelain may be distinguished by their colour.

5.3.1 Analysis of intact objects in the Ashmolean Museum, Oxford

Eighteen porcelain objects from four of the factories to which hue in the glaze is commonly ascribed (Chelsea, Bow, Derby, and Worcester), see Section 2.3.1, were analysed using spectrophotometry. The raw data are provided in Appendix A.8, and mean data for L^* , a^* and b^* are given below, Table 39. These mean data are plotted by factory, Figure 119, on a single axis to demonstrate brightness (L^*), and two axes to show hue (a^* green–red, b^* blue–yellow).

Table 39 - mean spectrophotometric data from eighteen porcelain objects

Factory	Sample		$L^*(D65)$	$a^*(D65)$	$b^*(D65)$
Chelsea	WA1967.28.151	μ	86.96	-0.89	2.845
		σ	1.61	0.04	0.02
		$\% \sigma$	1.85	4.77	0.75
	WA1971.351	μ	88.17	-0.55	5.11
		σ	1.02	0.07	0.07
		$\% \sigma$	1.15	12.86	1.38
	LI186.12	μ	86.615	-0.57	3.345
		σ	1.01	0.08	0.12
		$\% \sigma$	1.17	14.89	3.59
	LI186.14	μ	88.75	-0.965	2.92
		σ	1.23	0.08	0.16
		$\% \sigma$	1.39	8.06	5.33
Bow	LI1092.5	μ	86.43	-0.755	6.3
		σ	1.37	0.22	0.57
		$\% \sigma$	1.59	29.03	8.98
	LI1092.3	μ	83.21	-1.055	8.76
		σ	0.79	0.02	0.11
		$\% \sigma$	0.95	2.01	1.29
	LI1092.4	μ	84.37	-0.85	10.285
		σ	1.41	0.04	0.23
		$\% \sigma$	1.68	4.99	2.27
	LI1092.1	μ	85.205	-1.945	5.245
		σ	1.01	0.04	0.08
		$\% \sigma$	1.19	1.82	1.48

Results I: non-invasive techniques

Table 39 - mean spectrophotometric data from eighteen porcelain objects (continued)

Factory	Sample		L*(D65)	a*(D65)	b*(D65)
Derby	WA1971.375	μ	84.805	-2.59	5.61
		σ	1.24	0.11	0.04
		%σ	1.46	4.37	0.76
	WA1957.24.1.58	μ	87.005	-1.255	2.675
		σ	0.50	0.02	0.02
		%σ	0.58	1.69	0.79
	WA1957.24.1.59	μ	87.585	-0.1	5.235
		σ	0.95	0.03	0.19
		%σ	1.09	28.28	3.65
Worcester	WA1957.24.1.704	μ	85.485	-1.225	6.805
		σ	1.86	0.04	0.23
		%σ	2.18	2.89	3.43
	WA1957.24.1.397	μ	60.56	4.415	0.88
		σ	2.01	0.19	0.20
		%σ	3.32	4.32	22.50
	WA1957.24.1.681	μ	83.335	-1.06	4.535
		σ	1.24	0.06	0.06
		%σ	1.48	5.34	1.40
	WA1957.24.1.706	μ	83.555	-1.605	7.785
		σ	2.04	0.05	0.36
		%σ	2.45	3.08	4.63
	WA1957.24.1.599	μ	82.345	-1.195	4.37
		σ	1.66	0.04	0.14
		%σ	2.02	2.96	3.24
	1968.34	μ	84.48	-0.725	1.03
		σ	1.33	0.02	0.06
		%σ	1.57	2.93	5.49
	WA1957.24.1.773	μ	86.925	-2.06	5.04
		σ	0.83	0.01	0.07
		%σ	0.95	0.69	1.40

Results I: non-invasive techniques

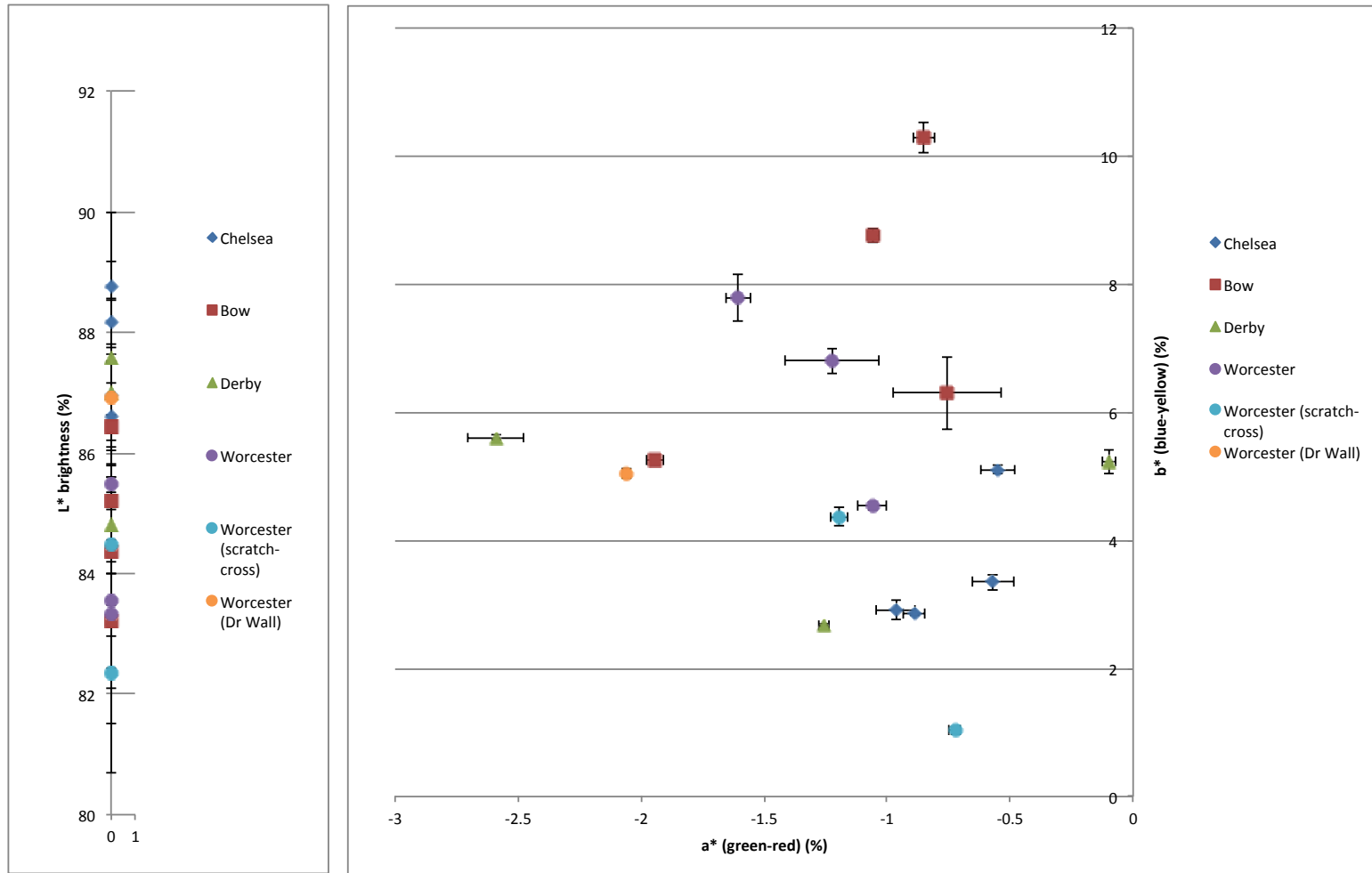


Figure 119 – lightness (left), and hue and chroma (right) of British soft-paste porcelain lead glazes

In all glazes, the level of brightness is high ($\mu = 85.602$; $\sigma = 2.079$), and no individual factory deviates consistently from the mean, see Figure 119. Chelsea and Derby appear to have generally higher brightness than Worcester and Bow in this limited range of samples.

In terms of hue, data from all factories are present within a relatively narrow range, and there are no distinct groups corresponding to factories. All factories plot very close to white (i.e. the a^* and b^* values are very low), and they reflect mostly yellow and green light, which may be attributed to copper (Cu) and iron (Fe) impurities in the paste or glaze, as these oxidise green. Percentage standard deviations from each sample mean are typically greatest on the x axis, and this is particularly the case for Worcester porcelain ($\% \sigma = 2-14$).

In general, Chelsea, Derby, and scratch-cross Worcester are closer to zero on both the a^* and b^* axes, see Figure 119, and therefore closer to a pure white hue. As the “scratch-cross” Worcester is lower on the b^* axis than Dr Wall-period and later Worcester pastes, this supports connoisseurs’ observations that the porcelain is cooler in hue. Bow and non-“scratch-cross” Worcester are slightly higher up the b^* axis towards a yellow hue, and this suggests that they may possess a slightly warmer “cream” tinge. However, these findings require support from more data obtained from a wider range of objects in order to be conclusive.

5.4 Summary and conclusions

In this chapter, two non-invasive analytical techniques – Hand-Held XRF spectroscopy and spectrophotometry – have been tested for their applicability to the characterisation of British porcelain. The aim was to determine whether these techniques are capable of measuring differences in composition or colour that might exhibit inter-factory variation that is consistent, and greater than intra-factory variation.

A well-characterised sample set has been analysed by XRF, to establish the extent to which the counts from the XRF spectra match the quantitative data from SEM-EDS/WDS, and the relationship between data generated by these techniques. The XRF identified the majority of elements present in these samples, and the data sets show a generally good correlation with the quantitative data.

Two sets of intact porcelain objects, and one set of archaeological sherds, were chosen to test connoisseurship hypotheses about certain factories or periods using Hand-Held XRF and spectrophotometry. The presence or absence of elements has been demonstrated to be useful in identifying compositional groups of glazes, overglaze polychrome enamels, and underglaze blue pigments, which may correspond to factories or periods. Colorimetric data provides some tentative support for the idea that porcelain glazes from certain factories or periods may exhibit differences in hue and brightness, although there is significant overlap between factory groups.

In both cases, it seems unlikely that these differences may be used to distinguish porcelain of unknown provenance to the same extent as quantitative data from SEM-EDS/WDS, which have been summarised in Section 3.4.

6 Results II: Laser Ablation Inductively Coupled Plasma Mass Spectroscopy

6.1 Introduction

In this chapter, the results of analysis by LA-ICPMS are presented. These are separated from the main body of results for two reasons: the first is that this analytical technique differs from the others, because the process of analysis requires the removal of a small amount of material, and thus it cannot be considered entirely non-destructive. Although the sampled area is typically invisible to the naked eye, this would still require that special permission be gained from the owner or authority in charge of the objects under examination. The second reason for examining the LA-ICPMS data separately is that they are greater in volume and complexity than the spectroscopic data discussed in the previous chapter. In dealing with quantitative data, the statistical techniques employed are of a different order from those employed in the treatment of qualitative data and the separation into two chapters helps to avoid the impression of comparing like with like.

The results of a methodological test to determine the suitability of the analytical settings and data processing routine are presented first. The results of analysis of the full sample set are then presented; multivariate statistical techniques are used to calculate the variables that have the greatest effect on variability within the data; these variables are then plotted against one another to identify clusters that correspond with similarity in composition and trends that could signify relationships. Finally, Rare Earth Element (REE) profiles and anomalies are explored, to identify the types of raw materials that may have been used in these porcelain pastes.

6.2 Laser Ablation Inductively Coupled Plasma Mass Spectroscopy

6.2.1 Methodological test

To test the effectiveness of the analytical method and calibration procedure, a set of 42 samples for which SEM-EDS data are available were analysed, and the elemental compositional data converted to weight per cent as oxides, in order that the data could be compared directly. The LA-ICPMS data are provided in Table 44, Table 46, Table 45 and Table 47, and the SEM-EDS data are in Appendix A.5. The results of the comparison are presented below, plotted by element (Figure 120).

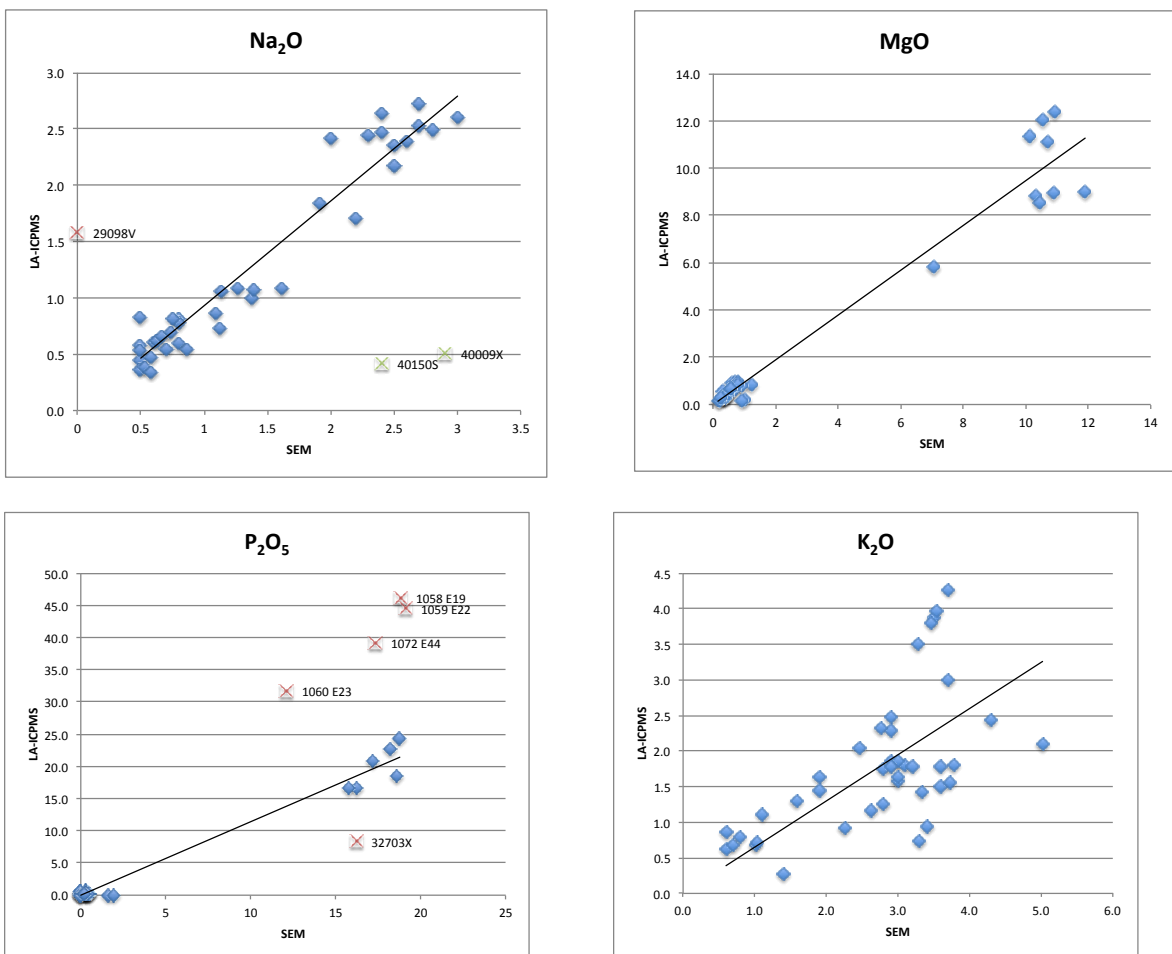


Figure 120 - plots of the SEM-EDS data against the LA-ICPMS data (both in weight per cent as oxides) for 42 of the 62 porcelain pastes for which fully quantitative data were available

Results II: Laser Ablation Inductively Coupled Plasma Mass Spectroscopy

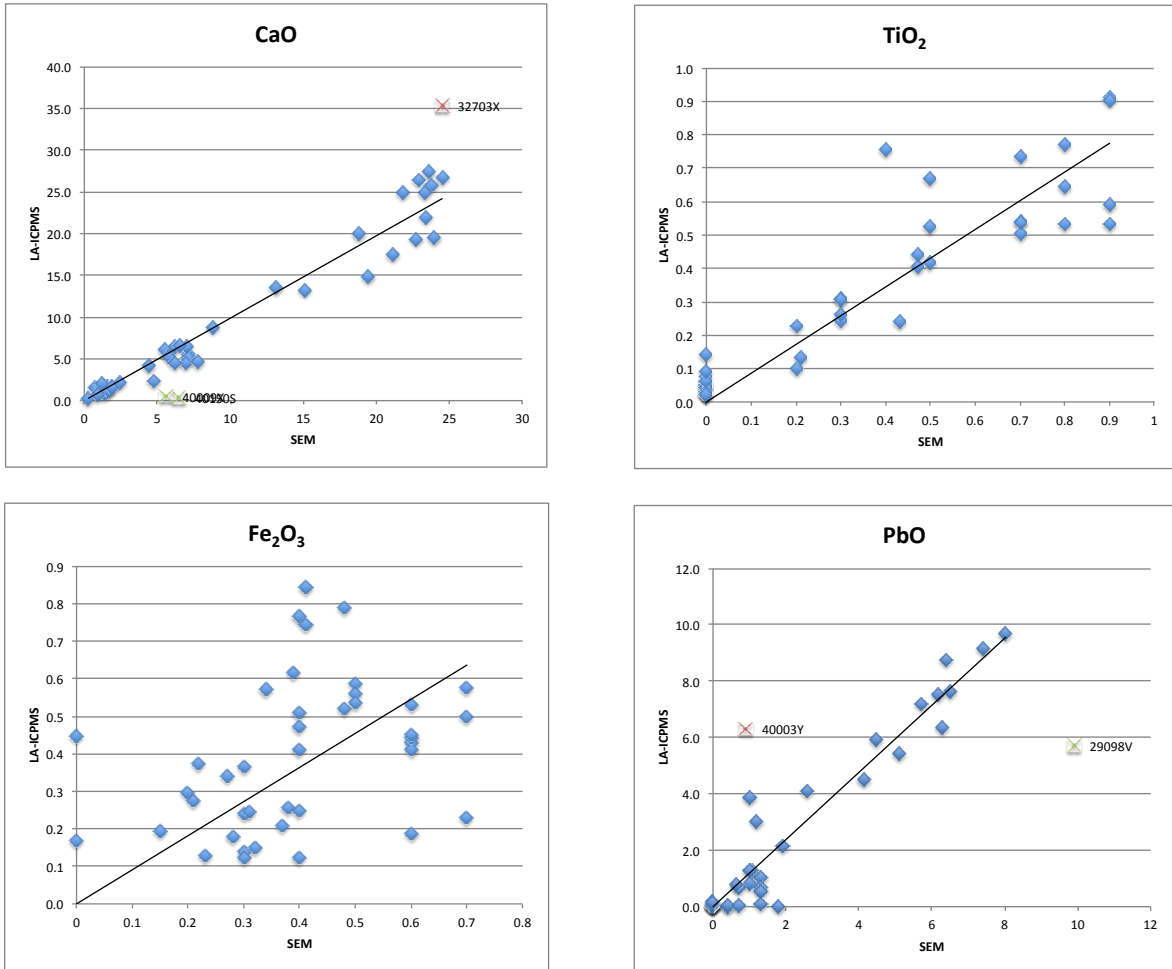


Figure 120 - plots of the SEM-EDS data against the LA-ICPMS data (both in weight percent as oxides) for 42 of the 62 porcelain pastes for which fully quantitative data were available (continued)

A strong linear relationship exists for most elements, and most of the LA-ICPMS results are approximately equal to the SEM-EDS ($y = x \pm 10\%$), see Table 40. Measurement of phosphorus by the ICP-MS is problematic, because it is monoisotopic, and it is affected by interferences with $^{15}\text{N}^{16}\text{O}^+$, and with $^{14}\text{N}^{16}\text{OH}^-$ (Wrobel et al, 2004; p. 240). Interferences that can affect LA-ICPMS analysis of these materials are discussed in Appendix A.2.4. Iron is affected by the very low quantities in which it is present in the glazes, which are close to the limits of quantification of the EDS.

In spite of the polycrystalline composition of the porcelain paste, the laser ablation sampling system appears to be capable of obtaining data that accurately represent the true elemental composition of the object.

Table 40 - linear operator (m) and coefficient of determination (R^2) for the relationship between the SEM-EDS and LA-ICPMS data for ten elements in porcelain pastes

Element	Na ₂ O	MgO	SiO ₂	Al ₂ O ₃	P ₂ O ₅	K ₂ O	CaO	TiO ₂	Fe ₂ O ₃	PbO
linear operator (m)	0.93	0.95	0.99	1.00	1.14	0.65	0.99	0.86	0.91	1.19
coefficient of determination (R^2)	0.93	0.96	0.87	0.82	0.98	0.36	0.95	0.83	0.07	0.93

The glaze results show a weaker correspondence between the data from LA-ICPMS and the published SEM-EDS data, see Figure 121 and Table 41. This may in part be due to the diameter of the sampled area, which in a few cases was greater than the thickness of the glaze, meaning that the data were contaminated by the underlying ceramic body. Thus, elements that are present in the glaze at concentrations significantly higher than the paste are underrepresented in the data (e.g. PbO, SnO₂), while those that are present at higher concentrations in the paste relative to the glaze are overrepresented (e.g. MgO, P₂O₅). The glazes being of different thicknesses, a variable amount of paste material may be included in analyses of different objects, and therefore it is difficult to compensate for the presence of these elements in the glaze data. These contaminated data were removed from consideration, and the remaining glaze data will be treated with caution.

Further differences between the LA-ICPMS data and those from SEM-EDS analysis may be attributed to compositional zoning in the glaze (Owen and Sandon, 1998; Owen, 1998; Owen and Sandon, 2002). The greater magnification power of the SEM, combined with the smaller spot size of the EDS or WDS, allow the analyst to target a specific area of the glaze (surface, middle, zone of interaction with the ceramic body), whereas this level of discrimination is not possible with Laser Ablation sampling. Therefore, the glaze data from LA-ICPMS analysis include the glaze composition from more than one compositional zone, and variation can be as great as 10% rsd for major and minor elements (Owen and Sandon, 1998; Owen, 1998; Owen and Sandon, 2002).

Results II: Laser Ablation Inductively Coupled Plasma Mass Spectroscopy

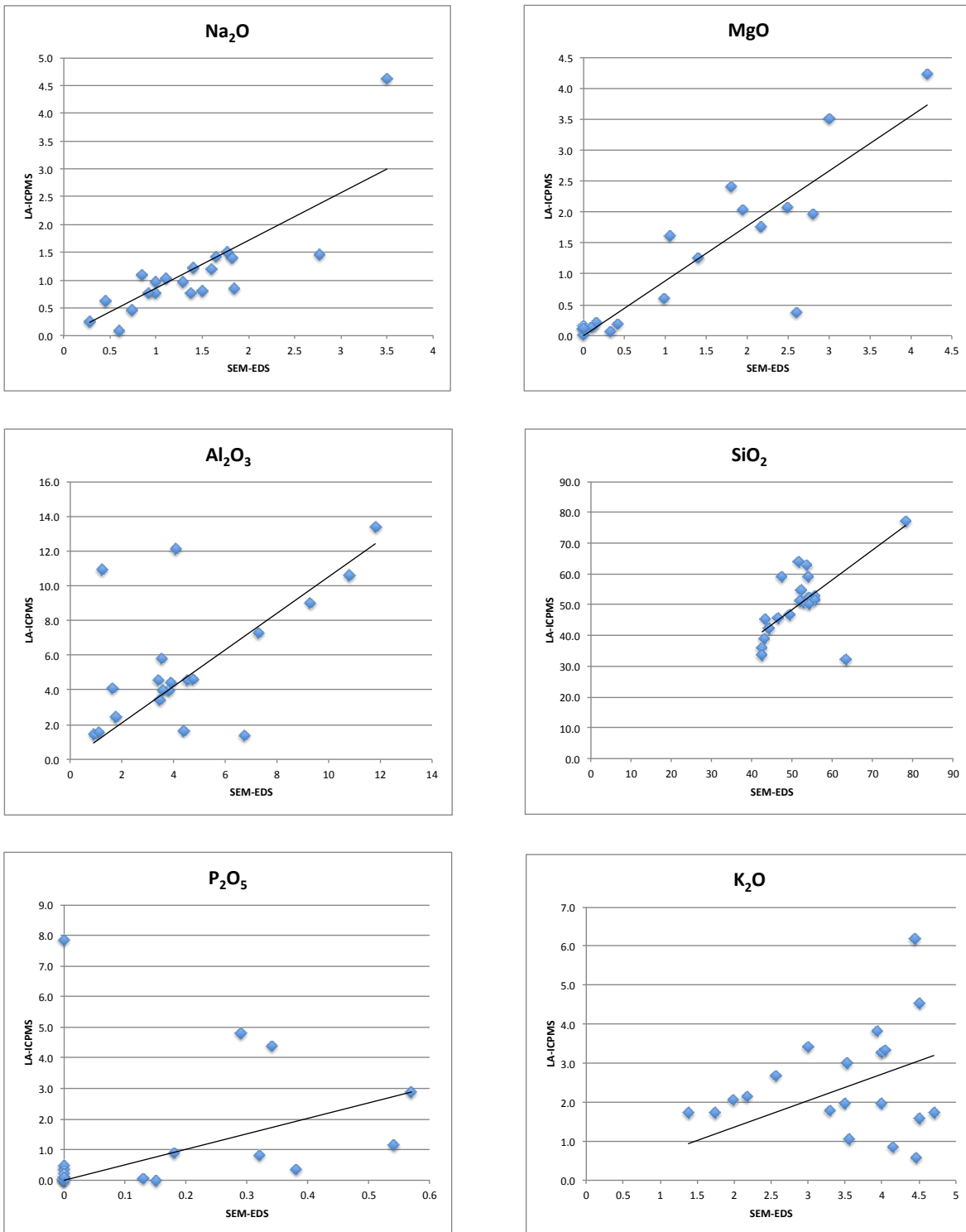


Figure 121 - plots of the SEM-EDS data against the LA-ICPMS data (both in weight percent as oxides) for 27 of the 61 porcelain glazes for which fully quantitative data were available, and which are securely uncontaminated by the underlying ceramic body

Results II: Laser Ablation Inductively Coupled Plasma Mass Spectroscopy

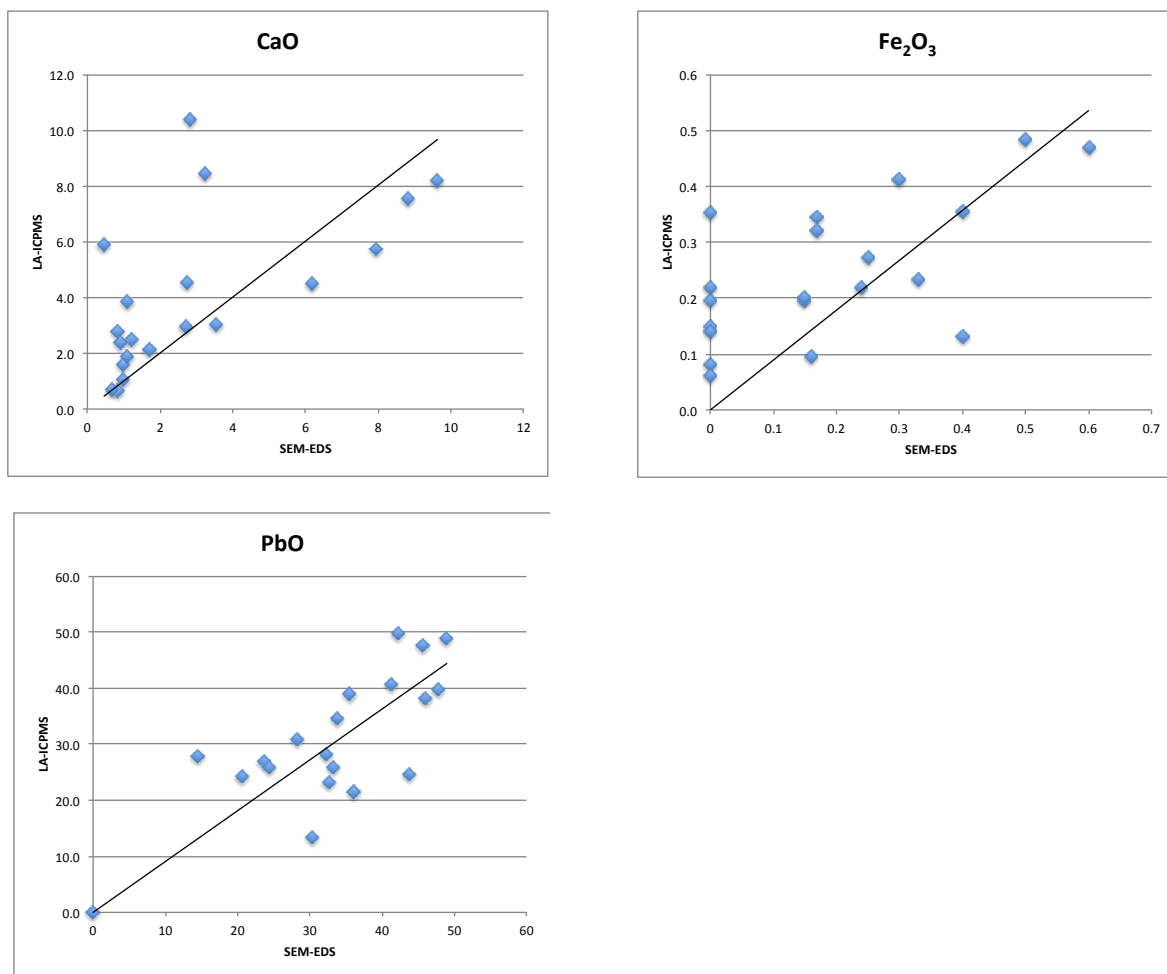


Figure 121 - plots of the SEM-EDS data against the LA-ICPMS data (both in weight percent as oxides) for 27 of the 61 porcelain glazes for which fully quantitative data were available (continued)

Table 41 - linear operator (m) and coefficient of determination (R^2) for the relationship between the SEM-EDS and LA-ICPMS data for nine elements present in porcelain glazes

Element	Na ₂ O	MgO	Al ₂ O ₃	SiO ₂	P ₂ O ₅	K ₂ O	CaO	Fe ₂ O ₃	PbO
linear operator (m)	0.86	0.89	1.05	0.97	5.06	0.68	1.00	0.89	0.91
coefficient of determination (R^2)	0.69	0.78	0.21	0.34	0.01	0.05	0.03	0.41	0.57

The accuracy of results and calibration in each run was measured by comparing the measured and expected values for three glass certified reference materials: Corning Museum of Glass (CMG) standard A, National Institute of Standards and Technology (NIST) standard 610 and NIST standard 612. The expected and measured values are compared in Table 65, and the mean values for the difference (Δ) between the measured and expected values for NIST 610, NIST 612 and CMG A are shown in Figure 122.

Results II: Laser Ablation Inductively Coupled Plasma Mass Spectroscopy

Table 42 - expected and mean measured values (μ) for NIST 610, NIST 612 and CMG A, with the mean difference ($\mu\Delta$) that has been used in Figure 122

	NIST 610				NIST 612				CMG A				
	Certified values	μ	σ	$\mu\Delta$	Certified values	μ	σ	$\mu\Delta$	Shortland et al (2007)	Wagner (2012)	μ	σ	$\mu\Delta$
Li	468	457	29	-2	40.2	39	3	-2	46.0	51.1	47	4	3
B	350	268	67	-14	34.3	30	4	-20	537.0	850.9	468	133	-3
Na	99406.53	102418	2306	2	101640.3	103663	2325	3	106083.1	99406.53	105133	8669	-1
Mg	432	479	72	-5	68	65	10	13	16043.4	15078.41	16009	2432	0
Al	10317.46	10524	344	1	10740.74	10867	230	2	5291.0	4338.62	5098	568	-2
Si	325548.8	325353	4091	-1	336758.5	334656	2422	0	310882.8	316767.87	311545	10211	0
P	543	421	117	-7	55	50	16	-7	341.0	370.92	548	340	3
K	464	384	94	9	62.3	69	23	-12	22639.0	28713.69	24095	22176	-2
Ca	81486.77	85411	6089	2	85060.75	86554	2389	5	35954.0	35310.94	36377	5818	-1
Ti	452	419	34	0	44	44	6	-7	4226.0	4427.80	4276	453	1
V	450	470	17	2	38.8	40	1	5	34.1	39.2	37	2	10
Cr	408	408	26	-1	36.4	38	9	0	17.9	20.52	21	6	8
Mn	444	449	33	-2	38.7	38	4	1	6921.0	8751.55	8025	798	16
Fe	458	473	87	-2	51	48	13	4	6537.0	6841.37	7063	2919	4
Co	375	451	30	6	35.5	38	3	20	1188.0	1336.48	1512	181	14
Ni	458.7	469	30	2	38.8	39	2	1	160.0	180.82	217	138	10
Cu	441	443	84	3	37.8	38	7	1	7842.0	8785.94	9772	2069	11
Zn	460	515	68	6	39.1	41	5	13	410.0	385.54	461	73	6
As	325	404	58	12	35.7	42	5	24	25.3	n/r	39	16	10
Rb	425.7	443	139	-6	31.4	32	11	-3	81.5	82.3	87	25	-1
Sr	515.5	522	31	0	78.4	78	3	1	860.0	896.8	976	93	14
Y	462	497	31	5	38.3	40	2	8	n/r	n/r	0	0	-
Zr	448	460	24	2	37.9	39	1	3	39.9	37.01	41	3	3
Nb	465	495	23	3	38.9	40	2	7	0.6	n/r	1	0	11

n/r = not reported

Results II: Laser Ablation Inductively Coupled Plasma Mass Spectroscopy

Table 42 - expected and mean measured values (μ) for NIST 610, NIST 612 and CMG A, with the mean difference ($\mu\Delta$) that has been used in Figure 122

NIST 610	NIST 610				NIST 612				CMG A				
	Certified values	μ	σ	$\mu\Delta$	Certified values	μ	σ	$\mu\Delta$	Shortland et al (2007)	Wagner (2012)	μ	σ	$\mu\Delta$
Mo	417	434	17	1	37.4	38	1	4	n/r	n/r	3	1	-
Ag	251	235	21	-9	22	20	2	-6	14.4	n/r	15	1	7
Sn	430	458	40	4	38.6	40	3	7	1194.0	1357.14	1686	373	15
Sb	396	452	47	7	34.7	37	6	15	10649.0	14001.81	15681	2616	23
Cs	366	417	32	9	42.7	47	4	14	0.2	n/r	0	0	18
Ba	452	438	30	-3	39.3	38	3	-3	3905.0	4121.86	4273	440	9
La	440	452	25	0	36	36	2	3	0.3	n/r	0	0	12
Ce	453	443	42	-4	38.4	37	2	-2	0.2	n/r	1	1	8
Pr	448	494	29	7	37.9	41	3	11	n/r	n/r	0	0	-
Nd	430	433	24	0	35.5	35	2	1	n/r	n/r	0	0	-
Sm	453	444	32	-2	37.7	37	2	-2	n/r	n/r	0	0	-
Eu	447	452	24	0	35.6	35	2	1	n/r	n/r	0	0	-
Gd	449	431	32	-3	37.3	36	2	-4	n/r	n/r	0	0	-
Tb	437	448	30	-3	37.6	36	2	3	n/r	n/r	0	0	-
Dy	437	444	31	1	35.5	36	2	2	n/r	n/r	0	0	-
Ho	449	455	35	-3	38.3	37	2	2	n/r	n/r	0	0	-
Er	455	445	28	-3	38	37	2	-2	n/r	n/r	0	0	-
Tm	435	443	30	-2	36.8	36	2	2	n/r	n/r	0	0	-
Yb	450	450	39	-4	39.2	38	3	0	n/r	n/r	0	0	-
Lu	439	455	31	-1	37	37	2	4	n/r	n/r	0	0	-
Hf	435	424	28	-3	36.7	36	2	-2	n/r	n/r	1	0	-
Pb	426	464	69	-6	38.57	36	6	-3	595.0	677.67	2059	3208	7
Bi	384	341	27	-6	30.2	28	2	-11	7.8	8.97	8	1	2
Th	457.2	453	34	-4	37.79	36	2	-1	0.3	n/r	0	0	-1
U	461.5	437	46	-7	37.38	35	2	-5	0.2	n/r	0	0	7

n/r = not reported

Results II: Laser Ablation Inductively Coupled Plasma Mass Spectroscopy

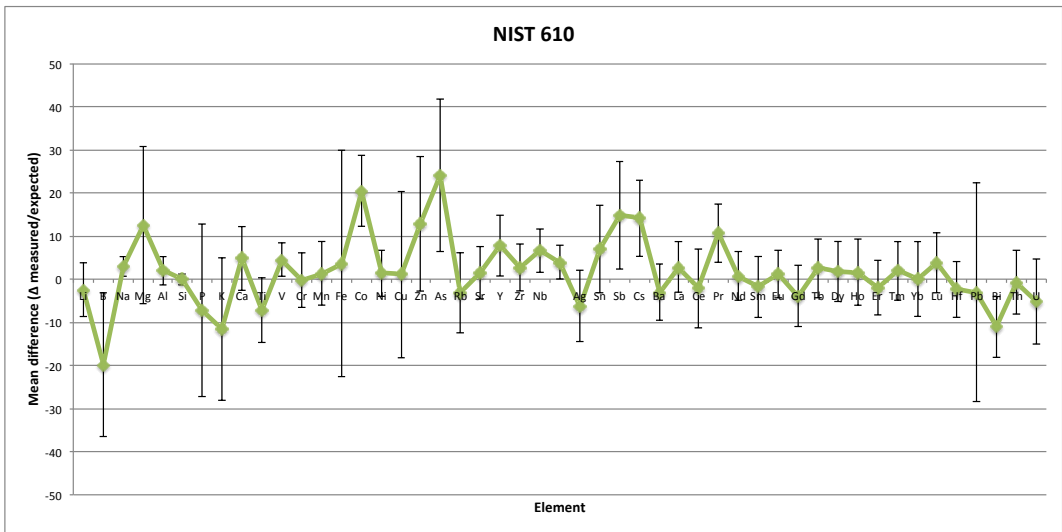
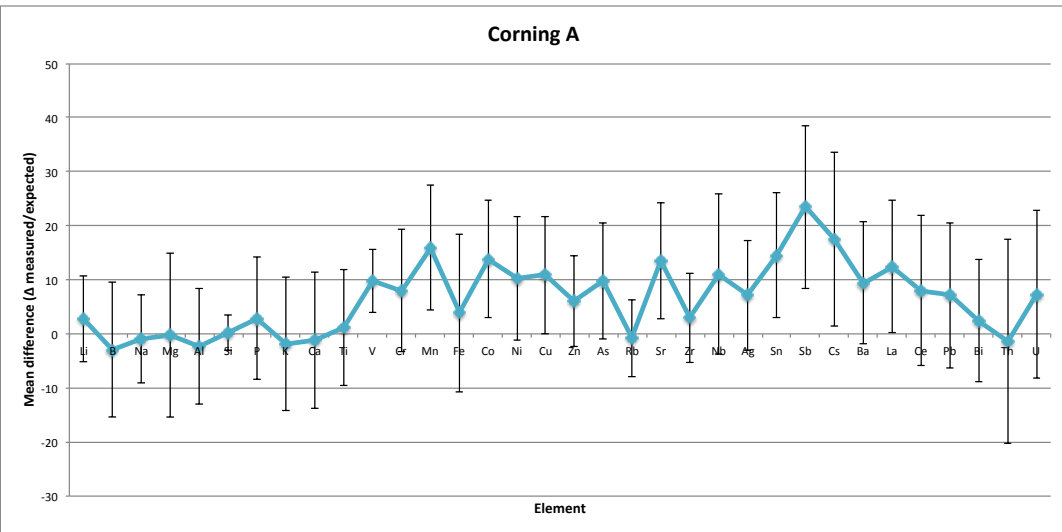
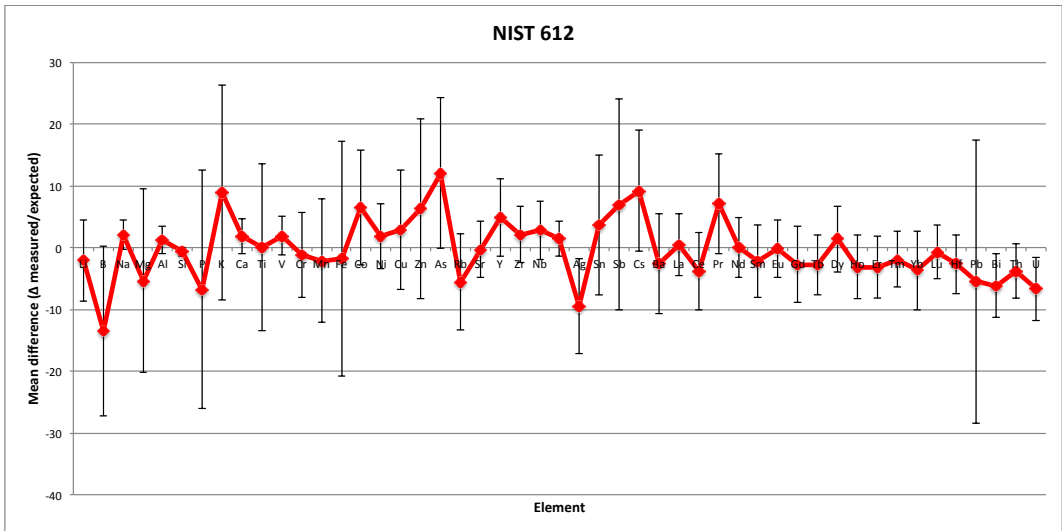


Figure 122 - mean difference (Δ) between calibrated LA-ICPMS data and reference data for 49 elements in three glass standards. Error bars represent a single standard deviation.



6.2.2 Analysis of porcelain bodies

The 58 mounted samples of porcelain, listed in Table 43, were analysed under the conditions that had been found to be effective in the methodological test. Tables of data for 49 elements measured in porcelain bodies are provided in Appendix A.9, and summarised below, as the major and minor elements in weight percent as oxides, trace element ratios, and rare earth element (chondrite normalised) profiles. The major and minor elemental compositional data are used to assess the paste recipe, based on the four compositional categories that are commonly employed to classify British soft-paste porcelain, which have been described in Section 2.3.2. The data are divided into these categories: phosphatic (Table 44); magnesian, (Table 46); frit, (Table 45); and SAC or hybrid hard-paste, (Table 47).

Table 43 - samples analysed using Laser Ablation Inductively Coupled Plasma Mass Spectroscopy

Sample	Factory	Paste	CRS	Eccles	V&A number	body	glaze
32699 W	Chelsea	glassy	746			*	*
32700 S	Worcester	soapstone	741			*	*
32701 Q	Plymouth	hard-paste	744			*	*
32702 Z	Pomona (Newcastle)	phosphatic				*	*
32703 X	Bow	phosphatic				*	*
32704 V	Chaffers (Liverpool)	soapstone	743			*	*
32705 T	Ball (Liverpool)	phosphatic				*	*
32706 R	Ball (Liverpool)	phosphatic				*	*
32707 P	Lowestoft	phosphatic				*	*
29102 W	Bristol	hard-paste		2	c352 1903	*	*
29099 T	Worcester	magnesian		26	c591 1919	*	*
29263 P	Worcester	magnesian		29	c517 1919	*	*
29101 Y	Lowestoft	phosphatic		8	c674 1920	*	*
29098 V	Longton hall	phosphatic		9	c8 1920	*	*
29103 U	Chelsea (red anchor)	glassy		7	c514 1919	*	*
29105 Q	Bow	phosphatic		10	c673 1920	*	*
29100 P	Bow	phosphatic		12	c590 1919	*	*
29104 S	Bow	phosphatic		14	c16 1920	*	*
29106 Z	Chelsea (gold anchor)	glassy		15	c511 1919	*	*

Results II: Laser Ablation Inductively Coupled Plasma Mass Spectroscopy

Table 43 - samples analysed using Laser Ablation Inductively Coupled Plasma Mass Spectroscopy
(continued)

Sample	Factory	Paste	CRS	Eccles	V&A number	body	glaze
36554 Q	Swansea	bone china	892			*	*
40149 P	Limehouse	SAC				*	*
40012 W	Limehouse	SAC				*	*
40011 Y	Limehouse	SAC				*	*
40010 P	Limehouse	SAC				*	*
40009 X	Limehouse	SAC				*	*
40008 Z	Limehouse	SAC				*	*
40007 Q	Limehouse	SAC				*	*
40006 S	Limehouse	SAC				*	*
40000 S	Limehouse	SAC				*	*
40004 W	Limehouse	SAC				*	*
40003 Y	Limehouse	SAC				*	*
40002 P	Limehouse	SAC				*	*
47122 R	'A'-marked	hard-paste				*	
1056	Crown Derby	bone china	1056	17		*	*
1057	Crown Derby	bone china	1057	18		*	*
1058	Pinxton	bone china	1058	19		*	*
1059	Nantgarw	bone china	1059	22		*	*
1060	Swansea	bone china	1060	23		*	*
1072	Coalport	bone china	1072	44		*	*
1062	Worcester	magnesian	1062	27		*	*
1063	Worcester	magnesian	1063	31		*	
1064	Worcester	magnesian	1064	32		*	*
1065	Worcester	magnesian	1065	34		*	
1066	Worcester	magnesian	1066	35		*	*
1067	Worcester	magnesian	1067	36		*	*
1068	Worcester	magnesian	1068	37		*	*
1069	Caughley	magnesian	1069	39		*	*
1070	Swansea	bone china	1070	40		*	*
1071	Swansea	bone china	1071	41		*	*
1053	New Hall	phosphatic	1053	3		*	*
1054	New Hall	phosphatic	1054	4		*	*
1055	Chelsea	glassy	1055	6		*	*
1076	Chelsea	glassy	1076			*	*

Results II: Laser Ablation Inductively Coupled Plasma Mass Spectroscopy

Table 44 - LA-ICPMS data for British porcelain phosphatic bodies in weight percent as oxides

Label	Factory	Na ₂ O	MgO	Al ₂ O ₃	SiO ₂	P ₂ O ₅	K ₂ O	CaO	TiO ₂	MnO	Fe ₂ O ₃	PbO
29105Q	Bow	0.77	0.71	8.28	41.65	18.55	1.11	27.44	0.42	0.00	0.59	0.07
29100P	Bow	0.37	0.40	5.65	49.50	16.60	0.69	25.72	0.23	0.00	0.45	0.03
29104S	Bow	0.54	0.37	6.04	48.11	16.59	0.62	26.82	0.26	0.00	0.37	0.03
32703X	Bow	0.83	0.54	5.98	47.39	8.33	0.86	35.43	0.24	0.00	0.14	0.00
29106Z	Chelsea	0.60	0.53	9.80	41.92	20.80	0.27	25.00	0.53	0.00	0.24	0.03
1072 E44	Coalport	1.08	0.41	9.75	30.27	39.27	1.30	17.47	0.06	0.00	0.27	0.00
1057 E18	Crown Derby	0.62	0.68	9.42	37.96	22.69	0.72	26.37	0.41	0.00	0.79	0.04
1056 E17	Crown Derby	0.66	0.68	9.06	37.93	24.37	0.79	24.90	0.44	0.00	0.75	0.18
32707P	Lowestoft	0.45	0.35	6.18	52.37	12.24	0.19	27.55	0.24	0.00	0.06	0.04
1059 E22	Nantgarw	0.73	0.29	9.13	24.18	44.45	1.45	19.45	0.02	0.00	0.19	0.03
1058 E19	Pinxton	0.39	0.44	6.83	25.37	46.13	0.68	19.41	0.24	0.00	0.37	0.05
1060 E23	Swansea	1.00	0.30	16.15	35.07	31.69	2.05	13.22	0.02	0.00	0.34	0.01

Table 45 - LA-ICPMS data for British porcelain frit bodies in weight percent as oxides

Label	Factory	Na ₂ O	MgO	Al ₂ O ₃	SiO ₂	P ₂ O ₅	K ₂ O	CaO	TiO ₂	MnO	Fe ₂ O ₃	PbO
32699W	Chelsea	0.45	0.25	4.67	71.44	0.11	2.44	13.55	0.31	0.07	0.41	5.42
29103U	Chelsea	0.58	0.29	4.14	67.87	0.16	3.88	20.01	0.31	0.07	0.30	2.17
66983 Y1	Chelsea	0.57	0.27	6.33	68.69	0.09	2.62	16.81	0.16	0.06	0.21	3.83
1055 E6	Chelsea	0.34	0.25	4.10	69.66	0.06	2.09	22.00	0.13	0.08	0.15	0.77
29101Y	Longton Hall	0.59	0.25	2.72	75.07	0.04	4.27	8.74	0.14	0.05	0.17	6.38
29098V	Longton Hall	1.59	0.33	2.60	76.91	0.00	6.63	4.88	0.10	0.04	0.12	5.73

Results II: Laser Ablation Inductively Coupled Plasma Mass Spectroscopy

Table 46 - LA-ICPMS data for British porcelain magnesian bodies in weight percent as oxides

Label	Factory	Na ₂ O	MgO	Al ₂ O ₃	SiO ₂	P ₂ O ₅	K ₂ O	CaO	TiO ₂	MnO	Fe ₂ O ₃	PbO
1069 E39	Caughley	0.71	8.61	5.63	73.39	0.07	4.15	1.04	0.07	0.04	1.53	4.60
32704V	Chaffers	1.72	8.99	4.43	78.55	0.01	2.48	2.44	0.06	0.09	0.23	0.12
32705T	Chaffers	0.78	9.91	2.87	67.64	0.00	9.38	7.55	0.44	0.17	0.30	2.18
32706R	Chaffers	2.15	7.79	3.85	77.40	1.14	1.15	4.70	0.06	0.05	0.16	1.99
32702Z	Pomona	0.70	10.01	3.01	74.02	0.17	2.00	1.40	0.05	0.05	0.43	7.75
29099T	Worcester	0.72	11.71	4.18	72.40	0.27	3.12	1.55	0.07	0.06	0.62	4.65
29263P	Worcester	0.71	11.04	3.29	70.41	0.15	3.63	1.08	0.06	0.04	0.87	8.31
1065 E34	Worcester	1.07	12.38	3.11	68.97	0.34	3.51	1.67	0.08	0.04	0.84	7.17
1064 E32	Worcester	1.08	11.33	2.84	67.41	0.33	3.97	2.28	0.04	0.05	0.62	9.66
1063 E31	Worcester	0.86	12.06	3.35	68.67	0.21	3.79	0.94	0.05	0.05	0.57	9.14
1062 E27	Worcester	0.55	11.14	2.80	76.32	0.19	2.32	1.22	0.05	0.04	0.52	4.48
1068 E37	Worcester	0.81	5.83	6.20	77.41	0.06	1.80	1.52	0.04	0.02	0.13	5.90
1067 E36	Worcester	0.69	8.83	3.04	75.85	0.14	1.17	1.61	0.06	0.05	0.24	7.52
1066 E35	Worcester	0.47	8.55	2.81	74.91	0.04	1.43	2.00	0.09	0.02	0.26	8.76
32700S	Worcester	0.81	8.97	3.30	73.91	0.06	2.99	1.67	0.05	0.04	0.12	7.63

Table 47 - LA-ICPMS data for British porcelain SAC and hybrid hard-paste bodies in weight percent as oxides

Label	Factory	Na ₂ O	MgO	Al ₂ O ₃	SiO ₂	P ₂ O ₅	K ₂ O	CaO	TiO ₂	MnO	Fe ₂ O ₃	PbO
47122R	'A'-marked	3.80	1.47	20.32	63.01	0.72	3.46	5.72	0.06	0.06	0.44	0.48
40419P	Limehouse	2.53	0.83	12.09	74.11	0.54	1.80	5.56	0.77	0.04	0.43	0.85
40150S	Limehouse	0.42	0.20	16.99	79.62	0.00	0.74	0.40	0.91	0.00	0.58	0.01
40012W	Limehouse	2.64	0.91	13.03	73.01	0.41	1.78	5.58	0.53	0.03	0.50	1.29
40011Y	Limehouse	2.35	0.81	11.26	74.79	0.45	1.78	6.18	0.50	0.02	0.41	1.03

Results II: Laser Ablation Inductively Coupled Plasma Mass Spectroscopy

Table 47 - LA-ICPMS data for British porcelain SAC and hybrid hard-paste bodies in weight percent as oxides (continued)

Label	Factory	Na₂O	MgO	Al₂O₃	SiO₂	P₂O₅	K₂O	CaO	TiO₂	MnO	Fe₂O₃	PbO
40010P	Limehouse	2.49	0.99	11.38	74.86	0.58	1.64	5.19	0.65	0.03	0.56	1.27
40009X	Limehouse	0.51	0.18	19.13	77.34	0.03	0.94	0.55	0.90	0.00	0.25	1.03
40008Z	Limehouse	2.60	0.63	10.02	75.90	0.12	2.30	6.54	0.54	0.02	0.19	1.66
40007Q	Limehouse	2.40	0.91	13.12	73.09	0.79	1.26	6.45	0.54	0.03	0.47	2.69
40006S	Limehouse	2.73	0.95	12.67	74.28	0.65	1.50	5.28	0.53	0.03	0.51	1.54
40000S	Limehouse	2.44	0.90	10.38	74.23	0.13	1.86	4.58	0.67	0.02	0.53	3.87
40004W	Limehouse	2.47	0.93	11.93	71.48	0.14	1.75	6.63	0.74	0.03	0.44	3.04
40003Y	Limehouse	2.17	0.79	11.41	71.43	0.13	1.86	4.44	0.59	0.02	0.45	6.31
40002P	Limehouse	2.42	0.87	10.88	73.51	0.09	1.78	4.66	0.76	0.02	0.53	4.09
1054 E4	New Hall	1.06	0.15	19.40	73.71	0.07	0.92	4.18	0.03	0.01	0.21	0.08
1053 E3	New Hall	1.85	0.16	24.96	70.01	0.19	1.56	0.71	0.02	0.01	0.18	0.13
32701Q	Plymouth	0.54	0.26	22.04	74.04	0.20	1.58	0.23	0.03	0.01	0.76	0.00
36554Q	Swansea	0.47	0.22	19.07	77.41	0.00	0.76	0.30	0.94	0.00	0.66	0.00
1070 E40	Swansea	1.14	2.63	7.23	85.60	0.13	2.36	0.46	0.04	0.00	0.15	0.15

Trace elements in porcelain pastes

Trace element ratios are used to characterise the porcelain pastes by their trace elemental composition, in preference to absolute amounts of the trace elements present. This is because the trace elements were not typically added deliberately as part of the paste recipe, but became included as contaminants in other raw materials, such as clay and quartz sand. Therefore, the amount of any given trace element present depends on the amount of the corresponding raw material. However, each raw material may contribute numerous trace elements, and in varying concentrations, depending on the processes that have been carried out to prepare it for inclusion in the paste, such as washing or filtration. Trace element ratios provide a more accurate means of comparing the trace elemental profile within and between factories.

For the purposes of this research, the definition of trace elements used is that defined by geology and archaeometry. In these disciplines, a trace element is an element that is present at <0.1 % (1000ppm) of an object or mineral phase (Rollinson, 1993; p. 102). Their low concentration means that an individual trace elements cannot be a stoichiometric component of the material, i.e. they do not individually contribute to the calculation of the sample composition in weight percent (White, 2013; p. 269). The trace elements measured in this analysis are illustrated below, see Figure 123.

The trace elements, with the exception of the rare earth elements (REEs), were plotted to demonstrate their distribution within the sample set, see Figure 124. Most show variation within a narrow range around the mean, but Ba, Sb, Sn, Zr, Sr, As, Zn, and Cu have outliers. The extent of the trace elements' pairwise correlation with one another was plotted, see Table 48, and are mostly low (<0.5).

Results II: Laser Ablation Inductively Coupled Plasma Mass Spectroscopy



Figure 123 - elements measured during analysis of British porcelain pastes and glazes using LA-ICPMS

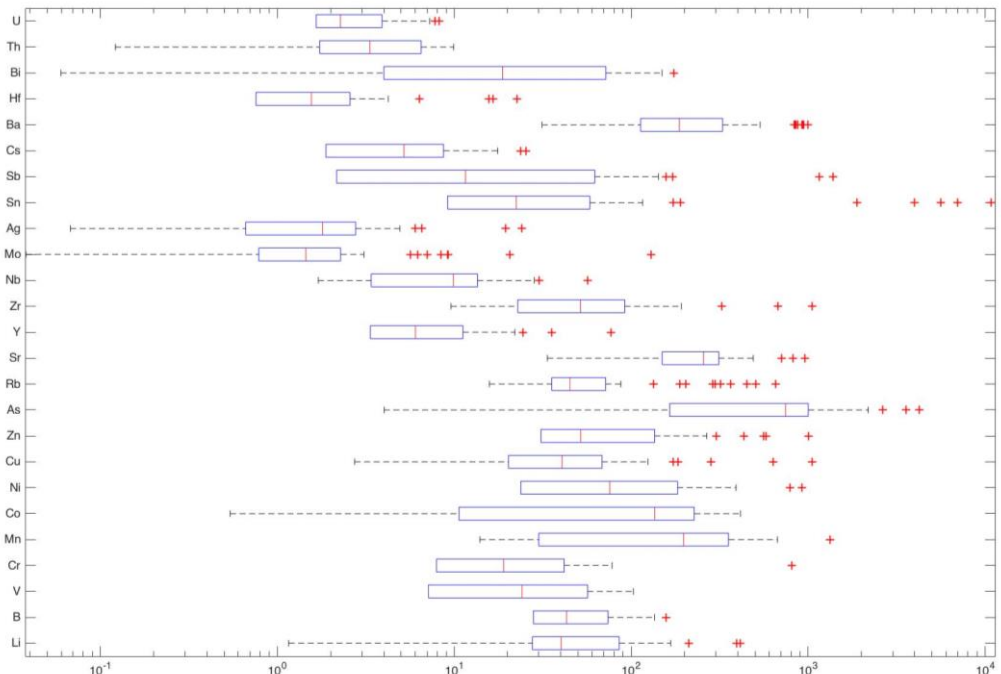


Figure 124 - illustrating the variability in each of the trace elements, minus REEs, in the porcelain pastes. To more clearly demonstrate the overall variability, a log scale has been used on the x axis (ppm).

A tentative relationship (>0.5) was identified between cobalt, nickel, arsenic, barium and bismuth, elements that have all been associated with the blue pigment smalt (discussed in Section 2.2.3, and characterised in terms of its major and minor elemental composition in Section 5.2.2). The majority of Limehouse samples and a Bow outlier are enriched in cobalt and in barium, see Figure 125, and these elements are present in a similar ratio (Co/Ba in Limehouse 0.3, Co/Ba in Bow 0.5), which suggests they may share a common origin or overlap. Pastes from these two factories demonstrate similar and consistent ratios between cobalt and nickel (Co/Ni in Limehouse 3-6; Co/Ni in Bow 2.5-3.5) and between cobalt and arsenic (Co/As in Limehouse 0.2-0.4; Co/As in Bow 0.2-0.3).

The other phosphatic and magnesian pastes belonging to factories that were known to have used ball clay or steatite (Bow, Chaffers, Chelsea, Liverpool (Ball), Lowestoft, Worcester, Pomona and Derby) contain some cobalt, but this is more strongly associated with bismuth, see Figure 126. Bow pastes once more show a consistent ratio between both of these elements (Co/Bi 3-4).

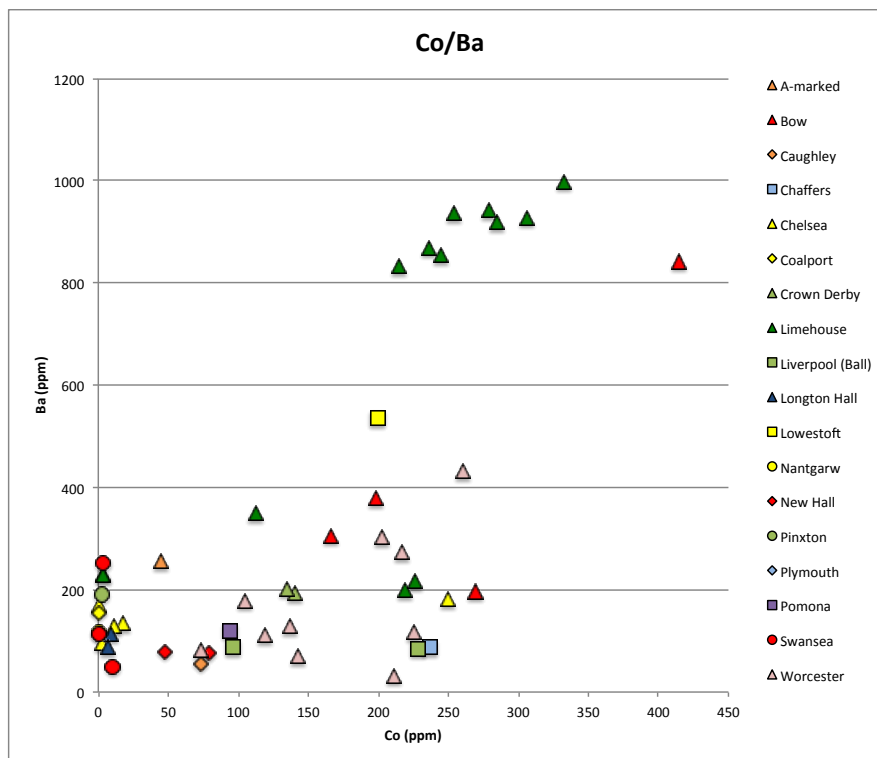


Figure 125 - cobalt vs bismuth in British porcelain pastes, by factory

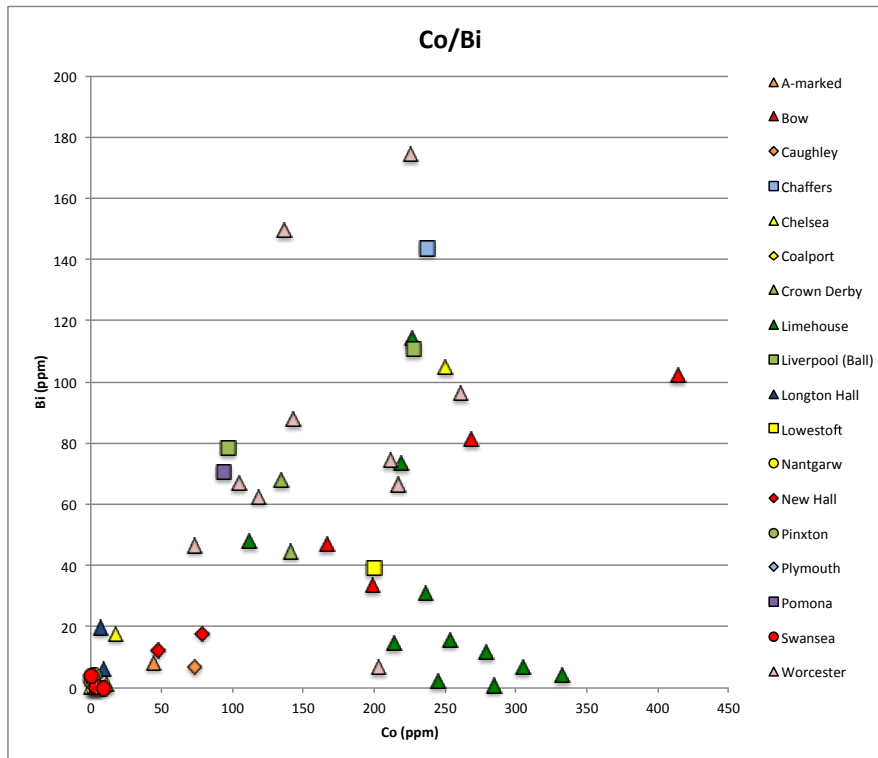


Figure 126 - cobalt vs bismuth in British porcelain pastes, by factory

Cobalt and nickel, along with scandium, titanium, vanadium, chromium, manganese, copper and zinc belong to the first series transition metals group, and in a geological system they behave in a similar manner, generally chalcophile but also found at trace levels in silicate minerals because of their compatibility. There is evidence for a linear trend in the relationship between copper and manganese in magnesian pastes, and those from Limehouse, see Figure 127. Chelsea porcelains contain relatively little copper (<50ppm), but are enriched in manganese relative to other pastes that included ball clay, including frit Longton Hall porcelain. Magnesian porcelain pastes are also significantly enriched in zinc, see Figure 128.

Results II: Laser Ablation Inductively Coupled Plasma Mass Spectroscopy

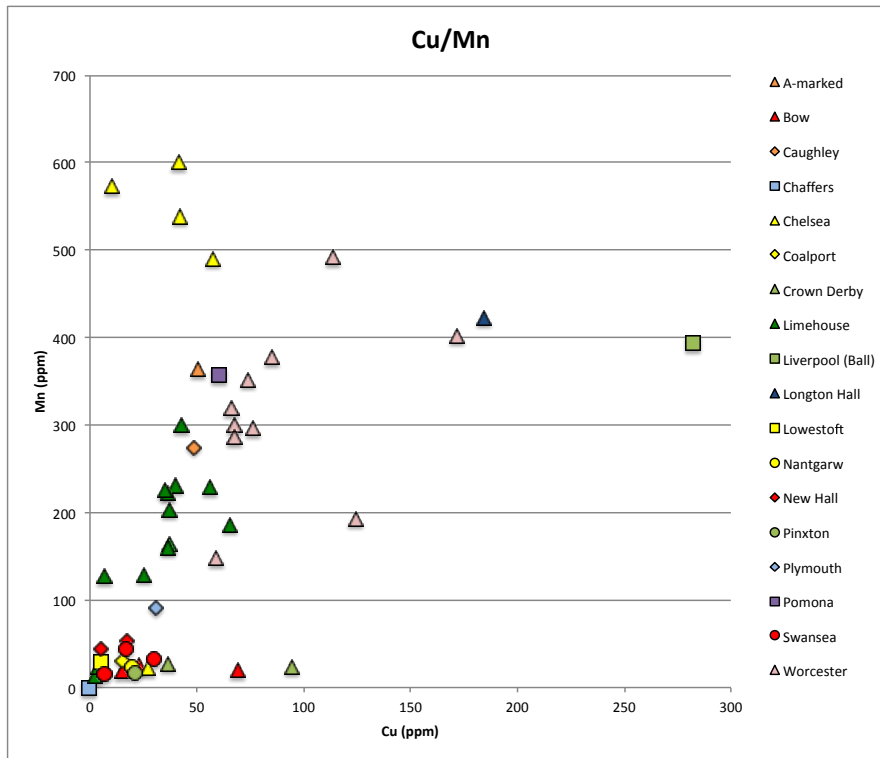


Figure 127 - copper vs manganese in British porcelain pastes, by factory

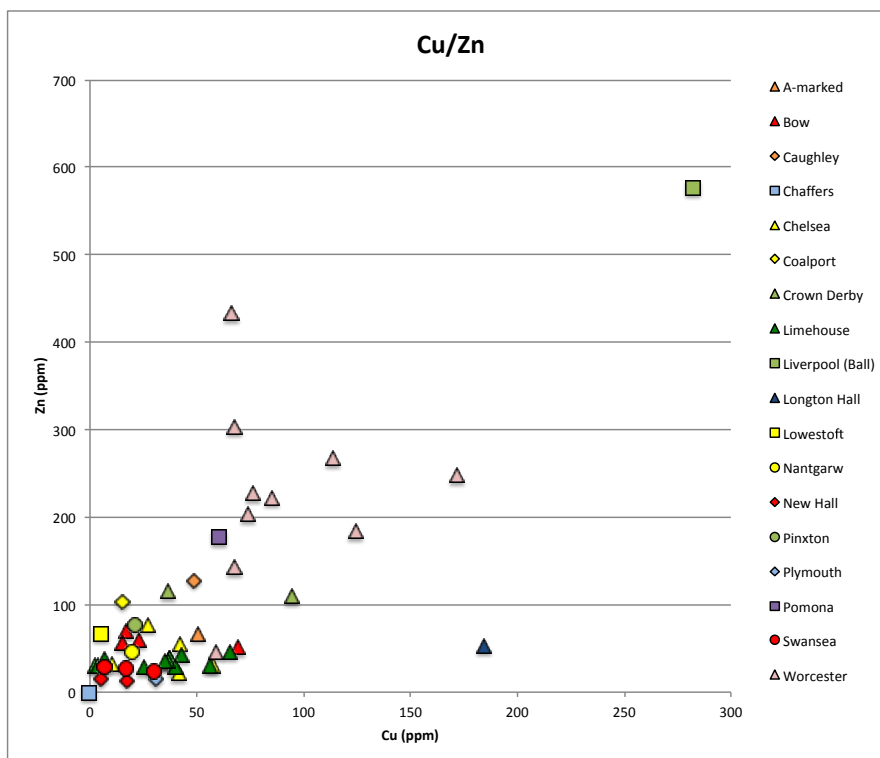


Figure 128 - copper vs zinc in British porcelain pastes, by factory

Zinc appears to be associated with magnesium, which was contributed by the steatite flux in magnesian porcelain, see Figure 129. Chaffers and Liverpool (Ball) porcelain has a relatively high ratio of magnesium to zinc (Mg/Zn 60-90) compared with Worcester, Pomona and Caughley (Mn/Zn 200-400). Crown Derby and Coalport bone china porcelain contains slightly more zinc, relative to magnesium, than the other china clay porcelain.

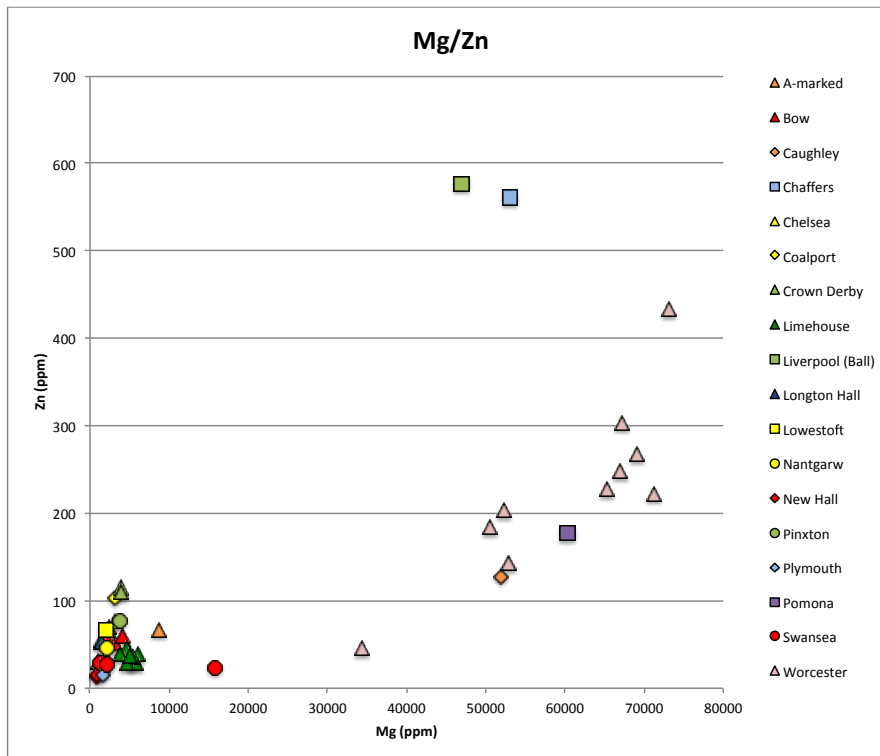


Figure 129 - magnesium vs zinc in British porcelain pastes, by factory

There is a linear trend between aluminium, an element that is contributed by clay, and niobium for most samples (Al/Nb 4000-8000), see Figure 130. A significant exception is the 'A'-marked sample, which is among the most aluminous samples analysed (Al_2O_3 22%), but contains relatively little niobium (Nb 2ppm). Outliers from Limehouse, Chaffers, New Hall, Swansea, Worcester and the Caughley and Plymouth samples are relatively enriched in niobium (Al/Nb 1300-3600). These niobium-enriched samples are also relatively depleted in titanium (Al/Ti 100-600), when compared with the other factories that used ball clay (Al/Ti 15-20), see Figure 131.

Results II: Laser Ablation Inductively Coupled Plasma Mass Spectroscopy

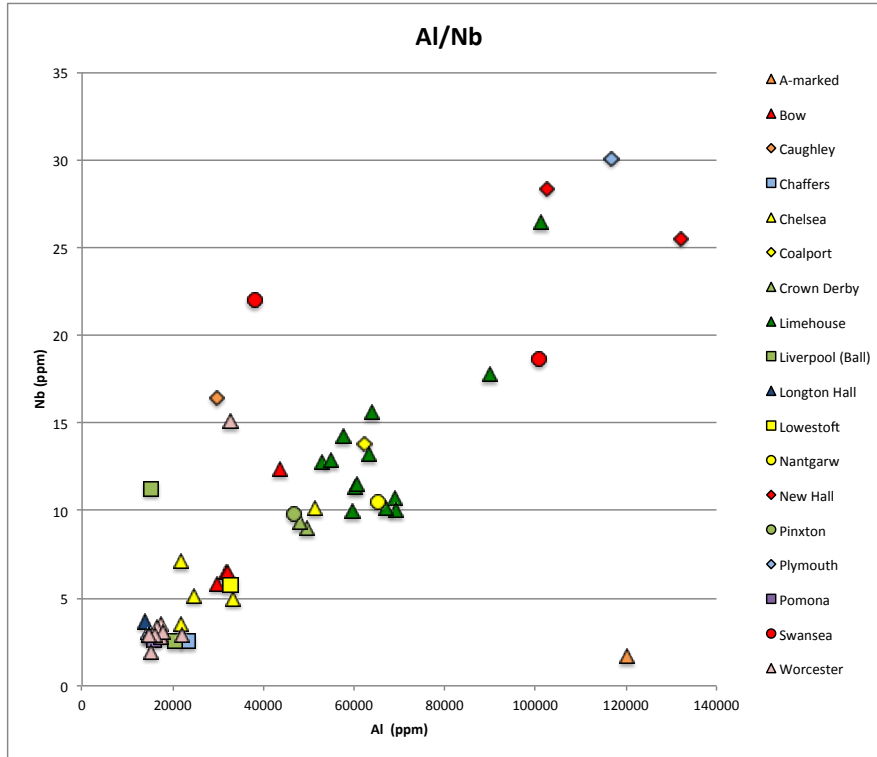


Figure 130 - aluminium vs niobium in British porcelain pastes, by factory

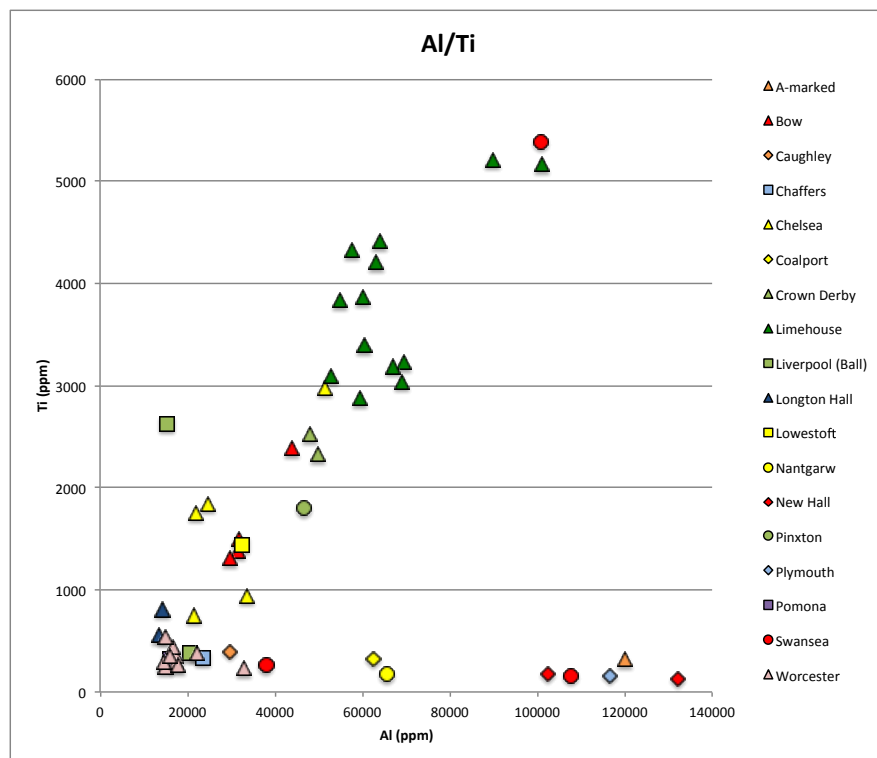


Figure 131 - aluminium vs titanium in British porcelain pastes, by factory

The magnesian factories (Caughley, Chaffers, Liverpool (Ball), Pomona and Worcester) generally contain little alumina ($Al_2O_3 < 6\%$), and are relatively depleted in titanium, although less so than the bone china and hybrid hard-paste porcelains containing china clay (Al/Ti 30-70).

Titanium is also associated in most pastes with zirconium (Figure 132) and hafnium (Figure 133), two high field strength lithophile elements that readily substitute for one another. This association is strongest in the pastes that used ball clay, and weakest in the magnesian porcelains, which tend to be enriched in zirconium and hafnium, relative to titanium. These two elements are found in virtually all samples at a consistent ratio (Zr/Hf 30-40), see Figure 134. Hafnium is relatively enriched in four samples (1058 E19 Pinxton, 32701Q Plymouth, 1060 E23 Swansea, 1067 E36 Worcester) that are also outliers in the titanium/zirconium and titanium/hafnium ratios illustrated in Figure 132 and Figure 133.

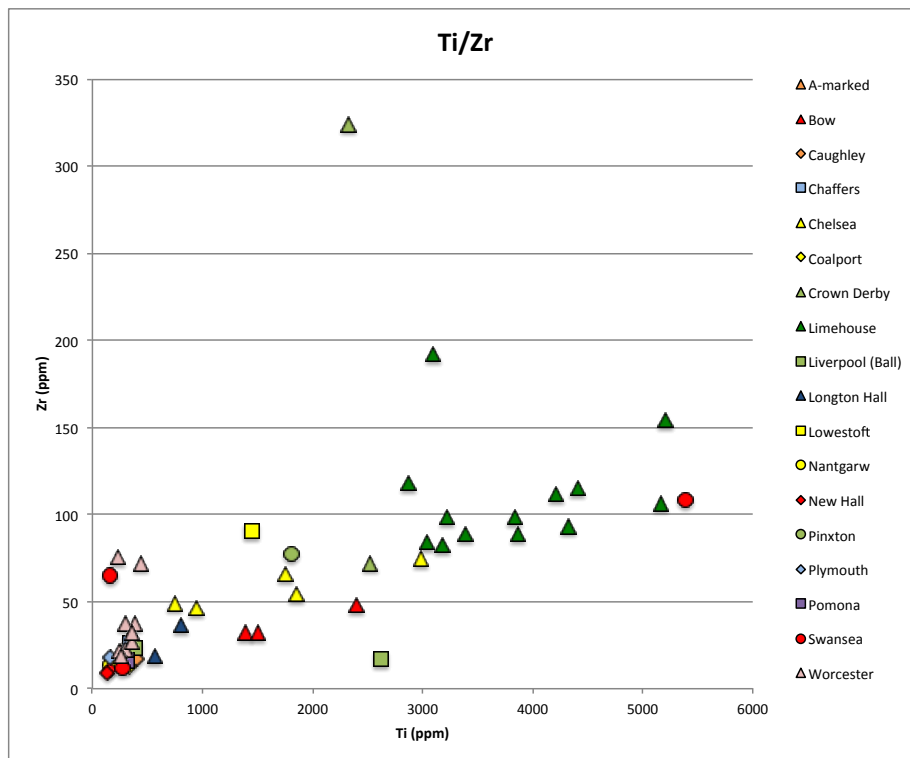


Figure 132 - titanium vs zirconium in British porcelain pastes, by factory

Results II: Laser Ablation Inductively Coupled Plasma Mass Spectroscopy

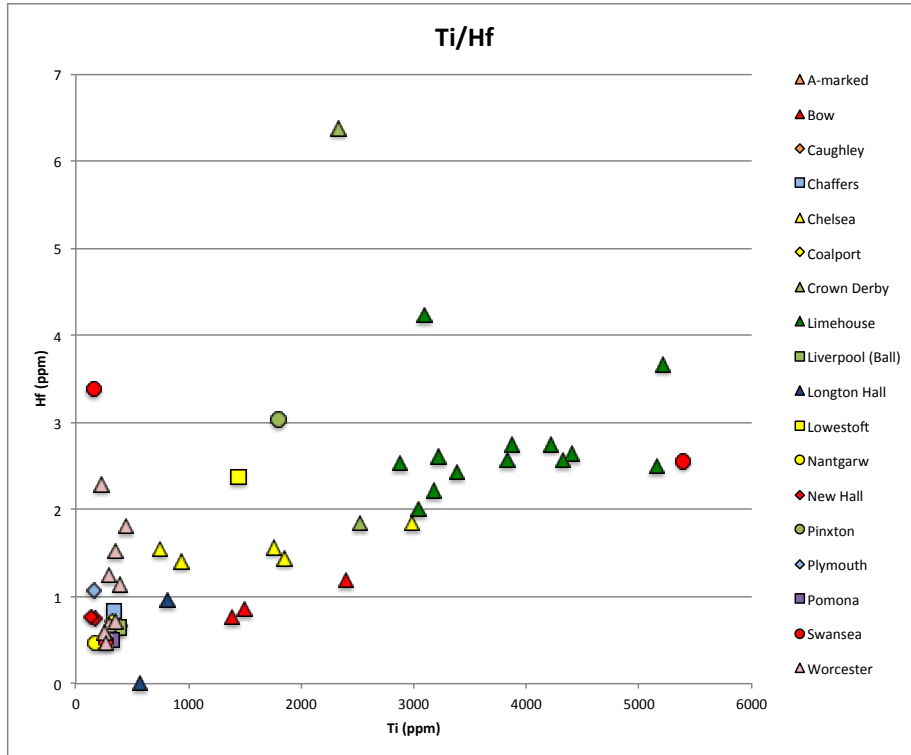


Figure 133 - titanium vs hafnium in British porcelain pastes, by factory

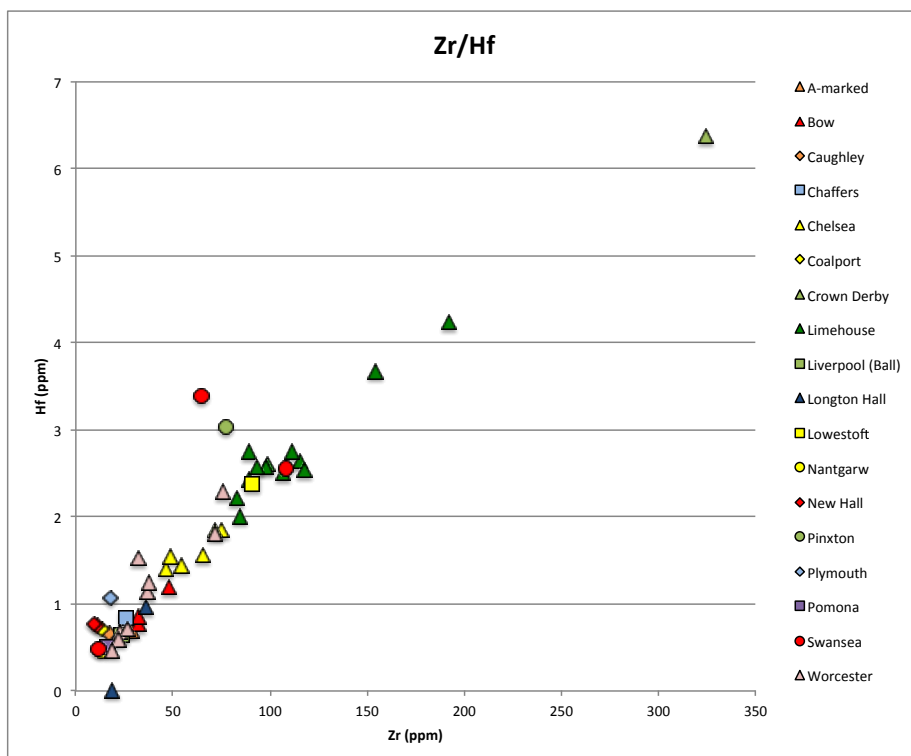


Figure 134 - zirconium vs hafnium in British porcelain pastes, by factory

Lead is present in magnesian pastes from Caughley, Pomona and Worcester, to which it was added as an additional flux (Tite and Bimson, 1991; Owen, 2003). It has also been found in frit pastes from Chelsea and Longton Hall, in which it is related to tin (Pb/Sn 5-9), see Figure 135. Tin is present in Chaffers and 'A'-marked porcelain pastes, but these contain negligible lead.

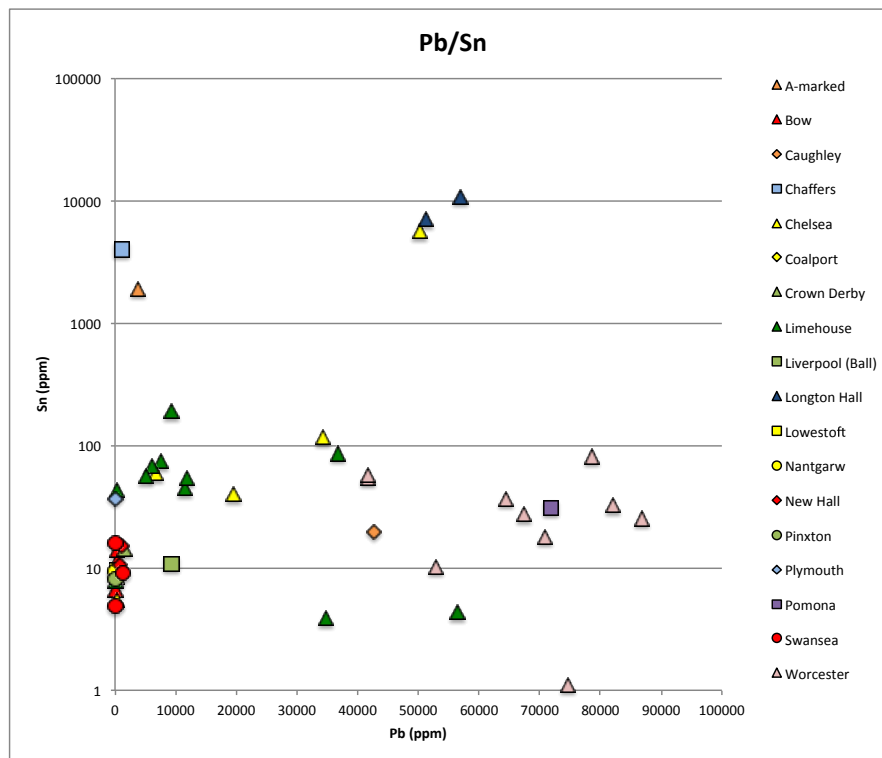


Figure 135 - lead vs tin in British porcelain pastes, by factory.

In order to more clearly illustrate compositional groups with different levels of tin, a logarithmic (base 10) scale has been used on the y axis.

Thorium and uranium are elements that are commonly used in provenancing studies, and are ubiquitous in geological materials (Allègre et al, 1986). Their stability in geological processes means that their relationship to one another is predictable within well-characterised raw materials (Turcotte et al, 2001), including granite (Aubert et al, 2001) zircon, (Kirkland et al, 2015) and basalts (O’Nions and McKenzie, 1993).

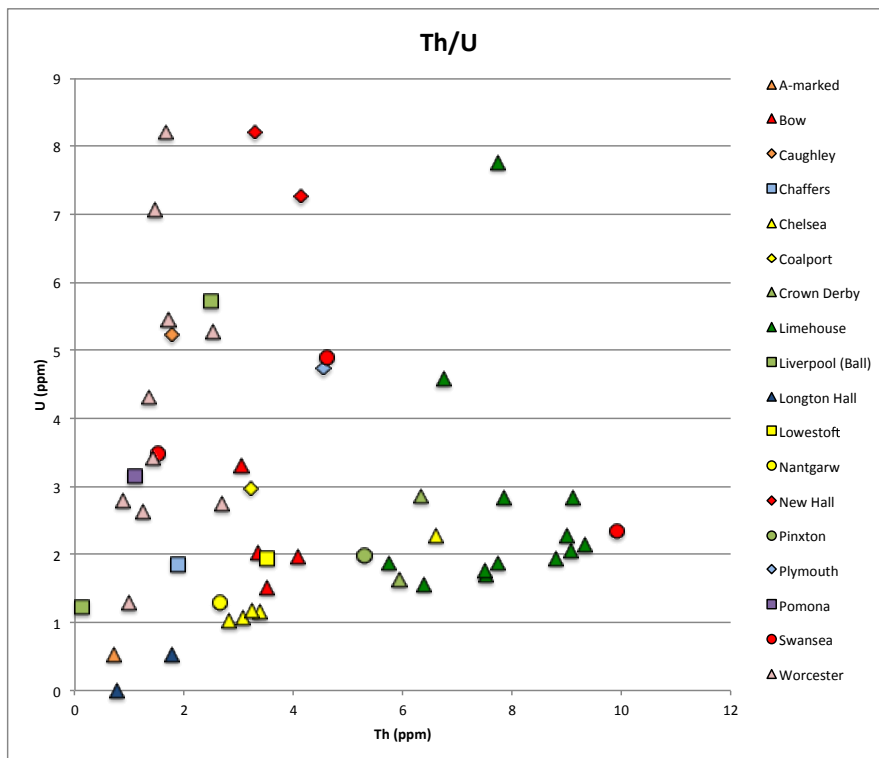


Figure 136 - thorium vs uranium in British porcelain pastes, by factory.

Of the factories for which more than one sample was available, most show significant variation in the Th/U ratio. Only porcelain from Chelsea is very stable with respect to its frit porcelain, which has a ratio similar to Bow, Lowestoft and Longton Hall. In general, bone ash porcelains and those that used ball clay in their pastes are enriched in thorium relative to uranium and show a linear trend in their relationship (Th/U 1.5-3.5). Magnesian pastes and those that used china clay are relatively enriched in uranium (Th/U <1), and vary more in their relationship to one another.

Rare Earth Elements in porcelain pastes

Rare Earth Elements (REE) are a class of metallic elements that include the lanthanides, i.e. the fifteen elements between lanthanum (La, 57) and lutetium (Lu, 71), plus two transition metals with similar material properties, scandium (Sc, 21) and yttrium (Y, 39) (Walters and Lusty, 2011). They are grouped in this manner because they share characteristics that mean that they are frequently found together in nature: the REEs easily form minerals, and so are not found naturally occurring as metallic elements, and their similar ionic radii and valence states mean that they may substitute one another easily in crystal structures (Walters and Lusty, 2011). As a consequence, they are commonly found as a group at trace levels in rocks everywhere on earth, in varying proportions relative to one another, depending on the conditions under which the mineral formed.

The ratios of REEs to one another can provide information as to the type of minerals that were present in the raw materials used in the porcelain paste and glaze. Similar ratios of REEs suggest that similar raw materials were used, whereas differences in REEs indicate that the raw materials or their proportions differ between objects.

Prior to creating profiles and ratios, REEs are often corrected with reference to the composition of a chondrite (Rollinson, 1993; pp. 135 - 136). These rocks have a mineral composition that has not been altered by processes of melting or fractionation, in the way that most minerals on earth have been, and therefore provide a baseline for REE distribution (Evensen et al, 1978). The raw REE data are reported in Appendix Table 39, and the values used in this normalisation are in Appendix Table 40. In the normalised results reported below (Table 49), the subscript c_N denotes that the REE data have been normalised to the chondrite.

Results II: Laser Ablation Inductively Coupled Plasma Mass Spectroscopy

Table 49 - Rare Earth Elements (REE) in British porcelain pastes. All values are chondrite normalised (CN).

Label	Factory	La	Ce	Pr	Nd	Sm	Eu	Gd	Tb	Dy	Ho	Er	Tm	Yb	Lu	(Ce/Ce*) _{cn}	(Eu/Eu*) _{cn}	Pr/Yb
47122R	A-marked	74	34	27	16	8	12	4	4	3	3	3	2	3	2	0.67	1.94	2.21
32703X	Bow	73	48	35	24	21	4	8	6	5	3	3	4	2	4	0.89	0.30	7.94
29105Q	Bow	76	54	45	34	19	9	11	8	7	6	5	5	6	4	0.90	0.60	4.83
29100P	Bow	62	46	37	27	16	8	18	20	19	17	15	14	13	14	0.94	0.49	4.49
29104S	Bow	63	46	36	26	14	7	8	5	5	4	3	2	4	4	0.92	0.66	5.05
1069 E39	Caughley	10	8	6	5	3	2	3	2	3	2	2	3	2	3	1.00	0.82	2.64
32706R	Chaffers	13	11	8	6	4	2	3	2	2	2	2	2	2	2	1.06	0.51	4.17
32699W	Chelsea	48	33	25	18	9	5	5	4	4	4	4	3	4	4	0.92	0.74	4.70
29103U	Chelsea	75	43	37	27	12	7	9	6	5	5	5	4	4	5	0.77	0.67	5.29
29106Z	Chelsea	110	79	58	44	22	12	11	8	7	7	7	6	8	8	0.94	0.75	4.70
66983 Y1	Chelsea	54	40	32	25	14	5	9	11	5	4	5	7	5	0	0.93	0.42	6.93
1055 E6	Chelsea	64	40	29	21	19	7	10	7	5	7	4	4	6	5	0.86	0.48	4.27
1072 E44	Coalport	39	29	24	18	11	5	5	3	3	2	2	1	3	1	0.92	0.60	5.14
1057 E18	Crown Derby	102	75	54	41	22	11	18	20	23	24	24	23	25	23	0.97	0.55	4.91
1056 E17	Crown Derby	98	72	52	39	22	10	10	9	8	7	8	7	8	7	0.96	0.65	4.99
40419P	Limehouse	147	106	76	55	28	18	13	9	9	9	9	7	11	9	0.95	0.86	4.29
40150S	Limehouse	183	133	92	65	36	19	17	12	11	9	11	9	13	13	0.97	0.70	4.91
40012W	Limehouse	105	75	55	39	20	10	11	8	7	5	6	9	8	8	0.94	0.65	5.35
40011Y	Limehouse	102	71	53	39	20	10	9	8	8	6	6	7	9	7	0.92	0.70	5.21
40010P	Limehouse	116	88	62	43	23	8	17	10	10	9	10	9	7	5	0.99	0.41	7.54
40009X	Limehouse	188	93	75	55	51	11	16	16	16	6	9	9	9	8	0.71	0.32	6.86
40008Z	Limehouse	13	10	6	5	8	3	5	3	4	1	3	3	2	3	1.03	0.49	2.02
40007Q	Limehouse	113	82	59	42	27	20	37	55	59	53	48	41	38	30	0.96	0.62	2.98
40006S	Limehouse	110	80	56	41	22	12	10	9	8	7	7	7	10	9	0.96	0.72	4.84
40000S	Limehouse	133	97	71	53	27	13	12	11	9	9	8	8	10	9	0.95	0.66	5.52

Results II: Laser Ablation Inductively Coupled Plasma Mass Spectroscopy

Table 49 - Rare Earth Elements (REE) in British porcelain pastes. All values are chondrite normalised (c_N) (continued)

Label	Factory	La	Ce	Pr	Nd	Sm	Eu	Gd	Tb	Dy	Ho	Er	Tm	Yb	Lu	(Ce/Ce*) c_N	(Eu/Eu*) c_N	Pr/Yb
40004W	Limehouse	146	105	78	59	29	13	17	14	12	13	13	13	14	13	0.94	0.57	5.85
40003Y	Limehouse	113	83	61	45	25	14	13	8	8	7	7	9	10	9	0.95	0.73	4.50
40002P	Limehouse	130	97	71	53	29	11	15	19	9	7	9	10	11	16	0.97	0.51	6.32
32706R	Liverpool (Ball)	13	11	8	6	4	2	3	2	2	2	2	2	2	2	1.06	0.51	4.17
29101Y	Longton Hall	37	26	20	15	10	4	7	4	5	4	4	4	4	3	0.90	0.43	5.63
32707P	Lowestoft	63	50	38	27	16	11	10	8	8	6	6	5	5	4	0.99	0.86	3.42
1059 E22	Nantgarw	15	13	10	8	5	2	3	2	2	1	1	1	1	2	1.04	0.54	4.49
1054 E4	New Hall	21	23	14	12	16	2	4	3	4	1	3	1	2	1	1.33	0.21	6.36
1053 E3	New Hall	47	43	24	13	9	2	6	5	2	1	1	2	0	0	1.20	0.28	11.26
1058 E19	Pinxton	77	58	42	30	15	8	9	7	6	5	7	8	9	8	0.97	0.64	5.37
32701Q	Plymouth	11	12	9	7	5	3	4	3	2	1	1	1	1	1	1.23	0.59	3.30
32702Z	Pomona	11	10	7	5	4	1	3	2	2	1	2	2	2	1	1.17	0.35	5.15
36554Q	Swansea	187	142	100	73	39	19	19	13	12	12	13	12	13	11	0.99	0.67	5.18
1060 E23	Swansea	18	16	12	10	7	5	4	3	3	2	2	3	4	4	1.07	0.81	2.61
1070 E40	Swansea	12	13	9	7	3	3	3	1	2	1	0	1	0	1	1.20	1.12	2.77
32700S	Worcester	187	126	80	58	50	11	15	13	13	5	7	9	9	12	0.94	0.33	7.47
29099T	Worcester	15	14	9	7	5	2	4	3	3	3	3	2	3	3	1.16	0.54	3.67
29263P	Worcester	13	13	9	6	5	1	3	3	3	2	3	2	3	3	1.15	0.24	9.13
1065 E34	Worcester	17	16	10	7	5	3	4	4	4	3	4	3	4	4	1.13	0.67	3.27
1064 E32	Worcester	12	10	7	6	4	2	2	2	2	2	2	2	2	2	1.03	0.74	3.20
1063 E31	Worcester	10	10	7	5	3	3	2	2	1	1	1	1	2	3	1.14	1.39	2.01
1062 E27	Worcester	10	10	6	4	2	2	2	3	2	2	2	2	3	3	1.20	0.84	3.83
1068 E37	Worcester	6	9	4	3	5	2	4	3	3	2	3	2	4	3	1.65	0.44	2.18
1067 E36	Worcester	16	14	8	6	4	3	2	5	4	2	3	3	3	2	1.19	1.09	2.49
1066 E35	Worcester	10	16	8	5	5	2	3	5	3	4	6	5	4	8	1.75	0.42	4.88

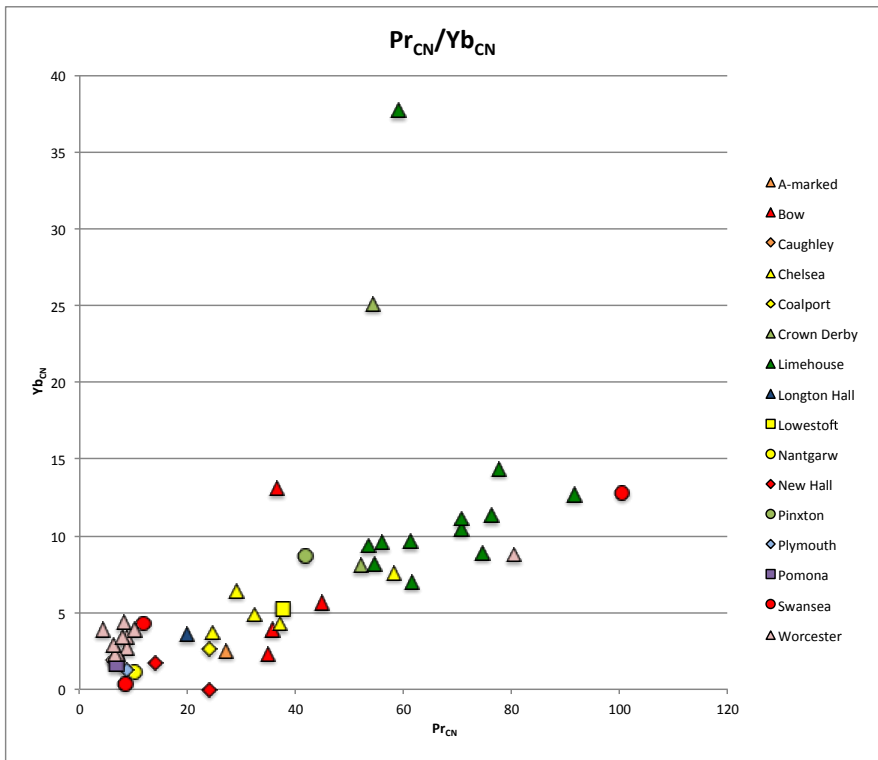


Figure 137 - Pr_{CN} vs Yb_{CN} in British porcelain pastes, by factory.

The ratio between praseodymium and ytterbium is used to illustrate the relationship between the light REEs (LREEs), and the heavy REEs (HREEs), and thus the extent to which fractionation of REEs differs between samples. In this case, the ratio shows a linear relationship, see Figure 137, with outliers from Crown Derby (1057 E18), Limehouse (40007Q), and Bow (29100P), which are relatively enriched in Yb_{CN}. The magnesian and hybrid hard-paste porcelains (Caughley, Chaffers, Liverpool (Ball), Plymouth, Pomona, Swansea, and Worcester) are the least enriched in REEs; phosphatic and bone-china porcelains and the ‘A’-marked sample contain slightly more; and the SAC porcelain from Limehouse and a Swansea outlier, are most enriched in these REEs.

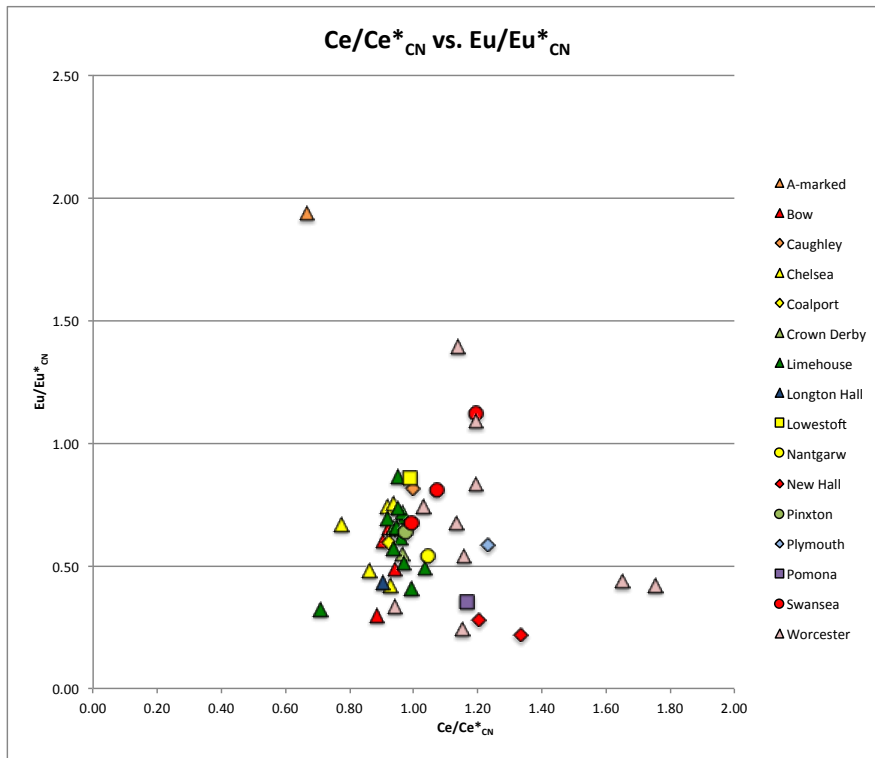


Figure 138 - Ce/Ce* vs Eu/Eu* in British porcelain pastes, by factory.

Cerium and europium are LREEs, both of which are affected by changes in valency that can result in these elements being relatively enriched or depleted in geological materials, relative to the other REEs. The cerium and europium anomalies in each sample can be measured by the ratio between the measured values (Ce_{CN} or Eu_{CN}) and the expected values, represented by half the sum of the two adjacent LREEs (Ce^*_{CN} or Eu^*_{CN}).

When these are plotted, the anomalous samples are clearly illustrated as outliers to the main group. Most of the samples have to some extent a negative Eu anomaly, and Ce can be either generally slightly enriched or depleted. The magnesian porcelains and the New Hall and Plymouth samples that used china clay form a group to the right of the main cluster, because they have a positive cerium anomaly. The 'A'-marked sample is distinct from both groups, higher on the y axis, due to a positive europium anomaly.

For factories where more than one sample was available for analysis (i.e. Bow, Chelsea, Limehouse, and Worcester), the REE profiles show a generally good agreement between objects attributed to the respective factories, see Figure 139. With the exception of one Limehouse sample (40007Q), all have greater LREE than HREE, and the bias is stronger in the phosphatic pastes (Bow) and frit pastes (Chelsea and Limehouse), than in magnesian (Worcester). There is an intriguing similarity between a Bow outlier (29100P) and Limehouse outlier (40007Q). Worcester porcelains show the greatest degree of fractionation within samples, and variability between samples.

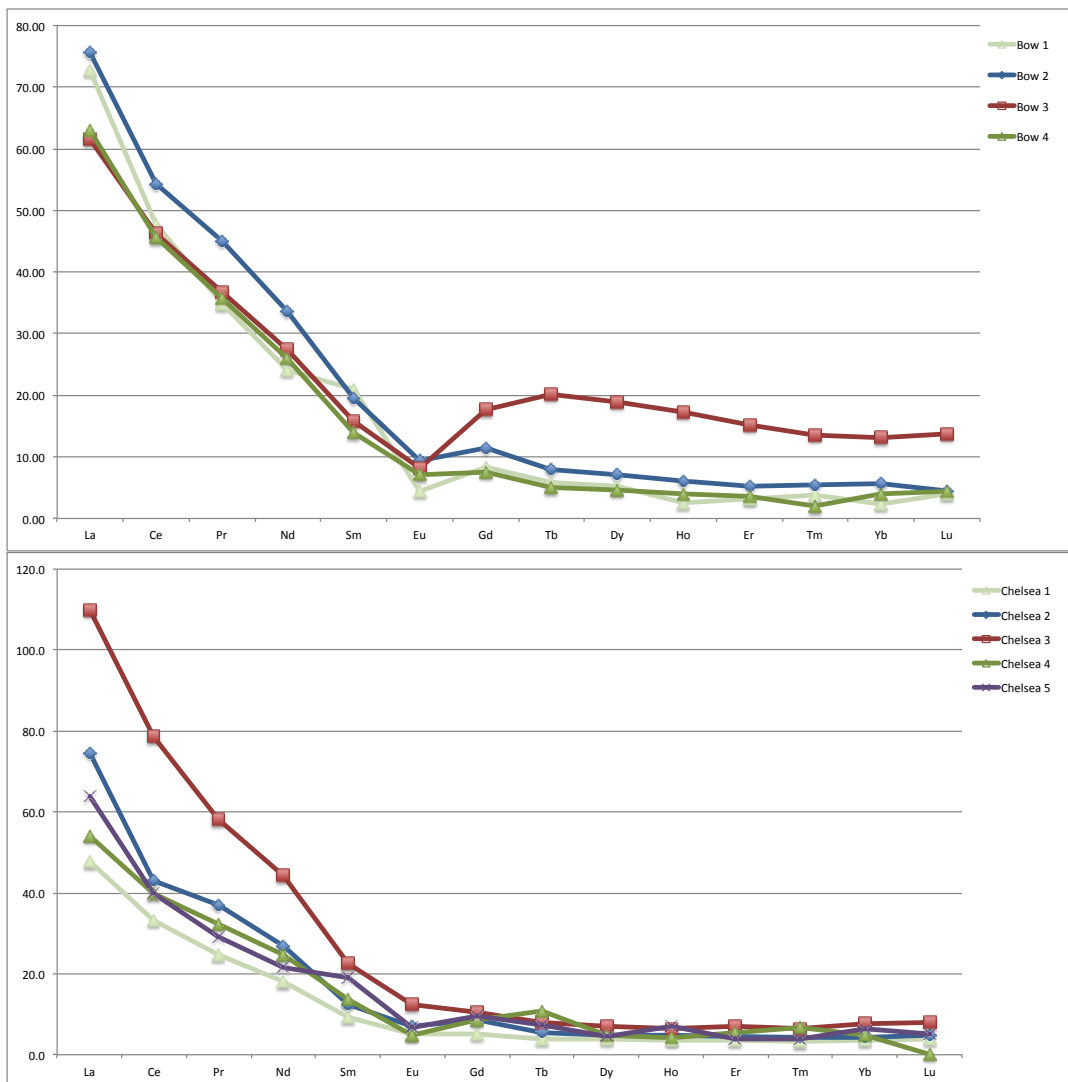


Figure 139 - REE_{CN} profiles for porcelain pastes from Worcester, Bow, Limehouse, and Chelsea.

Results II: Laser Ablation Inductively Coupled Plasma Mass Spectroscopy

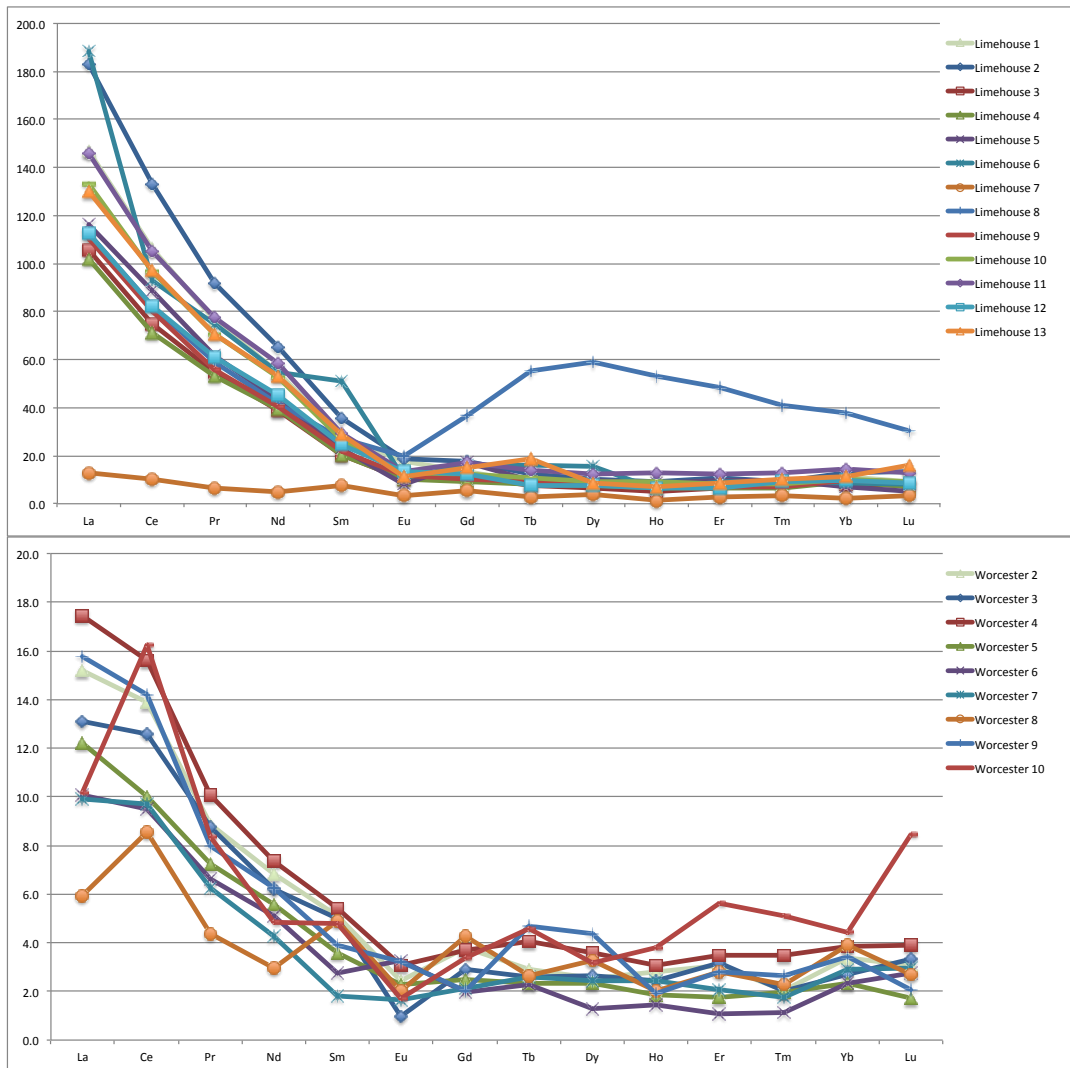


Figure 139 - REECN profiles for porcelain pastes from Worcester, Bow, Limehouse, and Chelsea. (continued)

Furthermore, the relationship between the REEs and aluminium appears to be strongly correlated with the paste type, see Figure 140. Limehouse and a bone china sample from Swansea are the most enriched in both REEs and aluminium, and Worcester, Nantgarw, Chaffers, Liverpool (Ball) and Caughley are the least enriched in both. The New Hall, Plymouth and 'A'-marked samples, and an outlier from Swansea, form a distinct group that contains high aluminium, but relatively little REEs. Bone china pastes from Coalport, Nantgarw and Swansea are also REE-depleted, relative to the amount of aluminium present.

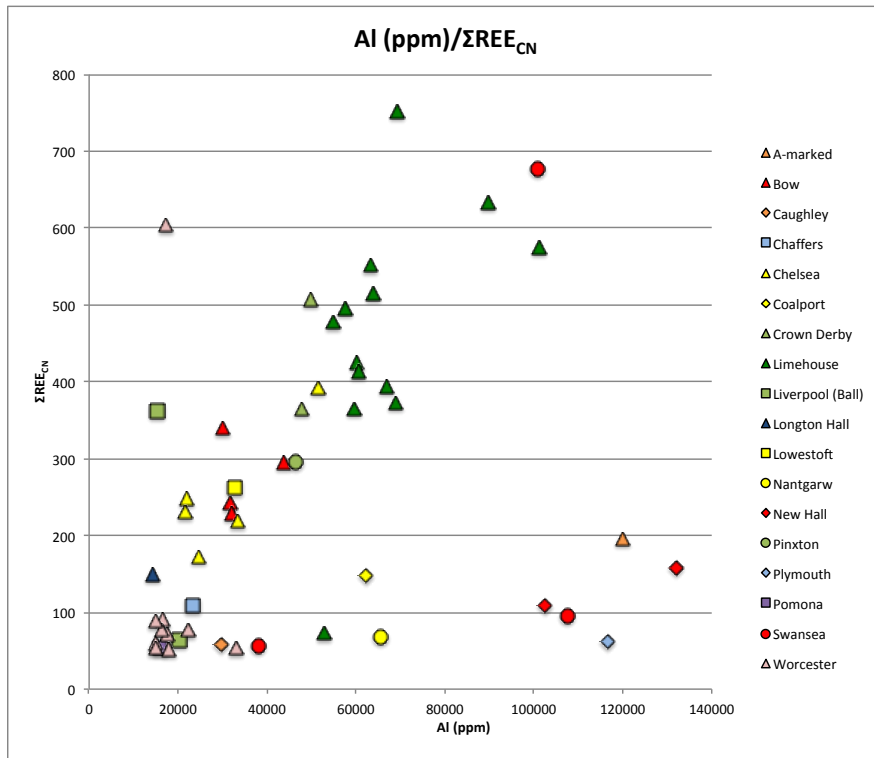


Figure 140 - Al (ppm) vs ΣREE_{CN} in British porcelain pastes.

To investigate this pattern further, the raw REE data were corrected again, this time to the upper continental crust (UCC) proxy MUQ (Kamber et al, 2005). This allows the REE composition to be examined in terms of its similarity to alluvial sediments, such as might be found in a secondary clay. The MUQ normalisation data are shown in Appendix Table 40, and the normalised data from the British porcelain pastes examined in this research are in Table 50. The subscript REE_{MUQ} will be used in the following results, in order to distinguish them from the chondrite-normalised data.

Results II: Laser Ablation Inductively Coupled Plasma Mass Spectroscopy

Table 50 - Rare Earth Elements (REE) in British porcelain pastes. All values are MUQ normalised (μUQ).

Label	Factory	La	Ce	Pr	Nd	Sm	Eu	Gd	Tb	Dy	Ho	Er	Tm	Yb	Lu	(Ce/Ce*)	(Eu/Eu*)	Pr/Yb
47122R	A-marked	0.54	0.29	0.30	0.22	0.18	0.44	0.14	0.14	0.13	0.12	0.12	0.09	0.13	0.11	0.70	2.78	2.34
32703X	Bow	0.42	0.36	0.44	0.35	0.28	0.27	0.24	0.20	0.17	0.19	0.18	0.17	0.13	0.19	0.83	1.03	3.50
29105Q	Bow	0.52	0.42	0.53	0.45	0.38	0.32	0.33	0.27	0.29	0.25	0.23	0.25	0.25	0.21	0.79	0.91	2.13
29100P	Bow	0.43	0.35	0.43	0.37	0.31	0.28	0.51	0.68	0.78	0.70	0.66	0.62	0.58	0.66	0.83	0.69	0.74
29104S	Bow	0.43	0.35	0.42	0.35	0.27	0.25	0.22	0.17	0.19	0.17	0.15	0.09	0.17	0.21	0.82	0.99	2.42
1069 E39	Caughley	0.07	0.07	0.07	0.06	0.06	0.08	0.09	0.09	0.12	0.10	0.11	0.16	0.10	0.14	0.99	1.11	0.70
32704V	Chaffers	0.13	0.14	0.17	0.13	0.19	0.01	0.14	0.11	0.13	0.14	0.15	0.15	0.15	0.20	0.97	0.07	1.12
32699W	Chelsea	0.35	0.29	0.27	0.25	0.20	0.19	0.16	0.14	0.16	0.16	0.17	0.16	0.18	0.20	0.93	1.06	1.47
29103U	Chelsea	0.52	0.33	0.44	0.36	0.24	0.24	0.25	0.19	0.20	0.20	0.20	0.20	0.19	0.23	0.69	0.99	2.29
29106Z	Chelsea	0.75	0.60	0.68	0.59	0.44	0.43	0.30	0.26	0.29	0.26	0.31	0.30	0.34	0.38	0.84	1.16	2.02
66983 Y1	Chelsea	0.37	0.31	0.38	0.33	0.27	0.16	0.25	0.37	0.20	0.17	0.24	0.32	0.22	0.00	0.81	0.63	1.75
1055 E6	Chelsea	0.44	0.31	0.34	0.29	0.37	0.24	0.28	0.25	0.19	0.29	0.17	0.19	0.29	0.24	0.78	0.73	1.20
1072 E44	Coalport	0.28	0.25	0.26	0.25	0.23	0.17	0.16	0.12	0.12	0.10	0.10	0.07	0.13	0.05	0.92	0.87	2.04
1057 E18	Crown Derby	0.70	0.58	0.64	0.55	0.44	0.38	0.53	0.67	0.93	0.97	1.07	1.07	1.11	1.11	0.86	0.80	0.58
1056 E17	Crown Derby	0.68	0.55	0.62	0.52	0.43	0.36	0.30	0.30	0.33	0.29	0.34	0.35	0.36	0.35	0.85	1.00	1.71
40419P	Limehouse	1.02	0.81	0.90	0.73	0.55	0.62	0.39	0.30	0.37	0.35	0.41	0.34	0.50	0.45	0.85	1.32	1.79
40150S	Limehouse	1.27	1.02	1.08	0.88	0.71	0.65	0.51	0.41	0.43	0.38	0.47	0.43	0.57	0.64	0.87	1.07	1.91
40012W	Limehouse	0.73	0.58	0.64	0.53	0.40	0.36	0.32	0.25	0.27	0.21	0.28	0.42	0.36	0.36	0.84	0.99	1.77
40011Y	Limehouse	0.71	0.55	0.63	0.53	0.40	0.36	0.27	0.27	0.32	0.26	0.28	0.31	0.41	0.34	0.82	1.07	1.52
40010P	Limehouse	0.85	0.76	0.68	0.60	0.50	0.29	0.54	0.36	0.40	0.38	0.47	0.46	0.35	0.26	1.00	0.57	1.95
40009X	Limehouse	1.09	0.95	1.02	0.85	0.67	0.67	0.43	0.45	0.44	0.41	0.41	0.41	0.49	0.55	0.89	1.21	2.11
40008Z	Limehouse	1.10	0.70	0.95	0.81	0.68	0.67	0.47	0.53	0.53	0.44	0.50	0.42	0.49	0.38	0.68	1.17	1.93
40007Q	Limehouse	0.82	0.71	0.65	0.58	0.59	0.71	1.15	2.01	2.45	2.37	2.29	1.98	1.87	1.52	0.97	0.82	0.35
40006S	Limehouse	0.80	0.69	0.61	0.56	0.47	0.41	0.33	0.34	0.34	0.32	0.33	0.33	0.48	0.47	0.97	1.05	1.29
40000S	Limehouse	0.92	0.74	0.84	0.71	0.52	0.45	0.36	0.35	0.38	0.38	0.36	0.38	0.46	0.43	0.84	1.01	1.81

Results II: Laser Ablation Inductively Coupled Plasma Mass Spectroscopy

Table 50 - Rare Earth Elements (REE) in British porcelain pastes. All values are MUQ normalised (μM). (continued)

Label	Factory	La	Ce	Pr	Nd	Sm	Eu	Gd	Tb	Dy	Ho	Er	Tm	Yb	Lu	(Ce/Ce*)	(Eu/Eu*)	Pr/Yb
40004W	Limehouse	1.01	0.81	0.92	0.79	0.58	0.46	0.50	0.47	0.51	0.54	0.55	0.59	0.64	0.62	0.84	0.86	1.43
40003Y	Limehouse	0.78	0.63	0.72	0.61	0.48	0.47	0.37	0.26	0.31	0.27	0.29	0.41	0.43	0.41	0.84	1.12	1.68
40002P	Limehouse	0.90	0.75	0.83	0.72	0.56	0.39	0.43	0.64	0.36	0.29	0.38	0.47	0.49	0.77	0.86	0.78	1.69
32705T	Liverpool (Ball)	0.01	0.19	1.03	0.78	0.00	0.14	0.00	2.08	0.00	0.05	5.66	0.00	0.23	0.00	0.36	-	4.39
32706R	Liverpool (Ball)	0.09	0.10	0.09	0.08	0.09	0.07	0.11	0.09	0.10	0.09	0.09	0.09	0.09	0.09	1.05	0.71	0.96
29101Y	Longton Hall	0.26	0.20	0.23	0.20	0.19	0.12	0.19	0.15	0.19	0.15	0.19	0.17	0.16	0.17	0.80	0.64	1.45
32707P	Lowestoft	0.46	0.43	0.41	0.37	0.34	0.39	0.31	0.30	0.32	0.28	0.27	0.26	0.26	0.22	0.99	1.21	1.58
1059 E22	Nantgarw	0.11	0.11	0.11	0.11	0.11	0.08	0.10	0.08	0.08	0.04	0.06	0.04	0.06	0.08	1.02	0.77	1.89
1054 E4	New Hall	0.14	0.18	0.17	0.17	0.32	0.08	0.12	0.10	0.17	0.04	0.11	0.04	0.08	0.04	1.15	0.34	2.12
1053 E3	New Hall	0.32	0.33	0.28	0.18	0.18	0.07	0.17	0.18	0.10	0.05	0.04	0.07	0.00	0.00	1.08	0.42	-
1058 E19	Pinxton	0.56	0.50	0.46	0.42	0.33	0.28	0.28	0.24	0.24	0.24	0.34	0.37	0.43	0.43	0.98	0.92	1.07
32701Q	Plymouth	0.08	0.10	0.10	0.10	0.12	0.09	0.11	0.10	0.08	0.06	0.06	0.05	0.06	0.05	1.19	0.83	1.52
32702Z	Pomona	0.08	0.09	0.07	0.07	0.08	0.05	0.11	0.09	0.07	0.06	0.08	0.09	0.08	0.07	1.16	0.49	0.90
36554Q	Swansea	1.29	1.09	1.19	0.97	0.76	0.68	0.55	0.44	0.51	0.47	0.55	0.55	0.57	0.54	0.88	1.03	2.09
1060 E23	Swansea	0.13	0.14	0.13	0.14	0.16	0.16	0.12	0.11	0.11	0.10	0.10	0.13	0.21	0.21	1.06	1.17	0.61
1070 E40	Swansea	0.09	0.11	0.09	0.09	0.06	0.11	0.09	0.04	0.07	0.07	0.02	0.05	0.02	0.05	1.17	1.51	4.90
32700S	Worcester	0.08	0.08	0.08	0.07	0.10	0.20	0.16	0.10	0.14	0.11	0.15	0.16	0.12	0.15	0.96	1.52	0.66
29099T	Worcester	0.11	0.11	0.10	0.09	0.10	0.08	0.11	0.10	0.10	0.12	0.13	0.09	0.15	0.15	1.02	0.80	0.69
29263P	Worcester	0.09	0.10	0.10	0.08	0.10	0.03	0.09	0.09	0.11	0.10	0.14	0.09	0.12	0.16	1.00	0.36	0.86
1065 E34	Worcester	0.12	0.12	0.12	0.10	0.11	0.11	0.11	0.14	0.15	0.13	0.15	0.16	0.17	0.19	1.00	0.99	0.69
1064 E32	Worcester	0.08	0.08	0.09	0.08	0.07	0.08	0.07	0.08	0.10	0.08	0.08	0.09	0.10	0.08	0.90	1.10	0.82
1063 E31	Worcester	0.07	0.07	0.08	0.07	0.05	0.12	0.06	0.08	0.05	0.06	0.05	0.05	0.10	0.13	0.99	2.05	0.76
1062 E27	Worcester	0.07	0.08	0.07	0.06	0.04	0.06	0.07	0.09	0.10	0.11	0.10	0.09	0.14	0.15	1.18	1.12	0.47
1068 E37	Worcester	0.04	0.07	0.05	0.04	0.10	0.07	0.12	0.09	0.13	0.08	0.12	0.11	0.17	0.13	1.41	0.63	0.30
1067 E36	Worcester	0.11	0.11	0.09	0.08	0.08	0.11	0.06	0.16	0.18	0.08	0.12	0.12	0.15	0.10	1.07	1.65	0.62
1066 E35	Worcester	0.07	0.13	0.10	0.07	0.10	0.06	0.10	0.15	0.13	0.16	0.25	0.24	0.20	0.40	1.48	0.62	0.50

The paste type appears to be correlated with the REE profile of the porcelain, and there are marked differences between factories. Magnesian porcelain pastes are slightly REE-enriched and, with the exception of Caughley and Worcester, show a slight positive cerium anomaly, and a negative europium anomaly, see Figure 141. Chaffers and Liverpool (Ball) are the most REE-enriched, and have a pronounced negative europium anomaly. Caughley is HREE-enriched, with greater fractionation in these elements than in the LREEs.

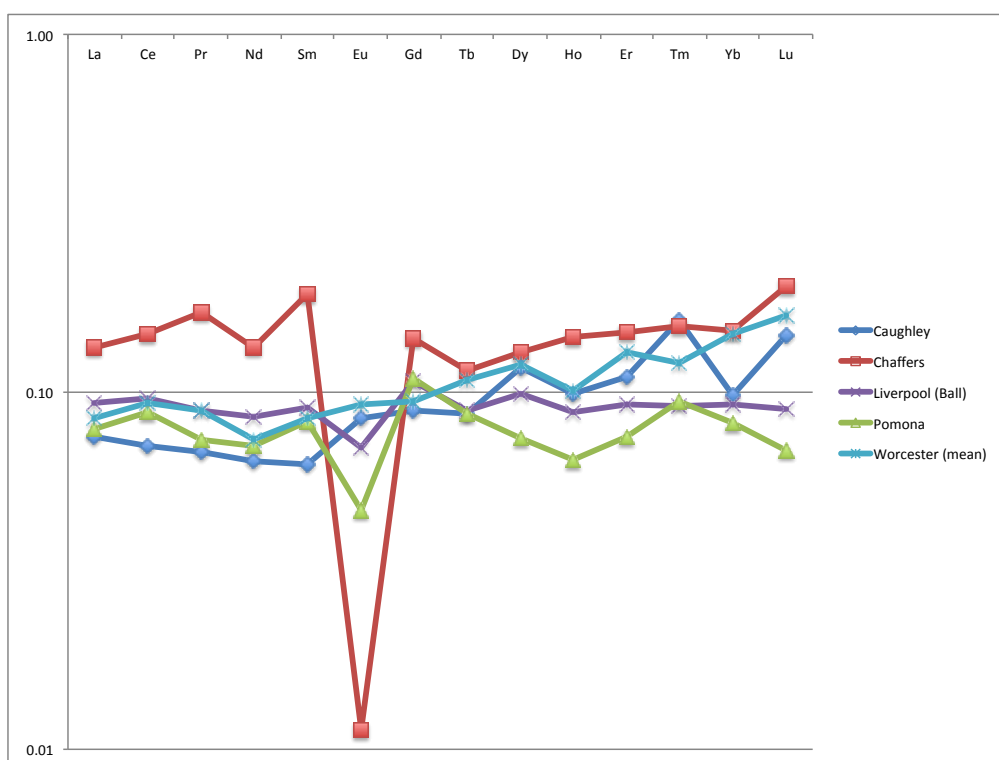


Figure 141 - REE_{MUQ} profiles for magnesian porcelain pastes from Caughley, Chaffers, Liverpool (Ball), Pomona, and Worcester. In order to more clearly illustrate the significant differences, a logarithmic (base 10) scale has been used on the y axis.

Phosphatic bodies are generally LREE-enriched, see Figure 142. Chelsea and Crown Derby are the most REE-enriched, and show significant overlap in their REE profiles. Bow, Lowestoft and Pinxton also share a similar pattern, with a slight negative europium anomaly. The bone china pastes (Coalport, Nantgarw and Swansea) are the least REE-enriched. Swansea has a similar profile to Pinxton, showing fractionation between the middle- and heavy-REEs. An anomalous paste from Crown Derby shows enrichment of the HREEs that is comparable with the profiles of the outliers from Bow and Limehouse, discussed below (Figure 144).

Results II: Laser Ablation Inductively Coupled Plasma Mass Spectroscopy

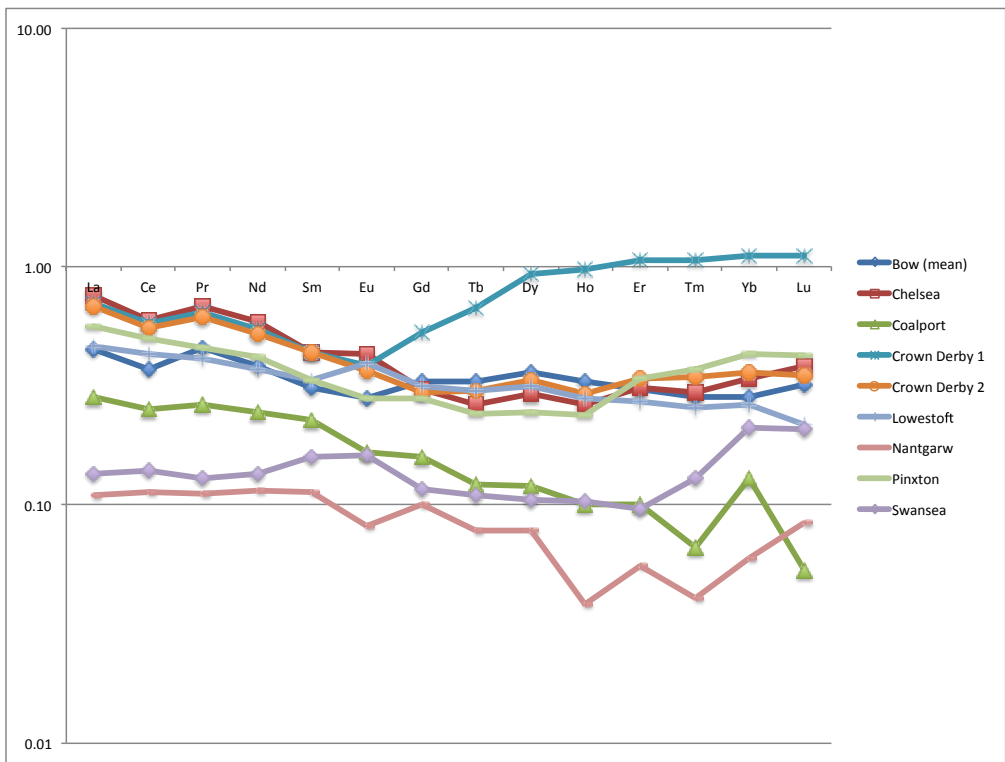


Figure 142 - REE_{MuQ} profiles for phosphatic porcelain pastes from Bow, Chelsea, Coalport, Derby, Lowestoft, Nantgarw, Pinxton and Swansea. In order to more clearly illustrate the significant differences, a logarithmic (base 10) scale has been used on the y axis.

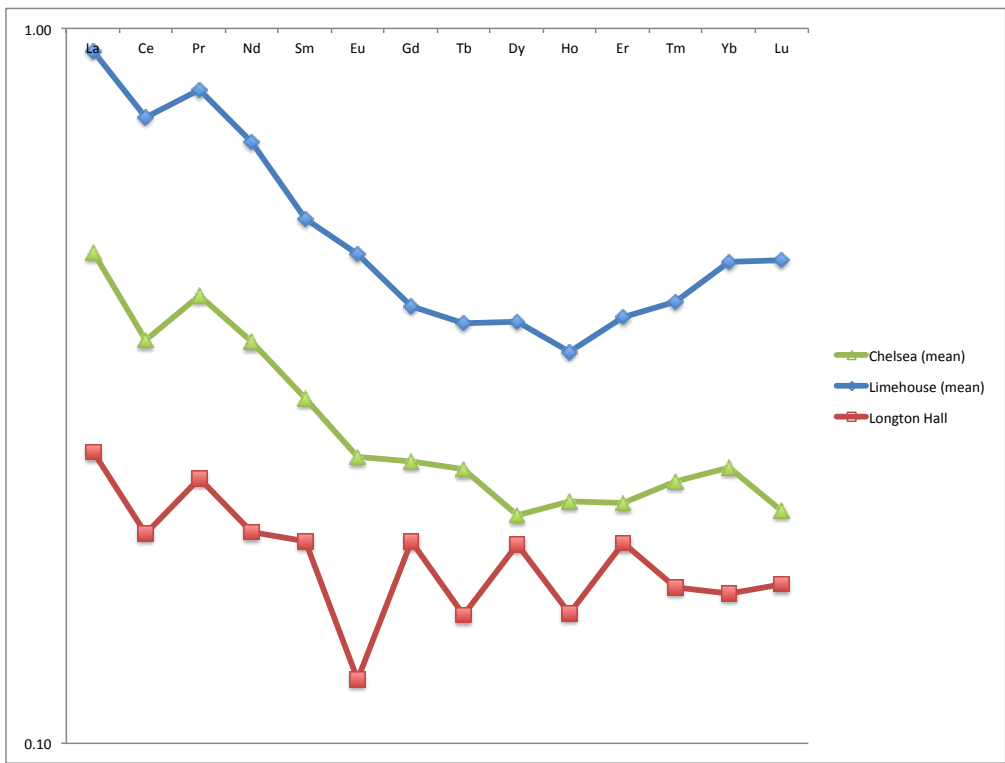


Figure 143 - REE_{MuQ} profiles for frit porcelain pastes from Chelsea and Longton Hall, plus SAC porcelain from Limehouse. In order to more clearly illustrate the significant differences, a logarithmic (base 10) scale has been used on the y axis.

Frit porcelains from Chelsea and Longton Hall are considered alongside SAC porcelain from Limehouse (Figure 143), because these are all thought to have used ball clay as a significant component of their paste. Chelsea and Limehouse have very similar REE profiles, with enrichment of the LREEs compared with the HREEs, a negative cerium anomaly and no significant europium anomaly. Longton Hall frit porcelain is not significantly enriched in REEs, and it is thought that the erratic distribution of this profile is due to these levels being too low to normalise successfully.

The outliers from Bow, Crown Derby and Limehouse considered here are significantly different from the mean values for these factories, but show similarities to one another. All are HREE-enriched, and have a slight negative cerium anomaly. The Bow and Derby pastes also have a slight negative europium anomaly.

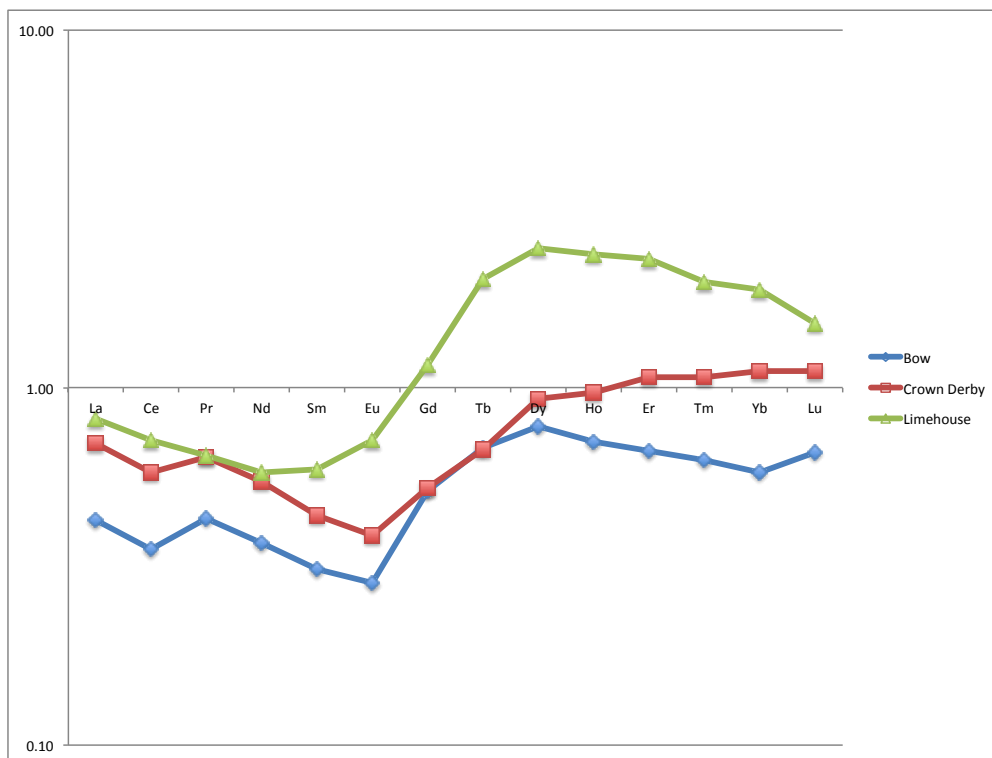


Figure 144 - REE_{MUQ} profiles for outliers from Bow and Limehouse, which were omitted from the calculations of mean values used in previous profiles. In order to more clearly illustrate the significant differences, a logarithmic (base 10) scale has been used on the y axis.

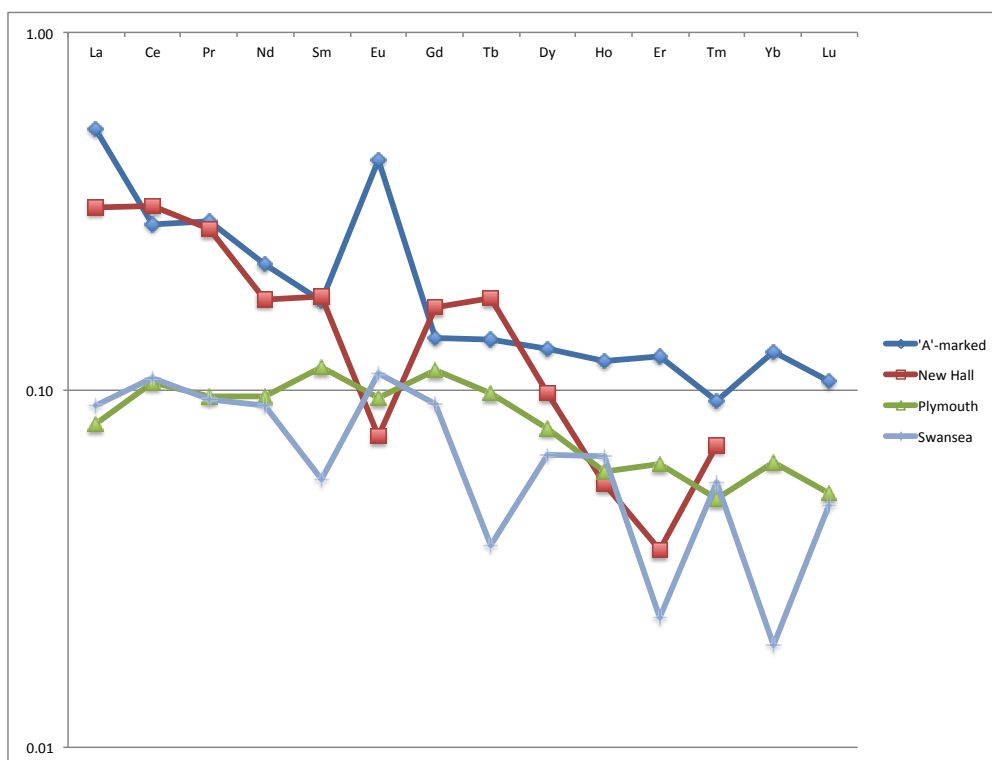


Figure 145 - REE_{MUQ} profiles for hybrid hard-paste porcelain pastes from the 'A'-marked group, New Hall, Plymouth, and Swansea. In order to more clearly illustrate the significant differences, a logarithmic (base 10) scale has been used on the y axis.

Hybrid hard-paste porcelains show the most variation in REE distribution of any paste type here examined, see Figure 145. They are all slightly LREE-enriched, and exhibit some fractionation. Plymouth and the 'A'-marked sample are relatively similar in their overall profile, but 'A'-marked porcelain has a negative cerium anomaly and a substantial positive europium anomaly, while Plymouth has a slight positive cerium anomaly and negative europium anomaly. New Hall and Swansea are more fractionated, showing a profile similar to that of Longton Hall porcelain (Figure 143).

6.2.3 Analysis of porcelain glazes

The glazes of the 51 glazed porcelain samples were analysed using LA-ICPMS; in each case, this was performed during the same run as the analysis of the body.

It has been demonstrated that the ICPMS data for these glazes do not compare well with the SEM-EDS data with regard to their major and minor elemental composition. This is thought to be due to the sampled area being greater in diameter than the glaze, resulting in contamination of the analysed material by the paste composition. However, the trace elemental data, including chondrite-normalised REEs, will be examined to see whether any characteristic features may be identified. The complete data for 49 elements measured in 35 of these glazes that appear to have been less affected by contamination are provided in Appendix A.9 and summarised below.

With the exception of a single object from William Cookworthy's Plymouth factory (32701Q), all of the porcelain glazes are of the high-lead type, see Table 51. Elements associated with the paste formula are found in many glazes: phosphorus and elevated calcium in the glazes of phosphatic porcelains; magnesium in those belonging to magnesian porcelains; and relatively high alumina in the glazes of SAC porcelains.

Results II: Laser Ablation Inductively Coupled Plasma Mass Spectroscopy

Table 51 - LA-ICPMS data for British porcelain glazes in weight percent as oxides

Label	Factory	Na ₂ O	MgO	Al ₂ O ₃	SiO ₂	P ₂ O ₅	K ₂ O	CaO	TiO ₂	Fe ₂ O ₃	PbO
32703X	Bow	0.7	0.1	1.2	37.4	0.1	2.0	1.6	0.1	0.0	56.0
29100P	Bow	0.1	0.0	1.6	45.4	7.8	1.7	3.8	0.0	0.1	38.3
1069 E39	Caughley	1.3	1.4	4.2	48.0	0.1	4.0	0.6	0.0	0.7	39.2
32704V	Chaffers	5.7	2.7	1.0	59.1	0.2	3.7	4.4	0.1	0.2	18.0
32699W	Chelsea	1.0	0.2	1.4	59.3	0.0	2.0	10.4	0.1	0.1	24.6
29106Z	Chelsea	1.2	0.0	0.5	73.1	0.4	2.9	3.7	0.0	0.5	17.5
1072 E44	Coalport	1.4	0.2	7.3	51.8	0.8	2.1	5.8	0.0	0.2	27.0
1057 E18	Crown Derby	0.5	0.1	2.4	42.3	0.9	3.3	2.2	0.1	0.1	47.6
1056 E17	Crown Derby	0.6	0.2	4.1	39.1	4.8	1.7	8.4	0.1	0.2	39.8
40419P	Limehouse	2.1	0.5	6.4	50.3	0.2	1.3	4.0	0.2	0.3	30.0
40012W	Limehouse	2.7	1.2	6.2	50.9	1.7	1.4	6.8	0.1	0.3	26.0
40010P	Limehouse	2.5	0.9	6.6	51.1	0.5	1.4	4.6	0.1	0.4	30.3
40008Z	Limehouse	3.5	1.0	7.2	56.5	0.1	2.3	6.8	0.1	0.2	20.0
40007Q	Limehouse	2.4	1.0	6.8	52.3	0.7	1.0	5.1	0.1	0.5	27.7
40000S	Limehouse	1.4	0.6	3.5	28.2	0.1	0.8	2.5	0.1	0.2	61.7
40004W	Limehouse	1.3	0.7	2.8	28.0	0.1	0.7	3.1	0.1	0.2	61.6
40003Y	Limehouse	0.6	0.1	1.5	16.6	0.0	0.4	0.5	0.0	0.1	78.0
40002P	Limehouse	1.6	0.7	3.7	28.1	0.1	0.9	2.7	0.0	0.2	61.0
32706R	Liverpool (Ball)	3.1	2.1	5.4	52.7	0.3	1.1	1.5	0.0	0.1	33.2
29101Y	Longton Hall	1.3	0.3	2.6	67.7	0.1	6.2	6.9	0.1	0.2	12.9
32707P	Lowestoft	0.4	0.0	1.1	42.9	0.1	1.8	0.8	0.0	0.0	50.5
1059 E22	Nantgarw	0.8	0.1	9.0	51.1	0.4	1.7	8.2	0.0	0.2	26.0
1054 E4	New Hall	0.9	0.2	17.4	55.5	0.1	0.8	10.2	0.1	0.1	14.4
1053 E3	New Hall	1.1	0.1	10.9	33.9	0.1	0.6	3.0	0.0	0.1	49.9

Results II: Laser Ablation Inductively Coupled Plasma Mass Spectroscopy

Table 51 - LA-ICPMS data for British porcelain glazes in weight percent as oxides (continued)

Label	Factory	Na₂O	MgO	Al₂O₃	SiO₂	P₂O₅	K₂O	CaO	TiO₂	Fe₂O₃	PbO
1058 E19	Pinxton	0.2	0.1	4.5	36.1	2.9	2.1	4.6	0.1	0.1	48.9
32701Q	Plymouth	0.8	2.4	13.4	77.2	0.5	2.0	2.9	0.0	0.5	0.0
32702Z	Pomona	0.9	2.7	6.0	50.4	0.1	2.0	1.2	0.1	0.4	35.7
1060 E23	Swansea	1.0	0.2	10.6	50.3	1.2	2.7	7.6	0.0	0.3	24.3
1071 E41	Swansea	14.7	0.6	1.4	32.4	4.4	6.2	4.5	0.2	2.0	27.9
32700S	Worcester	1.1	1.7	4.1	47.2	0.0	3.4	1.1	0.0	0.1	40.4
29099T	Worcester	1.2	2.0	3.9	50.8	0.2	3.4	1.6	0.0	0.5	34.5
29263P	Worcester	1.2	4.2	4.0	52.8	0.1	4.5	1.0	0.0	0.4	30.7
1064 E32	Worcester	1.0	2.1	3.4	59.0	0.0	3.0	1.9	0.0	0.2	28.2
1063 E31	Worcester	1.5	2.0	4.4	46.9	0.1	3.3	0.6	0.0	0.2	39.0
1062 E27	Worcester	1.4	1.6	4.6	45.7	0.1	3.8	0.7	0.0	0.3	40.7
1068 E37	Worcester	0.8	1.3	4.6	62.8	0.1	0.9	5.9	0.0	0.1	23.3
1067 E36	Worcester	0.8	1.8	5.8	64.1	0.0	1.0	2.8	0.0	0.3	21.5

Trace elements in porcelain glazes

Trace elements are important to consider in porcelain glazes, because it has been demonstrated that the major and minor elemental composition generally shows little intra-factory variation (this is discussed with reference to SEM-EDS/WDS data in Section 3.4.1, and HH-XRF data in Section 5.2.2). It is hoped that by comparing the trace elemental composition of the glaze with the paste, it may be discovered the extent to which common raw materials (e.g. silica, lead) were obtained from the same source, and whether the intra-factory variation in trace elements is greater than that present in major elements. The distribution of trace elements within the glazes is illustrated in Figure 146, and the correlation between these variables is shown in Table 52.

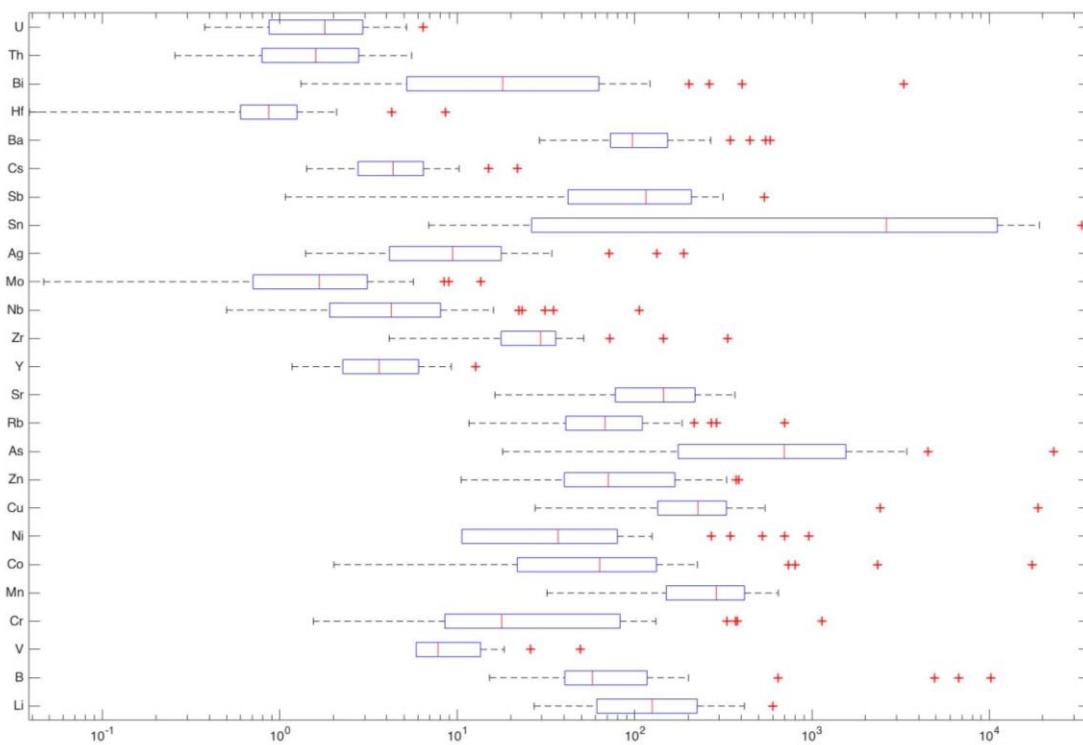


Figure 146 - boxplot illustrating the distribution of each of trace elements, minus REEs, in the porcelain glazes. To more clearly demonstrate the overall variability, a log scale has been used on the x axis (ppm).

The relationship that appears to exist between cobalt, copper and arsenic, and nickel and bismuth, was investigated and found to be due to the presence of two outliers (1057 E28 Crown Derby and 1071 E41 Swansea) that contained these elements abundantly compared with the other samples. This may be due to the presence of underglaze blue pigment that was not seen during analysis. These data having been removed, the elements exhibit no significant relationship.

A more robust linear trend exists between strontium and manganese (Figure 147) and strontium and cesium (Figure 148). These are interesting because they are prevalent in leaded and non-leaded glazes on porcelain from all paste types. The strongest relationship can be demonstrated in Limehouse and Worcester porcelain, which have high-lead glazes. Both elements are enriched in these porcelains, and depleted in unleaded glazes.

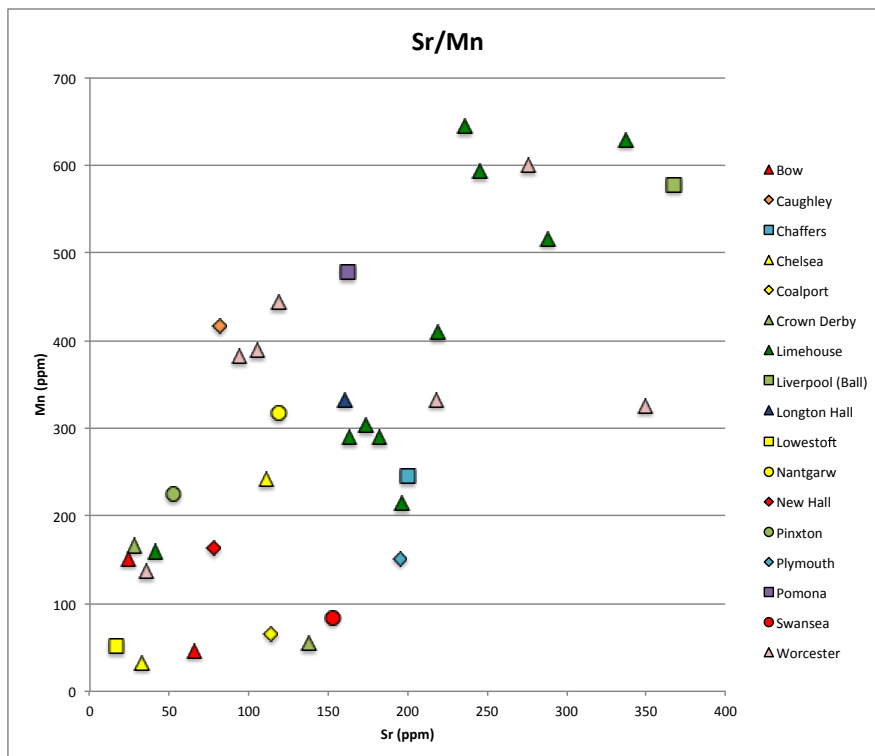


Figure 147 - strontium vs manganese in British porcelain glazes, by factory

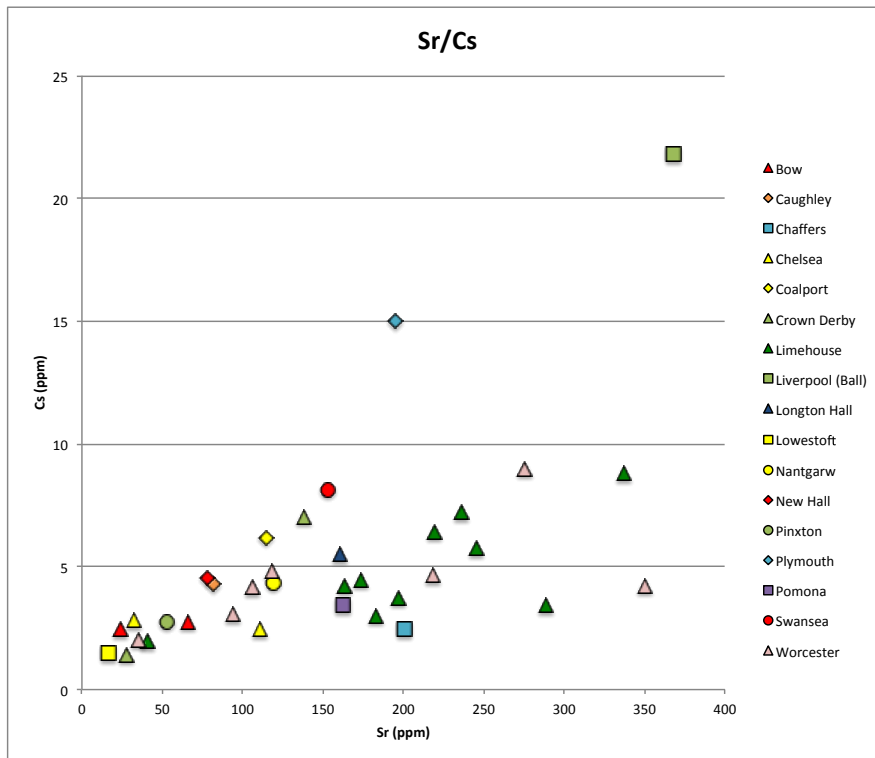


Figure 148 - strontium vs cesium in British porcelain glazes, by factory

The association between zirconium and hafnium that was found in the pastes also exists in the glazes (Figure 149). Both elements are enriched in two glazes from Bow and Limehouse, two glazes that also contain significant amounts of tin, see Figure 150. Tin and lead are related in Chaffers, Limehouse and Lowestoft glazes, and tin is not generally found in any low-lead (PbO 5-30%) or leadless (PbO <5%) glazes.

Results II: Laser Ablation Inductively Coupled Plasma Mass Spectroscopy

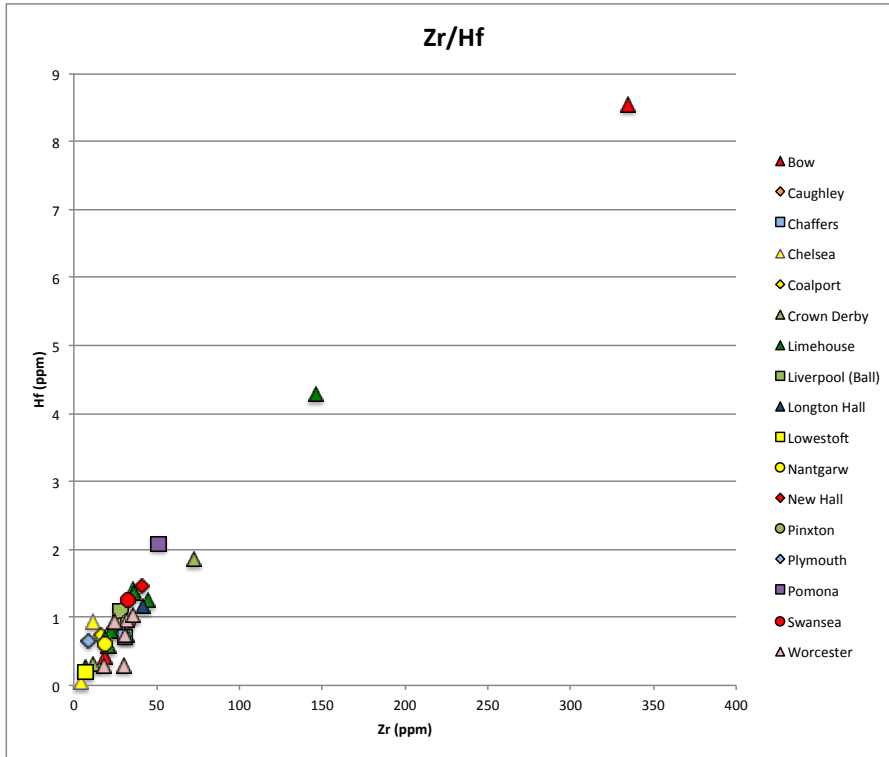


Figure 149 - zirconium vs hafnium in British porcelain glazes, by factory

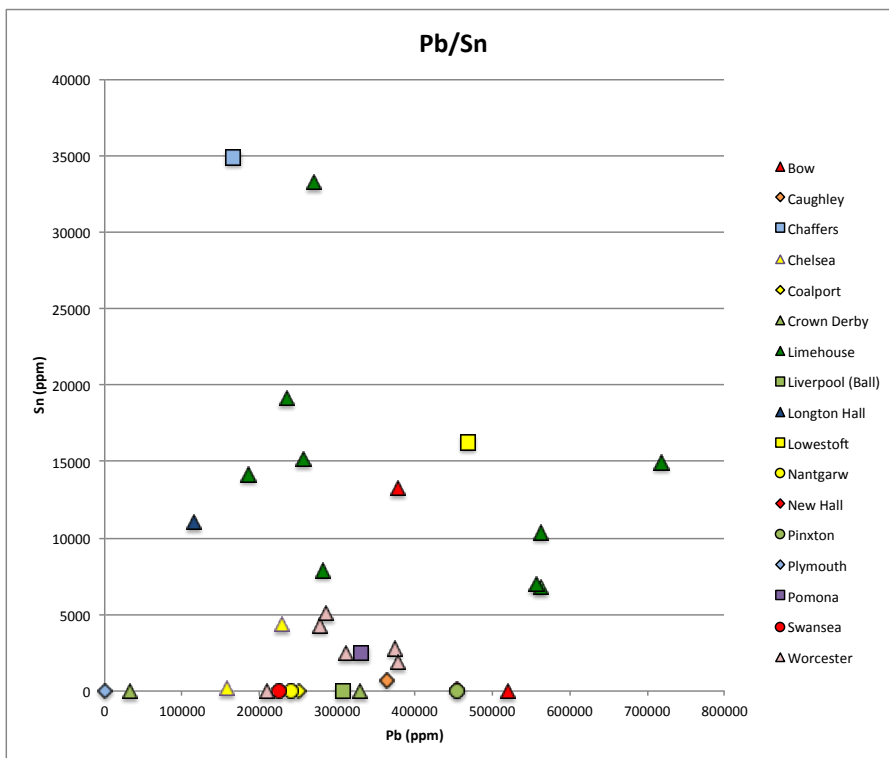


Figure 150 - lead vs tin in British porcelain glazes, by factory

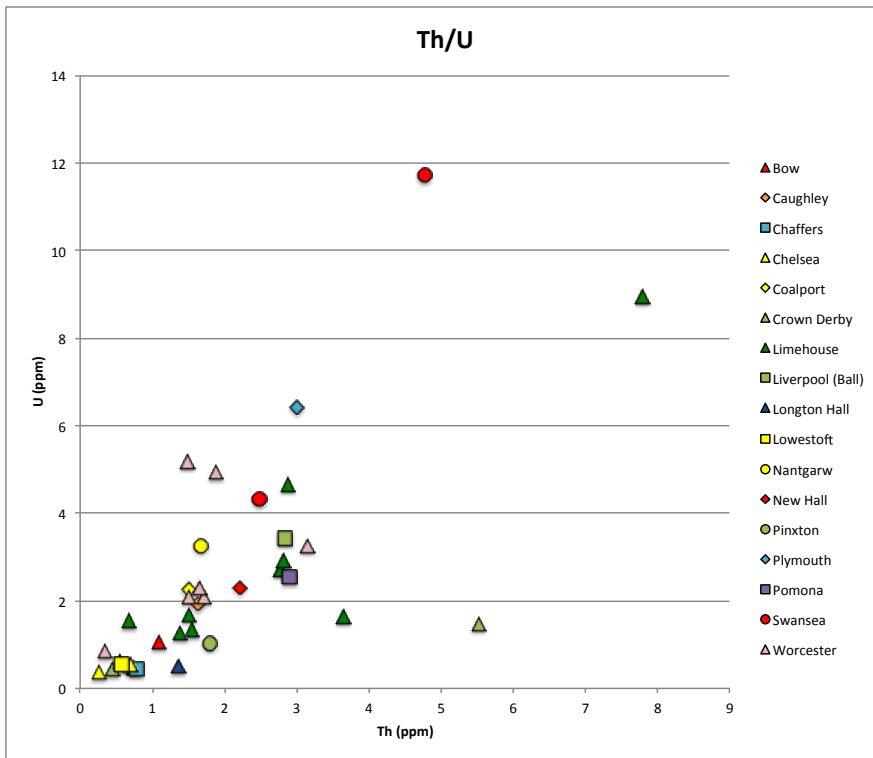


Figure 151 - thorium vs uranium in British porcelain glazes, by factory.

The relationship between Th and U is more straightforward in the glaze data than in the paste; there is a positive trend that exists among factories which have leaded glazes. The unleaded glaze of the Plymouth porcelain is relatively U-enriched, as are two Worcester outliers. A further outlier from Limehouse, and one Derby sample, are relatively Th-enriched. There are groups within the data that correspond to factories, such as Limehouse and Worcester, but there is also significant overlap between factories, especially where lower Th and U are present.

Rare Earth Elements in porcelain glazes

The chondrite-normalised REE data for glazes are presented in Table 53, and the raw data and normalisation values are in Appendix Table 43 and Appendix Table 40 respectively. Glazes in general are less REE-enriched than pastes, although this varies depending on the factory. As in the pastes, it is generally the glazes from Limehouse that contain the greatest concentrations of REEs. The ratio of Pr_{CN}/Yb_{CN} shows greater variation than that of the pastes, with significant outliers from Worcester and Limehouse, see Figure 152.

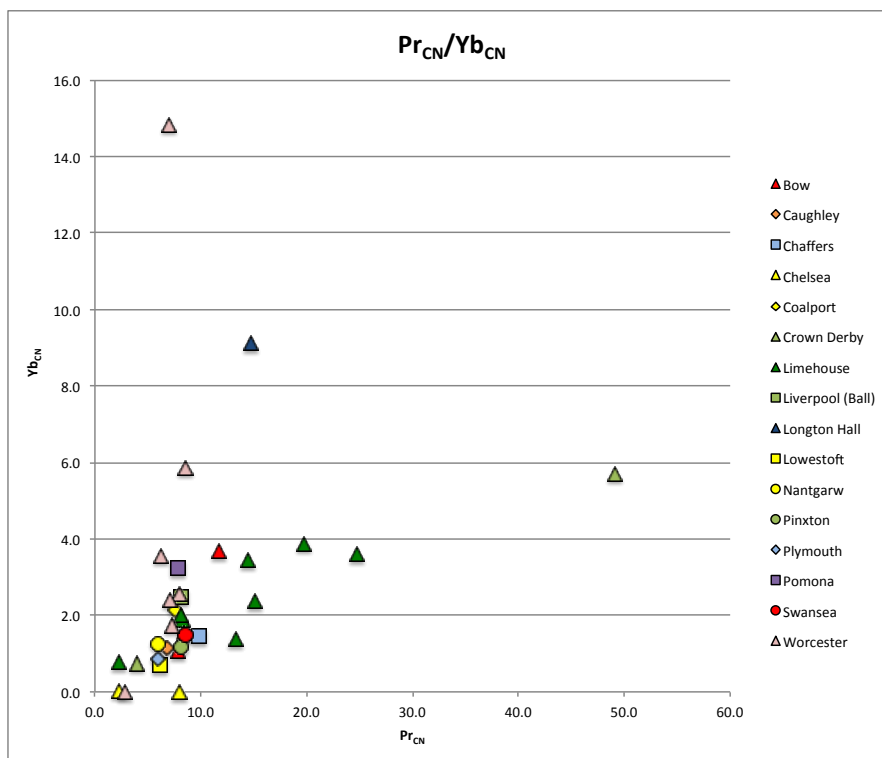


Figure 152 - Pr_{CN} vs Yb_{CN} in British porcelain glazes, by factory.

Results II: Laser Ablation Inductively Coupled Plasma Mass Spectroscopy

Table 53 - Rare Earth Elements (REE) in British porcelain glazes. All values are chondrite normalised (CN).

Label	Factory	La	Ce	Pr	Nd	Sm	Eu	Gd	Tb	Dy	Ho	Er	Tm	Yb	Lu	(Ce/Ce*) _{cn}	(Eu/Eu*) _{cn}	Pr/Yb
32703X	Bow	17.4	10.1	7.8	5.9	5.9	0.6	3.0	2.3	2.6	1.2	1.7	1.7	1.1	2.1	0.8	0.1	12.4
29100P	Bow	25.0	16.9	11.8	8.8	8.6	1.8	3.5	2.9	3.6	1.5	2.3	3.4	3.7	5.8	0.9	0.3	6.5
1069 E39	Caughley	15.9	10.1	6.9	5.7	6.8	1.1	3.5	3.0	3.8	1.1	1.9	2.7	1.1	3.2	0.9	0.2	6.2
32704V	Chaffers	20.9	13.0	9.9	6.9	8.3	1.0	3.6	2.2	2.6	1.1	1.7	2.1	1.5	2.5	0.8	0.2	10.2
32699W	Chelsea	16.5	14.7	8.0	5.0	4.2	9.9	14.0	0.6	2.2	0.6	1.7	1.5	0.0	10.5	1.2	1.1	0.8
29106Z	Chelsea	10.7	4.2	2.2	2.9	3.0	2.4	1.0	1.0	1.1	0.4	0.9	0.0	0.0	4.3	0.7	1.2	0.9
1072 E44	Coalport	18.8	9.7	7.6	6.2	6.9	1.3	2.6	1.9	2.4	1.0	1.4	1.5	2.1	0.8	0.7	0.3	6.0
1057 E18	Crown Derby	9.9	5.1	4.0	3.0	3.6	0.6	1.7	1.3	1.4	0.5	0.7	0.9	0.7	0.9	0.7	0.2	6.1
1056 E17	Crown Derby	117.6	75.3	49.2	35.2	31.0	5.9	9.2	7.7	7.8	3.4	5.1	6.6	5.7	6.8	0.9	0.3	8.3
40419P	Limehouse	62.2	38.2	24.8	18.3	17.6	4.4	6.0	4.2	5.6	2.1	2.9	3.1	3.6	4.2	0.9	0.4	5.6
40012W	Limehouse	40.7	17.9	13.3	8.5	6.7	2.1	3.4	2.2	2.1	0.6	1.1	3.0	1.4	1.8	0.7	0.4	6.3
40010P	Limehouse	34.2	23.9	15.1	11.1	14.8	1.0	8.0	6.2	6.1	2.1	3.5	3.3	2.4	2.3	1.0	0.1	15.2
40008Z	Limehouse	44.6	31.1	19.7	14.2	17.7	3.4	6.9	7.2	7.8	2.5	3.6	3.8	3.9	2.4	1.0	0.3	5.8
40007Q	Limehouse	31.7	21.7	14.5	10.5	13.2	2.5	6.2	6.8	7.4	2.3	2.9	3.9	3.4	2.9	0.9	0.3	5.9
40000S	Limehouse	20.1	13.3	8.3	6.3	6.5	1.3	3.0	3.4	3.6	1.5	1.6	1.4	1.9	1.2	0.9	0.3	6.5
40004W	Limehouse	19.7	13.0	8.5	6.4	6.3	0.7	3.6	2.8	3.1	1.1	1.6	1.9	1.5	1.6	0.9	0.1	11.7
40003Y	Limehouse	4.7	4.0	2.2	1.8	2.6	0.5	1.5	1.2	1.3	0.4	0.6	0.9	0.8	0.7	1.2	0.2	4.3
40002P	Limehouse	18.9	13.3	8.1	6.0	6.1	0.1	4.5	7.8	3.6	0.9	1.6	2.2	2.0	6.5	1.0	0.0	111.0
32706R	Liverpool (Ball)	18.7	10.9	8.1	7.4	10.2	1.6	6.0	5.6	6.0	2.1	3.1	3.0	2.5	3.2	0.8	0.2	5.0
29101Y	Longton Hall	36.6	19.9	14.7	11.2	11.1	1.9	5.1	3.6	6.7	4.0	7.7	9.9	9.1	9.8	0.8	0.2	7.8
32707P	Lowestoft	12.8	9.6	6.1	4.6	4.6	1.5	2.1	1.4	1.4	0.5	0.7	1.1	0.7	0.8	1.0	0.4	4.2
1059 E22	Nantgarw	13.3	7.4	6.0	4.7	3.3	0.2	3.6	1.2	2.0	0.3	2.7	0.3	1.3	5.5	0.8	0.1	25.9
1054 E4	New Hall	14.4	5.8	3.0	9.1	11.7	1.9	6.3	6.4	0.8	0.0	1.8	5.4	5.1	4.6	0.7	0.2	1.6
1053 E3	New Hall	21.8	11.6	2.9	5.5	2.0	0.7	2.1	2.0	1.7	0.0	0.3	0.0	2.8	1.5	0.9	0.3	4.4
1058 E19	Pinxton	19.2	12.4	8.2	6.3	4.0	0.9	3.0	2.3	1.9	0.6	1.3	1.8	1.2	1.1	0.9	0.3	8.6

Results II: Laser Ablation Inductively Coupled Plasma Mass Spectroscopy

Table 53 - Rare Earth Elements (REE) in British porcelain glazes. All values are chondrite normalised (C_N). (continued)

Label	Factory	La	Ce	Pr	Nd	Sm	Eu	Gd	Tb	Dy	Ho	Er	Tm	Yb	Lu	(Ce/Ce*) C_N	(Eu/Eu*) C_N	Pr/Yb
32701Q	Plymouth	13.0	8.8	6.0	4.3	4.7	0.5	1.5	1.3	1.2	0.4	0.6	0.8	0.9	0.8	0.9	0.2	11.8
32702Z	Pomona	18.8	11.4	7.8	6.7	10.4	1.0	6.2	5.7	6.4	2.2	3.2	4.1	3.2	3.5	0.9	0.1	7.5
1060 E23	Swansea	20.9	11.0	8.6	7.2	7.2	1.6	2.7	2.2	2.3	0.8	1.1	1.4	1.5	2.2	0.7	0.3	5.4
32700S	Worcester	15.7	11.3	7.3	5.6	8.9	2.7	5.5	4.1	4.5	1.5	2.3	2.4	1.8	2.3	1.0	0.4	2.7
29099T	Worcester	16.4	11.6	6.3	4.7	9.6	1.0	7.3	4.2	3.8	2.8	4.4	1.3	3.6	3.7	1.0	0.1	6.5
29263P	Worcester	16.5	12.0	8.0	6.1	8.5	0.9	4.7	4.8	5.3	1.7	2.8	3.0	2.6	3.3	1.0	0.1	9.2
1064 E32	Worcester	20.8	12.8	6.9	5.9	1.5	15.1	4.2	1.2	1.9	1.2	0.3	3.1	14.8	15.7	0.9	5.3	0.5
1062 E27	Worcester	14.9	11.3	7.1	5.2	6.0	1.4	4.3	4.7	4.8	1.9	2.4	2.2	2.4	2.5	1.0	0.3	5.0
1068 E37	Worcester	11.2	5.0	2.8	1.2	5.8	1.0	0.0	0.0	3.4	0.0	0.0	0.0	0.0	3.4	0.7	0.4	2.7
1067 E36	Worcester	25.2	9.6	8.5	3.9	6.3	8.0	4.4	3.5	6.1	1.8	1.9	10.9	5.9	7.6	0.6	1.5	1.1

The Ce/Ce^*_{CN} vs Eu/Eu^*_{CN} ratio exhibits some more interesting behaviours, see Figure 153, due to the presence of Ce and Eu anomalies within the glaze data. Most glazes are grouped together with a consistently low ratio of measured to expected europium, indicating that a slight negative europium anomaly is common in the data. Significant outliers are two Chelsea frit porcelain glazes, and two Worcester glazes. Most glazes have a slight positive Ce anomaly, however Limehouse and Chelsea have outliers at either end, which shows that there may be significant intra-factory variation in glaze REEs. The two Worcester outliers are also outliers in the plot of praseodymium vs ytterbium, as they are more enriched in HREE than any of the other glazes here examined.

The outliers from Worcester and Chelsea are striking, because these glazes share no other common distinguishing features, and the remaining Worcester glazes do not show this trait, see Figure 154.

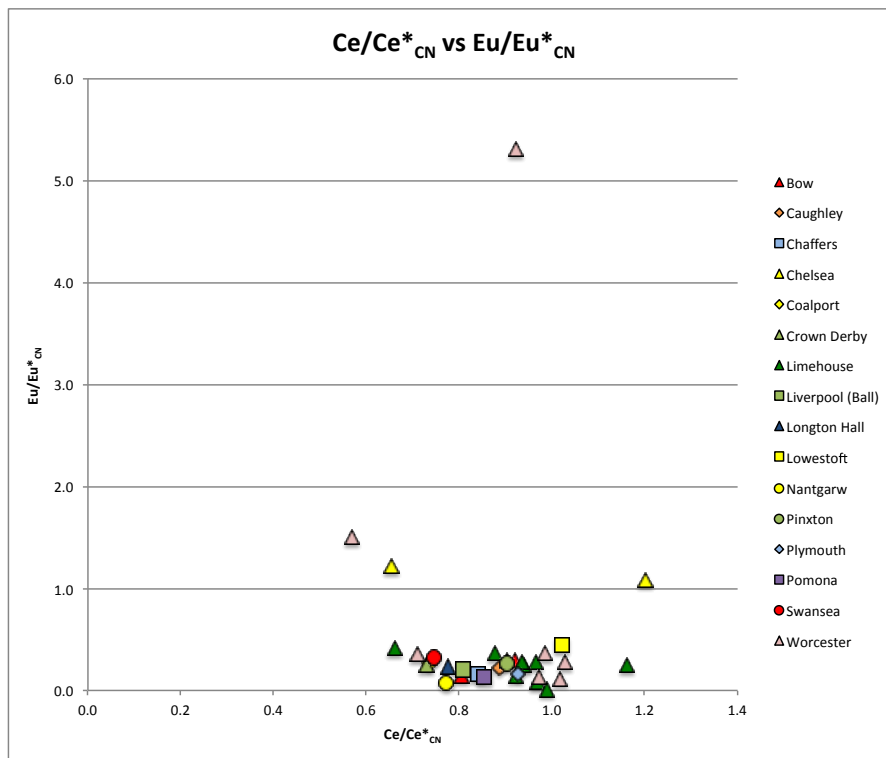


Figure 153 - Ce/Ce^*_{CN} vs Eu/Eu^*_{CN} in British porcelain glazes, by factory.

Results II: Laser Ablation Inductively Coupled Plasma Mass Spectroscopy



Figure 154 - REE_{CN} profiles for porcelain glazes from Bow, Chelsea, Limehouse, and Worcester.

Results II: Laser Ablation Inductively Coupled Plasma Mass Spectroscopy

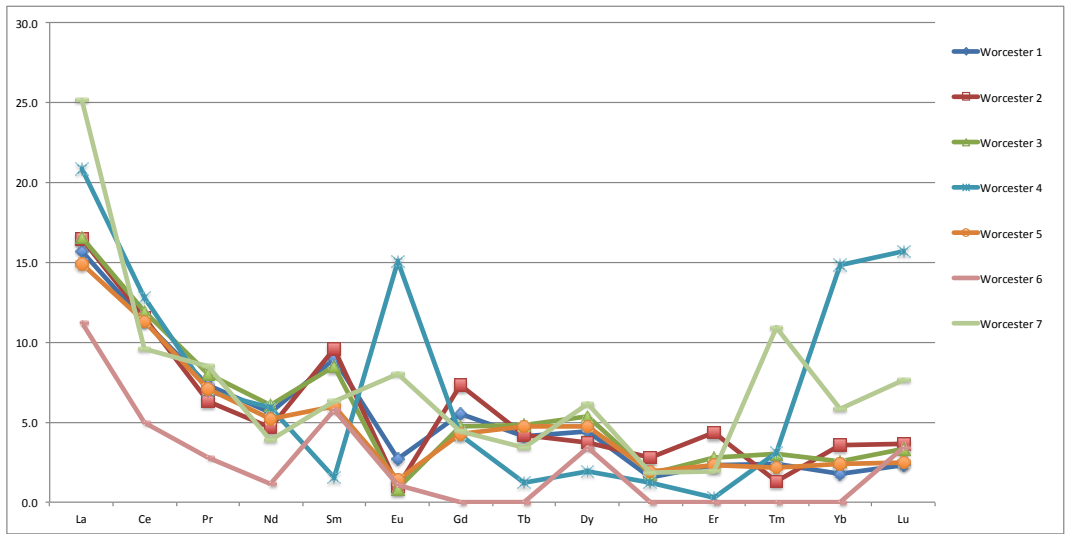


Figure 154 - REECN profiles for porcelain glazes from Bow, Chelsea, Limehouse, and Worcester. (continued)

The REEs present in the glazes show a greater degree of fractionation than the corresponding porcelain pastes. Enrichment of samarium and dysprosium is common, especially in Worcester glazes. The low-lead glazes exhibit less REE fractionation, see Figure 155, and the leadless Plymouth glaze the least of all.

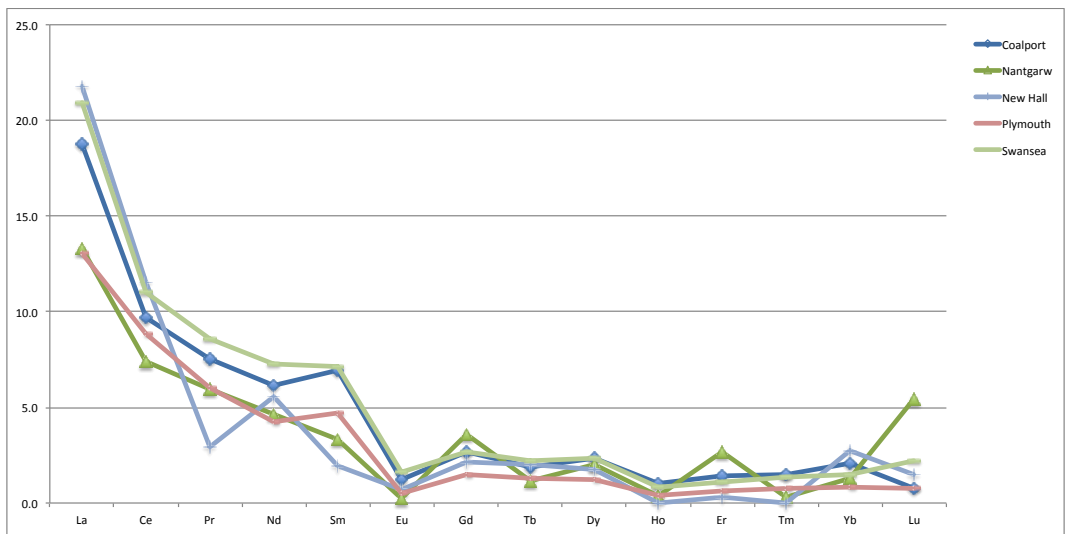


Figure 155 - REECN profile for low-lead and leadless porcelain glazes from Coalport, Nantgarw, New Hall, Plymouth, and Swansea

6.3 Summary and conclusions

In the methodological test, the LA-ICPMS data for the major and minor elements in the paste compare well with SEM-EDS data when converted to weight percent as oxides; the coefficient of determination (R^2) is better than 0.9 in most cases. Notable exceptions are potassium and iron. The paste composition compared much better than the glaze this is thought to be due to the much greater spot size of the laser ablation sampling system, which is generally deeper than the glaze in cross-section. This increases the risk of sample contamination by the surrounding paste and sample mount, and obscures the compositional zoning known to be present in porcelain glazes. As a result, some glaze data were exempted from this research, as they showed compositions that were not consistent with a porcelain glaze, and were assumed to have been contaminated.

The main sample set, comprising 58 samples, of which 57 were glazed, were analysed, and data for 49 elements were obtained. The major and minor elemental compositional data, calculated as weight percent as oxides, allow the paste type of the porcelain to be identified, as in SEM-EDS or WDS data.

Cobalt was found in pastes from Bow, Crown Derby, Limehouse, Lowestoft, and in all magnesian pastes. In the phosphatic and Limehouse pastes, it was strongly associated with barium, and in Bow, Crown Derby, Lowestoft and the magnesian pastes, it was also associated with bismuth.

Copper and manganese were found in Limehouse and magnesian pastes, and Chelsea frit pastes were enriched in manganese, but not copper. The magnesian pastes showed an association between copper, zinc and magnesium, through which Caughley, Pomona and Worcester were able to be distinguished from Chaffers and Liverpool (Ball).

Aluminium was found to be associated with niobium for all factories except the 'A'-marked sample. Aluminium was also associated with titanium, zirconium and hafnium for the magnesian pastes and those that are thought to have used ball clay, as opposed to china clay.

Lead was present in Chelsea frit and Limehouse pastes, in which it was associated with tin. Lead was found as an additional flux in magnesian pastes, but was not associated with tin.

In the ratio of thorium to uranium, this was relatively static for the china clay pastes, including the 'A'-marked group. The magnesian pastes and New Hall porcelain were relatively enriched in uranium, especially Caughley and Worcester. The ball clay pastes were relatively enriched in thorium, especially Swansea phosphatic and Limehouse.

The REE data were normalised to the chondrite, and the ratio of praseodymium to ytterbium was used to indicate the ratio of LREE to HREE. This was found to be fairly linear for the ball clay and china clay pastes, but the magnesian pastes showed no distinct pattern, and there were outliers from Bow, Crown Derby and Limehouse.

The ratio of measured to expected cerium against measured to expected europium was used to indicate the extent of anomalies caused by ionisation of these elements. A divide was evident between the magnesian pastes, New Hall and Plymouth, which tend to have no strong anomalies, and the phosphatic, frit and Limehouse SAC pastes, which tend to have negative cerium and europium anomalies. The 'A'-marked sample was a clear outlier in this case, due to a strong positive europium anomaly.

The REE profiles within each factory for which more than one sample was available, i.e. Bow, Chelsea, Limehouse and Worcester, were internally consistent. Worcester was the least enriched in REEs overall, and showed the most fractionation.

Aluminium was plotted against the sum of the REEs, and a relationship was found for the ball clay and bone china pastes. Therefore, the REE data were renormalized to the upper continental crust (UCC) proxy MUQ, and profiles were generated for each paste type, using the mean of groups from factories where more than one sample was available. While samples of the same paste type were generally more similar to one another than to samples from other paste types, differences were found between factories through their enrichment of LREEs or HREEs, the extent of fractionation within the sample, and the presence or absence of cerium and europium anomalies.

The patterns that were observed in the chondrite-normalised data were also evident in the MUQ-normalised data, and the latter made significantly different profiles easier to compare.

In the glazes, a relationship was found between strontium, manganese and cesium. The ratio of zirconium to hafnium was found to be similar to that present in the porcelain pastes, and consistent between samples. Lead and tin were found to be related in glazes from Bow, Limehouse and Lowestoft. The relationship between thorium and uranium was found to be more consistent than in the pastes, showing a positive linear trend in samples that have leaded glazes.

The REEs were normalised to the chondrite, and found to be generally less REE-enriched than the pastes. Limehouse, Bow, Crown Derby and Worcester low-lead glazes were found to be the most REE-enriched. The ratio of measured to expected cerium and europium was either just below or close to 1, illustrating that most glazes have a slight negative anomaly, or no significant anomaly, for both elements. Significant outliers were two Worcester and two Chelsea frit glazes, which have positive europium anomalies, but otherwise no evident similarities. Chelsea and Limehouse had glazes that have both positive and negative cerium anomalies.

The glaze REE profiles showed consistency for Bow and most Limehouse samples, even between low-lead and high-lead Limehouse glazes, but significant variation for Chelsea and Worcester glazes. The leadless glazes on Coalport, Nantgarw, New Hall, Plymouth and Swansea samples showed more similarity to one another.

It is concluded that there is evidence for some interesting patterns in the data, which might be used to gain information about different porcelain factories, and their sources of raw materials. However, more samples are needed to resolve the groupings, and demonstrate the range of intra-factory variation. These findings will be developed in greater detail in the following chapter.

7 Discussion: using multiple analytical techniques to characterise British porcelain

7.1 Introduction

This research has adopted an exploratory approach to the analysis of British porcelain; three analytical techniques have been used to obtain data from a wide range of material from different factories and periods. The aims were to build on the characterisation of British porcelain in general, and to identify the features that have the potential to provide characteristic data. This series of experiments with a variety of analytical techniques has been used to develop a novel methodology that is optimised for the analysis of this material type. In so doing, it has added to the understanding of this material, and the industry that produced it. All of these findings will be discussed in this chapter, following a summary of the background to the project, and the rationale to the selection of research questions.

First, the characteristics of British porcelain that have been discovered through a review of the existing data will be discussed, and the use of novel analytical techniques. Then the development of the novel analytical methodology will be discussed, from the rationale behind the choice of technique to the nature of the data gathered. The techniques are critically assessed, with regard to their suitability for use in the different contexts where British porcelain research is typically carried out, and also to determine the usefulness of the data thus collected.

The ultimate aim of this research has been to add to the existing state of knowledge about British porcelain as a class of ceramics, and as an historic event in British industrial development, using previously unexplored sources of scientific data. In the final section of this Discussion chapter, the achievements made in this direction are described.

7.2 Characterising British porcelain using multiple analytical techniques

7.2.1 Evaluating SEM-EDS data from published sources

The first question that was of interest to this research was to what extent the existing corpus of analytical data can be used to characterise British porcelain. Studies have been carried out that examine the output of a single factory through time, or compare two or more factories that operated in the same area or period, or which were somehow linked by an individual or transfer or technology; these are summarised in the Literature Review Sections 2.2.4 and 2.3.2. The present work has collected, for the first time, data from multiple published analytical studies of British porcelain. It has discovered that quantitative data for major and minor elements can be used to distinguish, not only paste types, but in some cases individual factories. These findings have been discussed in detail in the Meta-analysis, Chapter 3, and are summarised in Table 4 and Table 5.

Of the magnesian porcelains, Bovey Tracey can be distinguished by the presence of barium in the paste, due to the inclusion of barite, although it is not known whether this component was added deliberately, or whether it represents a contaminant present in a source of raw material that was not used by other magnesian-producing factories. Bow and Isleworth can be distinguished, not only from the other phosphatic porcelain, but also from one another. The paste of both appears to have been made with less potash and clay, due to the lower levels of potassium and aluminium in the products, when compared with later phosphatic porcelain including bone china. Furthermore, the ratio of potassium to aluminium is greater in Isleworth porcelain (0.2-0.5) than in Bow (0.1-0.2) (Figure 41).

From the small number of frit porcelains for which data were available, Chelsea can be distinguished on the basis of more crown glass in the formula; the ratio of silica to calcium is significantly lower than that of Derby, Longton Hall and Limehouse pastes, which have correspondingly higher lead from the use of flint glass (Figure 42).

'A'-marked porcelain can be distinguished from among the silicious-aluminous-calcic (SAC), hard-paste and hybrid hard-paste porcelains, on the basis of relatively large quantities of crown glass and clay in the paste ($\text{SiO}_2/\text{CaO} < 20$, $\text{SiO}_2/\text{Al}_2\text{O}_3 < 3$). Cookworthy's Plymouth porcelains belong in the same group, but used no glass, a similarly high proportion of clay ($\text{SiO}_2/\text{Al}_2\text{O}_3 < 7$), and greater amounts of silica ($\text{SiO}_2 > 70\%$). Both of these are shown as distinct groups in the ternary plot for this paste type (Figure 43).

Some distinction had been possible when comparing two or more factories in individual studies, and this research demonstrates that many of these conclusions are valid when all of the data are compiled. Furthermore, traditions of imitation and technology transfer can be traced between factories, through similarities in the paste composition.

An example of this can be found in the group of magnesian factories, where there is historical evidence for the involvement of Richard Podmore, a former employee of the Worcester factory, in the establishment of a porcelain factory in Liverpool in 1755 (Watney, 1964; Watney, 1995). The products of this factory, known by the name of the Master of the works, Richard Chaffers, and later Phillip Christian, show strong compositional similarities to Dr Wall-period Worcester, when compared with other magnesian-producing factories, such as Vauxhall and Bovey Tracey. They contain less magnesian flux (5-12% MgO), and less clay ($\text{Al}_2\text{O}_3 < 4\%$), and in this way they can be distinguished from Flight-period Worcester (1783 - 1793) and the porcelain produced by another ex-employee, Thomas Turner, at Caughley (Godden, 1970; pp. 435 - 436). These later magnesian porcelains (Flight-period Worcester and Caughley) contain more clay ($\text{Al}_2\text{O}_3 > 4\%$), and correspondingly less lead (PbO 1-5%, as opposed to 4-8%), and are compositionally very similar. This new formula with a greater proportion of the plastic components of the porcelain (i.e. clay) and decrease in the fluxing ingredients (i.e. steatite and lead) may have been a response to technological developments in kilns, which allowed higher temperatures to be reached and sustained safely, enabling the successful firing of less fertile pastes (Grant-Davidson, 1966). This possibility will be discussed in greater detail in Section 7.4.2.

Extensive compositional overlap is shown among the products of the Liverpool phosphatic porcelain factories, which operated in close proximity to one another, and were often run by members of the same family, the Penningtons. All of the products contain less bone ash flux than the London-based phosphatic factories, and correspondingly more silica ($\text{SiO}_2/(\text{CaO} + \text{P}_2\text{O}_5) > 1.2$) (Figure 38). Owen and Sandon found no way to distinguish these porcelains from one another reliably (Owen and Sandon, 1998), and this research upholds that finding, although the meta-analysis carried out as part of this research has demonstrated that it is possible to distinguish Liverpool phosphatic porcelains as a whole from other groups of the same paste type.

These findings rely entirely on the elemental composition of the ceramic paste; glazes have been found to show less inter-factory variation in composition, and fewer characteristic features, as discussed in Section 3.3, and summarised in Table 5. This may be attributed to the largely homogeneous recipe that was used in most cases. At the time when porcelain was developing as an industry in Britain, the transparent lead-rich glaze was already established, and was in use on earthenware and delftware (Watts, 2003). As a result, the major and minor elemental composition of the glaze is rarely characteristic of the factory of origin. Using the amount of lead flux present in the glaze, it appears to be possible to distinguish some factories. In the high-lead category ($\text{PbO} > 45\%$), are Bow, Chelsea, Derby and Lowestoft glazes; in the medium-lead category ($\text{PbO} 30\text{-}45\%$) are Isleworth, Limehouse and Chaffers; and in the low-lead category ($\text{PbO} 5\text{-}30\%$) are Nantgarw and Grainger glazes. All other factories fall under more than one category.

The meta-analysis concluded that some factories produced porcelain pastes with a unique elemental composition, indicating the use of formula that was different from the other factories producing porcelain of that paste type. In other cases, a distinction could be drawn between groups of factories operating in one tradition, such as Vauxhall and Bovey Tracey, and those in another, such as Worcester, Chaffers, Christian and Caughley. The glazes showed substantially less inter-factory variation in composition; the main distinguishing feature among the leaded glazes appears to be the absolute amount of lead present.

7.2.2 Trace elemental compositional data from LA-ICPMS analysis

In order to supplement these major and minor elemental compositional data, LA-ICPMS has been used to obtain a large suite of trace elements at very high precision down to low limits of detection. A set of 46 samples was used, comprising pieces from 14 factories, many of which had published SEM-EDS/WDS data that had been included in the meta-analysis in Chapter 3. It was hoped that the greater resolution in the data might produce more distinctions within and between sets of material with very similar composition. This has been the case with other types of archaeological materials, notably man-made glass and ceramic studies.

Provenance studies of British porcelain by the trace elemental composition of the paste is a complex matter, compared with the same process when applied to natural materials like obsidian and marble, or basic fired-clay ceramics. This is because of the mixture of raw materials that were used to create British porcelain (typically clay, silica and one or more fluxing substances), all of which contribute to the composition. Historical records exist that suggest some of the sources of clay and sand which were available for the manufacture of porcelain in the 18th century. Two sources of tertiary clay in Dorset were widely exploited for ceramic production throughout this period; one in Poole (Latham, 1979), and another in Bideford (de la Beche and Reeks, 1871; p.5). A white-firing clay was also found inland at Bovey Tracey (Massey, 2002), and another source further north at Brassington in Derbyshire (Housley, 1991). China clay was mined near St Stephens in Cornwall, along with porcelain stone (Hitchins and Drew, 1824; Owen, 1873; pp.vi-vii), and the steatite used in all magnesian porcelains, which was located at Gew Graze (Barrett, 1966; p.3). Another source of kaolinitic clay may have been imported from America, and there is evidence that this was used by Heylyn and Frye in London, and Cookworthy in Plymouth (Anderson, 1986). A well-known source of sand was Alum Bay on the Isle of Wight (Grosley, 1772; p.77), and flint was obtained from Brighton (Porter, 1832; p.36).

It has proved difficult to proceed from these records to establishing exactly which sources were in use by which factories, since documentary records patents and recipes that might tie a factory to a source of raw materials are scarce. Furthermore, when evaluating compositional data from the paste, it must be remembered that some constituents may have more than one source. Owen gives the example of small quantities of phosphorus found in Worcester magnesian porcelain, which may have been contributed by bone ash, as in phosphatic porcelains, or by apatite ($\text{Ca}_5(\text{PO}_4)_3$) that can be found in china clay (Owen, 1997).

Some patents exist for the production of porcelain at Bow and Plymouth; although these list the materials and general proportions used in their formulae, they are not generally specific as to the source of the materials. The Heylyn and Frye patent of 1744 identifies *uneka* (Tait, 1963; Freestone, 1996), and Cookworthy and Champion's patent of 1775 specifies the use of Cornish china clay (Mackenna, 1946; pp. 34-37), because these were the aspects of the formula that they were seeking to protect, but the sources of ingredients such as sand, flint and glass appear to be unimportant to the formula's patent.

It was therefore hoped that, by using these known matches between the raw material and the finished product as benchmarks, products of factories whose raw material sources are not presently known could be matched by comparison. Worcester, Plymouth, and Bow are used for this purpose, and represent the use of Cornish steatite, Cornish china clay and porcelain stone, and Dorset ball clay and Lynn sand respectively. Another important aim of this section of the research was to characterise porcelain from the 'A'-marked group, which have been found to be consistent with the first Bow patent, and therefore may have been made with clay imported from North Carolina, USA (Freestone, 1996). If this is the case, the trace elemental composition of this porcelain sample may have traits that are unique, when compared with British porcelain from the same period that was produced using clay sourced from Britain.

Three strategies were used on the LA-ICPMS data, in order to use them to characterise the samples: major and minor elemental composition, which is comparable with SEM-EDS/WDS data; trace element ratios; and chondrite-normalised or MUQ-normalised Rare Earth Elements (REE_{CN} or REE_{MUQ}) profiles. The findings of these aspects are summarised in Table 54, with respect to the paste types and factories in the sample set. It may be observed from this summary that the 'A'-marked sample is unique in several respects: the paste contains few trace elements, including the transition metals, zirconium and hafnium, indicating that a pure source of clay was used; it is depleted in strontium, relative to the paste which it most closely resembles (Plymouth); and the REE composition is significantly enriched in LREEs ($\Sigma LREE/\Sigma HREE > 2$) with a strong negative cerium anomaly and positive europium anomaly.

Among the porcelains for which a British source of clay may be assumed, the paste type, and therefore fluxing material, appears to have a substantial effect on the trace elemental composition of the object. Magnesian porcelain demonstrate a relationship between cobalt and bismuth, and between magnesium, copper and zinc. Uranium is enriched, relative to thorium. They are typically HREE-enriched with a positive cerium anomaly and negative europium anomaly.

Phosphatic porcelains fall into two groups, depending on the type of clay that was used in the paste. Phosphatic ball clay pastes (Bow, Chelsea, Crown Derby and Lowestoft) are relatively enriched in trace elements that accompany the alumina contributed by the clay, including titanium and the other transition metals, barium, zirconium and hafnium. Thorium is generally enriched, relative to uranium. They are generally LREE-enriched, although Lowestoft is a notable exception, and the presence and strength of anomalies varies between factories. The phosphatic or bone china pastes that contain china clay (Coalport, Nantgarw, Pinxton and Swansea) contain much lower levels of the trace elements that are associated with aluminium in the ball clay pastes. Thorium is enriched, relative to uranium. Coalport Nantgarw and Swansea are LREE-enriched, but Pinxton has an equal ratio of light to heavy REEs, and all three have a slight negative europium anomaly.

Discussion: using multiple analytical techniques to characterise British porcelain

Table 54 - summary of distinguishing features from the major and minor elemental, trace elemental, and MUQ-normalised REE composition of British porcelain samples analysed by LA-ICPMS

Type	Attribute	Factories
Major and minor elemental composition		
magnesian	5-10% PbO <1% PbO	Worcester, Caughley, Pomona Chaffers, Liverpool (Ball)
phosphatic	5-8% Al ₂ O ₃ , 0.2-0.4% TiO ₂ 9-20% Al ₂ O ₃ , 0.3-0.5% TiO ₂ 9-20% Al ₂ O ₃ , 0.03-0.05% TiO ₂	Bow, Lowestoft Chelsea, Crown Derby Coalport, Swansea
frit	CaO/PbO 2.5-10 CaO/PbO 0.5-1.5	Chelsea Longton Hall
SAC	TiO ₂ 0.02-0.05 TiO ₂ 0.5-0.9	A'-marked, New Hall, Plymouth, Swansea Limehouse
Trace elemental composition		
magnesian	Co/Ba 1-2, Co/Bi 1-3, Cu/Mn >1, Mg/Zn <100, Th/U <1 Co/Ba 1-2, Co/Bi 1-3, Cu/Mn <1, Mg/Zn >100, Th/U <1	Chaffers, Liverpool (Ball) Caughley, Pomona, Worcester
phosphatic	Co/Bi >1.5, Co/Ba >0.5, Al/Ti <100, Al/Zr <3000, Pb/Sn >10, V to As enriched, Bi >50ppm, Th/U >1 Co/Bi <1, Co/Ba <0.5, Al/Ti <30, Al/Zr >3000, Pb/Sn <10, V to As depleted, Bi <10ppm, Th/U >1	Bow, Chelsea, Crown Derby, Lowestoft Coalport, Pinxton, Swansea
frit	Cu/Mn <0.1, Al/Ti 10-30, Al/Zr 300-700, Sn <100ppm, Th/U 2.7-2.9 Cu/Mn 0.4-2.0, Al/Ti 15-25, Al/Zr 300-700, Sn <1000ppm, Th/U 3-7	Chelsea Longton Hall
SAC	Li >90ppm, Ba 100-250ppm, Al/Ti 370, Al/Zr 4000, Th/U 1.3, Ca/Sr 100, V to As depleted Li >90ppm, Ba 100-250ppm, Al/Ti 700, Al/Zr 7000, Th/U 0.9, Ca/Sr 10, V to As depleted Li 30-60ppm, Ba >300ppm, Co/Bi 10-100, Co/Ba 0.1-0.3, Al/Ti 15-20, Al/Zr 500-800, Pb/Sn 50-200, Th/U 1.5-4.5, V to As enriched Li 30-60ppm, Ba 50-80ppm, Al/Ti 600-900, Al/Zr 9000-13000, Th/U 0.4-0.5, Ca/Sr 50-200, V to As depleted Li 30-60ppm, Ba 50-80ppm, Al/Ti 20-100, Al/Zr 1000-3000, Th/U 0.4, Ca/Sr 20-100, V to As depleted	A'-marked Plymouth Limehouse New Hall Swansea

Discussion: using multiple analytical techniques to characterise British porcelain

Table 54 - summary of distinguishing features from the major and minor elemental, trace elemental, and MUQ-normalised REE composition of British porcelain samples analysed by LA-ICPMS (continued)

Type	Attribute	Factories
Rare Earth Elements (MUQ normalised)		
magnesian	HREE-enriched ($\Sigma\text{LREE}/\Sigma\text{HREE}$ 0.5), no anomalies	Caughley
	HREE-enriched ($\Sigma\text{LREE}/\Sigma\text{HREE}$ 0.3-0.7), positive Ce anomaly (1.1), negative Eu anomaly (0.1-0.7)	Chaffers, Liverpool (Ball)
	HREE-enriched ($\Sigma\text{LREE}/\Sigma\text{HREE}$ 0.7), positive Ce anomaly (1.2), negative Eu anomaly (0.5)	Pomona
	HREE-enriched ($\Sigma\text{LREE}/\Sigma\text{HREE}$ 0.3-0.7), Ce anomaly positive or negative (0.9-1.8), Eu anomaly positive or negative (0.6-2.0)	Worcester
phosphatic	LREE-enriched ($\Sigma\text{LREE}/\Sigma\text{HREE}$ 1.2-1.5), no anomalies	Bow
	LREE-enriched ($\Sigma\text{LREE}/\Sigma\text{HREE}$ 1.4), negative Ce anomaly (0.8), positive Eu anomaly (1.2)	Chelsea
	LREE-enriched ($\Sigma\text{LREE}/\Sigma\text{HREE}$ 1.7), negative Eu anomaly (0.8)	Coalport
	LREE-enriched ($\Sigma\text{LREE}/\Sigma\text{HREE}$ 1.2), negative Ce anomaly (0.8), negative Eu anomaly (0.8-0.9)	Crown Derby
	LREE/HREE equal (1), positive Eu anomaly (1.2)	Lowestoft
	LREE-enriched ($\Sigma\text{LREE}/\Sigma\text{HREE}$ 1.2), negative Eu anomaly (0.7)	Nantgarw
	LREE/HREE equal (1), negative Eu anomaly (0.9)	Pinxton
	LREE-enriched ($\Sigma\text{LREE}/\Sigma\text{HREE}$ 1.4), negative Eu anomaly (0.9)	Swansea
frit	LREE-enriched ($\Sigma\text{LREE}/\Sigma\text{HREE}$ 1.1-1.2), no anomalies	Chelsea
	HREE-enriched ($\Sigma\text{LREE}/\Sigma\text{HREE}$ 0.9), negative Eu anomaly (0.6)	Longton Hall
SAC	LREE-enriched ($\Sigma\text{LREE}/\Sigma\text{HREE}$ 2), negative Ce anomaly (0.7), positive Eu anomaly (2.7)	A ¹ -marked
	LREE-enriched ($\Sigma\text{LREE}/\Sigma\text{HREE}$ 1.1-1.5), negative Ce anomaly (0.8-0.9), Eu anomaly positive or negative (0.9-1.3)	Limehouse
	LREE-enriched ($\Sigma\text{LREE}/\Sigma\text{HREE}$ 1.5-2.0), positive Ce anomaly (1.1), negative Eu anomaly (0.3-0.4)	New Hall
	LREE/HREE equal (1), positive Ce anomaly (1.2), negative Eu anomaly (0.8)	Plymouth
	LREE-enriched ($\Sigma\text{LREE}/\Sigma\text{HREE}$ 1.4), positive Ce anomaly (1.2), positive Eu anomaly (1.5)	Swansea

Frit porcelains from Chelsea and Longton Hall differ in their ratio of calcium to lead, and therefore the proportions of two types of glass (crown or flint) that were used as the flux. Their ratios of trace elements such as titanium, zirconium and hafnium to aluminium are low and broadly similar, suggesting that a similar type of ball clay was used in both. Thorium is strongly enriched, relative to uranium. Neither shows substantial fractionation of the REEs, although Chelsea is slightly more LREE-enriched, and Longton Hall more HREE-enriched, and Longton Hall has a negative europium anomaly.

Limehouse porcelain belongs to the SAC group, but used ball clay instead of china clay, and so is considered separately from the others. Trace elements associated with aluminium are high in these pastes, and there is some evidence that it contains the blue pigment, smalt, which contributes cobalt, nickel, arsenic and barium. Thorium is significantly enriched, relative to uranium. It is slightly LREE-enriched, with a moderate negative cerium anomaly. Europium may be positive or negative.

Few samples of hybrid hard-paste SAC porcelains were available for analysis, but they show similarity in their major and minor elemental composition. They are generally low in the trace elements associated with aluminium, and therefore clay, 'A'-marked and Swansea especially so. Thorium is greater than uranium in the 'A'-marked sample, Plymouth has an approximately equal ratio of thorium to uranium, and in New Hall and Swansea, uranium is substantially lower than thorium. With the exception of Plymouth, they are LREE-enriched. Plymouth, New Hall and Swansea have positive cerium anomalies, New Hall and Plymouth have negative europium anomalies, and Swansea has a positive europium anomaly.

From these results it is possible to state that the clay is the main source of REEs (Figure 140), and to identify three main types of clay that were in use. The first is a ball clay that contains more impurities, and is relatively enriched in REEs, particularly LREEs. The second is a china clay that contains fewer impurities, and is relatively depleted in REEs, tending to have no significant anomalies.

The third source of clay, which was used only in the 'A'-marked sample, contains few trace impurities, including low levels of REEs, which are fractionated to the extent that the sum of the light REEs is double that of the heavy REEs, and which is distinguished still further by the presence of a significant positive europium anomaly. The steatite flux used by the magnesian-producing factories is characterised by the presence of the trace elements copper and zinc. It is depleted in REEs, and tends to be HREE-enriched with weak or no anomalies.

As with the major and minor elemental compositional data discussed above, the leaded porcelain glazes showed less variation than the pastes with respect to their trace elemental composition. A linear trend was demonstrated in the relationship between thorium and uranium, which suggests that these are being contributed by the same material in most cases. There is no apparent relationship between either of these elements and lead, which would have been contributed by the flux. Moderate levels of tin in some glazes from Bow, Lowestoft and Limehouse may suggest that this element was being added deliberately as an opacifier. The samples with tin in the glaze do not correspond directly with those that have significant amounts of tin in their paste. All glazes appeared to be less enriched in Rare Earth Elements than the pastes, and the REE_{CN} profiles exhibited a greater degree of fractionation. While this may be caused by the low limit of detection interfering with the normalisation process, another factor may be that an important source of REEs in these glazes was sand, which is a highly weathered and mixed geological material, and may possess a fractionated set of REEs.

The findings from this study are interesting, and make a significant contribution to the state of knowledge about British porcelain manufacture, which will be discussed in greater detail in section 7.4. As expected, trace elemental compositional data have a significantly greater power to discriminate between factories than major and minor elemental data. However, in most cases these findings are based on few samples from each factory and paste type, and therefore any conclusions drawn must therefore be preliminary, pending analysis of more samples from a broader range of factories and periods.

7.2.3 HH-XRF: qualitative elemental compositional data

As with any archaeological or historical material, the benefits of analysis must be balanced against the potential risks that it may present to the object. In the case of British porcelain, and other fine ceramics, it must be taken into account the value, both historical and monetary, of the object, which makes it preferable that they be preserved intact. In developing this methodology, therefore, the emphasis was on non-destructive and minimally-invasive analytical techniques. Additionally, two field-portable techniques have been explored, since these would reduce the need for the objects to be handled or moved as part of the analysis.

This requirement places restrictions upon the areas of porcelain objects that can be analysed; the paste is generally inaccessible through a lead-rich glaze. While the data meta-analysis (Section 3.2) has demonstrated that the paste is the aspect of British porcelain that provides the most characteristic data, it was hoped that collecting complementary data from the glaze, and other surface-level areas that have not been published in great detail such as enamels and gilding, would reveal other characteristic features.

One area in which this research has succeeded in advancing the characterisation of British porcelain is through elemental compositional analysis of the overglaze polychrome enamels. This has been carried out by HH-XRF analysis of intact objects in museum collections and antique shops; the bulk of the sample set was the Marshall Collection of Early Coloured Worcester porcelain. This provided a useful population for analysis, because most pieces are securely attributed to one factory (Worcester), and one period (the early period of the factory, between 1751-1783), which made it possible to characterise reliably the intra-factory variation in composition. Furthermore, this picture of the composition of genuine 18th century Worcester porcelain enamels has been used to identify later-decorated pieces, which are often similar in appearance and design, but appear to possess anachronistic enamel formulae.

As a result of the analysis of 71 objects in the Marshall collection, it was found that numerous enamel pigments and gilding formulae were in use for each of the colours tested throughout this period of the factory's existence. The reasons for this variety are not known for certain; from the analyst's observations, there is evidence for some link between the use of a specific formula, characterised by the presence or absence of elements, and the resulting pigment hue (compare, for instance, Figure 89 and Figure 90 with Figure 91 and Figure 92). However, a tandem study with spectrophotometry is recommended to quantify differences in pigment hue which might be associated with compositional variation.

Later-decorated pieces were identified by the presence of chromium and relatively high concentrations of zinc (Figure 79, Figure 80, and Figure 81); elements that were not isolated, nor available for use as pigments, until the early 19th century (Newman, 1997; Stiegelschmidt and Tomandl, 1985; Brongniart, 1898). They have been used successfully to characterise later-decorated porcelain objects from the Meissen and Vincennes-Sèvres factories, in analyses carried out using the same technique (Domoney, 2012).

A limited number of enamels on Worcester porcelain that was decorated at the studio of James Giles, in London, have also been analysed for comparison. The pigments and gilding in use by both factories are found to overlap significantly, in terms of the elements present, suggesting that similar formulae were in use. Further analyses, incorporating pigments from other factories and periods of the Worcester factory, may be able to resolve different formulae that were in use. Additionally, trace elemental compositional data of the enamels may allow different sources of materials, and proportions in which they were mixed, to be identified.

As part of this research, 140 intact porcelain objects attributed to 15 factories, and 37 sherds from 6 archaeologically-excavated factory sites have been analysed using HH-XRF. With the exception of the 71 polychrome-enamelled pieces from the Marshall collection, “blue and white” (i.e. glazed porcelain with underglaze blue decoration) was chosen, because this was the type of British porcelain most abundantly produced, and it was hoped to characterise a number of factories by the composition of the glaze and blue pigment.

Although the HH-XRF was unable to detect some of the lighter elements present in the glazes, namely sodium and magnesium, which are within the detectable range of SEM-EDS/WDS, a number of other elements were detected that are typically reported as below the limits of detection or quantification in the published data. These are titanium, manganese, iron and copper. The presence or absence of these elements at detectable levels allowed the glazes to be sorted into 11 compositional categories, some of which correspond with factories or regions.

Other diagnostic elements found in the glaze were: arsenic, which is strongly associated with porcelain from the Derby factory; barium, which has been found exclusively in Bovey Tracey porcelain; and bismuth, which has been detected only in Longton Hall porcelain. Significant levels of tin are normally, although not always, found in glazes from two factories based in London, namely Limehouse and Vauxhall.

If it is assumed that tin was added deliberately as an opacifying agent, that is, a substance that creates an opaque white glaze, then it may be that these London factories had trouble in obtaining a white paste, and the white glaze was used, as in contemporary delftware manufacture, to create a white appearance in the finished object. Both of these factories produced both frit and phosphatic porcelain pastes, and both are known to have performed extensive experimentation in order to arrive at a workable formula (Freestone, 1993; Owen et al, 2000). This being the case, it would not be surprising if one of the problems in some of their finished products was a less-than-white paste, and an opaque white glaze would correct this to some extent.

The presence of arsenic in Derby's glazes is not consistent with their ceramic pastes both before and after the Chelsea takeover, which have been found to contain no detectable arsenic (Owen and Barkla, 1997). It is known that the Derby factory at some point in its history exploited a local source of white-firing clay that was associated with lead mines, and it may be that the lead used in its glazes also came from this source (Houseley, 1991). If the lead ore present at this mine contained arsenic as a trace element, that may account for the presence of arsenic in the glaze, but not the paste, since the source of lead in the paste is likely to have been glass.

Likewise, Bovey Tracey and West Pans are two factories that are known to have used local sources of raw materials in their porcelains and other ceramics (Haggerty, 2008; p.11). Nicholas Crisp, the proprietor of the Bovey Tracey factory, had previously produced ceramics at a factory at Vauxhall, London (Watney, 1989). It may be assumed that the differences in composition between the products of Vauxhall and Bovey Tracey are partly due to a new experimental formula, which was devised in co-operation with William Cookworthy, who oversaw production of hard-paste porcelain at the Plymouth factory, and partly due to the use of local sources of clay and sand (Massey, 2002). Similarly, the difference in composition between porcelain produced at Longton Hall, Staffordshire, and at West Pans, Lothian, both of which were operated sequentially by William Littler, may be due to the exploitation of different sources of raw materials (Haggerty, 2008).

This study found, not only that Bovey Tracey and Vauxhall, and Longton Hall and West Pans glazes had distinct compositions, but also that those from Bovey Tracey and Longton Hall are entirely unique.

Analyses of the underglaze blue decoration on blue and white porcelain objects found confirmation for the commonly-known fact that the pigment in question was based on cobalt. It was also discovered that the presence or absence of other minor elements in the pigment produce ten compositional categories. Cobalt is a powerful chromophore, meaning that only a little is required to produce an intense blue colour (Eastaugh et al, 2008; p.351).

The presence of trace impurities associated with the cobalt ore, or to the materials with which it was mixed to produce the glassy substance, smalt, in which it was used, need not have substantially altered the colour of the finished blue pigment. Manganese, iron and nickel were found in the underglaze blue in quantities greater than the surrounding glaze, suggesting that they have been contributed by the pigment. Nickel, in particular, showed a co-increase when plotted against cobalt for most objects, see Figure 156.

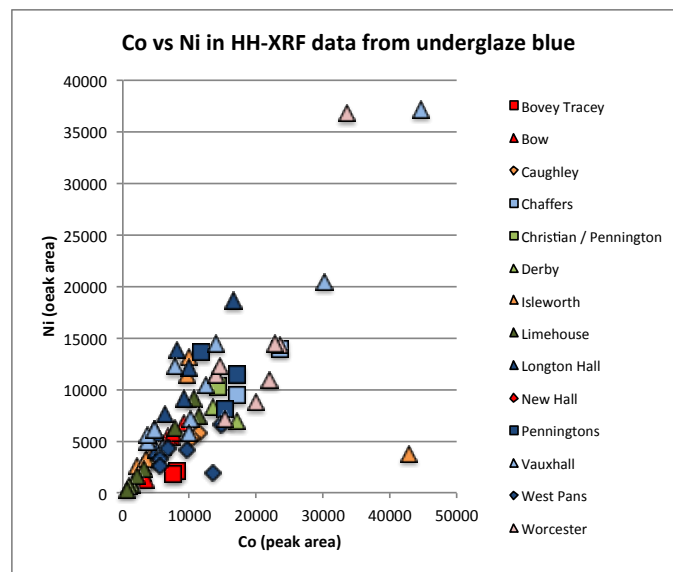


Figure 156 - cobalt versus nickel peak areas from HH-XRF analysis of underglaze blue

Once more, Bovey Tracey and West Pans porcelain were found to occupy unique compositional categories, with regard to the cobalt blue pigment. In both cases, manganese and arsenic accompany the pigment, although no consistent relationship between these two elements and the pigment can be discovered, see Figure 157 and Figure 158.

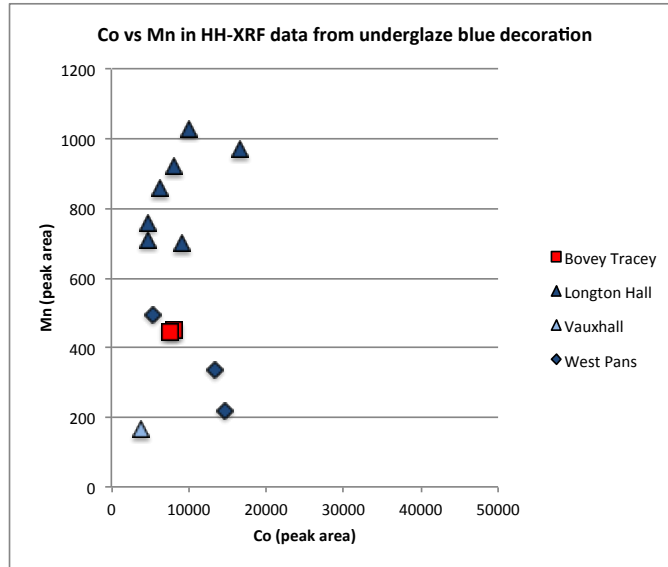


Figure 157 - cobalt versus manganese peak areas from HH-XRF analysis of underglaze blue on Crisp and Littler's soft-paste porcelains

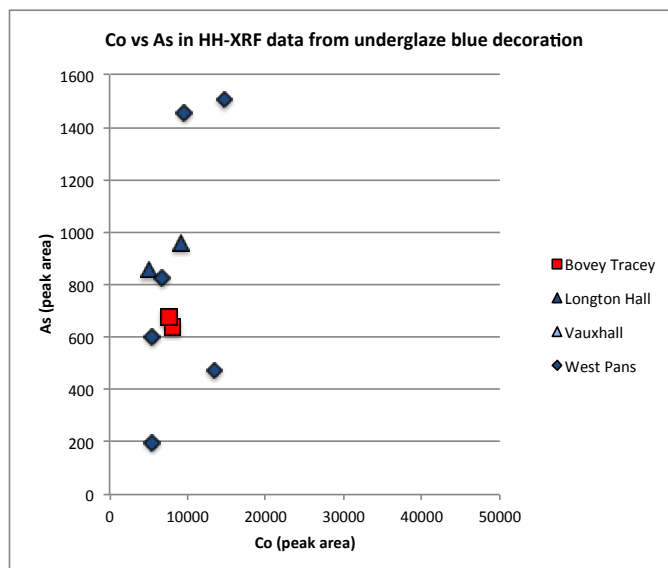


Figure 158 - cobalt versus arsenic peak areas from HH-XRF analysis of underglaze blue on Crisp and Littler's soft-paste porcelain

This finding may provide support for the theory that Nicholas Crisp and William Littler were experimenting with a source of cobalt ore (Turnbull, 1997; Haggerty, 2008). Throughout most of the 18th century, cobalt ore was imported by British industries, including porcelain, from mines in Saxony (Delamere, 2013; pp. 56 - 57).

There is evidence that Crisp and Littler were both individually in correspondence with Lord Alva, on whose land in Fife had been discovered a source of cobalt ore alongside the existing silver mines (Mallet, 1973; Turnbull, 1997). Both proprietors expressed interest in experimenting with this cobalt ore for the purposes of decorating their porcelain, and the presence of a unique underglaze blue composition that is common to both suggests that these experiments may have been successful, and the products brought to public sale. The discovery of three distinct compositional categories, occupied by underglaze blue pigments on porcelain from Bovey Tracey, New Hall and West Pans, give support for the use of non-destructive analysis of underglaze blue decoration as a means of distinguishing the products of these factories.

7.2.4 Spectrophotometry: hue and chroma of glazes

A pilot study was carried out to determine the extent to which the hue and chroma of the porcelains' surfaces varies within and between factories, and therefore the usefulness of colorimetric data for characterisation and provenance studies. Some evidence was found that porcelain from certain factories has a measurably warmer 'creamier' hue, and others have a cooler 'blue' hue. In particular, porcelain belonging to the "scratch-cross" group of Worcester porcelain was found to be cooler in hue than that from other periods of the same factory. This has been upheld by connoisseurs as a distinguishing feature of this group of porcelain (Dawson, 2007; p.21). Otherwise, however, inter-factory variation in hue and chroma was found to be as great as, or greater than, intra-factory variation, which would make colorimetry unhelpful for characterisation and provenance of British porcelain, when the glaze alone is relied upon.

7.2.5 Testing visual connoisseurship hypotheses: inter-factory versus intra-factory variation in glaze hue and major and minor elemental composition

When comparing the results of these two studies, the HH-XRF data clearly have greater power to discriminate between factories than those from the spectrophotometry data.

There is evidently potential for the techniques to be used in tandem when analysing polychrome enamelled wares, in order to assess the extent to which the composition of the pigment influences the hue and chroma of the resulting enamel. These findings could allow the spectrophotometer to be used as a screening technique for enamels, prior to analysis by HH-XRF, to identify pigments of interest to a given research question.

7.3 Developing a Non-Destructive Method for the Elemental Compositional Analysis of British Porcelain

In the interest of maximising the range and quality of elemental compositional data that can be gathered, while preserving intact porcelain objects, a method has been developed for the HH-XRF. As part of this work, a set of novel glass calibration standards has been created which shall allow data from the porcelain glaze and enamels to be calibrated, providing fully-quantitative elemental compositional data for 13 elements that are commonly present in porcelain glazes and enamels. Using the optimised method, it may in the future be possible to further distinguish porcelain glazes by XRF, which will be capable of producing results comparable with those collected by SEM-EDS/WDS analysis.

In this section, the selection of XRF spectroscopy as a technique is discussed, in the context of the scientific analysis of other archaeological materials. The advantages and disadvantages of the technique are described, and it is concluded that its usefulness is contingent upon an understanding of spectral interferences and limitations. The method has been developed with these limitations in mind and instrumental settings have been selected in order to minimise their impact. Finally, the effectiveness of the methodology is discussed, based on the data produced and how closely it compares with the SEM-EDS/WDS data for the same samples. The aim of this section is to critically assess the use of XRF for the analysis of British porcelain and the extent to which, with an optimised method and calibration standards, it may fulfil the requirements of precision and accuracy, as well as non-destructive analysis.

7.3.1 X-ray Fluorescence Spectroscopy in the study of archaeological materials

The purpose of this section is to discuss the reasons why XRF has been selected for the analysis of British porcelain. The history of XRF for the analysis of silicate and archaeological materials has been surveyed in section 2.4.2, so a brief summary will suffice for the purpose of this discussion, focussing on the favourable aspects of XRF for these sample types.

XRF has been used to a limited extent on British soft-paste porcelain, generally in circumstances where data are required but a sample for SEM-EDS cannot be taken (Watney et al, 1993; Freestone, 1996), or as a check against spectroscopic data (Owen, 1997; Owen and Day, 1998b). This means that the use of XRF for analysis of soft-paste porcelain is novel; an optimised methodology has never been developed for this type of sample, or used for the types of leaded glazes and enamels found on British soft-paste porcelain.

While the range of detectable elements is not as great as that of EDS or WDS as part of an SEM system, or ICPMS, the XRF produces compositional data for most major and minor elements present in British porcelain pastes with detection limits comparable to those of EDS. With a range of representative and matrix-matched standards, a calibration procedure can be carried out, in order to produce quantitative data that can be compared directly with SEM-EDS/WDS data. These factors make XRF an excellent candidate for the development of this optimised methodology.

7.3.2 Understanding XRF data

For XRF to be applied to the analysis of archaeological objects, it is not enough to push a button and publish the resulting data. The literature emphasises that XRF can be a reliable technique for elemental compositional analysis in art and archaeological applications, but that the data are limited by a number of interferences (Shackley, 2010; pp. 8-10; Calvo del Castillo and Strivay, 2012; pp. 70-72; Shugar and Mass, 2013; pp. 19-21; Scott et al, 2016).

These interferences occur in the interaction between the incident X-ray energy, the sample surface, the detector, and the air in between. Therefore, the first step in developing this method was to understand and to find ways to quantify these effects, in order to understand the potential and limitations of XRF.

Inelastic and elastic scatter, and Bremsstrahlung are inevitable phenomena that occur when the energy that produces the characteristic fluorescent energy in the sample react in other ways with the electrons in the surface of the sample, and the surrounding air. Their products in the spectra are predictable, and easy to identify with training, so, although they cannot be prevented, their spectral artefacts can be discounted during processing. It is possible to mitigate the effect of elastic scatter in cases where the user has a choice of X-ray sources, by selecting a source that will produce a peak in an area that does not overlap an element of interest.

Likewise, contamination lines will tend to appear in all spectra produced by any given instrument and, in the case of contamination from the excitation of machine components, cannot easily be removed. They can be identified using a blank run during each session of analysis, and the resulting counts removed from the total counts data. In this research, a pure silica blank was used for this purpose.

7.3.3 Evaluating XRF for use on British porcelain

This research has shown that most of the major and minor elements of interest in porcelain glazes can be detected using XRF analysis. The technique has been found to have a high level of accuracy and precision, meaning that samples analysed in different sessions may be compared directly, provided that the same analytical conditions are used, and that the sample matrices are similar. This makes the technique ideal for comparing samples of the same type in order to identify compositional groups using the presence or absence of elements, or ratios of counts. The simultaneous detection of all elements at once means that the user does not need to know the elements present in the sample prior to analysis, although some knowledge of the composition allows the user to select the best analytical conditions. Once collected, as this research has demonstrated, the data can be used as a qualitative indicator of the presence or absence of elements, or semi-quantitatively, to compare the relative abundance of elements in more than one sample through peak area or count ratios, and they are amenable to quantification.

XRF analysis is limited by interferences, some of which have been demonstrated to be surmountable by creating an optimised methodology, and by carrying out a calibration procedure to link the detected signal to an absolute compositional value. Others, such as the effect of the sample angle or air gap, have been quantified and found to have relatively little effect on the counts produced at the detector.

Low-Z elements suffer disproportionately from attenuation effects, but provided that they remain above the limit of quantification, and that the calibration standards are analysed under the same conditions, this can be corrected during calibration. The problem of peak overlap remains insurmountable without the use of a WDS detector, and can only be circumvented by selecting alternative peaks for the quantification of affected elements, such as cobalt, iron, arsenic and bismuth.

An obvious drawback to XRF analysis is the detection of low-Z elements under normal conditions. Elements that are known to be present in porcelain pastes and glazes, as well as historical glass and ceramics, notably sodium and magnesium, are unable to be detected by XRF analysis due to attenuation. Combined with the difficulty in quantifying elements for which significant peak overlaps apply (in the case of this methodology, arsenic and bismuth), and it may be impossible to quantify all of the stoichiometric components of the sample. In such cases, the elemental compositional data cannot be normalised to 100%, meaning that it is difficult to estimate the proportions of these light elements within one sample, much less to compare their abundances between samples.

However, this research has demonstrated that the characterisation of British porcelain pastes, glazes, enamels and underglaze blue pigment does not necessarily rely on these light elements. Indeed, the most helpful major and minor elements for identifying inter-factory variation appear to be: the clay and fluxing elements (aluminium, phosphorus, calcium, titanium and lead) in the case of the pastes; trace metals that may represent contaminants or deliberate additions to the formulae (manganese, cobalt, zinc, arsenic, tin, barium and bismuth) in the case of the glazes; and chromophores or associated elements (manganese, iron, cobalt, nickel, copper, arsenic and silver) in the case of the enamels, pigments and gilding. These elements are all well within the detectable and quantifiable range of XRF, and some inter-factory and intra-factory variation has been described using qualitative and quantitative data as part of this research.

The development of the standards and method has been successful, but a more rigorous test of its effectiveness for British porcelain is needed. Such an experiment would require that a large number ($n > 10$) of unweathered glazed porcelain samples were analysed by SEM-EDS on the surface of the glaze. The data thus obtained would be expected to be a closer fit with those from XRF analysis of the glaze surface.

7.4 Contributions to the narrative of technical and historical development of British porcelain in the 18th century

The ability to distinguish between British porcelain from different factories and periods is of use to curators, collectors and connoisseurs of these objects, and this research has shown that analytical data can complement the findings of art historical research and connoisseurship studies. In this section, these findings are expanded upon to discuss the ways in which analytical data can contribute to our understanding of the production of British porcelain from its inception in the 1740s to its obsolescence in the early 19th century, due to the development of hard-paste porcelain formulae for fine ceramics. These aspects will be discussed with regard to the data gathered from three factories individually through time, and comparing multiple factories that produced the same paste type. Finally, it will be discussed the contribution that this research has made to the story of the Eccles samples, which have played an important role in the recent history of the scientific examination of British porcelain.

7.4.1 Intra-factory variation

It has been proposed that the composition of porcelain from any given factory tend to be stable during a certain period in time, once a usable formula has been discovered (Freestone et al, 2003). This assumption is vital if factories are to be distinguished, or samples of unknown provenance assigned a factory of origin, based on the elemental or mineralogical composition of their paste. Therefore, an important initial objective of this research was to thoroughly characterise as many factories as possible by compiling the available data from published studies, this is described in detail in Chapter 3.

In this section, it will be discussed the extent to which the paste and glaze of selected factories have been found to change or remain stable in composition through time. The results of studies published before the current research are summarised first, and then any additional findings contributed by the analytical data obtained by this study are presented. Three factories have been selected, for which ample SEM-EDS/WDS data were available, and which have been characterised during this study by HH-XRF, and LA-ICPMS.

It will be concluded for each factory the characteristic factors that have previously been identified, and those which can be discovered from the data obtained using minimally invasive analytical techniques.

Worcester

Worcester porcelain has been well-characterised through time, in terms of the major and minor elemental composition of the paste and glaze. Owen has found that some early experimental pastes had a phosphatic composition, (Owen, 1998) which was supplanted by a magnesian formula once a soaprock mining license had been obtained through the purchase of the failed Lund's Bristol porcelain factory (Barrett, 1966; pp. 12-13). The composition changed through time from the Dr Wall period 1751 - 1783 to the Flight period 1783 - 1793, containing more magnesium, meaning that more steatite was added, and less lead, suggesting less flint glass (Owen, 1997). At the same time, the glaze formula changed to use less lead, and increasing silica (Owen, 1997).

However, this trend is difficult to identify in HH-XRF data from glazes, because the detection of lead is limited by the detector saturation effect, which occurs at around greater than 2,000,000 total counts, which is around 38% lead oxide in a soft-paste porcelain glaze. Worcester porcelain glazes are known to contain up to 48% lead oxide in earlier pieces, and this is indistinguishable by the HH-XRF from later glazes that contain between 38% and 44% lead oxide. Silica has been plotted against two elements that remains relatively stable through time, potassium (Figure 159) and calcium (Figure 160), to see whether an increase in silica from the Dr Wall period to the Flight period can be detected. There was significant overlap between these periods, and the relationship between these elements and silica does not appear to be time-dependent.

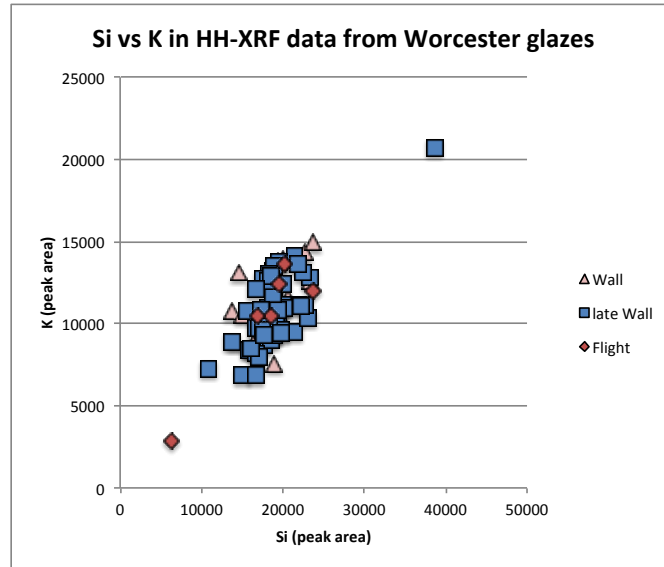


Figure 159 - silicon versus potassium peak areas from HH-XRF analysis of Worcester porcelain glazes

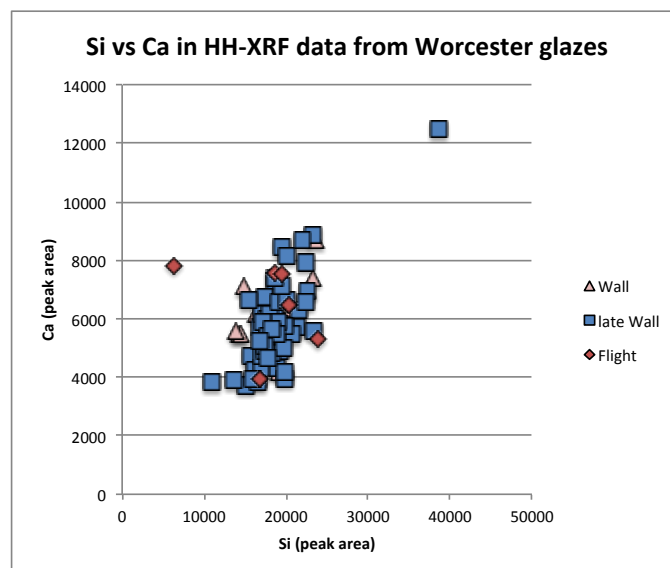


Figure 160 - silicon versus calcium peak areas from HH-XRF analysis of Worcester porcelain glazes

As part of this research, the overglaze polychrome enamels and gilding on Worcester porcelain have been characterised for the Dr Wall period. It has been demonstrated that compositionally similar pigments and gilding were employed by both factory decorators and the external decorating studio of James Giles, and that redecoration has been carried out in the 19th century in imitation of these mid-18th century enamelled pieces using different pigments.

Trace elemental compositional data for Worcester porcelain have shown it is relatively enriched in strontium and uranium. The normalised REE profile is highly fractionated and HREE-enriched, with positive cerium and negative europium anomalies, which appear to be characteristic of magnesian porcelain. The extent to which the trace elemental composition can be used to distinguish Worcester pastes from those of other magnesian porcelains will be discussed in greater detail in Section 7.4.2.

Through time, the Worcester paste contains less magnesium and associated trace elements, and more aluminium. This suggests that more clay was being incorporated into the body, the aluminium to titanium ratio of which suggests that a china clay was used.

Derby

Derby porcelain have also been well-characterised through time, in terms of the changes of paste type took place as part of the acquisition of the failing Chelsea factory in 1770 (Owen and Barkla, 1997). A lead-rich glassy paste had been used from the founding of the factory in 1750, which caused high levels of kiln failures, and a magnesian formula was experimented with from 1764-69 in an attempt to reduce costs (Owen and Barkla, 1997). It is unknown why this was unsuccessful, but it was abandoned in 1770 when the Chelsea phosphatic formula was adopted and used thereafter (Owen and Barkla, 1997). Glazes throughout this period were high in lead (40-50% PbO), and changed little because they were successful.

As a result of this research, it has been discovered that pre-Chelsea Derby glazes and underglaze blue pigment contain arsenic, which allow it to be distinguished from contemporary glassy porcelain from Longton Hall and later from West Pans.

Furthermore, the trace elemental composition of two phosphatic Derby sherds show similarities to phosphatic sherds from Chelsea, which suggests that similar raw materials were used by both factories in their production of the phosphatic formula. This might be expected, because both factories during this period were owned and operated by William Duesbury, who purchased the failing Chelsea factory in 1769 (Barrett and Thorpe, 1971).

Future analysis of more samples dating to before and after the Chelsea takeover, it may be possible to establish how quickly these recipe changes were implemented, and whether an experimental period preceded or followed. If samples from the early period of the factory could be obtained, they could be compared with the frit porcelains from Chelsea and it may be possible to answer the question of whether Derby obtained its raw materials, particularly lead and clay, from a local source.

Bow

A large sample of Bow porcelain, representing the entire life of the factory from 1743 to 1774 have been analysed by SEM-EDS (Ramsay and Ramsay, 2007). The paste composition has been found to change through time, decreasing the amount of bone ash flux that was used, and increasing the amount of silica (Ramsay and Ramsay, 2007). The glazes are also found to change, containing less lead and more silica through time (Ramsay et al, 2011).

As with the change in Worcester porcelain glazes, which also change to incorporate less lead through time, this is difficult to detect in the HH-XRF data, due to the saturation effect in the detector. It may be possible to detect the increase in silica by plotting silica against another element that remains static through time, such as potassium or calcium, but samples from the later period of the factory were not available in the current research. Nonetheless, it has found that Bow glazes from the early period of the factory (1752-65) can be distinguished from those on phosphatic porcelain from Isleworth, Lowestoft and the Liverpool factories based on the absence of manganese in the glaze and underglaze blue. This is discussed in greater detail with reference to inter-factory variation in phosphatic porcelains in section 7.4.2.

The trace elemental composition of Bow porcelain dated to the early 1750s, mid to late 1750s, early 1760s, and mid to late 1760s show no significant changes through time, which suggests that the same sources of raw materials were being exploited throughout this period.

One outlier, which dates to between 1755-1760, is relatively enriched in HREEs, but the major and minor elemental composition, and other aspects of the trace elemental composition, is not substantially different to the other samples of Bow porcelain that were produced before and afterwards. Certainly, these samples show no evidence of the significant compositional change that has been attributed to this period in the factory's history (Ramsay and Ramsay, 2007). The normalised REE profile of this outlier is similar to other outliers from Limehouse, dated 1747-1750, and Crown Derby, dated 1773-1790, but once more there are no other compositional similarities. Given that these pastes all used ball clay as the plastic component, it may be that there was some impurity in the clay that was more fractionated than the bulk composition of the deposit, and that periodically made its way into these ceramics.

7.4.2 Inter-factory variation

An important aim of this research has been to find new ways of distinguishing between factories that produced porcelains similar in appearance or composition. This has been accomplished using qualitative major and minor elemental compositional data from HH-XRF analysis, and quantitative trace elemental compositional data from LA-ICPMS. In this section, these findings are compiled and discussed in relation to the published fully-quantitative data. Specifically, it is discussed the extent to which these distinguishing features have advanced the characterisation of factories producing phosphatic and magnesian porcelain, and how they may contribute to our understanding of technological choices, sources of raw materials, transfer of workmen, skills, and formulae. The section will conclude with a review of the questions that remain to be answered, and recommendations for the steps that may be taken to inform their answers.

Inter-factory variation in quantitative and qualitative data

The distinguishing compositional features that are associated with porcelain from each factory, according to the published SEM-EDS/WDS data and the novel HH-XRF and LA-ICPMS data gathered as part of this research are shown in Table 55. Where alternative attribution can be made, based on these features, these are also given. Dates have been provided, which encompass the dates of the objects tested, where these are known, and it must be borne in mind that some of the longer-running factories, notably Bow, Chelsea, Derby and Worcester, are not characterised with regard to the entire lifespan of the factory.

Those that may be entirely distinguished using non-destructive or micro-destructive techniques, based on the data available, are: the 'A'-marked group, Bovey Tracey (magnesian pastes), Bow, Caughley (magnesian pastes), Chelsea (frit and phosphatic pastes), Cookworthy's Plymouth, Derby (phosphatic), Limehouse (SAC), Liverpool (Ball), Longton Hall, Lowestoft, New Hall and Worcester.

Discussion: using multiple analytical techniques to characterise British porcelain

Table 55 - compositional features that distinguish British porcelain using SEM-EDS/WDS, XRF and LA-ICPMS, sorted by factory

Factory	Date range tested	Technique	Area tested	Compositional indicators	Alternative Attributions
A ¹ -marked	pre-1744?	SEM-EDS/WDS	paste	SiO ₂ + Al ₂ O ₃ + CaO > 80%, SiO ₂ /CaO <20, SiO ₂ /Al ₂ O ₃ <4, TiO ₂ 0.02 - 0.05	n/a
		LA-ICPMS	paste	Al/Ti <400, Al/Zr <5000, LREE-enriched (Σ LREE/ Σ HREE 2), positive Eu anomaly (2.7)	n/a
Bovey Tracey (magnesian)	1767-1774	SEM-EDS/WDS	paste	MgO >5%, contains BaO	n/a
		SEM-EDS/WDS	glaze	PbO >45%, contains BaO, ZnO ₂	n/a
		HH-XRF	glaze	contains BaO, ZnO ₂	n/a
Bovey Tracey (phosphatic)	1767-1774	SEM-EDS/WDS	paste	CaO + P ₂ O ₅ >20%, SiO ₂ /(CaO + P ₂ O ₅) <1.2, K ₂ O + Al ₂ O ₃ >13%, SiO ₂ <40%	n/a
Bovey Tracey (hybrid hard-paste)	1767-1774	SEM-EDS/WDS	paste	SiO ₂ + Al ₂ O ₃ + CaO >80%, SiO ₂ /CaO >20, SiO ₂ /Al ₂ O ₃ <7, SiO ₂ >70%	Cookworthy's Plymouth/Bristol
		SEM-EDS/WDS	glaze	PbO <5%, Al ₂ O ₃ >15%	Cookworthy's Bristol
Bow	1740-1774	SEM-EDS/WDS	paste	CaO + P ₂ O ₅ >20%, Al ₂ O ₃ 5-8%, TiO ₂ 0.2-0.4%	Lowestoft
	1755-1770	SEM-EDS/WDS	glaze	PbO >45%, may contain SnO ₂ 0.5-3%	Sn present: Longton Hall; no Sn present: Caughley, Chelsea, Coalport, Derby, Liverpool factories, Longton Hall, Worcester
	1752-1765	HH-XRF	glaze	glaze contains no Mn, may contain Sn	Sn present: Longton Hall
	1755-70	LA-ICPMS	paste	Th/U >1, LREE-enriched (Σ LREE/ Σ HREE 1.2-1.5), no strong REE anomalies	n/a
Caughley (magnesian)	1772-1796	SEM-EDS/WDS	paste	MgO >5%, SiO ₂ /(MgO+CaO) 8-16, PbO <4%	Flight-period Worcester, Vauxhall
		SEM-EDS/WDS	glaze	PbO >30%	Bow, Chelsea, Coalport, Derby, Liverpool factories, Longton Hall, Worcester
		HH-XRF	glaze	contains Mn and As	Derby, Vauxhall
		LA-ICPMS	paste	Th/U <1, HREE-enriched (Σ LREE/ Σ HREE 0.5), no anomalies	n/a

Discussion: using multiple analytical techniques to characterise British porcelain

Table 55 - compositional features that distinguish British porcelain using SEM-EDS/WDS, XRF and LA-ICPMS, sorted by factory (continued)

Factory	Date range tested	Technique	Area tested	Compositional indicators	Alternative Attributions
Caughley (hybrid hard paste)	1796-1799	SEM-EDS/WDS	paste	SiO ₂ + Al ₂ O ₃ + CaO >80%, SiO ₂ /CaO >20, SiO ₂ /Al ₂ O ₃ <7, SiO ₂ <70%	Chamberlain's Worcester, Coalport, Grainger, Royal Worcester, Swansea
		SEM-EDS/WDS	glaze	PbO 5-30%, Al ₂ O ₃ + K ₂ O + CaO <15%	Grainger, Liverpool Brownlow Hill, Longton Hall, Nantgarw (SAC paste), Vauxhall
Chamberlain's Worcester	1783-1840	SEM-EDS/WDS	paste	SiO ₂ + Al ₂ O ₃ + CaO >80%, SiO ₂ /CaO >20, SiO ₂ /Al ₂ O ₃ <7, SiO ₂ <70%	Caughley, Coalport, Grainger, Royal Worcester, Swansea
	1783-1840	SEM-EDS/WDS	glaze	PbO <5%, Al ₂ O ₃ 8-13%, CaO >3%	Grainger, Royal Worcester
Chelsea (frit)	1745-1765	SEM-EDS/WDS	paste	PbO >5%, SiO ₂ /CaO <6, Al ₂ O ₃ >4%	n/a
		SEM-EDS/WDS	glaze	PbO >45%	Bow, Caughley, Coalport, Derby, Liverpool Brownlow Hill, Liverpool Gillbody, Liverpool Pennington, Longton Hall, Worcester
		LA-ICPMS	paste	Th/U 2.7-2.9, LREE-enriched (ΣLREE/ΣHREE 1.1-1.2), no strong anomalies	n/a
Chelsea (phosphatic)		LA-ICPMS	paste	CaO + P ₂ O ₅ >20%, Al ₂ O ₃ 9-20%, TiO ₂ 0.3-0.5%, Th/U >1, LREE-enriched (ΣLREE/ΣHREE 1.4), negative Ce anomaly (0.8), positive Eu anomaly (1.2)	n/a
Coalport	1795-1830	SEM-EDS/WDS	paste	CaO + P ₂ O ₅ >20%, SiO ₂ /CaO + P ₂ O ₅ <1.2, K ₂ O + Al ₂ O ₃ >13%, SiO ₂ ≥40%	Grainger, Nantgarw
	1799-1830	SEM-EDS/WDS	glaze	PbO 30-45%	Caughley, Chaffers, Isleworth, Limehouse, Liverpool factories, Worcester
		LA-ICPMS	paste	Al/Ti <30, Th/U >1, LREE-enriched (ΣLREE/ΣHREE 1.7), negative Eu anomaly (0.8)	Nantgarw, Swansea
Cookworthy's Plymouth/Bristol	1767-1774	SEM-EDS/WDS	paste	SiO ₂ + Al ₂ O ₃ + CaO >80%, SiO ₂ /CaO >20, SiO ₂ /Al ₂ O ₃ <7, SiO ₂ >70%	Bovey Tracey (hybrid hard paste)
	1768-1770	SEM-EDS/WDS	glaze	PbO <5%, Al ₂ O ₃ 8-13%, CaO <3%	n/a
		LA-ICPMS	paste	SiO ₂ + Al ₂ O ₃ + CaO > 80%, TiO ₂ 0.02 - 0.05, Th/U 0.9, LREE/HREE equal (1)	n/a

Discussion: using multiple analytical techniques to characterise British porcelain

Table 55 - compositional features that distinguish British porcelain using SEM-EDS/WDS, XRF and LA-ICPMS, sorted by factory (continued)

Factory	Date range tested	Technique	Area tested	Compositional indicators	Alternative Attributions
Derby (frit)	1750-1770	SEM-EDS/WDS	paste	PbO 5-20%, SiO ₂ /CaO >7	n/a
		SEM-EDS/WDS	glaze	PbO >45%	Bow, Caughley, Chaffers, Coalport, Liverpool factories, Longton Hall, Worcester
	1765-1770	HH-XRF	glaze	glaze contains As	Caughley, Chaffers, Isleworth, Lowestoft, Vauxhall
Derby (phosphatic)	1773-1791	LA-ICPMS	paste	CaO + P ₂ O ₅ >20%, Al ₂ O ₃ 9-20%, TiO ₂ 0.3-0.5%, Th/U >1, negative Ce and Eu anomalies	n/a
Grainger	1801-1830	SEM-EDS/WDS	paste	CaO + P ₂ O ₅ >20%, SiO ₂ /CaO + P ₂ O ₅ <1.2, K ₂ O + Al ₂ O ₃ >13%, SiO ₂ ≥40%	Caughley, Chamberlain's Worcester, Coalport, Nantgarw, Royal Worcester, Swansea,
		SEM-EDS/WDS	glaze	PbO <5%, Al ₂ O ₃ 8-13%, CaO >3%	Coalport, Royal Worcester
Isleworth	1770	SEM-EDS	paste	CaO + P ₂ O ₅ >20%, SiO ₂ /(CaO + P ₂ O ₅) <1.2, K ₂ O + Al ₂ O ₃ <11%, K ₂ O/Al ₂ O ₃ 0.2-0.5	n/a
		SEM-EDS	glaze	PbO 30-45%	Caughley, Chaffers, Coalport, Limehouse, Liverpool factories, Worcester contains Sn: Limehouse, Vauxhall; contains As: Chaffers, Derby, Lowesoft;
		HH-XRF	glaze	contains Mn, may contain Sn, As, Zn	contains Zn: Chaffers; contains neither Sn, As or Zn: Christian, Lowestoft, Reid, New Hall, Pennington, West Pans, Worcester
Limehouse (frit)	1745-1748	SEM-EDS/WDS	paste	SiO ₂ /CaO >7, PbO >20%	n/a
	1740-1750	SEM-EDS/WDS	glaze	PbO 30-45%	Caughley, Chaffers, Coalport, Isleworth, Liverpool factories, Worcester
Limehouse (SAC)	1745-1748	SEM-EDS/WDS	paste	SiO ₂ + Al ₂ O ₃ + CaO >80%, SiO ₂ /CaO <20, SiO ₂ /Al ₂ O ₃ >5, TiO ₂ 0.5-0.9%	n/a
	1745-46	SEM-EDS/WDS	glaze	PbO <5%, Al ₂ O ₃ <6%, contains no detectable Sn	n/a
		LA-ICPMS	paste	TiO ₂ 0.5-0.9, Th/U 1.5-4.5, LREE-enriched (ΣLREE/ΣHREE 1.1-1.5), negative Ce anomaly (0.8-0.9)	n/a

Discussion: using multiple analytical techniques to characterise British porcelain

Table 55 - compositional features that distinguish British porcelain using SEM-EDS/WDS, XRF and LA-ICPMS, sorted by factory (continued)

Factory	Date range tested	Technique	Area tested	Compositional indicators	Alternative Attributions
Liverpool (Ball)		LA-ICPMS	paste	MgO >5%, PbO <1%, Mg/Zn <100, Th/U <1, HREE-enriched ($\Sigma\text{LREE}/\Sigma\text{HREE}$ 0.3-0.7), positive Ce anomaly (~1.1), negative Eu anomaly (0.1-0.7)	n/a
Liverpool Chaffers / Christian	1765-1799	SEM-EDS/WDS	paste	MgO >5%, SiO ₂ /(MgO + CaO) 8-16, PbO >5%	Dr Wall-period Worcester
	1785-1778	SEM-EDS/WDS	glaze	PbO 30-45%	Caughley, Coalport, Isleworth, Limehouse, Liverpool factories, Worcester
		HH-XRF	glaze	glaze contains Mn, may contain As, Zn	Zn present: Isleworth; As present: Derby, Isleworth, Lowestoft; neither Zn nor As present: Isleworth, Lowestoft, Reid, New Hall, Liverpool factories, West Pans, Worcester
Liverpool Reid, Brownlow Hill, Gillbody, Penningtons	1755-1767	SEM-EDS/WDS	paste	CaO + P ₂ O ₅ >20%, SiO ₂ /(CaO + P ₂ O ₅) >1.2	n/a
	1765-70	SEM-EDS/WDS	glaze	PbO >30%	Bow, Caughley, Chelsea, Coalport, Derby, Isleworth, Limehouse, Longton Hall, Lowestoft, Worcester
		HH-XRF	glaze	contains Mn	Christian, Isleworth, Lowestoft, Reid, New Hall, West Pans, Worcester
		HH-XRF	glaze	contains Mn	Christian, Isleworth, Lowestoft, Reid, New Hall, West Pans, Worcester
Longton Hall	1755-1760	SEM-EDS	paste	PbO >5%, SiO ₂ /CaO <6, Al ₂ O ₃ ≤3.5%	West Pans
	1749-60	SEM-EDS	glaze	PbO >45%, contains Bi	n/a
		HH-XRF	glaze	contains Bi and Sn	n/a
		LA-ICPMS	paste	Th/U 3-7, HREE-enriched ($\Sigma\text{LREE}/\Sigma\text{HREE}$ 0.9), negative Eu anomaly (0.6)	n/a

Discussion: using multiple analytical techniques to characterise British porcelain

Table 55 - compositional features that distinguish British porcelain using SEM-EDS/WDS, XRF and LA-ICPMS, sorted by factory (continued)

Factory	Date range tested	Technique	Area tested	Compositional indicators	Alternative Attributions
Lowestoft	1770-1775	SEM-EDS/WDS	paste	CaO + P ₂ O ₅ >20%, Al ₂ O ₃ 5-8%, TiO ₂ 0.2-0.4%	Bow
		SEM-EDS/WDS	glaze	PbO >45%	Bow, Caughley, Chaffers, Coalport, Liverpool factories, Longton Hall, Worcester
	1770-1785	HH-XRF	glaze	contains Mn, may contain As	contains As: Chaffers, Derby, Isleworth; does not contain As: Christian, Isleworth, Reid, New Hall, Liverpool factories, West Pans, Worcester
		LA-ICPMS	paste	Al ₂ O ₃ 5-8%, Th/U >1, LREE/HREE equal (~1), positive Eu anomaly (1.2)	n/a
Nantgarw (SAC)		SEM-EDS/WDS	paste	SiO ₂ + Al ₂ O ₃ + CaO >80%, SiO ₂ /CaO <20, SiO ₂ /Al ₂ O ₃ >8, TiO ₂ <0.1%	n/a
		SEM-EDS/WDS	glaze	PbO 5-30%, Al ₂ O ₃ + K ₂ O + CaO <15%	Caughley, Grainger, Liverpool Brownlow Hill, Longton Hall, Vauxhall, Worcester
Nantgarw (phosphatic)		SEM-EDS/WDS	paste	CaO + P ₂ O ₅ >20%, SiO ₂ /(CaO + P ₂ O ₅) <1.2, K ₂ O + Al ₂ O ₃ >13%, SiO ₂ ≥40%	Coalport, Grainger
		SEM-EDS/WDS	glaze	PbO 5-30%, Al ₂ O ₃ + K ₂ O + CaO >15%, Na ₂ O <1%	Swansea
		LA-ICPMS	paste	TiO ₂ 0.03-0.05, Th/U >1, LREE-enriched (ΣLREE/ΣHREE 1.2), negative Eu anomaly (0.7)	Coalport, Swansea
New Hall		HH-XRF	glaze	contains Mn	Christian, Isleworth, Lowestoft, Reid, Liverpool Pennington, West Pans, Worcester
		LA-ICPMS	paste	SiO ₂ + Al ₂ O ₃ + CaO > 80%, TiO ₂ 0.02-0.05%, Th/U 0.4-0.5, LREE-enriched (1.5-2.0), positive Ce anomaly (1.1), negative Eu anomaly (0.3-0.4)	n/a
Swansea (SAC)	1814-1819	SEM-EDS/WDS	paste	CaO + P ₂ O ₅ >20%, SiO ₂ /CaO + P ₂ O ₅ <1.2, K ₂ O + Al ₂ O ₃ >13%, SiO ₂ ≥40%	Caughley, Chamberlain's Worcester, Coalport, Grainger, Nantgarw, Royal Worcester
		SEM-EDS/WDS	glaze	PbO 5-30%, Al ₂ O ₃ + K ₂ O + CaO >15%, Na ₂ O <1%	Nantgarw (phosphatic)
		LA-ICPMS	paste	TiO ₂ 0.02-0.05, Th/U 0.4, LREE-enriched (ΣLREE/ΣHREE 1.4, positive Eu anomaly (1.5)	n/a

Discussion: using multiple analytical techniques to characterise British porcelain

Table 55 - compositional features that distinguish British porcelain using SEM-EDS/WDS, XRF and LA-ICPMS, sorted by factory (continued)

Factory	Date range tested	Technique	Area tested	Compositional indicators	Alternative Attributions
Swansea (phosphatic)		LA-ICPMS	paste	TiO ₂ 0.03-0.05, Th/U >1, LREE-enriched (Σ LREE/ Σ HREE 1.4), negative Eu anomaly (0.9)	Coalport, Nantgarw
Vauxhall	1751-1764	SEM-EDS/WDS	paste	MgO >5%, SiO ₂ /(MgO+CaO) 8-16, PbO <4%	Chaffers, Flight-period Worcester
	1751-1764	SEM-EDS/WDS	glaze	PbO 5-30%, Al ₂ O ₃ + K ₂ O + CaO <15%	Caughley, Grainger, Liverpool Brownlow Hill, Longton Hall, Nantgarw (SAC), Worcester
	1757-60	HH-XRF	glaze	contains Mn and Sn, may contain As	contains As: n/a does not contain As: Isleworth, Limehouse
West Pans	1764-1777	SEM-EDS/WDS	paste	PbO >5%, SiO ₂ /CaO <6, Al ₂ O ₃ ≤3.5%	Longton Hall
		SEM-EDS/WDS	glaze	PbO 30-45%	Caughley, Chaffers, Isleworth, Limehouse, Liverpool factories, Worcester
		HH-XRF	glaze	contains Mn	Christian, Isleworth, Lowestoft, Reid, New Hall, Liverpool Penningtons, West Pans, Worcester
Worcester	1752-1813	SEM-EDS/WDS	paste	MgO >5%, SiO ₂ /(MgO + CaO) 8-16	Caughley, Chaffers, Vauxhall
		SEM-EDS/WDS	glaze	PbO 15-50%	Bow, Bovey Tracey, Caughley, Chelsea, Coalport, Derby, Grainger, Isleworth, Limehouse, Liverpool factories, Longton Hall, Lowestoft, Nantgarw, Vauxhall, West Pans, Worcester
	1756-1785	HH-XRF	glaze	glaze contains Mn	Christian, Isleworth, Lowestoft, Reid, New Hall, Liverpool Penningtons, West Pans, Worcester
		LA-ICPMS	paste	Cu/Mn <1, Mg/Zn >100, HREE-enriched (Σ LREE/ Σ HREE 0.3-0.7), Eu and Ce anomalies may be positive or negative	n/a

This research was carried out with the aim of developing a methodology for the analysis of British porcelain using a range of non-destructive techniques. Therefore, the distinguishing compositional features discussed above are displayed by analytical technique, in order to demonstrate the power that each technique has to identify inter-factory variation. The data used are: qualitative data from HH-XRF (Table 56 and Table 57), major and minor elemental compositional data from published SEM-EDS/WDS studies and novel LA-ICPMS analysis (Table 58 and Table 59), and trace elemental compositional data from LA-ICPMS (Table 60).

The major and minor elemental compositional data tables are similar to those compiled as a result of the meta-analysis of published data (Chapter 3, Table 4 and Table 5). However, the addition of the LA-ICPMS data have added factories for which data were not previously available (Chelsea phosphatic, Liverpool Ball, Lowestoft, New Hall, Pomona). They have supported many of the distinctions that were previously drawn, such as the difference between early phosphatic porcelain and later bone china, which will be discussed in greater detail in the following section. However, other apparently distinguishing features are no longer applicable; Pomona porcelain shares a compositional category with Dr Wall-period Worcester and Chaffers, while another Liverpool factory, Ball, appears compositionally indistinguishable from Flight-period Worcester, Vauxhall and Caughley porcelain. Bow can no longer be uniquely identified, due to compositional overlap with Chelsea, Derby (phosphatic pastes) and Lowestoft, and similarities between Cookworthy's hybrid hard-paste porcelain and that of Caughley, New Hall and Swansea make these difficult to distinguish from one another.

Trace elemental compositional analysis by LA-ICPMS appears to be the most effective means of identifying inter-factory variation. However this cannot be shown in full detail in Table 60, so for the full compositional categories for each of the factories, Table 55 should be consulted.

Discussion: using multiple analytical techniques to characterise British porcelain

Table 56 - compositional features that can be used to distinguish British porcelain glazes using XRF data

contains Al, Si, K, Ca, Ti, Fe, Cu, and Pb									
does not contain Mn	contains Mn								
Bow	contains Sn				does not contain Sn				
	contains Bi	does not contain Bi			contains As		does not contain As		
	Longton Hall	contains Ba	does not contain Ba		contains Co and Ni	does not contain Co or Ni	contains Zn	does not contain Zn	
		Bovey Tracey	contains Co and Ni	does not contain Co or Ni		Caughley Derby Vauxhall	Chaffers Derby Isleworth Lowestoft	Chaffers Isleworth	Christian Isleworth Lowestoft Liverpool Reid Liverpool Penningtons New Hall West Pans Worcester
			Limehouse	contains As	does not contain As				
Vauxhall	Isleworth Limehouse Vauxhall								

Discussion: using multiple analytical techniques to characterise British porcelain

Table 57 - compositional features that can be used to distinguish cobalt blue decoration on British porcelain using XRF data

contains Al, Si, K, Ca, Ti, Fe, Co, Ni, and Pb									
contains Mn				does not contain Mn					
contains As and Zn		does not contain As and Zn		contains Cu				does not contain Cu	
contains Cu	does not contain Cu	contains Sn	does not contain Sn	contains As		does not contain As		contains As	does not contain As
West Pans	Bovey Tracey	Limehouse	Caughley Chaffers Isleworth Liverpool Christian Liverpool Penningtons Limehouse Longton Hall Lowestoft Vauxhall	contains Sn	does not contain Sn	contains Zn	does not contain Zn	Derby Lowestoft Worcester	Bow Caughley Derby Isleworth Limehouse Liverpool Penningtons Liverpool Reid Vauxhall
				Longton Hall Vauxhall	Derby Worcester	New Hall	Bow Chaffers Isleworth Vauxhall		

Discussion: using multiple analytical techniques to characterise British porcelain

Table 58 - compositional categories for British porcelain pastes using major and minor elemental compositional data. All % data in these tables is absolute, and ratios are calculated from the absolute composition.

MgO >5%			
SiO ₂ /(MgO+CaO) 5-6		SiO ₂ /(MgO+CaO) 8-16	
contains BaO	does not contain BaO	PbO >5%	PbO <4%
Bovey Tracey	Dr Wall-period Worcester Lund's Bristol Vauxhall	Liverpool Chaffers Pomona Dr Wall-period Worcester	Caughley Flight-period Worcester Vauxhall Liverpool Ball

CaO + P₂O₅ >20%				
SiO ₂ /CaO + P ₂ O ₅ >1.2	SiO ₂ /CaO + P ₂ O ₅ <1.2			
Liverpool Brownlow Hill Liverpool Gillbody Liverpool Pennington	K ₂ O + Al ₂ O ₃ <11%		K ₂ O + Al ₂ O ₃ >13%	
	K ₂ O/Al ₂ O ₃ 0.2-0.5	K ₂ O/Al ₂ O ₃ 0.1-0.2	SiO ₂ >41%	SiO ₂ <40%
	Isleworth	Bow Chelsea Crown Derby Lowestoft	Coalport Grainger Nantgarw	Bovey Tracey Royal Worcester

PbO >5%			
SiO ₂ /CaO <6		SiO ₂ /CaO >7	
Al ₂ O ₃ >4%	Al ₂ O ₃ ≤3.5%	PbO >20%	PbO <20%
Chelsea	Longton Hall West Pans	Limehouse	Derby

SiO₂ + Al₂O₃ + CaO >80%					
SiO ₂ /CaO <20		SiO ₂ /CaO >20			
SiO ₂ /Al ₂ O ₃ <3	SiO ₂ /Al ₂ O ₃ >5	SiO ₂ /Al ₂ O ₃ <7		SiO ₂ /Al ₂ O ₃ >8	
A'-marked	Limehouse	SiO ₂ ≥70%	SiO ₂ <70%	TiO ₂ >0.3%	TiO ₂ <0.1%
		Caughley Cookworthy's Plymouth/Bristol New Hall Swansea	Caughley Chamberlain's Worcester Coalport Grainger Royal Worcester Swansea	Liverpool Brownlow Hill	Nantgarw

Discussion: using multiple analytical techniques to characterise British porcelain

Table 59 - compositional categories for British porcelain glazes using major and minor elemental compositional data. All % data in these tables is absolute, and ratios are calculated from the absolute composition.

PbO <5%				
Al ₂ O ₃ <6%		Al ₂ O ₃ 8-13%		Al ₂ O ₃ >15%
contains SnO ₂	contains no detectable SnO ₂	CaO <3%	CaO >3%	Bovey Tracey Bristol
Vauxhall	Limehouse	Plymouth	Grainger Royal Worcester	

PbO 5-30%			PbO > 30%	
Al ₂ O ₃ + K ₂ O + CaO >15%		Al ₂ O ₃ + K ₂ O + CaO <15%	PbO 30-45%	PbO >45%
Na ₂ O >1%	Na ₂ O <1%			
Bovey Tracey Royal Worcester	Nantgarw (phosphatic) Swansea	Caughley Grainger Liverpool Brownlow Hill Longton Hall Nantgarw (SAC paste) Vauxhall Worcester	Caughley Coalport Isleworth Limehouse Liverpool Brownlow Hill Liverpool Chaffers Liverpool Gillbody Liverpool Pennington Worcester	Bow Bovey Tracey Caughley Chelsea Coalport Derby Liverpool Brownlow Hill Liverpool Gillbody Liverpool Pennington Longton Hall Lowestoft Worcester

Discussion: using multiple analytical techniques to characterise British porcelain

Table 60 - compositional categories for British porcelain pastes using trace elemental compositional data.

All % data in these tables is absolute, and ratios are calculated from the absolute composition.

Th/U <1			Th/U >1						
Mg/Zn <100	Mg/Zn >100		Al/Ti ≤100			Al/Ti >100			
Chaffers Liverpool Ball	positive Ce anomaly, negative Eu anomaly	no positive Ce anomaly or negative Eu anomaly	Al/Zr ≤3000			Al/Zr >3000	negative Ce anomaly, positive Eu anomaly	positive Ce anomaly, negative Eu anomaly	
	Pomona, Worcester	Caughley, Worcester	HREE-enriched	LREE-enriched		Coalport Nantgarw Pinxton Swansea (phosphatic)	A'-marked	Plymouth	
			Longton Hall	negative Eu anomaly					no negative Eu anomaly
				negative Ce anomaly	no negative Ce anomaly				Bow Chelsea Limehouse Swansea
Crown Derby Limehouse	Coalport Lowestoft Nantgarw Pinxton Swansea New Hall								

Phosphatic factories: Bow, Isleworth and Lowestoft, the bone china factories

It has been established that Bow porcelain can be distinguished from that produced by Lowestoft by the presence of sulphur in the paste, which is attributed to the addition of gypsum ($\text{CaSO}_4 \cdot 2\text{H}_2\text{O}$) (Owen and Day, 1998). However, this element cannot be detected in the glaze using HH-XRF due to the extensive lead M peaks in the region where the peaks characteristic of sulphur should appear. Furthermore, this sulphur is not reported in any SEM-EDS data of Bow glazes, which suggests that it is not present at detectable levels.

However, it appears to be possible to distinguish porcelain from the three most prolific phosphatic porcelain factories using HH-XRF data of the glaze and underglaze blue. Bow appears to be unique in containing no detectable manganese in any of the glazes here analysed. This allows it to be distinguished from Isleworth and Lowestoft glazes, which always contain manganese. Lowestoft may be distinguished from most Isleworth and Bow glazes, because has no detectable tin. Furthermore, the underglaze blue pigment used by Lowestoft is the only one of the three that contains detectable levels of arsenic.

No Isleworth samples were available for LA-ICPMS analysis as part of this research, however there are compositional indicators that appear to distinguish Bow and Lowestoft by their paste composition. The relatively high levels of titanium in porcelain from both factories suggests that the clay used was a secondary clay, probably blue ball clay, based on a contemporary recipe from Bow, which will be discussed in greater detail in Section 7.4.3. There is documentary evidence that the Lowestoft factory used white-firing clay extracted from nearby Gunton, at least for the early years of the factory (1758 - 1764) (Brooks, 2001; pp. 14-15). Lowestoft pastes are enriched in barium, relative to niobium, strontium and calcium, which are present at the same levels as Bow and other phosphatic porcelains, including bone china. Trace elements associated with aluminium are also present at a lower ratio in Lowestoft paste, including titanium, zirconium and hafnium.

Furthermore the normalised REE profiles of these two factories' pastes differ; Bow porcelains are relatively LREE-enriched, and show a slight negative cerium anomaly that is not present in the Lowestoft porcelain here analysed, whereas the Lowestoft sample has a positive europium anomaly that has not been found in the Bow porcelain. This may be due to the use of different sources of clay, and another contributing factor may be the silica component; Bow is known to have used Lynn sand from King's Lynn, Norfolk (Tite and Bimson, 1991), while Lowestoft is thought to have used sand sourced more locally from Great Yarmouth (Brooks, 2001; pp. 29-30).

Bone china porcelains are easily distinguished from these early phosphatic factories, due to their use of china clay, which contains fewer impurities associated with aluminium. An unexpected result of this study is that Coalport, Nantgarw and Swansea bone china pastes can be distinguished by their REE profiles, as well as the ratio of thorium to uranium.

Magnesian factories: Worcester, Caughley, Richard Chaffers, Phillip Christian and Pomona

Mineralogical and elemental compositional data for Worcester, Caughley, Chaffers and Christian porcelain have demonstrated that it is possible to follow the transfer of technology from Worcester to each of the other factories, based on similarities between the early pastes of the new factories and the contemporary Worcester paste. Therefore, the composition of Chaffers early porcelain closely resembles that of Worcester of the 1750s, and Caughley magnesian porcelain is very similar to that of Worcester during the Flight period (1783 - 1793) (Owen and Sandon, 2003).

Owen and Sandon have shown that Caughley can be distinguished from the other magnesian factories, based on the proportions of magnesium to silica and alumina (Owen and Sandon, 2003), which suggests that less steatite was added to the paste, and correspondingly more clay and silica (Tite and Bimson, 1991). This was during the period when Cornish steatite was becoming scarce, and may therefore represent a cost-saving measure by the new factory.

Alternatively, it may be that Caughley's new kilns were superior in terms of the temperatures reached, and temperature control, enabling them to use less flux to achieve a successful firing (Grant-Davidson, 1966). The high levels of failed firings and kiln wastage experienced by Caughley during its early years appear to argue against the second theory (Owen and Sandon, 2003).

Chaffers and Christian porcelain can also be distinguished from contemporary Worcester on the basis of their mineralogy; the Liverpool factories' porcelain contain diopside ($\text{CaMgSi}_2\text{O}_6$), which has been interpreted as the inclusion of calcite in the paste formula (Owen and Sandon, 1998). However, this does not have any detectable influence on the major and minor elemental composition.

This research has demonstrated that Worcester glazes can be distinguished from Caughley, Chaffers and Christian because they appear to contain no detectable arsenic, when analysed by HH-XRF. The underglaze blue pigment that decorates Worcester porcelain does contain arsenic, which is rarely found in the blue pigments on Caughley, Chaffers and Christian porcelain.

All magnesian factories are thought to have used for their plastic component a soft porcelain stone that was associated with the steatite deposits from which their flux was extracted. This therefore gives them a lower level of titanium and other trace elements associated with aluminium than glassy and phosphatic porcelains that relied on secondary clays. These lower trace impurities in the paste may explain why magnesian porcelains rarely have tin in their glazes, because this element was commonly added to the glazes of phosphatic and glassy porcelains as an opacifier to conceal less-than-white pastes.

The trace elemental composition of the magnesian porcelains show some similarities; in all cases, magnesium is associated with zinc, although their ratio is significantly lower in Chaffers (Mn/Zn 60-100) pastes than in Caughley, Pomona and Worcester (Mn/Zn 200-400), which may mean that a different source of steatite was used, or that the steatite was processed differently prior to use, resulting in the retention of more trace elements. All magnesian pastes are enriched in uranium, relative to thorium, and

contain relatively low levels of REEs, which tend to be HREE-enriched with significant fractionation. Anomalies in cerium and europium are rare and tend to be low. Important exceptions are the Chaffers samples, which have strong negative europium anomalies, and outliers to the main Worcester group, which have positive cerium and europium anomalies.

Worcester porcelain can be further distinguished by its trace elemental composition, because it appears to be enriched in strontium and uranium, relative to calcium and thorium respectively, which are present at levels similar to other magnesian porcelains. This may be attributed to the greater quantity of steatite flux used in their early pastes (Owen, 1997). The variability in the REE profiles of Worcester porcelain through time remains unexplained, since the major, minor and other trace elemental composition is relatively static, with the exception of the increasing ratio of magnesium to lead.

This may may be a trait inherent in the steatite, which may weather differently depending on its position within the strata, or its exposure to air and water, in which case similar variability would be found within magnesian porcelains in general. This cannot be assessed for Caughley, Chaffers, Pomona or Liverpool (Ball) in the current research, due to the limited number of samples available.

7.4.3 Re-examining the Eccles samples: the contribution of trace elements

In this section, two important early studies of British porcelain using analytical techniques are revisited. Alongside the findings of this research, they will be critically assessed to determine what new technology and data can contribute to our understanding of British porcelain, and methods of characterising factories and objects.

One of the earliest technological studies of British porcelain was carried out by Eccles and Rackham (1922); in it they used wet chemical analytical techniques to characterise porcelain pastes from a range of factories. The same objects were revisited by Tite and Bimson (1991), using SEM-EDS and XRD in order to determine what more information could be gained using these techniques. The results obtained by Tite and Bimson (1991) agreed with those of Eccles and Rackham (1922) for the major elements (>8%) of most samples. They used model compositions for the constituent raw materials to calculate the proportions of these used to create the porcelain pastes. Their model raw material compositions are summarised in Table 61. They tested their calculated formulae for Bow and Nantgarw phosphatic porcelain against those reported by Josiah Wedgwood in his Experiment Book in 1759, and Dillwyn in his notebooks in 1815-17, and found agreement for the proportions of bone ash and silica. Likewise, the composition of magnesian porcelain produced at Worcester was compared with a recipe delivered by Richard Holdship in 1764, and good agreement was found for the major constituents. From these assumptions, it was possible to suggest the formulae that may have been used for magnesian porcelain from Vauxhall and Chaffers of Liverpool. The formulae provided by Tite and Bimson (1991) for all of the porcelains that they analysed in that work are summarised in Table 62.

Table 61 - model composition of porcelain raw materials, after Tite and Bimson (1991)

Raw material	Major and minor elemental	Source (after Tite and Bimson, 1991)
Blue ball clay (Dorset)	SiO ₂ 60%, Al ₂ O ₃ 37%, K ₂ O + Na ₂ O 3%	Holdridge, D A (1956) 'Ball clays and their properties', <i>Transactions of the British Ceramic Society</i> 55, pp. 369-440
Crown glass (French window glass)	SiO ₂ 70%, K ₂ O + Na ₂ O 15%, CaO 15%	Mackenzie, eds. (1875-7) <i>Chemistry as applied to arts and manufactures: 5, Glass</i> , pp. 1-11
Flint glass (English and French crystal)	SiO ₂ 60%, K ₂ O + Na ₂ O 10%, PbO 30%	Mackenzie, eds. (1875-7) <i>Chemistry as applied to arts and manufactures: 5, Glass</i> , pp. 1-11
Bone ash	CaO 57%, P ₂ O ₅ 43%	assumed 100% hydroxyapatite Ca ₅ (OH)(PO ₄) ₃
Soapstone	SiO ₂ 67%, MgO 33%	assumed 100% talc Mg ₃ Si ₄ O ₁₀ (OH) ₂

Table 62 - summary of formulae used in the porcelain samples analysed by Tite and Bimson (1991), according to the authors' interpretation

Factory	Date range	Source	Raw materials and proportions
Bow	1759	Josiah Wedgwood, Experiment Book	4 parts bone ash (47%), 4 parts Lynn sand (47%), ¼ part (3%) blue ball clay, ¼ part (3%) gypsum
Lowestoft	1770-75	assumed, based on Bow	40-45% bone ash, 25-40% silica, 20-30% blue ball clay
Chelsea	1760-65	assumed, based on Bow	40-45% bone ash, 25-40% silica, 20-30% blue ball clay
Nantgarw	1815-17	Dillwyn notebook	9 parts (25%) china stone, 12 (33%) parts china clay, 12 (33%) parts bone ash, 3 parts (8%) lime
Worcester	1764	correspondence between Richard Holdship (Worcester) and William Duesbury (Derby)	30-35% soapstone, 20% flint glass cullet, 15% crown glass cullet, 25-30% silica (sand or calcined and ground flint)
Vauxhall	1753-64	assumed, based on Worcester	25% soapstone 35% crown glass cullet, 35% silica (sand or calcined and ground flint)
Liverpool (Chaffers)	1756-65	assumed, based on Worcester	30-35% soapstone, 35-40% crown glass cullet, 25-30% silica (sand or calcined and ground flint)

It was concluded that porcelain of each paste type could be distinguished from other porcelain of the same paste type but from different factories, based on the elemental composition and mineralogy of the paste. This research has aimed to expand on these conclusions in two ways: by developing a methodology that will allow characteristic data to be obtained using non-invasive techniques (HH-XRF and spectrophotometry), and to identify further distinctive characteristics of the porcelain pastes using trace elemental compositional data, which will provide information on the development of the British porcelain industry through the manufacturers choices of technology and sources of raw material.

For this second objective, the Eccles samples have been analysed using LA-ICPMS. The LA-ICPMS data for the major and minor elements have been compared with the SEM-EDS data, and have been found to compare well with respect to the pastes, but less so the glazes. The trace elemental compositional data for the pastes were then examined in groups by type, in order to determine whether there are traits common to the products of certain factories that are not shared by others. These compositional distinctions have been linked where possible to sources of raw materials using the primary sources associated with the factory, where these were available. This process has been described in detail in sections 7.4.1 and 7.4.2 of this Discussion chapter, and the findings are expanded upon here in terms of their implications for the Eccles and Rackham (1922) and Tite and Bimson (1991) samples.

Eccles and Rackham stated that the Chelsea (29103U) and Longton Hall (29101Y and 29098V) samples had a frit paste, to which Tite and Bimson were able to add that these factories could be distinguished based on the proportions of the two types of glass cullet, crown glass and flint glass, that had been used in their formulation. They were also able to distinguish between two periods of the Chelsea factory, the red anchor period (represented by sample 29103U) and the triangle period (represented by sample 32699W), between which times a change in formula occurred. The trace elemental compositional data gathered during this research has confirmed that these two factories used a similar type of ball clay, based on the ratio of trace elements to aluminium, and similarities in their REE profiles.

The ratio of flint glass to crown glass was found to be greater in Longton Hall pastes, and this may account for the greater enrichment of thorium, relative to uranium, in these porcelains, while that of Chelsea is within the range of the phosphatic porcelain pastes that used ball clay. Alternatively, a different source of silica may have been in use at Longton Hall, which may have contributed to the unusual REE profile of this group. All other ball clay pastes are LREE-enriched with either no significant europium anomaly, or a slight positive anomaly for this element, including frit Chelsea pastes, whereas Longton Hall is uniquely HREE-enriched with a strong negative europium anomaly. From the SEM micrographs in Tite and Bimson (1991), there appear to be no morphological differences between the unreacted silica phases present in pastes from the two factories, both are angular in shape with diffused edges where melting has begun to occur during firing. These could be consistent with either sand or ground flint grains, but a different source used by Longton Hall is still a possibility. It would be interesting to compare the trace elemental composition of West Pans porcelain, the factory that was subsequently operated by Longton Hall's William Littler, and the major and minor composition of which is most similar to Longton Hall frit.

For phosphatic pastes, the Eccles and Rackham study was limited to Bow (29105Q, 29100P and 29104S), Lowestoft (29107X) and a gold-anchor period Chelsea (29106Z) sample, to which Tite and Bimson added another Bow sample from the same period (1750-1765, sample number 32703), a further Lowestoft (32707) and three Nantgarw samples (32846, 32847 and 32714). They were able to identify similar mineral phases in the bodies of the phosphatic pastes, in spite of the evident use of ball clay in the Bow, Chelsea and Lowestoft pastes, and china clay in Nantgarw. Silica and calcium phosphate are clearly the two important constituents in the formation of whitlockite phases in a glassy matrix, which characterises this paste type.

Later Bow (1765-70) was able to be distinguished from earlier pastes from that factory (1750-60) by the presence of gypsum in the later pastes, identified by ~2% sulphur dioxide. Unfortunately, sulphur was not able to be detected as part of this research using LA-ICPMS, because it is prone to spectral interferences when using a quadrupole MS without altering the carrier flow rate to promote the formation of oxides (Giner Martínez-Sierra et al, 2015). As a result, the normalisation of these Bow pastes may be inaccurate, due to the omission of a stoichiometric compound, and this distinction between periods cannot be made. However, this Bow samples appears to be in every other way compositionally identical to those of the earlier period.

The similarity between Bow and Lowestoft, and their distinction from the bone china porcelains, has been discussed in section 7.4.2. It builds upon the conclusions of Tite and Bimson by characterising the trace elemental profile of the two types of clay used, and identifying the presence of traces of tin and smalt in the Bow and Lowestoft pastes. While it is clearly possible to distinguish a phosphatic from a bone china porcelain using the major and minor elemental composition, this research demonstrates the discriminating power that the different clay types have upon the trace elemental composition and REE profile of the porcelain paste.

The magnesian porcelains were characterised by Eccles and Rackham through the identification of magnesium in the paste of two Worcester samples (29109T and 29623P). Tite and Bimson added to this by demonstrating that Worcester can be distinguished from magnesian Vauxhall (32706 and 32705) and Chaffers (32704) due to the presence of a higher concentration of lead (5-7% PbO) in these early (1750-1765) Worcester pastes. Vauxhall and Chaffers were also able to be distinguished, based on their ratio of steatite to crown glass. The Vauxhall samples were unavailable for this research, but magnesian porcelain from Caughley, Liverpool (Ball) and Pomona were compared with Worcester, the results of which are discussed in section 7.4.2. None of these factories match the composition of the Vauxhall porcelain, described by Tite and Bimson, although one sample from Liverpool (Ball) comes closest, in terms of their low magnesium to calcium ratio (MgO/CaO 1.3-1.6, as opposed to 4-8), caused by the presence of crown glass or glass frit.

This combined flux formula constitutes a hybrid magnesian-frit paste that does not fall into one compositional category, providing further support for Owen's (2007) classification scheme based on the chemical composition of the paste.

While compositional markers have been found that will enable factories to be distinguished by their trace elemental composition, it is remarkable how similar the trace element ratios and the REE profiles are between factories. It must be borne in mind that during the time when these ceramics were being manufactured, systems for quality control for raw materials were not as advanced as they now are. Clay, sand and cullet may have been visually inspected, and certainly washed or perhaps filtered, prior to inclusion in the ceramic paste. However, there were no reliable means of determining the chemical composition of the substance, and how well it matched what had previously been used. This variability in raw materials, as well as the lack of accurate means of measuring and controlling kiln temperatures, contributed to the high levels of wastage during firing, which for many factories was catastrophic.

Furthermore, each factory employed rigorous means of keeping their formula, the proportions of certain raw materials and their treatment, concealed from their competitors. This led to the diversity of pastes that are known to have been produced, and it also means that compositionally identical wares are most often the result of a transfer of workmen from one factory to another, because they took with them the proven formula from their previous place of employment. In spite of these circumstances, inter-factory variation in composition can be less than intra-factory variation, and the compositional and visual similarity between wares produced at different parts of the country, decades apart, can be sufficient to confound the connoisseur and the analyst. Trace elemental compositional data offer a solution to this problem by "fingerprinting" certain raw materials, and allowing the recipe of the product to be reconstructed, and the reliability of this method will increase greatly with the addition of more data from all factories and periods.

7.5 Summary

This chapter has collected the evidence from the analytical results collected in the preceding two chapters, and interpreted these against the existing scientific and historical evidence for British porcelain manufacture.

The analytical techniques used have been evaluated with regard to their usefulness for this material type., compared with the established method of SEM-EDS/WDS. While XRF produced ambiguous results in its initial test on ten archaeological porcelain sherds it has proven to be highly useful in answering certain research questions with regard to intact objects, and as a screening technique to identify samples for further analysis.

The trace elemental compositional data produced by LA-ICPMS have been demonstrated to add considerably to the characterisation and discrimination of objects from different factories, and there is potential for this technique to be used more extensively in the future to answer research questions in this field.

A case study that has been carried out as part of this research has been to revisit the Eccles samples, which were the subject of two of the most significant early technical studies of British porcelain, in order to demonstrate the impact of trace elemental data when added to the major and minor elemental and mineralogical data previously gathered.

This research has succeeded in developing a methodology for the analysis of British porcelain that fulfils the requirements of non-invasive analysis, and the results of which are comparable to the published data from SEM-EDS/WDS. Compositional criteria have been identified in the elemental compositional data that will enable certain factories and periods of manufacture to be identified using SEM-EDS/WDS, Hand-Held XRF, and LA-ICPMS. Furthermore, the data gathered during this study have further illuminated the development of British porcelain manufacture, and the transfer of technology and material across the country and through time.

8 Conclusions and recommendations

8.1 Conclusions

British porcelain has been the focus of study by historical methods, which has identified the existence of dozens of factories operating in competition with one another to produce fine ceramics in the style of the fashionable continental European and Far Eastern manufacturers. However, ceramic historians and fine art specialists have experienced difficulties in distinguishing between porcelain objects from different factories and periods; this situation is further complicated by the existence of later-decorated pieces and fakes (Sandon, 2009; p. 62; Elliot, 2006; pp. 98 - 102; Marno, 2008; Pearce, 2008 Manners, 2005).

Scientific analytical studies have demonstrated the existence of different types of paste composition, which are associated with the formulae used during manufacture. These studies have also allowed the products of certain factories to be distinguished from one another by the composition of their ceramic pastes, and thereby the formulae used, through SEM-EDS/WDS analysis. However, this method is limited by the dimensions of the SEM chamber and the vacuum conditions within, which require that the analyst remove a sample of material from the object under study. For this reason, SEM-EDS/WDS analysis has typically been used to characterise archaeological sherds and fragments from objects that the owner has given permission to sample.

The aim of this research has been to develop an analytical method using minimally-invasive analytical techniques, in order to characterise and distinguish the products of different porcelain factories operating in Britain during the mid- to late-18th and early-19th centuries. This has been accomplished by assessing the extent to which the data from each technique provide useful information about the objects' factory and period of origin, or the raw materials that may have been involved in their production. In this section, the most important findings from this research are stated, with regard to the applicability of each technique to the material, the effectiveness of the overall methodology, and the contribution that the novel data have made to our understanding of the history of the British porcelain industry.

8.1.1 Characterising and distinguishing British porcelain using multiple analytical techniques

Historical and technical review of British porcelain

Research into British porcelain has traditionally been based on historical and archaeological evidence, and a long tradition of connoisseurship, i.e. the identification of pieces, based on objective, human-measured traits. The past twenty-five years of research in this area have seen the development of a body of scientific knowledge, which is supported by, and in turn contributes to, connoisseurship, and archaeological and historical evidence. This was initially based on XRD, which gave insight into the mineralogy of the porcelain (Bimson, 1969; Tite and Bimson, 1991). By this method, the porcelain pastes could be categorised into three types, based on the formula used: phosphatic, which used a calcined animal-bone flux; magnesian, which incorporated soap-stone; and frit, which mixed the clay former with glass frit or cullet. Once SEM was brought into use for this purpose, the mineralogy could be explored further, using phase-contrast imaging. Furthermore, integrated spectroscopic systems, either EDS or WDS allowed bulk or spot analysis, in order to obtain quantitative elemental compositional data from the paste, and its individual mineral phases (Tite and Bimson, 1991; Watney et al, 1993; Owen, 1996; Freestone, 1996).

An early triumph for the use of SEM-EDS in the analysis of British porcelain was the identification of the 'A'-marked porcelain group with the product of the Bow first patent, which is described in detail in section 2.2.2. This group of porcelain had been the subject of intense interest to British porcelain collectors and scholars, and numerous theories had been put forward about its origin (Charleston and Mallet, 1971; Mallet, 1994).

Freestone carried out analysis on a sample of an 'A'-marked fluted cup using SEM-EDS, and the glaze of an 'A'-marked teapot using XRF, and concluded that the porcelain was probably English and from the 1740s or 1750s, on the basis of compositional similarity with Limehouse and Pomona porcelain (Freestone, 1996). Based on the purity of the clay used in the 'A'-marked porcelain, Freestone proposed that the source may have been the *uneka* clay imported from America, which was specified in the Bow first patent. This finding solved two mysteries about British porcelain at once: the origin of the 'A'-marked porcelain, and the survival of first patent Bow products.

Historical evidence for technological links between British porcelain factories have been supported by evidence from analysis, which can identify compositional similarities between the products of factories with known or suspected links that suggest the use of a shared formula. An excellent example was carried out by Owen et al, looking at the products of two factories known to have been operated by Nicholas Crisp, first at Vauxhall (1751-1763) and then at Bovey Tracey (1767-1774) (Owen et al, 2000). They found that Bovey Tracey magnesian porcelains are compositionally similar to those produced at Vauxhall, but employed a new ingredient, barite, which gives these porcelains a distinctive composition. Phosphatic porcelains were also produced at both factories, but those made at Bovey Tracey bear no resemblance to the few experimental Vauxhall examples, suggesting that Crisp had learned from his earlier failure, and was trying out a new formula.

Clearly, therefore, the application of SEM-EDS/WDS to these specific research questions has been of huge benefit to the study of this material type. There can be no doubt that elemental compositional data, and phase-contrast imaging, have answered a number of questions about the technology and raw materials of porcelain manufacture, and the development of the industry by the movement of individuals and ideas. However, these analytical findings remain limited in scope, because they have employed only archaeological material and objects that the analyst is free to sample using invasive methods.

Methodological development

Important achievements of this research include the development of the first specifically-designed method for the analysis of British porcelain, in order to achieve increased resolution in the data through the use of complementary analytical techniques that may be better suited to the material type. Porcelain from 24 factories, spanning a period from 1744 to 1840 has been analysed using complementary techniques to characterise the output of British soft-paste porcelain manufacture.

First, a meta-analysis of published quantitative elemental compositional data from porcelain bodies and glazes has found that nine factories may be distinguished reliably (Chapter 3). Of those that cannot be distinguished, this research presents some theories to explain why their paste formulae demonstrate close similarities, which are supported by documentary evidence indicating imitation or influence, shared management of factories, or the transfer of employees from one factory to another. For example, porcelain from Dr Wall-period Worcester is compositionally similar to that of Christian and Chaffers of Liverpool because the latter factories were established by defected workmen from Worcester. Later Flight-period Worcester porcelain differs consistently in composition from that of the earlier period, and is compositionally similar to porcelain from the Caughley factory, which was made under the advice of a former Worcester employee.

Spectrophotometry has been used to investigate the observation from visual connoisseurship that certain porcelains can be identified by the hue of their surface (Section 2.3.1). Porcelain from the “scratch-cross” group, said to have a grey hue, produces results indicative of a cooler hue, relative to Bow and Chelsea porcelain, which is said to have a creamier hue (Section 5.3). However, the overlap in values between wares from different factories makes colorimetry an impractical tool for characterisation if used independently of connoisseurship or compositional analysis.

Previous research conducted by Domoney (2012), which characterised 18th and 19th century continental European porcelains by the elemental composition of their coloured enamels, has been built upon to investigate British porcelain from the Worcester factory, which has been particularly subject to later (19th century) redecoration (Section 2.3.1). This research has found that HH-XRF is capable of detecting elements associated with 19th century redecoration of porcelain in green, turquoise, and claret overglaze enamels. For instance, chromium in green and turquoise enamels dates the pigments to the period after which this element was isolated in the early 19th century. Abundant zinc in enamels also indicates that they are later in date than they appear, since this substance was added to pigments from the 19th century onwards, in order to create a brighter colour.

Eighteen objects tested were found to have enamels that were consistent with 19th century decoration, of which connoisseurship had identified seven as “wrong” (Section 5.2.2). The compositional categories of pigments cannot currently be used to distinguish between factory-decorated and James Giles-decorated Worcester porcelain in any enamel colour or the gilding. Further analysis with more samples, using the optimised analytical method to obtain quantitative data from these pigments, may resolve these differences more clearly.

Expanding the method to include blue-and-white porcelain from a selection of factories and periods, this research finds that inter-factory variation in elemental composition of porcelain glazes is greater than intra-factory variation for three factories, namely Bow, Bovey Tracey and Longton Hall. This will allow unidentified objects from these factories to be attributed, based on the elemental composition of the glaze using HH-XRF analysis. Porcelain from thirteen further factories cannot presently be distinguished by the presence or absence of elements in their glazes, although interfactory differences are present (Section 5.2.2). In addition, the elemental composition of underglaze blue pigments used in three factories, namely Bovey Tracey, New Hall and West Pans, is distinctive. This suggests that they used an alternative source of cobalt ore, or that the techniques used to process the cobalt ore in creating the pigment were different.

Historical survey supports the former suggestion in the case of the Bovey Tracey and West Pans factories, which were said to have employed cobalt mined from Cornwall and Scotland respectively (Section 7.2.3).

It is concluded that HH-XRF analysis is a useful technique for the analysis of British porcelain, because it is able to identify most of the same elements available to SEM-EDS/WDS. The method is quick and flexible, since it involves no invasive sampling, and the equipment is field-portable, which has allowed analysis to be carried out inside the museum, archive or other premises where the objects are stored.

LA-ICPMS has been employed for the first time in the analysis of British porcelain to determine the extent to which British porcelain from a number of factories can be distinguished using the trace elemental composition, including rare earth elements (REEs), and to investigate whether imported clay from overseas may have been used in the manufacture of 'A'-marked porcelain (Section 6.2.2).

Differences have been found in the REE patterns shown by factories, which correspond with the use of steatite, and at least three different types of clay by different factories. The thorium/uranium ratio has been identified as a reliable means of distinguishing between the steatitic porcelains, in which uranium is enriched relative to thorium, and the other paste types in which clay represents the most significant plastic component, and where thorium is enriched relative to uranium. The ratios of aluminium to zirconium and to titanium have provided evidence to support the use of china clay by many later factories, and by Cookworthy in his Plymouth porcelain.

These trace impurities are found in greater concentrations in the factories that used ball clay (a secondary clay) than in those where china clay (a primary clay) is said to have been used. The 'A'-marked sample was found to be compositionally unique; a REE profile that is enriched in light rare earths (LREEs) with a strong positive europium anomaly are not found in any compositionally similar wares, or indeed any of the other British porcelain samples tested. This finding lends more support to the theory advanced by Freestone (1996), that these wares represent the products of the Heylyn and Frye patent of 1744, and that they were made using *uneka* clay from America.

This could be strengthened in future work by comparing the trace elemental composition of the 'A'-marked porcelain paste with those of ceramics that are known to have been made using *uneka* clay from North Carolina, where this particular factory is thought to have obtained its china clay.

These findings are based on a relatively small collection of samples, and demonstrate the power of LA-ICPMS for elemental compositional analysis. The major and minor elemental compositional data compare very well with that from SEM-EDS analysis, while the trace elements provide greater resolution between factories with similar major and minor compositions, including Bow and Lowestoft, and Longton Hall and Chelsea. The trace elemental composition has also allowed the identification of traits that are associated with the use of different sources of clay and fluxes.

The more data are gathered using this technique, particularly in cases where the source of raw materials is known, the more resolution will be gained of the compositional "signature" of certain raw materials. If the size of the sample chamber could be overcome as a limiting factor, this technique could entirely supplant SEM-EDS for compositional analysis, although the latter will still be used to gain information about the mineralogy and firing conditions of the pastes.

8.1.2 Developing a method for the fully-quantitative elemental compositional analysis of British porcelain using XRF

In the interest of maximising the range and quality of elemental compositional data which can be gathered, while preserving intact objects, a non-destructive method has been developed for the XRF, which is optimised for the analysis of British porcelain. As part of this work, a set of novel glass calibration standards has been created which should allow data from the porcelain glaze and enamels to be calibrated, providing fully-quantitative elemental compositional data for 14 elements of interest.

In the course of developing this method, it has been possible to investigate the challenges that affect the analysis of archaeological and historical materials, and to comment upon the extent to which these can be overcome.

Carrying out analyses under two current and voltage settings allows the optimal detection of low-Z and high-Z elements, which overcomes the challenge of the diverse compositional range of the pastes and glazes. The loss of low-Z elements through attenuation has been found to limit the characterisation of different glazes and enamels relatively little, and further losses through an increased air gap due to curved or deep surfaces may be compensated to some extent by analysing the standards for calibration under the same conditions.

8.1.3 Contributions to the narrative of the technological and historical development of British porcelain

Trace elemental compositional data have been used to identify features corresponding to the use of certain raw materials, as discussed above. This has made it possible to match porcelain pastes for which the raw materials are not known with those which have historical evidence for certain specific sources. In this way, sources of clay in particular can be proposed for 20 factories. It is suggested that china clay from St Stephens, Cornwall was used in the production of Coalport, Nantgarw, New Hall, Plymouth and Swansea porcelain, while ball clay, probably from Poole or Bideford in Dorset, was used for Bow, Chelsea, Derby and Longton Hall porcelain.

Although few samples were available for analysis, reliable differences were found between the REE profiles of Lowestoft and Bow porcelain, which are generally indistinguishable with respect to their major and minor elemental composition (Section 7.4.2). This is attributed to the use of clay from Grundon, Suffolk by the Lowestoft factory, and possibly sand from Great Yarmouth in the same area, whereas Bow is known to have obtained clay from one of the Dorset sources and sand from King's Lynn, Norfolk. The reliance on locally-sourced raw materials may explain the enigmatic location of the Lowestoft factory, which is apart from the clusters of contemporary porcelain factories.

Others were positioned close to the largest marketplace for their products (the London factories), or abundant sources of raw materials, such as clay (Bristol, Plymouth and Bovey Tracey) or timber and coal (the Welsh factories), or at canal transport hubs where a skilled ceramic-producing workforce existed (the Derbyshire, Worcestershire and Staffordshire factories).

An intriguing and unexpected finding of this research has been the variability in trace elemental composition among the magnesian porcelains, particularly with regard to their REEs (7.4.2). While all tend to be depleted in REEs, relative to the other pastes here analysed, and HREE-enriched where the other pastes tend to be LREE-enriched, these are the only similarities within the group. Anomalies in cerium and europium are not commonly found, and tend to be low, but the Chaffers factory is a significant exception with strong negative europium anomalies.

Worcester porcelain, for which the most samples were available for analysis, has different combinations of both positive and negative cerium and europium anomalies. These patterns must be examined further, and with greater numbers of samples from the four factories concerned. However, it is suggested that this difference is correlated with the greater presence of steatite as a flux in Worcester and Chaffers porcelain, relative to Caughley and Pomona. Furthermore, the variability of the trace elemental composition of the Worcester pastes may be a result of experimental formulae during the early Dr Wall period of the factory (1751-1783), during which time different sources or strata of steatite and porcelain stone may have been exploited, before the perfected formula was copied by Chaffers from 1756, and by Caughley from ca.1780.

It is also suggested that the Chaffers factory relied on another currently unknown source of steatite for its magnesian porcelains. This is based on the finding of Owen and Sandon (1998) that Chaffers pastes contain the mineral diopside ($\text{CaMgSi}_2\text{O}_6$), indicating the presence of calcite in the paste, and the supplementary finding in this work that the ratio of magnesium to zinc is significantly lower in Chaffers porcelain (Mg/Zn 60-100) than in those from Worcester, Caughley and Pomona (Mg/Zn 200-400).

This may represent the successful protection by Worcester of the Cornish source of steatite, the licenses for which it purchased from Lund's Bristol factory following the failure of the latter factory. If a 25-year license had been obtained at the time of Worcester's inception, it would have been in force at the time of Chaffers' foundation, but would have expired prior to the foundation of the Caughley and Pomona factories.

Finally, further evidence has been obtained to support the finding of Freestone (1996) that the 'A'-marked porcelain group represents the products of the Bow first patent, due to the unique REE profile of this paste, which is not consistent with any of the others obtained from contemporary and later British porcelain that was made using British sources of clay.

8.1.4 Summary

The findings of this work emphasise the compositional variation of British soft-paste porcelain by illustrating the broad range of types and sources of raw materials that were exploited in its manufacture during the mid- to late-17th century. The ingenuity of these manufacturers has created compositional diversity in their products, which is often strongly linked with the factory of origin, even when these were situated within a few miles of one another, as is the case of Bow, Isleworth, Vauxhall and Chelsea in the south east of the country, or Caughley and Coalport in the north west. This compositional variation is a gift to connoisseurs and collectors of British porcelain, since it provides the opportunity to gain a reliable provenance for an object, which can support future research into the products and history of this industry.

The compositional similarities between factories are equally fascinating, because they demonstrate the influence that one factory may have on many others through the spread of workmen and recipes. Since the formulation of the porcelain paste was generally a task carried out by one person, or a small group of people, it may be said that Dr Wall, the proprietor and chemist in charge of the Worcester porcelain factory, was responsible for Christian and Chaffers of Liverpool, and Caughley magnesian porcelain, which were derived from his recipe.

Similarly, William Cookworthy, another chemist who operated short-lived porcelain factories at Plymouth and Bristol, produced the first commercially-successful British hard-paste porcelain using the directions of Francois d'Entrecolles, and his formula was adopted at New Hall and subsequently most porcelain factories during the 19th century. The benefits of producing a successful porcelain formula extended beyond the proprietor's financial fortunes and contributed positively to the development of the fine ceramics industry in Britain at the beginning of the Industrial Revolution.

8.2 Recommendations for further work

This research has successfully achieved its stated objectives, which were to develop an optimised analytical methodology for British porcelain, which would enable characteristic data to be collected without destructive or invasive analysis, and to contribute new knowledge to our understanding of the British porcelain industry. This work has also illuminated some areas that would benefit from further research in the future, in the interests of expanding and resolving these objectives and other related research questions, which will be described in the following sections.

8.2.1 Refine and expand the XRF method

The XRF method that was developed as part of this research has been found to be effective for detecting and quantifying the elements of interest in porcelain glazes and enamels using a set of bespoke glass calibration standards. However, the method has demonstrated some disadvantages with regard to the detection of light elements and those with overlapping peaks, relative to spectroscopic analysis as part of an SEM system, which has previously been relied upon for analyses of this type. Furthermore, the method is yet to be tested on intact objects of British porcelain, and it would be interesting to see how practical it is for real-world analysis of this object type. This could be considered from the perspective of accessing objects, and the practical considerations of analysing curved and oddly-shaped objects, such as figures.

Further analysis on a range of glazes for which fully-quantitative data are available, for instance from LA-ICPMS or SEM-EDS, could investigate the extent to which peak overlaps for elements such as arsenic and lead, or iron and cobalt, affect the quantification of XRF data. In this way it could be determined whether there is a way of accurately quantifying arsenic in a high-lead glaze, or whether this must remain, as it is in the current method, a qualitative component of the glaze.

The method may also be relevant to the analysis of contemporary fine ceramics such as delftware and stoneware, which also employed leaded glazes and enamels, and underglaze blue decoration. These may help to resolve differences in the lead content of the glazes, which could be related to the area or period of manufacture, or to the type of object. For instance, a functional object such as a plate may have been glazed with a more siliceous, less leaded mixture in order to produce a harder glaze that is resilient to scratches and wear, whereas a decorative object such as a figure may have employed a higher-lead mixture that produced a softer glaze that could be fired at a lower temperature, thus reducing the risk of the complex form incurring damage in the kiln.

8.2.2 Identify a compositional chronology for enamelling and gilding

The HH-XRF data from this research have presented a tantalising glimpse into the complexity of enamel pigments and gilding in use on fine ceramics during this period, and their relationship with practices of added decoration and redecoration in the 19th century. Further research that incorporates objects from factories other than Worcester may help to resolve the differences between the pigment and gilding composition and whether these differ between factories and periods.

Furthermore, enamels on glass from the same period could be analysed using the same method, in order to test whether the same palette was used for both material types. A small number of painted enamelled and gilded glass objects were produced by James Giles' studio, which enamelled some of the porcelain analysed as part of this research, and a direct comparison could be made between the composition of Giles' porcelain and glass enamels and gilding.

8.2.3 Further LA-ICPMS analysis to include more pastes, glazes and cobalt blue

This pilot study using LA-ICPMS for British porcelain has revealed trace elemental compositional differences between objects with very similar major and minor elemental compositions, and this creates the possibility of a new method for the characterisation and distinction of British porcelain.

The patterns discovered here could be further resolved and tested by the incorporation of more objects from the factories here tested, and from other factories that operated during the same period.

The analysis of glazes in cross-section has been less successful, due to the relatively large analytical area of the laser ablation system. This may be resolved by positioning the laser perpendicular to the object's surface and analysing through the glaze.

Further experiments could determine whether the ablated area might be sufficiently deep to penetrate the glaze, in which case contamination by the paste would still need to be taken into account, or whether the analysed area is entirely glaze. This would also require that the thicknesses of glazes present on British porcelain should be more comprehensively characterised, perhaps using SEM or optical microscopy on samples mounted in cross-section.

If a method for the analysis of the glazes could be successfully developed, LA-ICPMS analysis could be expanded to include polychrome enamels and underglaze blue pigments, which would contribute to the characterisation of these areas that has been initiated with HH-XRF analysis as part of this research.

8.2.4 Compare trace elemental composition from porcelain pastes with geological materials and contemporary fine ceramics

It has been discussed as part of the literature review in this research the benefits that trace elemental compositional data have brought to archaeomaterials provenancing studies. Through comparison with objects of secure provenance, and with geological materials, aspects of the trace elemental composition of objects including obsidian and man-made glass, ceramics and metals have been identified that are indicative of a geographical area or period of origin.

In spite of its compositional complexity, this research has demonstrated that there is potential for the same to be achieved for British porcelain. Further research using LA-ICPMS analysis would allow the creation of a data-bank of porcelain pastes, glazes and geological raw materials that could allow such compositional traits to be identified. With the aid of such a data-bank, an object of unknown origin could be analysed using the same method, and a most likely origin could be suggested through comparison. This method would also contribute to our knowledge of the raw material sources and their proportions that were used in the formulation of pastes and glazes, by allowing the compositional “signature” of certain raw materials to be identified and compared within and between factory groups.

REFERENCES

- Adams, B and Thomas, A (1996) *A potworks in Devonshire: the history and products of the Bovey Tracey potteries 1750 - 1836*, Sayce Publishing, Bovey Tracey
- Adams, E (1991) *Bow porcelain*, Faber, London
- Adams, E (2001) *Chelsea porcelain*, British Museum, London
- Adan-Bayewitz, D, Asaro, F and Giauque, R D (1999) "Determining pottery provenance: application of a new high-precision X-ray fluorescence method and comparison with instrumental neutron activation analysis," *Archaeometry*, Blackwell Publishing Ltd, 41(1), pp. 1 - 24,
- Ahmon, J (2004) 'The Application of short-range 3D laser scanning for archaeological replica production: the Egyptian tomb of Seti I', *The Photogrammetric Record*, 19(106), pp.111 - 127
- Aitchison, J; Barcelo-Vidal, C; and Pawlowsky-Glahn, V (2002) 'Some comments on compositional data analysis in archaeometry, in particular the fallacies in Tangri and Wright's dismissal of logratio analysis', *Archaeometry* 44(2), pp. 295 - 304
- Alberghina, M F; Barraco, R; Brai, M; Schillaci, T; and Tranchina, L (2011) 'Integrated analytical methodologies for the study of corrosion processes in archaeological bronzes' *Spectrochimica Acta, Part B* 66, pp. 129 - 137
- Allègre, C J; Dupre, B; and Lewin, E (1986) 'Thorium/uranium ratio of the Earth', *Chemical Geology* 56(3), pp. 219 - 227
- Aloupi, E; Karydas, A G; and Paradellis, T (2000) 'Pigment analysis of wall paintings and ceramics from Greece and Cyprus: the optimum use of X-ray spectrometry on specific archaeological issues', *X-ray Spectrometry* 29, pp. 18 - 24
- Arabina, K D; Chakraborty, R; Cervera, M L; and de la Guardia, M (2006) 'Analytical techniques for the determination of bismuth in solid environmental samples', *Trends in Analytical Chemistry* 25(6), pp. 599 - 608

Aubert, D; Stille, P; and Probst, A (2001) 'REE fractionation during granite weathering and removal by waters and suspended loads: Sr and Nd isotopic evidence' *Geochimica et Cosmochimica Acta*, 65(3), pp. 387 - 406

Barker, D and Cole, S (1998) *Digging for Early Porcelain: the archaeology of six 18th-century British porcelain factories*, Art Books International

Barrett, F A (1966) *Worcester porcelain and Lund's Bristol*, Faber and Faber, London

Barrett, F A and Thorpe A L (1971) *Derby Porcelain 1750-1848*, Faber and Faber, London

Bartle, E K and Watling, R J. (2007) "Provenance determination of oriental porcelain using laser ablation-inductively coupled plasma-mass spectrometry.," *Journal of Forensic Sciences*, Blackwell Publishing, Inc., 52(2), pp. 341 - 348.

Baxter, M J (2001) 'Statistical modelling of artefact compositional data' *Archaeometry* 43(1), pp. 131 - 147

Baxter, M J; Beardah, C C; Papageorgiou, I; Cau, M A; Day, P M; and Kilikoglou, V (2008) 'On statistical approaches to the study of ceramic artefacts using geochemical and petrographic data', *Archaeometry* 50(1), pp. 142 - 157

Begg, P. (2000) *A treasury of Bow : a survey of the Bow factory from first patent until closure, 1744-1774*, Hawksburn [Vic.], Ceramics and Glass Circle of Australia.

Beurdeley, C and Beurdeley, M (1974) *A Connoisseur's Guide to Chinese Ceramics*, Harper and Row Publishers, USA

Bezur, A and Casadio, F (2013) 'The analysis of porcelain using handheld and portable X-ray fluorescence spectrometers' in Shugar and Mass eds., *Handheld XRF for Art and Archaeology*, Leuven University Press, pp. 249 - 312

Binns, R W (1865) *A Century of Potting in the City of Worcester (Being the History of the Royal Porcelain Works from 1751 to 1851)*, Bernard Quatrach, London

Bimson, M (1969) "The Examination of Ceramics by X-Ray Powder Diffraction," *Studies in Conservation*, Maney Publishing on behalf of the International Institute for Conservation of Historic and Artistic Works, 14(2), pp. 83 - 89

Boney, K (1957) *Liverpool Porcelain of the Eighteenth Century and its Makers*, B. I. Batsford, London

Bosco, G L (2012) 'Development and application of portable, Hand-Held X-ray fluorescence spectrometers' *Trends in Analytical Chemistry* 45, pp. 121 - 134

Brems, D and Degryse, P (2013) "Trace element analysis in provenancing Roman glass-making" *Archaeometry* 56(1), pp. 116 - 136

Brongniart, A (1898) *Colouring and decoration of ceramic ware*, Windsor and Kenfield, Chicago

Bronk, H and Freestone, I C (2001) "A Quasi Non-destructive Microsampling Technique for the Analysis of Intact Glass Objects By SEM/EDXA," *Archaeometry*, Blackwell Publishers Ltd, 43(4), pp. 517–527

Brooks, C J (2001) *China returns to Lowestoft: the story of Lowestoft porcelain*, Lowestoft, Jack Rose Old Lowestoft Society.

Brothwell, D R and Pollard, M eds., (2001) *An Introduction to Archaeological Sciences*, John Wiley & Sons, New York

Calvo del Castillo, H; and Strivay, D (2012) 'X-ray methods', in Edwards and Vandenabeele eds., *Analytical archaeometry: selected topics*, pp. 59 - 102

Carswell, J (2000) *Blue and White: Chinese Porcelain around the World*, The British Museum Press, London

Casadio, F, Bezur, A, Domoney, K, Eremin, K, Lee, L., Mass, J. L., Shortland, A., and Zumbulyadis, N (2012) "X-ray fluorescence applied to overglaze enamel decoration on eighteenth- and nineteenth-century porcelain from central Europe," *Studies in Conservation*, 57(1 Supplement1), pp. 61–72

Cassidy-Geiger, M eds. (2007) *Fragile Diplomacy: Meissen porcelain for European courts, ca. 1710 - 63*, Yale University Press, New Haven

Centeno, S A; Williams, V I; Little, N C; and Speakman, R J (2012) 'Characterisation of surface decorations on Prehispanic archaeological ceramics by Raman spectroscopy, FTIR, XRD, and XRF', *Vibrational Spectroscopy* 58, pp. 119 - 124

Charleston, R J and Mallet, J V G (1971) "A problematical group of 18th century porcelains," *Transactions of the English Ceramic Circle*, 8, pp. 80–121.

Chen, T, Rapp G, Jr, Jing, Z and He, N (1999) "Provenance Studies of the Earliest Chinese Protoporcelain Using Instrumental Neutron Activation Analysis," *Journal of Archaeological Science*, 26(8), pp. 1003–1015

Cheng, L; Li, R; Pan, Q; Li, G; Zhao, W; and Liu, Z (2009) 'Analysis of elemental maps from glaze to body of ancient Chinese Jun and Ru porcelain by micro-X-ray Fluorescence', *Nuclear Instruments and Methods in Physics Research B* 267(1), pp. 117 - 120

Chilton, M (2007) 'Dogs and Diplomats: Meissen porcelain in England, 1732 - 54' in Cassidy-Geiger eds. *Fragile Diplomacy: Meissen porcelain for European courts, ec. 1710 - 63*, Yale University Press, New Haven, pp. 275 - 300

Clark, R J H (2002) 'Pigment identification by spectroscopic means: an arts/science interface' *Comptes Rendus Chimie* 5, pp. 7 - 20

Clifford, T (1969) 'Derby biscuit', *Transactions of the English Ceramic Circle* 7(2), pp. 108 - 125

Colomban, P and Milande, V. (2006) "On-site Raman analysis of the earliest known Meissen porcelain and stoneware.," *Journal of Raman Spectroscopy*, John Wiley & Sons Ltd., 37(5), pp. 606–613.

Colomban, P (2012) 'The on-site/remote Raman analysis with mobile instruments: a review of drawbacks and success in cultural heritage studies and other associated fields', *Journal of Raman Spectroscopy* 43(11), pp. 1529 - 1535

Connors-Rowe, S A; Whitmore, P M and Morris, H R (2007) 'Optical brightness in black-and-white photographic paper: appearance and degradation', *Journal of the American Institute for Conservation*, 46(3), pp.199-213

Costa, B F O; Silva, A J M; Ramalho, A; Pereira, G and Ramos Silva, M (2012) 'X-ray compositional microanalysis and diffraction studies of Haltern 70 amphorae sherds' *X-Ray Spectrometry*, 41(2), pp.69-74

Craddock, P T (2009) *Scientific investigation of copies, fakes and forgeries*, Oxford; Burlington, MA, Elsevier / Butterworth-Heinemann.

Craig, N; Speakman, R J; Popelka-Filcoff, R S; Glascock, M D; Robertson, J D; Shackley, M S; and Aldenderfer, M S (2007) 'Comparison of XRF and pXRF for analysis of archaeological obsidian from southern Peru', *Journal of Archaeological Science*

Cui, J, Wood, N, Qin, D, Zhou, L, Ko, M, and Li, X (2012) "Chemical analysis of white porcelains from the Ding Kiln site, Hebei Province, China," *Journal of Archaeological Science*, Elsevier Ltd, 39(4), pp. 818–827

Cushion, J P; and Honey, W B (1996) *Handbook of pottery and porcelain marks*, Faber and Faber, London

Daniels, P (2007) *The origin & development of Bow porcelain, 1730-1747 : including the participation of the Royal Society, Andrew Duchè and the American contribution*, Resurgat Publishers, Faringdon

Danzer, K and Currie, L A (1998) 'Guidelines for calibration in analytical chemistry', *Pure and Applied Chemistry* 70(4), pp. 993 - 1014

Davis, M K; Jackson, T L; Shackley, M S; Teague, T; and Hampel, J H (2010) 'Factors affecting the Energy-Dispersive X-ray Fluorescence Analysis of Archaeological Obsidian' in Shackley eds. *X-ray Fluorescence Spectroscopy (XRF) in Geoarchaeology*, pp. 45 - 64

Dawson, A (2007) *The Art of Worcester Porcelain*, University Press of New England, Lebanon

de la Beche, H and Reeks, T (1871) *Catalogue of specimens in the Museum of Practical Geology, illustrative of the composition and manufacture of British pottery and porcelain, with a catalogue of clays by G Maw*, London

Delamere, F (2013) *Blue pigments: 5000 years of art and industry*, Archetype Publications, Ltd., London

Denoyer, E R; Freedman, K J; and Hager, J W (1991) 'Laser solid sampling for Inductively Coupled Plasma Mass Spectrometry' *Analytical Chemistry* 63, pp. 445 - 457

Deer, W A, Howie, R. A. and Zussman, J (1992) *An introduction to the rock-forming minerals*, Harlow, Essex, England; New York, NY, Longman Scientific & Technical ; Wiley.

Dias, M I, Prudêncio, M I, Pinto De Matos, M A and Rodrigues, A L (2013) "Tracing the origin of blue and white Chinese Porcelain ordered for the Portuguese market during the Ming dynasty using INAA," *Journal of Archaeological Science*, 40(7), pp. 3046–3057

Domoney, K; Shortland, A J; and Kuhn, S (2012) 'Characterisation of 18th-century Meissen porcelain using SEM-EDS', *Archaeometry* 54(3), pp. 454 - 474

Domoney, K (2012) *Non-Destructive Hand-Held X-Ray Fluorescence Analysis of Meissen and Vincennes-Sevres Porcelain: Characterisation, Dating and Attribution*, Cranfield Defence and Security, Cranfield University

Drakard, D eds. (1993) *Limehouse Ware Revealed*, English Ceramic Circle, London

Du Boulay, A (1984) *Chinese porcelain*, Weidenfeld and Nicholson, London

Dussubieux, L; Robertshaw, P; and Glascock, M D (2009) 'LA-ICP-MS analysis of African glass beads: laboratory inter-comparison with an emphasis on the impact of corrosion on data interpretation' *International Journal of Mass Spectrometry* 284, pp. 152 - 161

Dussubieux, L; Kusimba, C M; Gogte, V; Kusimba, S B; Gratuze, B; and Oka, R (2008) 'The trading of ancient glass beads: new analytical data from South Asian and East African soda-alumina glass beads', *Archaeometry* 50, pp. 797 - 821

Eastaugh, N; Walsh, V; Chaplin, T; and Siddal, R (2008) *Pigment Compendium*, Routledge

Eccles, H, and Rackham, B (1922) *Analysed specimens of English porcelain*, London, H.M. Stationery Off.

Edwards, D and Hampson, R (2005) *White salt-glazed stoneware of the British Isles*, Woodbridge, Suffolk, Antique Collectors' Club

Edwards, H G M; and Vandenaabeele, P eds. (2012) *Analytical archaeometry: selected topics*, Royal Society of Chemistry Publications, Cambridge

Elliot, G (2006) *Aspects of Ceramic History: A Series of Papers Focusing on the Ceramic Artifact As Evidence of Cultural and Technical Developments*, Gordon Elliot

Elliot, W (1939) 'Reproductions and fakes of English eighteenth-century ceramics', *Transactions of the English Ceramic Circle* 2(7), pp. 67 - 82

Evensen, N M; Hamilton, P J; and O'Nions, R K (1978) 'Rare earth abundances in chondritic meteorites', *Geochimica et Cosmochimica Acta* 42, pp. 1199 - 1212

Fairclough, O (2005) 'Buying ceramics and glass in the 1770s: the case of Sir Watkin Williams Wyn' *Transactions of the English Ceramic Circle* 19(1), pp. 46 - 70

Figueiredo, M O, Silva, T P and Veiga, J P (2012) 'A XANES study of cobalt speciation state in blue-and-white glazes from 16th to 17th century Chinese porcelains', *Journal of Electron Spectroscopy and Related Phenomena*, 185(3-4), pp. 97–102

Fisher, S W (1970) *English pottery and porcelain marks*, Flouham, Slough

Fitzhugh, E W eds. (1997) *Artists' pigments: a handbook of their history and characteristics*, National Gallery of Art, Washington

Fontana, D; Alberghinaa, M F; Barracoa, R; Basile, S; Tranchina, L; Braia, M; Guelid, A; Troja; S O; (2014) 'Historical pigments characterisation by quantitative X-ray fluorescence' *Journal of Cultural Heritage* 15, pp. 266 - 274

Frahm, E (2014) 'Characterizing Obsidian Sources with Portable XRF: Accuracy, Reproducibility, and Field Relationships in a Case Study from Armenia', *Journal of Archaeological Science* 49, pp. 105–125

Frahm, E (2012) 'Non-destructive sourcing of Bronze Age Near Eastern obsidian artefacts: redeveloping and reassessing Electron Microprobe analysis for obsidian sourcing', *Archaeometry*, 54(4), pp. 623–642.

Frahm, E and Doonan, R C P (2013) 'The technological versus methodological revolution of portable XRF in archaeology' *Journal of Archaeological Science* 40, pp. 1425 - 1434

Freestone, I C (2006) 'Glass production in Late Antiquity and the Early Islamic period: a geochemical perspective', in Maggetti and Messiga eds. *Geomaterials in Cultural Heritage*, The Geological Society, London

Freestone, I C (2001) 'The Science of Early British Porcelain', *Archaeological Papers of the American Anthropological Association*, pp. 19–27.

Freestone, I C (1996) 'A'-Marked Porcelain: Some Recent Scientific Work', *Transactions of the English Ceramic Circle*, 16(1), pp. 76–84

Freestone, I C (1993) 'A Technical Study of Limehouse Ware', in Drakard eds. *Limehouse Ware Revealed*, English Ceramic Circle, London

Freestone, I C and Gaimster, D R M eds. (1997) *Pottery in the Making*, British Museum Press, London

Freestone, I C; Joyner, L and Howard, R (2003) 'The Composition of Porcelain from the Isleworth Factory', *Transactions of the English Ceramic Circle* 18 (2), pp. 284–293

Freestone, I C and Middleton, A P (1987) 'Mineralogical applications of the analytical SEM in archaeology', *Mineralogical Magazine* 51, pp. 21 - 31

Freestone, I C; Pointing, M; and Hughes, M J (2002) 'The Origins Of Byzantine Glass From Maroni Petrera, Cyprus', *Archaeometry* 44, pp. 257 - 272

Forster, N and Grave, P (2013) 'Effects of elevated levels of lead in ceramics on provenancing studies using non-destructive PXRf: a case study in Byzantine Cypriot glazed ceramics', *X-ray Spectrometry* 42(6), pp. 480 - 486

Freund, K P (2013) "An assessment of the current applications and future directions of obsidian sourcing studies in archaeological research" *Archaeometry* 55(5), pp. 779–793

Gabszewicz, A (2000) *Made at New Canton Bow porcelain from the collection of the London borough of Newham*, Sealprint Ltd.

Gabszewicz, A and Freeman, G. (1982) *Bow porcelain: the collection formed by Geoffrey Freeman*, Lund Humphries, London

Gagnon, J E; Fryer, B J; Samson, I M; and Williams-Jones, A E (2008) 'Quantitative analysis of silicate certified reference materials by LA-ICPMS with and without an internal standard', *Journal of Analytical Atomic Spectrometry* 23, pp. 1529 - 1537

Gallagher, L J (1953) *China in the sixteenth century : the journals of Matthew Ricci, 1583-1610*, Random House, New York

Gerritsen, A and McDowall, S (2012) 'Material Culture and the Other: European Encounters with Chinese Porcelain, ca. 1650-1800', *Journal of World History*, 23:1

Gianini, R (2015) *Optimisation of the Laser Ablation ICP-MS technique to provenance and authenticate Chinese porcelain*, Cranfield Defence and Security, Cranfield University

Giner Martínez-Sierra, J; Galilea Sans Blas, O; Marchante Gayón, J M and Garcia Alonso, J I (2015) 'Sulfur analysis by inductively coupled plasma mass spectrometry: a review', *Spectrochimica Acta Part B: atomic spectroscopy*, pp. 35 - 52

Godden, G A (2004) *Godden's guide to English blue and white porcelain*, Antique Collectors Club, Woodbridge

Godden, G A (1993) *Godden's guide to European porcelain*, Barrie & Jenkins, London

Godden, G A (1990) *The handbook of British pottery and porcelain marks*, Barrie and Jenkins, London

Godfrey, E S. (1975) *The development of English glassmaking, 1560-1640*, Clarendon Press, Oxford

Godden, G A (1970) *Coalport and Coalbrookdale porcelains*, Jenkins, London

Goodale, N; Bailey, D G; Jones, G T; Prescott, C; Scholz, E; Stagliano, N; and Lewis, C (2012) 'pXRF: a study of inter-instrument performance', *Journal of Archaeological Science* 39(4), pp. 875 - 883

Goodhew, P J; Humphreys, J; and Beanland, R (2001) *Electron microscopy and analysis*, Taylor and Francis, Ltd., London

Grant-Davidson, W J (1966) 'Excavations at Caughley', *Transactions of the English Ceramic Circle* 6(3), pp. 268 - 278

Gratuze, B (1999) 'Obsidian characterization by Laser Ablation ICP-MS and its application to prehistoric trade in the Mediterranean and the Near East: sources and distribution of obsidian within the Aegean and Anatolia' *Journal of Archaeological Science* 26, pp. 869 - 881

Gratuze, B; Blet-Lemarquand, M; and Barrandon, J-N (2001) 'Mass spectrometry with laser sampling: a new tool to characterise archaeological materials' *Journal of Radioanalytical and Nuclear Chemistry* 247(3), pp. 645 - 656

Grosley, P J (1772) *A tour to London, or, new observations on England and its inhabitants, Volume 2*, Lockyer Davis, London

Guarneri, M; Danielis, A; Franucci, M; Ferri De Collibus, M; Fornetti, G and Mencattini, A (2014), '3D remote colorimetry and watershed segmentation techniques for fresco and artwork decay monitoring and preservation', *Journal of Archaeological Science*, 46, pp.182-190

Haggerty, G (2008) *Out of the Blue: 18th century Scottish porcelain*, City of Edinburgh Council, Edinburgh

Hanscombe, S (2010) *Jefferyes Hamett O'Neale : China Painter and Illustrator*, Elmhirst & Suttie Ltd., London

Halicz, L and Gunther, D (2004) 'Quantitative analysis of silicates using LA-ICP-MS with liquid calibration', *Journal of Analytical Atomic Spectrometry* 19, pp. 1539 - 1545

Hall, M E (2001) 'Pottery styles during the early Jomon period: geochemical perspectives on the Moroiso and Ukishima pottery styles' *Archaeometry* 43, pp. 59 - 75

Hall, E T (1960) 'X-ray fluorescent analysis applied to archaeology' *Archaeometry* 3(1), pp. 29 - 35

Harris, D C (2010) *Quantitative Chemical Analysis*, W H Freeman and Company, New York

Harrison-Hall, J (1997) 'Chinese porcelain from Jingdezhen' in Freestone, I C and Gaimster, D R M eds. *Pottery in the Making*, British Museum Press, London

He Li (2004) *Chinese ceramics : the new standard guide*, Thames and Hudson, London

Her Majesty's Stationery Office (1865) *1744: Manufacture of earthenware, Heylyn and Frye's specification*, patent No. 610

Hillis, M. (2011) *Liverpool porcelain 1756-1804*, Maurice Hillis, Great Britain

Hitchins, F and Drew, S (1824) *The History of Cornwall: From the Earliest Records and Traditions, to the Present Time*, Penaluna

Hochleitner, B; Desnica, V; Mantler, M; and Schreiner, M (2002) 'Historical pigments: a collection analysed with X-ray diffraction analysis and X-ray fluorescence analysis in order to create a database' *Spectrochimica Acta, Part B* 58, pp. 641 - 649

Hoffman, E; Charette, J; and Stroobant, V (1996) *Mass Spectrometry: principles and applications*, John Wiley & Sons, Chichester

Honey, W B (1933) *English Pottery and Porcelain*, A. & C. Black, Ltd., London

Horgnies, M; Bayle, M; Gueit, E; Darque-Ceretti, E and Aucouturier, M (2014) 'Microstructure and surface properties of frescoes based on lime and cement: the influence of the artists technique', *Archaeometry* 57(2), pp. 344 - 361

Housley, P P (1991) 'A study of Derbyshire raw materials and their possible relationship to the manufacture of porcelain at Derby', *Transactions of the English Ceramic Circle* 14, pp. 126 - 143

Howard, R (1998) 'Isleworth porcelain: recognition at last?', *Transactions of the English Ceramic Circle* 16(3), pp. 345 - 368

Howard, D S and Wallis, R R (1986) *The China Trade 1600 - 1860*, Royal Pavillion Art Gallery and Museum, Brighton

Hurlbutt, F (1926) *Bow Porcelain*, G. Bell and Sons Ltd., London

Hunt, R W G; and Pointer, M R (2011) *Measuring colour*, John Wiley & Sons, Chichester

Impey, O R; Pollard, A M; Wood, N; and Tregear, M (1983) 'An investigation into the provenance and technical properties of Tianqi porcelain', *Trade Ceramic Studies* 3, pp. 102 - 158

Jackson, S E (2001) 'The application of Nd:YAG lasers in LA-ICP-MS', in Sylvester, J P eds. *Laser Ablation-ICP-MS in the Earth Sciences: Principles and Applications*, pp. 29-45.

Janssens, K H A eds. (2013) *Modern methods for analysing archaeological and historical glass*, John Wiley & Sons, Ltd., Chichester

Janssens, K H A (2013) 'Electron Microscopy', in Janssens, K eds., *Modern methods for analysing archaeological and historical glass*, John Wiley & Sons Inc., Chichester, pp. 129 - 154

- Jay, W H and Orwa, J O (2012) 'Raman spectroscopy applied to early (ca. 1746-1754) English steatitic porcelains: a tentative study of compositions' *Journal of Raman Spectroscopy* 43(2), pp. 307–316
- Jenkins, R; Gould, R W; and Gedcke, D (1995) *Quantitative X-ray Spectrometry*, Practical Spectroscopy Series, Vol. 20, Marcel Dekker, Inc., New York
- Jones, R E (1986) *Greek and Cypriot pottery: a review of scientific studies*, British School at Athens Fitch Laboratory Occasional Paper 1, Athens
- Jörg, C J A (1982) *Porcelain and the Dutch China trade*, Martinus Nijhoff, The Hague
- Kelsall, R W, Hamley, I W and Geoghegan, M (2006) *Nanoscale science and technology*, John Wiley & Sons Ltd.
- Kerr, R and Wood, N (2004) 'Ceramic Technology' *Science and Civilisation in China, Vol. 5 Chemistry and Chemical Technology*, Cambridge University Press, Cambridge
- Kirkland, C L; Smithies, R H; Taylor, R J M; Evans, N; and McDonald, B (2015) 'Zircon Th/U ratios in magmatic environs' *Lithos* 212 - 215; pp. 397 - 414
- Kock, L D (2013) 'Raman analysis of glaze on various archaeological shard samples and intact Ming plates', *Journal of Raman Spectroscopy* 44(1), pp. 97–101.
- Lane, A (1954) *Italian porcelain, with a note on Buen Retiro*, London, Faber and Faber
- Lang, G (1995) *Pottery and porcelain marks*, Miller's, London
- Larkin, P J (2011) *IR and Raman Spectroscopy: principles and spectral interpretation*, Elsevier, Waltham
- Latham, J P M (1979) 'Dorset clay to Staffordshire pot', *Transactions of the English Ceramic Circle* 10(2), pp. 109 - 119
- Leung, P L; Stokes, M J; Tiemei, C; and Dashu, Q (2000): 'A study of ancient Chinese porcelain wares of the Song-Yuan dynasties from Cizhou and Ding kilns with Energy Dispersive X-Ray Fluorescence' *Archaeometry* 42 (1), pp. 129–140

Leung, P L and Luo, H (2000) 'A study of provenance and dating of ancient Chinese porcelain by X-ray fluorescence spectrometry', *X-Ray Spectrometry* 29(1), pp. 34–38.

Lewis, A (1954) 'Use of ultra-violet lamps for identification of porcelain', *Transactions of the English Ceramic Circle* 3(3), pp. 155 - 156

Lister, M (1699) *A Journey to Paris in the Year 1698 by Dr. Martin Lister*, Jacob Tonson, London

Ma, H, Zhu, J, Henderson, J and Li, N (2012) "Provenance of Zhangzhou export blue-and-white and its clay source," *Journal of Archaeological Science*, Elsevier Ltd, 39(5), pp. 1218–1226

MacKenna, F S (1946) *Cookworthy's Plymouth and Bristol porcelain*, F Lewis, Leigh-on-Sea

MacKenna, F S (1947) *Champion's Bristol porcelain*, F Lewis, Leigh-on-Sea

Maggetti, M (1982) 'Phase analysis and its significance for technology and origin', in Olin and Franklin eds., *Archaeological Ceramics*, pp. 121 - 133

Maggetti, M and Messiga, B eds., (2006) *Geomaterials in Cultural Heritage*, The Geological Society, London

Mallet, J V G (1994) 'The 'A' marked porcelains revisited', *Transactions of the English Ceramic Circle* 15(2), pp. 240 - 257

Mallet, J V G (1984) 'Rococo in English ceramics,' In Snodin, M. (ed.), *Rococo: art and design in Hogarth's England : [exhibition] 16 May - 30 Sept. 1984, the Victoria and Albert Museum*, Allanfeld & Schram.

Mallet, J V G (1974) 'Cookworthy's first Bristol factory of 1765,' *Transactions of the English Ceramic Circle*, 9(2), pp. 212–220

Mallet, J V G (1973) 'Studies in the Society's history and archives XCVII: Nicholas Crisp, founding member of the Society of Arts', *Journal of the Royal Society of Arts* Dec. 1972

Malmqvist, KG (1986) 'Comparison between PIXE and XRF for applications in art and archaeology', *Nuclear Instruments and Methods in Physics Research B* 14(1), pp. 86 - 92

Mallory-Greenough, L M; and Greenough, J D (2004) 'Applications of earth science techniques to archaeological problems' *Canadian Journal of Earth Sciences* 41(6), pp. 655 - 657

Mallory-Greenough, L M; Greenough, J D; and Owen J V (1998) 'New data for old pots: trace-element characterization of ancient Egyptian pottery using ICP-MS', *Journal of Archaeological Science* 25, pp. 85 - 97

Manners, Errol (2005) "Some continental influences on English porcelain," *Transactions of the English Ceramic Circle*, 19(3), pp. 429–470.

Mantler, M and Schreiner, M (2000) 'X-ray fluorescence spectrometry in art and archaeology', *X-ray Spectrometry* 29(1), pp. 3 - 17

Markowicz, A (2013) 'Quantification and Correction Procedures' in Potts and West eds. *Portable X-ray Fluorescence Spectrometry: Capabilities for In Situ Analysis*, Royal Society of Chemistry Publishing, Cambridge, pp. 13-38

Marno, F (2008) 'The shells of Bow and Derby', *Transactions of the English Ceramic Circle* 20(2), pp. 361 - 368

Marshall, H R (1954) *Coloured Worcester porcelain of the first period, 1751 - 1783*, Ceramic Books, Newport

Massey, R (2002) 'Nicholas Crisp at Bovey Tracey', *Transactions of the English Ceramic Circle* 18(10), pp. 96 - 115

Massey, R (2001) 'The size and scale of Eighteenth century English porcelain factories', *Transactions of the English Ceramic Circle* 17(3), pp. 442 - 466

Massey, R; Marno, F; and Spero, S (2007) *Ceramics of Vauxhall: 18th century pottery and porcelain*, The English Ceramic Circle, London

Meeks, N; Cartwright, C; and Meek, A eds. (2012) *Historical technology, materials, and conservation: SEM and microanalysis*, Archetype Publications, London

Menzhausen, I (1990) *Early Meissen porcelain in Dresden*, Thames and Hudson, London

Miao, J M, Lu, C L, Li, H E and Chen, T M (2012) 'Non-destructive analysis of 'original' Song dynasty Guan wares and later imitations from the Palace Museum collections, Beijing', *Archaeometry*, 54(6), pp. 955–973

Milazzo, M. (2003) "Radiation applications in art and archaeometry X-ray fluorescence applications to archaeometry. Possibility of obtaining non-destructive quantitative analyses.," *Nuclear Instruments & Methods in Physics Research, Section B: Beam Interactions with Materials and Atoms*, Elsevier Science B.V., 213, pp. 683–692.

Moioli, P., & Seccaroni, C. (2000). 'Analysis of Art Objects Using a Portable X-Ray Fluorescence Spectrometer', *X-Ray Spectrometry* 29, pp. 48-52

Miliani, C, Doherty, B, Daveri, A, Loesch, A, Ulbricht, H, Brunetti, B G, Sgamellotti, A (2009) 'In situ non-invasive investigation on the painting techniques of early Meissen Stoneware', *Spectrochimica Acta, Part A: Molecular and Biomolecular Spectroscopy*, Elsevier B.V., 73A(4), pp. 587–592.

Moretti, C, & Hreglich, S (1984). 'Opacification and colouring of glass by the use of 'anime'' *Glass Technology* 26(6), pp. 277 - 282

Morton Nance, E (1935) "Soap rock licenses" *Transactions of the English Ceramic Circle*, 1(3), pp.73-85

Moseley, H J G (1913) 'The high-frequency spectra of the elements', *Philosophical Magazine* 26 (156), pp. 1024 - 1034

Mountford, A (1969) 'Thomas Briand - a stranger', *Transactions of the English Ceramic Circle* 7(2), pp. 87 - 104

Neelmeijer, C and Roscher, R (2012) 'PIXE–RBS survey of a Meissen porcelain snuff box: first version or not?,' *X-Ray Spectrometry* 41(2), pp. 93–97

Neff, H (2003) 'Synthesising analytical data - spatial results from pottery provenancing investigation' in Brothwell and Pollard eds., *An Introduction to Archaeological Sciences*, pp. 733 - 747

Neff, H (2001) 'Analysis of plumbate pottery sherds by Laser Ablation Inductively Coupled Plasma Mass Spectrometry (LA-ICPMS)', *Journal of Archaeological Science* 30, pp. 21 - 35

Newman, R (1997) 'Chromium oxide greens', in Fitzhugh, E W eds. *Artists' pigments: a handbook of their history and characteristics* 3, pp. 273-294

Olin, J S; and Franklin, J D (1982) *Archaeological ceramics*, Smithsonian Institute Press, Washington D.C.

Olsen, S L (1988) 'Applications of Scanning Electron Microscopy in Archaeology', *Advances in Electronics and Electron Physics* 71, pp. 357 - 380

O'niions, R K; and McKenzie, D (1993) 'Estimates of mantle thorium/uranium ratios from Th U, and Pb isotope abundances in basaltic melts', *Philosophical Transactions of the Royal Society A*, 342(1663), pp. pp. 65 - 77

Oswald, A, Hildyard, R. J. C. and Hughes, R. G. (1982) *English brown stoneware, 1670-1900*, London, Faber and Faber.

Owen, H (1873) *Two Centuries of Ceramic Art in Bristol (Being a History of the Manufacture of "The True Porcelain" by Richard Champion)*, Bell and Daldy, London

Owen, J V (2007) 'A new classification scheme for eighteenth-century American and British soft-paste porcelains', *Ceramics in America*, pp. 121 - 1140

Owen, J V (2003) 'The geochemistry of Worcester porcelain from Dr. Wall to royal Worcester: 150 years of innovation', *Historical Archaeology*, 37(4), pp. 84-96.

Owen, J V (2002) 'Antique porcelain 101: a primer on the chemical analysis and interpretation of eighteenth-century British wares' *Ceramics in America*.

Owen, J V (2001a) 'Geochemical and Mineralogical Distinctions between Bonnin and Morris (Philadelphia, 1770-1772) Porcelain and Some Contemporary British Phosphatic Wares' *Geoarchaeology - An International Journal*, 16(7), pp. 785–802.

Owen, J V (2001b) 'Provenience of eighteenth-century British porcelain sherds from sites 3B and 4E, Fortress of Louisbourg, Nova Scotia: constraints from mineralogy, bulk paste and glaze compositions' *Historical Archaeology*, 35(2), pp. 108–121.

Owen, J V (1998) 'On the earliest products (ca.1751 - 1752) of the Worcester Porcelain Factory: evidence from sherds from the Warmstry House site, England,' *Historical Archaeology*, 32(4), pp. 63–75.

Owen, J V (1997) 'Quantification of early Worcester porcelain recipes and the distinction between Dr Wall- and flight-period wares,' *Journal of Archaeological Science*, 24(4), pp. 301–310.

Owen, J V (1996) 'Compositional constraints on the identification of eighteenth-century porcelain sherds from Fort Beausejour, New Brunswick, and Grassy Island, Nova Scotia', *Transactions of the English Ceramic Circle* 30(4), pp. 88 - 100

Owen, J V; Adams, B and Stephenson, R (2000) 'Nicholas Crisp's 'Porcellien': A Petrological Comparison of Sherds from the Vauxhall (London; ca. 1751-1764) and Indeo Pottery (Bovey Tracey, Devonshire; ca. 1767-1774) Factory Sites,' *Geoarchaeology - An International Journal*, 15(1), pp. 43–78.

Owen, J V and Barkla, R (1997) 'Compositional Characteristics of 18th Century Derby Porcelains: Recipe Changes, Phase Transformations, and Melt Fertility,' *Journal of Archaeological Science*, 24(2), pp. 127–140.

Owen, J V and Day, T E (1998a) '18th century phosphatic porcelain : Bow and Lowestoft. Further confirmation of their compositional distinction,' *Transactions of the English Ceramic Circle*, 16(3), pp. 342–345.

Owen, J V and Day, T E (1998b) 'Assessing and correcting the effects of the chemical weathering of potsherds: a case study using soft-paste porcelain wasters from Longton Hall (Staffordshire) factory site', *Geoarchaeology* 13(3), pp. 265-286

Owen, J V and Day, T E (1994) 'Estimation of the bulk composition of fine-grained media from microchemical and backscatter-image analysis: application to biscuit wares from the Bow factory site, London' *Archaeometry*, 36(2), pp. 217–226.

Owen, J V and Hillis, M (2003) 'From London to Liverpool: Evidence for a Limehouse-Reid porcelain connection based on the analysis of sherds from the Brownlow Hill (ca. 1755-1767) factory site' *Geoarchaeology*, 18(8), pp. 851–882.

Owen, J V and Hunter, R (2009) 'Too little, too late: the geochemistry of a 1773 Philadelphia porcelain openwork basket,' *Journal of Archaeological Science*, 36(2), pp. 333–342.

Owen, J V, Meek, A and Hoffman, W (2011) 'Geochemistry of sauceboats excavated from Independence National Historical Park (Philadelphia): Evidence for a Bonnin and Morris (c. 1770-73) provenance and implications for the development of nascent American porcelain wares' *Journal of Archaeological Science*, 38(9), pp. 2340–2351.

Owen, J V and Morrison, M L (1999) 'Sagged Phosphatic Nantgarw Porcelain (ca. 1813-1820): Casualty of Overfiring or a Fertile Paste?' *Geoarchaeology* 14(4), pp. 313–332

Owen, J V and Sandon, J (2003) 'A rose by any other name: a geochemical comparison of Caughley (c. 1772-99), Coalport (John Rose & Co.; c. 1799-1837), and rival porcelains based on sherds from the factory sites' *Post Medieval Archaeology* 37(1), pp. 79 - 89

Owen, J V and Sandon, J (1998) 'Petrology of Gilbody, Pennington and Christian/Pennington (18th century Liverpool) porcelains and their distinction from some contemporary phosphatic and magnesian/plombian British wares' *Journal of Archaeological Science*, 25(4), pp. 359 - 375

Owen, J V, Wilstead, J O, Williams, R W and Day, T E (1998) 'A tale of two cities: Compositional characteristics of some Nantgarw and Swansea porcelains and their implications for kiln wastage' *Journal of Archaeological Science*, 25(4), pp. 359–375

Papageorgiou, I; Baxter, M J; and Cau, M A (2001) 'Model-based cluster analysis of artefact compositional data' *Archaeometry* 43(4), pp. 571 - 588

Pauls-Eisenbeiss, E (1972) *German porcelain of the 18th century*, Barrie and Jenkins, London

Pearce, J (2008) 'English porcelain of the 18th century in archaeologically excavated assemblages from London' *Transactions of the English Ceramic Circle* 20(2), pp. 273 - 314

Perrott, E G (1997) *Pottery and porcelain marks: European, oriental, and U.S.A, in chronological order*, Gemini, Bath

Pessanha, S; Guilherme, A; and Carvalho, M L (2009) 'Comparison of matrix effects on portable and stationary XRF spectrometers for cultural heritage samples' *Applied Physics A* 97, pp.497–505

Phil Trans R. Soc. (1665) 'An Intimation of a Way, Found in Europe to Make China-Dishes' accessed online at <http://rstl.royalsocietypublishing.org> , 06/07/14 12:24

Phillips, S C and Speakman, R J (2009) 'Initial source evaluation of archaeological obsidian from the Kuril Islands of the Russian Far East using portable XRF', *Journal of Archaeological Science* 36(6), pp. 1256 - 1263

Pietsch, U and Banz, C (2010) *Triumph of the blue swords: Meissen porcelain for aristocracy and bourgeoisie 1710–1815*, Staatliche Kunstsammlungen Dresden, Dresden

Pietsch, U (2010) 'Meissen porcelain: making a brilliant entrance', in Pietsch and Banz eds., *Triumph of the blue swords: Meissen porcelain for aristocracy and bourgeoisie 1710 - 1815*, Staatliche Kunstsammerlungen Dresden

Poche, E (1975) *Porcelain marks of the world*, Hamlyn, London

Polvorinos Del Rio, A and Castaing, J (2010) 'Lustre-decorated Ceramics from a 15th to 16th century production in Seville', *Archaeometry*, 52(1), pp.83-98

Porter, G R (1832) *A treatise on the progressive improvement and present state of the manufacture of porcelain*, Longman & Co., London

Potts P J and West, M (2008) *Portable X-ray Fluorescence Spectrometry: capabilities for in-situ analysis*, Royal Society of Chemistry Publishing, Cambridge

Rackham, B (1937) 'Some unusual Worcester pieces', *Transactions of the English Ceramic Circle* 1(5), pp. 50–55

Ramsay, W R H and Ramsay, E G (2008) "A case for the production of the earliest commercial hard-paste porcelains in the English-speaking world by Edward Heylyn and Thomas Frye in about 1743," *Proceedings of the Royal Society of Victoria* 120(1), pp. 236–256.

Ramsay, W R H and Ramsay, E G (2007) "A classification of Bow porcelain from first patent to closure: c.1743–1774," *Proceedings of the Royal Society of Victoria* 119(1), pp. 1–68.

Ramsay, W R H, Ramsay, E G and Girvan, L (2011) "Lund's Bristol Porcelain:and both are called fine ornamental white china.," Bow Porcelain, [online] accessed online at [http://www.bowporcelain.net/Lunds Bristol Porcelain - and both are called fine ornamental white china.pdf](http://www.bowporcelain.net/Lunds%20Bristol%20Porcelain%20-%20and%20both%20are%20called%20fine%20ornamental%20white%20china.pdf) , 19/02/13 09:42

Ramsay, W R H, Daniels, P and Ramsay, E G (2013) *The Limehouse porcelain factory: its output, antecedents and the influence of the Royal Society of London on the evolution of English porcelain based on composition and technology*, Invercargill, Craigs Design and Print.

Ramsay, W R H, Ramsay, E G, and Gabsewicz, A (2003) "The chemistry of 'A'-marked porcelains and its relation to the Heylyn and Frye patent of 1744," *Transactions of the English Ceramic Circle* 18(2), p. 264.

Ramsay, W R H; Sutton, K; and Ramsay, E G (2011) 'Bow porcelain: glaze compositions associated with the phosphatic wares ~1742-1774', *Proceedings of the Royal Society of Victoria* 123(2), pp. 161 - 171

Ricciardi, P, Colombari, P, Fabbri, B and Milandè, V. (2009) "Towards the establishment of a Raman database of early European porcelain.," *e-Preservation Science*, 6, pp. 22–26

Rollinson, H R (1993) *Using Geochemical Data: evaluation, presentation, interpretation*, Longman Scientific and Technical, Harlow

Rousseau, (2002) 'Debate on some algorithms relating concentration to intensity in XRF spectrometry' *The Rigaku Journal* 19(1), pp. 25 - 34

Rousseau, R M and Boivin, J A (1998) 'The fundamental algorithm: a natural extension of the Sherman equation Part 1: theory', *The Rigaku Journal* 15(1), pp. 13 - 28

Rousseau, R M; Willis, J P; and Duncan, A R (1996) 'Practical XRF calibration procedures for major and trace elements', *X-ray Spectrometry* 25(4), pp. 179 - 189

Russo, R E; Mao, X; Liu, H; Gonzales, J; and Mao, S S (2002) 'Laser ablation in analytical chemistry - a review', *Talanta* 57, pp. 425 - 451

Sandon, H (1980) *The illustrated guide to Worcester porcelain, 1751 - 1793*, H Jenkins, London

Sandon, J (2009) *Worcester porcelain*, Shire, Oxford

Sandon, J. (1997) *Antique porcelain*, Antique Collectors' Club, Woodbridge

Sandon, J (1993) *The dictionary of Worcester porcelain*, Antique Collectors' Club, Woodbridge

Sawczak, M; Kamińska, A; Rabczuk, G; Ferretti, M; Jendrzewski, R; and Śliwiński, G (2009) 'Complementary use of the Raman and XRF techniques for non-destructive analysis of historical paint layers', *Applied Surface Science* 255(10), pp. 5542 - 5545

Scott, R B; Eekelers, K and Degryse, P (2016) 'Quantitative Chemical Analysis of Archaeological Slag Material Using Handheld X-Ray Fluorescence Spectrometry', *Applied Spectroscopy* 70(1), pp. 94-109

Shackley, S M (2010) "Is there reliability and validity in portable X-Ray Fluorescence (XRF) Spectrometry (PXRF)?" *The SAA Archaeological Record*, 10(5), pp. 17–20.

Shackley, M S eds, (2010) *X-ray Fluorescence Spectrometry (XRF) in Geoarchaeology*, Springer-Verlag, New York

Shackley, M S eds. (1998) *Archaeological obsidian studies: method and theory*, Plenum Press, New York

Shugar, A and Mass, J eds. (2013) *Handheld XRF for Art and Archaeology*, Leuven University Press, Leuven

Shortland, A; Rogers, N; and Eremin, K (2007) 'Trace Element discriminants between Egyptian and Mesopotamian Late Bronze Age glasses' *Journal of Archaeological Science* 34, pp. 781 - 789

Smirniou, M and Rehren, T (2013) 'Shades of blue e cobalt-copper coloured blue glass from New Kingdom Egypt and the Mycenaean world: a matter of production or colourant source?', *Journal of Archaeological Science* 40, pp. 4731 - 4743

Smith, D (2013) 'Handheld X-ray fluorescence analysis of Renaissance bronzes: practical approaches to quantification and acquisition' in Shugar and Mass eds. pp.37 - 74

Snodin, M (1984) *Rococo: art and design in Hogarth's England: [exhibition] 16 May-30 Sept. 1984, the Victoria and Albert Museum, Totowa, Allanfeld & Schram.*

Spataro, M; Meeks, N; Bimson, M; Dawson, A; and Ambers, J (2009) 'Early porcelain in 17th century England: non-destructive examination of two jars from Burghley House' *The British Museum Technical Research Bulletin* 3, pp. 37 - 46

Speakman, R J and Neff, H (2005) *Laser Ablation ICP-MS in Archaeological Research*, University of New Mexico Press, Albuquerque

Speakman, R J and Shackley, M S (2013) 'Silo science and portable XRF in archaeology: a response to Frahm' *Journal of Archaeological Science* 40, pp. 1435 - 1443

Spero, S (2006) *Lund's Bristol and early Worcester porcelain, 1750-58 : the A.J. Smith Collection*, London, C and J Smith.

Spero, S (2005) 'What we do not know about 18th century English porcelain' , *Transactions of the English Ceramic Circle* 19(2), pp. 316 - 342

Spero, S (1986) 'Reattributing some 'Worcester' porcelain at the Ashmolean Museum', *Ceramics: the international journal of ceramics and glass* 2, pp. 83 - 91

Stevenson, T (1990) 'A review of Chelsea, Chelsea-Derby, and Derby knife and fork hafts', *Transactions of the English Ceramic Circle* 14(1), pp. 50 - 58

Stoneham, D and Stoneham, M (2010) "Beating the forger: authenticating ceramic antiques," *Contemporary Physics* 51(5), pp. 397–411

Stretton, N (1970) 'The Indio Pottery at Bovey Tracey', *Transactions of the English Ceramic Circle* 8(2), pp. 124 - 144

Sylvester, J P eds. (2001) *Laser Ablation-ICP-MS in the Earth Sciences: Principles and Applications*, Mineralogical Association of Canada, University of Michigan

Tait, H (1963) 'The Bow Factory under Alderman Arnold and Thomas Frye 1747-1759', *Transactions of the English Ceramic Circle* 5(4), pp. 195 - 216

Tate, J (1986) 'Some problems in analysing museum material by non-destructive surface sensitive techniques' *Nuclear Instruments and Methods in Physics Research B* 14(1), pp. 20 - 23

Thompson, A; Attwood, D; Gullikson, E; Howells, M; Kim, K J; Kirz, J; Kortright, J; Lindau, I; Liu, Y; Pianetta, P; Robinson, A; Scofield, J; Underwood, J; Williams, G and

Winich, H (2009) *Centre for X-ray Optics and Advanced Light Source X-ray data booklet*, Lawrence Berkeley National Laboratory, University of California, Berkeley

Tichane, R (1983) *Ching-te-chen: views of a porcelain city*, Painted Post, New York

Tite, M S, Freestone, I and Wood, N (2012) "an Investigation Into the Relationship Between the Raw Materials Used in the Production of Chinese Porcelain and Stoneware Bodies and the Resulting Microstructures," *Archaeometry* 54(1), pp. 1–19

Tite, M S and Bimson, M (1991) "A technological study of English porcelains," *Archaeometry* 1749, pp. 3–27

Toppin, A J (1954) 'The proprietors of the Early Bristol China Factory: Identified as William Miller and Benjamin Lund', *Transactions of the English Ceramic Circle* 4(1), pp. 129 - 140

Trentelman, K; Bouchard, M; Ganio, M; Namowicz, C; Schmidt Patterson, C; and Walton, M (2010) 'The examination of works of art using *in situ* XRF line and area scans' *X-ray Spectrometry* 39, pp. 159 - 166

Turco, F; Davit, P; Maritano, C; Operti, L; Fenoglio, G; and Agostino, A (2015) 'XRF characterisation of 18th century Piedmontese porcelains from the Palazzo Madama Museum (Torino, Italy)' *Archaeometry* (forthcoming)

Turcotte, D L; Paul D; and White, W M (2001) 'Thorium-uranium systematics require layered mantle convection', *Journal of Geophysical Research* 106(B3), pp. 4265 - 4276

Turnbull, J (1997) 'Scottish cobalt and Nicholas Crisp', *Transactions of the English Ceramic Circle* 16(2), pp. 144 - 151

Tykot, R H (1996) 'Obsidian procurement and distribution in the Central and Western Mediterranean', *Journal of Mediterranean Archaeology* 9, pp. 39 - 82

Tykot, R H and Young, S M M (1996) 'Archaeological applications of inductively coupled plasma mass spectrometry' in Orna, M V eds., *Archaeological Chemistry*, ACS Symposium series 625, pp. 116 - 130

Uda, M; Demortier, G; and Nakai, I eds. (2005) *X-rays for Archaeology*, Springer, Netherlands

Uda, M (2005) 'Characterisation of pigments used in ancient Egypt' in Uda et al eds. *X-rays for Archaeology*, Springer, pp. 3 - 26

Valpy, N (1984) "Extracts from 18th century London newspapers," *Transactions of the English Ceramic Circle* 12(1), pp. 58–89.

Van Elteren, J; Tennent, N; and Šelih, V (2009) 'Multi-element quantification of ancient / historic glasses by laser ablation inductively coupled plasma mass spectrometry using sum normalization calibration', *Analytica Chimica Acta* 644, pp. 1–9

Wagner, B and Jedral, W (2011) 'Open ablation cell for LA-ICP-MS investigations of historic objects', *Journal of Analytical Atomic Spectrometry* 26, pp. 2058-2063

Walters, A and Lusty, P (2011) 'Rare earth elements', British Geological Survey commodity profile, available at www.mineralsuk.com accessed 29/10/2015

Watney, B M (1997) *Liverpool Porcelain of the Eighteenth Century*, Richard Dennie, Somerset

Watney, B M (1995) 'Bone ash and soapstone porcelains from the Chaffers production line', *Transactions of the English Ceramic Circle* 16(1), pp. 85 - 108

Watney, B M (1973) *English Blue and White Porcelain of the 18th Century*, Faber and Faber, London

Watney, B M (1964) 'The porcelain of Chaffers, Christian and Pennington', *Transactions of the English Ceramic Circle* 5(5), pp. 269 - 296

Watney, B M (1959) 'Four groups of porcelain, possibly Liverpool', *Transactions of the English Ceramic Circle* 4(5), pp. 13 - 25

Watney, B M, Middleton, A P and Cowell, M R (1993) "Excavations at the Longton Hall porcelain factory. Part III: the porcelain and other ceramic finds," *Post-Medieval Archaeology* 27, pp. 57–109

Watts, A (2003) 'Developments in glaze composition and application in Staffordshire during the 18th century', *Transactions of the English Ceramic Circle* 18(2), pp. 248 - 252

Weber, J (2010) ' "...that other nations must be amazed by it..." Saxon porcelain in European diplomacy', in Pietsch and Banz eds., *Triumph of the blue swords: Meissen porcelain for aristocracy and bourgeoisie 1710 - 1815*, Staatliche Kunstsammlungen Dresden, pp. 152 - 160

Wen, R; Wang, C S; Mao, Z W; Huang, Y Y; and Pollard, A M (2007) "The chemical composition of blue pigment on Chinese blue-and-white porcelain of the Yuan and Ming dynasties (ad 1271-1644).," *Archaeometry* 49(1), pp. 101–115.

White, M (2007) 'A Bovey Tracey fuddling cup', *Transactions of the English Ceramic Circle* 19(3), pp. 501 - 507

White, W M (2013) *Geochemistry*, Wiley-Blackwell, Chichester

Williams, I J (1931) *A Guide to the Collection of Welsh Porcelain (Nantgarw and Swansea)*, National Museum of Wales, Cardiff

Williams-Thorpe, O (1995) "Obsidian in the Mediterranean and the Near East: a provenancing success story" *Archaeometry* 37(2), pp. 217-248

Wood, N (1999) *Chinese glazes: their origins, chemistry, and recreation*, A & C Black, London

Wu, J; Leung, P L; Li, J Z; Stokes, M J; and Li, M T W (2000) 'EDXRF studies on blue and white Chinese porcelain samples from the Yuan, Ming, and Qing dynasties' *X-ray Spectrometry* 29, pp. 239 - 244

Wysecki, G; and Stiles, W S (1982) *Color Science*, John Wiley & Sons, Inc., New York

Xie, G; Feng, S; Feng, X; Li, Y; Han, H; Wang, Y; Zhu, J; Yan, L; Li, L (2009) "Study on the elemental features of ancient Chinese white porcelain at Jingdezhen by INAA," *Nuclear Instruments and Methods in Physics Research Section B: Beam Interactions with Materials and Atoms* 267(5), pp. 821–824

Xie, G; Feng, S; Feng, X; Wang, Y; Zhu, J; Yan, L; Li, Y; Han, H (2007) "Study on ancient Chinese imitated GE ware by INAA and WDXRF," *Nuclear Instruments and Methods in Physics Research, Section B: Beam Interactions with Materials and Atoms* 264(1), pp. 103–108

Yang, Y; Feng, M; Ling, X; Zhenwei, M; Wang, C; Sun, X; and Guo, M (2005) 'Microstructural analysis of the color-generating mechanism in Ru ware, modern copies, and its differentiation with Jun ware', *Journal of Archaeological Science* 32(2), pp. 301 - 310

Yin, M, Rehren, T and Zheng, J (2011) "The earliest high-fired glazed ceramics in China: the composition of the proto-porcelain from Zhejiang during the Shang and Zhou periods (c. 1700–221 BC)," *Journal of Archaeological Science* 38(9), pp. 2352–2365

Young, H (1999a) "Evidence for wood and coal firing and the design of kilns in the 18th C porcelain industry," *Transactions of the English Ceramic Circle*, 17(1), p. 1.

Young, H. (1999b) *English porcelain, 1745-95: its makers, design, marketing and consumption*, London, V&A Publications.

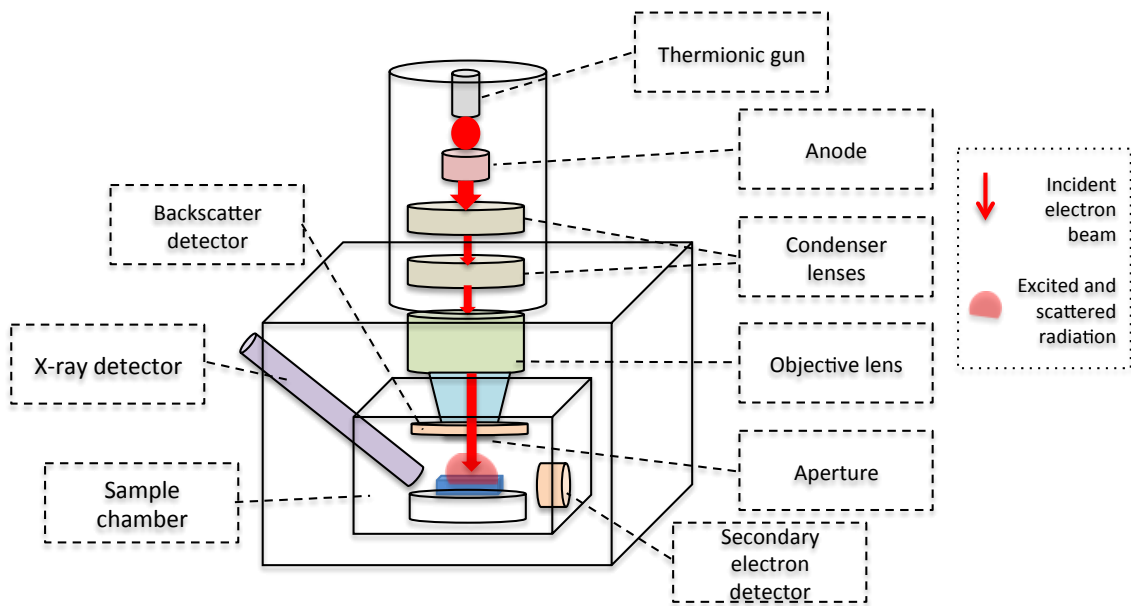
Yu, K N and Miao, J M (1998) "Multivariate analysis of the energy dispersive X-ray fluorescence results from blue and white Chinese porcelains.," *Archaeometry* 40(2), pp. 331–339.

Yu, K N and Miao, J M (1996) "Non-destructive analysis of Jingdezhen blue and white porcelains of the Ming Dynasty using EDXRF" *X-Ray Spectrometry* 25(6), pp. 281–285.

APPENDICES

A.1 Scanning Electron Microscopy theory and instrumentation

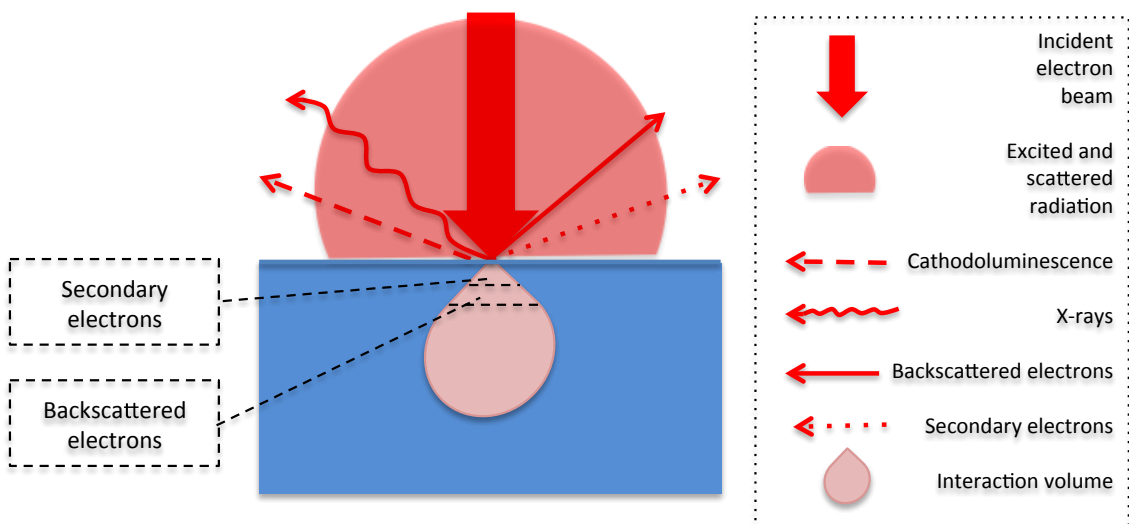
A Scanning Electron Microscope operates using principles similar to optical microscopy, that is, the use of a focused beam of energy to form an enlarged image of a surface. An important difference is that a directed beam of electrons is subject to much greater scattering by gas molecules than a beam of photons, and therefore analysis must be carried out in a vacuum of $>10^{-10}$ Pa (Goodhew et al, 2001; pp. 16 - 17). Electrons are generated using a thermionic gun, the voltage of which is controlled by reducing or increasing the area at the tip of the filament (Goodhew et al, 2001; pp. 24 - 25). The current is also controlled to a high degree of precision, and this combination of settings allows clear images to be produced of a wide range of sample materials. The beam of electrons is further directed and focused towards the surface of the sample by a series of electromagnetic lenses, see Appendix Figure 1 (Goodhew et al, 2001; pp. 27 - 28).



Appendix Figure 1 - diagram of a Scanning Electron Microscope, illustrating the path of the incident electron beam from the thermionic gun to the sample surface

Upon reaching the sample surface, the incident electrons react with the atoms that comprise the sample in two ways:

1. Elastic scattering: the incident electron is deflected by the surface atoms, changing direction but without any significant change in energy (Goodhew et al, 2001; p. 30)
2. Inelastic scattering: any interaction which causes the incident electron to lose a detectable amount of energy. Most of this energy is converted to heat in the sample surface, but a small proportion of the incident electron energy can produce X-rays, fluorescent energy, or secondary electron emission at the surface of the sample, see Appendix Figure 2 (Goodhew et al, 2001; pp. 31 - 32).



Appendix Figure 2 - illustration of the types of interaction that occur when a beam of electrons impact a sample surface under vacuum conditions

As in X-ray fluorescence analysis, the surface atoms are excited by the incident energy, and cathodoluminescence and characteristic X-rays are also given off in the same way, see Appendix A.3. However, the characteristic types of interactions, for the purpose of Scanning Electron Microscopy, are elastic scattering, whereby the backscattered electrons are detected, and the inelastic scattering interactions that produce secondary electrons.

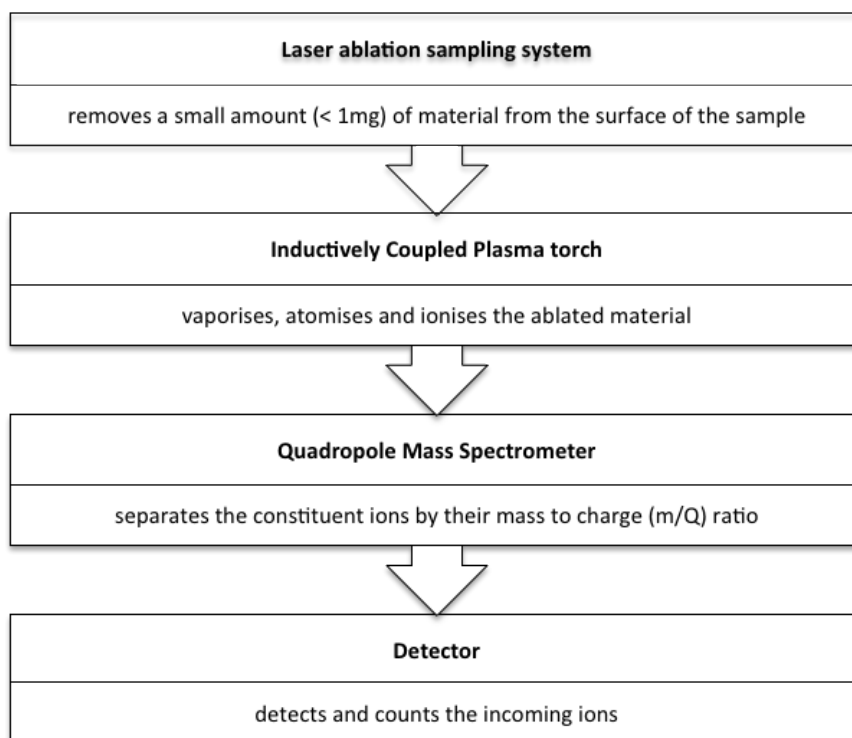
Secondary electrons provide topographical information about the surface of the sample, because the yield of electrons is greatest when the emitting surface is perpendicular to the detector (Goodhew et al, 2001; pp. 145 - 146). Backscattered electrons are used to determine the topography of the sample in terms of the relative Z-number of the elements that comprise its surface; the intensity of the backscattered electron is greatest for very high-Z elements, and these appear brighter in colour on backscattered electron view, while lower-Z elements appear progressively darker (Goodhew et al, 2001; pp. 146 - 148). This phenomenon is also referred to as phase-contrast view, because it allows the analyst to identify the compositional phases in the sample surface, such as mineral phases, in the case of a ceramic paste (Janssens, 2013; p. 130).

In the field of archaeological science, spectroscopic microprobes are frequently used alongside SEM, in order to obtain quantitative elemental compositional data from the sample under analysis. The two most popular are Energy-Dispersive Spectroscopy (EDS) and Wavelength-Dispersive Spectroscopy (WDS); both of these rely on the characteristic X-ray energy that is emitted by the sample surface, following excitation, in the same way as Energy-Dispersive, and Wavelength-Dispersive, XRF Spectroscopy. One important difference is that the vacuum conditions inside the sample chamber allow the detection and quantification of low-Z elements, up to sodium (Na, 11). EDS comprises a silicon (Si, 14) or germanium (Ge, 32) detector, which collects the incoming X-ray energy across a range of voltages simultaneously (Goodhew et al, 2001; pp. 176 - 177). WDS employs a crystal spectrometer, which diffracts the X-ray energy, functioning as a filter between the sample surface and the detector, in order to collect X-rays of a certain wavelength at any one time (Goodhew et al, 2001; pp. 181 - 182). This results in increased peak resolution and detection of light elements, but takes more time, and the WDS instruments are generally more expensive. In both methods, the data are plotted on a spectrum, with the X-ray energy in keV along the x-axis, and the number of counts detected along the y-axis. The peaks thus produced are characteristic of the elements present, and their quantities within the analysed area.

A.2 Laser Ablation Inductively Coupled Plasma Mass Spectroscopy (LA-ICPMS) theory and instrumentation

Mass spectroscopy is a separation technique of analysis, meaning that it works by separating the sample material according to its mass/charge ratio (m/Q), which is characteristic of the elements present and their relative intensity. When used in tandem with a laser ablation sampling system and inductively-coupled plasma torch for ionisation, see Appendix Figure 3, the technique can be used with very little sample preparation on solid materials to produce quantitative elemental compositional data with very high accuracy and precision. In addition, the ablated area is sufficiently small that the technique may be seen as almost non-destructive.

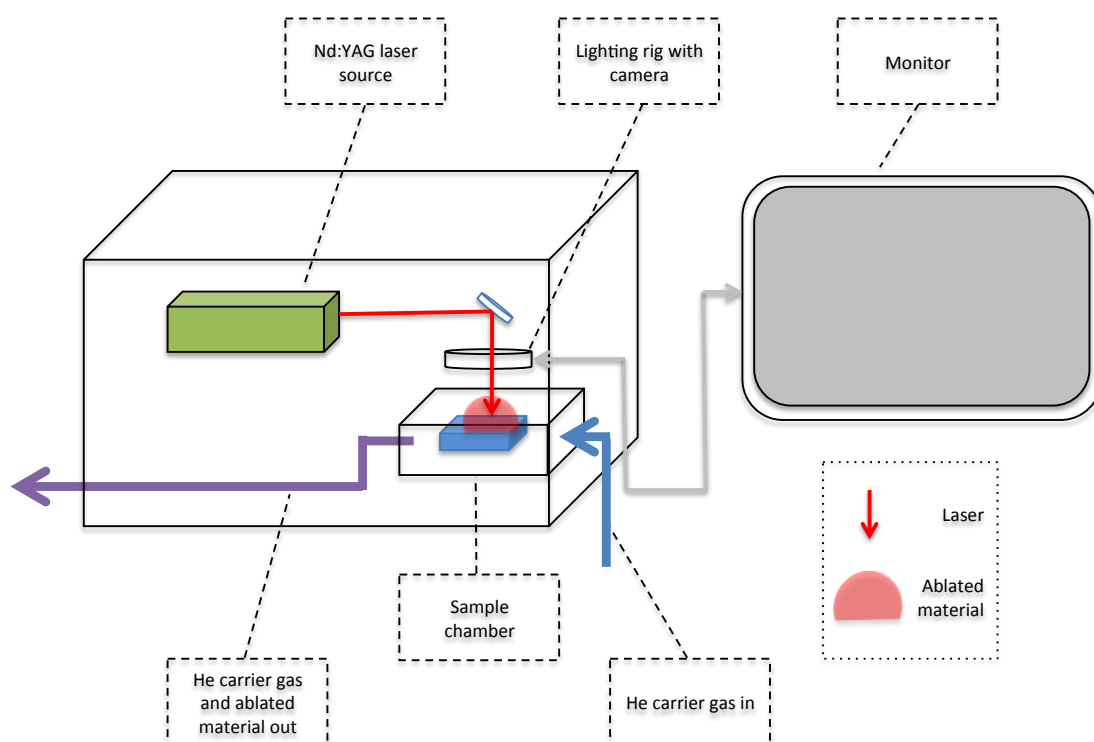
In this section of the appendix, it will be explained the theory of each part of the LA-ICPMS technique, and the instrumentation of the specific systems used in this thesis will be described.



Appendix Figure 3 - diagram of the sections of the Laser Ablation Inductively Coupled Plasma Mass Spectroscopy technique

A.2.1 Laser Ablation sampling system

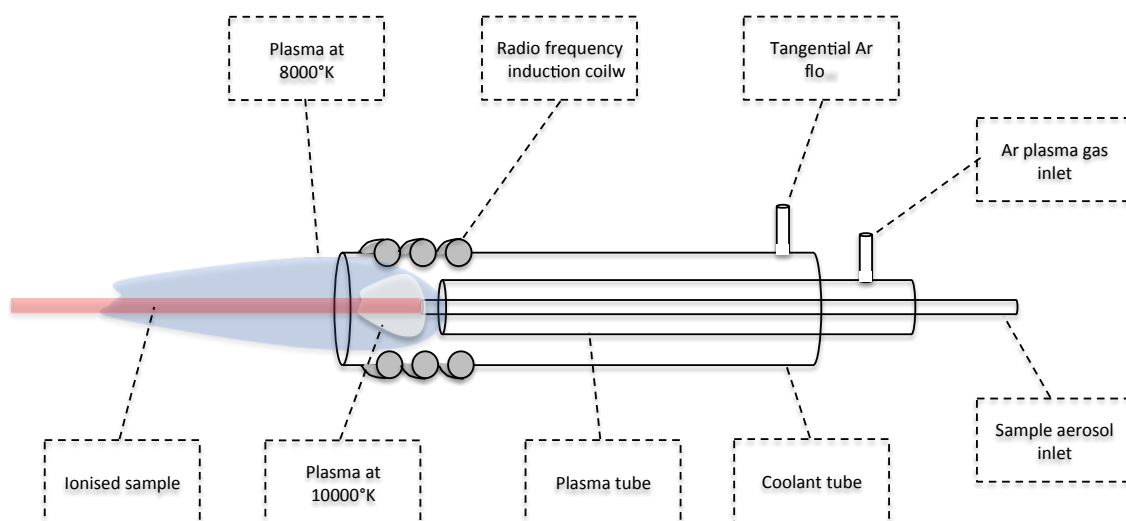
This sampling system comprises a chamber into which the sample is placed; when sealed, this chamber is airtight, allowing the carrier gas to be introduced at a variable pressure. A lighting rig with a camera allows the laser spot to be focused and directed at the surface of the sample, and through the software, allows the user to select spots for analysis. A neodymium-doped yttrium aluminium garnet (Nd:YAG) crystal is used as the lasing medium, through which a pulsed laser beam is directed towards the sample surface. On the surface, a small quantity of sample material - the volume varies, depending on the sample matrix and constituent elements - is irradiated and thereby heated, resulting in evaporation or sublimation. The evaporated material is then carried by the gas that flows through the sample chamber towards the ionisation system.



A.2.2 Inductively Coupled Plasma ionisation system

This system begins with the sample in an aerosol, i.e. fine particles of sample in a gas, or a vapour, i.e. fine particles of sample in a liquid, in order to allow as much sample as possible to come into contact with the plasma.

The plasma torch may be seen as the final stage of transformation for the sample before it enters the mass spectrometer; the plasma breaks down any remaining structures of sample matrix and most molecules, and it excites the sample atoms to produce ions. The plasma torch comprises a high-powered radio-frequency generator, connected to a supply of electricity, with a quartz crystal interface to the plasma gas, see Appendix Figure 4.



Appendix Figure 4 - diagram of a plasma torch, showing the main gas inlet tubes. The flow of gas and sample aerosol is from right to left.

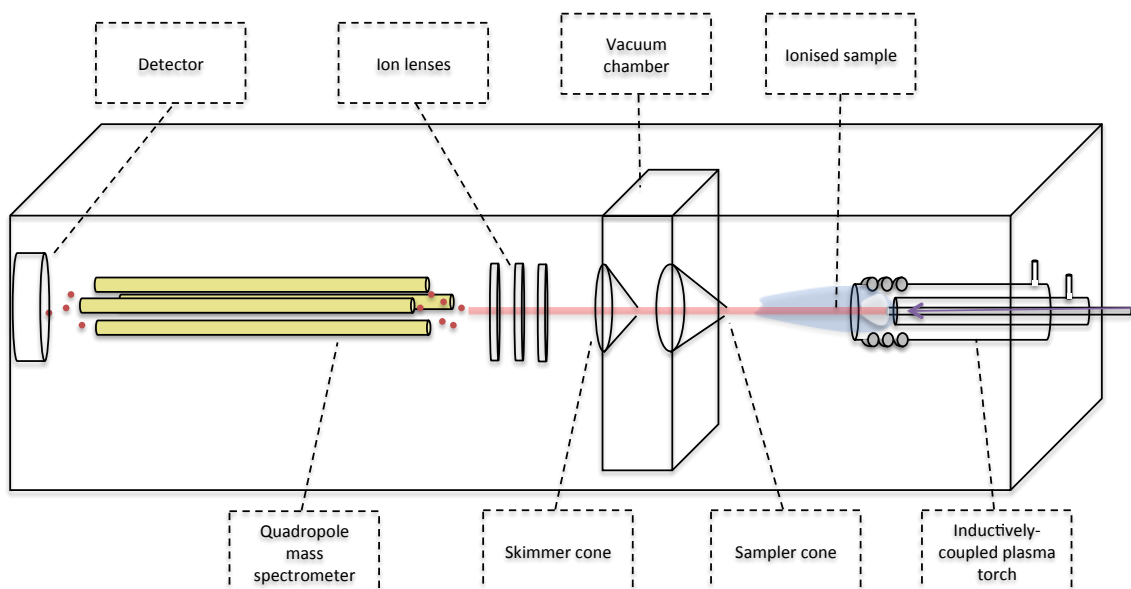
The application of the electromagnetic current to the gas produces a plasma, which is a dense, high-temperature, electrically-neutral medium of positively charged gas atoms and free electrons, formed at the mouth of the torch. The plasma transfers electrical energy to the sample aerosol, causing it to break down and ionise.

Argon is commonly chosen as the plasma gas, because it is monoatomic and inert, meaning that it will not form compounds with the sample atoms (Hoffman et al, 1996; pp. 21 - 22). A further flow of Ar, introduced tangentially to the plasma gas flow, causes the base of the plasma to form a vortex, into which the sample carrier gas can be introduced by a third gas flow. Having left the ICP torch, the ions are fed through a water-cooled sampling cone, which has a small orifice to focus the stream of particles as they are pumped through by a rotary pump.

From the ICP torch to the mass analyser chamber, each stage of the ion sampling interface is at a lower atmospheric pressure, to force the ion beam to move through, see Appendix Figure 5. A second cone, called the skimmer cone, streamlines the beam and further reduces the amount of material that will be introduced to the mass analyser. The ion beam is focused once more using a series of electric fields, called ion focusing lenses, which cause the ion beam to accelerate.

A.2.3 Quadrupole Mass Spectrometer

A mass spectrometer (MS) is the name given to an analytical instrument that separates a sample, in order to characterise it by the mass to charge ratio (m/Q) and relative abundance of the constituent ions. A quadrupole analyser achieves this separation by varying the stability of the ions' trajectories through the instrument, so that ions of different m/Q arrive at the detector at different points in time. The device consists of four rods, onto which the ion focusing lenses interface, so that the sample ions are accelerated along the z axis, and enter the space between the quadrupole rods, see Appendix Figure 5.



Appendix Figure 5 - diagram of an inductively coupled plasma quadrupole ion source, which interfaces through a series of ion lenses with a quadrupole mass spectrometer. In this image, the direction of travel for the sample (represented by a red line) is from right to left.

The poles carry an electric field, the radiofrequency of which is manipulated during the time during when the sample ions are passing through, causing the sample ions to alter their flight along the x and y axes. The selection of analytical parameters, while setting up an experiment involving QMS analysis of a sample, must aim to create sufficient separation that the constituent ions may be resolved, without losing too much of the sample through collisions by ions on unstable flights. In the analyses carried out as part of this research, a large number of elements were expected to be found, including large atomic-number elements, which produce many ions of slightly different m/Q when separated. The scan acquisition mode was therefore felt to be the most appropriate, since this varies the quadrupole potential progressively through the analysis time, while the detector scans through the complete spectra between two limit masses.

If the resolution of the detector peaks is sufficient, the elemental composition of the sample can be obtained for most elements (Li - U, with the exception of O), to low limits of detection (<10ppm in most cases) (Hoffman et al, 1996; p. 32).

A.2.4 Sources of interference in LA-ICPMS analysis of ceramic and vitreous materials

The objective of data calibration is to transform raw counts data from LA-ICPMS spectra (m/Q vs relative intensity) into elemental compositional data (typically in parts per million) that accurately represent the composition of the sample material. In this section, the obstacles to calibration and the mitigating actions are addressed, then the possible calibration strategies are surveyed, and the process that was selected for this research is described. The challenge that calibration aims to overcome is that the counts received by the detector are not accurately representative of the sample composition, due to a number of interfering processes (Denoyer et al, 1991). These interferences are summarised in Appendix Table 1, and can be separated broadly into two categories, based on the effect that they have on the data.

Appendix Table 1 - sources of interference encountered in LA-ICPMS analysis of glass and porcelain samples, and the mitigating actions taken in this research to avoid these effects.

Source of interference	Effect on data	Mitigation
spectroscopic: isobaric interference	conflation of two or more overlapping isotopes, increase of one isotope to the detriment of the other	prediction and correction, calibration with certified reference materials
spectroscopic: polyatomic interference	presence of polyatomic ions, which interfere with analyte ions with the same mass to charge ratio	varying plasma radio-frequency (<i>rf</i>) power during analysis, correction using subtraction from a blank, calibration with certified reference materials
non-spectroscopic: variation in matrix density within and between samples	lower-density matrix permits a greater ablated area, and therefore more ablated material; higher-density matrix results in less ablated material	calibration with matrix-matched standards, selection of multiple spots for analysis
non-spectroscopic: sample fractionation	variable response of plasma to volatile analytes, resulting in an increased signal relative to stable analytes	variation of analytical conditions (e.g. nebuliser gas flow, radiofrequency power of plasma), selection of stable ionic species for analysis
non-spectroscopic: contamination	elements not present in sample, or present at lower concentrations, are included in spectra	correction using subtraction from a blank

Spectroscopic interferences are those caused by the presence of atomic and molecular ions that have the same mass as an analyte, thereby creating a misleading number of counts for that m/Q region of the spectrum. The spectroscopic interferences that might be expected to occur in the current research are shown in Appendix Table 2.

Appendix Table 2 - spectroscopic interferences from isobaric polyatomic ions that may be formed during LA-ICPMS analysis of glass or ceramic materials (Russo et al, 2002)

Analyte	Isobaric Interferences	Analyte	Isobaric Interferences
⁵¹ V	²⁵ Mg ²⁶ Mg ⁺ , ¹¹ B ⁴⁰ Ar ⁺	¹¹⁸ Sn	⁵⁹ Co ⁵⁹ Co ⁺
⁶³ Cu	⁴⁷ Ti ¹⁶ O ⁺	¹³⁷ Ba	¹²¹ Sb ¹⁶ O ⁺
⁶⁶ Zn	⁵⁰ Ti ¹⁶ O ⁺ , ²⁶ Mg ⁴⁰ Ar ⁺	¹³⁹ La	¹²³ Sb ¹⁶ O ⁺
⁷⁵ As	⁵⁹ Co ¹⁶ O ⁺	¹⁴⁰ Ce	¹²⁴ Sn ¹⁶ O ⁺
⁶⁹ Ga	¹³⁸ Ba ⁺	¹⁵³ Eu	¹³⁷ Ba ¹⁶ O ⁺
⁸⁸ Sr	⁴⁸ Ti ⁴⁰ Ar ⁺	¹⁵⁷ Gd	¹¹⁷ Sn ⁴⁰ Ar ⁺
⁸⁹ Y	⁴⁹ Ti ⁴⁰ Ar ⁺	¹⁵⁹ Tb	¹¹⁹ Sn ⁴⁰ Ar ⁺
⁹⁰ Zr	⁵⁰ Ti ⁴⁰ Ar ⁺	¹⁶³ Dy	¹²³ Sb ⁴⁰ Ar ⁺
⁹³ Nb	⁴⁶ Ti ⁴⁷ Ti ⁺	¹⁷⁵ Lu	¹³⁵ Ba ⁴⁰ Ar ⁺
¹¹⁵ In	⁷⁵ As ⁴⁰ Ar ⁺	²³⁸ U	¹¹⁸ Sn ¹²⁰ Sn ⁺

Non-spectroscopic interferences are effects that take place in the laser ablation, sample transport, ionisation by the plasma, or transport of the ion beam; these effects may reduce or enhance disproportionately parts of the analytical signal. These effects can typically be mitigated by calibrating the data using matrix-matched standards, and by varying the plasma radio-frequency power during analysis. Additionally, problematic isotopes can often be circumvented by selecting stable isotopes of the element for measurement, see Appendix Figure 6.

As in X-ray Fluorescence spectroscopy, contamination also occurs through the carrier gas, the sample chamber environment, or any other part of the system. Where this is systematic, it can usually be identified and subtracted through the use of an analytical blank, i.e. collecting signal at the detector, without engaging the laser ablation system.

A.2.5 Calibration procedure for LA-ICPMS data

The most commonly used calibration strategies employ matrix-matched standards to produce calibration curves, using the measured (x) and expected (y) values to arrive at a conversion factor (m) that can be used to convert measured values from unknown samples, see Appendix Equation 2 (Danzer and Currie, 1998).

Where few matrix-matched standards are available, or in cases where the samples are likely to vary somewhat from the composition of the standards, internal calibration is used to correct the analytical signal of the unknown sample through comparison with that of the standards for a single element common to both.

$$y_i = mx_i + c$$

Appendix Equation 1 - calculation to relate observed and expected values for standards in an external calibration by linear regression. Where:

y = expected value for analyte i

m = the linear operator, equal to the slope of the line

x = the measured value for analyte i

c = sensitivity, equal to the intercept of the line with the y axis

The method selected for this research is sum normalisation calibration, which is the simultaneous measurement of a suite of elements, the data from which are normalised to 100% as oxides. Variants of this method have been used with great success to calibrate LA-ICPMS data from analyses carried out on archaeological and cultural heritage materials (Gratuze et al, 2001; Halicz and Gunther, 2004; Gagnon et al, 2008; Dussubieux et al, 2008; Dussubieux et al, 2009; van Elteren et al, 2009). This research follows that used by van Elteren (2009) and Giannini (2015).

Correction by subtraction from a blank having been carried out, an internal standard element, Si, is used to standardise the analytical signal in counts per second, relative to those of the glass standard NIST 612, see Appendix Equation 2.

$$I_i(\text{corr}) = \frac{I_i}{(I_{i=IS}/c_{i=IS})}$$

Appendix Equation 2 - process to correct the raw signal intensity in counts per second (cps) for each constituent oxide (1 to n). Where:

I_i = raw signal intensity for oxide i in the sample

I_{i=IS} = raw intensity for the internal standard (Si)

c_{i=IS} = known concentration of oxide i in the internal standard

A response factor (F_i) is then calculated for each element present in the sample, see Appendix Equation 3 and Appendix Equation 4, in order to convert these corrected signal intensities to elemental concentration data, by using the known concentrations of each element in the glass standards j.

$$I_{i,j}(\text{corr}) = \frac{I_{i,j}}{(I_{i=IS,j}/c_{i=IS,j})}$$

Appendix Equation 3 - process to correct the raw signal intensity in cps for each constituent oxide (1 to n) in the glass standards. Where:

I_{ij}(corr) = corrected signal intensity for oxide i in the glass standards j

I_{ij} = raw signal intensity for oxide i in the glass standards j

I_{i=IS,j} = raw intensity of the internal standard in the glass standards j

c_{i=IS,j} = known concentration of the internal standard in the glass standards j

$$F_i = \frac{\sum_{j=1}^m c_{i,j} I_{i,j}(\text{corr})}{\sum_{j=1}^m (c_{i,j})^2}$$

Appendix Equation 4 - process to calculate the response factor (F_i) for each element present in the sample. Where:

F_i = response factor for i

Σ^m_{j=1} = sum of the points for each of the glass standards j

c_{i,j} = known concentration of oxide i in the glass standards j

I_{ij}(corr) = corrected signal intensity of oxide i in glass standard j

The values for each element in the unknown samples having been multiplied by the response factor, see Appendix Equation 5, the resulting elements as oxides may be normalised to 100%, see Appendix Equation 6.

$$C_i = \frac{I_i(\text{corr})}{F_i}$$

Appendix Equation 5 - process to calculate the elemental oxide concentration in the sample using the response factor. Where:

c_i = concentration of element i as oxide in the sample

$I_i(\text{corr})$ = corrected intensity for element i

F_i = response factor for element i

$$C_{i,norm} = \frac{C_i}{\sum_{i=1}^n C_i} \times 100$$

Appendix Equation 6 - process of sum normalisation for the elemental oxide concentration in the sample.

Where:

$c_{i,norm}$ = normalised concentration of element i

c_i = concentration of element i

$\sum_{i=1}^n$ = the sum of the elemental oxides measured in the sample

A.3 X-Ray Fluorescence Spectroscopy theory and instrumentation

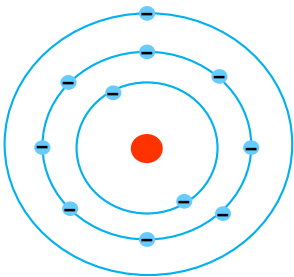
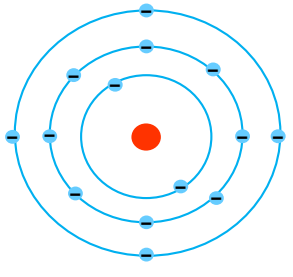
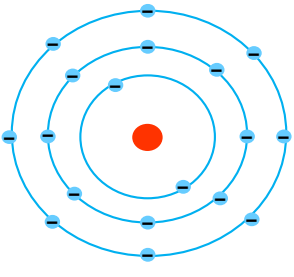
X-ray Fluorescence Spectroscopy (XRF) is a technique that uses short-wavelength (i.e. high-energy and high frequency) electromagnetic radiation to excite an atom within a sample, causing it to emit a packet of characteristic energy in the form of a photon (Jenkins et al, 1995; pp. 7 – 8). When this occurs in the surface of a sample under analysis, this fluorescent energy is detected by the instrument and plotted as a spectrum, with the energy on the x-axis and the relative intensity on the y-axis. XRF is frequently used in analysing archaeological objects, as it provides a wide range of elemental compositional data, with the benefits of quick, non-destructive, and inexpensive instrumentation.

A.3.1 The structure of an atom

An atom is the smallest individual component of an element; it is an electrically neutral structure comprising three types of packets of energy, called subatomic particles. The core, called a nucleus, of the atom consists of protons, which are positively charged, and neutrons, which are neutral (Daintith, 2008; p. 47). Existing in orbitals surrounding the nucleus are electrons, which are negatively charged (Daintith, 2008; p. 386). In order for the atom to retain its neutrality, the number of electrons is equal to the number of protons. The number of neutrons is usually equal to the number of protons, and it is the number of neutrons that gives the atom its atomic number (Z) (Daintith, 2008; p. 48).

As the atomic number increases, the number of protons and electrons also increase, and the number and configuration of electrons gives the element its material properties. This is shown by the periodic table of the elements, which displays the elements from left to right, and top to bottom, by increasing atomic number, see Appendix Figure 7.

Appendix Table 3 - electron configuration for sodium (Na, 11), silicon (Si, 14) and argon (Ar, 18)

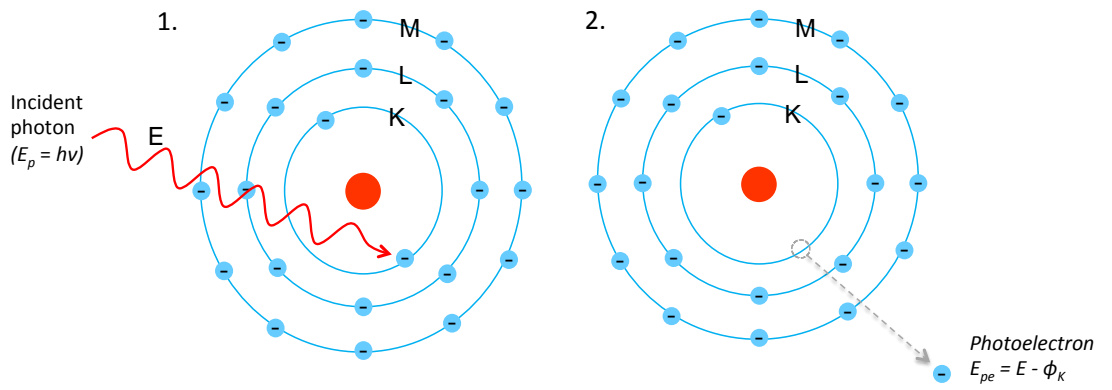
	Na	Si	Ar
Z	11	14	18
K	2	2	2
L	8	8	8
M	1	4	8
electron shell structure (Bohr model)			

The inner electrons are more tightly bound to the nucleus due to their proximity to the positively-charged protons. The further away an electron is from the nucleus, the weaker its bond to the protons. This means that larger atoms are generally less stable and more reactive than smaller atoms in their group, and it also causes them to interact in more complex ways with X-rays.

A.3.2 The reaction of X-rays with electrons: characteristic radiation

When an X-ray photon impacts an electron in one of the inner shells (K, L), the energy of the photon may be raised, and it may detach from its shell, see Appendix Figure 9. This causes the atom to become briefly positively charged, at which point it is called a positively charged ion, or cation (Jenkins et al, 1995; p. 13). In order to maintain equilibrium, an electron from an outer shell drops to fill the vacancy. As the energy required to dislodge an electron increases with proximity to the nucleus, a packet of energy called a photoelectron is discharged by the transition, and the energy of this photon is equal to the difference between the higher and lower energy electrons (Jenkins et al, 1995; p. 13), see Appendix Figure 10.

Appendix 3: XRF theory and instrumentation



Appendix Figure 9 - interaction between an atom and an incident photon from X-radiation. Where:

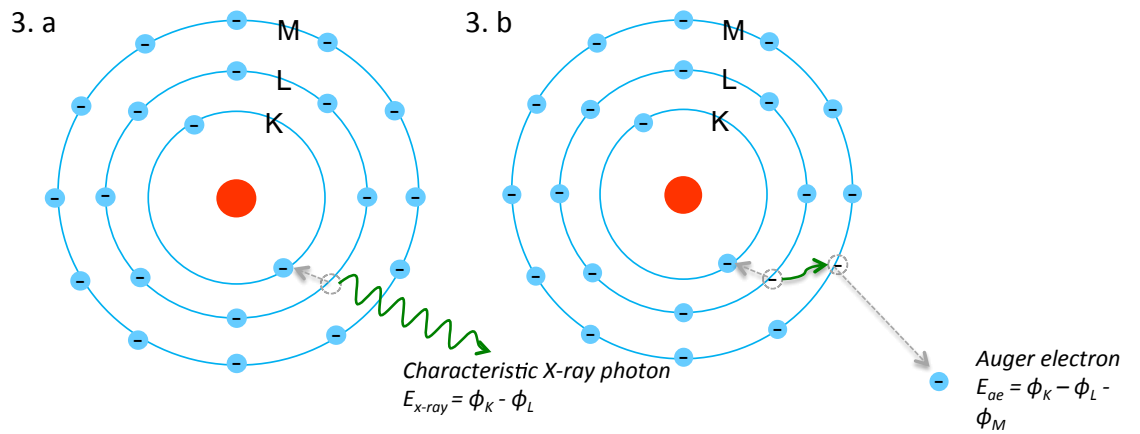
E = energy

ϕ = binding energy of the electron in transit

h = Planck's constant

ν = frequency

pe = photoelectron



Appendix Figure 10 - photoelectric effect (3. a) and Auger effect (3. b) within the atom illustrated in

Appendix Figure 9. Where:

E = energy

ϕ = binding energy of the electron in transit

ae = auger electron

κ = k shell

L = L shell

M = M shell

Alternatively, the difference in binding energies may be equalised by the transition of an electron from a higher shell of the same atom, known as an Auger electron (Jenkins et al, 1995; p. 13). In this case, the energy that is ultimately released is equal to the binding energy of the core electron, minus the binding energy of the first electron and the second electron to undergo transition, see Appendix Figure 10.

In larger atoms, transitions may occur between any of a number of shells, and therefore a number of different energies of photon may be emitted. These transitions are named for the lines that they produce on the resulting spectrum, see Appendix Table 4.

Appendix Table 4 - electron shell transitions, according to Siegbahn notation

Shell of excited atom	Shell of transitioning atom	Resulting emission line (Siegbahn notation)
K	L	K- α
K	M	K- β
K	N	K- γ
L	M	L- α
L	N	L- β
M	N	M- α

Fluorescent radiation is produced when the incident X-ray excites the electrons in the inner electron shells of atoms in the surface of the sample, causing a shell transition within the atom to fill the vacancy. The binding energy of the electron in transit is released as a photon, the energy of which is characteristic of the atom of origin. The fluorescent effect is more likely to occur in some elements, typically those with a higher atomic number, while lower energy elements are more likely to emit an Auger electron; this likelihood is denoted by the fluorescent yield, which is between 0 and 1 (Jenkins et al, 1995; p. 13).

A.3.3 The reaction of X-rays with electrons: other reactions

The collision of the incident X-ray with electrons in outer shells of atoms may instead result in a recoil with returning energy equal to that of the portion of energy received from the primary photon. This species of scatter is known as inelastic (or incoherent) Compton scatter, and results in a broad, poorly-defined peak at a fixed distance (0.024Å) from the elemental (coherently-scattered) lines.

When the incident X-ray is deflected by the surface atoms without electronic interaction, it may be returned to the detector without any change in its energy. This scatter is known as elastic (or coherent) Rayleigh scatter, and it produces a peak in the spectrum which is characteristic of the source (for example, rhodium).

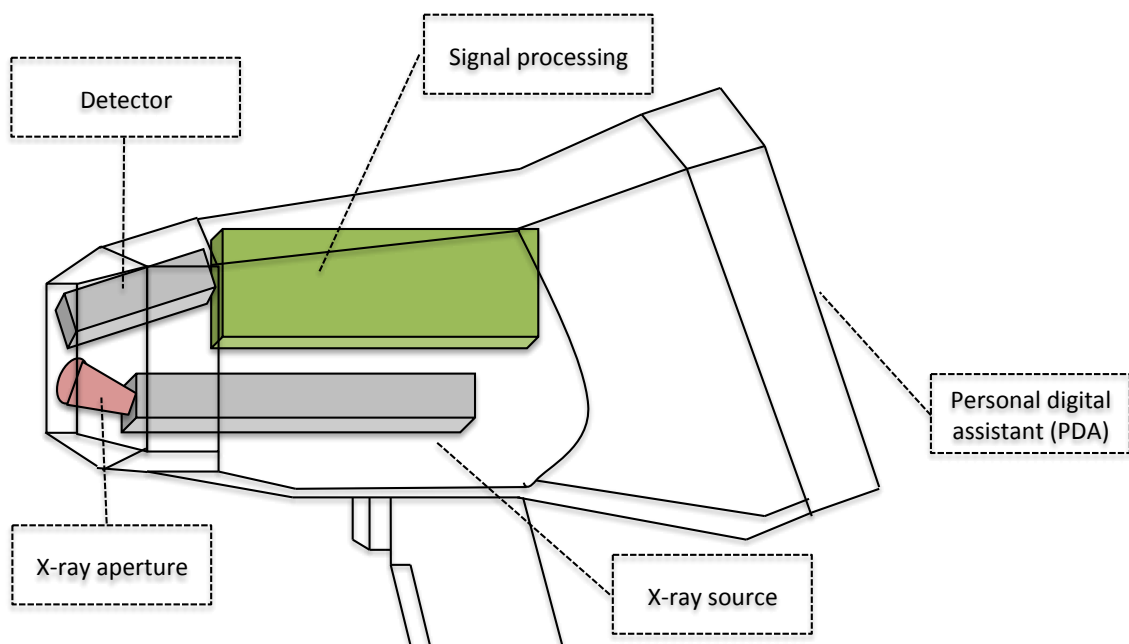
The deceleration of electrons as they collide with the nuclei of the X-ray tube anode causes continuous radiation at variable energy levels, this phenomenon is termed Bremsstrahlung, meaning 'braking radiation'. Bremsstrahlung manifests on the spectra as a continuous and relatively low-level "background". The energy limits of the radiation, and therefore the extent of the spectral background, are inversely proportional to the atomic number of the element which produces the scatter, meaning that the majority of instruments, which use a high-Z target such as rhodium (Rh, 45), will not be able to calculate reliably elements lower-Z than sodium (Na, 11)¹. The volume of the background is also determined by the sample matrix; a light sample matrix, such as leaf, bone, or paper, has been found to produce a higher background than a dense matrix, such as copper or gold alloys (Pessanha et al, 2009).

High frequency of incident or fluorescent radiation striking the detector can also produce the photoelectric effect on the detector, whereby the metal that comprises the detector absorbs the energy of a photon that is greater than the binding energy of one of its electrons, and this electron is released as a free particle. This produces a peak at a predictable location in the spectrum, known as an escape peak.

¹ Low-Z <18, mid-Z 18 – 41, high-Z >41 (Shackley, 2010; p. 24)

A.3.4 X-Ray Fluorescence Spectrometer instrumentation

The XRF systems used in this research is an Oxford Instruments X-MET5100 Hand-Held XRF. The instrument is shaped like a gun, with a handle topped by a trigger that controls the emission of X-rays, and two openings at the end of the barrel, one of which contains the X-ray aperture, and the other the detector behind a Mylar window, to protect it from contamination, see Appendix Figure 11. A personal digital assistant (PDA) at the butt allows the user to control the settings, and to view the data in real time, or manipulate the spectra after analysis. After analysis, the user exports the data to a computer for analysis using Bruker Systems ARTAX Spectra software², from which peaks may be identified, and peak intensities may be generated from up to 20 spectra at once. This software requires a slightly different document format from that generated by the X-MET integrated software, and so a text conversion program³ was written by David Wall, a doctoral candidate at Cranfield University, which creates a copy of the Hand-Held XRF data file that is readable by the Bruker Systems software.

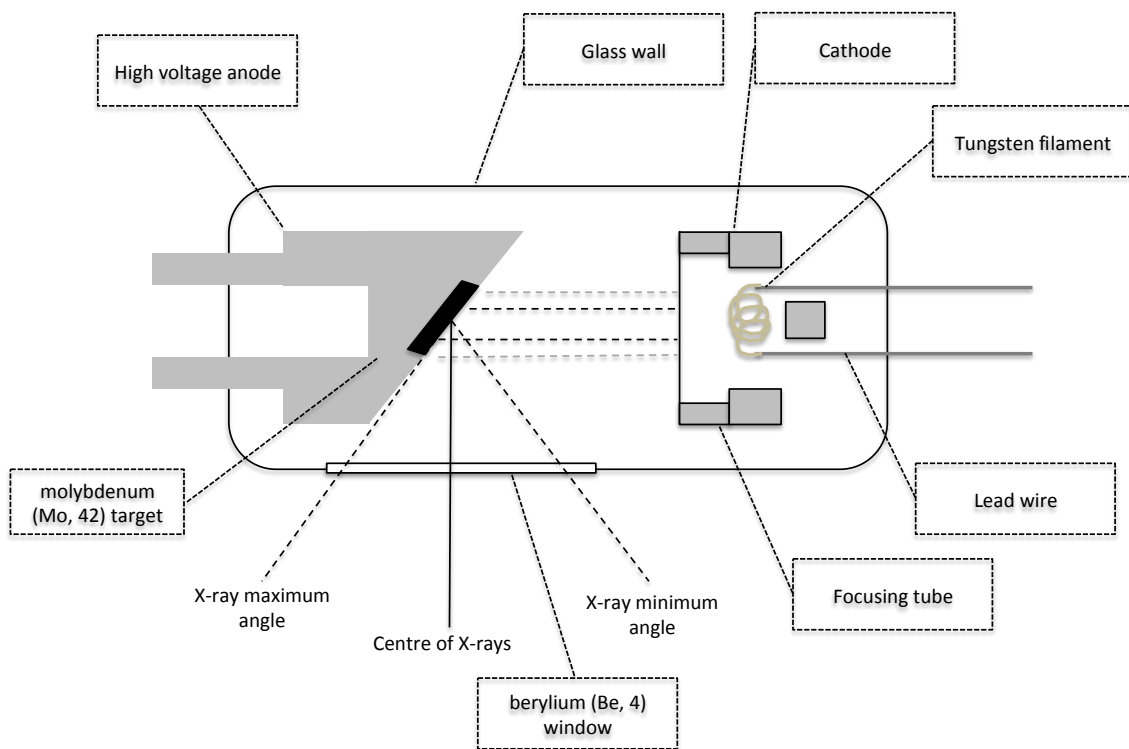


Appendix Figure 11 - diagram of the Oxford Instruments X-MET5100 Hand-Held XRF instrument

² Version 7.2, © Bruker Systems

³ using Java 6 v.1.6.032

There are two main sources of excitation energy that are commonly used in XRF spectroscopy: a sealed X-ray tube, and an X-ray or γ -ray emitting radioisotope. The latter is considered more energy efficient, as the X-rays are produced without constant application of electricity from another source; however, this also makes them less safe to transport and use, because the X-ray source cannot be turned off. Furthermore, the range of radiation that can be produced is more limited, because the source will give off energy at a constant rate that cannot be substantially amplified, and can only be decreased through the use of filters (Jenkins et al, 1995; pp. 41 – 42),



Appendix Figure 12 - diagram of an X-ray tube

Sealed X-ray tubes are more versatile; they operate by bombarding a high voltage anode with electricity from a heated metal cathode, see Appendix Figure 12. At the centre of the anode is a target material, typically a heavy metal, the electrons of which are excited by the energy from the cathode, and emit X-ray photons through the photoelectric effect.

The X-ray photons are directed by the angle of the target, through a non-attenuating window, and towards the sample surface. Scattering also takes place within the anode, producing *bremsstrahlung*, or braking radiation, which manifests as a continuous background signal in the resulting X-ray spectra, see A.3.3. This reaction takes place within a vacuum, both in order to prevent the interaction of electrons and resulting X-ray photons with the air, and to minimise the accumulation of heat in the components.

A.3.5 X-Ray Fluorescence spectra

The scattered and fluorescent energy emitted from the sample is collected by a detector, which is positioned close to the sample, adjacent to the X-ray emission aperture. This is typically a silicon drift detector (SDD); a solid-state material, which is ionised by the incoming energy, and the charge is collected and then translated into a series of pulses. These pulses are used to generate a spectrum, where the energy of the pulse is plotted on the x-axis, and the frequency of pulses of that specific energy is the y-axis. Therefore, the x-axis gives the characteristic energy of the atom from which the photon originated, and the y-axis gives the relative abundance of this atom. The relationship between the frequency of energy emitted and the element of origin is defined by Moseley's Law, see Appendix Equation 7. The frequency of the photon is derived from its energy energy using the Planck-Einstein relation, see Appendix Equation 8.

$$\nu = k_1(Z - k_2)^2$$

Appendix Equation 7 - Moseley's law, defining the relationship between the frequency of a fluorescent photon and the atomic number and transition of the element of origin. Where:

ν = frequency

k_1 = a constant unique to the K transition

Z = the atomic number of the element of origin

k_2 = a constant unique to the K transition

$$E = \frac{hc}{\lambda}$$

Appendix Equation 8 - the Planck-Einstein relation, describing the relationship between the wavelength and the energy of a photon. Where:

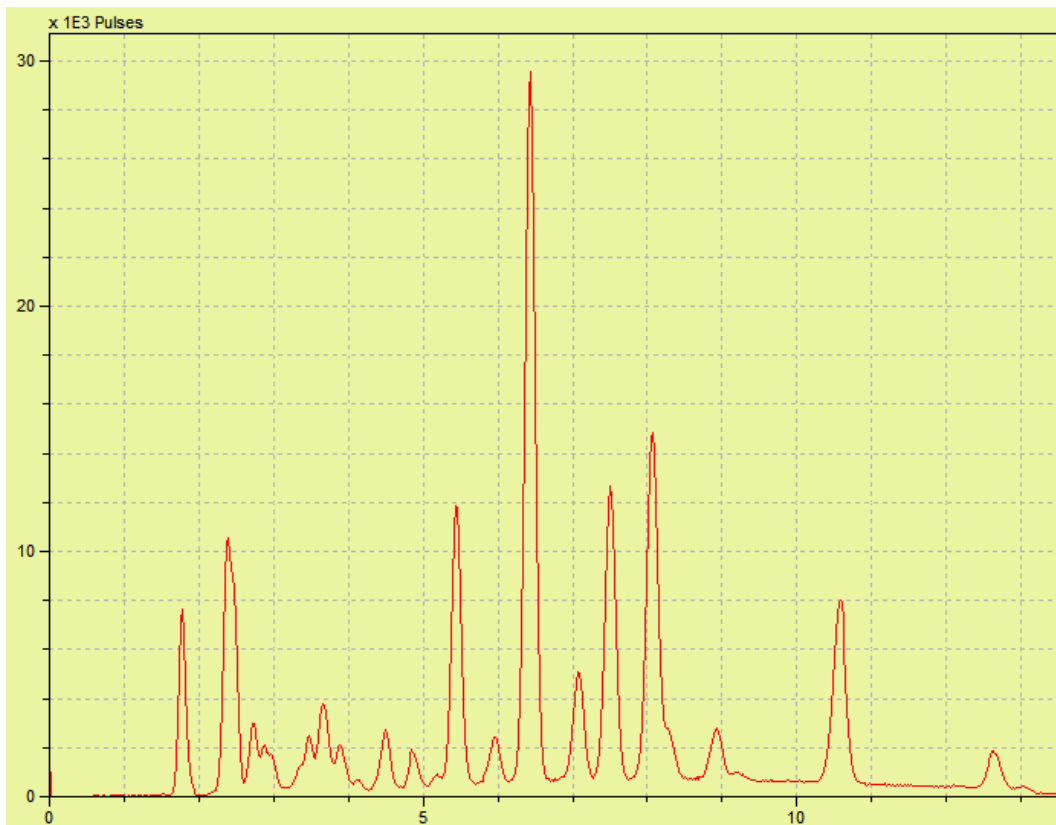
E = energy

h = Planck's constant

c = speed of light

λ = wavelength

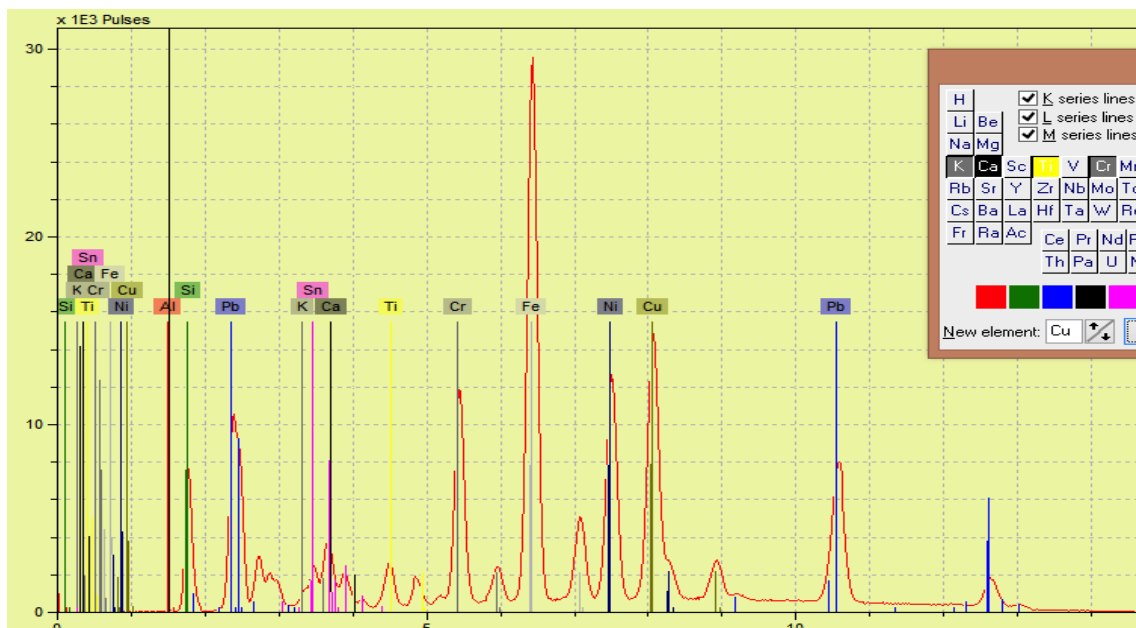
These calculations are carried out by the Bruker Systems ARTAX software, rendering the spectrum as a continuous line, with peaks produced by the energy received by the detector, see Appendix Figure 13. The user can then manually identify the peaks as elements, see Appendix Figure 14. In the case of overlapping peaks, comparing spectra with similar peaks allows the user to assess the ratio of K-α to K-β, or L-α to L-β, and therefore whether there are two elements present or one.



Appendix Figure 13 - an XRF spectrum, produced using Bruker Artax software (version 7.2)

In the case of overlapping peak areas, the software is capable of resolving some elements that occupy adjacent regions of interest (ROI), such as Mn K β (6.49 keV) and Fe K α (6.39 keV). However, the overlap of Pb L α (10.45 – 10.55 keV) and As K α (10.54 keV) cannot be distinguished automatically, even when both elements have been identified by the operator. In this case, it is necessary to calculate the peak area for As using the region of interest (ROI) tool, which is part of the ARTAX software, to select the area of the As K β peak. This value is then copied and pasted to an Excel spreadsheet, and used to calculate the peak area for As K α ; the peak area ratio of K α :K β should be 7:1 (Oxford Instruments, 2010).

For the remaining elements in the spectrum, the software then employs a line of best fit, which encompasses the elements identified and then calculates the peak area using the unidentified data as a baseline. The peak area data may be exported as a spreadsheet for further processing and display.



Appendix Figure 14 - an XRF spectrum with tags to identify the peaks as elements, produced using Bruker ARTAX software (version 7.2)

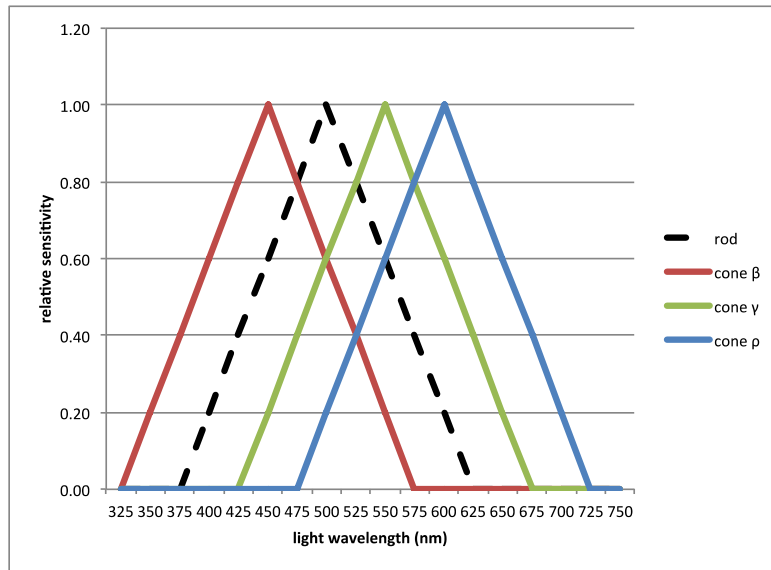
A.4 Spectrophotometer theory and instrumentation

Spectrophotometry is a technique that is used to characterise materials in terms of the reaction that occurs when they are exposed to visible light, and thereby the colour of the material. Colour is the perception of light of a given wavelength within the visible area of the electromagnetic spectrum, from violet at 400nm to red at 800nm. The human eye is able to distinguish up to ten million colours, based on the following three attributes (Hunt and Pointer, 2011; pp. 9 - 10):

- **Brightness:** the amount of light that appears to be present, either emitted or reflected from the object
- **Hue:** the similarity of the object's colour to one or two of the perceived colours, red, yellow, green, and blue
- **Chroma:** the colourfulness of the object, meaning the extent to which the object exhibits its hue

In human sight, these attributes are relative; this means that the perceived brightness of an object appears greater against a dark background, or less against a bright background, and the perceived hue and chroma also vary, depending on the hue and chroma of surrounding objects or ambient light. The eye receives colour through four different types of receptors, each of which reacts to a different wavelength of light, overlapping with one another to allow total colour vision, see Appendix Figure 15 (Hunt and Pointer, 2011; pp. 6 - 7).

Colour may be objectively measured using photometry, meaning 'light measurement'; spectrophotometry measures not merely the brightness of the light, but also its colour, based on the wavelength or frequency on the electromagnetic spectrum (Wysecki and Stiles, 1982; p. 249). A spectrophotometric instrument achieves this by illuminating the sample area using a standard illuminant, which is a well-characterised light source, and measuring the reflected light. The difference between the incident light, which is typically white, and the reflected light is the colour of the sample.

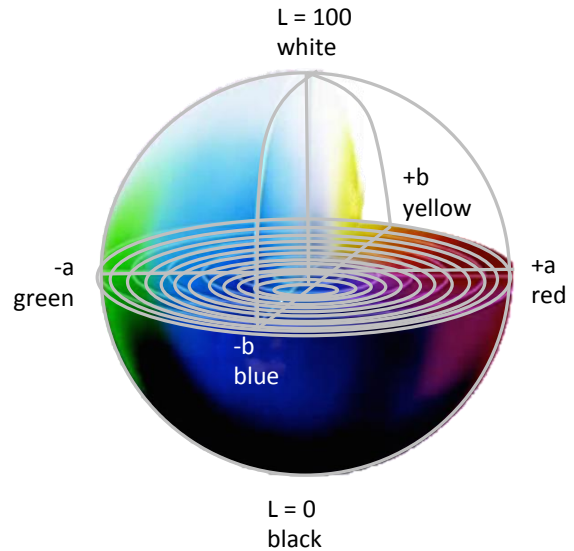


Appendix Figure 15 - the spectral sensitivity of the human eye, based on the four types of photo-sensitive structures; rods, β cones, γ cones, and α cones.

The Konica Minolta CM-700d Hand-Held spectrophotometer device used in this study employs the CIE $L^*a^*b^*$ colour space, a convention that was developed by the *Commission Internationale de l'Éclairage* (International Commission on Illumination) in the mid-20th century. This colour space is designed to correspond with the perception of colour by the human eye, whereby the response from the γ cone that measures to the strength of the light is denoted by a value L^* , the ρ cone response, measuring the red or green hue, is denoted as value a^* , and the β cone response, measuring the yellow or blue hue, is denoted as value b^* . The correspondence between the components of this colour space are nonlinear, but are calibrated to the perceptual difference of the human eye. Therefore the distance between any two points on the CIE $L^*a^*b^*$ colour space can be approximated to the perceptual difference between those two colours by a working eye. Using this method, the reflected light measured by the spectrophotometer is converted to tristimulus values, whereby every colour has a value on three axes in order to plot it in three-dimensional space, see Appendix Figure 16 (Hunt and Pointer, 2011; pp. 53 - 57):

- Lightness: a vertical axis describing the relative luminance of the sample, ranging from black ($L = 0$) to white ($L = 100$), with shades of grey between.

- a: a diametric axis representing hue, where this falls between red ($a = 100$) and green ($a = -100$)
- b: a diametric axis representing hue, where this falls between yellow ($b = 100$) and blue ($b = -100$)



*Appendix Figure 16 - Commission Internationale de l'Eclairage (CIE) $L^*a^*b^*$ colour space, showing the axes upon which measured colour values are plotted*

In interpreting quantitative CIE $L^*a^*b^*$ data, the values for these three components may be read to discover the approximate colour of the object, for instance: $L = 25$; $a = 40$; $b = -90$, this colour may be assumed to be dark or dull, because there is a low value for L , it likely to be purple in colour, because it is positive on the a axis (i.e. red), and negative on the b axis (i.e. blue). Furthermore, a number of points may be plotted on two charts, one representing a vs. b , and a linear scale representing L , in order to determine how similar or different their perceived colours may be.

A.5 porcelain paste and glaze data from published sources

Appendix Table 5 - elemental compositional data of porcelain pastes, obtained from mounted sections using SEM-EDS (Tite and Bimson, Freestone, Middleton and Cowell, Ramsay) and SEM with EDS and WDS (Owen)

Ref	Paste	Sherd	SiO ₂	TiO ₂	Al ₂ O ₃	FeO	MgO	CaO	Na ₂ O	K ₂ O	P ₂ O ₅	PbO	SO ₂
'A'-marked													
Ramsay and Gabszewicz (2003)	proto-porcelain	A-m 1	63.50	<lod	19.50	0.60	1.20	6.10	4.20	3.60	0.50	0.40	<lod
Ramsay and Gabszewicz (2003)	proto-porcelain	A-m 2	59.80	<lod	26.60	0.30	1.17	5.89	3.87	2.87	<lod	<lod	<lod
Ramsay and Gabszewicz (2003)	proto-porcelain	A-m 3	65.20	0.20	19.80	0.30	1.30	5.40	4.60	2.20	<lod	0.60	0.40
Ramsay and Gabszewicz (2003)	proto-porcelain	A-m 4	63.60	<lod	23.20	0.30	1.30	5.10	4.30	2.10	<lod	<lod	<lod
Bovey Tracey													
Owen et al (2000)	true porcelain	BT5	63.00	<lod	30.60	0.50	0.30	0.30	1.10	3.80	0.30	<lod	<lod
Owen et al (2000)	true porcelain	BT6	62.60	<lod	30.90	0.50	0.30	0.40	1.10	3.80	0.30	<lod	<lod
Owen et al (2000)	true porcelain	BT11	77.60	<lod	17.20	0.50	0.20	0.30	1.10	2.60	0.30	<lod	0.10
Owen et al (2000)	phosphatic	BT11	38.80	<lod	14.20	0.30	0.60	24.30	1.40	2.00	18.30	<lod	<lod
Owen et al (2000)	phosphatic	BT2	37.00	<lod	14.40	0.30	0.60	25.30	1.30	1.80	19.20	<lod	<lod
Owen et al (2000)	phosphatic	BT3	37.30	<lod	13.90	0.30	0.60	25.40	1.30	1.70	19.50	<lod	<lod
Owen et al (2000)	phosphatic	BT4	38.10	<lod	14.20	0.30	0.60	24.80	1.30	1.80	18.80	<lod	<lod
Owen et al (2000)	magnesian	BT7	65.20	<lod	3.20	0.40	8.10	8.50	0.40	2.60	2.30	6.10	1.30
Owen et al (2000)	magnesian	BT8	64.90	<lod	3.10	0.40	7.50	8.00	0.40	2.50	2.10	6.70	1.50
Owen et al (2000)	magnesian	BT9	63.50	<lod	3.10	0.40	8.00	8.60	0.40	2.50	2.70	6.20	1.80
Owen et al (2000)	magnesian	BT10	65.30	<lod	3.30	0.40	8.10	7.90	0.50	2.30	2.10	5.80	1.30
Owen et al (2000)	magnesian	BT12	75.40	<lod	3.10	0.30	5.70	4.40	1.40	3.70	<lod	5.90	<lod
Bow													
Tite and Bimson (1991)	phosphatic	E10	45.60	0.50	8.70	0.50	0.60	23.60	0.80	1.10	18.60	<lod	<lod
Tite and Bimson (1991)	phosphatic	E12	50.70	0.20	5.60	<lod	0.40	23.80	0.50	0.70	15.80	<lod	2.00
Tite and Bimson (1991)	phosphatic	E14	49.20	0.30	5.60	0.30	0.30	24.50	0.50	0.60	16.20	0.40	2.10

Appendix 5: porcelain paste and glaze data from published sources

Appendix Table 5 - elemental compositional data of porcelain pastes, obtained from mounted sections using SEM-EDS (Tite and Bimson, Freestone, Middleton and Cowell, Ramsay) and SEM with EDS and WDS (Owen)

Ref	Paste	Sherd	SiO ₂	TiO ₂	Al ₂ O ₃	FeO	MgO	CaO	Na ₂ O	K ₂ O	P ₂ O ₅	PbO	SO ₂
Bow (continued)													
Tite and Bimson (1991)	phosphatic	745	51.20	0.30	5.60	0.30	0.60	23.20	0.60	0.60	15.30	0.40	1.90
Owen (1998) i	phosphatic	mean	53.40	0.30	4.60	0.20	0.40	22.20	0.70	0.60	14.70	-	2.80
Freestone (2000)	phosphatic	mean	51.20	0.30	5.60	0.30	0.60	23.20	0.60	0.60	15.30	0.40	1.90
Ramsay and Ramsay (2011)	phosphatic	sauceboat	46.40	0.30	8.50	0.40	0.40	23.00	0.67	0.95	19.40	<lod	<lod
Ramsay and Ramsay (2011)	phosphatic	coffee cup	58.40	0.20	4.30	0.20	0.40	18.80	0.70	0.50	14.90	<lod	1.60
Ramsay and Ramsay (2011)	phosphatic	leaf dish	50.31	0.30	5.30	0.30	0.30	22.87	0.85	0.55	16.28	0.20	2.75
Ramsay and Ramsay (2011)	phosphatic	bowl	50.80	0.30	4.70	0.30	0.40	22.60	0.20	0.70	17.90	<lod	2.10
Ramsay and Ramsay (2011)	magnesian	tea cannister	52.90	<lod	32.60	2.90	4.60	0.30	2.00	2.70	0.10	<lod	1.90
Ramsay and Ramsay (2011)	phosphatic	B9	48.34	0.44	5.00	0.18	0.33	22.65	0.88	0.68	18.43	<LOD	3.08
Ramsay and Ramsay (2011)	phosphatic	B10	43.27	0.61	9.71	0.24	0.72	22.79	1.15	0.69	20.00	0.13	0.74
Ramsay and Ramsay (2011)	phosphatic	B30	40.04	0.40	6.70	0.30	0.60	25.30	0.30	2.70	20.00	1.70	2.00
Ramsay and Ramsay (2011)	phosphatic	B64	47.77	0.30	7.08	0.41	0.36	21.49	0.49	1.25	19.00	1.30	0.55
Ramsay and Ramsay (2011)	phosphatic	B68	46.92	0.18	7.11	0.52	0.34	21.16	0.55	1.49	15.07	2.55	4.14
Ramsay et al (2013)	Si-Al	13	81.00	0.80	14.70	0.30	0.30	0.30	0.30	1.70	0.20	<lod	0.20
Ramsay et al (2013)	Si-Al-Ca	14	59.70	<lod	27.70	0.10	0.30	7.30	3.70	1.20	<lod	<lod	<lod
Ramsay et al (2013)	Al-Mg-P-Pb	15	36.90	0.50	33.00	0.80	3.10	8.90	4.20	1.70	2.70	8.30	<lod
Ramsay et al (2013)	Si-Al	13	52.50	<lod	5.50	<lod	0.60	2.50	3.30	3.30	<lod	32.50	<lod
Ramsay et al (2013)	Si-Al-Ca	14	44.50	<lod	<lod	<lod	<lod	0.30	2.00	3.00	<lod	50.00	<lod
Ramsay et al (2013)	Al-Mg-P-Pb	15	74.40	<lod	8.30	0.40	1.50	10.70	2.20	2.50	<lod	<lod	<lod

Appendix 5: porcelain paste and glaze data from published sources

Appendix Table 5 - elemental compositional data of porcelain pastes, obtained from mounted sections using SEM-EDS (Tite and Bimson, Freestone, Middleton and Cowell, Ramsay) and SEM with EDS and WDS (Owen)

Ref	Paste	Sherd	SiO ₂	TiO ₂	Al ₂ O ₃	FeO	MgO	CaO	Na ₂ O	K ₂ O	P ₂ O ₅	PbO	SO ₂
Lund's Bristol													
Ramsay et al (2011)	magnesian	leaf pickle dish	57.00	<lod	2.00	<lod	8.00	10.50	0.30	3.00	10.50	9.50	<lod
Ramsay et al (2011)	magnesian	pickle dish	62.30	<lod	3.30	<lod	20.00	8.70	1.70	3.30	6.00	4.50	<lod
Ramsay et al (2011)	magnesian	sauceboat	67.60	<lod	4.60	<lod	13.30	2.60	1.60	1.15	2.00	8.00	<lod
Ramsay et al (2011)	magnesian	sherd	60.70	<lod	2.40	<lod	15.00	10.90	2.20	1.60	6.70	<lod	<lod
Ramsay et al (2011)	magnesian	Lu Tung Pin	66.80	<lod	3.60	<lod	11.40	0.50	0.50	4.40	<lod	13.20	<lod
Ramsay et al (2011)	magnesian	sauceboat	68.00	<lod	3.00	<lod	12.30	1.30	1.00	3.30	<lod	10.90	<lod
Ramsay et al (2011)	magnesian	sauceboat	60.80	<lod	2.80	<lod	11.50	10.00	2.00	2.00	7.10	3.50	<lod
Ramsay et al (2011)	magnesian	pickle dish	58.00	<lod	3.00	<lod	7.00	8.00	0.30	3.00	7.00	14.00	<lod
Ramsay et al, 2013	Mg-P-Pb	12	55.90	<lod	3.50	<lod	13.90	7.00	2.00	2.50	5.00	10.40	<lod
Ramsay et al, 2013	Mg-P-Pb	12	55.00	<lod	4.00	<lod	3.00	1.00	3.00	4.00	<lod	29.00	<lod
Caughley													
Owen and Sandon (2003)	magnesian	CY2	73.60	<lod	5.50	0.40	9.80	1.90	1.70	2.10	0.40	4.40	0.20
Owen and Sandon (2003)	magnesian	CY7	77.00	<lod	5.30	0.40	8.40	1.90	2.00	2.70	0.60	1.60	0.20
Owen and Sandon (2003)	magnesian	CY8	76.40	<lod	4.20	0.40	10.70	1.50	1.40	2.40	0.50	2.30	0.20
Owen and Sandon (2003)	magnesian	CY9	77.90	<lod	5.00	0.30	5.80	1.10	1.50	2.50	0.20	5.40	0.20
Owen and Sandon (2003)	magnesian	CY10	73.60	<lod	4.50	0.40	11.00	1.50	1.70	2.30	0.50	4.10	0.40
Owen and Sandon (2003)	magnesian	CY11	77.00	<lod	4.90	0.40	8.90	1.60	1.70	2.70	0.40	2.10	0.30
Owen and Sandon (2003)	magnesian	CY13	73.50	<lod	5.90	0.10	8.40	0.80	1.00	3.40	<lod	6.80	<lod
Owen and Sandon (2003)	magnesian	CY15	75.20	<lod	3.80	0.50	10.90	2.80	1.60	2.90	0.10	2.00	<lod
Owen and Sandon (2003)	magnesian	CY16	75.20	<lod	3.40	0.10	9.40	1.20	1.10	2.20	<lod	7.20	<lod
Owen and Sandon (2003)	magnesian	CY18	76.20	<lod	5.40	0.40	9.60	1.80	2.20	2.40	0.50	1.30	0.20
Owen and Sandon (2003)	magnesian	CY19	79.00	<lod	5.10	0.30	8.00	1.60	2.00	2.50	0.30	1.30	<lod

Appendix 5: porcelain paste and glaze data from published sources

Appendix Table 5 - elemental compositional data of porcelain pastes, obtained from mounted sections using SEM-EDS (Tite and Bimson, Freestone, Middleton and Cowell, Ramsay) and SEM with EDS and WDS (Owen)

Ref	Paste	Sherd	SiO ₂	TiO ₂	Al ₂ O ₃	FeO	MgO	CaO	Na ₂ O	K ₂ O	P ₂ O ₅	PbO	SO ₂
Caughley (continued)													
Owen and Sandon (2003)	magnesian	CY20	77.40	<lod	5.40	0.20	7.60	1.80	1.80	2.60	0.40	2.40	0.20
Owen and Sandon (2003)	true porcelain	CY3	70.70	<lod	23.40	0.40	0.40	0.50	1.40	2.90	0.30	<lod	0.10
Owen and Sandon (2003)	true porcelain	CY4	74.90	<lod	19.80	0.20	0.10	0.60	1.30	2.70	0.30	<lod	0.10
Owen and Sandon (2003)	true porcelain	CY5	76.10	<lod	18.10	0.20	0.10	0.50	1.60	3.00	0.30	<lod	0.10
Owen and Sandon (2003)	true porcelain	CY6	75.00	<lod	19.30	0.20	0.20	0.40	1.40	3.00	0.40	<lod	0.10
Owen and Sandon (2003)	true porcelain	CY12	77.00	<lod	17.40	0.20	0.10	0.60	1.50	2.80	0.30	<lod	0.10
Owen and Sandon (2003)	true porcelain	CY14	74.80	<lod	19.60	0.20	0.40	0.40	1.50	2.90	0.20	<lod	<lod
Owen and Sandon (2003)	true porcelain	CY17	73.80	<lod	20.00	0.10	0.10	1.60	1.60	2.60	0.20	<lod	<lod
Owen and Sandon (2003)	true porcelain	CY21	74.20	<lod	20.00	0.20	0.20	0.40	1.60	2.90	0.30	<lod	<lod
Chamberlain's Worcester													
Owen (2003)	SAC	CW1	76.10	<lod	18.70	0.30	0.20	1.10	1.10	2.20	0.30	<lod	0.20
Owen (2003)	SAC	CW2	78.50	<lod	16.70	0.30	0.20	0.70	0.70	2.40	0.30	<lod	0.10
Chelsea													
Tite and Bimson (1991)	frit	E7	70.30	0.30	4.10	0.20	0.40	18.80	0.50	3.50	<lod	1.90	<lod
Tite and Bimson (1991)	frit	746	71.70	0.30	4.30	0.40	0.30	13.10	0.50	4.30	<lod	5.10	<lod
Tite and Bimson (1991)	phosphatic	E15	46.40	0.50	11.30	0.30	0.50	21.80	0.60	1.40	17.20	<lod	<lod
Freestone (2000)	glassy	mean	62.80	0.20	4.90	0.20	0.30	20.10	0.80	5.30	0.30	4.40	0.30
Coalport													
Freestone (2000)	bone china	mean	43.00	<0.2	13.60	<0.2	0.50	17.40	1.60	1.60	21.20	<0.3	<0.2
Owen and Sandon (2003)	phosphatic	COAL3	50.70	<lod	12.60	0.20	0.40	19.00	0.70	1.50	14.80	<lod	<lod
Owen and Sandon (2003)	phosphatic	COAL4	45.50	<lod	12.80	<lod	0.50	21.10	0.80	2.10	16.20	<lod	<lod
Owen and Sandon (2003)	phosphatic	COAL5	41.90	<lod	14.80	0.20	0.50	22.20	0.80	1.90	17.70	<lod	<lod

Appendix 5: porcelain paste and glaze data from published sources

Appendix Table 5 - elemental compositional data of porcelain pastes, obtained from mounted sections using SEM-EDS (Tite and Bimson, Freestone, Middleton and Cowell, Ramsay) and SEM with EDS and WDS (Owen)

Ref	Paste	Sherd	SiO ₂	TiO ₂	Al ₂ O ₃	FeO	MgO	CaO	Na ₂ O	K ₂ O	P ₂ O ₅	PbO	SO ₂
Coalport (continued)													
Owen and Sandon (2003)	phosphatic	COAL9	40.50	<lod	15.00	0.30	0.50	23.30	0.60	1.60	18.20	<lod	<lod
Owen and Sandon (2003)	phosphatic	COAL10	43.00	<lod	15.20	0.10	0.40	21.40	1.10	1.90	16.80	<lod	<lod
Owen and Sandon (2003)	phosphatic	COAL14	48.30	<lod	11.70	0.20	0.40	20.50	0.70	1.30	16.90	<lod	<lod
Owen and Sandon (2003)	phosphatic	COAL15	49.40	<lod	12.20	0.20	0.40	19.60	0.80	1.20	16.20	<lod	<lod
Owen and Sandon (2003)	phosphatic	COAL18	43.70	<lod	12.90	0.20	0.40	21.90	1.10	1.70	18.00	<lod	<lod
Owen and Sandon (2003)	phosphatic	COAL20	43.40	<lod	12.80	0.20	0.40	22.10	1.10	2.10	17.80	<lod	<lod
Owen and Sandon (2003)	phosphatic	COAL21	41.80	<lod	15.80	0.30	0.50	21.20	1.10	2.20	17.00	<lod	<lod
Owen and Sandon (2003)	phosphatic	COAL22	51.00	<lod	11.40	0.20	0.40	19.20	0.70	1.30	15.70	<lod	<lod
Owen and Sandon (2003)	phosphatic	COAL24	42.30	<lod	14.50	0.20	0.60	21.40	0.50	2.20	18.30	<lod	<lod
Owen and Sandon (2003)	phosphatic	COAL27	44.40	<lod	13.40	0.30	0.50	21.40	1.20	2.00	16.90	<lod	<lod
Owen and Sandon (2003)	phosphatic	COAL29	42.40	<lod	12.80	0.20	0.50	22.70	1.10	1.70	18.60	<lod	<lod
Owen and Sandon (2003)	phosphatic	COAL32	43.20	<lod	13.40	0.40	0.30	22.00	1.20	1.80	17.60	<lod	<lod
Owen and Sandon (2003)	phosphatic	COAL33	46.90	<lod	12.10	0.20	0.40	20.70	0.90	1.40	17.30	<lod	<lod
Owen and Sandon (2003)	phosphatic	COAL34	42.10	<lod	12.60	0.20	0.50	22.80	1.10	1.80	18.90	<lod	<lod
Owen and Sandon (2003)	true porcelain	COAL1	76.00	<lod	19.10	0.20	0.20	0.50	1.20	2.60	0.20	<lod	<lod
Owen and Sandon (2003)	true porcelain	COAL2	75.00	<lod	19.70	0.20	0.20	0.50	1.30	2.70	0.30	<lod	<lod
Owen and Sandon (2003)	true porcelain	COAL6	75.60	<lod	19.10	0.10	0.10	0.60	1.40	2.50	0.30	<lod	<lod
Owen and Sandon (2003)	true porcelain	COAL7	75.40	<lod	18.80	0.10	0.10	0.60	1.60	2.90	0.30	<lod	<lod
Owen and Sandon (2003)	true porcelain	COAL8	75.80	<lod	18.60	0.20	0.20	0.50	1.50	2.90	0.30	<lod	<lod
Owen and Sandon (2003)	true porcelain	COAL11	75.00	<lod	18.70	0.20	0.20	0.60	1.60	3.20	0.40	<lod	<lod
Owen and Sandon (2003)	true porcelain	COAL12	75.50	<lod	18.90	0.10	0.10	0.50	1.60	2.90	0.30	<lod	<lod
Owen and Sandon (2003)	true porcelain	COAL13	74.20	<lod	19.10	0.10	0.10	1.30	1.20	2.60	1.10	<lod	<lod

Appendix 5: porcelain paste and glaze data from published sources

Appendix Table 5 - elemental compositional data of porcelain pastes, obtained from mounted sections using SEM-EDS (Tite and Bimson, Freestone, Middleton and Cowell, Ramsay) and SEM with EDS and WDS (Owen)

Ref	Paste	Sherd	SiO ₂	TiO ₂	Al ₂ O ₃	FeO	MgO	CaO	Na ₂ O	K ₂ O	P ₂ O ₅	PbO	SO ₂
Coalport (continued)													
Owen and Sandon (2003)	true porcelain	COAL16	75.20	<lod	20.80	0.20	0.20	0.50	0.40	2.20	0.20	<lod	<lod
Owen and Sandon (2003)	true porcelain	COAL17	74.30	<lod	19.70	0.20	0.20	0.90	1.40	2.70	0.50	<lod	<lod
Owen and Sandon (2003)	true porcelain	COAL19	73.80	<lod	22.30	0.20	0.20	0.50	0.30	2.10	0.20	<lod	<lod
Owen and Sandon (2003)	true porcelain	COAL23	74.20	<lod	19.30	0.20	0.20	1.20	1.30	2.70	0.80	<lod	<lod
Owen and Sandon (2003)	true porcelain	COAL25A	76.00	<lod	18.20	0.20	0.20	0.70	1.30	2.90	0.40	<lod	<lod
Owen and Sandon (2003)	true porcelain	COAL25B	74.00	<lod	17.60	0.20	0.20	2.30	1.40	2.50	1.60	<lod	<lod
Owen and Sandon (2003)	true porcelain	COAL26	74.60	<lod	18.30	0.20	0.20	1.50	1.40	2.60	1.00	<lod	<lod
Owen and Sandon (2003)	true porcelain	COAL28	74.10	<lod	19.10	0.20	0.20	1.30	1.40	2.50	1.00	<lod	<lod
Owen and Sandon (2003)	true porcelain	COAL30	71.50	<lod	17.80	0.20	0.20	3.50	1.30	2.60	2.70	<lod	<lod
Owen and Sandon (2003)	true porcelain	COAL31	75.40	<lod	18.70	0.10	0.10	1.20	1.10	2.40	0.70		
Cookworthy													
Owen et al (2000)	true porcelain	CK1	64.20	<lod	28.00	0.60	0.50	0.80	1.40	4.10	0.40	<lod	<lod
Owen et al (2000)	true porcelain	CK2	68.90	<lod	24.90	0.50	0.30	0.30	0.90	3.90	0.30	<lod	<lod
Derby													
Owen and Barkla (1997)	frit	I.1	79.90	0.20	2.70	0.20	0.20	2.70	0.20	1.80	1.60	11.10	0.10
Owen and Barkla (1997)	frit	I.2	70.00	0.20	4.00	0.30	0.20	9.50	0.30	2.30	<lod	13.10	<lod
Owen and Barkla (1997)	frit	I.50	71.00	0.10	4.10	0.20	0.30	6.80	0.20	2.60	0.30	13.50	0.90
Owen and Barkla (1997)	frit	II.4	71.10	0.10	3.50	0.30	1.20	6.40	0.20	2.30	2.60	12.30	<lod
Owen and Barkla (1997)	frit	II.7	70.30	0.20	3.50	0.30	0.30	1.40	0.30	2.50	2.50	18.20	0.40
Owen and Barkla (1997)	frit	II.9.1	72.50	0.10	3.80	0.20	0.30	4.70	0.20	2.70	0.40	14.70	0.20
Owen and Barkla (1997)	bone china	I.11	38.50	0.10	15.10	0.30	0.50	23.00	1.10	2.00	17.80	1.60	<lod
Owen and Barkla (1997)	phosphatic	II.1	51.50	0.50	10.00	0.40	0.60	19.90	0.80	0.80	14.20	1.40	<lod

Appendix 5: porcelain paste and glaze data from published sources

Appendix Table 5 - elemental compositional data of porcelain pastes, obtained from mounted sections using SEM-EDS (Tite and Bimson, Freestone, Middleton and Cowell, Ramsay) and SEM with EDS and WDS (Owen)

Ref	Paste	Sherd	SiO ₂	TiO ₂	Al ₂ O ₃	FeO	MgO	CaO	Na ₂ O	K ₂ O	P ₂ O ₅	PbO	SO ₂
Derby (continued)													
Owen and Barkla (1997)	phosphatic	II.2	47.90	0.40	9.80	0.30	0.60	21.10	0.80	0.70	16.20	2.30	<lod
Owen and Barkla (1997)	phosphatic	II.3	45.80	0.40	9.70	0.40	0.60	23.70	0.80	0.80	17.20	0.60	<lod
Owen and Barkla (1997)	phosphatic	II.5	47.70	0.40	9.70	0.40	0.60	21.30	0.90	0.70	16.60	1.60	<lod
Owen and Barkla (1997)	phosphatic	II.6	46.30	0.40	10.90	0.40	0.60	22.40	0.60	0.90	16.30	1.00	<lod
Owen and Barkla (1997)	phosphatic	II.8.1	42.00	0.50	10.40	0.50	0.60	23.10	0.70	2.30	18.80	0.90	<lod
Owen and Barkla (1997)	glassy	I.40	76.60	0.20	2.90	0.20	0.40	3.30	0.20	2.20	2.40	11.20	0.40
Owen and Barkla (1997)	glassy	I.45.3	81.00	0.10	3.70	0.20	0.10	0.10	0.20	2.40	0.20	11.70	0.10
Owen and Barkla (1997)	glassy	I.48	76.40	0.20	4.40	0.20	0.20	1.70	0.10	3.10	0.10	13.00	0.20
Grainger													
Owen (2003)	bone china	G1	42.10	<lod	17.50	0.30	0.50	19.80	1.40	2.50	15.80	<lod	<lod
Owen (2003)	true porcelain	G2	77.00	<lod	17.50	0.40	0.20	0.90	0.70	2.60	0.40	<lod	0.20
Owen (2003)	bone china	G3	40.50	<lod	16.90	0.20	0.50	21.20	1.50	2.30	17.00	<lod	<lod
Owen (2003)	true porcelain	G4	75.90	<lod	18.30	0.30	0.20	1.50	2.20	2.20	0.70	<lod	0.20
Isleworth													
Freestone et al (2003)	phosphatic	BM1	43.00	0.40	5.90	0.60	0.50	24.30	0.60	2.20	17.40	3.00	2.50
Freestone et al (2003)	phosphatic	BM2	36.80	0.30	7.40	0.30	0.70	28.10	0.90	2.40	17.30	4.20	2.10
Freestone et al (2003)	phosphatic	BM3	33.70	0.40	8.00	0.60	0.50	23.60	0.80	1.60	13.80	2.90	14.70
Freestone et al (2003)	phosphatic	BM4	36.90	0.30	8.20	0.30	0.70	27.90	0.70	1.90	18.10	2.80	2.50
Freestone et al (2003)	phosphatic	BM5	38.50	0.30	8.00	0.40	0.50	27.80	0.70	1.60	16.40	3.20	2.90
Freestone et al (2003)	phosphatic	BM6	37.30	0.40	8.30	0.40	0.80	28.20	0.90	1.80	17.20	3.10	2.30
Freestone et al (2003)	phosphatic	BM7	42.70	0.40	7.70	0.30	0.60	22.40	1.20	2.20	17.10	3.00	2.50
Freestone et al (2003)	phosphatic	BM8	37.20	0.40	8.80	0.40	0.60	25.40	0.70	2.30	18.20	3.60	2.90

Appendix 5: porcelain paste and glaze data from published sources

Appendix Table 5 - elemental compositional data of porcelain pastes, obtained from mounted sections using SEM-EDS (Tite and Bimson, Freestone, Middleton and Cowell, Ramsay) and SEM with EDS and WDS (Owen)

Ref	Paste	Sherd	SiO ₂	TiO ₂	Al ₂ O ₃	FeO	MgO	CaO	Na ₂ O	K ₂ O	P ₂ O ₅	PbO	SO ₂
Isleworth (continued)													
Freestone et al (2003)	phosphatic	BM9	49.30	0.60	6.10	0.40	0.40	20.40	0.60	1.80	14.80	3.20	2.60
Freestone et al (2003)	phosphatic	BM10	36.50	0.30	7.30	0.30	0.70	29.00	0.80	1.60	18.00	2.90	3.00
Freestone et al (2003)	phosphatic	BM11	41.10	0.30	5.60	0.40	0.40	26.60	0.60	2.60	18.70	2.20	2.00
Freestone et al (2003)	phosphatic	BM12	39.50	0.40	8.10	0.40	0.60	26.00	0.60	1.90	16.90	3.30	2.50
Freestone et al (2003)	phosphatic	BM13	46.90	0.40	7.50	0.50	0.50	20.80	0.60	2.20	14.10	3.80	2.90
Freestone et al (2003)	phosphatic	BM14	80.80	0.50	8.20	0.30	1.10	1.20	1.20	3.30	<0.2	3.30	<0.2
Limehouse													
Freestone (2000)	clay-rich	mean	72.40	0.80	10.70	0.50	0.70	7.10	2.80	3.00	<0.2	1.00	<0.2
Ramsay et al (2013)	Si-Al	1	76.10	0.70	16.00	0.50	0.20	0.50	0.70	1.30	0.10	3.80	0.10
Ramsay et al (2013)	Si-Al	2	78.10	1.00	16.90	0.70	0.20	0.40	0.60	1.40	0.20	<lod	0.30
Ramsay et al (2013)	Si-Al-Ca	3	73.30	0.50	10.70	0.50	1.00	6.70	2.50	2.90	0.30	1.20	<lod
Ramsay et al (2013)	Si-Al-Ca	4	72.50	0.80	10.80	0.70	1.00	6.20	2.50	3.30	0.10	1.30	<lod
Ramsay et al (2013)	Si-Al-Ca	5	74.80	0.40	11.60	0.20	<lod	6.80	2.70	2.70	<lod	1.30	<lod
Ramsay et al (2013)	Si-Al-Ca	6	71.80	0.50	12.20	0.20	0.60	8.10	3.30	3.00	<lod	0.30	<lod
Ramsay et al (2013)	Si-Al-Ca	7	73.60	<lod	12.70	<lod	<lod	7.50	3.00	3.00	<lod	<lod	<lod
Ramsay et al (2013)	Si-Al-Ca	8	74.40	0.20	10.80	1.00	0.70	7.70	2.00	3.10	<lod	<lod	<lod
Ramsay et al (2013)	Si-Al-Ca	9	73.70	0.60	12.30	0.30	0.30	7.00	2.70	2.00	0.20	0.20	<lod
Ramsay et al (2013)	Mg-P	10	62.00	<lod	3.10	0.20	12.50	8.80	3.70	2.70	6.70	<lod	0.50
Ramsay et al (2013)	Mg-P	11	69.60	<lod	2.70	<lod	9.40	9.80	1.00	1.70	4.70	0.38	<lod
Liverpool Brownlow Hill													
Owen and Hillis (2003)	phosphatic	BH1	58.90	0.40	9.70	0.50	0.50	15.70	0.70	1.80	11.70	<lod	<lod
Owen and Hillis (2003)	phosphatic	BH2	61.40	0.50	8.70	0.40	0.60	14.90	0.80	1.70	11.10	<lod	<lod

Appendix 5: porcelain paste and glaze data from published sources

Appendix Table 5 - elemental compositional data of porcelain pastes, obtained from mounted sections using SEM-EDS (Tite and Bimson, Freestone, Middleton and Cowell, Ramsay) and SEM with EDS and WDS (Owen)

Ref	Paste	Sherd	SiO ₂	TiO ₂	Al ₂ O ₃	FeO	MgO	CaO	Na ₂ O	K ₂ O	P ₂ O ₅	PbO	SO ₂
Liverpool Brownlow Hill (continued)													
Owen and Hillis (2003)	phosphatic	BH3	60.10	0.40	8.00	0.30	0.40	16.40	0.50	1.20	12.70	<lod	<lod
Owen and Hillis (2003)	phosphatic	BH4	55.20	0.30	6.40	0.30	0.40	18.80	0.70	2.40	15.50	<lod	<lod
Owen and Hillis (2003)	phosphatic	BH5	57.70	0.30	6.50	0.50	0.50	18.00	2.00	0.80	13.70	<lod	<lod
Owen and Hillis (2003)	phosphatic	BH6	58.80	0.40	9.70	0.40	0.50	15.90	0.60	1.80	11.80	<lod	<lod
Owen and Hillis (2003)	phosphatic	BH8	59.70	0.40	8.80	0.40	0.50	16.00	0.50	1.50	12.20	<lod	<lod
Owen and Hillis (2003)	phosphatic	BH9	61.10	0.40	8.30	0.30	0.40	25.60	0.50	1.20	12.10	<lod	<lod
Owen and Hillis (2003)	phosphatic	BH10	58.70	0.40	9.90	0.50	0.50	15.70	0.60	1.90	11.80	<lod	<lod
Owen and Hillis (2003)	phosphatic	BH11	55.90	0.30	6.80	0.50	0.50	18.70	1.80	1.10	14.30	<lod	<lod
Owen and Hillis (2003)	phosphatic	BH12	59.80	0.40	10.00	0.50	0.50	15.00	0.70	1.90	11.20	<lod	<lod
Owen and Hillis (2003)	phosphatic	BH13	51.00	0.20	5.80	0.40	0.50	22.70	1.10	2.00	16.20	<lod	<lod
Owen and Hillis (2003)	phosphatic	BH14	61.10	0.50	11.00	0.40	0.40	14.20	0.60	1.30	10.60	<lod	<lod
Owen and Hillis (2003)	phosphatic	BH16	57.80	0.20	6.00	0.50	0.60	18.10	1.90	1.10	13.80	<lod	<lod
Owen and Hillis (2003)	phosphatic	BH17	56.00	0.50	10.50	0.40	0.40	16.60	0.50	2.10	12.90	<lod	<lod
Owen and Hillis (2003)	phosphatic	BH21	57.60	0.30	5.90	0.30	0.50	28.50	0.70	1.00	15.00	<lod	<lod
Owen and Hillis (2003)	silicious aluminous	BH15	71.50	0.90	20.60	0.80	0.40	0.40	0.70	2.90	<lod	1.80	<lod
Liverpool Chaffers													
Owen and Sandon (1998)	phosphatic	LCP4	50.70	0.40	10.70	0.40	0.60	18.90	1.00	2.60	14.60	<lod	0.10
Owen and Sandon (1998)	magnesian	LCP1	75.70	0.10	2.60	0.40	8.30	2.00	1.20	2.00	0.20	7.40	0.10
Owen and Sandon (1998)	magnesian	LCP2	75.80	0.10	2.80	0.40	7.80	2.00	1.00	2.60	0.20	7.30	0.10
Owen and Sandon (1998)	magnesian	LCP3	75.90	0.10	2.90	0.40	7.90	1.40	1.30	2.50	0.30	7.20	0.20
Owen and Sandon (1998)	magnesian	LCP5	74.40	0.10	3.00	0.40	9.40	2.00	1.00	1.40	0.20	7.70	0.20

Appendix 5: porcelain paste and glaze data from published sources

Appendix Table 5 - elemental compositional data of porcelain pastes, obtained from mounted sections using SEM-EDS (Tite and Bimson, Freestone, Middleton and Cowell, Ramsay) and SEM with EDS and WDS (Owen)

Ref	Paste	Sherd	SiO ₂	TiO ₂	Al ₂ O ₃	FeO	MgO	CaO	Na ₂ O	K ₂ O	P ₂ O ₅	PbO	SO ₂
Liverpool Gillbody													
Owen and Sandon (1998)	phosphatic	LG1	59.40	0.40	8.60	0.30	0.40	16.80	0.50	1.00	12.70	<lod	<lod
Owen and Sandon (1998)	phosphatic	LG2	56.00	0.40	7.40	0.30	0.50	19.20	0.60	0.80	14.80	<lod	<lod
Owen and Sandon (1998)	phosphatic	LG3	55.60	0.50	8.70	0.40	0.50	18.40	0.50	1.10	14.30	<lod	<lod
Owen and Sandon (1998)	phosphatic	LG4	57.80	0.50	9.30	0.30	0.40	17.10	0.50	1.10	13.10	<lod	<lod
Liverpool Pennington													
Owen and Sandon (1998)	phosphatic	LP1	50.90	0.40	10.80	0.50	0.50	20.10	0.70	1.10	15.00	<lod	0.10
Owen and Sandon (1998)	phosphatic	LP2	46.50	0.50	11.60	0.50	0.60	21.50	0.80	1.10	16.70	<lod	0.10
Owen and Sandon (1998)	phosphatic	LP3	46.80	0.50	11.10	0.50	0.80	22.00	1.10	1.80	15.00	<lod	0.30
Owen and Sandon (1998)	phosphatic	LP4	51.60	0.50	11.90	0.50	0.50	19.80	0.70	1.30	13.00	<lod	0.10
Longton Hall													
Tite and Bimson (1991)	frit	E8	77.20	<lod	2.90	<lod	0.30	8.80	0.80	3.70	<lod	6.30	<lod
Tite and Bimson (1991)	frit	E9	62.90	0.20	3.20	0.30	0.30	194.00	<lod	1.90	1.90	9.90	<lod
Lowestoft													
Tite and Bimson (1991)	phosphatic	742	45.50	0.30	7.50	0.30	0.80	24.10	1.00	1.10	19.40	<lod	<lod
Tite and Bimson (1991)	phosphatic	E16	43.20	0.30	8.00	0.40	0.60	25.30	0.80	1.20	20.20	<lod	<lod
Owen (1998) i	phosphatic	mean	42.10	0.20	6.90	0.30	0.70	27.60	0.90	0.70	20.50	<lod	<lod
Nantgarw													
Tite and Bimson (1991)	phosphatic	N14-1	43.80	<lod	12.50	<lod	0.60	22.50	0.90	2.50	17.40	<lod	<lod
Tite and Bimson (1991)	phosphatic	N18-4	45.00	<lod	13.30	0.40	0.50	21.20	1.20	2.20	16.40	<lod	<lod
Tite and Bimson (1991)	phosphatic	N18-7	44.60	<lod	13.30	0.20	0.70	21.90	0.70	2.20	16.40	<lod	<lod
Owen et al (1998)	phosphatic	N1	43.90	<lod	12.50	0.20	0.40	23.00	0.40	2.30	17.30	<lod	<lod
Owen et al (1998)	phosphatic	N3	43.90	<lod	12.30	0.20	0.50	22.80	0.40	2.50	17.50	<lod	<lod

Appendix 5: porcelain paste and glaze data from published sources

Appendix Table 5 - elemental compositional data of porcelain pastes, obtained from mounted sections using SEM-EDS (Tite and Bimson, Freestone, Middleton and Cowell, Ramsay) and SEM with EDS and WDS (Owen)

Ref	Paste	Sherd	SiO ₂	TiO ₂	Al ₂ O ₃	FeO	MgO	CaO	Na ₂ O	K ₂ O	P ₂ O ₅	PbO	SO ₂
Nantgarw (continued)													
Owen et al (1998)	phosphatic	N5	45.00	<lod	13.00	0.20	0.40	22.50	0.40	2.20	16.90	<lod	<lod
Owen et al (1998)	phosphatic	N6	45.20	<lod	13.00	0.20	0.40	23.70	0.40	2.40	16.70	<lod	<lod
Owen et al (1998)	phosphatic	N7	42.80	<lod	13.00	0.30	0.50	22.80	0.40	2.30	17.90	<lod	<lod
Owen et al (1998)	phosphatic	N8	44.40	<lod	13.00	0.30	0.40	22.20	0.40	2.20	17.10	<lod	<lod
Owen et al (1998)	phosphatic	N9	43.70	<lod	12.30	0.20	0.40	23.60	0.40	1.20	18.20	<lod	<lod
Owen et al (1998)	phosphatic	N10	39.00	<lod	13.10	0.10	0.40	25.60	0.40	2.00	19.40	<lod	<lod
Owen and Morrison (1999)	phosphatic	N11	45.70	<lod	13.80	0.20	0.50	21.40	0.50	1.70	15.40	<lod	0.70
Owen and Morrison (1999)	phosphatic	N12	46.10	<lod	14.00	0.20	0.60	21.00	0.50	1.80	15.00	<lod	0.80
Owen and Morrison (1999)	phosphatic	N13	43.70	<lod	12.70	0.20	0.50	22.90	0.40	2.40	17.10	<lod	0.20
Owen and Morrison (1999)	phosphatic	N14-1	42.40	<lod	13.40	0.20	0.40	23.70	0.40	1.90	17.40	<lod	0.20
Owen and Morrison (1999)	phosphatic	N23	39.00	<lod	13.30	0.20	0.40	25.50	0.40	2.00	19.10	<lod	0.10
Owen and Morrison (1999)	phosphatic	N24	41.10	<lod	13.30	0.20	0.40	24.30	0.50	2.30	17.80	<lod	0.10
Owen and Morrison (1999)	phosphatic	N37	45.50	<lod	12.10	0.20	0.40	21.80	0.60	2.9	16.30	<lod	0.10
Owen and Morrison (1999)	silicious porcelain	N25	80.70	<lod	9.00	0.10	2.20	0.50	1.50	5.40	0.50	<lod	0.10
Owen and Morrison (1999)	silicious porcelain	N43	80.50	<lod	9.30	0.10	2.20	0.40	1.50	5.40	0.40	<lod	0.20
Owen and Morrison (1999)	silicious porcelain	N44	80.30	<lod	9.30	0.20	1.80	0.60	1.50	5.50	0.50	<lod	0.10
Royal Worcester													
Owen (2003)	phosphatic	W30	37.50	<lod	14.00	0.30	0.60	25.00	1.00	1.80	19.80	<lod	0.10
Owen (2003)	phosphatic	W31	31.90	<lod	13.90	0.20	0.60	27.70	1.40	1.70	22.40	<lod	<lod
Owen (2003)	phosphatic	W45	32.40	<lod	13.10	0.20	0.60	26.00	1.40	1.60	21.40	3.20	<lod
Owen (2003)	hybrid hard-paste	W34	76.00	<lod	18.30	0.30	0.30	1.80	0.80	1.80	0.50	<lod	0.10
Owen (2003)	hybrid hard-paste	W36	75.30	<lod	18.90	0.50	0.30	1.40	0.90	2.00	0.40	<lod	0.20

Appendix 5: porcelain paste and glaze data from published sources

Appendix Table 5 - elemental compositional data of porcelain pastes, obtained from mounted sections using SEM-EDS (Tite and Bimson, Freestone, Middleton and Cowell, Ramsay) and SEM with EDS and WDS (Owen)

Ref	Paste	Sherd	SiO ₂	TiO ₂	Al ₂ O ₃	FeO	MgO	CaO	Na ₂ O	K ₂ O	P ₂ O ₅	PbO	SO ₂
Swansea													
Owen et al (1998)	white glass	S1	68.00	<lod	8.20	0.10	0.20	9.70	10.90	2.50	<lod	<lod	0.20
Owen et al (1998)	silicious porcelain	S2	71.10	0.40	24.90	0.70	0.20	0.30	0.40	1.60	0.20	<lod	0.20
Owen et al (1998)	silicious porcelain	S3	73.80	0.40	21.60	0.80	0.20	0.30	0.60	1.60	0.20	<lod	0.40
Owen et al (1998)	silicious porcelain	S4	70.70	0.40	24.50	0.70	0.20	0.40	0.70	1.80	0.10	<lod	0.30
Owen et al (1998)	silicious porcelain	S5	70.50	0.40	25.10	0.70	0.20	0.30	0.50	1.70	0.20	<lod	0.30
Owen et al (1998)	silicious porcelain	S6	71.70	0.30	23.90	0.60	0.20	0.20	0.60	1.90	0.20	<lod	0.30
Owen et al (1998)	silicious porcelain	S7	73.60	0.40	22.10	0.60	0.20	0.30	0.60	1.70	0.20	<lod	0.30
Owen et al (1998)	silicious porcelain	S8	70.00	0.50	25.40	0.70	0.20	0.40	0.50	1.70	0.20	<lod	0.40
Owen et al (1998)	phosphatic	S9	42.50	<lod	20.00	0.30	0.40	16.70	1.40	2.80	13.00	<lod	0.10
Vauxhall													
Tite and Bimson (1991)	magnesian	739	78.20	<lod	4.40	0.50	10.00	2.10	1.50	3.00	<lod	0.30	<lod
Owen et al (2000)	magnesian	Vx5	75.60	0.10	3.40	0.60	9.10	2.10	1.70	2.80	0.20	3.90	0.10
Owen et al (2000)	magnesian	Vx1	70.80	0.10	2.70	0.60	7.50	9.10	0.80	3.90	1.40	2.70	0.20
Owen et al (2000)	magnesian	Vx2	72.10	0.10	3.00	0.30	8.20	9.60	0.90	4.30	0.20	0.60	0.50
Owen et al (2000)	magnesian	Vx4	68.80	0.10	2.70	0.70	7.80	9.10	1.00	4.80	0.20	4.20	0.30
Owen et al (2000)	phosphatic	Vx3	52.20	0.40	9.60	0.30	0.40	18.50	0.90	1.20	14.70	1.60	<lod
Worcester													
Tite and Bimson (1991)	magnesian	E26	74.10	0.30	3.80	0.40	10.80	1.90	1.00	2.80	<lod	4.90	<lod
Tite and Bimson (1991)	magnesian	E29	72.80	0.20	3.30	0.30	10.70	1.20	1.00	3.30	<lod	7.20	<lod
Tite and Bimson (1991)	magnesian	741	72.60	<lod	3.50	0.40	10.90	1.60	0.80	3.70	<lod	6.50	<lod
Owen (1997)	magnesian	W1	69.60	<lod	3.60	0.30	11.50	1.40	1.30	3.40	0.30	8.60	<lod
Owen (1997)	magnesian	W5	69.20	<lod	3.60	0.40	11.50	2.10	1.60	4.00	0.40	7.20	<lod

Appendix 5: porcelain paste and glaze data from published sources

Appendix Table 5 - elemental compositional data of porcelain pastes, obtained from mounted sections using SEM-EDS (Tite and Bimson, Freestone, Middleton and Cowell, Ramsay) and SEM with EDS and WDS (Owen)

Ref	Paste	Sherd	SiO ₂	TiO ₂	Al ₂ O ₃	FeO	MgO	CaO	Na ₂ O	K ₂ O	P ₂ O ₅	PbO	SO ₂
Worcester (continued)													
Owen (1997)	magnesian	W6	69.60	<lod	4.10	0.40	12.80	1.50	1.50	2.90	0.30	6.90	<lod
Owen (1997)	magnesian	W7	72.80	<lod	3.60	0.40	11.60	1.70	1.20	2.90	0.30	5.40	<lod
Owen (1997)	magnesian	W8	70.60	<lod	4.30	0.40	13.40	1.40	1.50	3.00	0.30	5.00	<lod
Owen (1997)	magnesian	W10	69.80	<lod	3.20	0.40	11.80	2.10	1.60	3.80	0.30	7.00	<lod
Owen (1997)	magnesian	W2	72.10	<lod	7.30	0.20	6.90	0.50	1.10	5.90	0.30	5.70	<lod
Owen (1997)	magnesian	W3	70.60	<lod	7.50	0.20	7.60	0.60	1.00	6.70	0.30	5.50	<lod
Owen (1997)	magnesian	W4	72.50	<lod	6.20	0.30	7.80	1.00	0.90	3.70	0.40	7.20	<lod
Owen (1998) ii	magnesian	W11	75.50	<lod	3.20	0.40	10.70	2.80	1.60	2.70	0.30	2.70	<lod
Owen (1998) ii	magnesian	W12	60.70	<lod	2.40	0.50	15.00	10.90	2.20	1.60	6.70	<lod	<lod
Owen (1998) ii	phosphatic	W13	79.30	<lod	3.80	0.50	0.50	6.00	0.60	3.40	4.60	0.90	0.40
Owen (1998) ii	phosphatic	W14	82.40	<lod	4.00	0.40	0.40	4.90	0.60	3.20	2.70	1.20	0.20
Owen (2003)	phosphatic	NW1	74.40	<lod	20.30	0.60	0.30	0.20	0.40	1.80	<lod	<lod	0.20
Owen (2003)	phosphatic	NW2	79.00	<lod	16.70	0.50	0.30	0.20	0.80	1.20	<lod	<lod	0.10
Owen (2003)	phosphatic	NW8	75.00	<lod	3.80	0.40	0.70	5.00	0.80	3.80	2.90	7.60	0.10
Owen (2003)	mangesian	W46	76.00	<lod	4.00	0.60	9.40	3.40	1.00	3.60	1.30	0.50	0.20
Owen (2003)	mangesian	W47	75.40	<lod	3.60	0.60	8.20	4.00	0.90	3.80	2.40	0.50	0.20
Owen (2003)	mangesian	W44E	70.10	<lod	3.50	0.60	6.80	3.20	1.20	4.10	1.90	8.30	0.40
Owen (2003)	mangesian	W44C	60.00	<lod	3.60	0.40	16.50	6.80	2.30	2.20	3.80	5.20	0.20
Owen (2003)	mangesian	NW3	62.50	<lod	5.20	0.80	8.20	2.80	1.20	1.90	0.10	17.10	0.10
Owen (2003)	mangesian	W40A	83.90	<lod	12.10	0.50	1.00	0.50	0.20	0.90	0.30	<lod	0.20
Owen (2003)	mangesian	W40C	54.80	<lod	21.00	6.20	2.20	0.60	0.70	4.10	0.30	7.90	0.30
Owen (2003)	mangesian	NW4	74.40	<lod	3.10	0.40	8.40	2.10	1.20	4.80	0.40	4.90	0.10

Appendix 5: porcelain paste and glaze data from published sources

Appendix Table 5 - elemental compositional data of porcelain pastes, obtained from mounted sections using SEM-EDS (Tite and Bimson, Freestone, Middleton and Cowell, Ramsay) and SEM with EDS and WDS (Owen)

Ref	Paste	Sherd	SiO ₂	TiO ₂	Al ₂ O ₃	FeO	MgO	CaO	Na ₂ O	K ₂ O	P ₂ O ₅	PbO	SO ₂
Worcester (continued)													
Owen (2003)	mangesian	NW5	74.70	<lod	3.80	0.50	9.30	3.10	1.00	3.50	0.60	3.40	<lod
Owen (2003)	mangesian	NW6	70.90	<lod	3.10	0.30	10.70	1.90	1.20	3.20	0.10	8.50	<lod
Owen (2003)	mangesian	NW9	76.00	<lod	2.00	0.20	9.90	2.10	0.40	2.30	1.10	5.90	<lod
Owen (2003)	mangesian	NW7	70.00	<lod	3.00	0.40	10.40	1.50	1.20	2.40	<lod	10.80	<lod
Owen (2003)	mangesian	W40B	72.20	<lod	3.50	0.40	12.20	2.50	1.60	2.50	0.40	4.30	0.30
Owen (2003)	mangesian	W44A	71.50	<lod	3.00	0.30	10.60	2.00	1.20	3.50	0.30	7.40	0.10
Owen (2003)	mangesian	W44B	73.10	<lod	3.00	0.30	9.30	1.80	1.00	3.90	0.40	7.00	0.20
Owen (2003)	mangesian	W44D	75.30	<lod	3.20	0.40	10.80	1.30	0.90	2.70	0.30	5.00	0.10
Owen (2003)	mangesian	W16	71.40	<lod	2.70	0.40	10.40	1.70	0.90	2.20	0.30	9.60	0.30
Owen (2003)	mangesian	W17	68.20	<lod	3.10	0.40	10.20	2.50	1.60	3.90	0.40	9.60	0.20
Owen (2003)	mangesian	W18	71.60	<lod	7.00	0.20	7.50	0.50	1.00	5.70	0.30	5.90	0.30
Owen (2003)	mangesian	W19A	74.70	<lod	6.40	0.40	8.30	1.40	0.80	3.50	0.60	3.60	0.20
Owen (2003)	mangesian	W19B	73.20	<lod	6.30	0.30	7.90	1.40	0.90	3.40	0.50	5.90	0.20
Owen (2003)	mangesian	W20	74.60	<lod	6.00	0.20	7.70	0.50	0.90	3.80	0.30	5.80	0.10
Owen (2003)	mangesian	W42	68.80	<lod	4.10	0.50	11.60	2.20	1.50	3.00	0.30	7.80	0.10
Owen (2003)	mangesian	W43	74.00	<lod	5.90	0.30	7.60	1.10	0.80	3.90	0.40	5.80	0.10
Owen (2003)	mangesian	W21	73.20	<lod	6.40	0.40	7.80	1.20	0.80	4.30	0.50	5.30	0.10
Owen (2003)	mangesian	W22	73.60	<lod	6.60	0.20	7.90	0.80	0.90	4.10	0.20	5.40	0.40
Owen (2003)	mangesian	W26	75.90	<lod	5.70	0.50	6.50	0.60	0.90	3.40	0.30	5.90	0.10
Owen (2003)	mangesian	W32	70.60	<lod	8.50	0.20	8.00	0.70	1.30	5.80	0.30	4.30	0.20
Owen (2003)	mangesian	W33	71.30	<lod	7.90	0.20	7.00	0.60	1.30	5.60	0.20	5.70	0.10
Owen (2003)	mangesian	W37	70.60	<lod	8.10	0.20	7.40	0.60	1.10	5.90	0.30	5.40	0.30
Owen (2003)	mangesian	W38	82.10	<lod	7.80	0.20	4.50	0.50	2.80	1.60	0.40	<lod	<lod
Owen (2003)	mangesian	W39	81.70	<lod	7.90	0.20	4.40	0.90	2.80	1.70	0.20	<lod	<lod

Appendix 5: porcelain paste and glaze data from published sources

Appendix Table 5 - elemental compositional data of porcelain pastes, obtained from mounted sections using SEM-EDS (Tite and Bimson, Freestone, Middleton and Cowell, Ramsay) and SEM with EDS and WDS (Owen)

Ref	Paste	Sherd	SiO ₂	TiO ₂	Al ₂ O ₃	FeO	MgO	CaO	Na ₂ O	K ₂ O	P ₂ O ₅	PbO	SO ₂
Worcester (continued)													
Owen (2003)	mangesian	W23	72.50	<lod	7.10	0.20	7.00	0.30	1.20	4.60	0.30	6.70	0.20
Owen (2003)	mangesian	W35	75.20	<lod	6.10	0.20	7.10	0.60	1.10	3.80	0.30	5.30	0.20
Owen (2003)	mangesian	W24	74.40	<lod	7.00	0.30	5.40	0.60	0.60	4.70	0.40	6.60	0.20
Owen (2003)	phosphatic	W25	27.90	<lod	11.50	0.20	0.60	31.60	1.20	1.40	25.50	<lod	<lod
Owen (2003)	phosphatic	W28	30.30	<lod	12.10	0.20	0.60	30.20	0.90	1.50	24.10	<lod	<lod
Owen (2003)	phosphatic	W29	44.10	<lod	14.90	0.30	0.40	20.80	1.20	2.00	16.10	<lod	<lod
Owen (2003)	mangesian	W41A	75.10	<lod	5.80	0.40	7.40	1.30	0.90	3.80	0.30	4.80	0.10
Owen (2003)	mangesian	W41B	71.30	<lod	3.20	0.40	9.70	2.00	1.30	3.30	0.30	8.20	0.20
Ramsay et al (2011)	mangesian	mean	71.00	<lod	3.80	<lod	12.20	1.70	1.50	3.40	0.30	5.80	<lod
Freestone (2000)	mangesian	mean	72.30	<lod	3.40	0.40	11.00	1.90	1.40	3.30	0.30	5.70	0.30

Appendix 5: porcelain paste and glaze data from published sources

Appendix Table 6 - elemental composition of porcelain glazes, obtained from powdered glaze (Ramsay and Gabszewicz; Ramsay et al; Tite and Bimson) and mounted sections (Owen et al; Middleton and Cowell)

Ref.	Paste	Sherd	SiO ₂	Al ₂ O ₃	FeO	MgO	CaO	PbO	Na ₂ O	K ₂ O	P ₂ O ₅	SO ₃
'A'-marked												
Ramsay and Gabszewicz (2003)	proto-porcelain	A-m 3	68.10	11.70	0.60	1.00	13.60	0.40	2.20	2.20	<lod	<lod
Bovey Tracey												
Owen et al (2000)	true porcelain	BT5	73.52	16.70	0.56	0.51	1.73	<lod	1.07	5.35	<lod	<lod
Owen et al (2000)	true porcelain	BT6	74.57	15.85	0.53	0.45	1.74	<lod	1.15	5.30	<lod	<lod
Owen et al (2000)	true porcelain	BT11	73.15	16.73	1.00	0.45	2.90	<lod	1.10	3.51	<lod	<lod
Owen et al (2000)	magnesian plombian	BT12	47.40	0.29	<lod	1.66	1.63	45.25	1.12	2.63	<lod	<lod
Owen et al (2000)	phosphatic	BT11	60.61	10.33	0.40	0.40	10.24	13.85	1.12	3.04	<lod	<lod
Owen et al (2000)	phosphatic	BT2	60.65	11.30	1.52	0.24	10.05	11.50	1.21	2.78	<lod	<lod
Owen et al (2000)	phosphatic	BT3	60.74	12.25	1.21	1.12	10.44	10.44	1.77	3.70	<lod	0.53
Owen et al (2000)	phosphatic	BT4	58.70	11.89	<lod	0.26	8.66	8.66	1.13	3.30	<lod	<lod
Bow												
Tite and Bimson (1991)	phosphatic	E10	37.20	0.90	<lod	<lod	0.70	55.80	0.60	4.80	<lod	<lod
Tite and Bimson (1991)	phosphatic	E12	43.30	1.10	0.40	<lod	1.10	46.10	0.60	4.70	<lod	<lod
Tite and Bimson (1991)	phosphatic	E14	42.20	0.60	0.50	<lod	0.90	48.70	0.50	4.10	<lod	<lod
Tite and Bimson (1991)	phosphatic	745	43.00	1.20	<lod	<lod	0.70	46.50	0.90	5.00	<lod	<lod
Ramsay et al (2011)	phosphatic	B30	38.51	0.16	0.11	<lod	3.27	53.03	0.26	1.29	2.21	1.07
Ramsay et al (2011)	phosphatic	B30	44.35	0.31	0.13	0.08	1.66	50.02	0.26	2.94	<lod	0.22
Ramsay et al (2011)	phosphatic	B41	50.99	1.19	0.07	0.48	0.50	41.39	0.81	4.43	<lod	<lod
Ramsay et al (2011)	phosphatic	B18	51.36	0.46	0.21	0.16	1.68	40.11	4.00	4.14	<lod	1.38
Ramsay et al (2011)	phosphatic	B30	38.51	0.16	0.11	<lod	3.27	53.03	0.26	1.29	2.21	1.07
Ramsay et al (2011)	phosphatic	B64	34.55	0.42	0.01	0.37	2.07	58.23	0.30	0.84	0.43	2.73
Ramsay et al (2011)	phosphatic	B68	46.43	<lod	0.06	0.75	3.29	44.74	1.34	2.00	0.03	1.39
Ramsay et al (2011)	phosphatic	B18	44.35	0.31	0.13	0.08	1.66	50.02	0.26	2.94	<lod	0.22

Appendix 5: porcelain paste and glaze data from published sources

Appendix Table 6 - elemental composition of porcelain glazes, obtained from powdered glaze (Ramsay and Gabszewicz; Ramsay et al; Tite and Bimson) and mounted sections (Owen et al; Middleton and Cowell)

Ref.	Paste	Sherd	SiO ₂	Al ₂ O ₃	FeO	MgO	CaO	PbO	Na ₂ O	K ₂ O	P ₂ O ₅	SO ₃
Bow (continued)												
Ramsay et al (2011)	phosphatic	B41	44.53	0.50	0.42	<lod	1.61	49.59	0.53	2.76	0.02	0.02
Ramsay et al (2011)	phosphatic	B11	45.78	0.12	0.07	<lod	1.03	47.56	0.12	3.81	0.14	1.38
Ramsay et al (2011)	phosphatic	B16	51.30	0.85	0.15	0.06	1.74	41.35	0.59	3.51	<lod	0.41
Ramsay et al (2011)	phosphatic	B20	42.53	0.92	0.14	0.27	0.26	50.62	0.31	4.57	<lod	0.39
Ramsay et al (2011)	phosphatic	B32	47.30	1.69	0.21	0.13	4.44	45.27	0.17	0.57	<lod	<lod
Ramsay et al (2011)	phosphatic	B33	39.33	0.17	0.08	0.32	3.42	50.61	0.61	2.44	2.86	0.16
Ramsay et al (2011)	phosphatic	B62	36.65	0.11	0.03	0.12	1.42	58.33	0.08	1.80	0.16	1.30
Ramsay et al (2011)	phosphatic	B66	43.31	0.44	0.39	<lod	1.58	49.50	<lod	1.00	<lod	3.79
Ramsay et al (2011)	phosphatic	B71	46.08	0.01	0.15	0.03	1.21	49.43	<lod	2.54	<lod	0.41
Ramsay et al (2011)	phosphatic	B73	46.84	1.04	0.20	0.59	2.92	44.63	0.85	1.32	<lod	1.60
Ramsay et al (2011)	phosphatic	B75	46.44	0.84	0.16	0.24	1.74	47.72	0.19	1.24	0.12	1.35
Ramsay et al (2011)	phosphatic	E10	37.20	0.90	<lod	<lod	0.70	55.80	0.60	4.80	<lod	<lod
Ramsay et al (2011)	phosphatic	B18	51.36	0.46	0.21	0.16	1.68	40.11	0.40	4.14	<lod	1.38
Ramsay et al (2011)	phosphatic	B3	48.63	0.79	0.05	<lod	1.67	43.24	0.59	4.00	0.19	0.90
Ramsay et al (2011)	phosphatic	B27	50.85	0.79	0.13	<lod	1.47	42.83	0.13	3.33	0.20	0.24
Ramsay et al (2011)	phosphatic	B41	50.99	1.19	0.07	0.48	0.50	41.39	0.81	4.43	<lod	<lod
Ramsay et al (2011)	phosphatic	B42	53.87	0.74	0.79	0.65	2.29	35.71	1.18	4.66	<lod	<lod
Ramsay et al (2011)	phosphatic	B61	46.67	0.60	0.15	0.04	4.00	44.51	0.61	2.13	0.08	1.16
Ramsay et al (2011)	phosphatic	B77	49.05	0.60	0.11	0.40	0.72	44.23	0.32	2.58	<lod	1.83
Ramsay et al (2011)	phosphatic	E12	43.30	1.10	0.40	<lod	1.10	46.10	0.60	4.70	<lod	<lod
Ramsay et al (2011)	phosphatic	E14	42.20	0.60	0.50	<lod	0.90	48.70	0.50	4.10	<lod	<lod
Ramsay et al (2011)	phosphatic	745	43.00	1.20	<lod	<lod	0.70	46.50	0.90	5.00	<lod	<lod

Appendix 5: porcelain paste and glaze data from published sources

Appendix Table 6 - elemental composition of porcelain glazes, obtained from powdered glaze (Ramsay and Gabszewicz; Ramsay et al; Tite and Bimson) and mounted sections (Owen et al; Middleton and Cowell)

Ref.	Paste	Sherd	SiO ₂	Al ₂ O ₃	FeO	MgO	CaO	PbO	Na ₂ O	K ₂ O	P ₂ O ₅	SO ₃
Bristol												
Tite and Bimson (1991)	true porcelain	E2	71.10	16.80	0.50	2.30	3.60	<lod	1.50	4.20	<lod	<lod
Ramsay et al (2011)	magnesian plombian	sauceboat	55.80	5.00	<lod	1.50	2.00	28.00	4.20	3.20	<lod	<lod
Ramsay et al (2011)	magnesian plombian	pickle dish	49.30	3.00	<lod	1.70	1.50	40.00	0.30	3.80	0.30	<lod
Ramsay et al (2011)	magnesian plombian	ivy leaf pickle dish	52.30	4.00	0.30	1.70	1.00	35.00	0.30	5.30	0.30	<lod
Ramsay et al (2011)	magnesian plombian	pickle dish	58.60	6.00	0.10	1.30	3.00	23.20	3.70	4.00	0.10	<lod
Ramsay et al (2011)	magnesian plombian	Lu Tung Pin	60.50	3.50	<lod	3.00	0.50	25.50	1.00	5.50	<lod	<lod
Ramsay et al (2011)	magnesian plombian	sauceboat	58.30	4.20	<lod	2.70	1.00	27.70	1.20	5.00	<lod	<lod
Caughley												
Owen and Sandon (2003)	magnesian plombian	CY9	63.37	5.81	<lod	2.45	1.06	22.83	0.69	2.63	<lod	1.55
Owen and Sandon (2003)	magnesian plombian	CY7	61.15	5.70	<lod	2.78	1.21	21.37	2.88	3.42	<lod	1.35
Owen and Sandon (2003)	magnesian plombian	CY10	58.99	6.16	0.54	1.57	1.05	28.53	0.90	2.68	<lod	<lod
Owen and Sandon (2003)	magnesian plombian	CY11	65.91	5.62	<lod	3.49	1.48	19.56	0.91	2.84	<lod	1.04
Owen and Sandon (2003)	magnesian plombian	CY19	62.59	5.08	<lod	3.04	<lod	19.42	1.48	3.42	<lod	0.70
Owen and Sandon (2003)	magnesian plombian	CY20	63.68	6.14	0.37	2.85	1.22	20.42	1.33	3.23	<lod	1.07
Owen and Sandon (2003)	true porcelain	CY5	54.00	8.81	<lod	<lod	0.42	25.58	2.77	3.62	<lod	1.79
Owen and Sandon (2003)	true porcelain	CY6	49.50	5.14	<lod	0.27	0.79	40.68	1.70	1.91	<lod	1.72
Owen and Sandon (2003)	true porcelain	CY12	52.25	6.98	<lod	<lod	0.79	33.73	0.97	2.58	<lod	2.08
Owen and Sandon (2003)	true porcelain	CY21	41.82	10.77	<lod	<lod	0.34	43.54	0.99	1.35	<lod	<lod
Chelsea												
Tite and Bimson (1991)	phosphatic	E15	47.80	0.50	0.40	<lod	2.30	43.10	0.90	5.00	<lod	<lod
Tite and Bimson (1991)	frit	746	47.30	0.90	<lod	<lod	2.80	43.70	1.00	3.50	<lod	<lod

Appendix 5: porcelain paste and glaze data from published sources

Appendix Table 6 - elemental composition of porcelain glazes, obtained from powdered glaze (Ramsay and Gabszewicz; Ramsay et al; Tite and Bimson) and mounted sections (Owen et al; Middleton and Cowell)

Ref.	Paste	Sherd	SiO ₂	Al ₂ O ₃	FeO	MgO	CaO	PbO	Na ₂ O	K ₂ O	P ₂ O ₅	SO ₃
Coalport												
Owen and Sandon (2003)	true porcelain	COAL17	53.30	8.85	<lod	<lod	0.94	30.75	1.60	2.53	<lod	1.39
Owen and Sandon (2003)	true porcelain	COAL23	51.20	8.78	<lod	<lod	1.08	33.30	2.02	3.06	<lod	1.20
Owen and Sandon (2003)	phosphatic	COAL3	46.21	5.44	<lod	<lod	2.16	43.98	1.01	2.11	<lod	<lod
Owen and Sandon (2003)	phosphatic	COAL15	51.62	5.63	<lod	<lod	3.67	33.74	0.71	1.56	<lod	<lod
Owen and Sandon (2003)	phosphatic	COAL21	57.48	15.06	<lod	0.22	10.53	3.58	1.47	4.96	<lod	1.26
Owen and Sandon (2003)	phosphatic	COAL33	45.28	4.91	<lod	<lod	2.90	38.82	1.21	2.54	<lod	<lod
Derby												
Owen and Barkla (1997)	frit	I.1	40.92	0.74	<lod	0.47	2.66	50.96	0.46	2.75	<lod	<lod
Owen and Barkla (1997)	frit	II.7	42.43	0.85	<lod	0.42	2.52	50.51	0.44	3.55	<lod	<lod
Owen and Barkla (1997)	frit	II.9.1	47.38	1.22	<lod	0.38	3.52	44.57	0.34	3.28	<lod	<lod
Owen and Barkla (1997)	phosphatic	II.8.1	44.90	1.07	<lod	0.53	3.47	47.80	0.37	2.13	<lod	<lod
Grainger												
Owen, J V (2003)	phosphatic	G1	53.85	6.22	<lod	<lod	3.40	10.55	0.67	1.28	<lod	<lod
Owen, J V (2003)	phosphatic	G3	60.05	9.61	<lod	0.34	4.52	<lod	0.87	1.65	<lod	1.21
Owen, J V (2003)	true porcelain	G4	51.63	8.34	<lod	<lod	3.38	13.82	0.75	1.20	<lod	1.46
Freestone et al (2003)	bone ash	BM1	47.3	0.8	0.1	<0.1	1.0	41.2	1.1	4.8	<0.2	3.3
Freestone et al (2003)	bone ash	BM2	49.4	1.8	<0.1	<0.1	1.3	39.5	1.6	5.5	<0.2	0.8
Freestone et al (2003)	bone ash	BM4	46.6	1.7	0.1	0.1	0.8	41.3	1.9	6.8	<0.2	0.2
Freestone et al (2003)	bone ash	BM6	49.6	1.6	0.1	<0.1	0.7	40.0	1.2	6.4	<0.2	0.2
Freestone et al (2003)	bone ash	BM7	50.0	1.9	0.2	<0.1	0.6	39.9	1.4	5.9	<0.2	<0.1
Freestone et al (2003)	bone ash	BM8	47.2	2.4	0.1	<0.1	1.0	41.9	1.0	5.3	<0.2	<0.1

Appendix 5: porcelain paste and glaze data from published sources

Appendix Table 6 - elemental composition of porcelain glazes, obtained from powdered glaze (Ramsay and Gabszewicz; Ramsay et al; Tite and Bimson) and mounted sections (Owen et al; Middleton and Cowell)

Ref.	Paste	Sherd	SiO ₂	Al ₂ O ₃	FeO	MgO	CaO	PbO	Na ₂ O	K ₂ O	P ₂ O ₅	SO ₃
Isleworth												
Freestone et al (2003)	bone ash	BM9	49.1	0.4	0.2	0.1	1.2	39.0	1.4	6.4	0.2	<0.1
Freestone et al (2003)	bone ash	BM11	49.5	1.0	0.1	<0.1	1.3	40.7	1.5	5.7	<0.2	<0.1
Freestone et al (2003)	bone ash	BM12	48.9	1.6	n.d.	<0.1	1.4	41.2	1.3	5.4	<0.2	<0.1
Freestone et al (2003)	bone ash	BM13	49.4	0.3	0.1	<0.1	1.6	40.8	1.6	5.8	n.d.	0.2
Limehouse												
Owen and Hillis (2003)	phosphatic	LHOUSE1	72.70	4.30	0.50	2.40	11.00	<lod	4.90	3.90	-	<lod
Owen and Hillis (2003)	phosphatic	LHOUSE2	73.50	5.40	0.50	2.20	7.70	0.50	5.10	4.00	-	<lod
Owen and Hillis (2003)	SAC	LHOUSE3	48.20	6.70	0.40	1.10	4.70	30.60	3.00	2.50	<lod	<lod
Tite and Bimson (1991)	magnesian	743	54.20	4.40	<lod	3.00	1.20	30.40	3.50	3.30	<lod	<lod
Liverpool factories – Brownlow Hill												
Owen and Hillis (2003)	phosphatic	BH1	55.08	5.40	0.43	0.57	7.59	27.50	0.49	1.67	<lod	0.76
Owen and Hillis (2003)	phosphatic	BH2	56.71	4.43	2.40	0.16	2.26	28.50	0.59	2.97	<lod	0.52
Owen and Hillis (2003)	phosphatic	BH3	47.97	1.26	0.59	1.90	5.32	35.20	1.52	3.12	<lod	0.49
Owen and Hillis (2003)	phosphatic	BH4	46.69	1.34	<lod	0.35	4.67	43.95	0.64	2.35	<lod	<lod
Owen and Hillis (2003)	phosphatic	BH8	49.90	5.28	0.30	0.48	4.33	35.59	0.62	2.69	<lod	0.53
Owen and Hillis (2003)	phosphatic	BH9	49.95	1.33	0.41	1.61	3.90	36.49	0.83	2.46	<lod	0.74
Owen and Hillis (2003)	phosphatic	BH10	53.69	4.31	0.55	0.74	5.75	32.40	0.56	1.98	<lod	0.51
Owen and Hillis (2003)	phosphatic	BH11	47.59	1.62	0.36	1.39	4.31	40.01	1.79	1.81	<lod	0.50
Owen and Hillis (2003)	phosphatic	BH12	54.12	4.44	0.34	0.55	5.12	31.04	0.58	2.83	<lod	<lod
Owen and Hillis (2003)	phosphatic	BH14	46.57	1.14	0.27	1.28	2.65	40.69	1.41	4.02	<lod	<lod
Owen and Hillis (2003)	phosphatic	BH21	44.94	0.94	<lod	<lod	3.61	48.43	0.61	1.93	<lod	<lod

Appendix 5: porcelain paste and glaze data from published sources

Appendix Table 6 - elemental composition of porcelain glazes, obtained from powdered glaze (Ramsay and Gabszewicz; Ramsay et al; Tite and Bimson) and mounted sections (Owen et al; Middleton and Cowell)

Ref.	Paste	Sherd	SiO ₂	Al ₂ O ₃	FeO	MgO	CaO	PbO	Na ₂ O	K ₂ O	P ₂ O ₅	SO ₃
Liverpool factories – Brownlow Hill (continued)												
Owen and Hillis (2003)	SAC	BH7	60.94	1.11	<lod	0.23	2.48	31.94	0.38	0.92	<lod	<lod
Owen and Hillis (2003)	SAC	BH18	53.71	1.94	<lod	<lod	2.06	35.82	1.06	1.53	<lod	<lod
Owen and Hillis (2003)	SAC	BH20	45.29	0.56	<lod	<lod	1.32	48.51	0.51	3.82	<lod	<lod
Liverpool factories – Chaffers												
Owen and Sandon (1998)	magnesian plombian	LCP2 in	51.69	2.50	<lod	1.99	0.33	40.42	0.88	2.92	<lod	<lod
Owen and Sandon (1998)	magnesian plombian	LPC2 mid	50.25	3.42	<lod	1.95	0.46	39.88	1.22	3.62	<lod	<lod
Owen and Sandon (1998)	magnesian plombian	LCP2 out	47.86	2.86	<lod	2.31	0.43	42.32	1.14	3.38	<lod	<lod
Owen and Sandon (1998)	magnesian plombian	LCP5 in	50.99	2.18	2.31	2.51	0.64	35.34	1.07	4.33	<lod	<lod
Owen and Sandon (1998)	magnesian plombian	LCP5 mid	50.85	2.06	1.94	2.26	0.76	37.94	1.16	3.97	<lod	<lod
Owen and Sandon (1998)	magnesian plombian	LCP5 out	50.41	4.36	0.56	0.85	0.58	36.30	1.23	4.52	<lod	<lod
Liverpool factories - Gilbody												
Owen and Sandon (1998)	phosphatic	LG1 in	47.65	0.80	<lod	0.46	1.32	44.91	0.75	4.55	<lod	<lod
Owen and Sandon (1998)	phosphatic	LG1 mid	50.13	0.47	<lod	0.56	1.36	44.03	0.73	4.57	<lod	<lod
Owen and Sandon (1998)	phosphatic	LG1 out	47.00	0.37	<lod	0.33	0.95	45.81	0.57	4.80	<lod	0.98
Liverpool factories – Pennington												
Owen and Sandon (1998)	phosphatic	LP3 in	49.04	5.80	<lod	<lod	3.39	36.61	0.80	3.46	<lod	<lod
Owen and Sandon (1998)	phosphatic	LP3 mid	46.63	4.09	<lod	<lod	1.63	45.05	0.71	2.92	<lod	<lod
Owen and Sandon (1998)	phosphatic	LP3 out	45.10	3.40	<lod	0.32	1.60	46.87	0.86	2.58	<lod	<lod
Longton Hall												
Tite and Bimson (1991)	frit	E8	62.30	1.90	<lod	0.60	5.50	18.00	2.00	7.10	<lod	<lod
Tite and Bimson (1991)	frit	E9	42.10	0.50	<lod	0.80	2.90	45.90	0.50	4.20	<lod	<lod
Middleton and Cowell (1993)	frit	929	41.40	<lod	<lod	<lod	1.90	47.50	0.40	4.00	<lod	0.60

Appendix 5: porcelain paste and glaze data from published sources

Appendix Table 6 - elemental composition of porcelain glazes, obtained from powdered glaze (Ramsay and Gabszewicz; Ramsay et al; Tite and Bimson) and mounted sections (Owen et al; Middleton and Cowell)

Ref.	Paste	Sherd	SiO ₂	Al ₂ O ₃	FeO	MgO	CaO	PbO	Na ₂ O	K ₂ O	P ₂ O ₅	SO ₃
Longton Hall (continued)												
Middleton and Cowell (1993)	frit	931	51.90	1.40	<lod	0.50	11.10	25.10	0.90	3.70	1.00	0.60
Middleton and Cowell (1993)	frit	888	51.70	0.60	<lod	<lod	6.30	30.00	0.70	5.10	<lod	0.50
Middleton and Cowell (1993)	frit	914	53.20	1.50	<lod	0.50	9.70	27.00	1.00	4.10	1.00	0.90
Lowestoft												
Tite and Bimson (1991)	phosphatic	742	40.70	1.40	<lod	0.50	1.70	51.40	0.90	2.80	<lod	<lod
Tite and Bimson (1991)	phosphatic	E16	43.50	1.60	<lod	<lod	2.00	47.60	0.80	3.70	<lod	<lod
Nantgarw												
Tite and Bimson (1991)	phosphatic	N14-1	60.00	12.90	0.40	0.30	11.00	11.10	0.70	3.30	0.30	<lod
Tite and Bimson (1991)	phosphatic	N18-1	61.60	11.30	0.50	0.40	8.80	12.80	0.70	2.30	0.80	<lod
Tite and Bimson (1991)	phosphatic	N18-7	62.60	11.40	<lod	0.30	10.40	11.30	0.70	2.10	1.20	<lod
Owen and Morrison (1999)	SAC	N25	67.84	6.99	<lod	2.87	1.05	15.44	1.08	4.30	0.42	<lod
Owen and Morrison (1999)	SAC	N43	65.99	6.34	<lod	1.64	0.87	14.96	2.74	6.12	0.34	<lod
Owen and Morrison (1999)	SAC	N44	68.34	7.36	<lod	2.59	0.87	14.39	1.29	5.16	<lod	<lod
Pomona												
Owen and Hillis (2003)	SAC	POMONA1	48.43	6.61	<lod	<lod	1.32	38.50	0.59	2.98	<lod	0.93
Owen and Hillis (2003)	SAC	POMONA2	28.98	1.31	0.59	0.59	0.51	46.24	0.49	<lod	<lod	0.43
Plymouth - Cookworthy												
Tite and Bimson (1991)	true porcelain	744	78.10	11.80	0.60	1.80	2.70	<lod	1.00	4.00	<lod	<lod
Owen, Adams and Stephenson (2000)	true porcelain	Ck1	80.00	11.11	0.82	1.33	0.80	<lod	1.32	4.60	<lod	<lod
Owen, Adams and Stephenson (2000)	true porcelain	Ck2	77.75	13.56	0.82	0.67	0.71	<lod	1.08	5.98	<lod	<lod

Appendix 5: porcelain paste and glaze data from published sources

Appendix Table 6 - elemental composition of porcelain glazes, obtained from powdered glaze (Ramsay and Gabszewicz; Ramsay et al; Tite and Bimson) and mounted sections (Owen et al; Middleton and Cowell)

Ref.	Paste	Sherd	SiO ₂	Al ₂ O ₃	FeO	MgO	CaO	PbO	Na ₂ O	K ₂ O	P ₂ O ₅	SO ₃
Royal Worcester												
Owen (2003)	phosphatic plombian	W31	57.46	14.72	<lod	0.20	10.17	0.61	1.81	4.94	<lod	<lod
Owen (2003)	true porcelain	W36	49.96	11.98	0.55	<lod	6.28	24.31	1.05	2.20	<lod	<lod
Owen (2003)	phosphatic	W45	50.74	11.99	0.45	0.29	9.75	16.89	1.55	3.25	<lod	1.30
Swansea												
Owen et al (1998)	phosphatic	S9 out	64.50	8.17	0.45	0.28	7.11	13.32	0.54	2.63	0.35	<lod
Owen et al (1998)	phosphatic	S9 in	59.93	10.19	0.37	0.29	8.61	13.63	0.73	2.83	0.45	0.41
Vauxhall												
Tite and Bimson (1991)	magnesian plombian	739	63.90	1.60	0.40	3.40	3.00	14.00	5.40	4.20	<lod	<lod
Tite and Bimson (1991)	magnesian plombian	738	60.30	1.40	0.30	2.80	6.40	14.30	2.10	8.30	0.60	<lod
Owen, Adams and Stephenson (2000)	magnesian plombian	Vx5	64.07	0.68	<lod	3.00	4.43	17.05	5.62	4.38	<lod	0.76
Owen, Adams and Stephenson (2000)	magnesian plombian	Vx4	57.95	1.37	0.39	4.04	6.00	20.05	2.40	7.12	<lod	<lod
Owen, Adams and Stephenson (2000)	phosphatic	Vx3	50.13	0.98	0.97	1.26	5.33	5.33	0.84	1.29	<lod	<lod
West Pans												
Middleton and Cowell (1993)	frit	936	53.00	0.60	<lod	0.50	4.80	34.20	0.50	5.10	0.30	0.70
Middleton and Cowell (1993)	frit	937	53.00	0.30	<lod	0.30	6.00	33.30	0.60	4.90	0.40	0.90
Middleton and Cowell (1993)	frit	940	48.90	<lod	<lod	<lod	3.40	39.80	0.40	6.30	<lod	0.70
Worcester												
Tite and Bimson (1991)	magnesian plombian	E26	52.70	3.80	0.50	2.80	1.00	33.80	1.60	3.00	<lod	<lod
Tite and Bimson (1991)	magnesian plombian	E29	55.60	3.60	0.40	4.20	1.00	28.30	1.40	4.50	<lod	<lod
Tite and Bimson (1991)	magnesian plombian	741	52.30	4.10	0.30	2.60	0.90	33.30	1.50	4.50	<lod	<lod
Owen and Hillis (2003)	SAC	W15 out	42.44	9.25	0.19	0.07	<lod	47.08	0.13	0.84	<lod	<lod
Owen and Hillis (2003)	SAC	NW1	40.18	8.60	0.53	0.15	0.18	48.77	0.26	0.66	-	<lod

Appendix 5: porcelain paste and glaze data from published sources

Appendix Table 6 - elemental composition of porcelain glazes, obtained from powdered glaze (Ramsay and Gabszewicz; Ramsay et al; Tite and Bimson) and mounted sections (Owen et al; Middleton and Cowell)

Ref.	Paste	Sherd	SiO ₂	Al ₂ O ₃	FeO	MgO	CaO	PbO	Na ₂ O	K ₂ O	P ₂ O ₅	SO ₃
Worcester (continued)												
Owen (2003)	magnesian plombian	W16	53.01	3.59	<lod	3.30	1.25	33.24	1.09	3.81	<lod	<lod
Owen (2003)	magnesian plombian	W17	49.92	3.02	1.08	3.12	1.46	29.96	1.24	4.02	<lod	<lod
Owen (2003)	magnesian plombian	W18	49.34	4.86	<lod	1.26	0.41	38.60	1.08	4.89	<lod	<lod
Owen (1997)	hybrid magnesian phosphatic	W5	49.88	3.51	0.92	1.52	0.84	36.46	1.60	3.67	<lod	<lod
Owen (1997)	hybrid magnesian phosphatic	W7	47.73	2.68	0.47	2.07	0.94	40.58	1.58	2.69	<lod	<lod
Owen (1997)	hybrid magnesian phosphatic	W10	51.33	3.19	0.43	2.39	0.85	37.52	0.87	2.96	<lod	<lod
Owen (1998)	magnesian plombian	W11 out	51.70	3.88	<lod	2.53	0.97	38.50	0.88	2.21	<lod	<lod
Owen (1998)	magnesian plombian	W11 mid	52.64	4.59	<lod	2.23	2.41	37.00	0.85	2.41	<lod	0.77
Owen (1998)	magnesian plombian	W11 in	51.85	3.94	<lod	1.86	0.77	38.40	0.84	2.36	<lod	0.76
Owen (1998)	magnesian plombian	W12 out	52.13	3.88	<lod	1.35	0.80	37.93	1.10	2.53	<lod	<lod
Owen (1998)	magnesian plombian	W12 mid	49.42	2.71	<lod	2.65	1.34	39.03	1.25	2.60	<lod	1.16
Owen (1998)	magnesian plombian	W12 in	53.68	3.68	<lod	4.87	3.06	30.70	1.46	3.60	<lod	0.92
Owen (1998)	phosphatic	W13 out	44.69	7.51	<lod	0.22	<lod	47.32	<lod	0.67	<lod	<lod
Owen (1998)	phosphatic	W13 mid	41.68	8.74	0.56	<lod	<lod	50.23	<lod	0.67	<lod	<lod
Owen (1998)	phosphatic	W13 in	42.24	11.78	<lod	<lod	<lod	45.10	0.40	1.20	<lod	<lod
Owen (2003)	stone china	NW1	40.18	8.60	0.53	0.15	0.18	48.77	0.26	0.66	<lod	<lod
Owen (2003)	magnesian plombian	W46	47.24	3.69	<lod	1.93	0.78	41.26	0.78	2.78	<lod	1.45
Owen (2003)	magnesian plombian	W47	55.14	3.24	0.37	3.64	1.72	26.63	0.09	4.37	1.05	<lod
Owen (2003)	magnesian plombian	W44E	51.14	3.54	0.51	2.37	0.76	34.53	0.71	3.32	<lod	1.20
Owen (2003)	magnesian plombian	NW4	57.47	5.39	0.32	2.50	0.92	26.86	0.76	4.70	<lod	<lod
Owen (2003)	magnesian plombian	NW5	66.68	4.59	0.49	7.08	0.76	14.72	1.00	4.21	<lod	<lod
Owen (2003)	magnesian plombian	NW6	53.98	3.14	0.15	3.78	1.15	32.87	0.98	2.93	0.10	0.45

Appendix 5: porcelain paste and glaze data from published sources

Appendix Table 6 - elemental composition of porcelain glazes, obtained from powdered glaze (Ramsay and Gabszewicz; Ramsay et al; Tite and Bimson) and mounted sections (Owen et al; Middleton and Cowell)

Ref.	Paste	Sherd	SiO ₂	Al ₂ O ₃	FeO	MgO	CaO	PbO	Na ₂ O	K ₂ O	P ₂ O ₅	SO ₃
Worcester (continued)												
Owen (2003)	magnesian plombian	NW7	53.16	3.40	<lod	3.79	1.26	33.23	1.43	3.31	<lod	<lod
Owen (2003)	magnesian plombian	NW9	56.16	3.68	0.14	2.93	1.13	30.34	0.52	4.58	0.24	<lod
Owen (1997)	hybrid magnesian phosphatic	W3	52.58	4.51	<lod	0.48	0.28	35.36	0.53	4.01	<lod	<lod
Owen (1997)	hybrid magnesian phosphatic	W4	52.85	3.50	0.81	1.35	0.65	33.85	1.44	3.76	<lod	<lod
Owen (2003)	magnesian plombian	W21	55.72	3.92	0.68	4.58	0.49	23.93	0.51	4.15	<lod	<lod
Owen (2003)	magnesian plombian	W22	51.95	4.08	<lod	1.93	0.70	34.78	0.93	4.05	<lod	<lod
Owen (2003)	magnesian plombian	W26	54.39	4.82	<lod	2.61	0.42	31.36	0.94	5.04	<lod	<lod
Owen (2003)	magnesian plombian	W37	43.69	3.83	<lod	0.77	<lod	47.99	0.73	2.95	<lod	<lod
Owen (2003)	magnesian plombian	W23	49.84	4.51	0.41	1.62	1.07	38.44	3.75	<lod	<lod	1.01
Owen (2003)	magnesian plombian	W24	45.57	3.56	<lod	0.84	0.70	44.08	0.92	3.88	<lod	<lod
Owen (2003)	phosphatic	W25	51.31	3.74	0.94	1.92	0.38	35.58	1.04	3.97	<lod	<lod
Owen (2003)	phosphatic	W25	55.50	11.15	<lod	<lod	7.06	14.05	1.01	3.55	<lod	<lod
Owen (1997)	hybrid magnesian phosphatic	W9B	45.67	3.40	<lod	2.88	1.28	44.02	0.54	1.97	<lod	<lod
Owen (2003)	magnesian plombian	W44A	41.75	2.55	0.79	1.15	0.80	44.96	0.50	3.01	<lod	1.38
Owen (2003)	magnesian plombian	W44B	54.16	3.50	0.39	3.41	1.28	30.64	0.77	4.06	<lod	1.72
Owen (2003)	magnesian plombian	W44D	58.00	4.83	0.35	1.96	0.63	26.89	0.74	3.81	<lod	1.75
Owen (2003)	magnesian plombian	W43	59.53	4.19	<lod	1.02	0.46	27.63	0.76	4.01	<lod	1.71
Worcester - Chamberlain												
Owen (2003)	true porcelain	CW1	56.44	5.90	0.45	0.40	1.39	32.05	1.00	3.30	<lod	<lod
Owen (2003)	true porcelain	CW2	58.52	8.92	<lod	0.29	1.13	24.08	0.65	3.85	<lod	<lod

A.6 Sample catalogue

Session	Sample	Factory	object type	assigned date	Image
2013-08-12	927 Marshall Collection, Ashmolean Museum	Worcester	teapot and lid	later (C19th)	
2013-08-12	929 Marshall Collection, Ashmolean Museum	Worcester	tureen, lid, stand, ladle	1768-72	
2013-08-12	930 Marshall Collection, Ashmolean Museum	Worcester	vase	1770-72	
2013-08-12	932 Marshall Collection, Ashmolean Museum	Worcester	knife and fork	~1775	
2013-08-12	934 Marshall Collection, Ashmolean Museum	Worcester	mug	~1770	
2013-08-12	1005 Marshall Collection, Ashmolean Museum	Worcester	cake plate	1775-80	

Appendix 6: Sample catalogue

Session	Sample	Factory	object type	assigned date	Image
2013-08-12	1006 Marshall Collection, Ashmolean Museum	Worcester	coffee cup	~1770	
2013-08-12	1010 Marshall Collection, Ashmolean Museum	Worcester	dessert dish	~1770	no image available
2013-08-12	1012 Marshall Collection, Ashmolean Museum	Worcester	tea bowl and saucer	1780-85	
2013-08-12	1014 Marshall Collection, Ashmolean Museum	Worcester	plate	later (C19th)	
2013-08-12	1016 Marshall Collection, Ashmolean Museum	Worcester	plate	c19th	
2013-09-08	DJG1 Stockspring Antiques, Kensington	Derby	dish	1765-68	

Appendix 6: Sample catalogue

Session	Sample	Factory	object type	assigned date	Image
2013-09-08	DJG2 Stockspring Antiques, Kensington	Derby	dish	1765-70	
2013-09-08	UDV1 Stockspring Antiques, Kensington	Unknown	cup		
2013-09-08	WJG1 Stockspring Antiques, Kensington	Worcester	saucer	1768-73	
2013-09-08	WJG3 Stockspring Antiques, Kensington	Worcester	plate	1765-70	
2013-09-08	WJG5 Stockspring Antiques, Kensington	Worcester	teacup	1763-68	
2013-09-08	WJG6 Stockspring Antiques, Kensington	Worcester	spoon rest	1763-68	

Appendix 6: Sample catalogue

Session	Sample	Factory	object type	assigned date	Image
2013-09-08	WJG7 Stockspring Antiques, Kensington	Worcester	teacup	1770-75	
2013-09-08	WJG8 Stockspring Antiques, Kensington	Worcester	dish	1763-68	
2013-09-08	WJG9 Stockspring Antiques, Kensington	Worcester	plate	1765-70	
2013-09-08	WUK1 Stockspring Antiques, Kensington	Worcester	cup	1770-75	
2013-09-08	WUK2 Stockspring Antiques, Kensington	Worcester	teapot	ca.1770	
2013-09-08	WWR1 Stockspring Antiques, Kensington	Worcester	saucer	ca.1770	

Appendix 6: Sample catalogue

Session	Sample	Factory	object type	assigned date	Image
2013-09-08	WWR2 Stockspring Antiques, Kensington	Worcester	saucer	ca.1770	
2013-09-18	WON1 Stockspring Antiques, Kensington	Worcester	plate	1768-70	
2013-09-18	WUK3 Stockspring Antiques, Kensington	Worcester	cup	ca.1775	
2013-09-18	WWR3 Stockspring Antiques, Kensington	Worcester		ca.1765	no image available
2013-09-18	WWR4 Stockspring Antiques, Kensington	Worcester	coffee pot		
2013-09-18	WWR5 Stockspring Antiques, Kensington	Worcester	vase		

Appendix 6: Sample catalogue

Session	Sample	Factory	object type	assigned date	Image
2013-09-18	WWR6 Stockspring Antiques, Kensington	Worcester			no image available
2013-09-19	BT sb1 Nick Panes' collection	Bovey Tracey	sauceboat		
2013-09-19	Bow mg1 Nick Panes' collection	Bow	mug	1760s	
2013-09-19	Bow pl1 Nick Panes' collection	Bow	plate	1760s	
2013-09-19	Bow pl2 Nick Panes' collection	Bow	plate	1752-54	
2013-09-19	Bow pl3 Nick Panes' collection	Bow	plate	1760s	

Appendix 6: Sample catalogue

Session	Sample	Factory	object type	assigned date	Image
2013-09-19	Bow sb1 Nick Panes' collection	Bow	sauceboat	1750s	
2013-09-19	Bow sb2 Nick Panes' collection	Bow	sauceboat	1755-57	
2013-09-19	Bow sb3 Nick Panes' collection	Bow	sauceboat	1760-65	
2013-09-19	Bow sb4 Nick Panes' collection	Bow	sauceboat	1762-65	
2013-09-19	Bow sb5 Nick Panes' collection	Bow	sauceboat	1770-75	
2013-09-19	Bow sb6 Nick Panes' collection	Bow	sauceboat	1770-75	
2013-09-19	Bow sb7 Nick Panes' collection	Bow	sauceboat	1750-52	
2013-09-19	Cha sb1 Nick Panes' collection	Chaffers	sauceboat	c1758	
2013-09-19	Cha tb1 Nick Panes' collection	Chaffers	teabowl	c1758	

Appendix 6: Sample catalogue

Session	Sample	Factory	object type	assigned date	Image
2013-09-19	Cpen sb1 Nick Panes' collection	Christian Pennington	sauceboat	1765-78	
2013-09-19	Lgil sb1 Nick Panes' collection	Gillbody	sauceboat	1755-60	
2013-09-19	Isl sb1 Nick Panes' collection	Isleworth	sauceboat	c.1770	
2013-09-19	Isl sb2 Nick Panes' collection	Isleworth	sauceboat	c.1770	
2013-09-19	Isl tb1 Nick Panes' collection	Isleworth	teabowl	c.1770	
2013-09-19	Jpen pl1 g Nick Panes' collection I	James Pennington	plate	1765-70	
2013-09-19	Jpen sb1 Nick Panes' collection	James Pennington	sauceboat	1765-70	

Appendix 6: Sample catalogue

Session	Sample	Factory	object type	assigned date	Image
2013-09-19	JoPen mg1 Nick Panes' collection	John Pennington	mug	1775-85	
2013-09-19	JoPen sb1 Nick Panes' collection	John Pennington	sauceboat	1775-85	
2013-09-19	Lhse sb1 Nick Panes' collection	Limehouse	sauceboat	1745-46	
2013-09-19	Lhse sb2 Nick Panes' collection	Limehouse	sauceboat	1745-46	
2013-09-19	Lowe sb1 Nick Panes' collection	Lowestoft	sauceboat	1760-65	
2013-09-19	Lowe sc1 Nick Panes' collection	Lowestoft	saucer	1780s	
2013-09-19	LRd tb1 Nick Panes' collection	Reid	teabowl	1758-60	

Appendix 6: Sample catalogue

Session	Sample	Factory	object type	assigned date	Image
2013-09-19	Spn sb1 Nick Panes' collection	Seth Pennington	sauceboat		
2013-09-19	Vx mg1 Nick Panes' collection	Vauxhall	mug	1757-60	
2013-09-19	Vx sb1 Nick Panes' collection	Vauxhall	sauceboat	1756-58	
2013-09-19	Vx sb2 Nick Panes' collection	Vauxhall	sauceboat	1755-58	
2013-09-19	Worcs mg1 Nick Panes' collection	Worcester	mug	1770-85	
2013-09-19	Worcs mg2 Nick Panes' collection	Worcester	mug	1765-70	

Appendix 6: Sample catalogue

Session	Sample	Factory	object type	assigned date	Image
2013-09-19	Worcs sb1 Nick Panes' collection	Worcester	sauceboat	1750s	
2013-09-19	Worcs sb2 Nick Panes' collection	Worcester	sauceboat	1750s	
2013-09-19	Worcs sb3 Nick Panes' collection	Worcester	sauceboat		
2013-09-19	Worcs sb4 Nick Panes' collection	Worcester	sauceboat	1765-70	
2013-09-19	Worcs sb5 Nick Panes' collection	Worcester	sauceboat	1755-56	
2013-09-19	Worcs tb1 Nick Panes' collection	Worcester	teabowl	1772-85	
2013-09-19	Worcs tc1 Nick Panes' collection	Worcester	teacup	1760-80	
2013-09-19	Bri sb1 Nick Panes' collection	Bristol	sauceboat	1767-82	

Appendix 6: Sample catalogue

Session	Sample	Factory	object type	assigned date	Image
2013-09-19	Bri sb2 Nick Panes' collection	Bristol	sauceboat	1767-82	
2013-09-30	77 Marshall Collection, Ashmolean Museum	Worcester	tea canister	1772-75	
2013-09-30	79 Marshall Collection, Ashmolean Museum	Worcester	oval basket	1775-0	
2013-09-30	98 Marshall Collection, Ashmolean Museum	Worcester	creamboat	c19th	
2013-09-30	122 Marshall Collection, Ashmolean Museum	Worcester	leaf dish	c19th	
2013-09-30	123 Marshall Collection, Ashmolean Museum	Worcester	mug	c19th	

Appendix 6: Sample catalogue

Session	Sample	Factory	object type	assigned date	Image
2013-09-30	138 Marshall Collection, Ashmolean Museum	Worcester	tureen and lid	c19th	
2013-09-30	611 Marshall Collection, Ashmolean Museum	Worcester	bowl	1775-80, grounds possibly later	
2013-09-30	926 Marshall Collection, Ashmolean Museum	Worcester	spoon tray	~1765	
2013-09-30	928 Marshall Collection, Ashmolean Museum	Worcester	cake plate	~1770	
2013-09-30	931 Marshall Collection, Ashmolean Museum	Worcester	small plate	~1770	
2013-09-30	933 Marshall Collection, Ashmolean Museum	Worcester	plate	~1775	

Appendix 6: Sample catalogue

Session	Sample	Factory	object type	assigned date	Image
2013-09-30	1001 Marshall Collection, Ashmolean Museum	Worcester	small plate	~1770	
2013-09-30	1003 Marshall Collection, Ashmolean Museum	Worcester	small plate	1775-80	
2013-09-30	1004 Marshall Collection, Ashmolean Museum	Worcester	cake plate	1775-80	
2013-09-30	1005 Marshall Collection, Ashmolean Museum	Worcester	small plate	1775-80	
2013-09-30	1007 Marshall Collection, Ashmolean Museum	Worcester	tea bowl	~1770	
2013-09-30	1009 Marshall Collection, Ashmolean Museum	Worcester	leaf dish	~1775	

Appendix 6: Sample catalogue

Session	Sample	Factory	object type	assigned date	Image
2013-09-30	1011 Marshall Collection, Ashmolean Museum	Worcester	beaker	~1770	
2013-09-30	1013 Marshall Collection, Ashmolean Museum	Worcester	sucrier stand	1770-75	
2013-09-30	1015 Marshall Collection, Ashmolean Museum	Worcester	teacup and saucer	1775-80	
2013-11-11	839 Marshall Collection, Ashmolean Museum	Worcester	saucer		no image available
2013-11-11	891 Marshall Collection, Ashmolean Museum	Worcester	tureen, lid, stand	~1775	
2013-11-11	892 Marshall Collection, Ashmolean Museum	Worcester	cake plate	1775-80	

Appendix 6: Sample catalogue

Session	Sample	Factory	object type	assigned date	Image
2013-11-11	893 Marshall Collection, Ashmolean Museum	Worcester	dish	1775-80	
2013-11-11	1008 Marshall Collection, Ashmolean Museum	Worcester	tea cup		no image available
2013-11-18	701 Marshall Collection, Ashmolean Museum	Worcester	cup and saucer	~1772 Giles	
2013-11-18	706 Marshall Collection, Ashmolean Museum	Worcester	plate	1770-72 Giles	
2013-11-18	708 Marshall Collection, Ashmolean Museum	Worcester	plate	~1770 Giles, ground possibly later	
2013-11-18	855 Marshall Collection, Ashmolean Museum	Worcester	sauceboat		
2013-11-18	849 Marshall Collection, Ashmolean Museum	Worcester	cup and saucer	c19th	

Appendix 6: Sample catalogue

Session	Sample	Factory	object type	assigned date	Image
2013-11-18	887 Marshall Collection, Ashmolean Museum	Worcester	dish	~1765	
2013-11-18	919 Marshall Collection, Ashmolean Museum	Worcester	tea cup, coffee cup and saucer	1770-75	
2013-11-18	920 Marshall Collection, Ashmolean Museum	Worcester	cup and saucer	~1772	
2013-11-18	921 Marshall Collection, Ashmolean Museum	Worcester	small jug		
2014-02-24	240 Marshall Collection, Ashmolean Museum	Worcester	urn	~1765	

Appendix 6: Sample catalogue

Session	Sample	Factory	object type	assigned date	Image
2014-02-24	292 Marshall Collection, Ashmolean Museum	Worcester	King of Prussia' saucer	1780-85	
2014-02-24	571 Marshall Collection, Ashmolean Museum	Worcester	egg strainer	~1796	
2014-02-24	574 Marshall Collection, Ashmolean Museum	Worcester	saucer	~1778-82	
2014-02-24	576 Marshall Collection, Ashmolean Museum	Worcester	leaf dish	1770-72	
2014-02-24	577 Marshall Collection, Ashmolean Museum	Worcester	saucer	1778-82	

Appendix 6: Sample catalogue

Session	Sample	Factory	object type	assigned date	Image
2014-02-24	696 Marshall Collection, Ashmolean Museum	Worcester	saucer	~1770 Giles	
2014-02-24	697 Marshall Collection, Ashmolean Museum	Worcester	spoon tray	~1770 Giles	
2014-02-24	698 Marshall Collection, Ashmolean Museum	Worcester	plate	~1772 Giles	
2014-02-24	699 Marshall Collection, Ashmolean Museum	Worcester	spoon tray	~1770 Giles	
2014-02-24	700 Marshall Collection, Ashmolean Museum	Worcester	plate	~1772 Giles	
2014-02-24	702 Marshall Collection, Ashmolean Museum	Worcester	plate	~1770 Giles	

Appendix 6: Sample catalogue

Session	Sample	Factory	object type	assigned date	Image
2014-02-24	703 Marshall Collection, Ashmolean Museum	Worcester	plate	~1770 Giles	
2014-02-24	704 Marshall Collection, Ashmolean Museum	Worcester	plate	1770-72 Giles	
2014-02-24	705 Marshall Collection, Ashmolean Museum	Worcester	saucer	1775-80 Giles	
2014-03-17	65 Marshall Collection, Ashmolean Museum	Worcester	coffee cup and saucer	O'Neale?, ~1785	
2014-03-17	111 Marshall Collection, Ashmolean Museum	Worcester	cup and saucer	~1770	
2014-03-17	377 Marshall Collection, Ashmolean Museum	Worcester	cream jug	1778-80	

Appendix 6: Sample catalogue

Session	Sample	Factory	object type	assigned date	Image
2014-03-17	480 Marshall Collection, Ashmolean Museum	Worcester	rectangular dish	1770-80	
2014-03-17	617 Marshall Collection, Ashmolean Museum	Worcester	teapot stand	1775-80	
2014-03-17	620 Marshall Collection, Ashmolean Museum	Worcester	cup and saucer	1775-80	
2014-03-17	804 Marshall Collection, Ashmolean Museum	Worcester	cake plate	1770-75, possibly Giles	
2014-03-17	826 Marshall Collection, Ashmolean Museum	Worcester	candlestick	1775-80, experimental? Outside dec?	
2014-03-17	829 Marshall Collection, Ashmolean Museum	Worcester	tobacco jar	1778-80, Dutch-style decoration?	
2014-03-17	914 Marshall Collection, Ashmolean Museum	Worcester	tea cup, coffee cup and saucer	1775-80, decoration removed - redecorated	

Appendix 6: Sample catalogue

Session	Sample	Factory	object type	assigned date	Image
2014-05-28	BT cp Rosalie Wise Sharp collection	Bovey Tracey	cup		
2014-05-28	Cy tc1 Nick Panes' collection	Caughley	teacup	1775-99	
2014-05-28	Cy tc2 Nick Panes' collection	Caughley	teacup	1775-99	
2014-05-28	Dby sb2 Nick Panes' collection	Derby	sauceboat		
2014-05-28	Dby vase Nick Panes' collection	Derby	vase		no image available
2014-05-28	LH frag2 National Museum of Scotland	Longton Hall	archaeologi cal sherd	1749-60	
2014-05-28	LH frag3 National Museum of Scotland	Longton Hall	archaeologi cal sherd	1749-60	

Appendix 6: Sample catalogue

Session	Sample	Factory	object type	assigned date	Image
2014-05-28	LH frag4 National Museum of Scotland	Longton Hall	archaeological sherd	1749-60	
2014-05-28	LH frag5 National Museum of Scotland	Longton Hall	archaeological sherd	1749-60	
2014-05-28	LH frag6 National Museum of Scotland	Longton Hall	archaeological sherd	1749-60	
2014-05-28	LH frag1 National Museum of Scotland	Longton Hall	archaeological sherd	1749-60	
2014-05-28	LH mg1 Nick Panes' collection	Longton Hall	mug	1749-60	

Appendix 6: Sample catalogue

Session	Sample	Factory	object type	assigned date	Image
2014-05-28	LH sb1 Nick Panes' collection	Longton Hall	sauceboat	1749-60	
2014-05-28	Lowe frag1 National Museum of Scotland	Lowestoft	archaeological sherd	1761-65	
2014-05-28	Lowe tb1 Nick Panes' collection	Lowestoft	teabowl	1780s	no image available
2014-05-28	UK mg1 Nick Panes' collection	Unknown	mug		
2014-05-28	UK pl1 Nick Panes' collection	Unknown	plate		
2014-05-28	UK sb1 Nick Panes' collection	Unknown	sauceboat		

Appendix 6: Sample catalogue

Session	Sample	Factory	object type	assigned date	Image
2014-05-28	UK sb2 Nick Panes' collection	Unknown	sauceboat		
2014-05-28	WP frag1 National Museum of Scotland	West Pans	archaeological sherd	1764-77	
2014-05-28	WP frag2 National Museum of Scotland	West Pans	archaeological sherd	1764-77	
2014-05-28	WP frag3 National Museum of Scotland	West Pans	archaeological sherd	1764-77	
2014-05-28	WP frag4 National Museum of Scotland	West Pans	archaeological sherd	1764-77	
2014-05-28	WP frag5 National Museum of Scotland	West Pans	archaeological sherd	1764-77	

Appendix 6: Sample catalogue

Session	Sample	Factory	object type	assigned date	Image
2014-05-28	WP frag6 National Museum of Scotland	West Pans	archaeological sherd	1764-77	
2015-01-21	HNB1 LAARC/MOLA	Bow	archaeological sherd		no image available
2015-01-21	HNB2 LAARC/MOLA	Bow	archaeological sherd		no image available
2015-01-21	HNB3 LAARC/MOLA	Bow	archaeological sherd		no image available
2015-01-21	HNB4 LAARC/MOLA	Bow	archaeological sherd		no image available
2015-01-21	Dby bskt	Derby	basket		no image available
2015-01-21	Dby sb1	Derby	sauceboat		no image available
2015-01-21	Dby tc1	Derby	teacup		no image available
2015-01-21	GAH1 LAARC/MOLA	Isleworth	archaeological sherd		no image available
2015-01-21	GAH2 LAARC/MOLA	Isleworth	archaeological sherd		no image available
2015-01-21	GAH3 LAARC/MOLA	Isleworth	archaeological sherd		no image available
2015-01-21	GAH4 LAARC/MOLA	Isleworth	archaeological sherd		no image available
2015-01-21	GAH5 LAARC/MOLA	Isleworth	archaeological sherd		no image available
2015-01-21	GAH6 LAARC/MOLA	Isleworth	archaeological sherd		no image available
2015-01-21	GAH7 LAARC/MOLA	Isleworth	archaeological sherd		no image available
2015-01-21	LLK1 LAARC/MOLA	Limehouse	archaeological sherd		no image available
2015-01-21	LLK2 LAARC/MOLA	Limehouse	archaeological sherd		no image available
2015-01-21	LLK3 LAARC/MOLA	Limehouse	archaeological sherd		no image available
2015-01-21	LLK4 LAARC/MOLA	Limehouse	archaeological sherd		no image available
2015-01-21	LLK5 LAARC/MOLA	Limehouse	archaeological sherd		no image available
2015-01-21	LLK6 LAARC/MOLA	Limehouse	archaeological sherd		no image available
2015-01-21	LLK7 LAARC/MOLA	Limehouse	archaeological sherd		no image available

Appendix 6: Sample catalogue

Session	Sample	Factory	object type	assigned date	Image
2015-01-21	NH sc1 Roger Pomfrett's collection	New Hall	saucer		no image available
2015-01-21	NH sc2 Roger Pomfrett's collection	New Hall	saucer		no image available
2015-01-21	NH sc3 Roger Pomfrett's collection	New Hall	saucer		no image available
2015-01-21	NH tb1 Roger Pomfrett's collection	New Hall	teabowl		no image available
2015-01-21	EMB1 LAARC/MOLA	Vauxhall	archaeological sherd		no image available
2015-01-21	EMB2 LAARC/MOLA	Vauxhall	archaeological sherd		no image available
2015-01-21	EMB3 LAARC/MOLA	Vauxhall	archaeological sherd		no image available
2015-01-21	EMB4 LAARC/MOLA	Vauxhall	archaeological sherd		no image available
2015-01-21	EMB5 LAARC/MOLA	Vauxhall	archaeological sherd		no image available
2015-01-21	EMB6 LAARC/MOLA	Vauxhall	archaeological sherd		no image available
2015-01-21	EMB7 LAARC/MOLA	Vauxhall	archaeological sherd		no image available
2015-01-21	EMB9 LAARC/MOLA	Vauxhall	archaeological sherd		no image available
2015-01-21	EMB8 LAARC/MOLA	Vauxhall	archaeological sherd		no image available

A.7 Hand-Held X-ray Fluorescence spectroscopy data and example spectra

Appendix Table 7 - peak area data from XRF analysis of ten glazed porcelain sherds, used in a methodological test

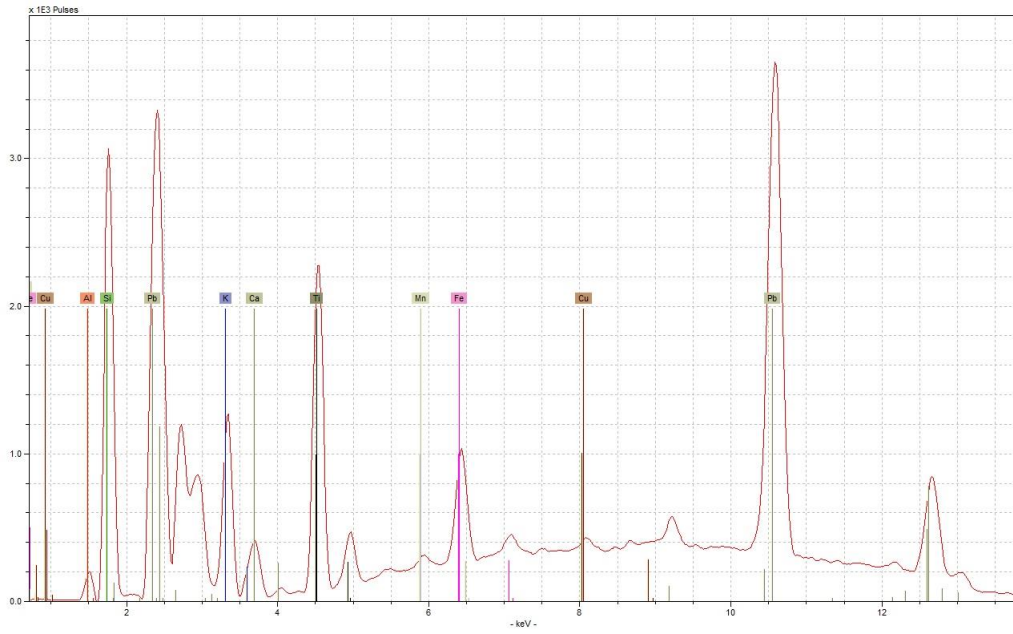
Sample	Al (K)	Si (K)	K (K)	Ca (K)	Ti (K)	Mn (K)	Fe (K)	Cu (K)	Zn (K)	Pb (L)
CY4 1	353	5356	3666	1774	82520	nd	11108	nd	nd	60058
CY4 2	879	16647	8956	3006	16751	nd	7109	nd	nd	137335
CY4 3	811	16201	8961	2996	21105	nd	7130	nd	nd	137811
μ	681	12735	7194	2592	40125	-	8449	-	-	111735
σ	286	6394	3056	708	36779	-	2303	-	-	44754
CY5 1	1045	26231	15162	4676	474	1256	5188	1733	nd	179435
CY5 2	1093	26070	14009	4198	501	1313	5074	1858	nd	177387
CY5 3	918	25470	14956	4837	470	1381	5230	1935	nd	179755
μ	1019	25924	14709	4570	482	1317	5164	1842	-	178859
σ	90	401	615	332	17	63	81	102	-	1285
CY6 1	589	19210	6698	6648	648	1697	14401	3280	1490	164752
CY6 2	435	16854	5815	5409	707	1816	12175	3067	1251	158990
CY6 3	629	22142	8611	6509	884	2148	6740	2815	4700	140949
μ	551	19402	7041	6189	746	1887	11105	3054	2480	154897
σ	102	2649	1429	679	123	234	3941	233	1926	12418
CY8 1	570	20409	10588	5991	619	1698	9951	2119	1263	165676
CY8 2	599	20076	10321	6280	722	1660	10393	1853	1295	166320
CY8 3	593	20829	10263	6501	729	1466	10217	1977	1484	168106
μ	587	20438	10391	6257	690	1608	10187	1983	1347	166701
σ	15	377	173	256	62	124	223	133	119	1259
CY9 1	796	26944	13921	6345	625	1744	9448	1994	1151	167971
CY9 2	672	22113	13688	5883	645	1552	8829	1457	1142	165095
CY9 3	742	25962	13518	6306	662	1795	9295	1551	962	163047
μ	737	25006	13709	6178	644	1697	9191	1667	1085	165371
σ	62	2553	202	256	19	128	322	287	107	2474
CY11 1	557	24395	14493	9678	1115	1966	10987	1089	1628	150523
CY11 2	491	20434	12547	8598	878	1761	9940	1384	1460	139627
CY11 3	502	23372	13633	9706	938	1717	11338	1395	1556	147974
μ	517	22734	13558	9327	977	1815	10755	1289	1548	146041
σ	35	2056	975	632	123	133	727	174	84	5699
CY12 1	702	17294	9014	4436	451	1266	4050	1945	nd	174992
CY12 2	630	15525	8577	4212	444	1236	3995	1793	nd	166010
CY12 3	770	19534	9437	4699	487	1270	4659	2097	nd	176381
μ	701	17451	9009	4449	461	1257	4235	1945	-	172461
σ	70	2009	430	244	23	19	369	152	-	5630

Appendix 7: Hand-Held XRF data

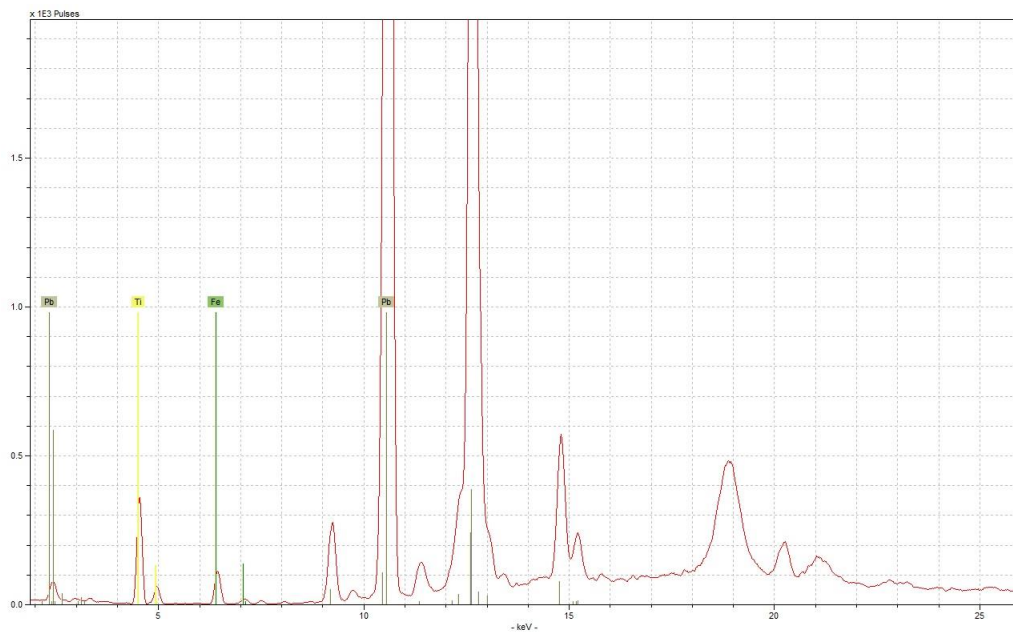
Appendix Table 7 - peak area data from XRF analysis of ten glazed porcelain sherds, used in a methodological test (continued)

Sample	Al (K)	Si (K)	K (K)	Ca (K)	Ti (K)	Mn (K)	Fe (K)	Cu (K)	Zn (K)	Pb (L)
LP3 1	430	15975	8867	6484	494	1841	5378	1401	nd	194380
LP3 2	458	16157	8992	6334	573	2047	5295	1495	nd	193590
LP3 3	412	15939	8979	6467	418	1973	5178	1625	nd	194129
μ	433	16024	8946	6428	495	1954	5284	1507	-	194033
σ	23	117	69	82	78	104	100	112	-	404
W12 1	380	16125	11153	9525	1393	1904	7280	1298	7007	158762
W12 2	428	14303	10018	10837	1286	2040	7026	1203	6123	144546
W12 3	284	16232	11218	7122	1294	2003	6950	1317	8554	165485
μ	364	15553	10796	9161	1324	1982	7085	1273	7228	156264
σ	73	1084	675	1884	60	70	173	61	1230	10691
W15 1	826	16615	3597	2296	6152	12114	7859	1341	917	193000
W15 2	723	16737	3700	2265	6140	11595	7582	1537	996	190626
W15 3	861	17306	3678	2280	6261	10964	7987	1100	891	192515
μ	803	16886	3658	2280	6184	11558	7809	1326	935	192047
σ	72	369	54	16	67	576	207	219	55	1254

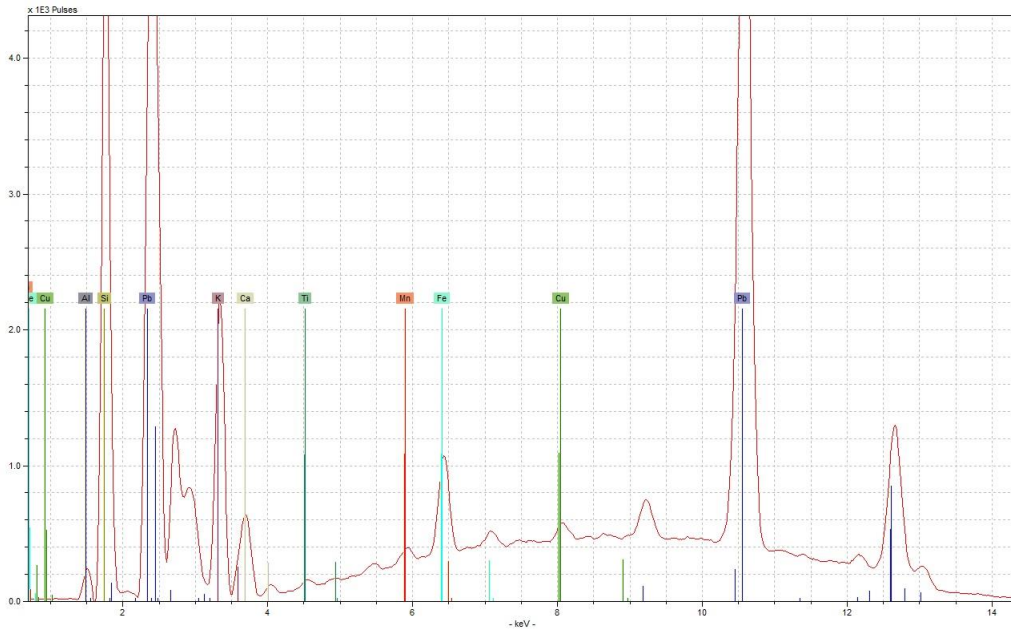
Appendix 7: Hand-Held XRF data



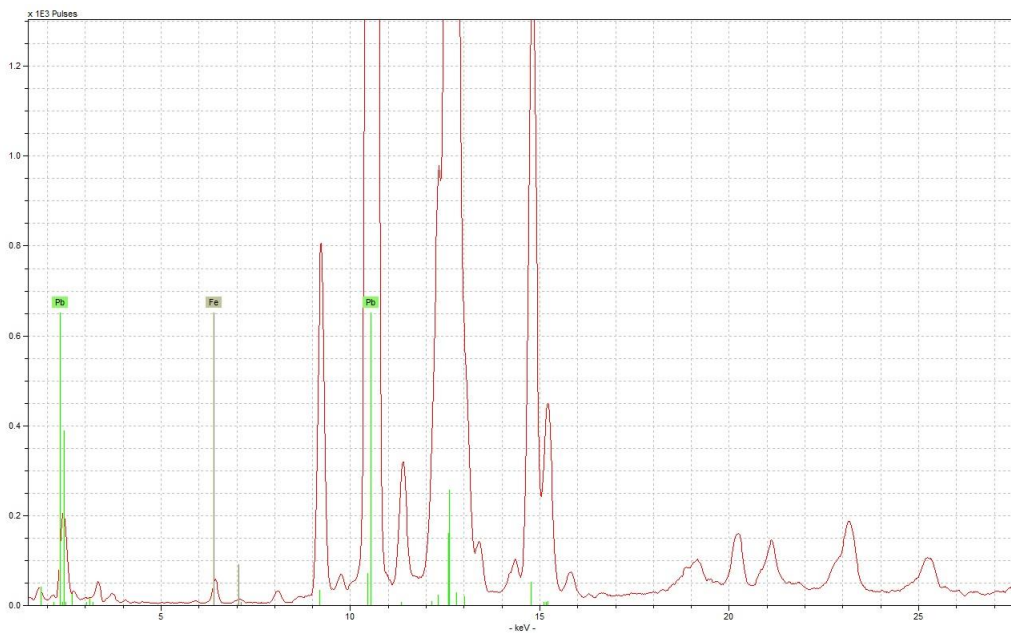
Appendix Figure 17 - example spectra for the glaze of sherd CY4, obtained under the low-voltage (upper) and high-voltage (lower) conditions



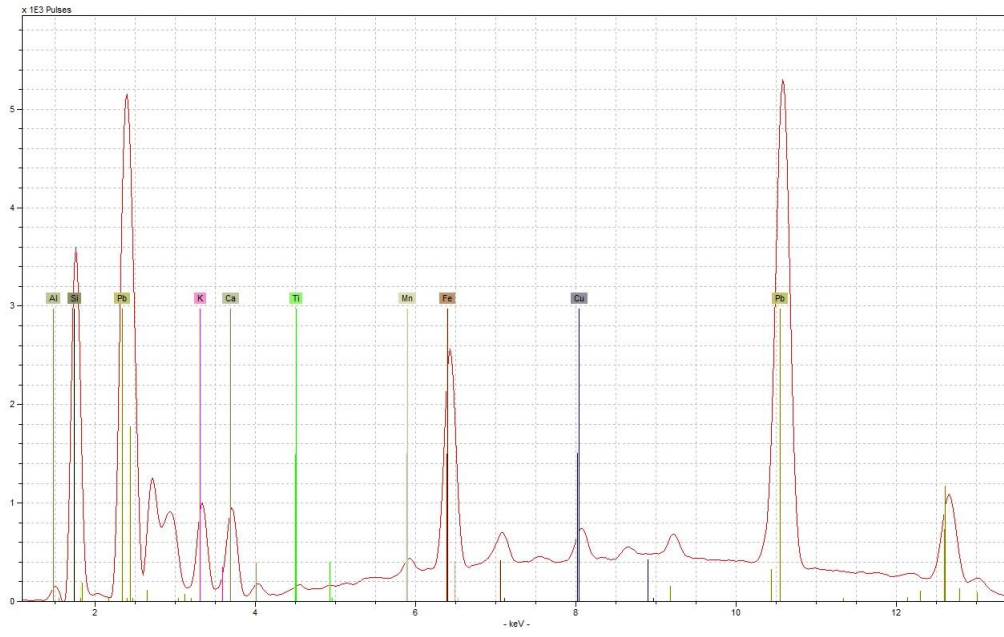
Appendix 7: Hand-Held XRF data



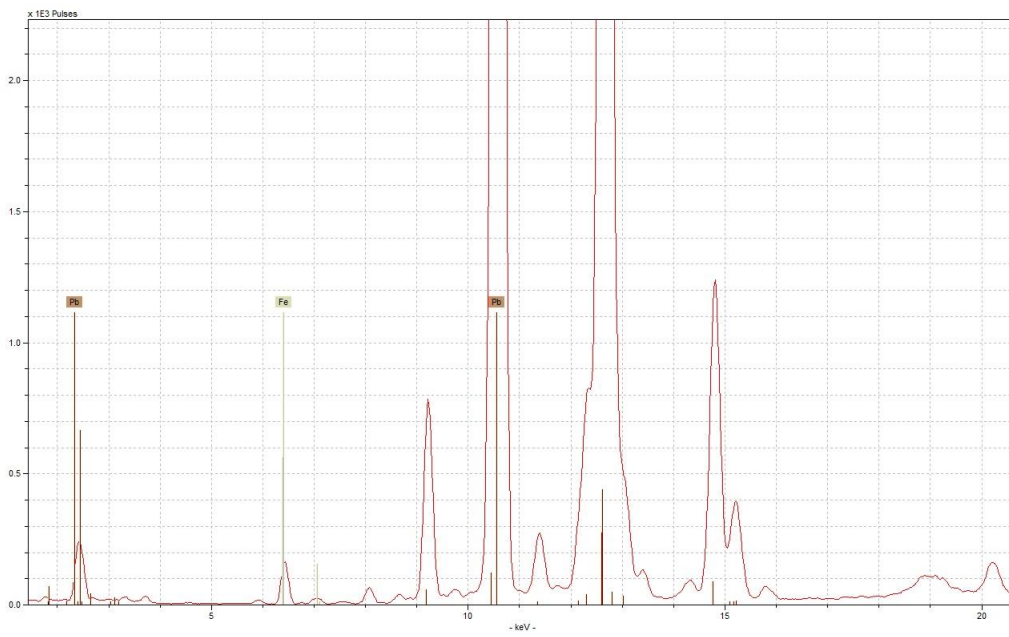
Appendix Figure 18 - example spectra for the glaze of sherds CY5, obtained under the low-voltage (upper) and high-voltage (lower) conditions



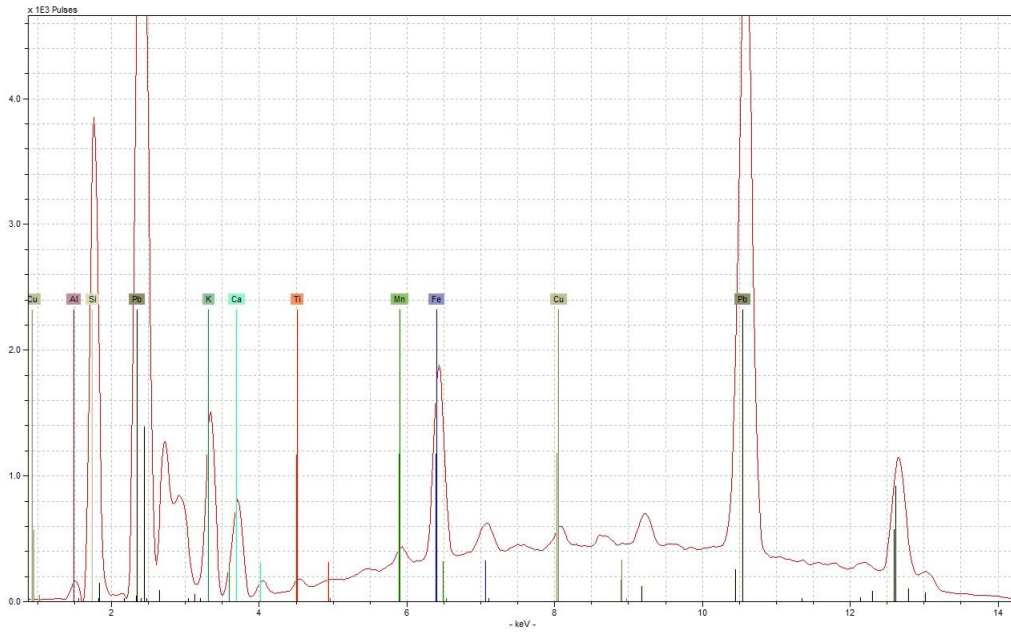
Appendix 7: Hand-Held XRF data



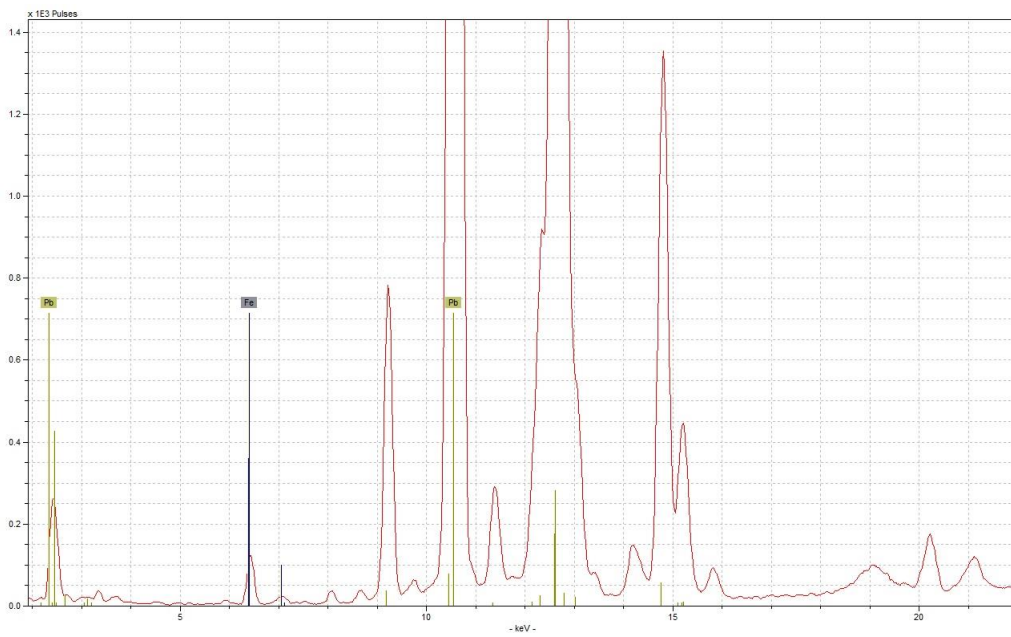
Appendix Figure 19 - example spectra from the glaze of sherd CY6, obtained under the low-voltage (upper) and high-voltage (lower) conditions



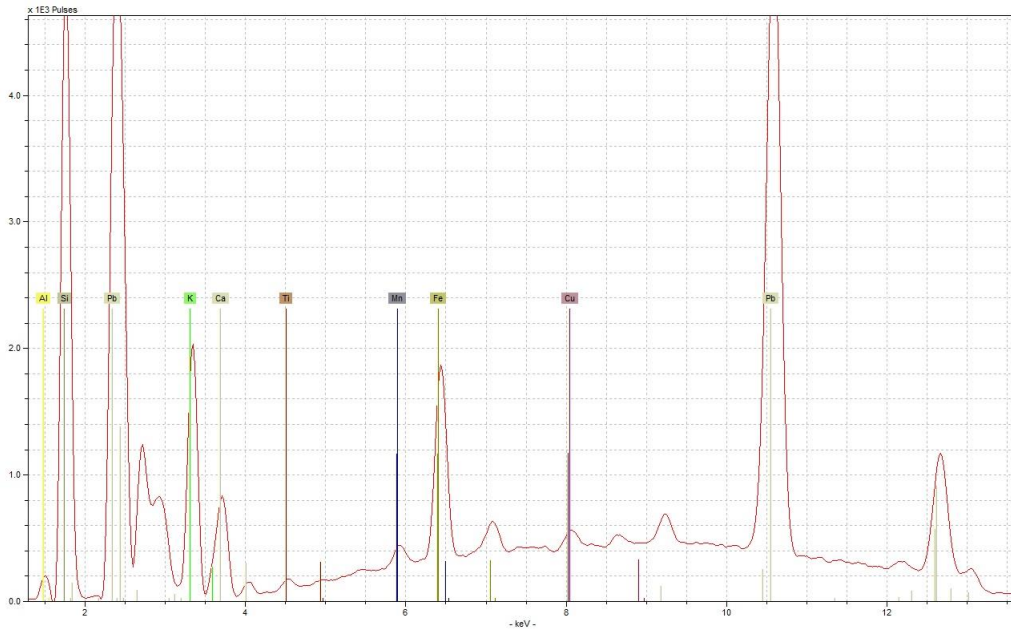
Appendix 7: Hand-Held XRF data



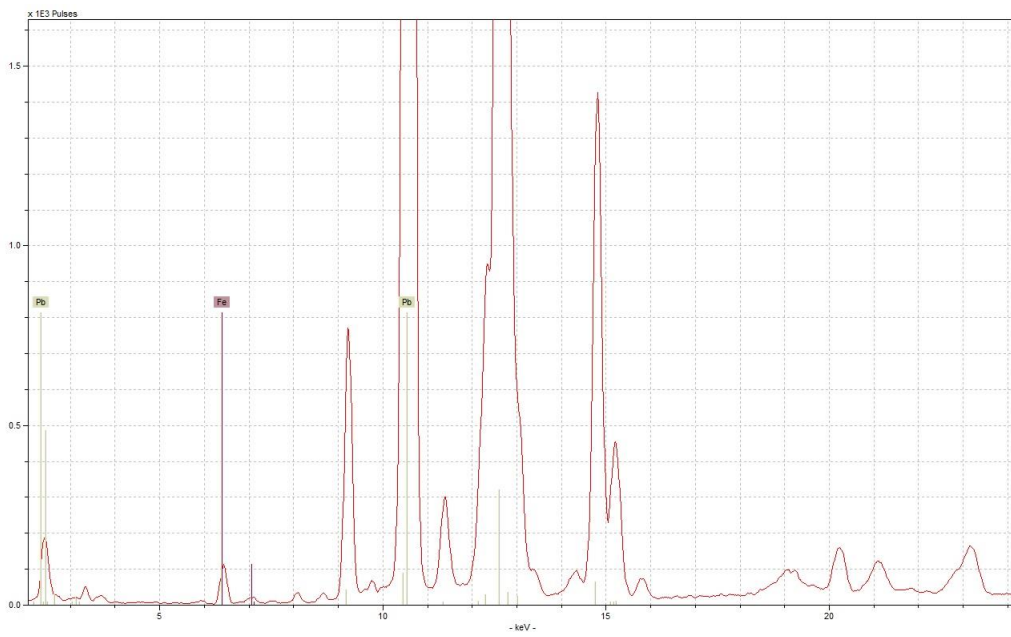
Appendix Figure 20 - example spectra from the glaze of sherds CY8, obtained under low-voltage (upper) and high-voltage (lower) conditions



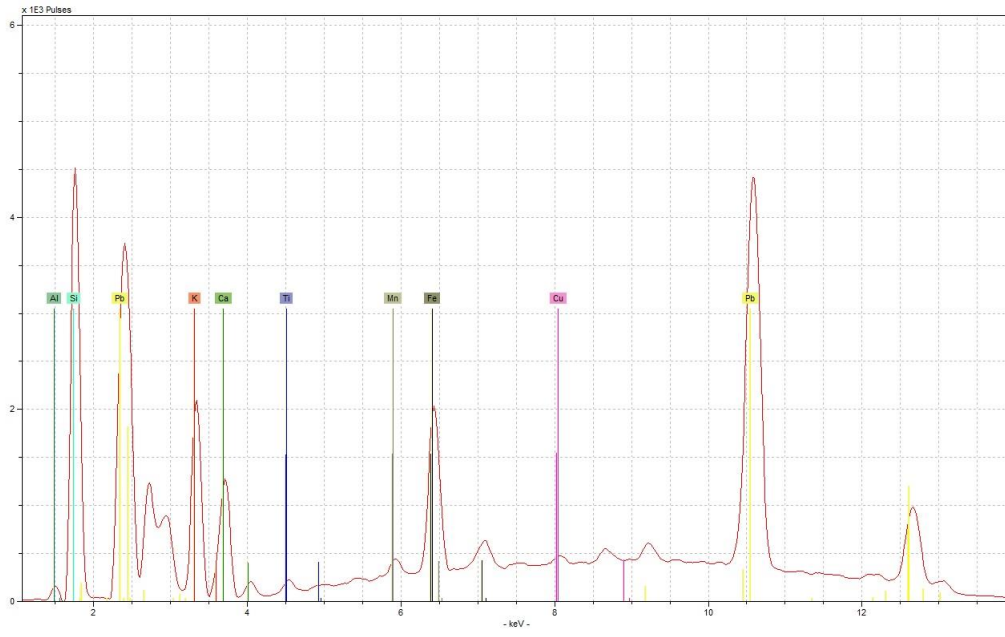
Appendix 7: Hand-Held XRF data



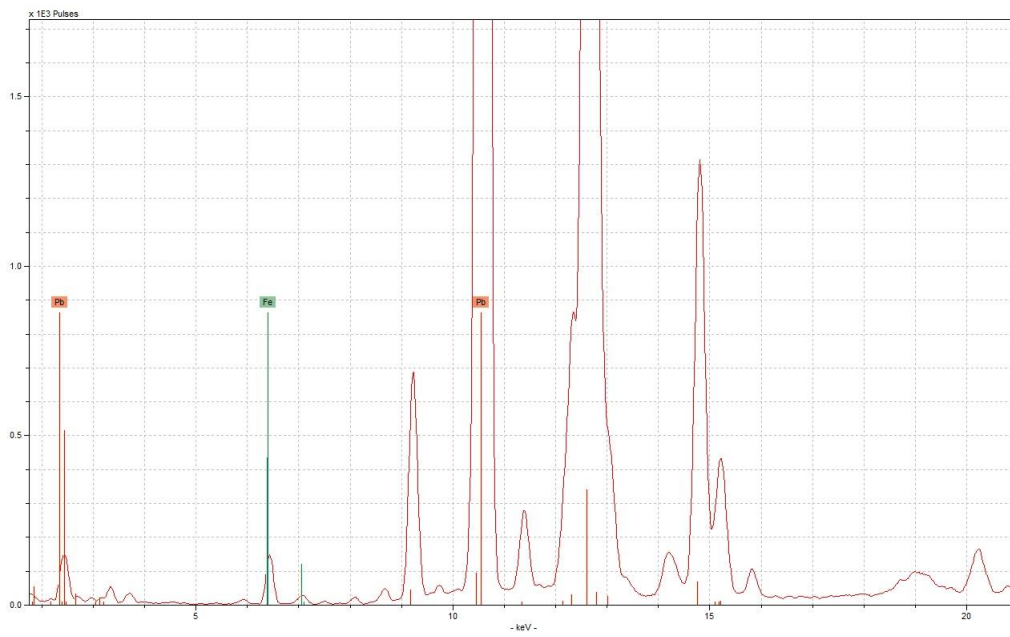
Appendix Figure 21 - example spectra from the glaze of sherds CY9, obtained under low-voltage (upper) and high-voltage (lower) conditions



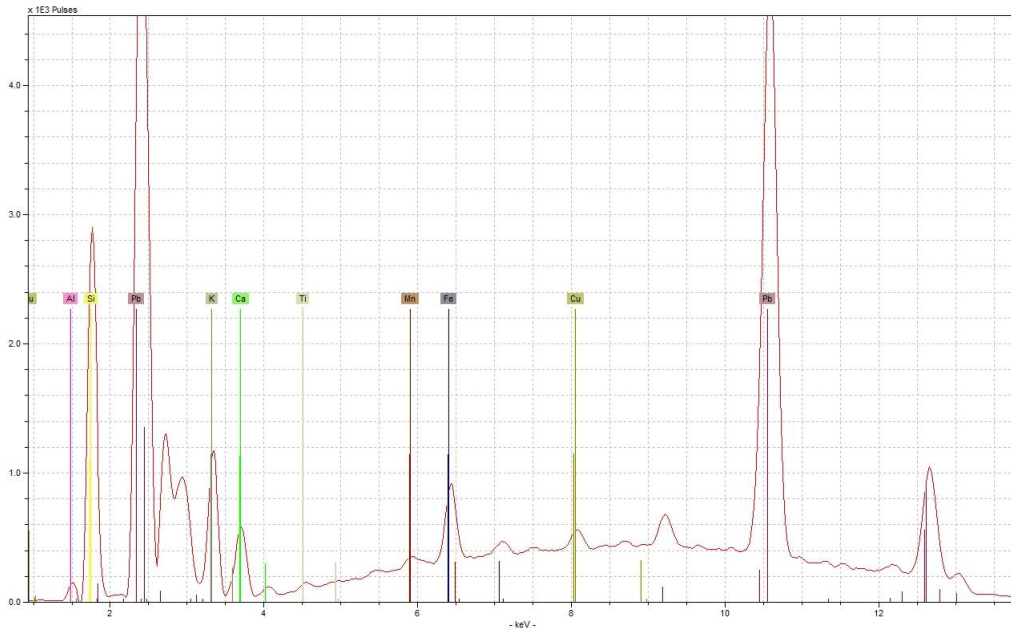
Appendix 7: Hand-Held XRF data



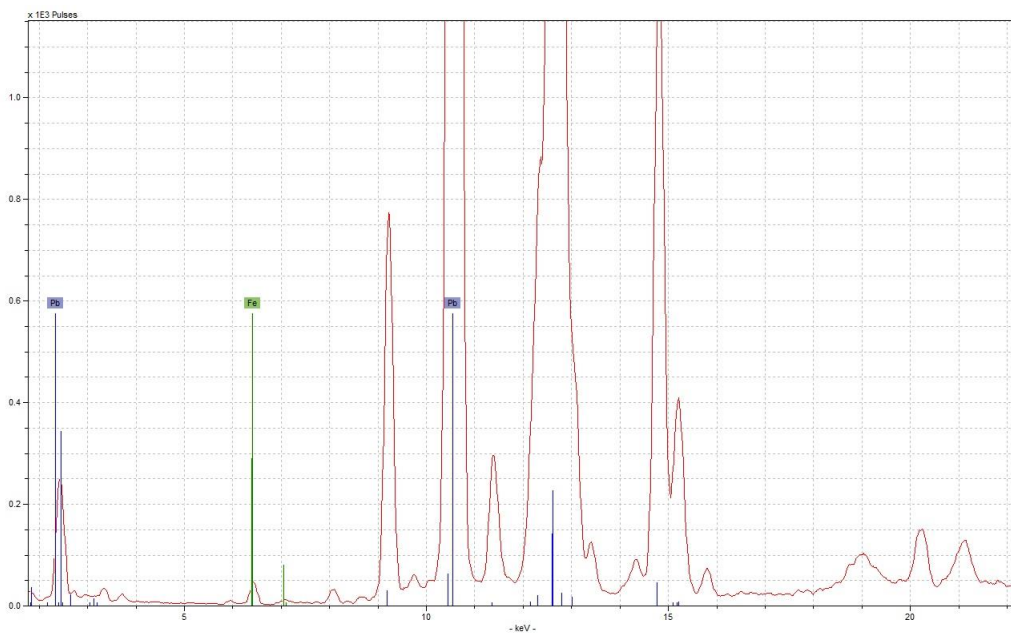
Appendix Figure 22 - example spectra from the glaze of sherd CY11, obtained under low-voltage (upper) and high-voltage (lower) conditions



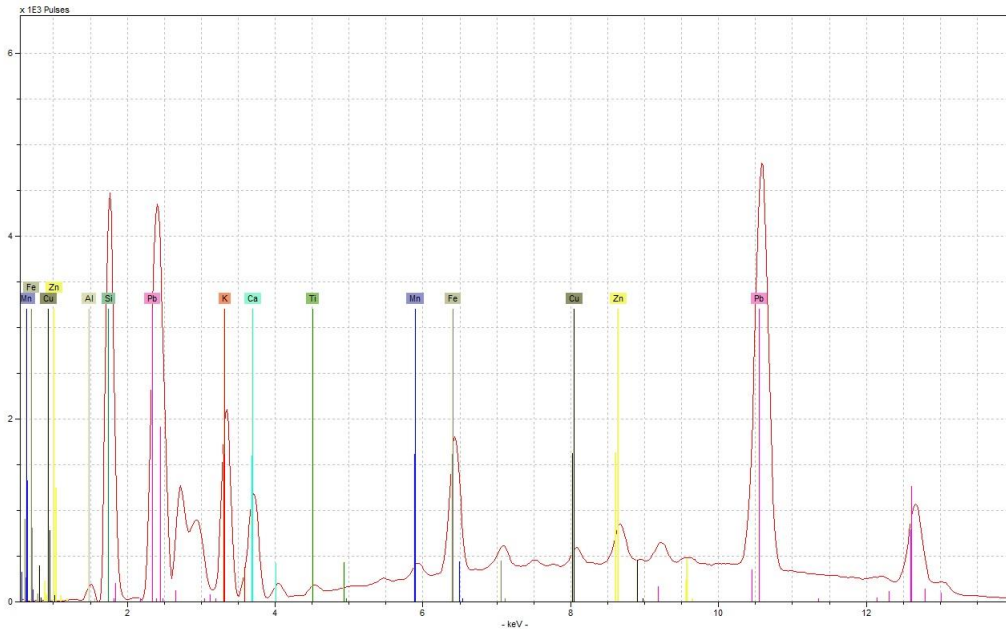
Appendix 7: Hand-Held XRF data



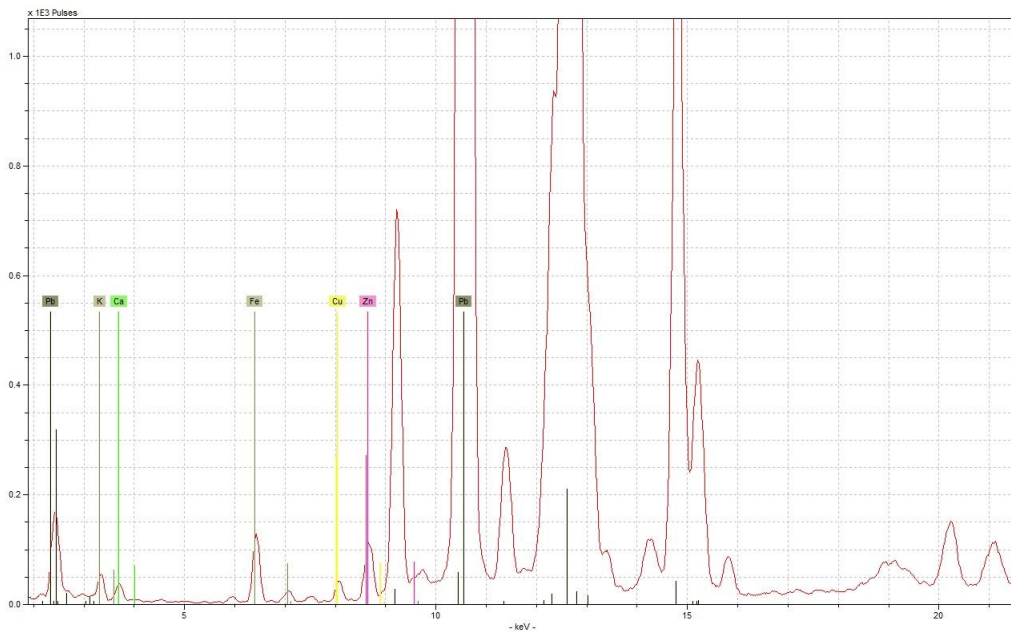
Appendix Figure 23 - example spectra from the glaze of sherd CY12, obtained under low-voltage (upper) and high-voltage (lower) conditions



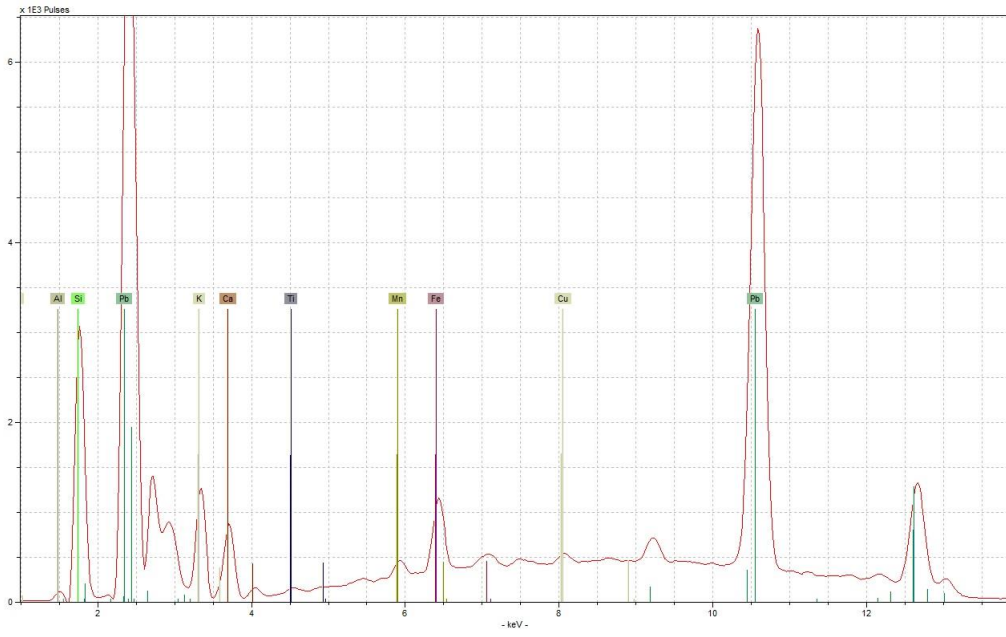
Appendix 7: Hand-Held XRF data



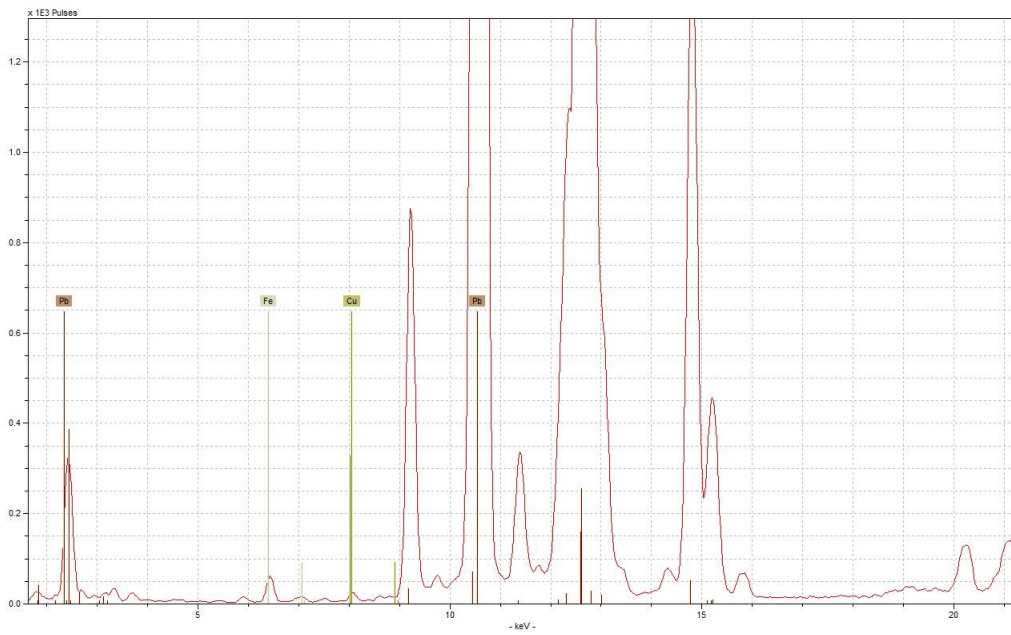
Appendix Figure 24 - example spectra from the glaze of sherd CY20, obtained under low-voltage condition (upper) and high-voltage (lower) conditions



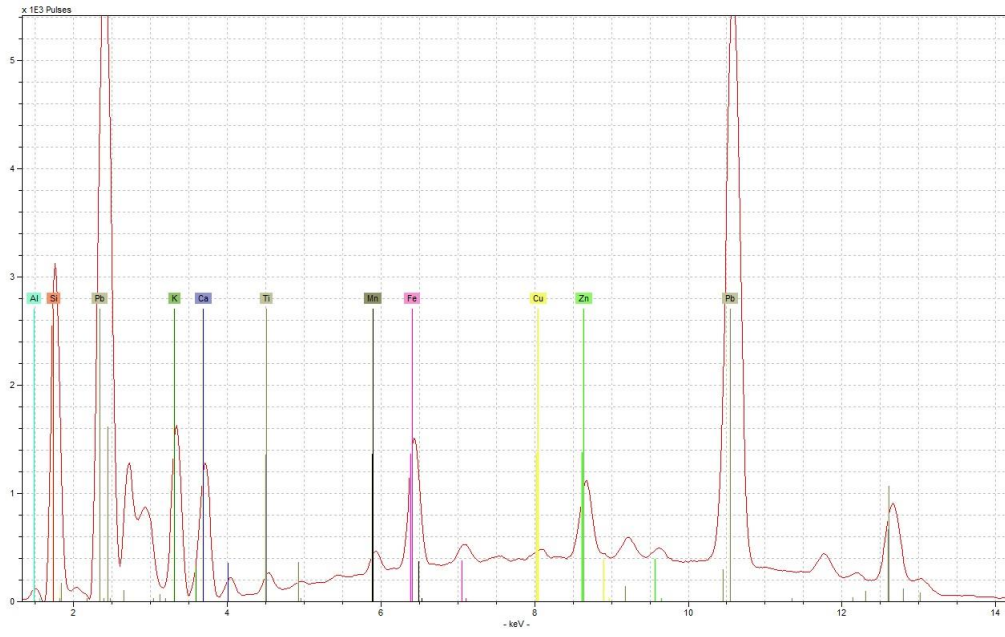
Appendix 7: Hand-Held XRF data



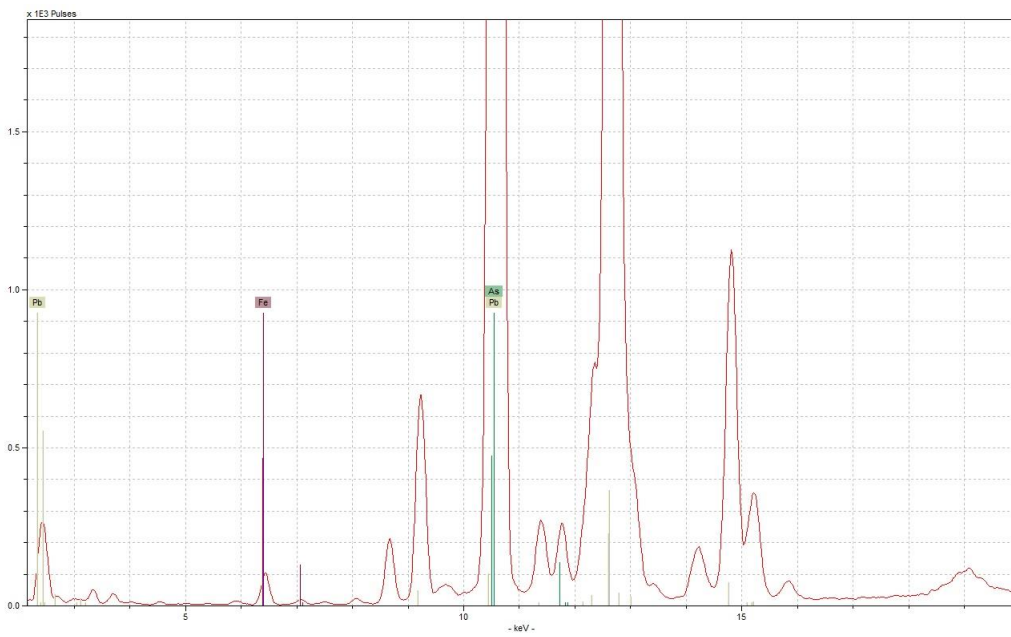
Appendix Figure 25 - example spectra from the glaze of sherd LP3, obtained under low voltage (upper) and high-voltage (lower) conditions



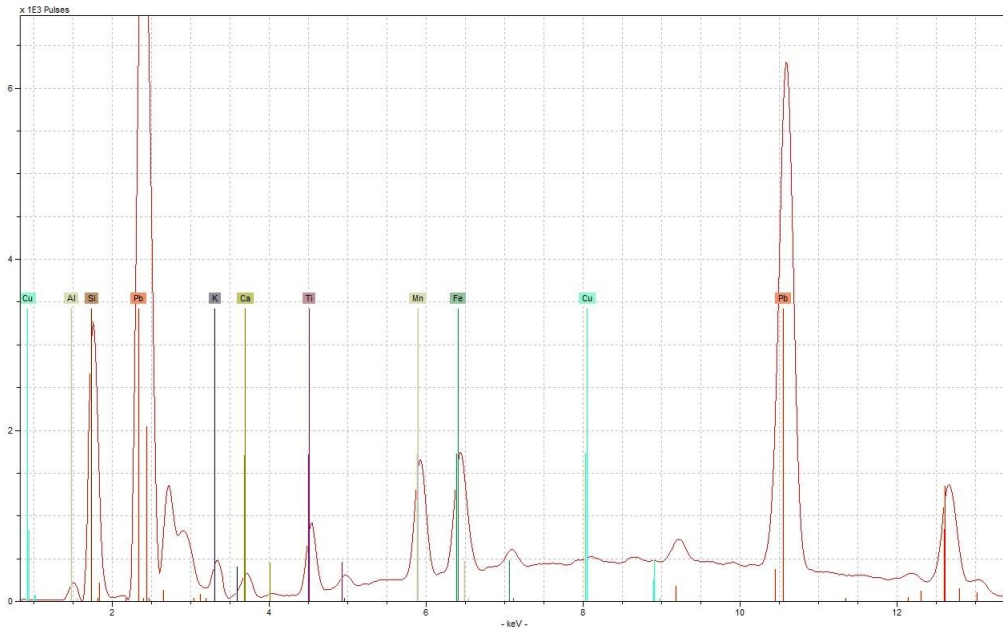
Appendix 7: Hand-Held XRF data



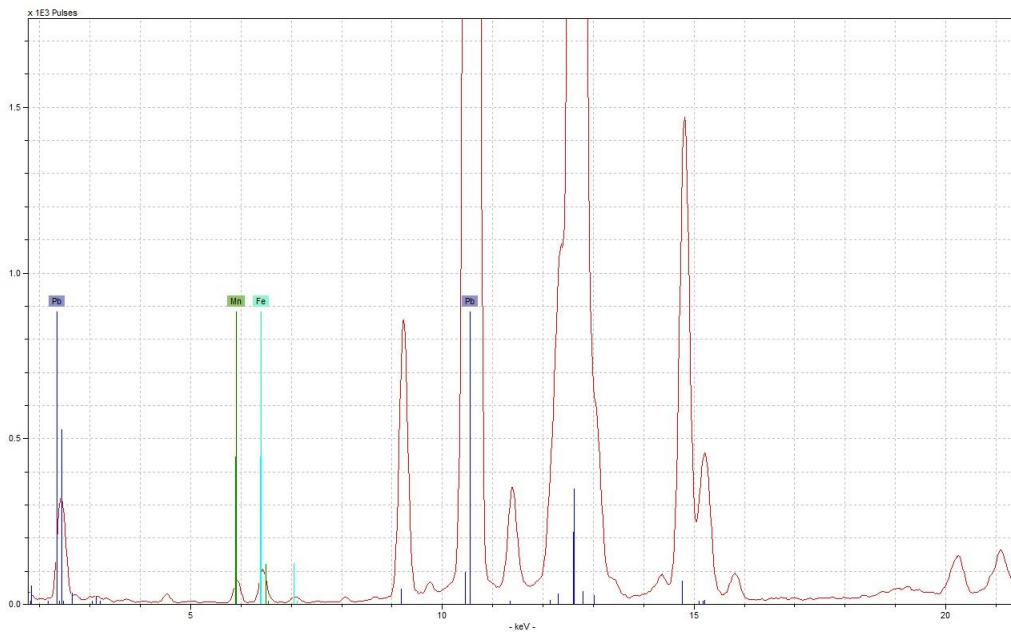
Appendix Figure 26 - example spectra from the glaze of sherds W12, obtained under low-voltage (upper) and high-voltage (lower) conditions



Appendix 7: Hand-Held XRF data



Appendix Figure 27 - example spectra from the glaze of sherds W15, obtained under low-voltage (upper) and high-voltage (lower) conditions

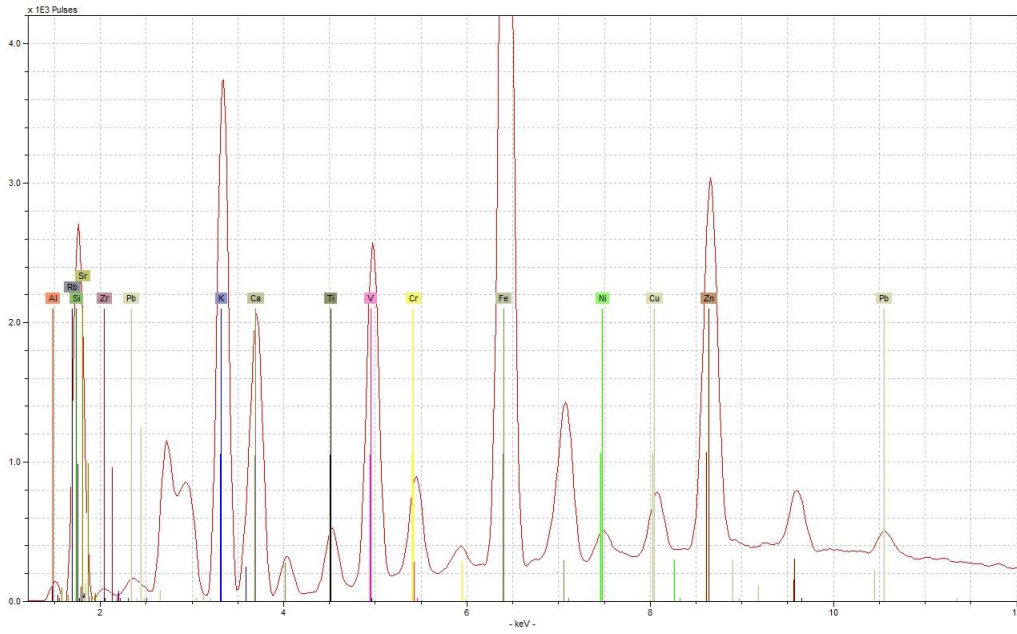


Appendix 7: Hand-Held XRF data

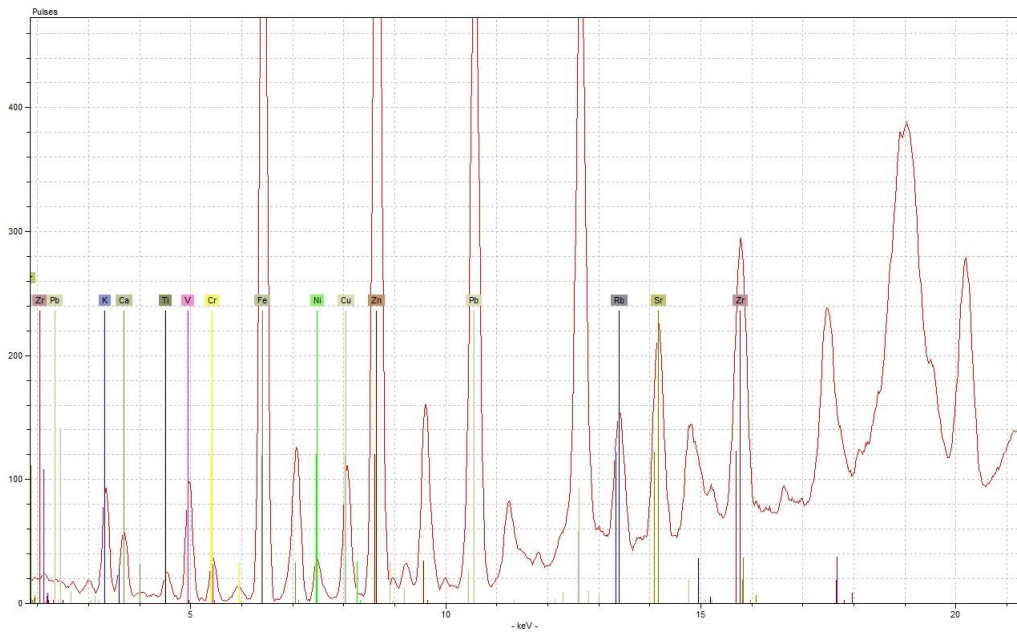
Appendix Table 8 - peak area data from Hand-Held XRF analysis of Oxford Instruments #3a2 soil standard over five sessions of analysis

Session	Sample	Al (K)	Si (K)	K (K)	Ca (K)	Ti (K)	Cr (K)	Fe (K)	Ni (K)	Cu (K)	Zn (K)	Rb (K)	Sr (K)	Zr (K)	Pb (L)
Aug-13	3a2 1	312	286	25835	15619	3533	2559	60558	2006	3936	24790	1292	2071	2077	5703
Aug-13	3a2 2	366	490	26007	15363	3301	3095	60920	1719	4150	24723	1387	2154	2543	5755
Aug-13	3a2 3	331	417	27489	16833	3568	2174	63075	1809	4243	25745	1472	2148	1719	5986
Sep-13	3a2 1	285	498	27594	16272	3541	2011	63130	1844	4051	25093	1392	2196	1059	6174
Sep-13	3a2 2	336	389	27517	16792	3614	1921	63455	2168	4096	25380	1367	2137	1475	5971
Sep-13	3a2 3	272	539	26478	15761	3468	2811	61829	2038	4165	24471	1457	2107	2142	5989
Feb-14	3a2 1	387	368	27348	16296	3459	1713	62886	2115	4258	24905	1420	2131	1599	5897
Feb-14	3a2 2	234	485	26708	16354	3463	2080	62700	1951	4275	25407	1424	2088	1769	5844
Feb-14	3a2 3	398	369	27963	16389	3567	2496	63893	1795	4179	25517	1400	2249	2784	6063
May-14	3a2 1	270	363	27264	16784	3479	1643	63260	1879	4002	24907	1467	2193	1567	6091
May-14	3a2 2	222	323	27732	16601	3721	1745	63133	1720	3918	25095	1518	2208	1490	5973
May-14	3a2 3	329	362	27890	16232	3652	2619	65006	2087	4530	26699	1444	2253	2617	6302
Jan-15	3a2 1	375	439	27886	16292	3687	2786	64813	2063	4487	26751	1447	2175	2480	6223
Jan-15	3a2 2	348	417	28149	16809	3777	2717	66150	2247	4553	26887	1514	2283	2144	6238
Jan-15	3a2 3	327	425	27999	16319	3810	2754	65292	2187	4502	27141	1501	2190	2308	6207

Appendix 7: Hand-Held XRF data



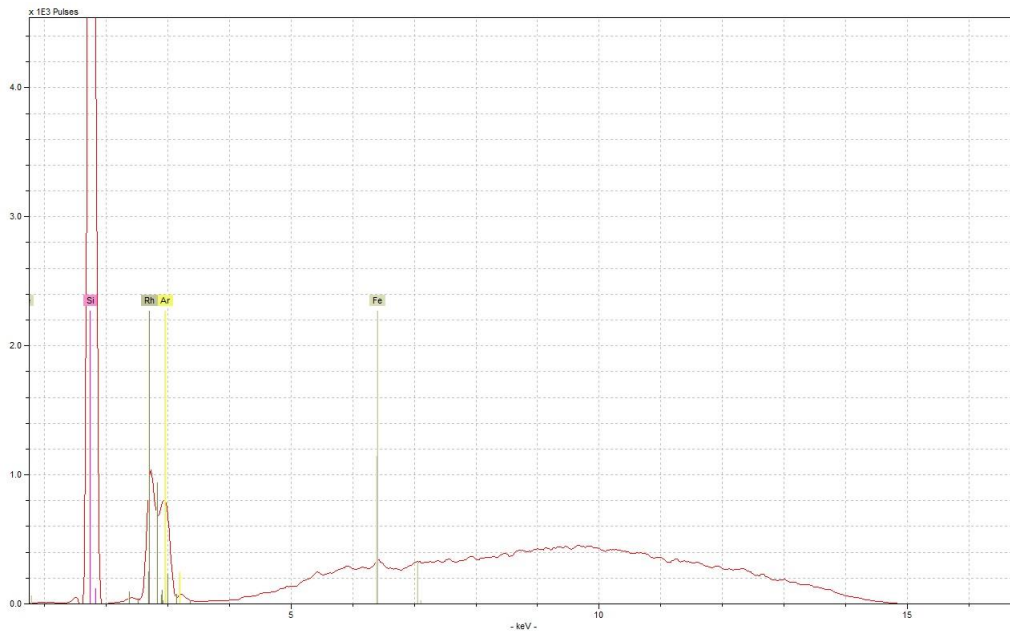
Appendix Figure 28 - example spectra from analyses of Oxford Instrument soil standard #3a2, obtained under low-voltage (upper) and high-voltage (lower) conditions



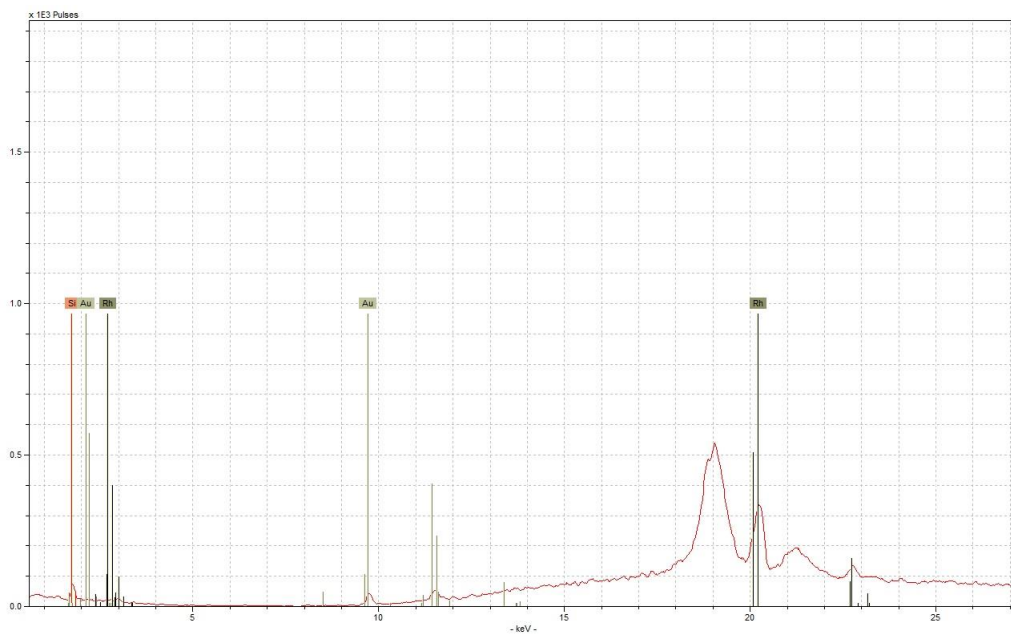
Appendix Table 9 - certified values for Oxford Instruments soil standard #3a2, analysed by XMET5100 HH-XRF under the SOIL LE condition for 240 seconds, mean of four analyses, calculated using the software's empirical calibration programme

	%				ppm										
	Al	Si	K	Ca	Cr	Ni	Cu	Zn	As	Se	Mo	Cd	Sb	Hg	Pb
μ	4.42	26.99	2.20	0.66	589	194	457	2683	49	89	195	102	35	118	1883
σ	0.04	0.08	0.01	>0.01	19	6	6	15	8	2	3	8	4	4	12

Appendix 7: Hand-Held XRF data



Appendix Figure 29 - example spectra from analyses of a silicon disk, obtained under the low-voltage (upper) and high-voltage (lower) conditions



Appendix Table 10 - contamination, silicon and rhodium peaks from analyses of a silicon disk, obtained under the low-voltage (upper) and high-voltage (lower) conditions

	Si (K)	Ar (K)	Fe (K)	Au (L)	Rh (L)
45 keV	3	29	40	422	28
15 keV	425	2517	1415	2145	3081

Appendix 7: Hand-Held XRF data

Appendix Table 11 - peak area data from Hand-Held XRF analysis of glazes on porcelain objects and sherds

Sample	Al (K)	Si (K)	P (K)	K (K)	Ca (K)	Ti (K)	Mn (K)	Fe (K)	Co (K)	Ni (K)	Cu (K)	Zn (K)	As (K)	Sn (K)	Ba (K)	Pb (L)	Bi (L)
Bovey Tracey																	
BT cp	113	21093	<lod	15124	20239	7034	1560	10464	<lod	<lod	1848	10454	<lod	8268	3803	163137	<lod
BT sb1	192	32865	<lod	13859	16871	6578	1866	11990	<lod	<lod	2118	9609	<lod	7805	2573	156055	<lod
Bow																	
Bow mg1	102	15161	<lod	10652	5796	446	<lod	2713	<lod	<lod	1502	<lod	<lod	5025	<lod	196040	<lod
Bow mg2	162	12252	<lod	6910	7554	609	1918	4795	<lod	<lod	3647	<lod	<lod	2551	<lod	186758	<lod
Bow pl1	90	14934	<lod	17340	5392	418	<lod	2245	<lod	<lod	1479	<lod	<lod	5255	<lod	194217	<lod
Bow pl2	62	14865	<lod	13477	4925	263	<lod	2263	<lod	<lod	1578	<lod	<lod	5135	<lod	189631	<lod
Bow pl3	112	16283	<lod	22899	8832	366	<lod	2076	<lod	<lod	1570	<lod	<lod	4624	<lod	197173	<lod
Bow pl4	146	15716	<lod	8211	8153	740	<lod	2947	<lod	<lod	1301	<lod	<lod	4936	<lod	194436	<lod
Bow sb1	62	13455	<lod	9053	6515	309	<lod	2556	<lod	<lod	1486	<lod	<lod	3274	<lod	200808	<lod
Bow sb2	124	11444	<lod	11474	4142	246	<lod	2039	<lod	<lod	1269	<lod	<lod	4242	<lod	190461	<lod
Bow sb3	71	11157	<lod	10815	6155	623	<lod	2476	<lod	<lod	1255	<lod	<lod	3679	<lod	180539	<lod
Bow sb4	147	15188	<lod	11966	4240	356	<lod	2541	<lod	<lod	980	<lod	<lod	4625	<lod	194135	<lod
Bow sb5	107	10928	<lod	9756	3629	424	<lod	2032	<lod	<lod	1126	<lod	<lod	3596	<lod	178753	<lod
Bow sb6	72	13436	<lod	10559	3543	345	<lod	2497	<lod	<lod	1141	<lod	<lod	4282	<lod	188887	<lod
Bow sb7	15	11668	<lod	11842	4143	301	<lod	1824	<lod	<lod	1405	<lod	<lod	4057	<lod	180668	<lod
BUK1	104	14305	<lod	8751	7044	437	<lod	2737	<lod	<lod	1478	<lod	<lod	4155	<lod	193350	<lod
HNB1	126	13133	1244	6645	21923	627	<lod	3120	<lod	<lod	594	<lod	<lod	<lod	<lod	174555	<lod
HNB2	214	9174	1076	5912	37075	454	<lod	13182	<lod	<lod	261	<lod	<lod	<lod	<lod	126311	<lod
HNB3	77	9597	<lod	2887	9774	464	<lod	2189	<lod	<lod	412	<lod	<lod	<lod	<lod	177471	<lod
HNB4	210	18153	<lod	6721	17193	514	<lod	3183	<lod	<lod	736	<lod	<lod	5922	<lod	193011	<lod

Appendix 7: Hand-Held XRF data

Appendix Table 11 - peak area data from Hand-Held XRF analysis of glazes on porcelain objects and sherds (continued)

Sample	Al (K)	Si (K)	P (K)	K (K)	Ca (K)	Ti (K)	Mn (K)	Fe (K)	Co (K)	Ni (K)	Cu (K)	Zn (K)	As (K)	Sn (K)	Ba (K)	Pb (L)	Bi (L)
Caughley																	
Cy tc1	394	25430	<lod	11913	7078	757	1815	8931	2298	1596	966	1182	530	<lod	<lod	168641	<lod
Cy tc2	399	21571	<lod	11825	5105	733	1578	9944	<lod	<lod	1456	<lod	<lod	<lod	<lod	155843	<lod
Chaffers																	
Cha sb1	358	20524	<lod	10078	4523	566	3021	8677	<lod	<lod	4718	<lod	211	<lod	<lod	173835	<lod
Cha tb1	276	19093	<lod	14350	5374	542	3105	7908	<lod	<lod	7761	1113	<lod	<lod	<lod	175872	<lod
Christian/Pennington																	
Cpen sb1	170	12840	<lod	11493	4961	481	2037	5939	<lod	<lod	4485	<lod	<lod	<lod	<lod	167575	<lod
Derby																	
Dby bskt	172	18107	<lod	14211	10932	525	1195	3943	<lod	<lod	694	<lod	254	<lod	<lod	176460	<lod
Dby sb1	175	17320	<lod	13732	13721	504	1264	6251	2802	1915	1302	<lod	198	<lod	<lod	180678	<lod
Dby tc1	73	18186	<lod	12368	15875	512	1828	3563	<lod	<lod	1144	<lod	744	<lod	<lod	187088	<lod
DJG1	121	12132	<lod	8388	7157	372	1229	2018	<lod	<lod	825	<lod	673	<lod	<lod	199389	<lod
DJG2	53	12573	<lod	11393	14390	601	1038	2633	<lod	<lod	952	<lod	571	<lod	<lod	181568	<lod
dby vase2	68	14241	<lod	10314	7602	402	1715	2989	<lod	<lod	1062	<lod	559	<lod	<lod	188854	<lod
Liverpool Gillbody																	
Lgil sb1	153	14977	<lod	8489	8503	784	2907	3728	<lod	<lod	1051	<lod	<lod	<lod	<lod	<lod	<lod
Isleworth																	
GAH1	177	14901	<lod	12332	5839	387	2106	4560	<lod	<lod	890	<lod	<lod	<lod	<lod	187580	<lod
GAH2	889	26324	<lod	12900	40133	606	1073	8370	<lod	<lod	1376	<lod	<lod	<lod	<lod	117348	<lod
GAH3	62	13805	<lod	12454	3845	243	1638	2610	<lod	<lod	612	<lod	<lod	<lod	<lod	172729	<lod
GAH4	184	18054	<lod	11872	5585	438	2050	4762	<lod	<lod	945	<lod	<lod	<lod	<lod	189265	<lod
GAH5	629	20207	<lod	11660	10011	1724	1836	5260	<lod	<lod	905	4259	<lod	<lod	<lod	175283	<lod
GAH6	162	17846	<lod	9507	6319	400	1584	3282	<lod	<lod	500	<lod	<lod	<lod	<lod	175964	<lod

Appendix 7: Hand-Held XRF data

Appendix Table 11 - peak area data from Hand-Held XRF analysis of glazes on porcelain objects and sherds (continued)

Sample	Al (K)	Si (K)	P (K)	K (K)	Ca (K)	Ti (K)	Mn (K)	Fe (K)	Co (K)	Ni (K)	Cu (K)	Zn (K)	As (K)	Sn (K)	Ba (K)	Pb (L)	Bi (L)
Isleworth (continued)																	
GAH7	242	17934	<lod	11252	9450	455	1834	4565	<lod	<lod	911	<lod	<lod	<lod	<lod	177515	<lod
Isl sb1	123	14786	<lod	14450	3093	436	1705	2983	<lod	<lod	860	<lod	<lod	<lod	<lod	180270	<lod
Isl sb2	104	18317	<lod	13494	5062	468	1730	3300	<lod	<lod	940	<lod	<lod	<lod	<lod	191690	<lod
Isl tb1	33	17122	<lod	15523	7214	542	609	2750	<lod	<lod	1403	<lod	<lod	4886	<lod	196343	<lod
Liverpool James Pennington																	
Jpen pl1	309	14889	<lod	5832	9797	549	2054	5284	<lod	<lod	4542	<lod	<lod	<lod	<lod	191023	<lod
Jpen sb1	295	14033	<lod	8049	4143	422	2443	8375	<lod	<lod	1971	<lod	<lod	<lod	<lod	183926	<lod
Liverpool John Pennington																	
JoPen mg1	237	16768	<lod	8616	12090	569	2473	5433	<lod	<lod	9237	<lod	<lod	<lod	<lod	184751	<lod
JoPen sb1	345	19493	<lod	12600	8491	564	1736	5505	<lod	<lod	2536	<lod	<lod	<lod	<lod	182082	<lod
Limehouse																	
Lhse sb1	648	24486	<lod	12543	17614	846	2123	8737	<lod	<lod	1076	<lod	<lod	4960	<lod	165771	<lod
Lhse sb2	412	18602	<lod	9986	9832	992	2037	7790	<lod	<lod	2783	1223	<lod	2871	<lod	174950	<lod
LLK1	359	19537	<lod	6955	16659	747	1977	5480	<lod	<lod	1578	<lod	483	7959	<lod	178689	<lod
LLK2	168	12991	<lod	5795	11124	472	1713	4458	<lod	<lod	1766	<lod	674	7363	<lod	172886	<lod
LLK3	347	15971	<lod	5583	14441	600	1964	5052	<lod	<lod	1619	<lod	206	8000	<lod	184128	<lod
LLK4	219	8169	<lod	4510	14341	524	1732	5298	<lod	<lod	892	<lod	<lod	4208	<lod	101859	<lod
LLK5	96	6879	<lod	2311	9972	541	934	3142	<lod	<lod	621	<lod	<lod	2476	<lod	65742	<lod
LLK6	511	22201	<lod	8906	28200	878	2902	9620	<lod	<lod	1950	<lod	<lod	8144	<lod	169521	<lod
LLK7	209	8978	<lod	4849	14180	532	1980	6006	<lod	<lod	988	<lod	<lod	2789	<lod	118902	<lod
Longton Hall																	
LH frag2	260	14750	<lod	15439	65207	2065	<lod	7080	<lod	<lod	908	<lod	<lod	10760	<lod	147023	<lod
LH frag3	257	16859	<lod	18181	76915	2146	<lod	8147	<lod	<lod	939	<lod	<lod	11243	<lod	163814	<lod

Appendix 7: Hand-Held XRF data

Appendix Table 11 - peak area data from Hand-Held XRF analysis of glazes on porcelain objects and sherds (continued)

Appendix 7: Hand-Held XRF data

Appendix Table 11 - peak area data from Hand-Held XRF analysis of glazes on porcelain objects and sherds (continued)

Sample	Al (K)	Si (K)	P (K)	K (K)	Ca (K)	Ti (K)	Mn (K)	Fe (K)	Co (K)	Ni (K)	Cu (K)	Zn (K)	As (K)	Sn (K)	Ba (K)	Pb (L)	Bi (L)
Longton Hall (continued)																	
LH frag4	253	17915	<lod	11239	71933	2042	<lod	9547	<lod	<lod	1245	<lod	<lod	8373	<lod	163614	<lod
LH frag5	209	15651	<lod	16485	75479	2008	<lod	7147	<lod	<lod	1245	<lod	<lod	10757	<lod	160979	<lod
LH frag6	137	17392	<lod	15251	63594	1367	<lod	6050	<lod	<lod	1164	<lod	<lod	11803	<lod	168329	<lod
LH frag1	380	14283	<lod	15226	59359	2125	<lod	8509	<lod	<lod	1140	<lod	<lod	10792	<lod	166506	<lod
LH mg1	67	16702	<lod	9526	27862	773	1105	4555	<lod	<lod	866	<lod	1022	3865	<lod	189109	<lod
LH sb1	152	17097	<lod	8759	33871	761	1424	6513	2563	2180	991	<lod	1240	3451	<lod	179319	<lod
Lowestoft																	
Lowe sb1	166	14049	<lod	3899	14474	541	1072	4439	<lod	<lod	922	<lod	524	<lod	<lod	193897	<lod
Lowe sc1	82	9007	<lod	2550	8534	383	1009	2058	<lod	<lod	1240	<lod	<lod	<lod	<lod	125629	<lod
Lowe frag1	122	9275	523	7589	8025	482	859	2778	<lod	<lod	619	<lod	<lod	<lod	<lod	131457	<lod
New Hall																	
NH sc1	792	22408	123	9751	29843	420	851	4042	<lod	<lod	1011	<lod	<lod	<lod	<lod	177480	<lod
NH sc2	1249	30559	323	20463	32453	489	1309	7798	<lod	<lod	1212	1385	<lod	<lod	<lod	129066	<lod
NH sc3	821	30257	352	13607	30429	354	1022	3966	<lod	<lod	1166	<lod	<lod	<lod	<lod	182828	<lod
NH tb1	1108	26528	58	15140	27906	455	1072	5072	<lod	<lod	1203	<lod	<lod	<lod	<lod	159039	<lod
Liverpool Reid																	
LRd sb1	139	17646	<lod	12854	16991	570	1863	7673	<lod	<lod	1819	<lod	<lod	<lod	<lod	185492	<lod
Liverpool Pennington																	
Spen sb1	404	16222	<lod	4594	11670	686	1894	5373	<lod	<lod	1728	<lod	<lod	<lod	<lod	187127	<lod
Vauxhall																	
EMB1	562	26441	402	30391	41366	737	1802	10265	<lod	<lod	7261	<lod	229	2245	<lod	128382	<lod
EMB2	684	38658	2582	21842	53375	1410	2211	14523	<lod	<lod	7036	<lod	387	2693	<lod	131493	<lod
EMB3	452	28864	36	32205	34810	774	1916	9490	<lod	<lod	9818	<lod	225	2377	<lod	123503	<lod
Sample	Al (K)	Si (K)	P (K)	K (K)	Ca (K)	Ti (K)	Mn (K)	Fe (K)	Co (K)	Ni (K)	Cu (K)	Zn (K)	As (K)	Sn (K)	Ba (K)	Pb (L)	Bi (L)

Appendix 7: Hand-Held XRF data

Vauxhall (continued)																	
EMB4	177	28185	<lod	16502	16507	1322	2340	15433	<lod	<lod	28966	<lod	<lod	2462	<lod	74076	<lod
EMB5	413	16037	<lod	4565	14352	1087	1117	7646	<lod	<lod	503	<lod	267	<lod	<lod	162801	<lod
EMB6	506	30674	<lod	34336	28828	915	2020	8101	<lod	<lod	7961	<lod	<lod	16266	<lod	125063	<lod
EMB7	223	20836	<lod	14708	34956	1954	1043	17414	<lod	<lod	2333	<lod	<lod	18177	<lod	159198	<lod
EMB9	130	19311	<lod	14660	32789	1616	1068	17605	<lod	<lod	2424	<lod	<lod	15923	<lod	146878	<lod
Vx mg1	108	18551	<lod	17021	26804	870	1654	6341	1762	2020	1908	982	<lod	5611	<lod	154053	<lod
Vx sb1	160	22023	<lod	18695	30509	3421	1731	6669	<lod	<lod	3855	<lod	<lod	6659	1105	144260	<lod
Vx sb2	140	26368	<lod	16322	26597	611	1054	5850	1457	1087	4070	805	<lod	6294	<lod	149642	<lod
West Pans																	
WP frag1	229	15438	<lod	15249	21767	523	1477	3518	<lod	<lod	896	<lod	<lod	<lod	<lod	163473	20968
WP frag2	400	16132	<lod	17208	14309	577	1544	3021	<lod	<lod	841	<lod	<lod	<lod	<lod	167740	21830
WP frag3	339	18667	202	13444	43329	1152	1825	8559	<lod	<lod	623	<lod	<lod	<lod	<lod	157486	21287
WP frag4	319	20192	<lod	11800	25278	996	1419	4265	<lod	<lod	516	<lod	<lod	<lod	<lod	158279	21453
WP frag5	201	10544	96	13629	13671	535	1254	2852	<lod	<lod	437	<lod	<lod	<lod	<lod	152109	20572
WP frag6	181	15061	<lod	15521	19726	675	1465	3716	<lod	<lod	540	<lod	<lod	<lod	<lod	160560	22752
Worcester																	
1001	389	17787	<lod	8703	5125	567	1971	5886	<lod	<lod	1574	<lod	<lod	<lod	<lod	192703	<lod
1003	299	15802	<lod	8409	4718	484	1829	5697	<lod	<lod	1060	<lod	<lod	<lod	<lod	182202	<lod
1004	359	17125	<lod	10417	5333	615	1717	5547	<lod	<lod	1214	<lod	<lod	<lod	<lod	175601	<lod
1005	220	21344	<lod	9551	5689	665	1890	6494	<lod	<lod	1106	<lod	<lod	<lod	<lod	183160	<lod
1006	255	18440	<lod	10061	5723	464	1928	5641	<lod	<lod	1366	<lod	<lod	<lod	<lod	196207	<lod
1007	288	17790	<lod	10078	4839	554	1835	5172	<lod	<lod	1124	<lod	<lod	<lod	<lod	197426	<lod

Appendix 7: Hand-Held XRF data

Appendix Table 11 - peak area data from Hand-Held XRF analysis of glazes on porcelain objects and sherds (continued)

Sample	Al (K)	Si (K)	P (K)	K (K)	Ca (K)	Ti (K)	Mn (K)	Fe (K)	Co (K)	Ni (K)	Cu (K)	Zn (K)	As (K)	Sn (K)	Ba (K)	Pb (L)	Bi (L)
Worcester (continued)																	
1007	288	17790	<lod	10078	4839	554	1835	5172	<lod	<lod	1124	<lod	<lod	<lod	<lod	197426	<lod
1010	327	17007	<lod	10693	6198	529	1719	6108	<lod	<lod	1157	<lod	<lod	<lod	<lod	185453	<lod
1012	322	18618	<lod	10449	7605	746	1640	6668	<lod	<lod	907	<lod	<lod	<lod	<lod	171264	<lod
1013	265	18225	<lod	10025	6001	534	2056	5420	<lod	<lod	1352	<lod	<lod	<lod	<lod	193066	<lod
1014	282	23188	<lod	10335	8884	603	1953	5749	<lod	<lod	1010	<lod	<lod	<lod	<lod	187755	<lod
1015	279	18567	<lod	8978	6239	561	1884	5957	<lod	<lod	1469	<lod	<lod	<lod	<lod	186892	<lod
1016	280	16186	<lod	8438	4222	427	1538	5123	<lod	<lod	1197	<lod	<lod	<lod	<lod	191611	<lod
111	282	21463	<lod	14160	6275	565	1559	6030	<lod	<lod	1311	<lod	<lod	<lod	<lod	160843	<lod
122	334	22582	<lod	14346	7011	686	2206	6827	<lod	<lod	1008	<lod	<lod	<lod	<lod	182823	<lod
138	176	10962	<lod	7300	3819	446	1565	4318	<lod	<lod	949	<lod	499	<lod	<lod	155774	<lod
1016	280	16186	<lod	8438	4222	427	1538	5123	<lod	<lod	1197	<lod	<lod	<lod	<lod	191611	<lod
111	282	21463	<lod	14160	6275	565	1559	6030	<lod	<lod	1311	<lod	<lod	<lod	<lod	160843	<lod
122	334	22582	<lod	14346	7011	686	2206	6827	<lod	<lod	1008	<lod	<lod	<lod	<lod	182823	<lod
138	176	10962	<lod	7300	3819	446	1565	4318	<lod	<lod	949	<lod	499	<lod	<lod	155774	<lod
240	249	19326	<lod	13827	6155	529	2051	7559	<lod	<lod	1215	<lod	<lod	<lod	<lod	185355	<lod
292	248	16399	<lod	8930	4236	565	2027	6460	<lod	<lod	1006	<lod	176	<lod	<lod	181482	<lod
377	358	22680	<lod	11164	6931	640	2514	8533	<lod	<lod	1318	<lod	536	<lod	<lod	165364	<lod
480	370	17602	<lod	10081	6027	573	1911	5633	<lod	<lod	1266	<lod	208	<lod	<lod	183707	<lod
571	636	23796	<lod	11994	5279	699	1504	10037	<lod	<lod	1367	<lod	<lod	<lod	<lod	168624	<lod
574	336	18113	<lod	10951	5160	658	1566	7152	<lod	<lod	841	<lod	174	<lod	<lod	177881	<lod
576	336	16627	<lod	8206	3982	527	1775	6831	<lod	<lod	1263	<lod	118	<lod	<lod	185087	<lod
577	245	19322	<lod	10091	5813	601	1863	6112	<lod	<lod	1224	<lod	481	<lod	<lod	191990	<lod
611	242	18889	<lod	9354	4291	611	1775	6594	<lod	<lod	1120	1458	391	<lod	<lod	185142	<lod
617	289	17958	<lod	10170	6173	666	1947	5597	<lod	<lod	1154	<lod	601	<lod	<lod	189690	<lod

Appendix 7: Hand-Held XRF data

Appendix Table 11 - peak area data from Hand-Held XRF analysis of glazes on porcelain objects and sherds (continued)

Sample	Al (K)	Si (K)	P (K)	K (K)	Ca (K)	Ti (K)	Mn (K)	Fe (K)	Co (K)	Ni (K)	Cu (K)	Zn (K)	As (K)	Sn (K)	Ba (K)	Pb (L)	Bi (L)
Worcester (continued)																	
620	295	18124	<lod	10411	5861	590	2552	6216	<lod	<lod	3872	<lod	<lod	<lod	<lod	182403	<lod
65	310	20208	<lod	13643	6447	440	1696	5053	<lod	<lod	1898	<lod	<lod	<lod	<lod	178140	<lod
696	390	18860	<lod	12064	5392	583	2321	6112	<lod	<lod	1301	<lod	<lod	<lod	<lod	191722	<lod
697	346	19575	<lod	13756	8467	518	2050	7051	<lod	<lod	1396	<lod	<lod	<lod	<lod	177898	<lod
698	355	19969	<lod	10996	5765	652	2067	7066	<lod	<lod	1227	<lod	<lod	<lod	<lod	186987	<lod
699	331	19028	<lod	13483	5898	481	1600	5557	<lod	<lod	1087	<lod	<lod	<lod	<lod	180502	<lod
700	245	15037	<lod	6829	3730	448	1829	5543	<lod	<lod	1121	<lod	<lod	<lod	<lod	195614	<lod
701	300	17034	<lod	7939	4314	517	2165	6247	<lod	<lod	1600	<lod	<lod	<lod	<lod	196658	<lod
702	309	18258	<lod	12964	5520	585	1763	5322	<lod	<lod	1200	<lod	<lod	<lod	<lod	191821	<lod
704	295	17468	<lod	12657	6751	566	1825	5392	<lod	<lod	1002	<lod	<lod	<lod	<lod	185002	<lod
705	439	22297	<lod	11064	6599	796	1879	7120	<lod	<lod	1256	<lod	333	<lod	<lod	180961	<lod
706	219	17879	<lod	10095	5453	645	2086	5848	<lod	<lod	1446	<lod	<lod	<lod	<lod	190871	<lod
708	333	23361	<lod	12767	5571	723	2579	7695	<lod	<lod	1500	<lod	<lod	<lod	<lod	187419	<lod
79	310	19215	<lod	10019	4906	543	1754	6601	<lod	<lod	1067	<lod	<lod	<lod	<lod	192865	<lod
804	321	17403	<lod	9648	5055	536	1764	5447	<lod	<lod	1065	<lod	<lod	<lod	<lod	193642	<lod
826	291	17085	<lod	10267	5881	560	1489	5602	<lod	<lod	875	<lod	<lod	<lod	<lod	152823	<lod
829	420	18973	<lod	9364	6606	570	1866	11663	<lod	<lod	749	<lod	225	<lod	<lod	170786	<lod
849	271	18646	<lod	11289	6003	402	2109	5402	<lod	<lod	1329	<lod	<lod	<lod	<lod	194697	<lod
855	158	14255	<lod	8861	5451	395	1456	4650	<lod	<lod	947	<lod	<lod	<lod	<lod	142363	<lod
887	290	20579	<lod	11611	6364	542	2069	5646	<lod	<lod	1218	<lod	<lod	<lod	<lod	187021	<lod
891d	298	17791	<lod	10143	5419	556	1864	5888	<lod	<lod	1411	<lod	<lod	<lod	<lod	190557	<lod
893	265	16981	<lod	9724	4693	540	1879	5476	<lod	<lod	837	<lod	269	<lod	<lod	181839	<lod
914	265	19983	<lod	11014	3927	607	2027	4649	<lod	<lod	1236	<lod	71	<lod	<lod	185053	<lod
919 sc	406	19820	<lod	9666	4203	584	2019	7107	<lod	<lod	1333	<lod	215	<lod	<lod	186559	<lod

Appendix 7: Hand-Held XRF data

Appendix Table 11 - peak area data from Hand-Held XRF analysis of glazes on porcelain objects and sherds (continued)

Sample	Al (K)	Si (K)	P (K)	K (K)	Ca (K)	Ti (K)	Mn (K)	Fe (K)	Co (K)	Ni (K)	Cu (K)	Zn (K)	As (K)	Sn (K)	Ba (K)	Pb (L)	Bi (L)
Worcester (continued)																	
920	311	18285	<lod	9974	4817	510	2382	6085	<lod	<lod	1641	<lod	<lod	<lod	<lod	193951	<lod
926	327	18891	<lod	9770	4613	494	1937	5717	<lod	<lod	1399	<lod	87	<lod	<lod	191835	<lod
927 lid	156	6302	<lod	2811	7793	271	2308	14935	<lod	<lod	915	<lod	<lod	<lod	<lod	86877	<lod
927 teapot	354	19471	<lod	12398	7498	619	1912	7046	<lod	<lod	1718	<lod	<lod	<lod	<lod	183960	<lod
929 ladle	667	38569	<lod	20681	12464	1174	3929	16732	<lod	<lod	2178	<lod	549	<lod	<lod	355768	<lod
929 lid	431	20152	<lod	10977	6669	637	1969	8455	<lod	<lod	1049	<lod	323	<lod	<lod	177995	<lod
931	296	19689	<lod	9443	4998	620	1963	6763	<lod	<lod	1612	<lod	174	<lod	<lod	186520	<lod
933	214	19434	<lod	10851	7098	696	1792	6855	<lod	<lod	1223	<lod	<lod	<lod	<lod	185167	<lod
934	238	15546	<lod	10701	6660	573	1840	5780	<lod	<lod	1785	<lod	<lod	<lod	<lod	169372	<lod
WJG1	256	18838	<lod	11726	5495	613	2496	5905	<lod	<lod	1443	<lod	<lod	<lod	<lod	191411	<lod
WJG3	231	18445	<lod	12375	6297	464	1812	5874	<lod	<lod	911	<lod	<lod	<lod	<lod	183344	<lod
WJG4	284	16666	<lod	9789	6872	489	1788	6189	<lod	<lod	2425	<lod	<lod	<lod	<lod	179142	<lod
WJG5	301	14517	<lod	13068	5456	461	2036	4792	<lod	<lod	942	<lod	<lod	<lod	<lod	177313	<lod
WJG6	262	13763	<lod	10776	5564	504	1772	5060	<lod	<lod	639	<lod	<lod	<lod	<lod	163332	<lod
WJG7	272	17363	<lod	10802	4875	362	1739	5235	<lod	<lod	1165	<lod	<lod	<lod	<lod	185593	<lod
WJG8	346	23262	<lod	12612	7415	726	1835	7397	<lod	<lod	919	<lod	<lod	<lod	<lod	184114	<lod
WON1	450	35040	<lod	7575	4186	913	4076	9695	<lod	<lod	2851	<lod	<lod	<lod	<lod	195856	<lod
Worce mg1	324	17438	<lod	9632	5074	569	2009	5967	<lod	<lod	1162	<lod	<lod	<lod	<lod	191988	<lod
Worcs mg2	287	16409	<lod	8827	6186	618	1655	6934	<lod	<lod	1958	<lod	<lod	<lod	<lod	186445	<lod
Worcs sb1	429	19517	<lod	10529	6520	528	2316	7563	<lod	<lod	1569	<lod	<lod	<lod	<lod	177208	<lod
Worcs sb2	404	19166	<lod	10004	7339	479	1979	9253	<lod	<lod	1060	<lod	<lod	<lod	<lod	167288	<lod
Worcs sb3	308	16716	<lod	7367	5878	518	2323	7167	<lod	<lod	947	<lod	<lod	<lod	<lod	185275	<lod
Worcs sb4 glaze	263	17452	<lod	9533	6243	418	2015	6174	<lod	<lod	1164	<lod	<lod	<lod	<lod	188556	<lod

Appendix 7: Hand-Held XRF data

Appendix Table 11 - peak area data from Hand-Held XRF analysis of glazes on porcelain objects and sherds (continued)

Sample	Al (K)	Si (K)	P (K)	K (K)	Ca (K)	Ti (K)	Mn (K)	Fe (K)	Co (K)	Ni (K)	Cu (K)	Zn (K)	As (K)	Sn (K)	Ba (K)	Pb (L)	Bi (L)
Worcester (continued)																	
Worcs sb5 glaze	173	14982	<lod	10533	7094	416	1935	5803	<lod	<lod	712	<lod	<lod	<lod	<lod	166004	<lod
Worcs tb1 glaze	447	21908	<lod	13637	8701	621	2427	8742	<lod	<lod	1515	<lod	<lod	<lod	<lod	178670	<lod
Worcs tc1 glaze	383	23634	<lod	14997	8687	571	1845	7840	<lod	<lod	1245	<lod	<lod	<lod	<lod	179329	<lod
WUK1 glaze	277	18167	<lod	12581	5643	629	1668	5216	<lod	<lod	1241	<lod	<lod	<lod	<lod	190700	<lod
WUK2 glaze	218	18633	<lod	12929	7411	597	1703	6180	<lod	<lod	753	<lod	<lod	<lod	<lod	165168	<lod
WUK3 glaze	291	16722	<lod	12098	5214	514	2250	5398	<lod	<lod	1621	<lod	<lod	<lod	<lod	179520	<lod
WWR1 glaze	301	17740	<lod	9277	4680	370	2355	5297	<lod	<lod	1216	<lod	<lod	<lod	<lod	196223	<lod
WWR2 glaze	246	13682	<lod	8941	3874	471	2130	5014	<lod	<lod	1098	<lod	<lod	<lod	<lod	174412	<lod
WWR3 glaze	37	126	<lod	252	180	37	115	535	<lod	<lod	172	<lod	<lod	<lod	<lod	63422	<lod
WWR4 glaze	403	20852	<lod	12539	6685	510	1830	7089	<lod	<lod	1213	<lod	<lod	<lod	<lod	189041	<lod
WWR5 glaze	369	19842	<lod	12418	7586	506	1843	6640	<lod	<lod	1135	<lod	<lod	<lod	<lod	169497	<lod

Appendix 7: Hand-Held XRF data

Appendix Table 12 - peak area data from Hand-Held XRF analysis of underglaze blue on porcelain objects and sherds

Sample	Al (K)	Si (K)	K (K)	Ca (K)	Ti (K)	Mn (K)	Fe (K)	Co (K)	Ni (K)	Cu (K)	Zn (K)	As (K)	Sn (K)	Ba (K)	Pb (L)
Bovey Tracey															
BTr cp bl	189	22970	1926	20427	8155	2009	14414	8163	2136	2756	12108	641	7353	3805	156063
BTr sb1 bl	139	23410	1759	19388	6828	2311	13256	7594	1796	1761	11099	676	6943	2593	152408
Bow															
Bow mg1 bl	119	14665	9703	7178	521	<lod	7131	11150	5829	2047	<lod	<lod	4307	<lod	189709
Bow mg2 bl	321	14336	1155	8179	562	2067	8195	9070	6821	3651	<lod	<lod	<lod	<lod	188247
Bow pl1 bl	114	14698	15368	5158	641	<lod	3217	2991	1987	2600	<lod	<lod	5093	<lod	191703
Bow pl3 bl	189	15372	8832	7655	688	<lod	6864	7411	5516	1602	<lod	<lod	4437	<lod	194292
Bow sb1 bl	103	12814	1083	712	443	<lod	4013	3344	1223	1417	<lod	<lod	<lod	<lod	195907
Bow sb2 bl	123	13613	12923	4672	886	<lod	4087	6713	5419	1827	<lod	<lod	4424	<lod	196252
Bow sb3 bl	116	13875	9800	5411	439	<lod	4910	7588	5755	1833	<lod	<lod	4272	<lod	187359
Bow sb5 bl	141	11656	10911	3519	491	<lod	3931	4808	3563	1335	<lod	<lod	3713	<lod	183959
Bow sb7 bl	100	13876	8421	6064	501	<lod	3907	3687	3231	1452	<lod	<lod	3853	<lod	189867
Caughley															
Cy tc1 bl	375	20885	1321	5474	653	1516	11079	13696	7346	660	784	<lod	<lod	<lod	170073
Cy tc2 bl	436	23435	1062	6151	796	1883	13147	10269	5249	1106	1321	<lod	<lod	<lod	172406
Chaffers															
Cha sb1 bl	322	19376	1045	3962	619	3126	19328	17171	9382	3837	764	<lod	<lod	<lod	178663
Cha tb1 bl	236	17311	1168	5269	566	3072	11795	23639	13946	9446	744	<lod	<lod	<lod	171361
Liverpool (Christian)															
Cpen sb1 bl	254	15710	1184	5544	528	2346	10711	14175	10248	4275	720	<lod	<lod	<lod	180100
Derby															
Dby bskt1 bl	241	19640	1138	14023	560	1113	5231	3747	3216	921	<lod	377	<lod	<lod	178382
Dby sb1 bl	263	20265	1316	13566	492	1270	8421	16223	10224	2288	<lod	339	<lod	<lod	181037
Dby tc1 bl	135	15928	1073	13592	390	1468	5082	17174	6900	982	<lod	697	<lod	<lod	188289

Appendix 7: Hand-Held XRF data

Appendix Table 12 - peak area data from Hand-Held XRF analysis of underglaze blue on porcelain objects and sherds (continued)

Sample	Al (K)	Si (K)	K (K)	Ca (K)	Ti (K)	Mn (K)	Fe (K)	Co (K)	Ni (K)	Cu (K)	Zn (K)	As (K)	Sn (K)	Ba (K)	Pb (L)
Derby (continued)															
Dby sb1 bl	230	16417	1156	13420	550	1398	5223	8394	6727	1756	<lod	904	<lod	<lod	195797
Dby vase1 bl	120	16012	1206	9736	459	1721	4951	14513	6007	959	<lod	714	<lod	<lod	195339
Isleworth															
GAH 1 bl	345	18699	1982	15965	603	2166	13278	2818	2611	1349	<lod	<lod	<lod	<lod	191610
GAH 2 bl	773	23114	1164	33647	1031	960	8252	42762	3699	1305	<lod	<lod	<lod	<lod	104732
GAH 5 bl	537	21029	1856	8173	415	1811	6212	4641	4219	1297	<lod	<lod	<lod	<lod	194238
GAH 6 bl	268	20925	1342	9180	536	1606	7912	9976	13119	1645	<lod	<lod	<lod	<lod	185479
Isl sb1 bl	125	16585	1485	4396	433	2151	3593	2142	2612	3248	<lod	<lod	<lod	<lod	193104
Isl sb2 bl	203	18869	1324	6702	530	1959	4562	9656	11391	1910	<lod	<lod	<lod	<lod	187809
Isl tb1 bl	123	15768	1807	1524	465	<lod	4409	3454	3226	2268	<lod	<lod	<lod	<lod	196016
Liverpool (James Pennington)															
Jpen sb1 bl	434	15378	1240	4651	547	2654	15006	11739	13576	2193	<lod	<lod	<lod	<lod	192352
Liverpool (John Pennington)															
JoPen mg1 bl	329	15576	1458	5408	474	2470	6070	15196	8127	5527	<lod	<lod	<lod	<lod	30150
JoPen sb1 bl	268	13852	1266	6638	551	2205	8337	16991	11522	3399	<lod	<lod	<lod	<lod	187241
Limehouse															
Lhse sb1 bl	718	26495	1387	21463	1007	2484	9164	1311	697	1176	<lod	<lod	4909	<lod	167198
Lhse sb2 bl	352	15686	1358	8738	1426	1743	12031	7845	6329	2398	<lod	<lod	2326	<lod	160514
LLK 1 bl	284	15850	1801	14752	591	1999	5885	10585	9107	1637	<lod	<lod	7716	<lod	184283
LLK 4 bl	641	20593	1564	23051	782	2230	9217	3151	2202	865	<lod	<lod	7060	<lod	145221
LLK 5 bl	466	29316	1551	15426	769	1852	6267	2262	1615	1359	<lod	<lod	8409	<lod	181652
LLK 6 bl	436	14444	1610	21074	680	2379	6807	752	611	1647	<lod	<lod	7796	<lod	149621
LLK 7 bl	168	5737	417	4823	190	743	2591	487	288	364	<lod	<lod	1634	<lod	62390

Appendix 7: Hand-Held XRF data

Appendix Table 12 - peak area data from Hand-Held XRF analysis of underglaze blue on porcelain objects and sherds (continued)

Sample	Al (K)	Si (K)	K (K)	Ca (K)	Ti (K)	Mn (K)	Fe (K)	Co (K)	Ni (K)	Cu (K)	Zn (K)	As (K)	Sn (K)	Ba (K)	Pb (L)
Longton Hall															
LH 1 bl	228	16290	2541	48819	1247	922	13157	8077	<lod	3038	<lod	<lod	9665	<lod	155649
LH 2 bl	303	18540	1984	56524	1393	710	9355	4788	6046	1158	<lod	<lod	9590	<lod	149438
LH 3 bl	205	15212	2149	62964	1552	758	8906	4791	5797	1203	<lod	<lod	11934	<lod	145969
LH 4 bl	146	16914	2186	62050	1655	969	19239	16619	18597	1312	<lod	<lod	10887	<lod	158434
LH 5 bl	159	14615	2761	91614	2214	1030	11295	9988	12053	1425	<lod	<lod	14450	<lod	150513
LH 6 bl	178	20791	2072	58293	1373	860	12653	6362	7649	1395	<lod	<lod	11044	<lod	168712
LH mg1 bl	77	13551	1746	21450	688	1208	11005	9196	9143	1362	<lod	1980	4302	<lod	197519
LH sb1 bl	62	18244	1700	34760	827	1503	9514	7660	6314	1208	<lod	2097	4014	<lod	190944
Lowestoft															
Lowe sb1 bl	243	13129	972	7448	476	906	7221	11296	7525	885	<lod	848	<lod	<lod	198998
Lowe sc1 bl	164	13789	1276	8506	578	1623	4698	8561	6446	4231	<lod	<lod	<lod	<lod	194868
Lowe tb1 bl	171	14336	1162	4799	599	1624	3387	6777	4433	3075	<lod	<lod	<lod	<lod	196636
New Hall															
NH sc1 bl	848	19677	1131	32032	252	857	3643	4698	<lod	1392	<lod	<lod	<lod	<lod	183189
NH sc2 bl	834	18499	1185	24975	411	857	6097	42462	<lod	2982	<lod	<lod	<lod	<lod	136531
Liverpool (Reid)															
LRd sb1 bl	149	15437	1248	14307	482	1844	7751	7192	5187	1820	<lod	<lod	<lod	<lod	178421
LRd tb1 bl	621	26755	1127	8041	638	2927	13017	21075	10892	1137	<lod	1571	2236	<lod	181951
Liverpool (Seth Pennington)															
Spen sb1 bl	443	16225	1105	13051	862	1621	7126	22279	7977	1167	<lod	<lod	<lod	<lod	188957
Vauxhall															
EMB 1 bl	374	27352	1821	39550	830	1738	31761	44548	37134	9468	<lod	<lod	<lod	<lod	133897
EMB 2 bl	629	34258	1621	50332	1406	2171	17104	6089	4387	5928	<lod	<lod	<lod	<lod	140697
EMB 3 bl	401	31832	2023	34469	705	1939	15177	12337	10412	10489	<lod	<lod	<lod	<lod	130971

Appendix 7: Hand-Held XRF data

Appendix Table 12 - peak area data from Hand-Held XRF analysis of underglaze blue on porcelain objects and sherds (continued)

Sample	Al (K)	Si (K)	K (K)	Ca (K)	Ti (K)	Mn (K)	Fe (K)	Co (K)	Ni (K)	Cu (K)	Zn (K)	As (K)	Sn (K)	Ba (K)	Pb (L)
Vauxhall (continued)															
EMB 4 bl	171	24805	1871	20727	1314	1516	28433	30090	20494	23977	<lod	<lod	<lod	<lod	83590
EMB 5 bl	337	17394	1784	12679	809	996	4825	3752	5021	371	<lod	<lod	<lod	<lod	188955
EMB 6 bl	358	28687	2125	29902	835	1972	10314	10217	7053	6812	<lod	<lod	<lod	<lod	132235
EMB 7 bl	278	19781	2336	29617	1731	1209	19022	3749	5603	3379	<lod	<lod	<lod	<lod	153832
EMB 8 bl	1973	40039	1037	85539	950	49417	28645	5317	912	277	<lod	<lod	<lod	<lod	533
EMB 9 bl	245	19700	2584	29298	1619	1048	23434	7852	12348	2970	<lod	<lod	<lod	<lod	156763
Vx sb1 bl	113	21840	1867	33192	3591	1833	10318	4851	6060	3772	<lod	<lod	<lod	905	157393
Vx sb2 bl	130	27473	1886	28303	585	1362	7241	11435	6886	4251	<lod	155	<lod	<lod	152801
West Pans															
WP 1 bl	272	15129	1918	22308	675	1332	5941	6821	4309	1614	1738	825	3802	<lod	175506
WP 2 bl	171	17169	1420	21160	721	1565	5640	9662	4133	2464	2236	1453	2461	<lod	188755
WP 3 bl	162	15932	1309	17634	646	1456	3561	5493	3312	1067	682	194	2293	<lod	176974
WP 4 bl	272	21732	1345	18966	806	1756	5470	13383	1996	1680	609	471	2891	<lod	190882
WP 5 bl	257	16669	1542	9297	514	1748	3297	5387	2564	2039	1683	602	3130	<lod	200080
WP 6 bl	213	20144	1585	23307	816	1684	6115	14653	6662	2449	3401	1506	2453	<lod	193790
Worcester															
Worcs mg1 bl	224	13254	1488	5520	535	1815	19878	23411	14249	1530	<lod	1274	<lod	<lod	184727
Worcs mg2 bl	324	17860	1563	6547	780	1540	18967	22795	14400	1774	<lod	895	<lod	<lod	187900
Worcs sb2 bl	480	21210	1192	9175	687	1985	18396	13977	11385	1223	<lod	475	<lod	<lod	175243
Worcs sb3 bl	337	17889	1619	7192	686	2050	15004	14512	12351	1330	<lod	614	<lod	<lod	179905
Worcs sb4 bl	289	18474	1534	7175	468	1836	14825	21846	11002	1501	<lod	212	<lod	<lod	188009
Worcs sb5 bl	328	18259	1605	8576	851	1864	15917	15392	7132	1074	<lod	1360	<lod	<lod	176921
Worcs tb1 bl	251	19214	1411	12034	590	2087	16025	19908	8857	1318	<lod	940	<lod	<lod	180137
Worcs tc1 bl	415	21149	1477	10695	554	1642	25270	33522	36816	1780	<lod	612	<lod	<lod	174322

Appendix 7: Hand-Held XRF data

Appendix Table 13 - peak area data from Hand-Held XRF analysis of underglaze blue subtracted from glaze data

Sample	K (K)	Ca (K)	Ti (K)	Mn (K)	Fe (K)	Co (K)	Ni (K)	Cu (K)	Zn (K)	As (K)	Sn (K)	Pb (L)
Bovey Tracey												
BT cp bl	<lod	188	1121	449	3950	8163	2136	908	1654	641	<lod	<lod
BT sb1 bl	<lod	2517	250	445	1266	7594	1796	<lod	1490	676	<lod	<lod
Bow												
Bow mg1 bl	<lod	625	<lod	149	3400	9070	6821	<lod	<lod	<lod	<lod	<lod
Bow pl1 bl	<lod	<lod	223	<lod	972	2991	1987	1121	<lod	<lod	<lod	<lod
Bow pl3 bl	<lod	<lod	322	<lod	4788	7411	5516	<lod	<lod	<lod	<lod	<lod
Bow sb1 bl	<lod	<lod	134	<lod	1457	3344	1223	<lod	<lod	<lod	<lod	<lod
Bow sb2 bl	1449	530	640	<lod	2048	6713	5419	558	<lod	<lod	182	<lod
Bow sb3 bl	<lod	<lod	<lod	<lod	2434	7588	5755	578	<lod	<lod	593	<lod
Bow sb5 bl	1155	<lod	<lod	<lod	1899	4808	3563	209	<lod	<lod	117	<lod
Bow sb7 bl	<lod	1921	200	<lod	2083	3687	3231	<lod	<lod	<lod	<lod	<lod
Caughley												
Cy tc1 bl	<lod	<lod	<lod	<lod	2148	11398	5750	<lod	<lod	<lod	<lod	<lod
Cy tc2 bl	<lod	1046	<lod	305	3203	10269	5249	<lod	1321	<lod	<lod	16563
Chaffers												
Cha sb1 bl	<lod	<lod	<lod	105	10651	17171	9382	<lod	764	<lod	<lod	<lod
Cha tb1 bl	<lod	<lod	<lod	<lod	3887	23639	13946	1685	<lod	<lod	<lod	<lod
Liverpool (Christian)												
Cpen sb1 bl	<lod	583	<lod	309	4772	14175	10248	<lod	720	<lod	<lod	12525
Derby												
Dby bskt bl	<lod	3091	<lod	<lod	1288	3747	3216	227	<lod	123	<lod	<lod
Dby sb1 bl	<lod	<lod	<lod	<lod	2170	13421	8309	986	<lod	141	<lod	<lod
Dby tc1 bl	<lod	<lod	<lod	<lod	1519	17174	6900	<lod	<lod	<lod	<lod	<lod
dby vase2 bl	<lod	2134	<lod	<lod	1962	14513	6007	<lod	<lod	155	<lod	<lod

Appendix 7: Hand-Held XRF data

Appendix Table 13 - peak area data from Hand-Held XRF analysis of underglaze blue subtracted from glaze data (continued)

Sample	K (K)	Ca (K)	Ti (K)	Mn (K)	Fe (K)	Co (K)	Ni (K)	Cu (K)	Zn (K)	As (K)	Sn (K)	Pb (L)
Isleworth												
GAH1 bl	<lod	10126	216	<lod	8718	2818	2611	459	<lod	<lod	<lod	<lod
GAH2 bl	<lod	<lod	425	<lod	<lod	42762	3699	<lod	<lod	<lod	<lod	<lod
GAH5 bl	<lod	<lod	<lod	<lod	952	4641	4219	392	<lod	<lod	<lod	18955
GAH6 bl	<lod	2861	136	<lod	4630	9976	13119	1145	<lod	<lod	<lod	<lod
Isl sb1 bl	<lod	1303	<lod	446	610	2142	2612	2388	<lod	<lod	<lod	12834
Isl sb2 bl	<lod	1640	<lod	229	1262	9656	11391	970	<lod	<lod	<lod	<lod
Isl tb1 bl	<lod	<lod	<lod	<lod	1659	3454	3226	865	<lod	<lod	<lod	<lod
Liverpool (James Pennington)												
Jpen sb1 bl	<lod	508	125	211	6631	11739	13576	222	<lod	<lod	<lod	<lod
Liverpool (John Pennington)												
JoPen mg1 bl	<lod	<lod	<lod	<lod	637	15196	8127	<lod	<lod	<lod	<lod	<lod
JoPen sb1 bl	<lod	<lod	<lod	469	2832	16991	11522	863	<lod	<lod	<lod	<lod
Limehouse												
Lhse sb1 bl	<lod	3849	161	361	427	1311	697	100	<lod	<lod	<lod	<lod
Lhse sb2 bl	<lod	<lod	434	<lod	4241	7845	6329	<lod	<lod	<lod	<lod	<lod
LLK1 bl	<lod	<lod	<lod	<lod	405	10585	9107	<lod	<lod	<lod	<lod	<lod
LLK4 bl	<lod	8710	258	498	3919	3151	2202	<lod	<lod	<lod	2852	43362
LLK5 bl	<lod	5454	228	918	3125	2262	1615	738	<lod	<lod	5933	115910
LLK6 bl	<lod	<lod	<lod	<lod	<lod	752	611	<lod	<lod	<lod	<lod	<lod
LLK7 bl	<lod	<lod	<lod	<lod	<lod	487	288	<lod	<lod	<lod	<lod	<lod
Longton Hall												
LH frag1 bl	<lod	<lod	<lod	922	4648	8077	13739	1898	<lod	<lod	<lod	<lod
LH frag2 bl	<lod	<lod	<lod	710	2275	4788	6046	250	<lod	<lod	<lod	<lod
LH frag3 bl	<lod	<lod	<lod	758	759	4791	5797	264	<lod	<lod	691	<lod

Appendix 7: Hand-Held XRF data

Appendix Table 13 - peak area data from Hand-Held XRF analysis of underglaze blue subtracted from glaze data (continued)

Sample	K (K)	Ca (K)	Ti (K)	Mn (K)	Fe (K)	Co (K)	Ni (K)	Cu (K)	Zn (K)	As (K)	Sn (K)	Pb (L)
Longton Hall (continued)												
LH frag4 bl	<lod	<lod	<lod	969	9692	16619	18597	<lod	<lod	<lod	2514	<lod
LH frag5 bl	<lod	16135	206	1030	4148	9988	12053	180	<lod	<lod	3693	<lod
LH frag6 bl	<lod	<lod	<lod	860	6603	6362	7649	231	<lod	<lod	<lod	<lod
LH mg1 bl	<lod	<lod	<lod	103	6450	9196	9143	496	<lod	958	437	<lod
LH sb1 bl	<lod	889	<lod	<lod	3001	5097	4134	217	<lod	857	563	11625
Lowestoft												
Lowe sb1 bl	<lod	<lod	<lod	<lod	2782	11296	7525	<lod	<lod	324	<lod	<lod
Lowe sc1 bl	<lod	<lod	195	614	2640	8561	6446	2991	<lod	<lod	<lod	69239
New Hall												
NH sc1 bl	<lod	2189	<lod	<lod	<lod	4698	<lod	381	<lod	<lod	<lod	<lod
NH sc2 bl	<lod	<lod	<lod	<lod	<lod	42462	<lod	1770	<lod	<lod	<lod	<lod
Liverpool (Reid)												
LRd sb1 bl	<lod	<lod	<lod	<lod	<lod	7192	5187	<lod	<lod	<lod	<lod	<lod
Liverpool (Seth Pennington)												
Spn sb1 bl	<lod	1381	176	<lod	1753	22279	7977	<lod	<lod	<lod	<lod	<lod
Vauxhall												
EMB1 bl	<lod	<lod	<lod	<lod	21496	44548	37134	2207	<lod	<lod	<lod	<lod
EMB2 bl	<lod	<lod	<lod	<lod	2581	6089	4387	<lod	<lod	<lod	<lod	<lod
EMB3 bl	<lod	<lod	<lod	<lod	5687	12337	10412	671	<lod	<lod	<lod	<lod
EMB4 bl	<lod	4220	<lod	<lod	13000	30090	20494	<lod	<lod	<lod	<lod	<lod
EMB5 bl	<lod	<lod	<lod	<lod	<lod	3752	5021	<lod	<lod	<lod	<lod	26154
EMB6 bl	<lod	1074	<lod	<lod	2213	10217	7053	<lod	<lod	<lod	<lod	<lod
EMB7 bl	<lod	<lod	<lod	166	1608	3749	5603	1046	<lod	<lod	<lod	<lod
EMB9 bl	<lod	<lod	<lod	<lod	5829	7852	12348	546	<lod	<lod	<lod	<lod

Appendix 7: Hand-Held XRF data

Appendix Table 13 - peak area data from Hand-Held XRF analysis of underglaze blue subtracted from glaze data (continued)

Sample	K (K)	Ca (K)	Ti (K)	Mn (K)	Fe (K)	Co (K)	Ni (K)	Cu (K)	Zn (K)	As (K)	Sn (K)	Pb (L)
Vauxhall (continued)												
Vx mg1 bl	<lod	766	274	<lod	8636	14104	14502	1121	<lod	1490	821	11361
Vx sb1 bl	<lod	2683	170	102	3649	4851	6060	<lod	<lod	<lod	<lod	13133
Vx sb2 bl	<lod	1706	<lod	308	1391	9978	5799	<lod	<lod	<lod	<lod	<lod
West Pans												
WP frag1 bl	<lod	541	152	<lod	2423	6821	4309	718	1738	825	3802	12033
WP frag2 bl	<lod	6851	144	<lod	2619	9662	4133	1623	2236	1453	2461	21015
WP frag3 bl	<lod	<lod	<lod	<lod	218	5493	3312	444	682	194	2293	19488
WP frag4 bl	<lod	<lod	<lod	337	1205	13383	1996	1164	609	471	2891	32603
WP frag5 bl	<lod	<lod	<lod	494	445	5387	2564	1602	1683	602	3130	47971
WP frag6 bl	<lod	3581	141	219	2399	14653	6662	1909	3401	1506	2453	33230
Worcester												
Worcs mg1 bl	<lod	446	<lod	<lod	13911	23411	14249	368	<lod	1274	<lod	<lod
Worcs mg2 bl	<lod	361	162	<lod	12033	22795	14400	<lod	<lod	895	<lod	<lod
Worcs sb2 bl	<lod	1836	208	<lod	9143	13977	11385	163	<lod	475	<lod	<lod
Worcs sb3 bl	<lod	1314	168	<lod	7837	14512	12351	383	<lod	614	<lod	<lod
Worcs sb4 bl	<lod	932	<lod	<lod	8651	21846	11002	337	<lod	212	<lod	<lod
Worcs sb5 bl	<lod	1482	435	<lod	10114	15392	7132	362	<lod	1360	<lod	10917
Worcs tb1 bl	<lod	3333	<lod	<lod	7283	19908	8857	<lod	<lod	940	<lod	<lod
Worcs tc1 bl	<lod	2008	<lod	<lod	17430	33522	36816	535	<lod	612	<lod	<lod

Appendix 7: Hand-Held XRF data

Appendix Table 14 - peak area data from Hand-Held XRF analysis of overglaze blue enamel

Sample	Al (K)	Si (K)	K (K)	Ca (K)	Ti (K)	Cr (K)	Mn (K)	Fe (K)	Co (K)	Ni (K)	Cu (K)	Zn (K)	As (K)	Sn (K)	Pb (L)
Worcester															
111 bl 1	345	18459	14537	6934	634	<lod	1645	24528	39002	31282	1162	855	1025	<lod	175965
111 bl 2	299	16890	10966	4706	657	<lod	1772	12516	16678	5378	1048	845	613	<lod	175704
292 bl	195	9801	5784	6426	1084	10615	2023	26422	21653	3330	19682	56888	<lod	2835	175590
377 bl	<lod	29214	29995	42893	1459	<lod	8630	17122	41843	3226	3396	<lod	1493	<lod	153242
65 bl	146	14779	10862	4759	420	<lod	1557	6568	29248	4425	1069	<lod	<lod	<lod	180913
804 bl	114	19073	35312	5912	1010	<lod	2066	3960	59292	2438	<lod	<lod	2816	<lod	184280
WJG6 bl	107	12875	7627	4946	1290	<lod	3270	12806	10043	1794	9833	<lod	623	<lod	181344
WJG8 bl	<lod	15297	11338	5904	779	<lod	1367	14101	15789	849	710	<lod	531	<lod	170552
WJG9 bl	<lod	13282	9559	4143	342	<lod	1095	4520	24004	1410	9497	<lod	1334	<lod	190202
WUK1 bl	<lod	17283	13358	6086	488	<lod	1556	17531	20698	16071	1425	<lod	938	<lod	176786
WWR1 bl	<lod	15607	9485	5208	412	<lod	1861	9351	9547	7215	1189	<lod	610	<lod	188838
WWR2 bl	394	18487	10045	4863	449	<lod	2217	5615	2200	1640	1455	<lod	<lod	<lod	193971
WWR5 bl	199	12354	7669	8374	1616	<lod	4061	11416	10626	3395	8411	<lod	<lod	3816	182564

Appendix 7: Hand-Held XRF data

Appendix Table 15 - peak area data from Hand-Held XRF analysis of overglaze green enamel grounds and borders

Sample	Al (K)	Si (K)	K (K)	Ca (K)	Ti (K)	Cr (K)	Mn (K)	Fe (K)	Co (K)	Ni (K)	Cu (K)	Zn (K)	Sn (K)	Pb (L)
Worcester														
1005 grgd 2	97	9056	3734	8331	650	<lod	1040	8017	<lod	<lod	81160	<lod	10744	153526
1010 grgd	119	10832	5352	11125	611	<lod	1003	8242	<lod	<lod	92276	<lod	10341	157000
1012 grgd	111	9513	5541	11354	731	<lod	850	4039	<lod	<lod	97314	<lod	11237	165865
1012 grgd lid	105	9634	5449	11393	724	<lod	652	4158	<lod	<lod	98591	<lod	11227	166454
1014 grgd	99	4770	3302	6919	510	<lod	860	3054	<lod	<lod	62152	<lod	9536	130041
1016 grgd	217	9712	5659	13279	893	<lod	825	5308	<lod	<lod	79243	<lod	10280	163110
927 grgd tp	189	13369	8329	10375	829	5749	642	9135	2188	680	43906	5883	5344	178093
927 grgd tp	195	12009	8392	10327	766	4288	551	7280	1734	664	39882	4970	5292	173698
927 grgd tp	195	12652	8717	9412	901	3322	661	7071	1469	575	32222	4229	5171	175022
929 st grgd	86	9580	5303	10036	787	<lod	860	9336	<lod	<lod	82167	<lod	11410	152170
929 t grgd	181	17978	6844	13705	835	<lod	958	11083	<lod	<lod	99153	<lod	14763	171007
929 tld grgd	85	12895	6129	11738	855	<lod	908	11065	<lod	<lod	84174	<lod	12641	155179
929 tt grgd	137	18422	7996	15121	876	<lod	856	13253	<lod	<lod	99913	<lod	14115	172382
930 grgd	119	13470	8455	17393	1070	<lod	876	10107	<lod	<lod	90264	<lod	11024	165239
932 grgd	357	14136	19591	39697	1980	79545	1162	7907	12662	1556	1948	24408	4310	52262
934 grgd	97	13297	6313	10033	756	<lod	885	9292	<lod	<lod	103521	<lod	11409	166662

Appendix 7: Hand-Held XRF data

Appendix Table 16 - peak area data from Hand-Held XRF analysis of overglaze green painted enamels

Sample	Al (K)	Si (K)	K (K)	Ca (K)	Ti (K)	Cr (K)	Mn (K)	Fe (K)	Co (K)	Ni (K)	Cu (K)	Zn (K)	Sn (K)	Pb (L)
Worcester														
1010 gre	198	12069	4008	8447	825	<lod	6887	5928	<lod	<lod	43976	<lod	4516	185247
1012 gre	148	14576	8075	10360	707	7588	941	10619	842	378	16598	2010	2920	168549
1014 gre	263	11267	5056	9712	955	6260	614	9117	4595	469	25092	7289	3358	185782
1016 gre	246	12739	5457	5191	414	<lod	4680	6767	<lod	<lod	21355	<lod	<lod	190897
292 gre	240	10607	6004	7353	1185	8739	2301	18805	6398	2573	10814	4843	2862	182961
480 gre	119	7504	3014	8221	909	6611	762	4132	5033	413	1959	15574	3016	177516
617 gre	288	15388	8387	10145	798	<lod	1492	7620	1135	<lod	27649	<lod	<lod	183119
620 gre	390	16371	8069	5499	452	<lod	2230	5901	<lod	<lod	5831	<lod	<lod	181740
65 gre	275	14886	8669	4805	639	<lod	2114	6168	4156	<lod	22305	<lod	<lod	190329
696 gre	252	14139	10400	10862	749	<lod	1487	7771	<lod	<lod	28997	<lod	4220	176407
697 gre	153	14539	7566	11917	554	<lod	2633	12582	3038	1896	67015	<lod	4250	175509
698 gre	290	14826	6199	7315	594	<lod	1749	7323	1692	<lod	26563	<lod	<lod	187517
699 gre	97	10963	3414	7328	764	<lod	1213	6825	<lod	<lod	65035	<lod	3673	191074
702 gre	65	9765	2623	7526	684	<lod	1285	6940	<lod	<lod	46396	<lod	3543	185531
703 gre	148	7673	3677	9138	561	<lod	1284	5040	1001	<lod	31732	<lod	<lod	160960
704 gre	156	12924	6501	7766	589	<lod	1766	5989	<lod	<lod	29447	<lod	<lod	186005
705 gre	231	14515	6523	7348	831	3859	626	6766	2946	419	20101	12793	3072	178010
804 gre	96	10059	2163	6704	574	<lod	1441	6607	<lod	<lod	58079	<lod	<lod	189778
826 gre	146	8621	3141	4347	360	<lod	1035	5529	<lod	<lod	21846	<lod	<lod	153885

Appendix 7: Hand-Held XRF data

Appendix Table 16 - peak area data from Hand-Held XRF analysis of overglaze green painted enamels (continued)

Sample	Al (K)	Si (K)	K (K)	Ca (K)	Ti (K)	Cr (K)	Mn (K)	Fe (K)	Co (K)	Ni (K)	Cu (K)	Zn (K)	Sn (K)	Pb (L)
Worcester (continued)														
829 gre	102	10149	1600	5926	496	<lod	2644	10970	<lod	<lod	41868	<lod	<lod	186384
914 gre	161	14545	10342	5775	821	7133	679	5255	1513	639	1470	18675	2760	181860
927 gre ld	96	8008	4927	7813	525	<lod	1398	4026	<lod	<lod	57109	<lod	7983	157063
927 gre tp	233	13470	8778	11269	829	<lod	2140	9147	<lod	<lod	45467	<lod	5344	178093
927 gre tp	219	12096	8876	11225	766	<lod	1768	7544	<lod	<lod	41553	<lod	5292	173698
929 gre st	218	12946	5145	6015	603	<lod	3440	8454	<lod	<lod	25867	<lod	<lod	186988
929 gre tld	171	12605	4295	4002	464	<lod	3843	8549	<lod	<lod	44552	<lod	<lod	189127
929 gre tt	235	12482	5526	4859	503	<lod	1971	7080	<lod	<lod	28560	<lod	<lod	181465
930 gre	125	13777	9796	20617	914	<lod	808	10646	<lod	<lod	99224	<lod	12778	161674
932 gre	339	14339	19077	42512	1610	79471	1778	8139	12386	1222	1412	24133	4098	49614
934 gre	185	12679	6500	10539	693	<lod	2667	12185	<lod	<lod	14308	<lod	3242	187592
WJG4 gre	203	13919	6909	6418	599	<lod	1697	6369	<lod	<lod	18583	<lod	<lod	182305
WJG6 gre	419	20140	10278	6842	714	<lod	1935	7431	<lod	<lod	11419	<lod	<lod	182478
WJG8 gre	347	20231	10013	6119	658	<lod	2263	7358	<lod	<lod	6080	<lod	<lod	178919
WJG9 gre	138	14476	7242	11732	424	<lod	5006	23769	<lod	<lod	78321	<lod	<lod	172450
WON1 gre	245	7308	2031	6757	8192	<lod	4150	5933	<lod	<lod	15639	<lod	<lod	193733
WUK2 gre	161	13206	10278	6212	498	<lod	2717	17252	<lod	<lod	53591	<lod	<lod	171570
WWR5 gre	310	15714	9539	7962	514	<lod	3444	6184	<lod	<lod	20855	<lod	<lod	176496
WWR6 gre	316	17505	10950	6852	714	<lod	2126	6939	<lod	<lod	4084	<lod	<lod	185691

Appendix 7: Hand-Held XRF data

Appendix Table 17 - peak area data from Hand-Held XRF analysis of overglaze orange enamels

Sample	Al (K)	Si (K)	K (K)	Ca (K)	Ti (K)	Mn (K)	Fe (K)	Ni (K)	Cu (K)	Zn (K)	Sn (K)	Pb (L)
Worcester												
111 or	256	13862	12501	6232	786	1875	56686	2082	1468	<lod	<lod	178631
377 or	210	15916	7919	7107	597	1948	36019	<lod	1890	<lod	<lod	173437
826 or	304	12983	10617	6622	723	1679	36087	<lod	1403	1974	<lod	147640
829 or	118	11260	2788	10771	442	2998	37741	<lod	2730	886	<lod	181847
WJG2 or	57	4526	8369	10616	1592	1739	60793	<lod	1793	<lod	3353	184000
WJG4 or	288	16946	10150	7565	661	1900	18417	<lod	1358	<lod	<lod	185904

Appendix 7: Hand-Held XRF data

Appendix Table 18 - peak area data from Hand-Held XRF analysis of overglaze pink enamels

Sample	Al (K)	Si (K)	K (K)	Ca (K)	Ti (K)	Mn (K)	Fe (K)	Zn (K)	As (K)	Sn (K)	Ba (K)	Au (L)	Pb (L)
Worcester													
480 pn	259	15357	10197	12465	13513	2346	4363	5823	<lod	3519	173	<lod	186303
574 pn	143	10350	9020	10587	1516	1400	4942	<lod	<lod	2556	<lod	<lod	163992
617 pn	356	17202	11388	8077	666	1801	6409	<lod	563	<lod	<lod	<lod	189255
65 pn	124	12121	8166	4899	319	3185	3975	<lod	<lod	<lod	<lod	24352	164400
696 pn	165	12516	11935	11358	820	1966	5256	2331	<lod	3169	<lod	11874	174023
697 pn	<lod	11098	8885	8882	459	5521	6441	<lod	<lod	<lod	<lod	31610	134496
698 pn	197	16063	8711	8938	507	2756	6836	<lod	<lod	<lod	<lod	<lod	180997
699 pn	107	15630	8539	3793	435	1714	9718	<lod	<lod	<lod	<lod	<lod	190350
702 pn	180	15911	12882	12489	565	3109	5600	<lod	<lod	<lod	<lod	<lod	186310
703 pn	206	10239	8546	5350	478	1635	8802	<lod	<lod	<lod	<lod	<lod	152742
704 pn	143	17605	12156	9442	527	3434	5578	<lod	<lod	<lod	<lod	<lod	188955
804 pn	191	17498	8008	4378	481	2108	4796	<lod	<lod	<lod	<lod	<lod	189221
DJG1 pn	109	12672	9471	8410	422	1711	3439	<lod	<lod	<lod	<lod	10920	189732
WJG1 pn	<lod	11613	7628	3336	341	2040	6620	<lod	<lod	<lod	<lod	<lod	173933
WJG2 pn	<lod	5029	8013	9546	1453	3962	5859	<lod	<lod	<lod	<lod	<lod	188385
WJG4 pn	<lod	12055	5175	3246	310	1602	4307	<lod	<lod	<lod	<lod	<lod	163334
WJG5 pn	216	13747	9994	5985	489	4406	7573	<lod	<lod	<lod	<lod	<lod	180976
WJG6 pn	168	21386	13543	16205	579	5008	6956	<lod	<lod	<lod	<lod	<lod	182506
WJG8 pn	219	20690	9999	5724	762	2159	19424	<lod	<lod	<lod	<lod	<lod	179454
WWR5 pn	248	15674	9681	11095	375	2668	6174	<lod	<lod	<lod	<lod	<lod	171367
WWR6 pn	168	15528	7850	4511	643	2261	7248	<lod	<lod	<lod	<lod	<lod	187612

Appendix 7: Hand-Held XRF data

Appendix Table 19 - peak area data from Hand-Held XRF analysis of overglaze purple enamels

	Al (K)	Si (K)	K (K)	Ca (K)	Ti (K)	Mn (K)	Fe (K)	Co (K)	Ni (K)	Cu (K)	Zn (K)	As (K)	Sn (K)	Pb (L)
Worcester														
WJG3 pur	201	13562	6735	7215	392	2059	9526	3628	2350	<lod	<lod	<lod	<lod	188420
WJG8 pur	131	12771	4688	5096	772	1633	7687	14676	965	<lod	<lod	<lod	<lod	187665
WJG9 pur	350	16009	8484	5446	745	6437	5642	626	602	1612	<lod	<lod	<lod	186261
WUK1 pur	167	11221	7376	5775	623	3881	5440	910	470	995	<lod	<lod	<lod	169406
WUK2 pur	116	13888	10017	4686	393	1938	5172	2611	2263	<lod	<lod	<lod	<lod	164000
WWR6 pur	271	16026	9988	7419	720	1710	6015	473	597	1311	2046	551	3071	184620

Appendix Table 20 - peak area data from Hand-Held XRF analysis of overglaze red enamels

	Al (K)	Si (K)	K (K)	Ca (K)	Ti (K)	Cr (K)	Mn (K)	Fe (K)	Cu (K)	Zn (K)	Sn (K)	Ba (K)	Pb (L)
Worcester													
576 red	328	15926	8020	4094	416	<lod	2969	14678	3608	<lod	<lod	<lod	190438
620 red	229	9945	5925	4120	465	<lod	2739	17786	11126	<lod	<lod	<lod	162338
620 red	244	12013	6135	4946	670	<lod	5217	21881	16535	<lod	<lod	<lod	188399
65 red	218	14245	9828	6518	508	<lod	1518	24172	3480	<lod	<lod	<lod	187538
705 red	201	11076	4924	6733	1476	1212	371	69816	2574	15775	2601	147	181887
WJG8 red	321	15840	7873	5600	467	<lod	1808	37742	1568	<lod	<lod	<lod	180643
WWR1 red	183	8713	6696	3280	644	<lod	1719	71181	1459	<lod	<lod	<lod	180180
WWR5 red	348	14695	12348	8846	640	<lod	2048	45199	1554	<lod	<lod	<lod	172888

Appendix 7: Hand-Held XRF data

Appendix Table 21 - peak area data from Hand-Held XRF analysis of overglaze turquoise enamels

	Al (K)	Si (K)	K (K)	Ca (K)	Ti (K)	Cr (K)	Mn (K)	Fe (K)	Co (K)	Ni (K)	Cu (K)	Zn (K)	As (K)	Sn (K)	Au (K)	Pb (L)
Worcester																
576 tqgd	199	13371	14722	4345	487	<lod	7786	22013	4381	5687	83519	<lod	518	<lod	<lod	171966
577 tqgd	68	9237	4985	2614	335	<lod	707	3700	<lod	<lod	133627	<lod	<lod	<lod	<lod	147790
620 tqgd	87	12453	8107	9143	558	<lod	1293	4837	<lod	<lod	74040	<lod	<lod	5645	<lod	147452
65 tqgd	163	12875	8340	2867	439	<lod	1110	3916	3350	797	49459	<lod	490	<lod	<lod	191377
698 tqgd	143	12418	10391	8559	474	<lod	791	4866	<lod	<lod	87675	<lod	3217	<lod	<lod	181957
699 tqgd	86	10677	7325	4077	430	<lod	1605	4699	<lod	<lod	55820	<lod	1254	<lod	<lod	168289
700 tqgd	179	16954	37320	29289	1522	<lod	1044	4383	<lod	<lod	87275	3704	<lod	9467	<lod	159813
701 tqgd cp	131	13502	10947	7838	383	<lod	652	4994	<lod	<lod	91119	<lod	3600	<lod	<lod	189974
702 tqgd	84	11447	8078	4506	513	<lod	2009	6065	2426	<lod	76817	<lod	<lod	<lod	19402	162542
703 tqgd	113	12781	10971	7451	428	<lod	426	4139	<lod	<lod	90287	<lod	3541	<lod	<lod	183519
704 tqgd	128	15560	11291	4890	442	<lod	1435	6392	3430	425	89611	<lod	1182	<lod	<lod	185442
705 tqgd	84	11723	8150	12459	627	<lod	781	3544	<lod	<lod	35723	<lod	1755	9519	<lod	187085
914 tqgq	282	14833	10050	4138	476	7126	1153	4615	<lod	<lod	2851	7630	<lod	<lod	18200	170100
919 tqgd sc	120	14044	35296	27700	1551	<lod	1023	5434	<lod	<lod	104648	4037	<lod	7206	<lod	151823
WJG5 tqe	179	13415	10442	5499	534	<lod	4316	6951	<lod	<lod	18254	<lod	<lod	<lod	<lod	176328

Appendix 7: Hand-Held XRF data

Appendix Table 22 - peak area data from Hand-Held XRF analysis of overglaze yellow enamels

	Al (K)	Si (K)	K (K)	Ca (K)	Ti (K)	Cr (K)	Mn (K)	Fe (K)	Co (K)	Ni (K)	Cu (K)	Zn (K)	As (K)	Sn (K)	Sb (K)	Au (K)	Pb (L)
Worcester																	
240 yelgd	162	8176	3514	8795	722	<lod	1852	5972	<lod	<lod	1992	678	<lod	2641	<lod	<lod	182283
292 yel	273	11176	6653	9924	1419	9446	1927	15342	7202	2731	1599	4266	<lod	3094	<lod	<lod	189942
480 yel	234	12886	6333	10884	733	<lod	1776	5946	<lod	<lod	1897	2320	<lod	3156	<lod	<lod	190682
65 yel	80	12381	7205	7887	530	<lod	1520	15426	<lod	<lod	3562	743	<lod	3114	<lod	<lod	188891
696 yel	172	10343	7421	9383	1358	17702	860	19196	<lod	<lod	5388	31087	<lod	3088	<lod	<lod	178711
697 yel	112	14649	9530	11896	710	<lod	1924	10780	<lod	<lod	6647	1103	<lod	2895	<lod	<lod	181169
698 yel	191	15601	8094	10280	783	<lod	2050	19478	<lod	<lod	1716	1543	<lod	2787	<lod	<lod	184759
699 yel	115	10832	5953	17697	1414	<lod	2000	11766	<lod	<lod	2917	931	3920	3780	709	<lod	184405
702 yel	114	9594	5263	16800	1196	<lod	1769	9299	<lod	<lod	2180	1106	3739	3642	696	<lod	181879
703 yel	81	5872	3733	13573	941	<lod	1773	6516	<lod	<lod	2169	522	2997	2096	488	<lod	149567
704 yel	67	10111	5967	16866	1388	<lod	1942	12302	<lod	<lod	1989	823	3647	3420	620	<lod	182040
705 yel	103	6669	3863	4734	858	3508	459	5449	<lod	<lod	13957	12072	<lod	1782	<lod	5506	136697
829 yel	170	11872	3410	9230	805	<lod	6213	33265	<lod	<lod	8954	1041	2902	2537	393	<lod	179768
914 yel	212	11920	9046	7631	938	12446	717	4843	<lod	<lod	1801	33638	<lod	2904	<lod	1817	185283
DJG1 yel	310	14104	7086	9894	1690	<lod	1337	11739	<lod	<lod	2761	652	526	3421	<lod	<lod	195996
WJG1 yel	77	6935	4781	8574	654	<lod	1816	23268	<lod	<lod	7730	507	3931	2417	325	<lod	157964
WJG6 yel	172	13128	6225	8796	1245	<lod	3040	6443	<lod	<lod	16670	1501	3738	3156	328	<lod	181924
WWR2 yel	150	9014	2996	6840	885	<lod	1766	4497	<lod	<lod	1605	608	3027	2500	155	<lod	176643
WWR5 yel	236	9648	3104	10352	700	<lod	5736	6169	2410	2338	2853	<lod	<lod	3686	<lod	<lod	187041

Appendix 7: Hand-Held XRF data

Appendix Table 23 - peak area data from Hand-Held XRF analysis of gilding

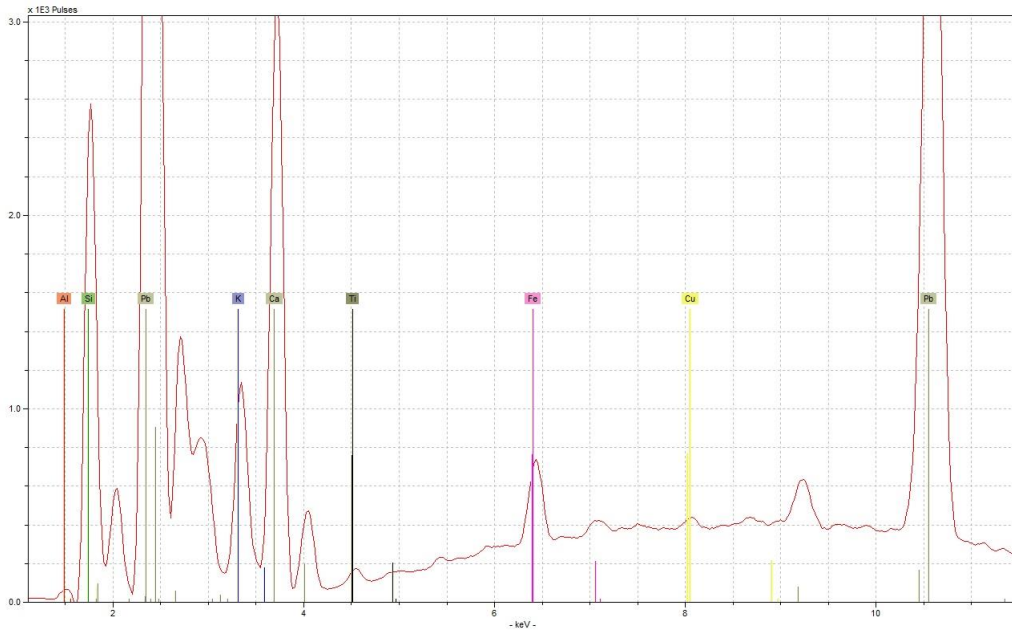
	Al (K)	Si (K)	K (K)	Ca (K)	Ti (K)	Mn (K)	Fe (K)	Cu (K)	Ag (K)	Sn (K)	Au (L)	Pb (L)
Bow												
BUK1 au	88	6332	4623	4449	300	1732	3714	2273	<lod	<lod	36675	117716
Worcester												
1016 au	169	10376	6354	4046	318	3111	7149	1890	<lod	<lod	18783	160522
480 au	201	15839	9708	5411	681	2744	4783	1821	<lod	<lod	26391	166883
571 au	461	16776	11489	5272	602	1911	9725	1915	<lod	<lod	6954	157137
574 au	377	18196	11732	6160	645	1970	7100	1193	<lod	<lod	6605	176664
576 au	294	16868	8972	2972	440	1946	7199	1705	<lod	<lod	3894	177679
617 au	439	17890	11035	6587	616	2260	5889	1614	<lod	<lod	7961	185838
65 au	296	12071	7819	4873	369	1110	4204	2208	<lod	<lod	9053	138013
698 au	253	13228	8721	7226	517	2676	7229	2224	<lod	<lod	36895	152442
704 au	328	18039	13618	6600	677	2481	5751	1736	<lod	<lod	10050	178536
705 au	209	13409	8180	5696	570	2410	6276	1395	<lod	<lod	13926	151825
WJG7 au	179	13540	7823	3693	320	4862	7258	3050	<lod	<lod	41577	152016
WWR1 au	171	12776	7819	4003	316	4545	4539	2485	<lod	<lod	30043	165022
1006 au	104	10555	6246	3622	474	3403	6093	3628	14127	<lod	347135	519706
1010 au	167	12341	8075	4671	458	3272	6734	2152	1455	<lod	34313	144437
577 au	131	11685	7918	4585	433	3256	6439	2654	1327	<lod	29065	165557
696 au	125	9042	7745	3859	381	6004	5255	5918	1195	<lod	46922	124150
703 au	217	12204	10319	5724	637	2921	5782	1890	952	<lod	34529	136974
934 au	84	9968	6907	4036	439	5128	7150	3613	2378	<lod	75696	106881
WJG9 au	38	6647	3657	2403	370	6267	11607	4694	2051	<lod	98434	103154
699 au	301	17678	16641	7307	632	1762	9555	3506	<lod	<lod	5780	178197
WJG5 au	153	13531	10247	5156	534	4029	17170	12369	<lod	<lod	21283	167827

Appendix 7: Hand-Held XRF data

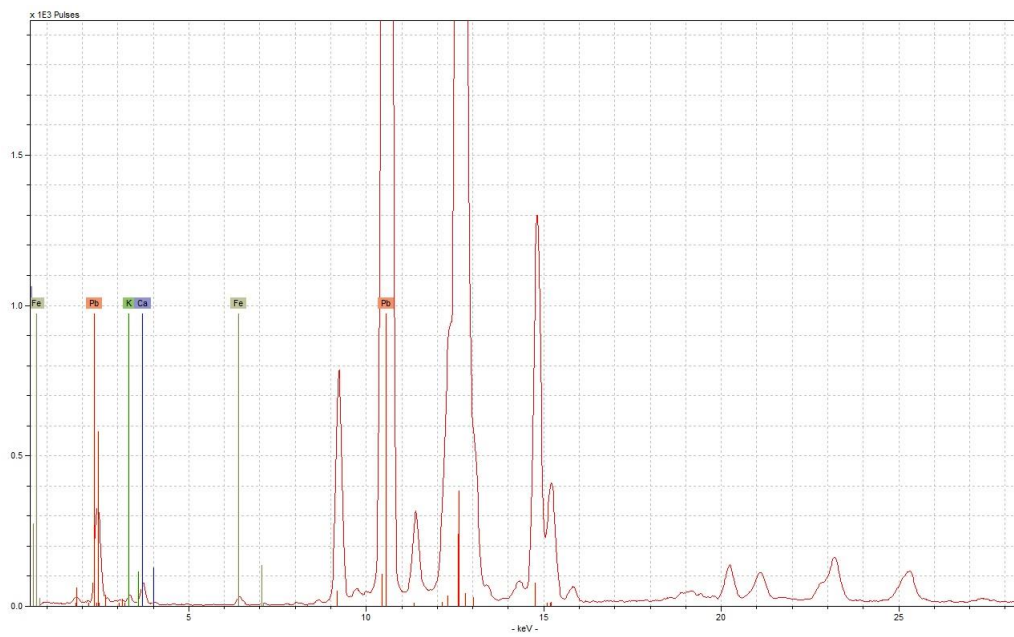
Appendix Table 23 - peak area data from Hand-Held XRF analysis of gilding (continued)

	Al (K)	Si (K)	K (K)	Ca (K)	Ti (K)	Mn (K)	Fe (K)	Cu (K)	Ag (K)	Sn (K)	Au (L)	Pb (L)
Worcester (continued)												
700 au	48	7650	9792	15535	884	4345	3864	48115	<lod	5173	48099	101697
914 au	6	2203	3123	3450	108	6833	4725	18844	<lod	2800	134693	63523
919 au sc	2	3152	2836	5335	163	5975	4670	25017	<lod	2626	149403	41595
702 au	18	3608	4048	2535	609	4769	2638	39137	2921	<lod	109868	86342
804 au	26	3586	4003	1646	572	6606	1486	6140	4389	<lod	128334	62155

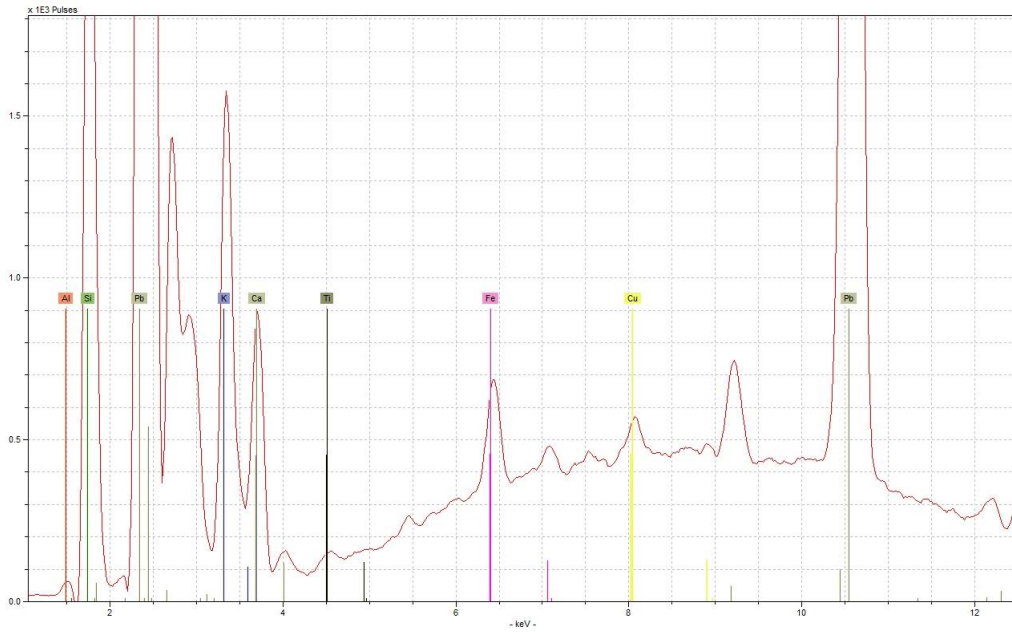
Appendix 7: Hand-Held XRF data



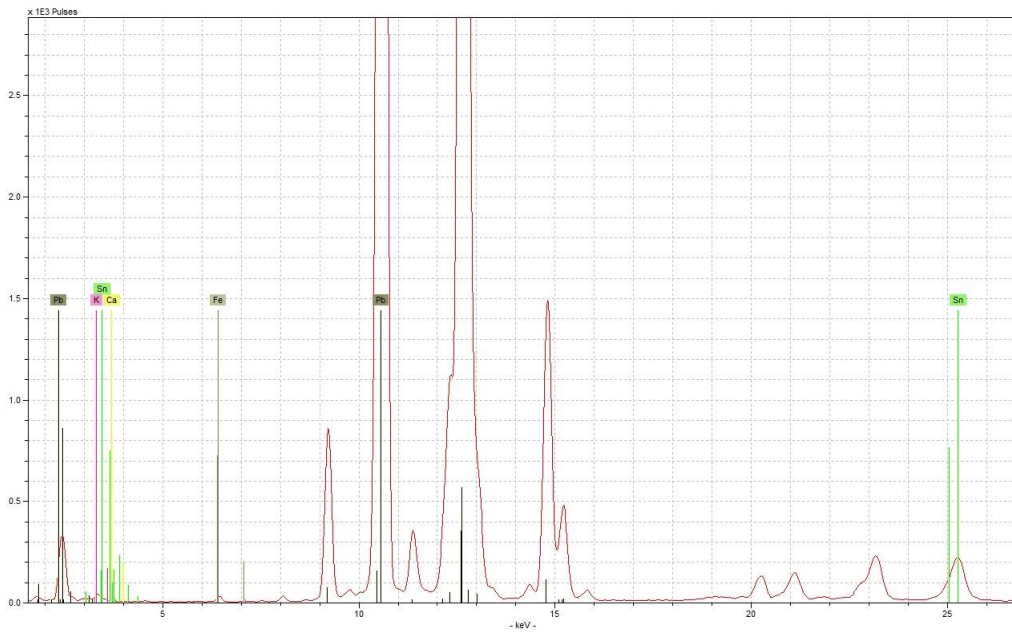
Appendix Figure 30 - example spectrum for glaze type 1 from HNB sherd 1, obtained under low voltage condition (upper), and high voltage condition (lower)



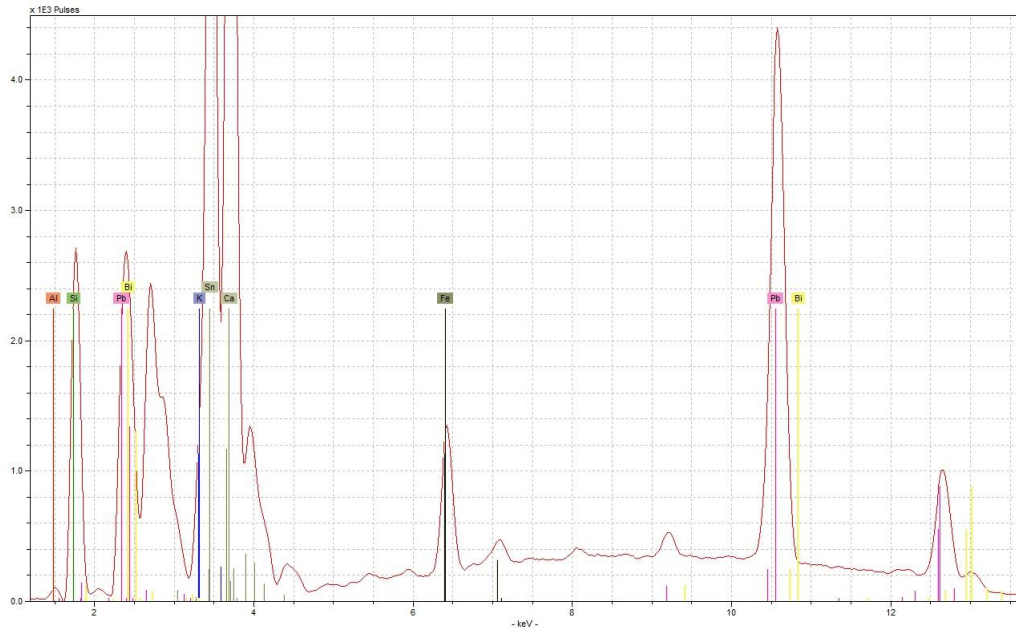
Appendix 7: Hand-Held XRF data



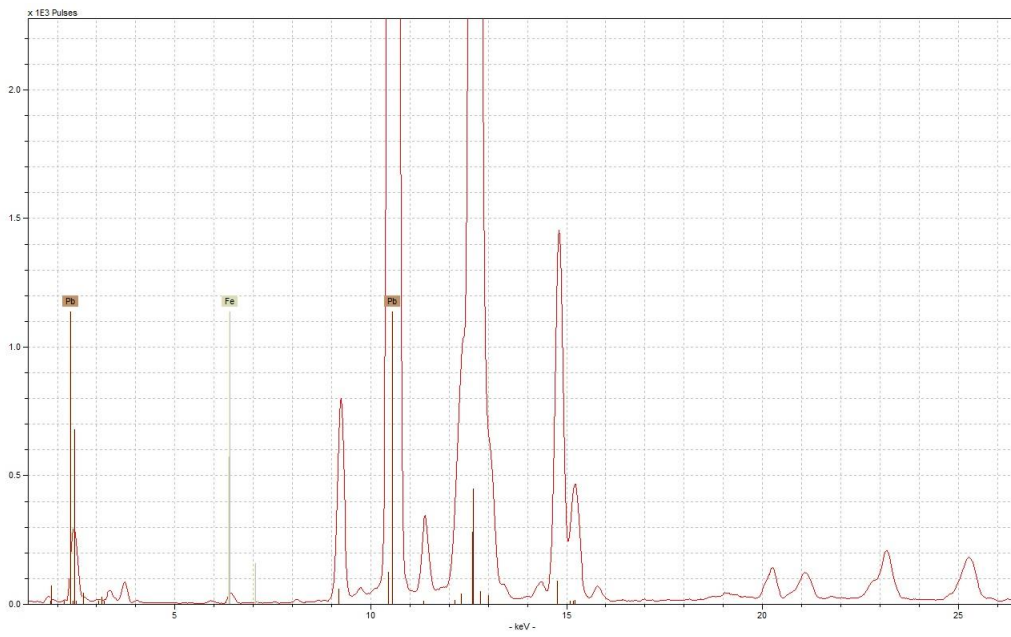
Appendix Figure 31 - example spectrum for glaze type 2 from Bow mg1, obtained under low voltage condition (upper), and high voltage condition (lower)



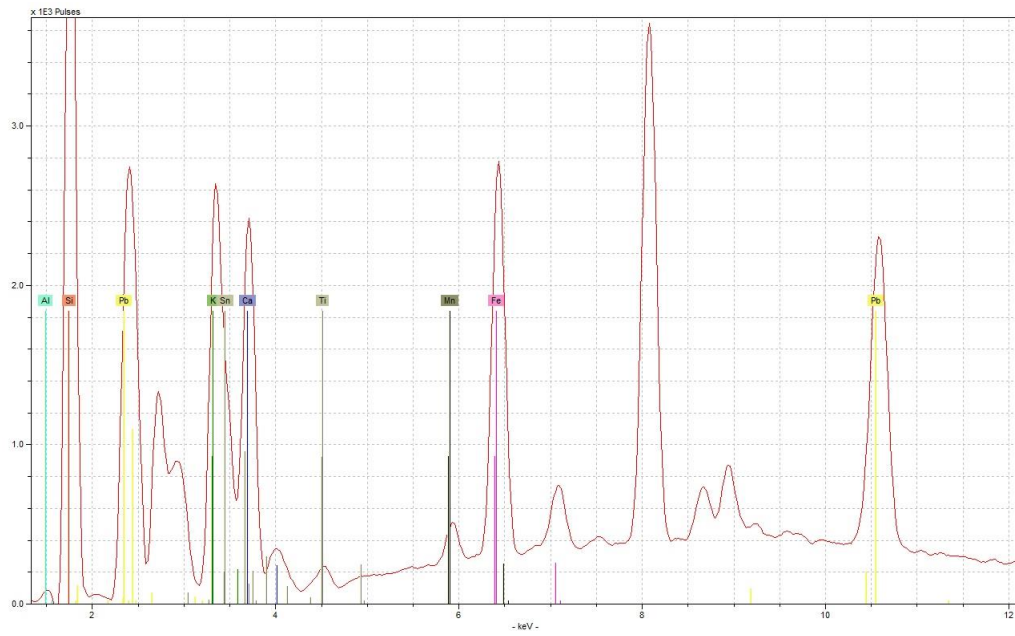
Appendix 7: Hand-Held XRF data



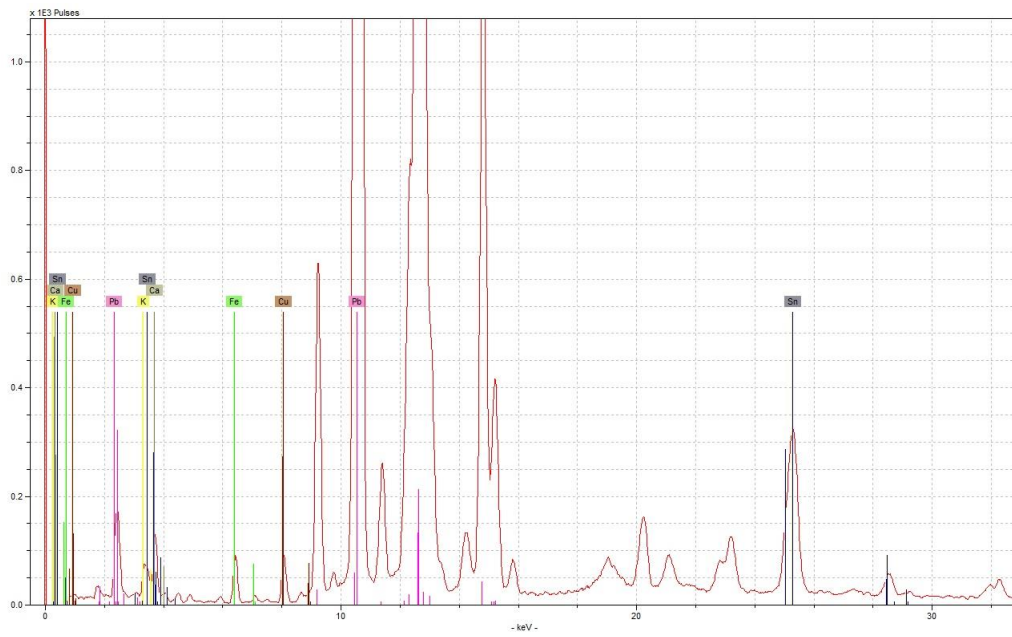
Appendix Figure 32 - example spectrum for glaze type 3 from LH 1, obtained under low voltage condition (upper), and high voltage condition (lower)



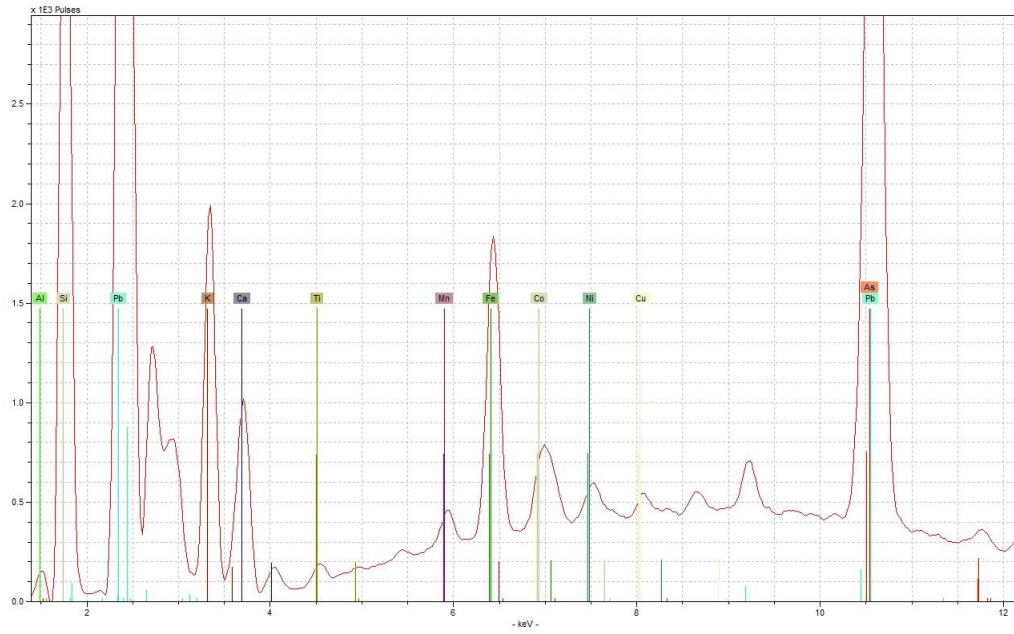
Appendix 7: Hand-Held XRF data



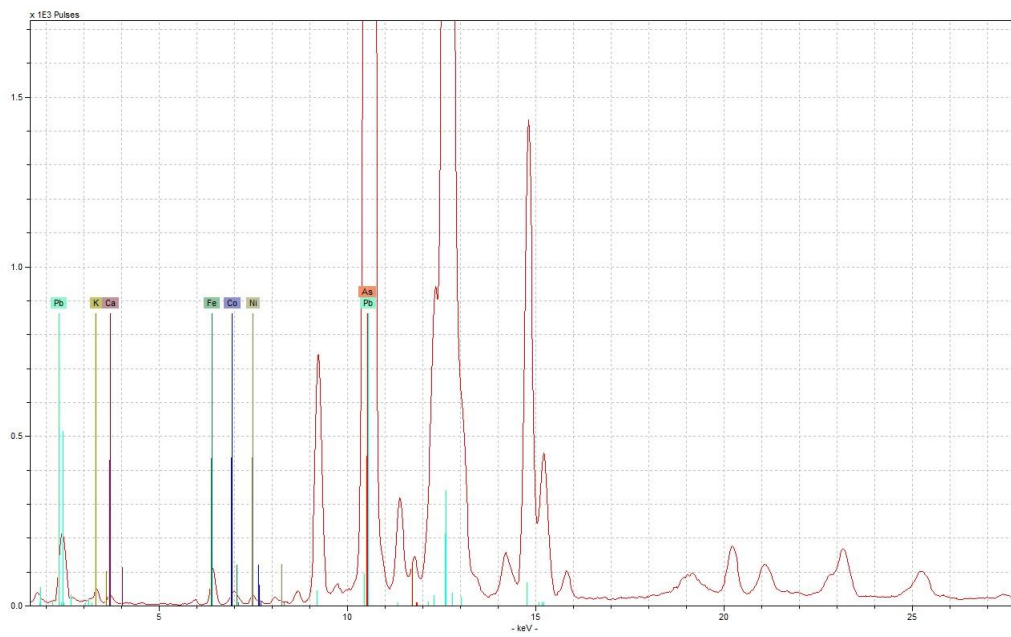
Appendix Figure 33 - example spectrum for glaze type 4 from EMB frag 4, obtained under low voltage condition (upper), and high voltage condition (lower)



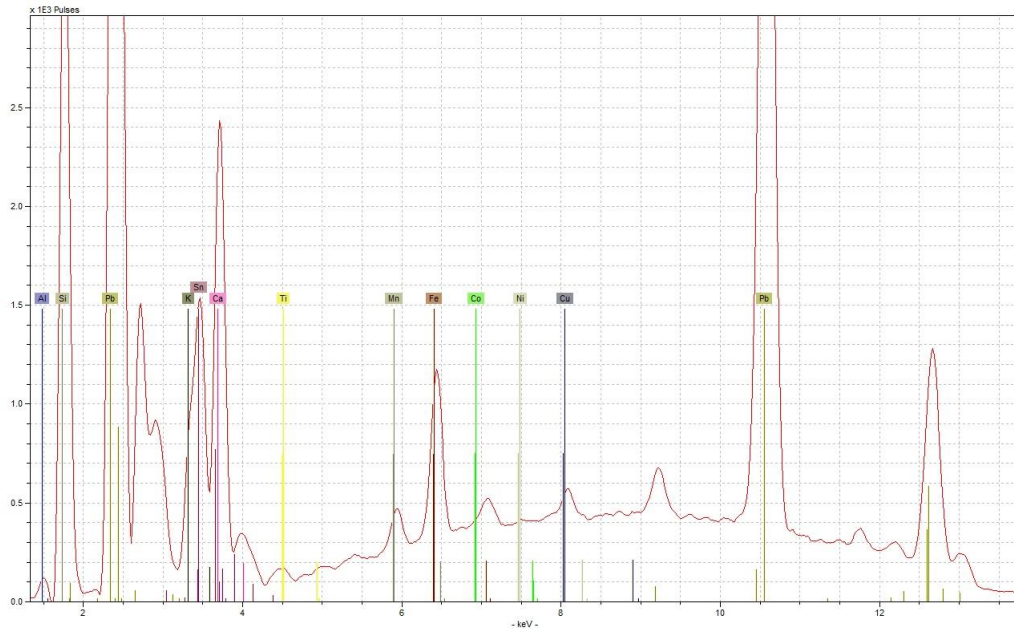
Appendix 7: Hand-Held XRF data



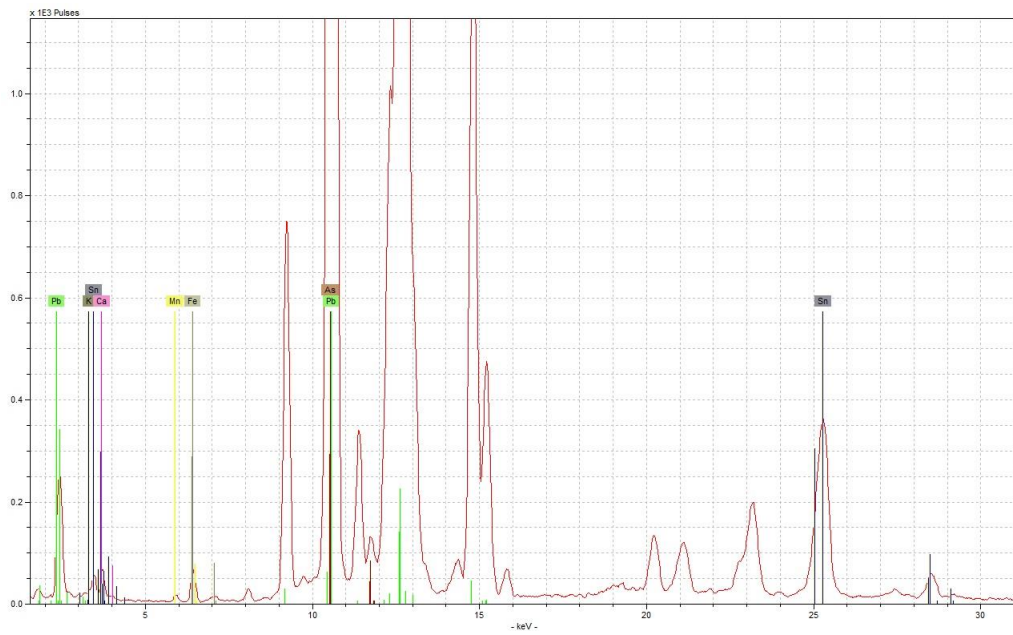
Appendix Figure 34 - example spectrum for glaze type 5 from Cy tc1, obtained under low voltage condition (upper), and high voltage condition (lower)



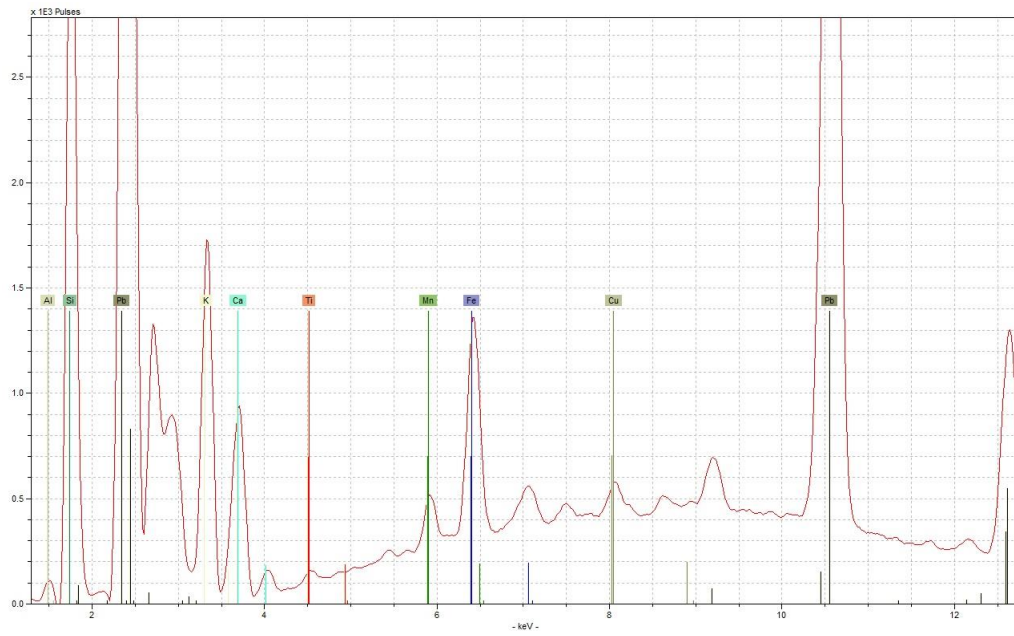
Appendix 7: Hand-Held XRF data



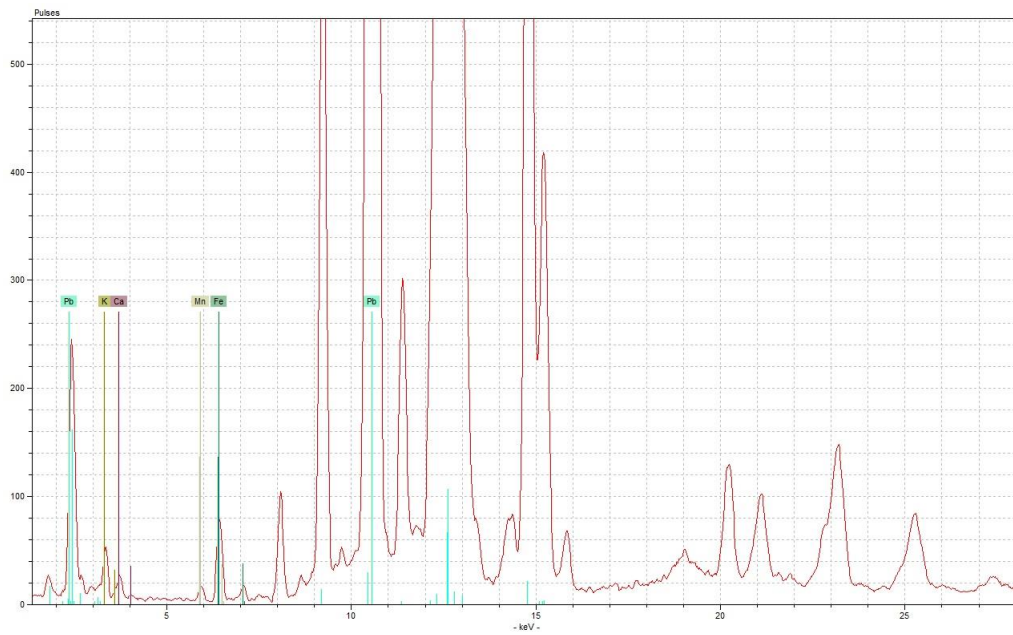
Appendix Figure 35 - example spectrum for glaze type 6 from LLK sherd 1, obtained under low voltage condition (upper), and low voltage condition (lower)



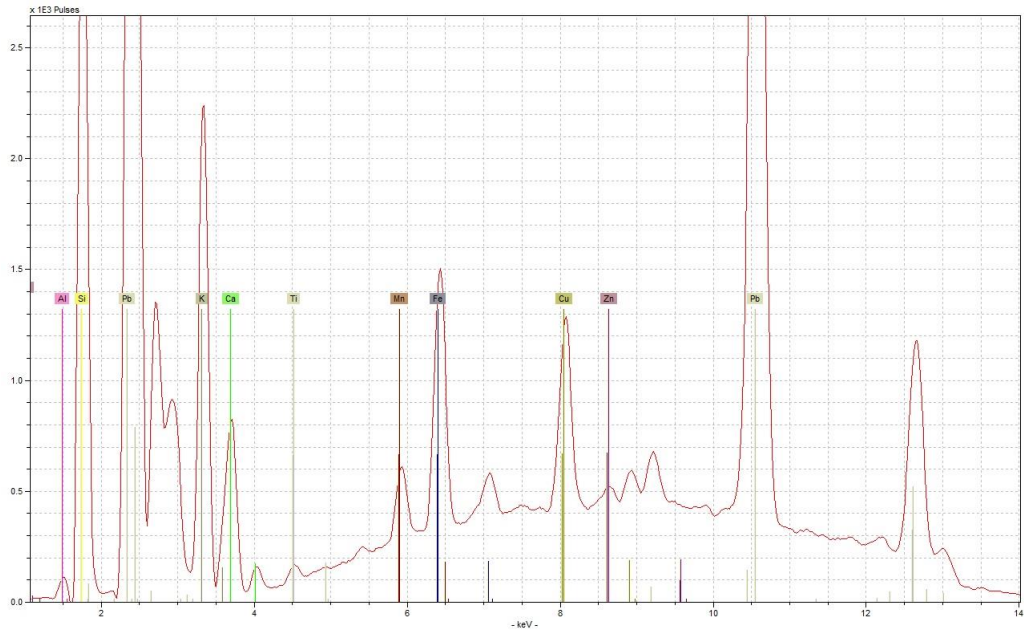
Appendix 7: Hand-Held XRF data



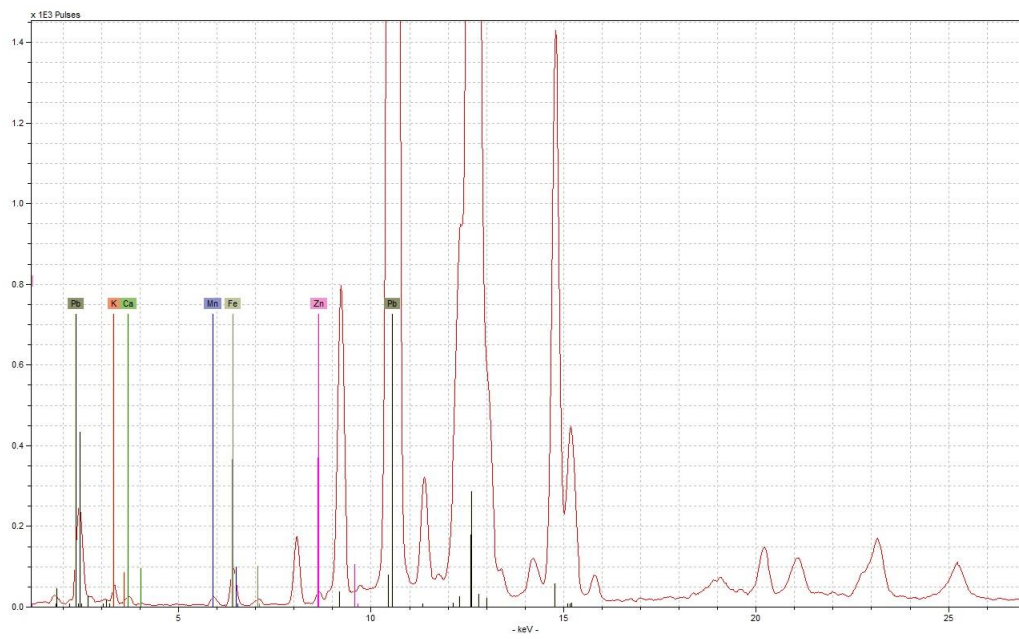
Appendix Figure 36 - example spectrum for glaze type 7 from Worcs sb1, obtained under low voltage condition (upper), and high voltage condition (lower)



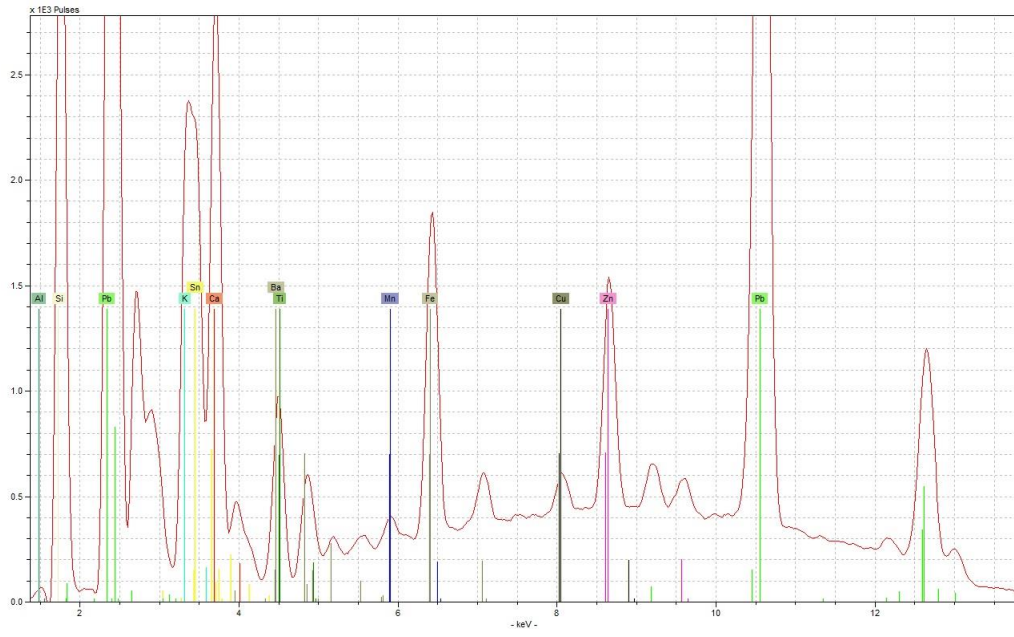
Appendix 7: Hand-Held XRF data



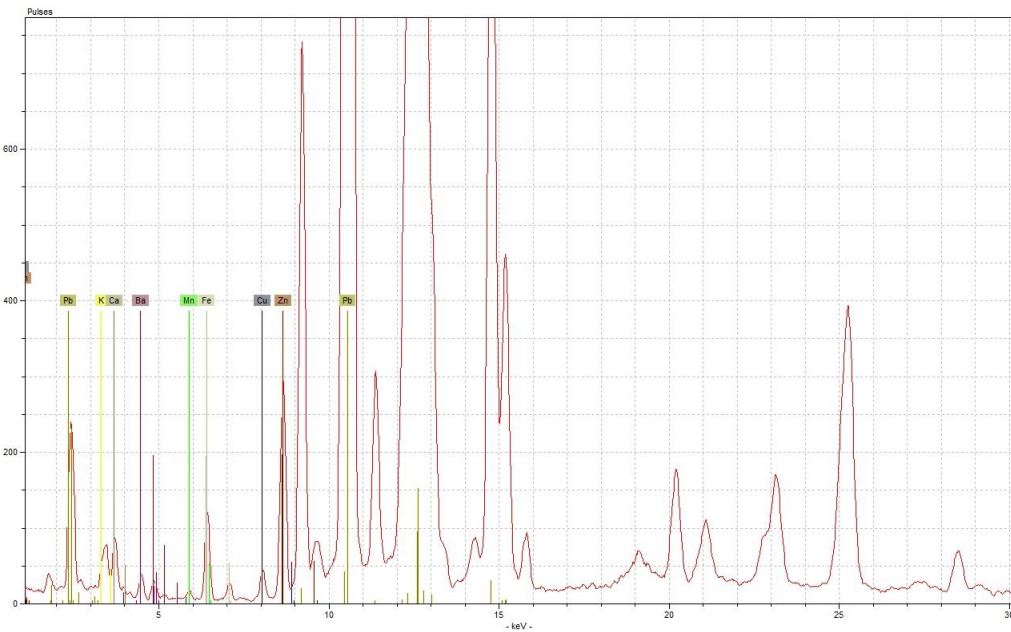
Appendix Figure 37 - example spectrum for glaze type 8 from Cha tb1, obtained under low voltage condition (upper), and high voltage condition (lower)



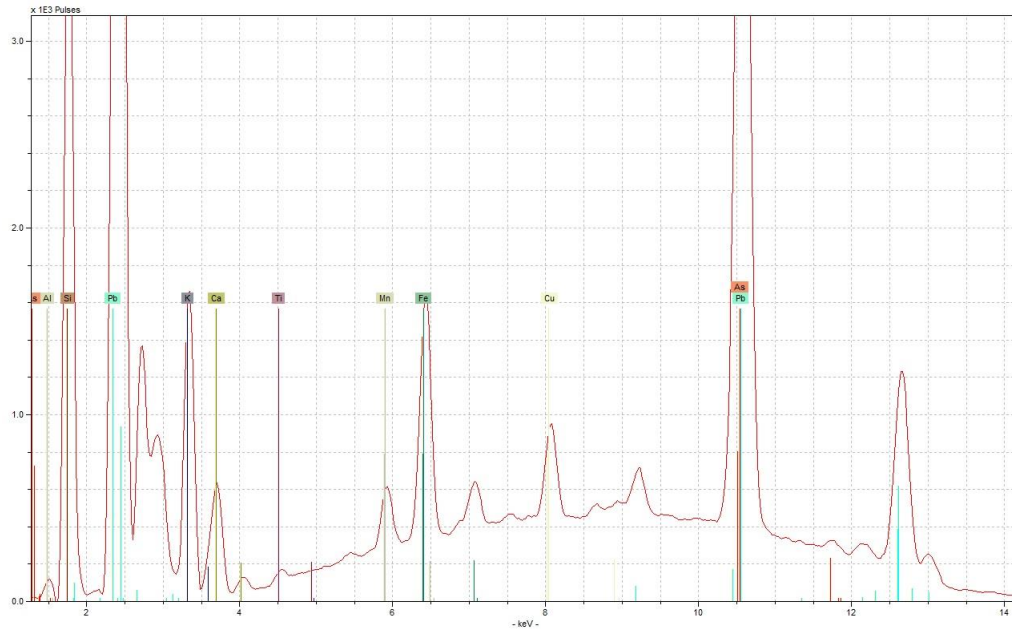
Appendix 7: Hand-Held XRF data



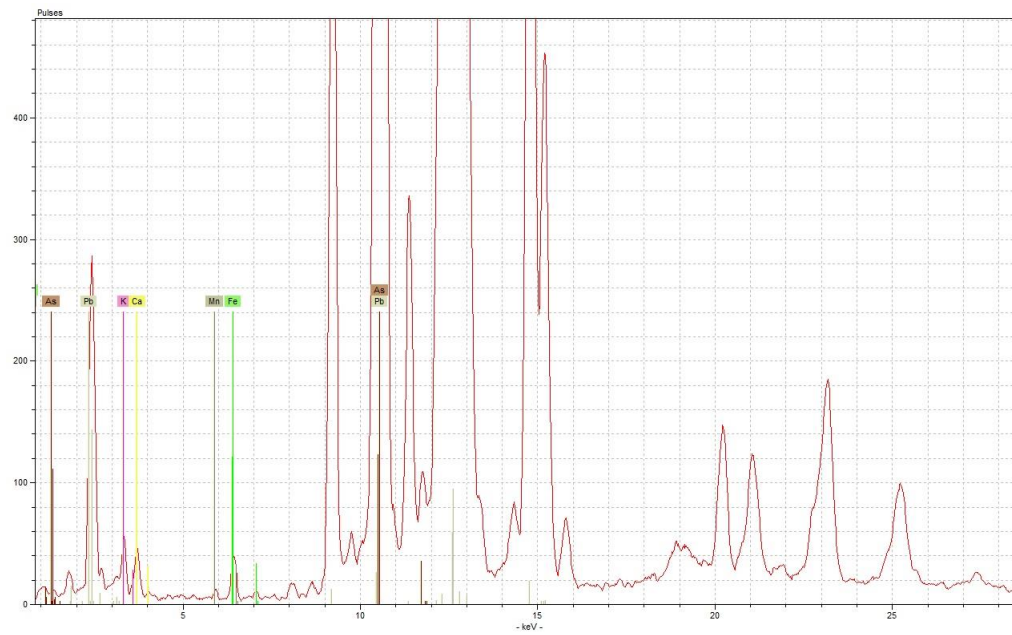
Appendix Figure 38 - example spectrum for glaze type 9 from BTr sb1, obtained under low voltage condition (upper), and high voltage condition (lower)



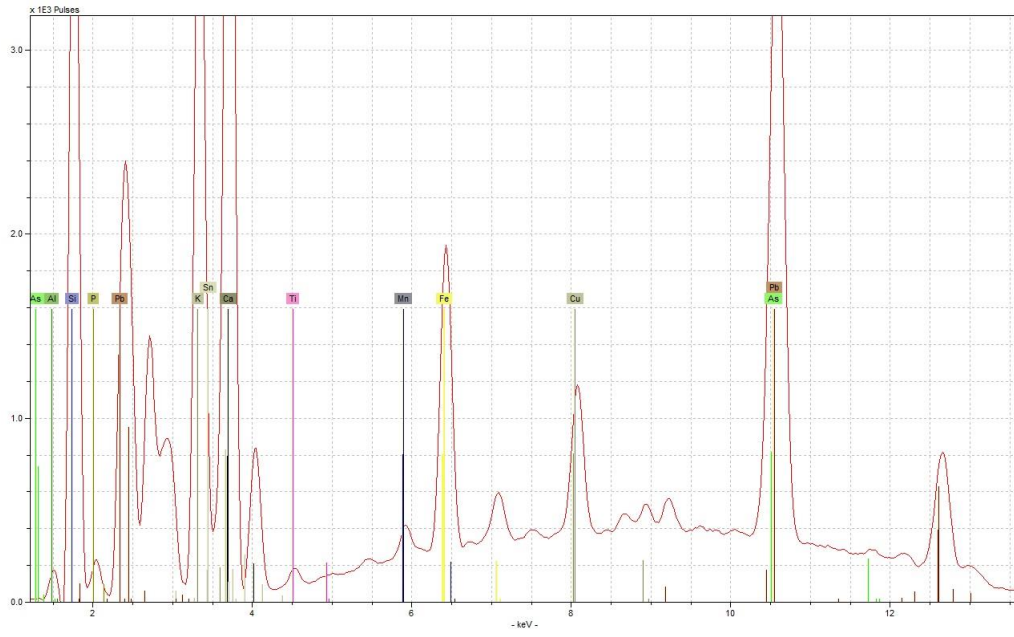
Appendix 7: Hand-Held XRF data



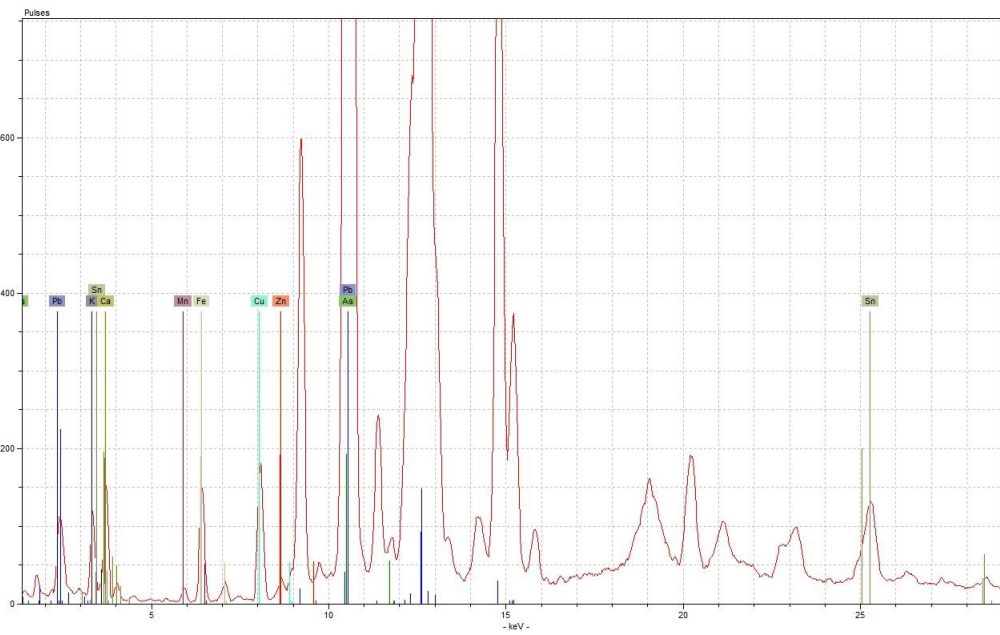
Appendix Figure 39 - example spectrum for glaze type 10 from Cha sb1, obtained under low voltage condition (upper), and high voltage condition (lower)



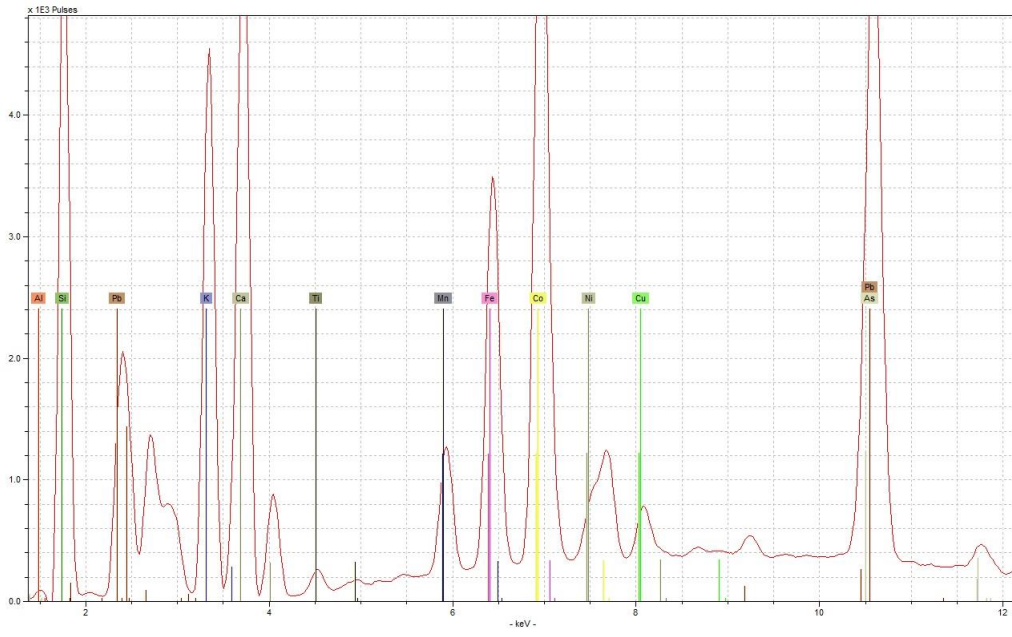
Appendix 7: Hand-Held XRF data



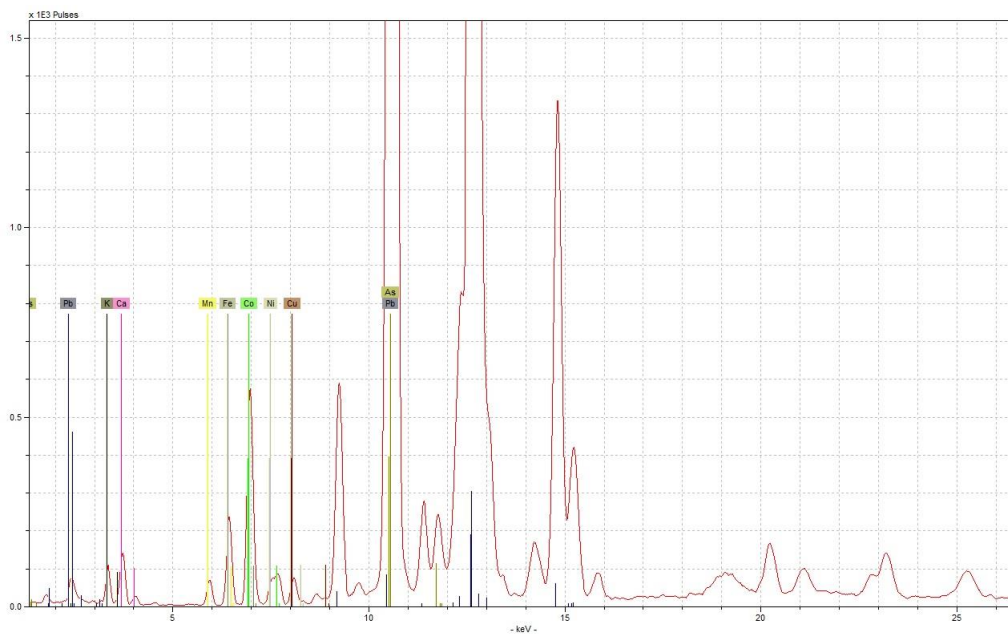
Appendix Figure 40 - example spectrum for glaze type 11 from EMB sherd 1, obtained under low voltage condition (upper), and high voltage condition (lower)



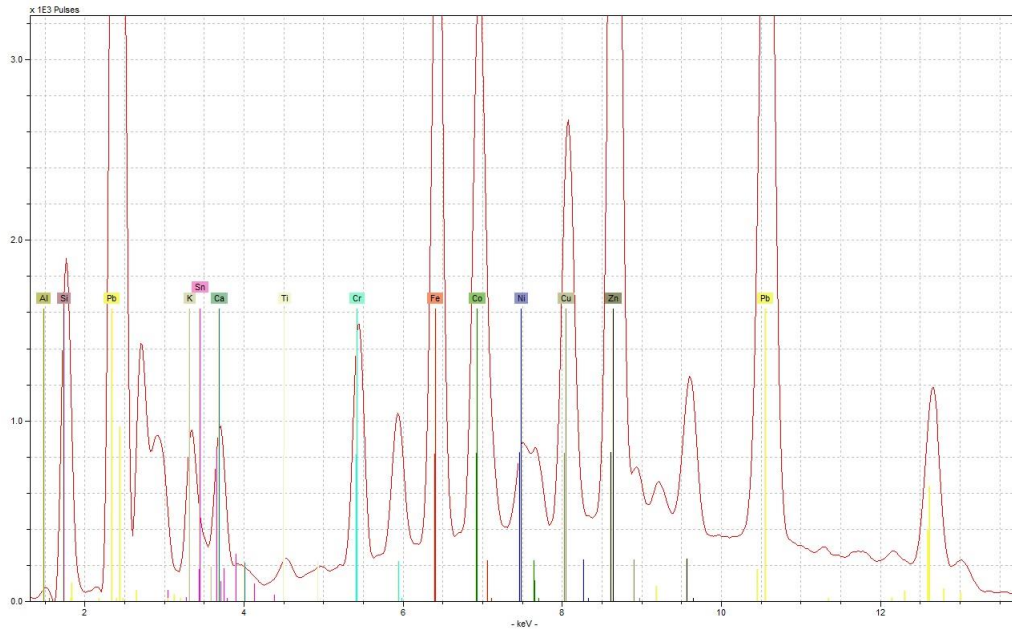
Appendix 7: Hand-Held XRF data



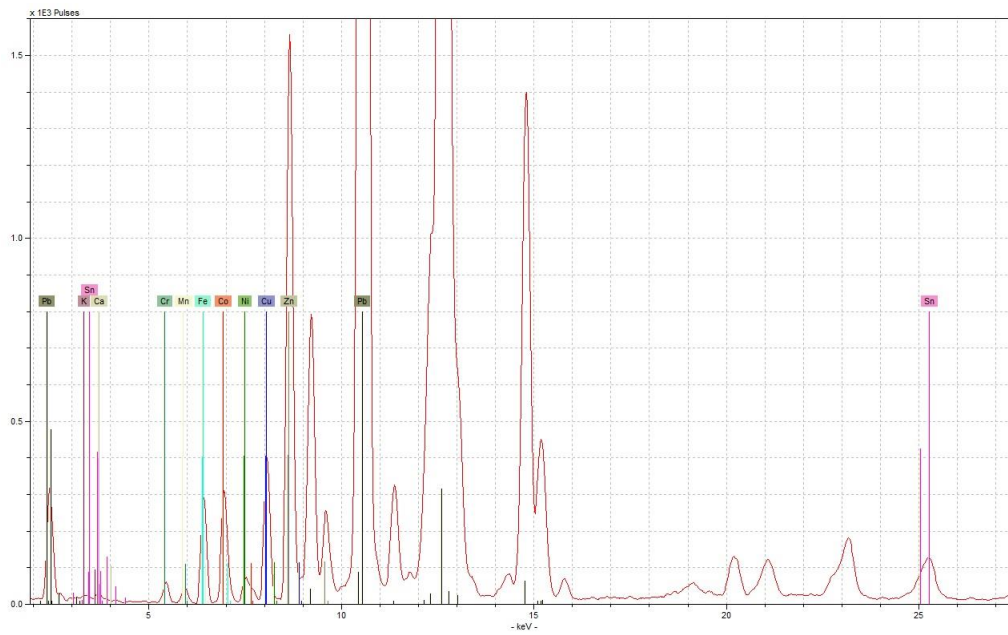
Appendix Figure 41 - example spectrum for blue enamel type 1 from 377, obtained under low voltage condition (upper), and high voltage condition (lower)



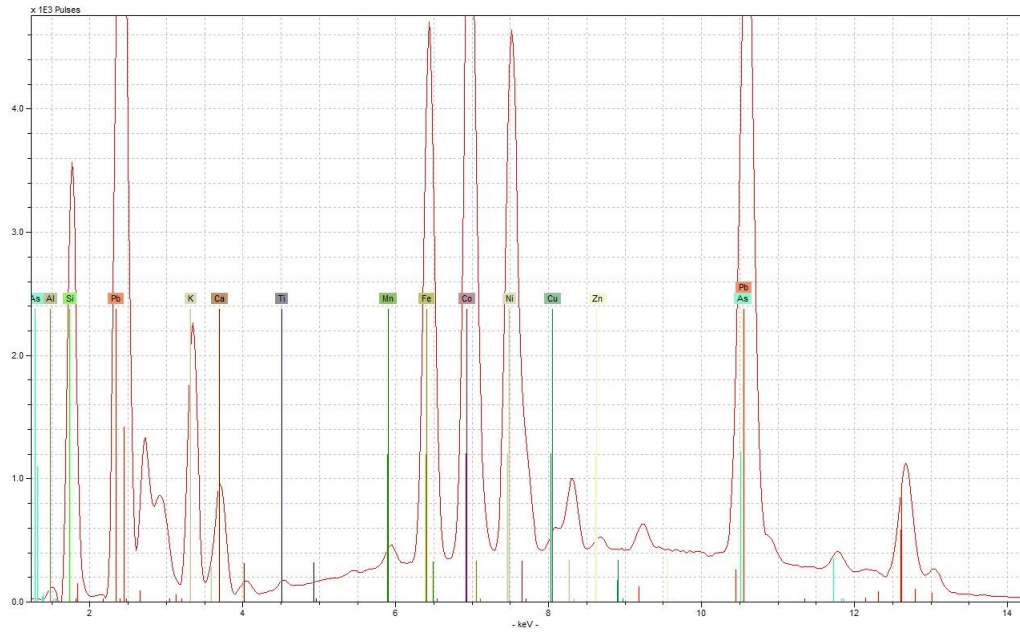
Appendix 7: Hand-Held XRF data



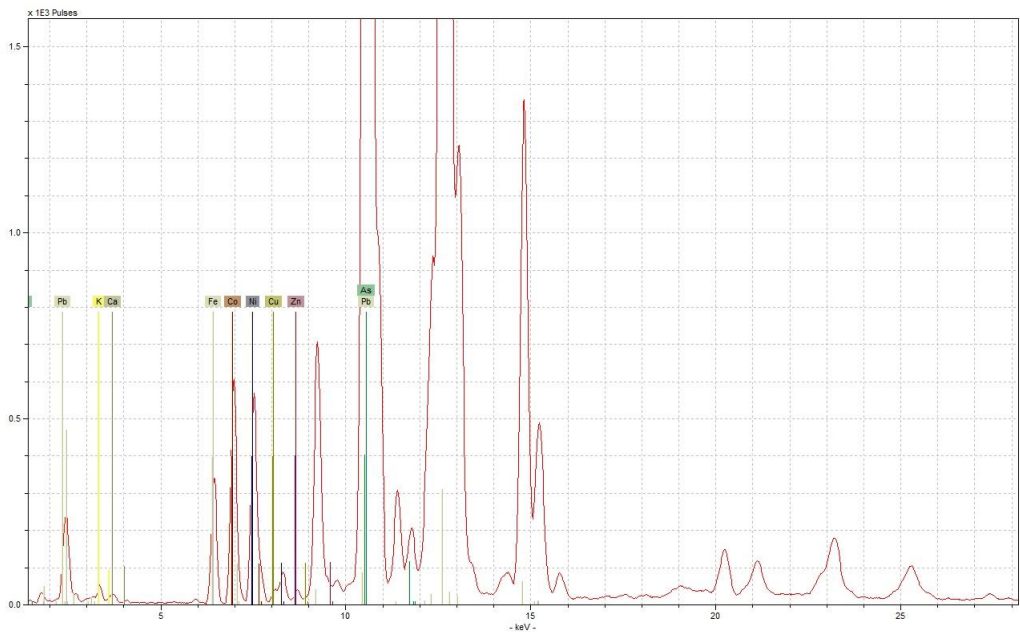
Appendix Figure 42 - example spectrum for blue enamel type 2 from 292, obtained using low voltage condition (upper), and high voltage condition (lower)



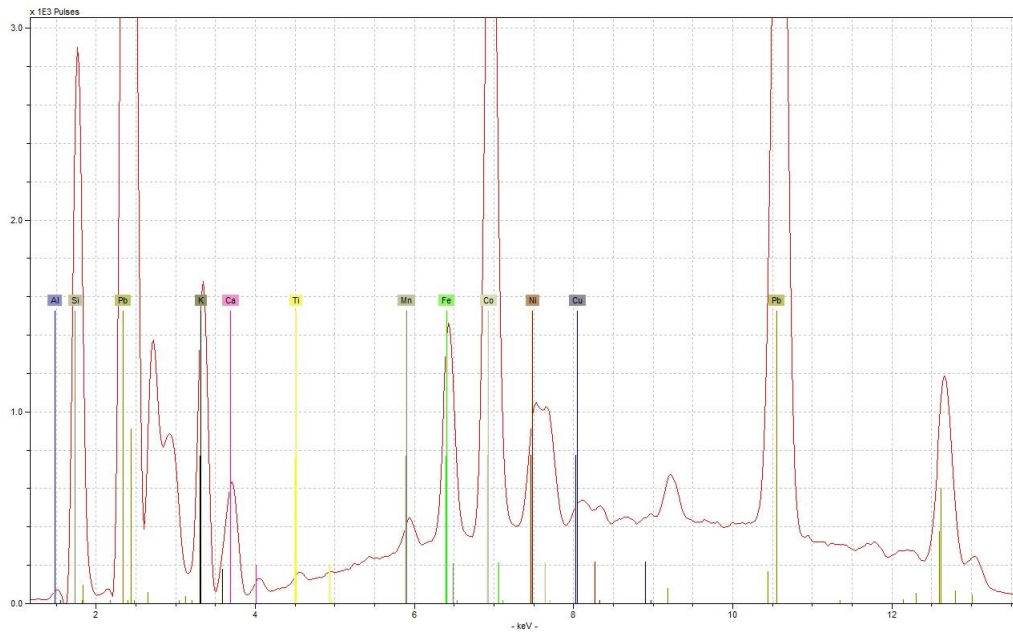
Appendix 7: Hand-Held XRF data



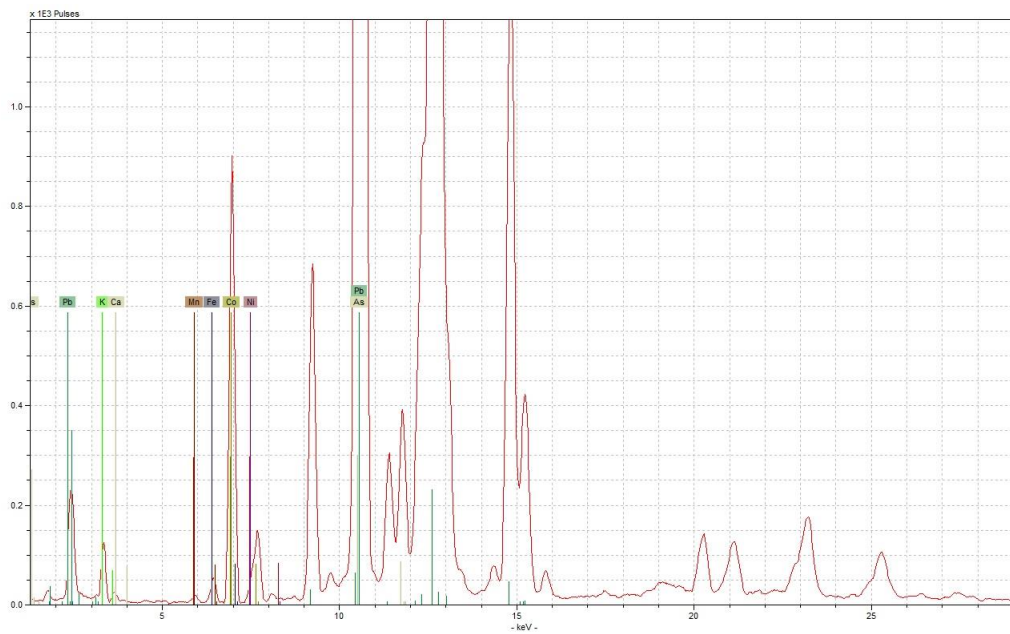
Appendix Figure 43 - example spectrum for blue enamel type 3 from 111, obtained using low voltage condition (upper), and high voltage condition (lower)



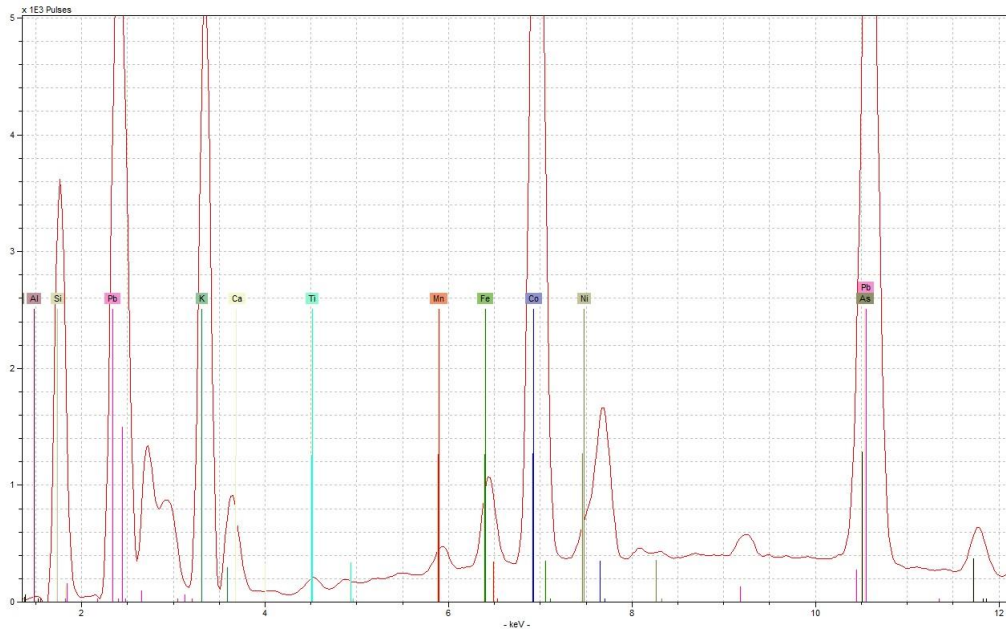
Appendix 7: Hand-Held XRF data



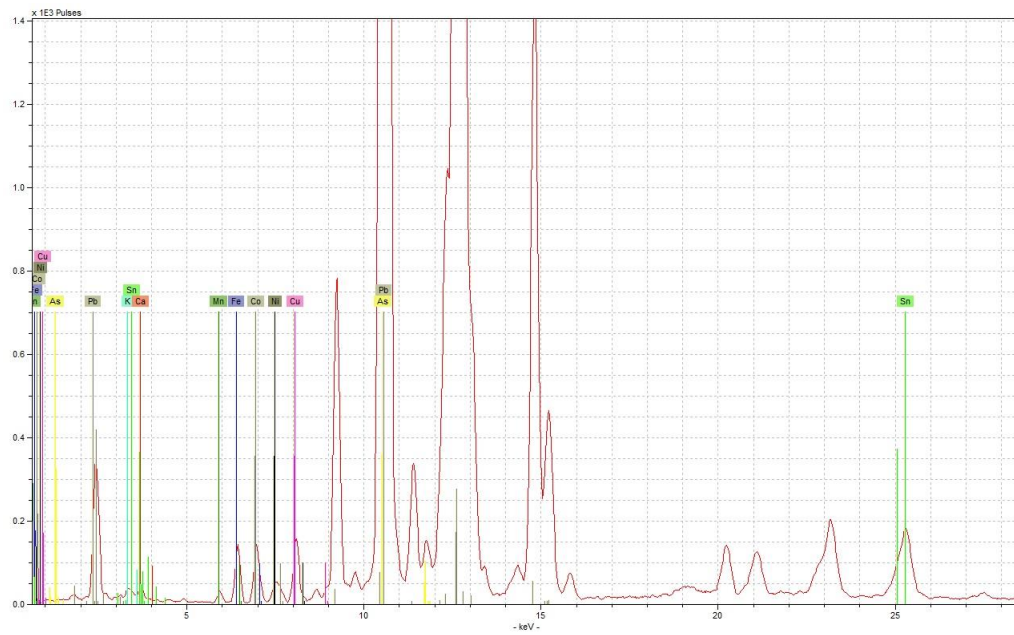
Appendix Figure 44 - example spectrum for blue enamel type 4 from 65, obtained using low voltage condition (upper), and high voltage condition (lower)



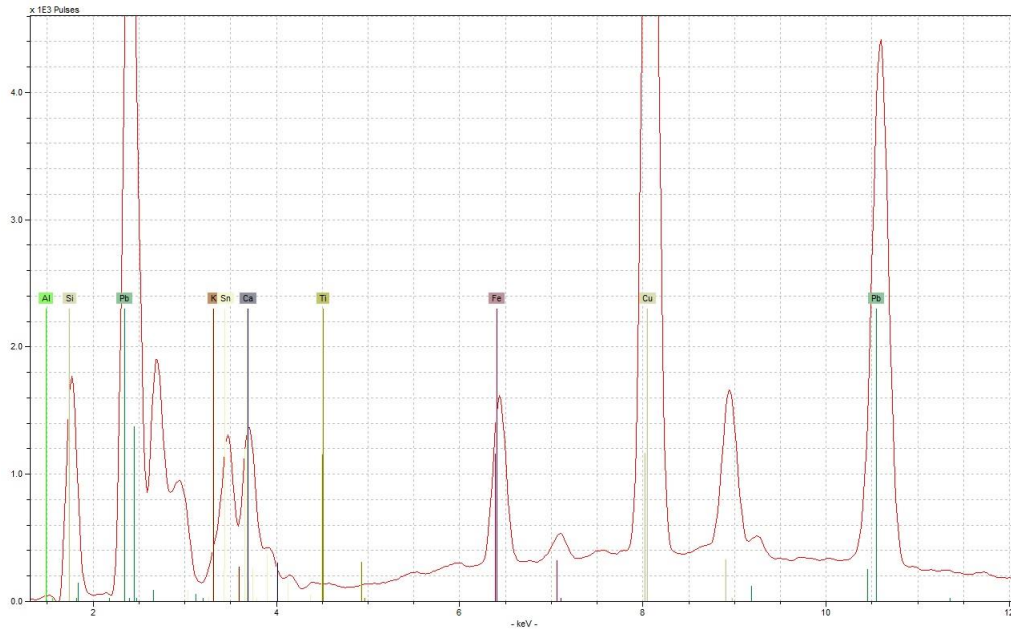
Appendix 7: Hand-Held XRF data



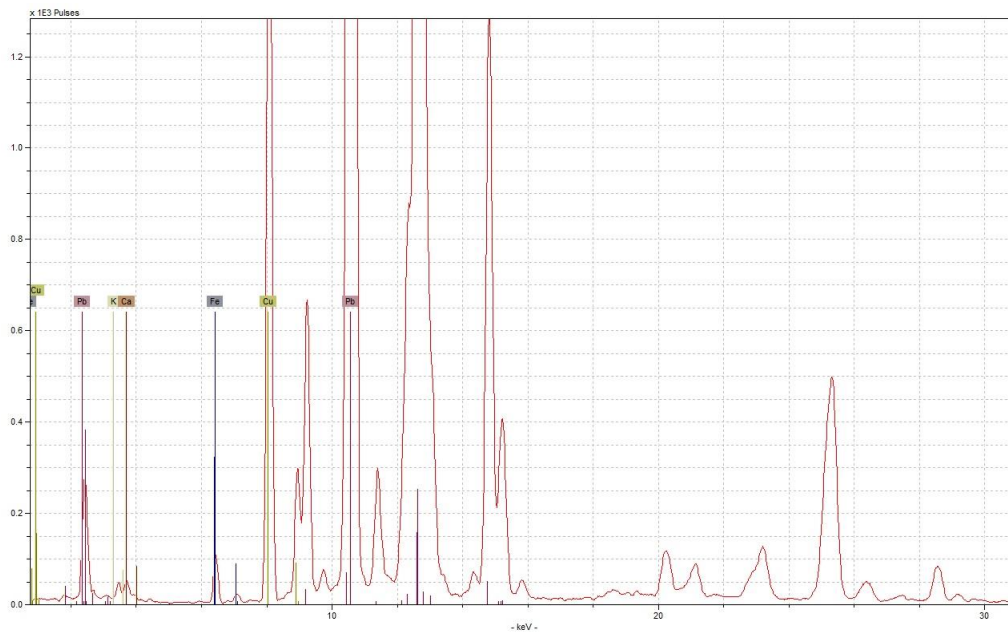
Appendix Figure 45 - example spectrum for blue enamel type 5 from 804, obtained under low voltage condition (upper), and high voltage condition (lower)



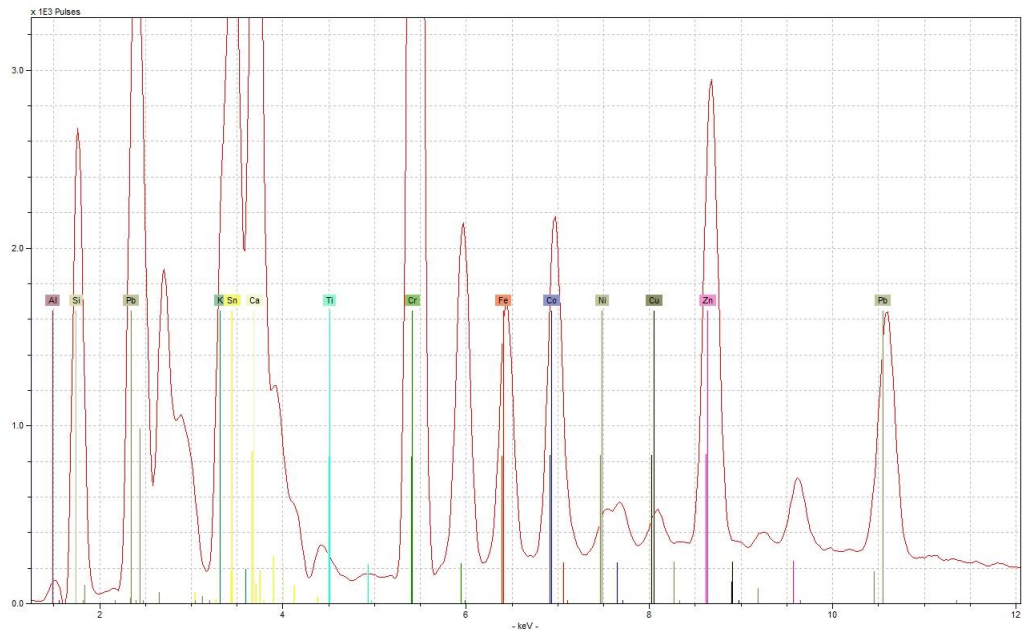
Appendix 7: Hand-Held XRF data



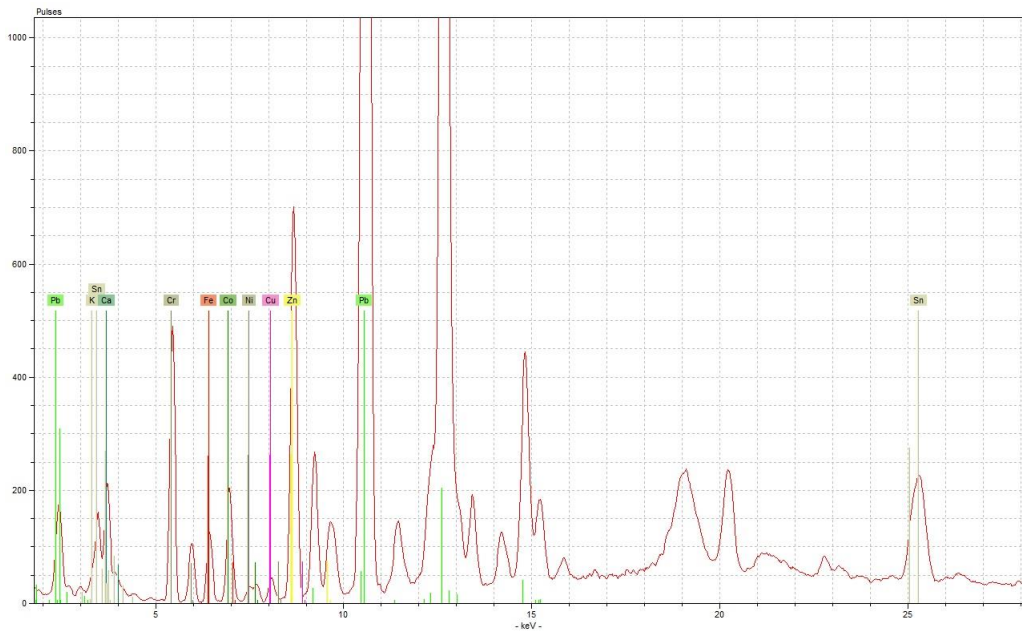
Appendix Figure 46 - example spectrum for green ground/border type 1 from 1005, obtained under low voltage condition (upper), and high voltage condition (lower)



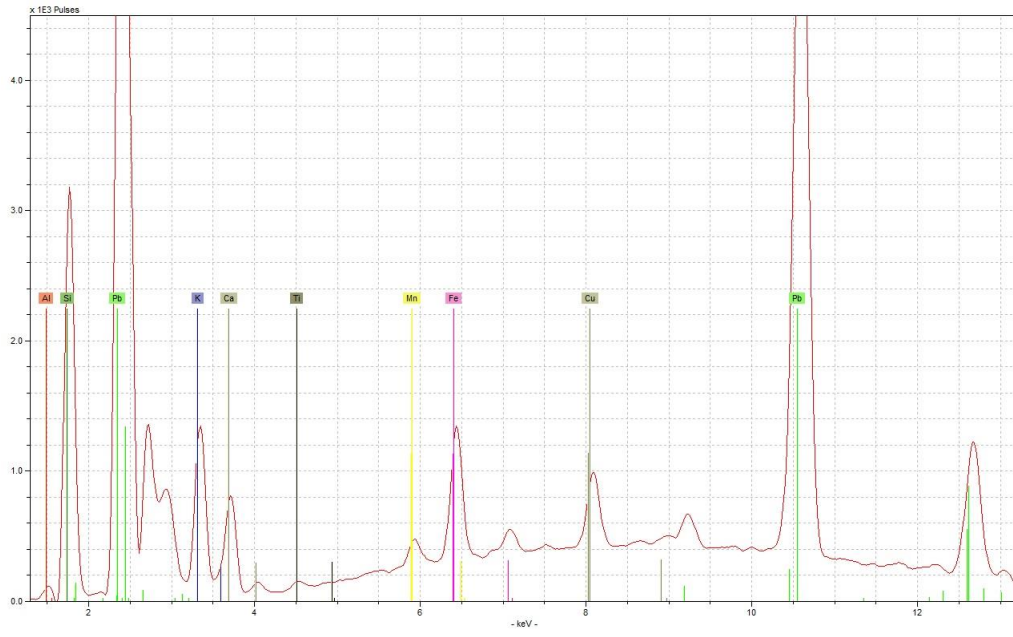
Appendix 7: Hand-Held XRF data



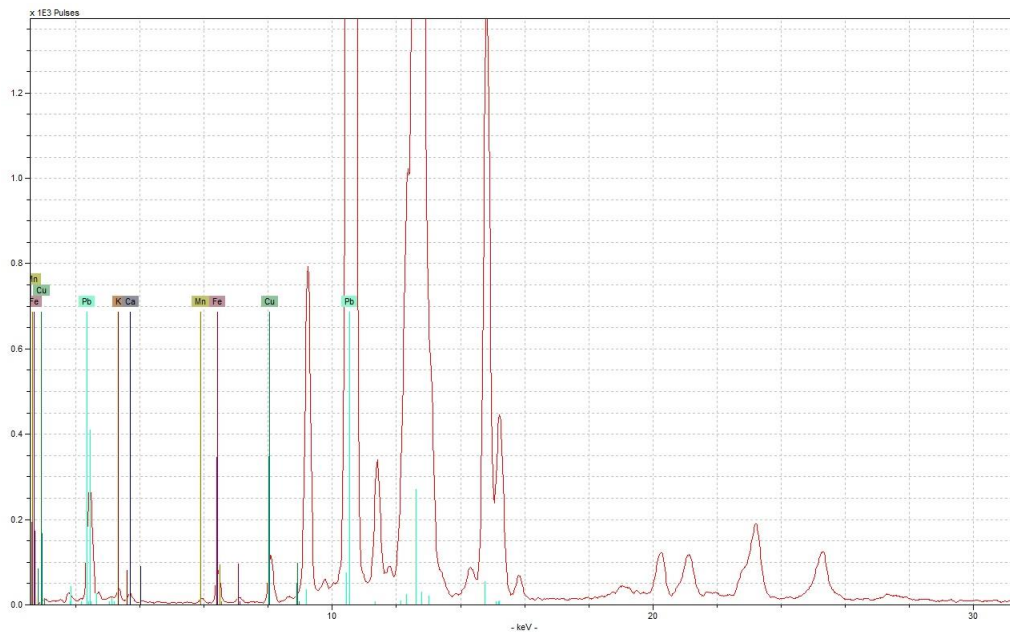
Appendix Figure 47 - example spectrum for green ground/border type 2 from 932, obtained under low voltage condition (upper), and high voltage condition (lower)



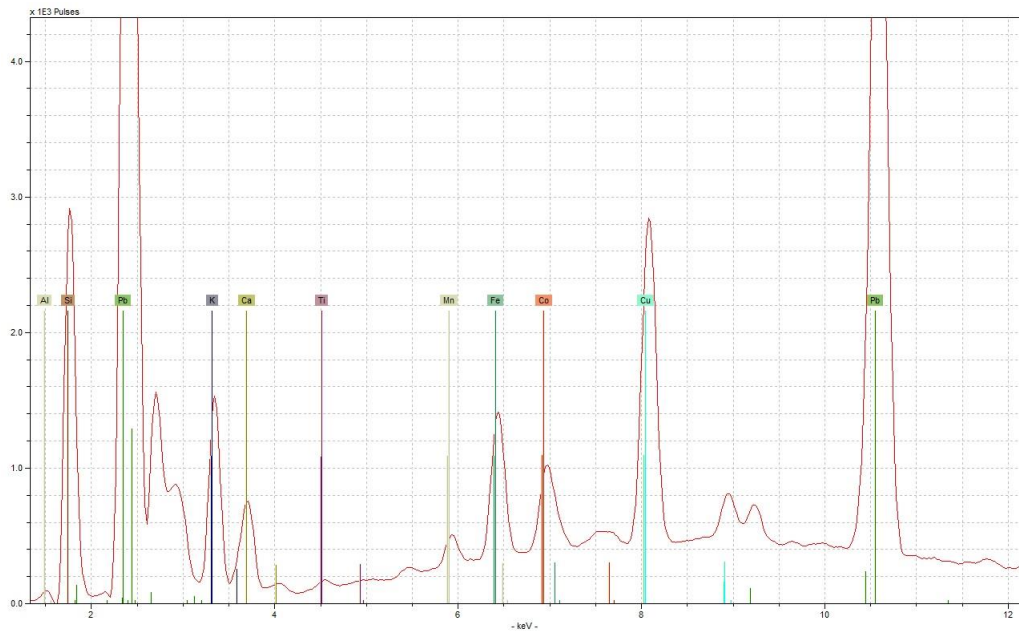
Appendix 7: Hand-Held XRF data



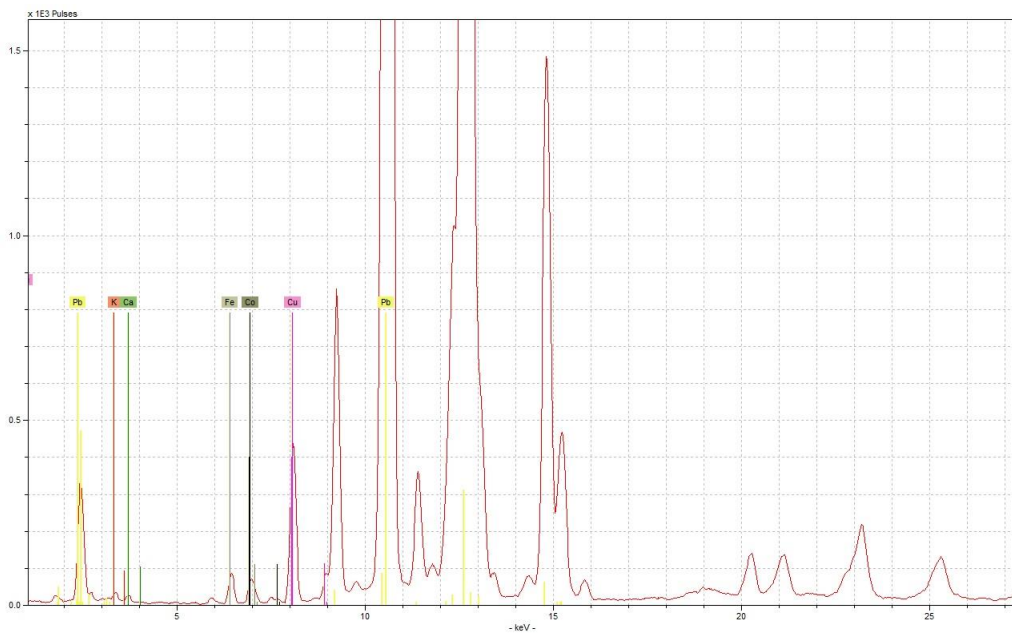
Appendix Figure 48 - example spectrum for green painted enamel type 1 from 620, obtained under low voltage condition (upper), and high voltage condition (lower)



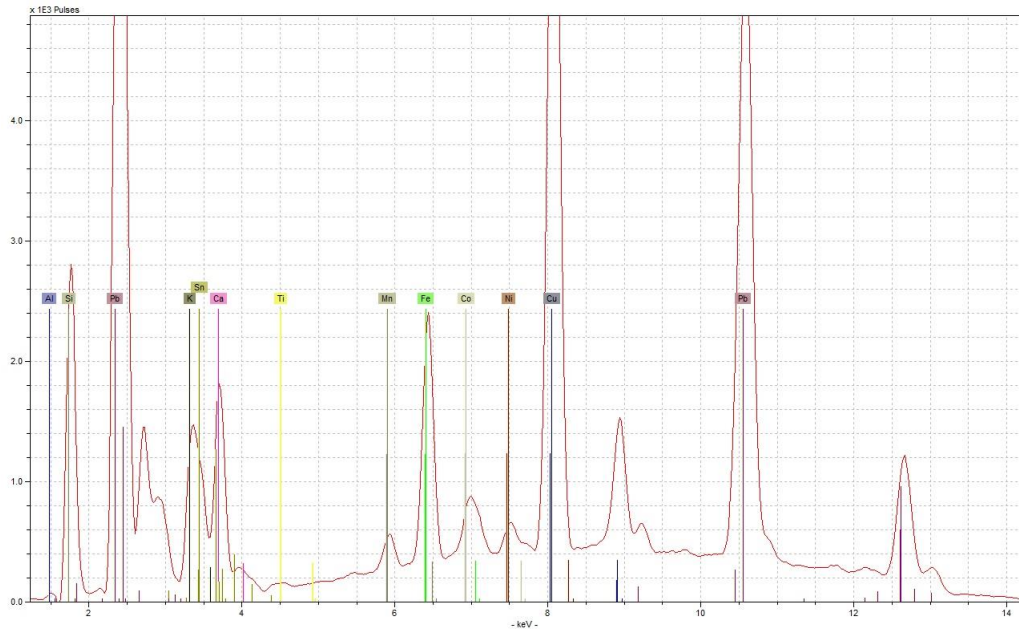
Appendix 7: Hand-Held XRF data



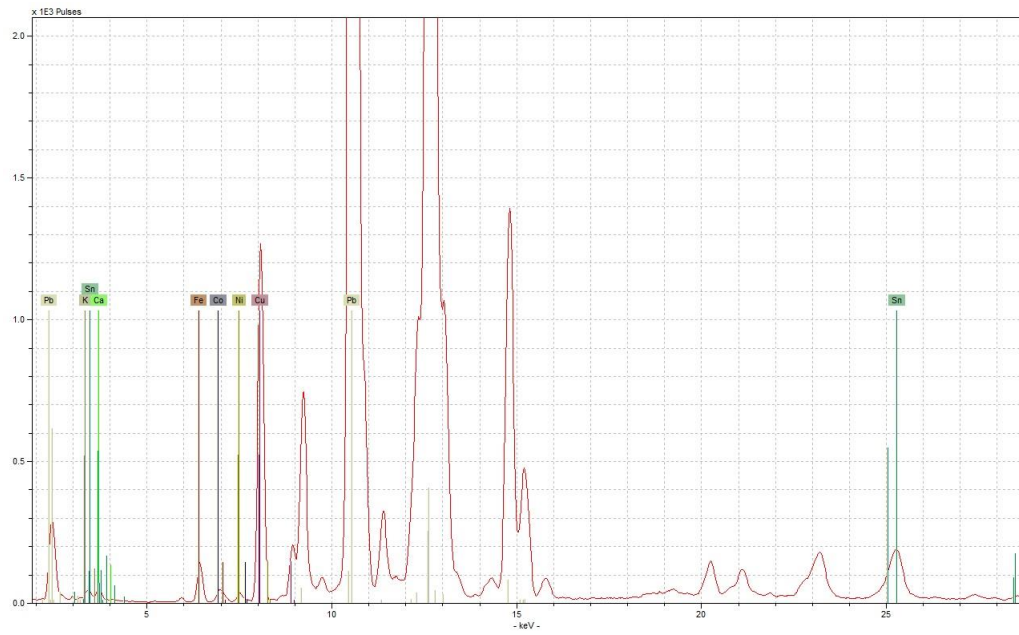
Appendix Figure 49 - example spectrum for green painted enamel type 2 from 65, obtained under low voltage condition (upper), and high voltage condition (lower)



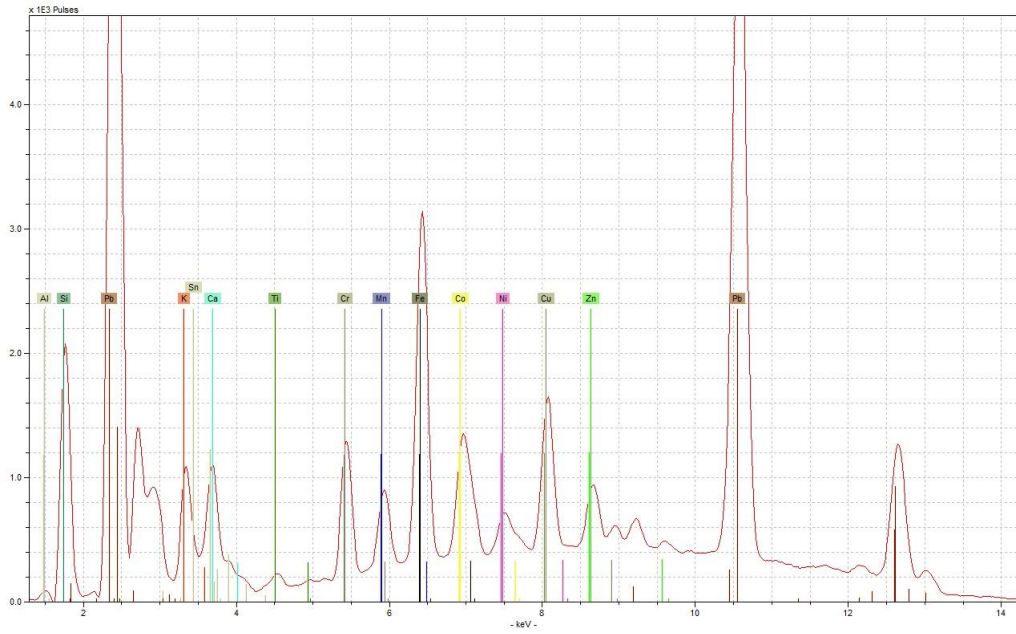
Appendix 7: Hand-Held XRF data



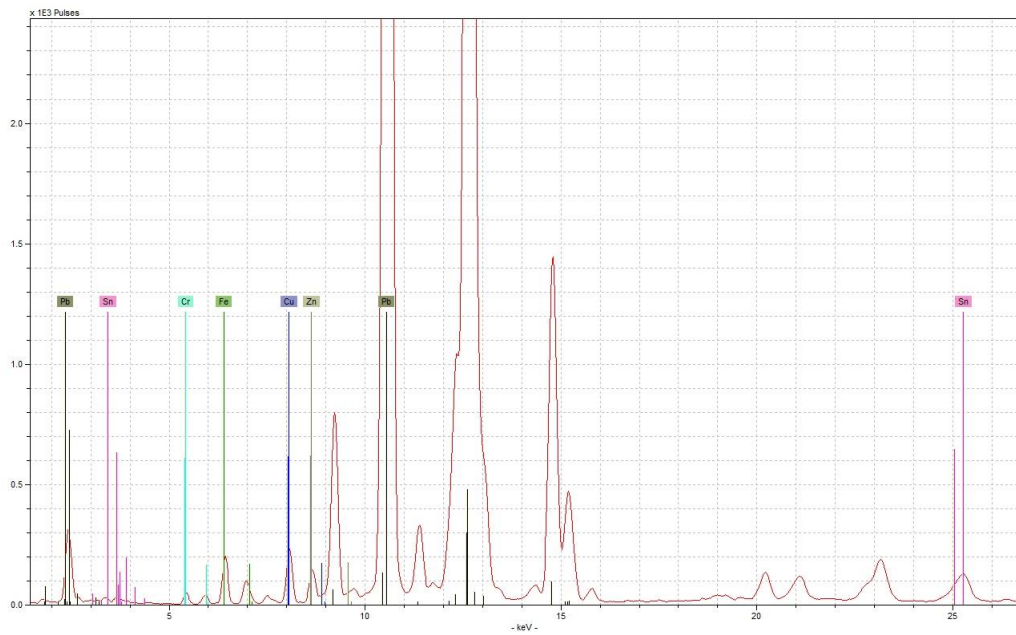
Appendix Figure 50 - example spectrum for green painted enamel type 3 from 697, obtained under low voltage condition (upper), and high voltage condition (lower)



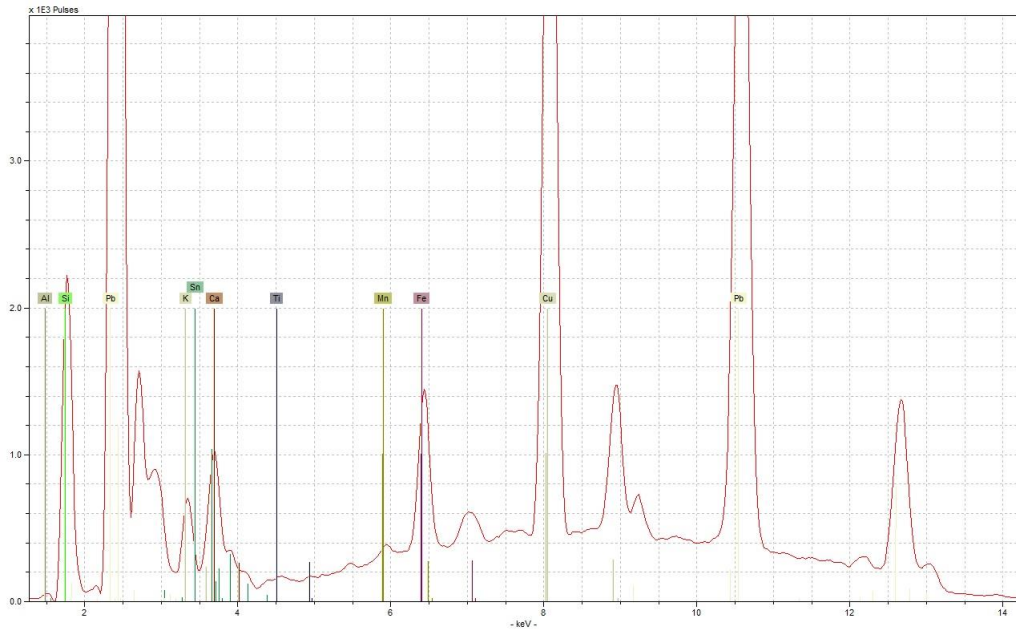
Appendix 7: Hand-Held XRF data



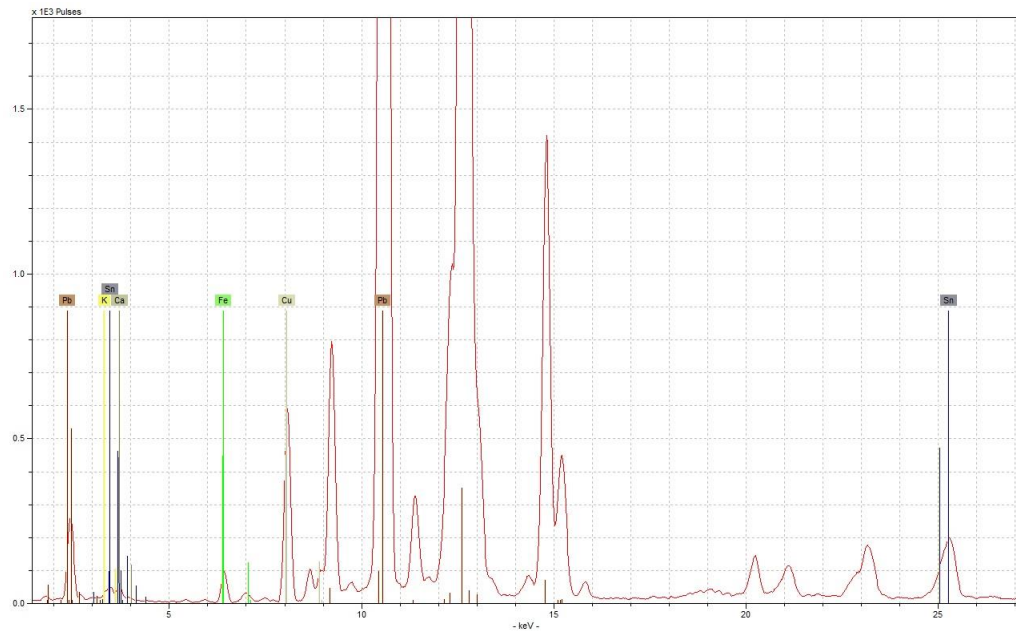
Appendix Figure 51 - example spectrum for green painted enamel type 4 from 292, obtained under low voltage condition (upper), and high voltage condition (lower)



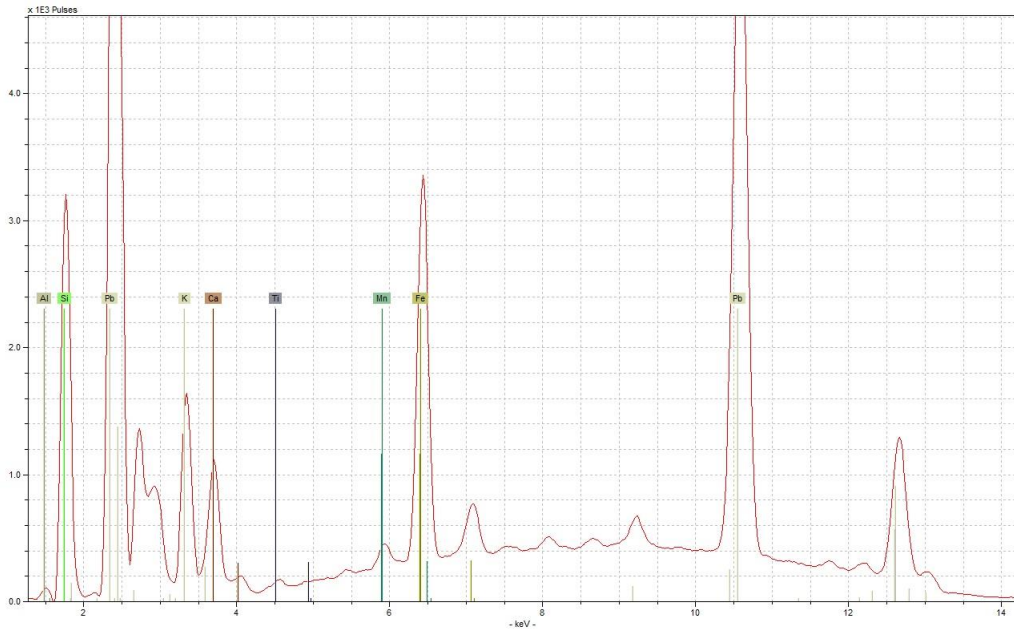
Appendix 7: Hand-Held XRF data



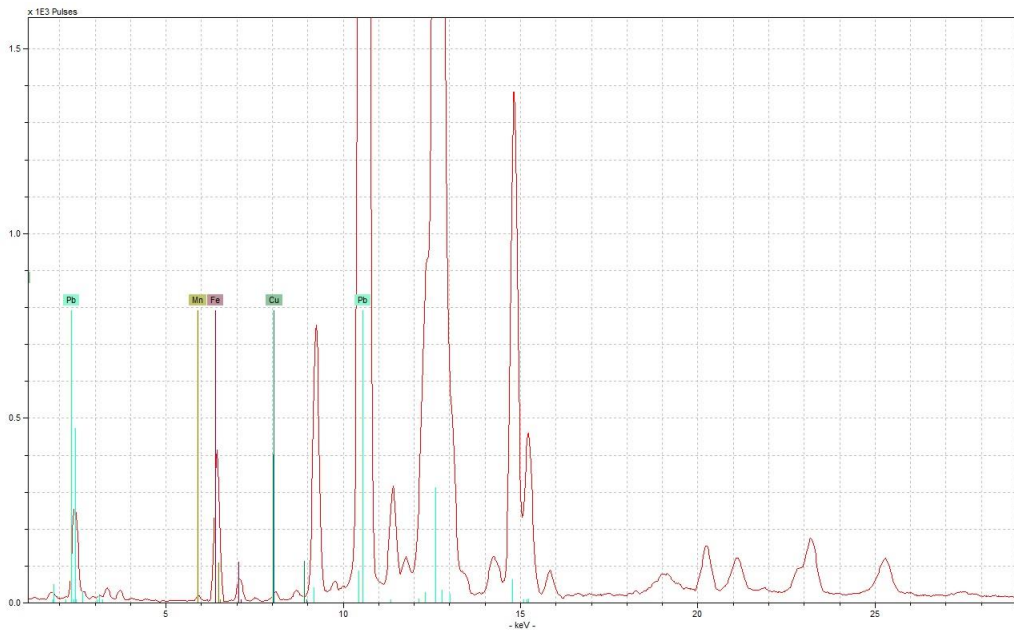
Appendix Figure 52 - example spectrum for green painted enamel type 5 from 699, obtained under low voltage condition (upper), and high voltage condition (lower)



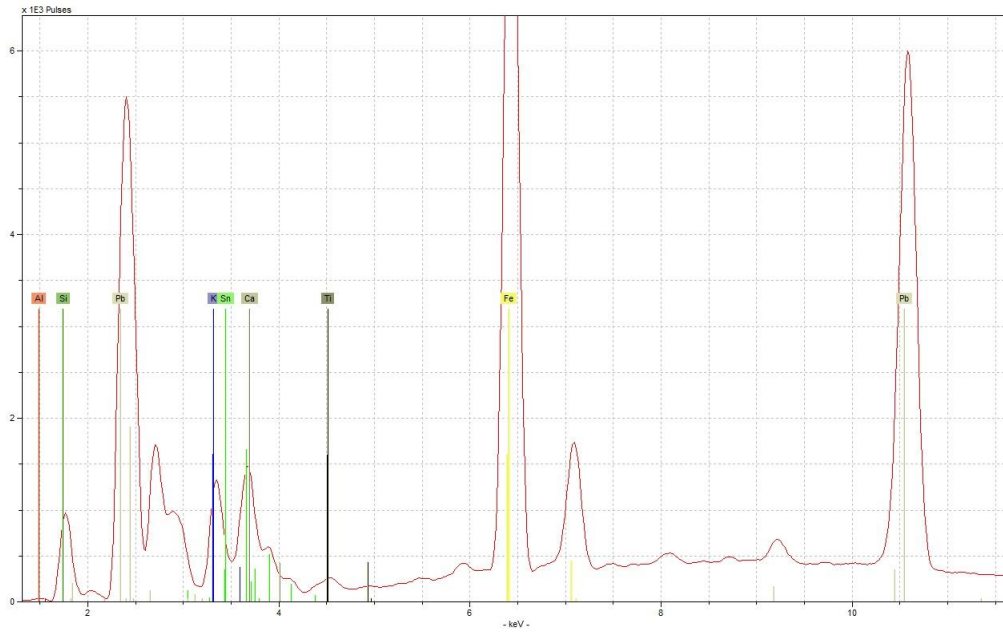
Appendix 7: Hand-Held XRF data



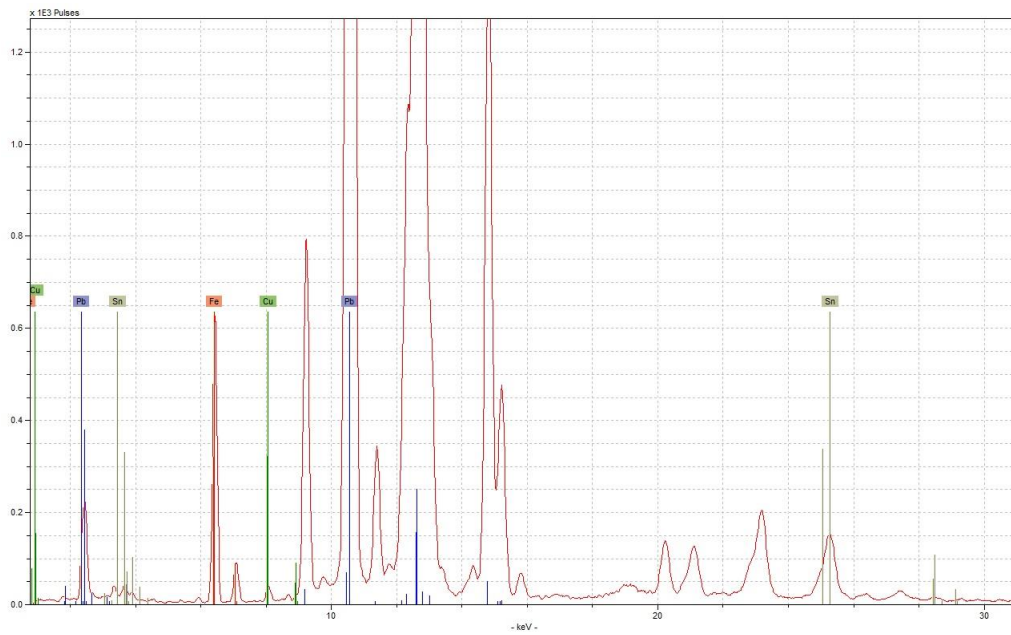
Appendix Figure 53 - example spectrum for orange enamel type 1 from WJG4, obtained under low voltage condition (upper), and high voltage condition (lower)



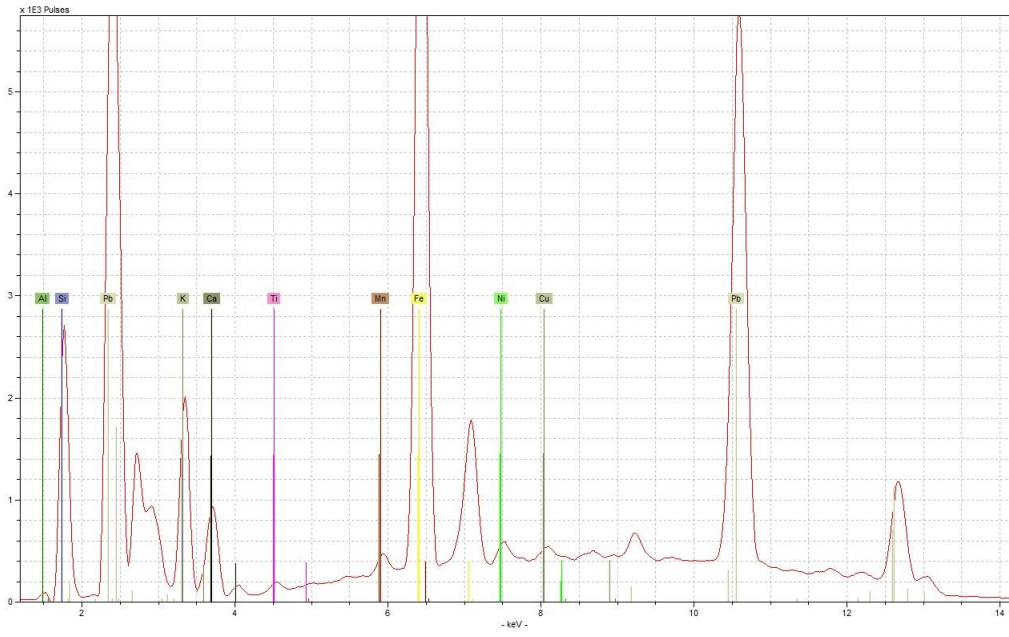
Appendix 7: Hand-Held XRF data



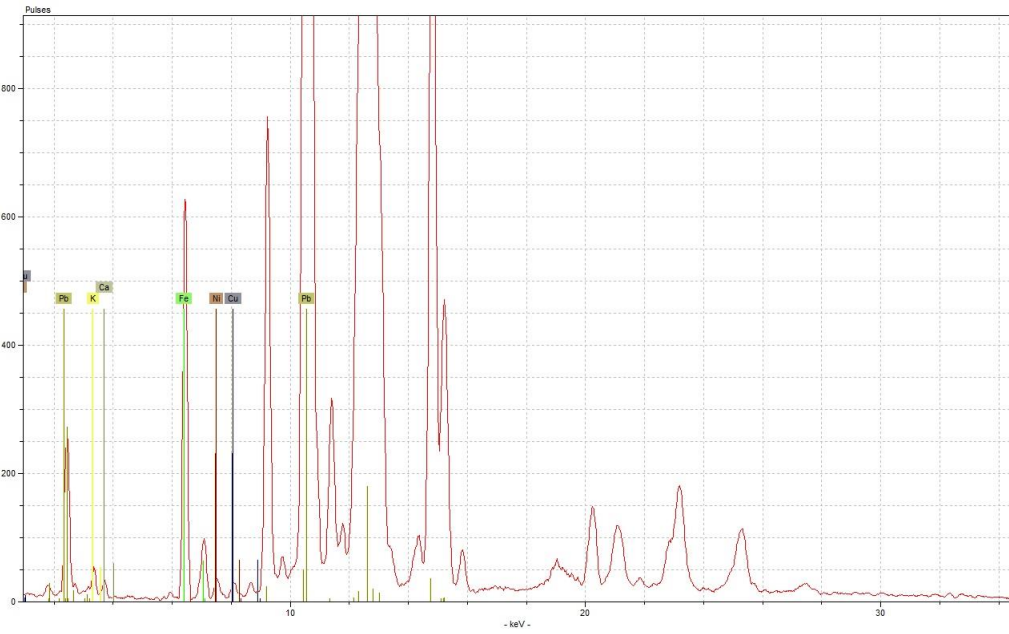
Appendix Figure 54 - example spectrum for orange enamel type 2 from WJG1, obtained under low voltage condition (upper), and high voltage condition (lower)



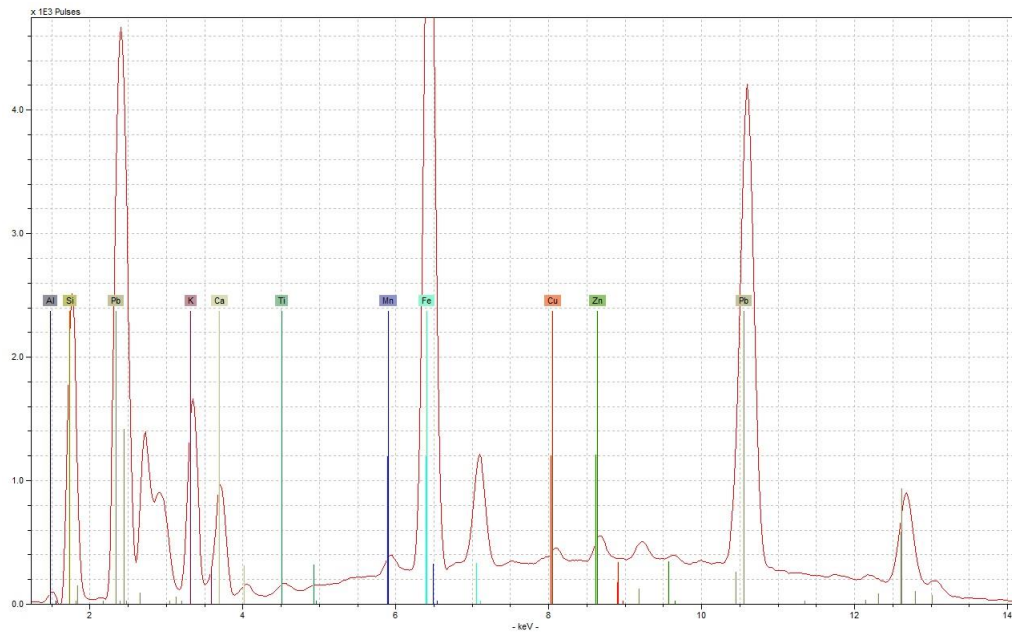
Appendix 7: Hand-Held XRF data



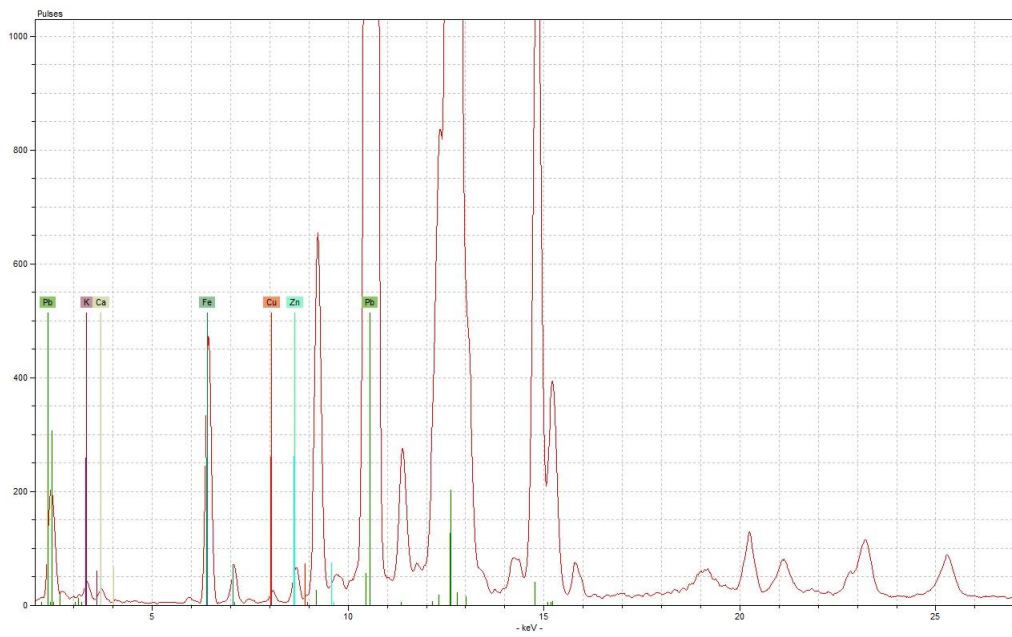
Appendix Figure 55 - example spectrum for orange enamel type 3 from 111, obtained under low voltage condition (upper), and high voltage condition (lower)



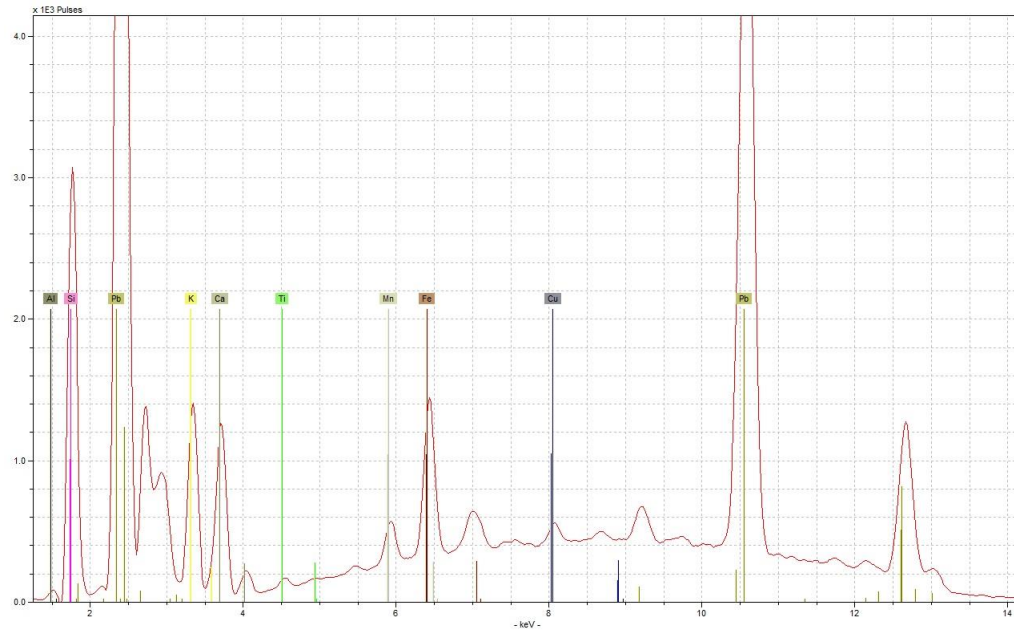
Appendix 7: Hand-Held XRF data



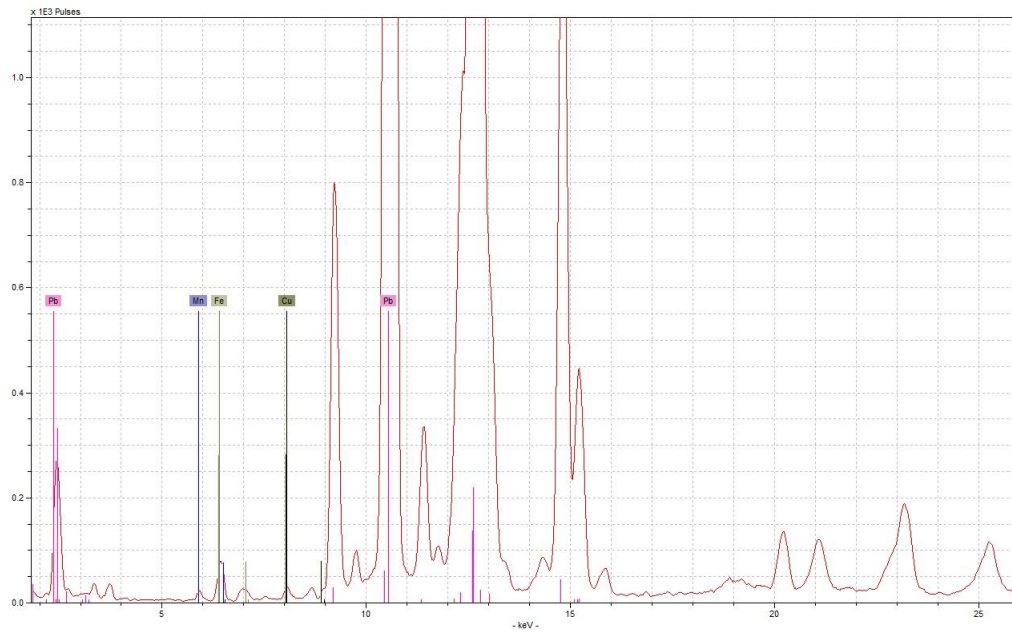
Appendix Figure 56 - example spectrum for orange enamel type 4 from 826, obtained under low voltage condition (upper), and high voltage condition (lower)



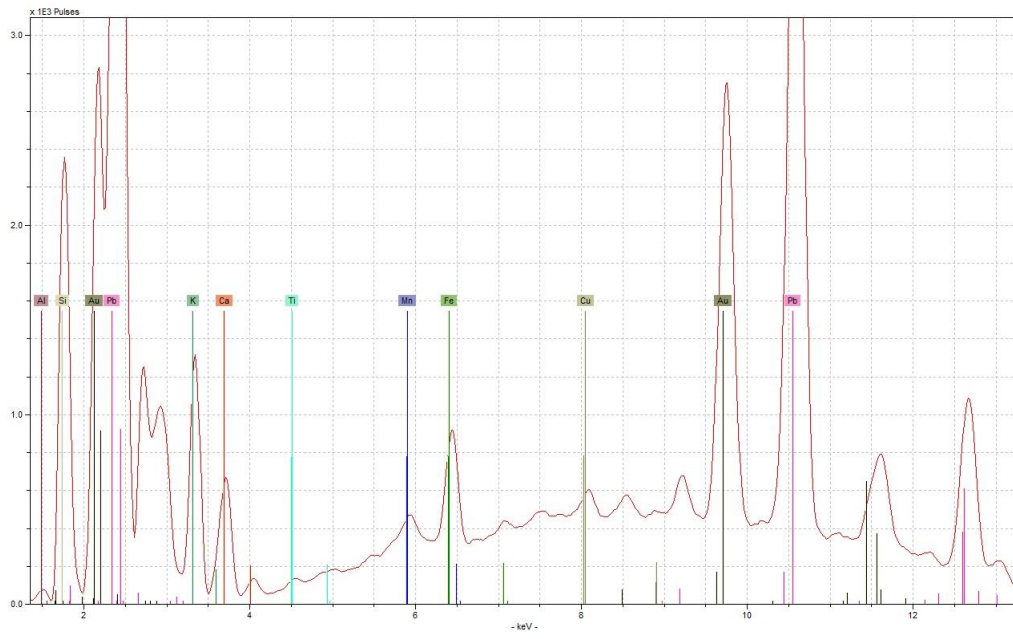
Appendix 7: Hand-Held XRF data



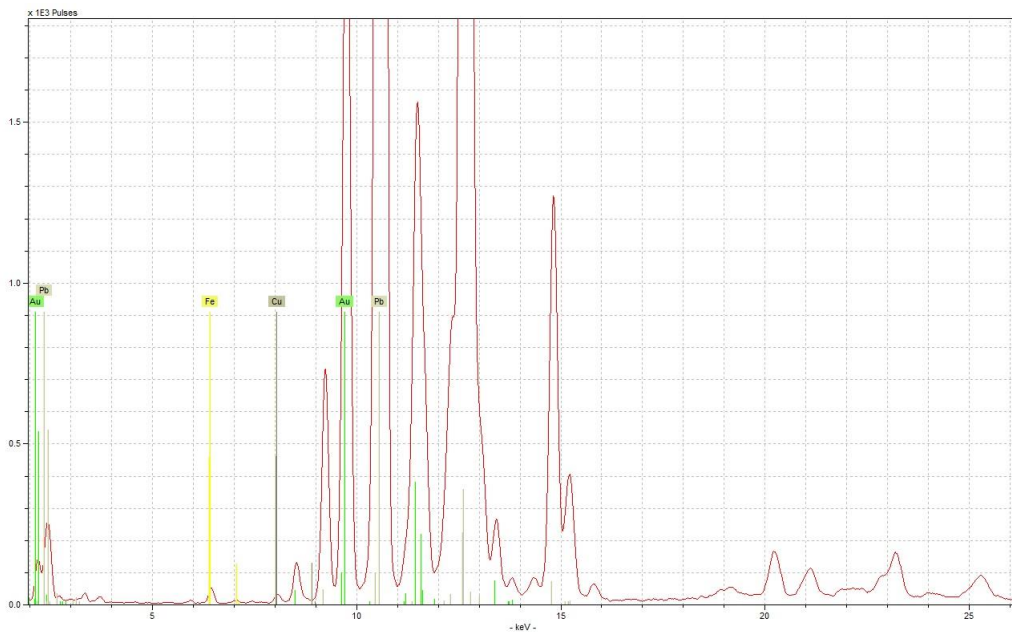
Appendix Figure 57 - example spectrum for pink enamel type 1 from 698, obtained under low voltage condition (upper), and high voltage condition (lower)



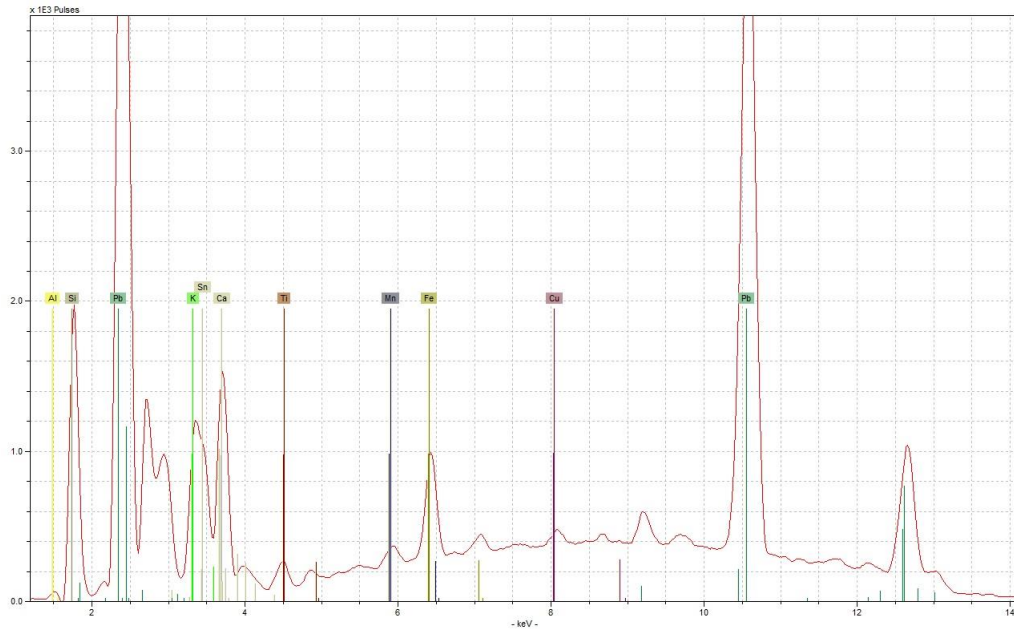
Appendix 7: Hand-Held XRF data



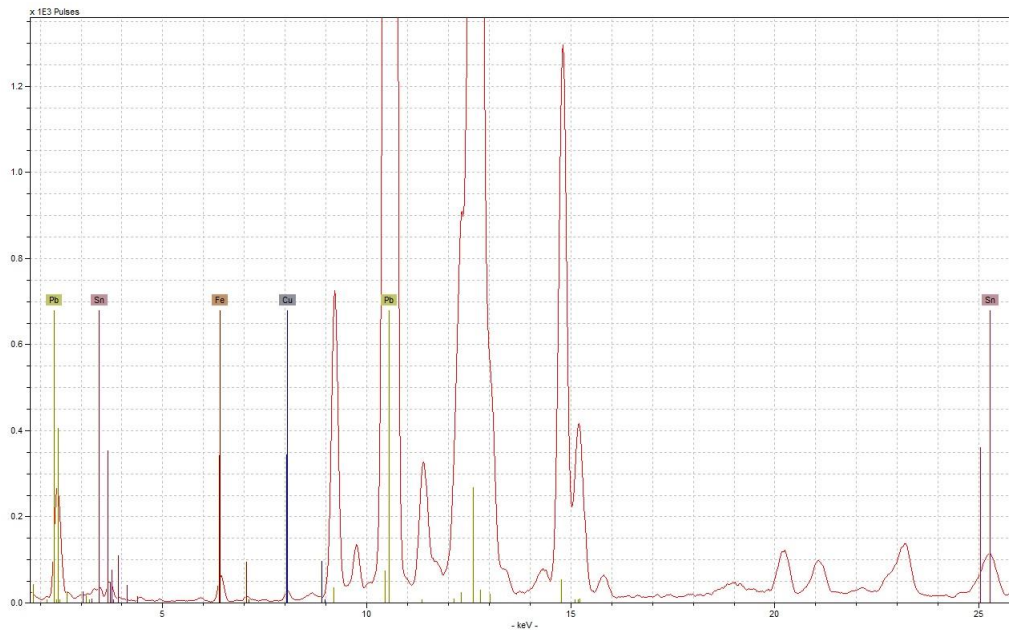
Appendix Figure 58 - example spectrum for pink enamel type 2 from 65, obtained under low voltage condition (upper), and high voltage condition (lower)



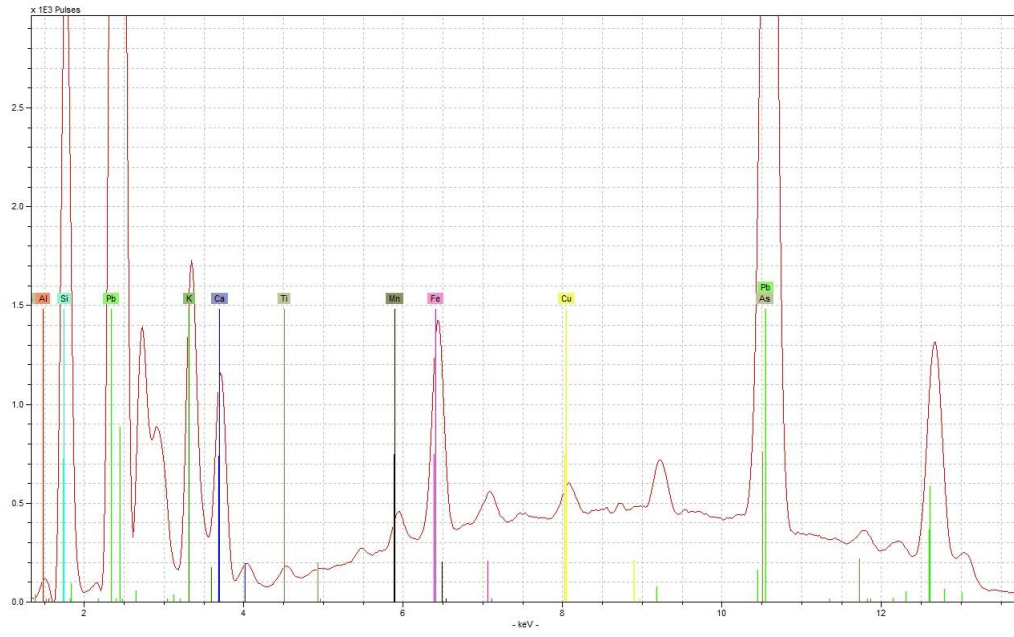
Appendix 7: Hand-Held XRF data



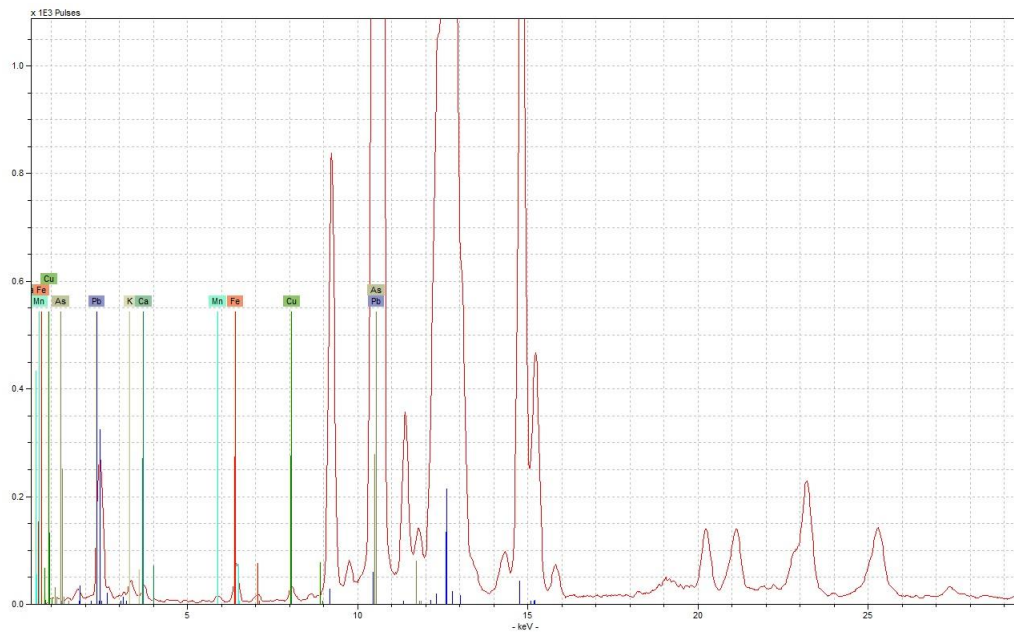
Appendix Figure 59 - example spectrum for pink enamel type 3 from 574, obtained under low voltage condition (upper), and high voltage condition (lower)



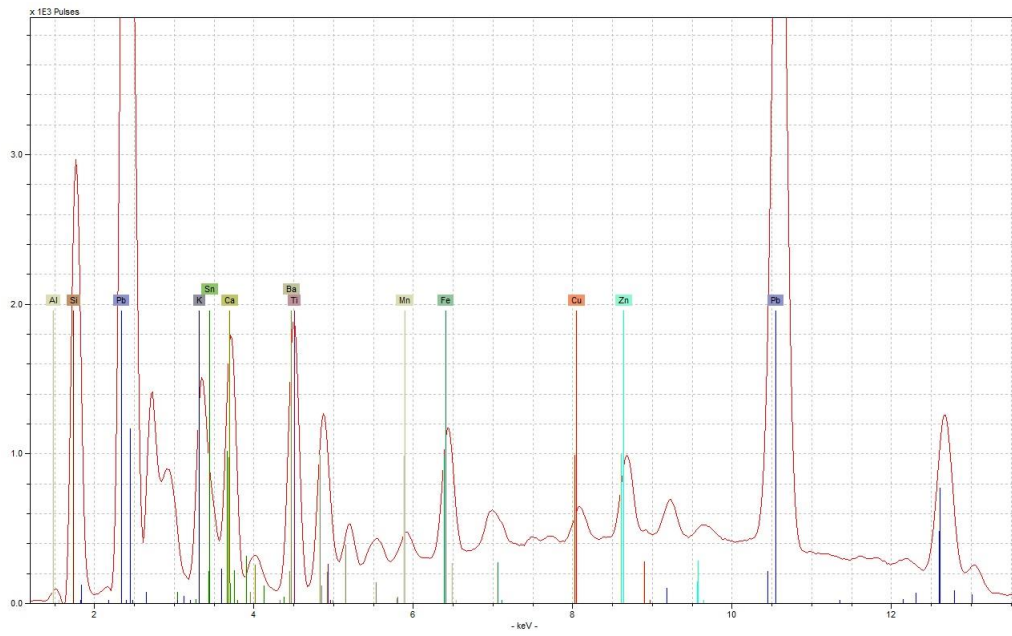
Appendix 7: Hand-Held XRF data



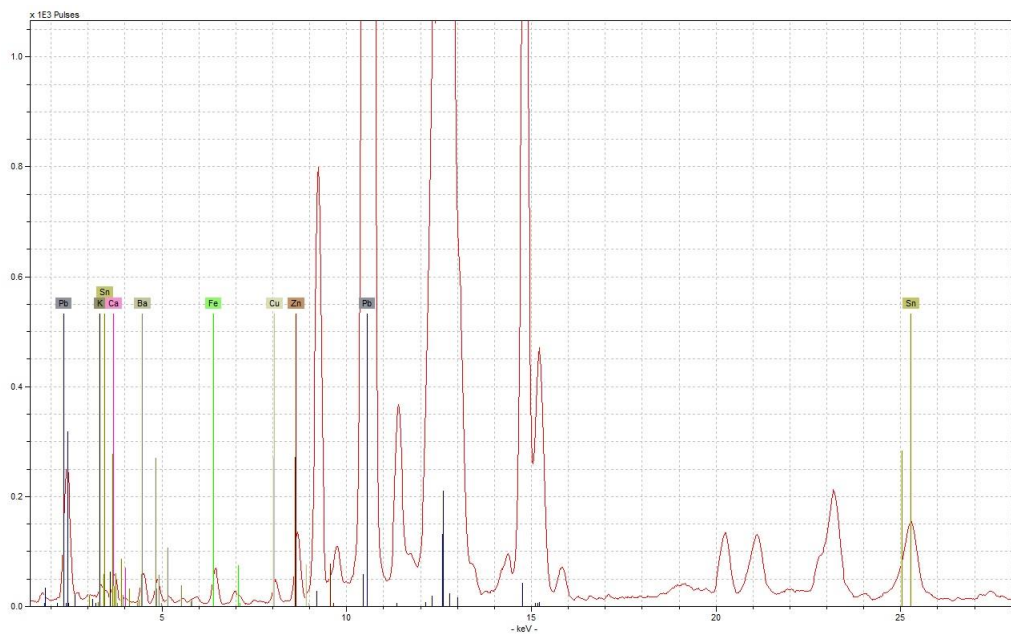
Appendix Figure 60 - example spectrum for pink enamel type 4 from 617, obtained under low voltage condition (upper), and high voltage condition (lower)



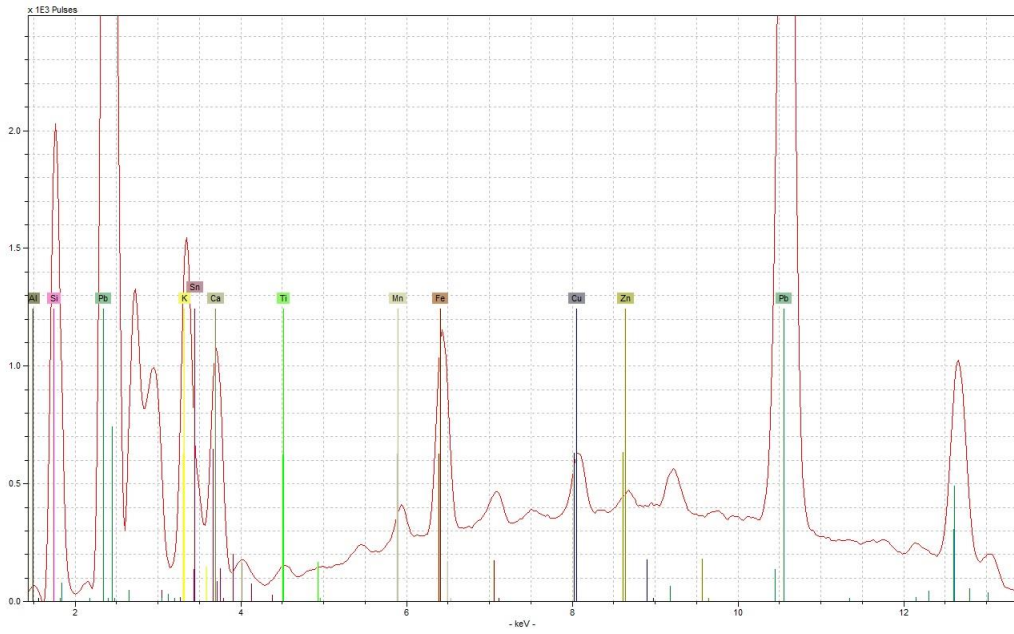
Appendix 7: Hand-Held XRF data



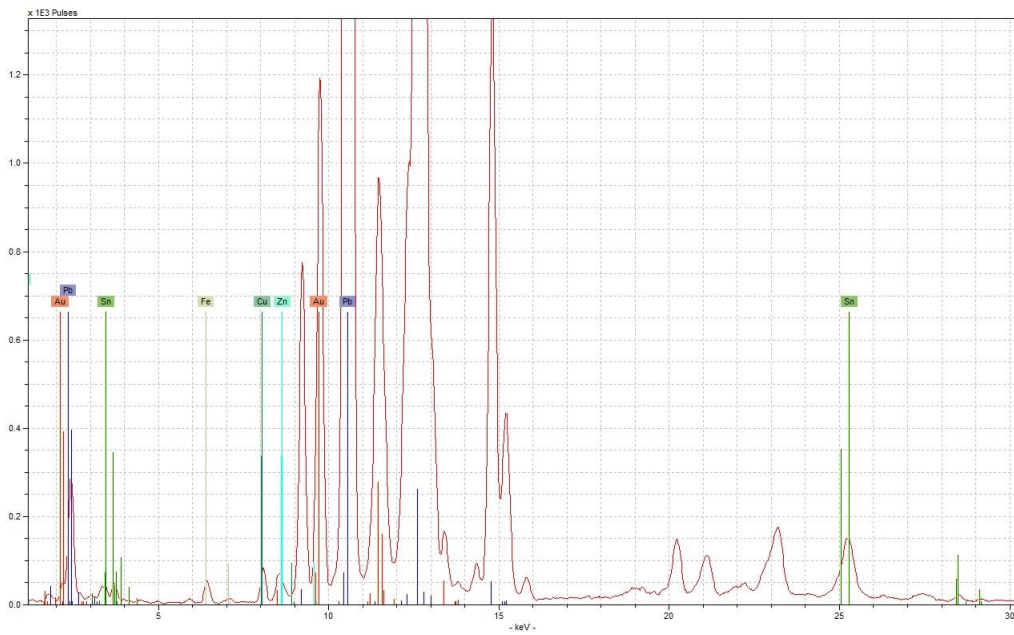
Appendix Figure 61 - example spectrum for pink enamel type 5 from 480, obtained under low voltage condition (upper), and high voltage condition (lower)



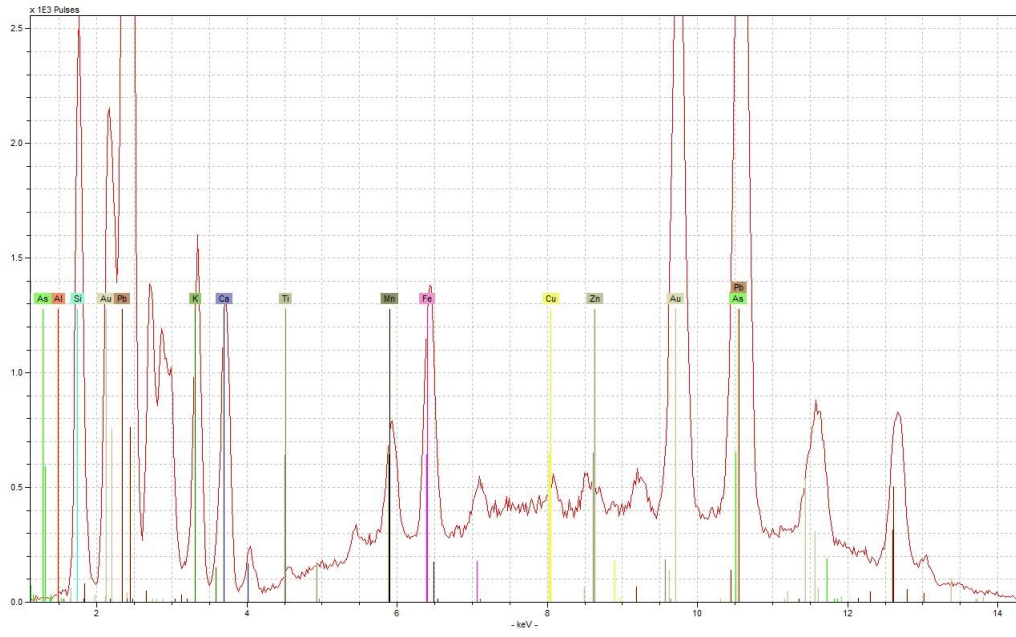
Appendix 7: Hand-Held XRF data



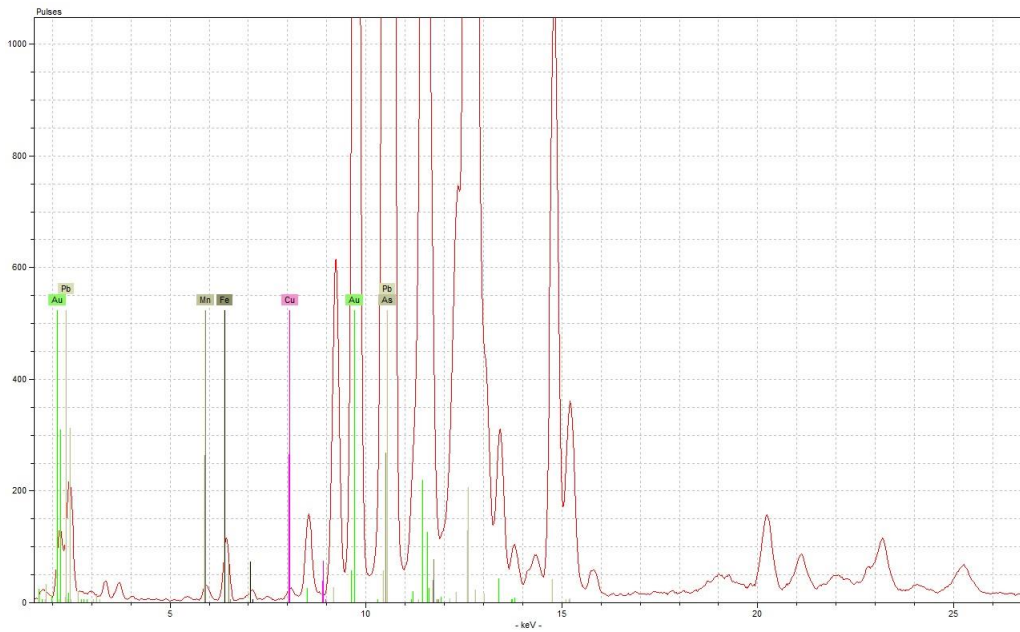
Appendix Figure 62 - example spectrum for pink enamel type 6 from 696, obtained under low voltage condition (upper), and high voltage condition (lower)



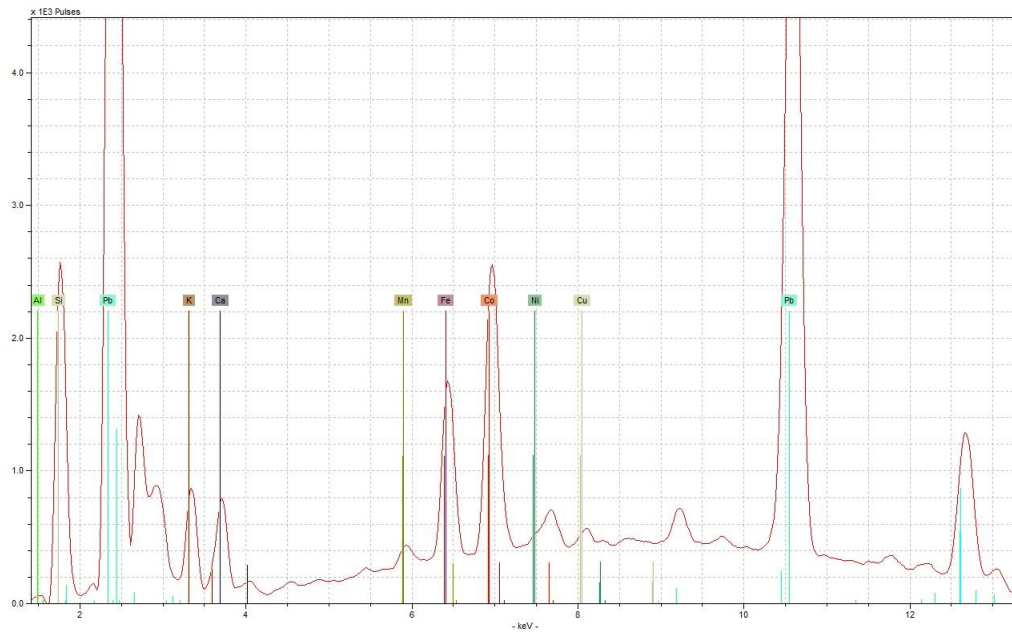
Appendix 7: Hand-Held XRF data



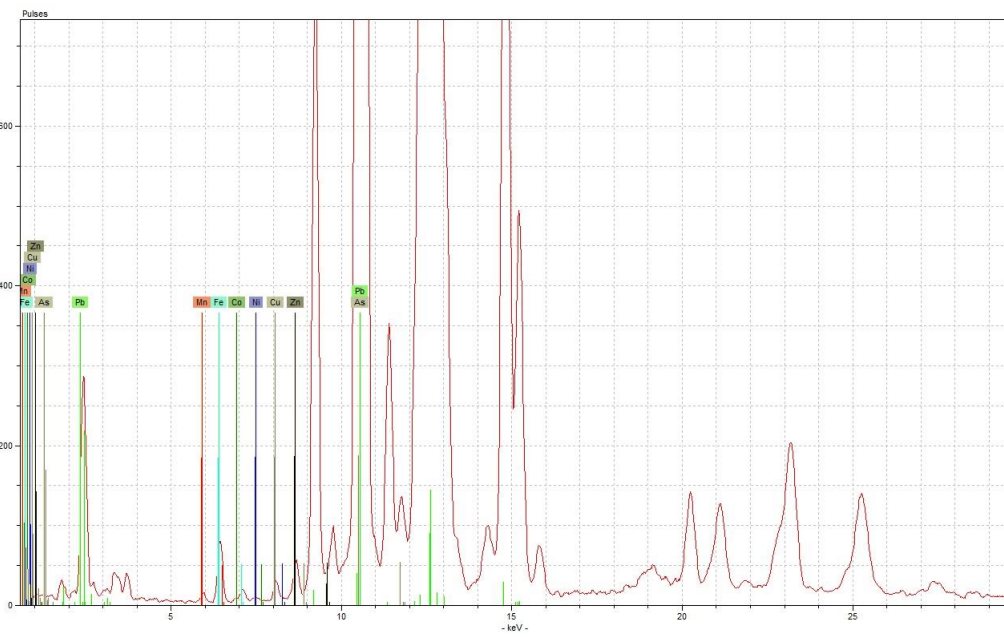
Appendix Figure 63 - example spectrum for pink enamel type 7 from 697, obtained under low voltage condition (upper), and high voltage condition (lower)



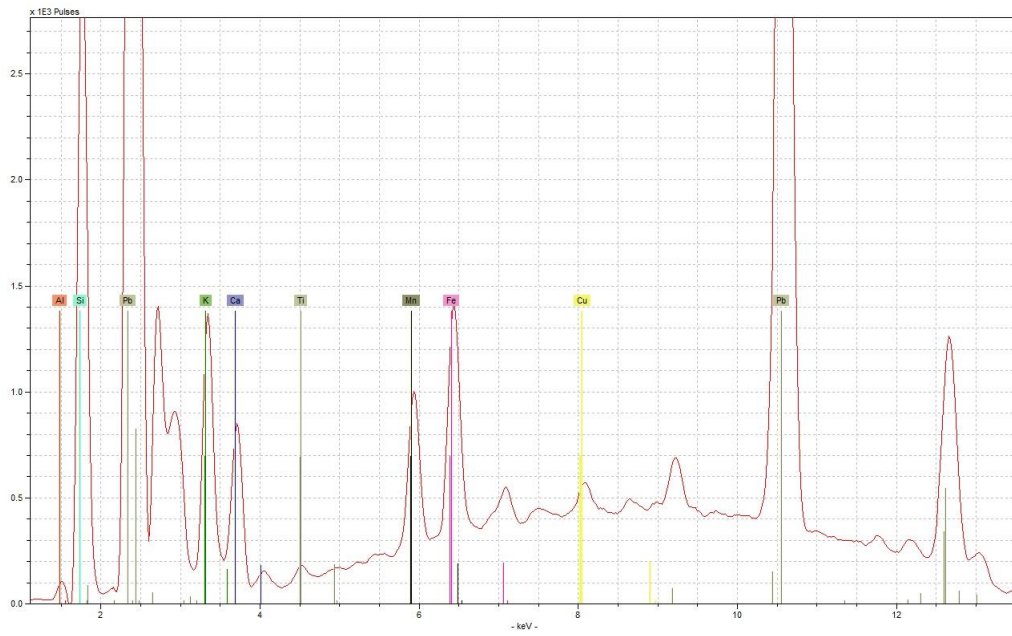
Appendix 7: Hand-Held XRF data



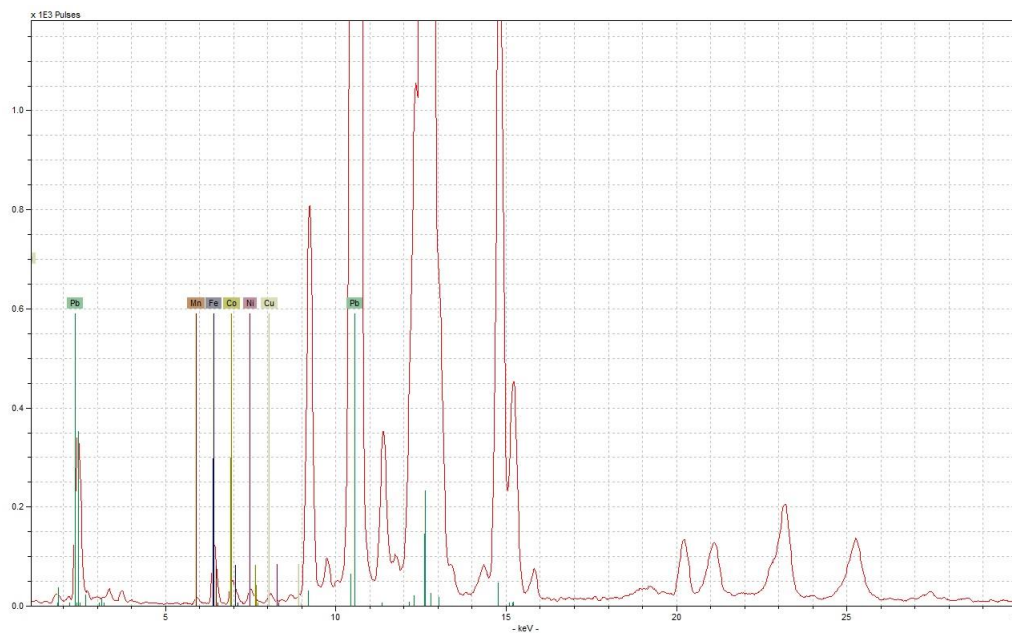
Appendix Figure 64 - example spectrum for purple enamel type 1 from WJG8, obtained under low voltage condition (upper), and high voltage condition (lower)



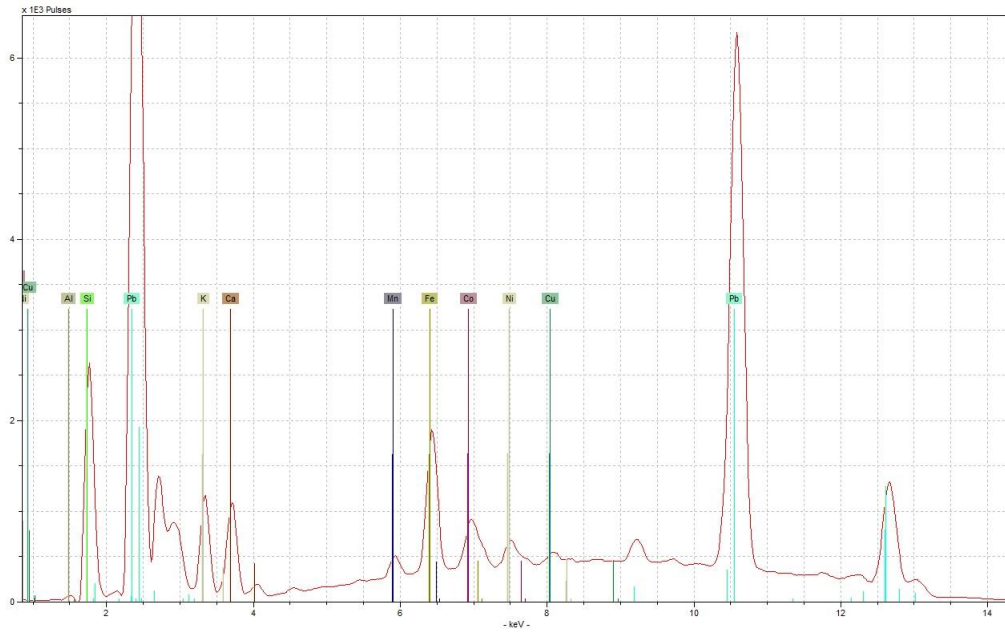
Appendix 7: Hand-Held XRF data



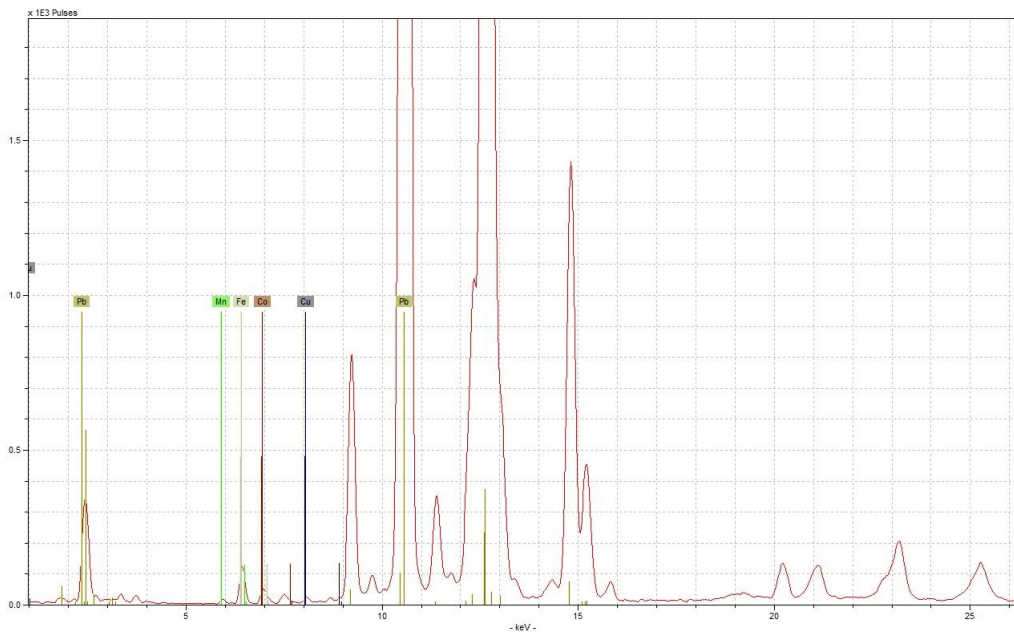
Appendix Figure 65 - example spectrum for purple enamel type 2 from WJG9, obtained under low voltage condition (upper), and high voltage condition (lower)



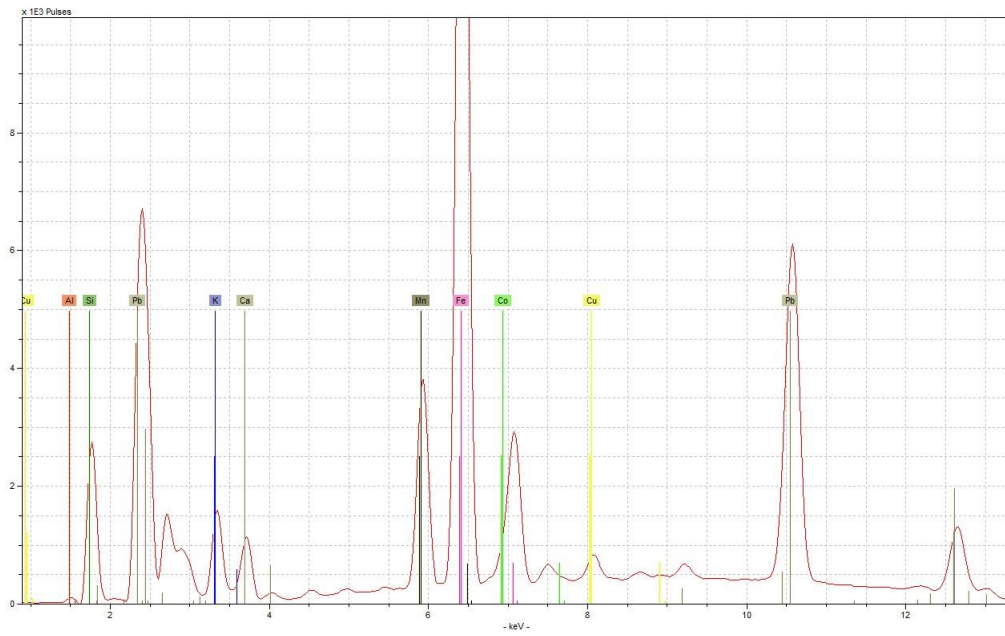
Appendix 7: Hand-Held XRF data



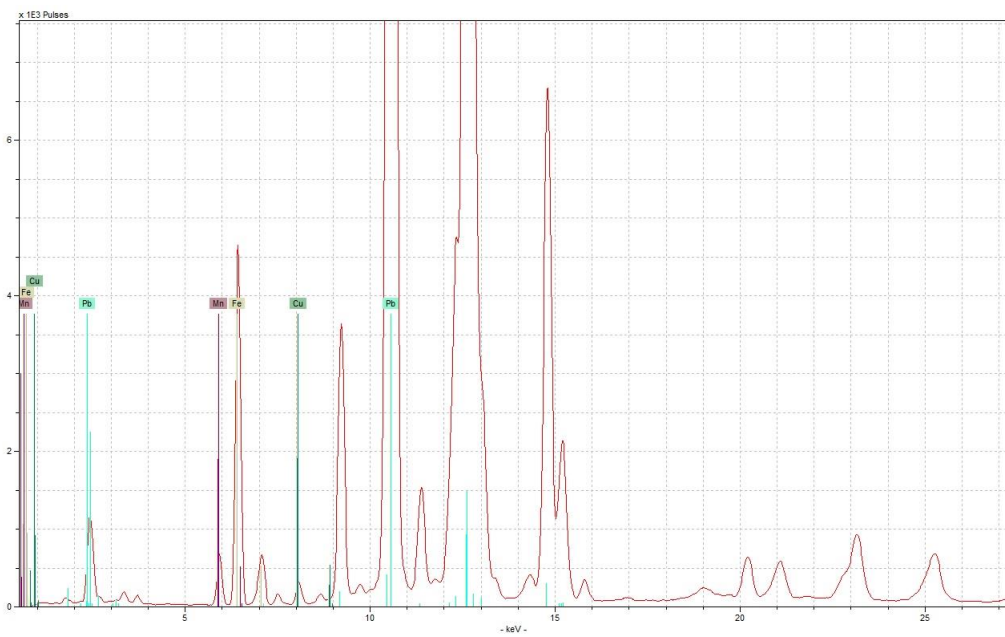
Appendix Figure 66 - example spectrum for purple enamel type 3 from WJG3, obtained under low voltage condition (upper) and high voltage condition (lower)



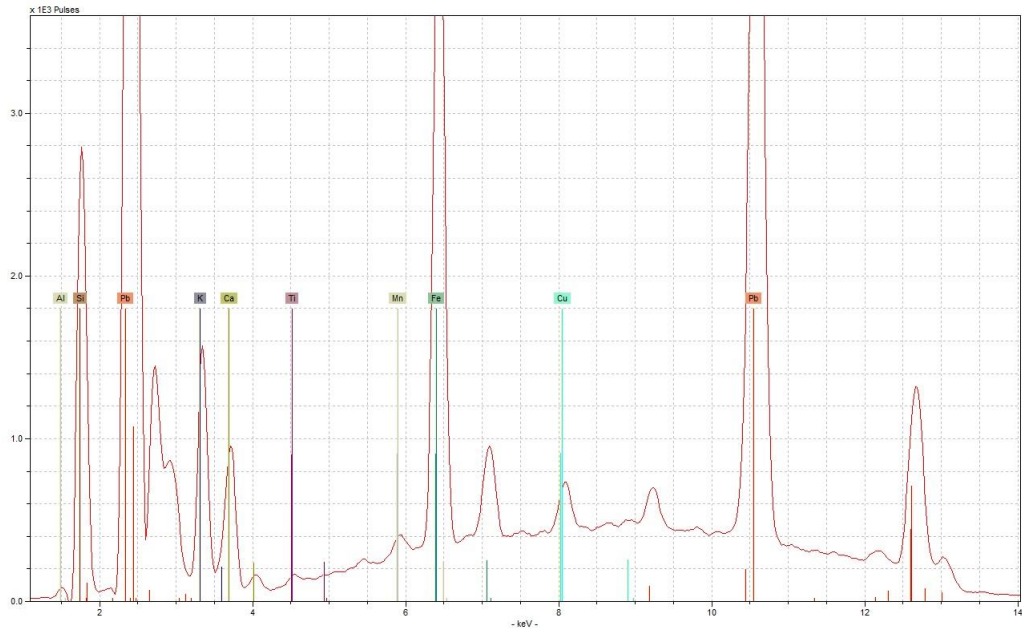
Appendix 7: Hand-Held XRF data



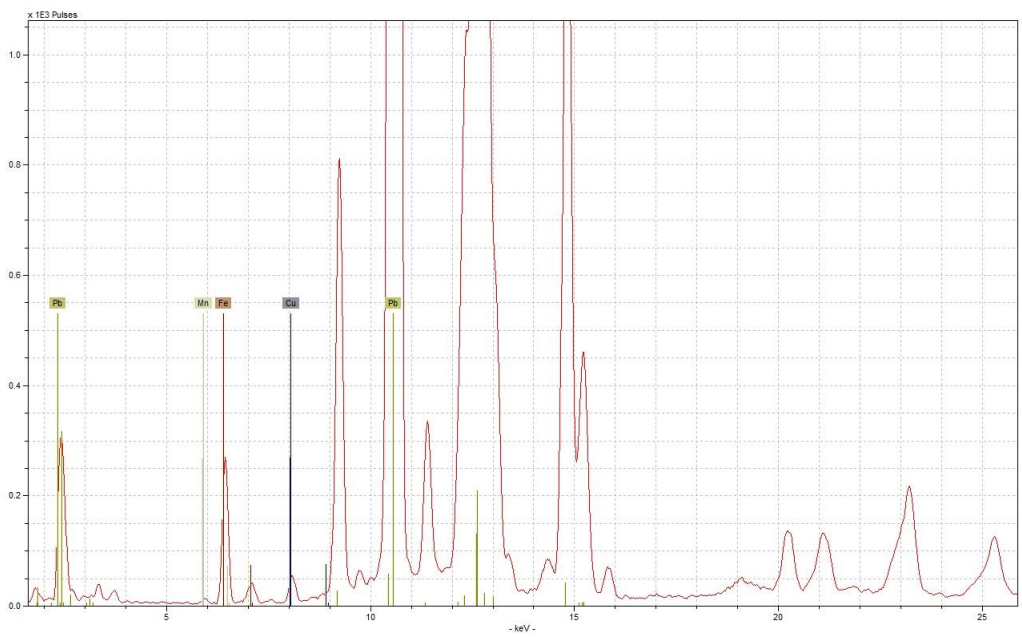
Appendix Figure 67 - example spectrum for purple enamel type 4 from WWR3, obtained under low voltage condition (upper) and high voltage condition (lower)



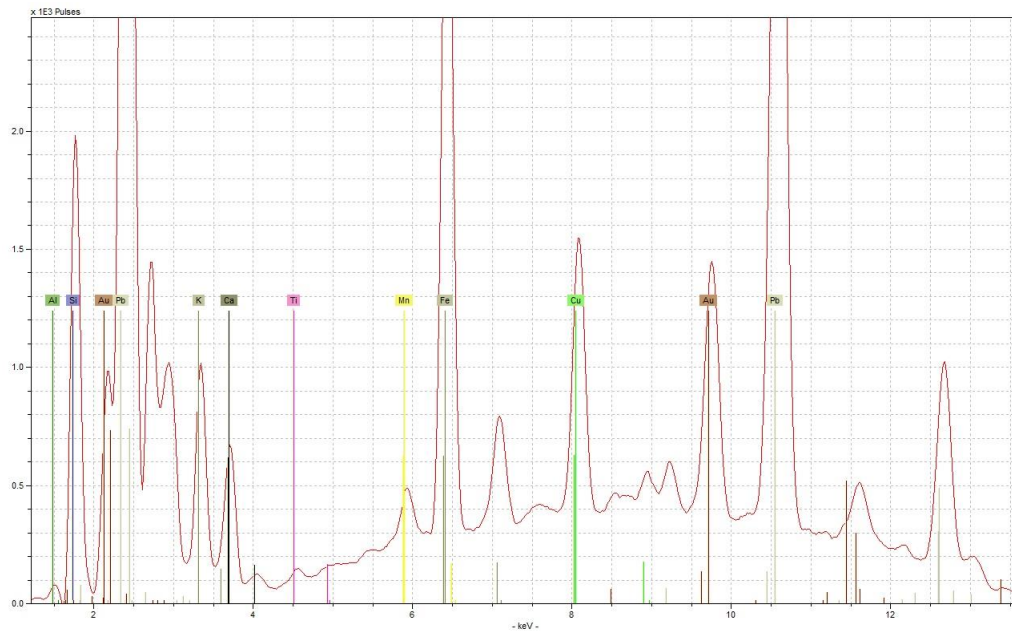
Appendix 7: Hand-Held XRF data



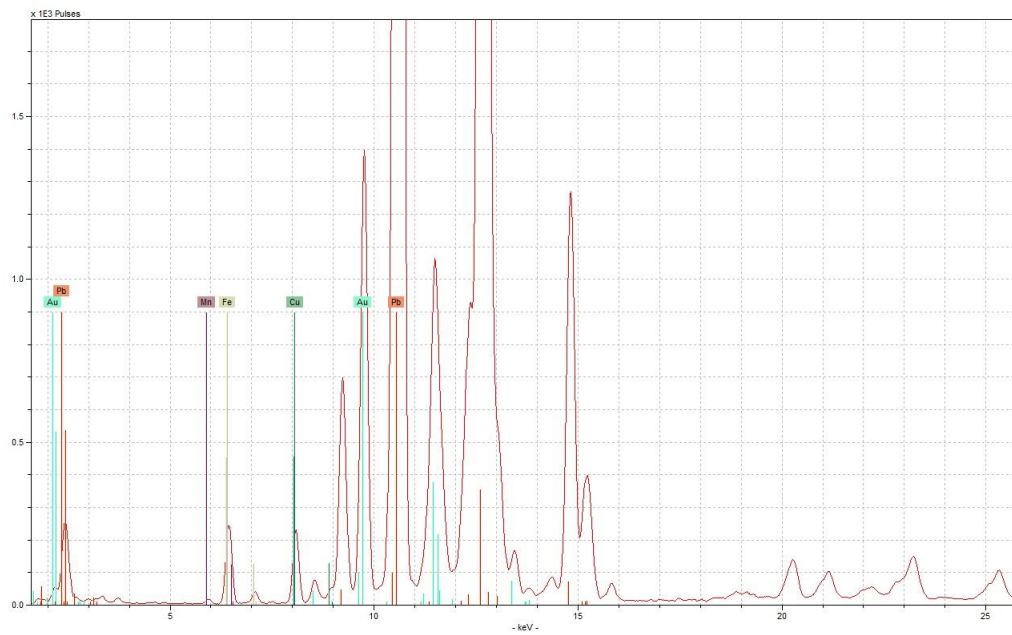
Appendix Figure 68 - example spectrum for red enamel type 1 from 65, obtained under low voltage condition (upper), and high voltage condition (lower)



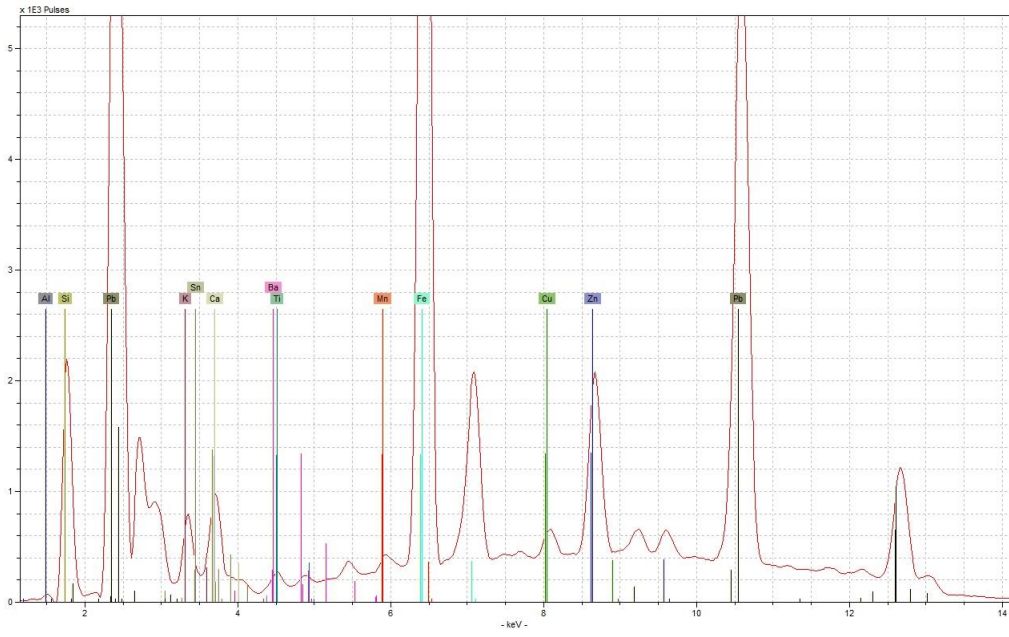
Appendix 7: Hand-Held XRF data



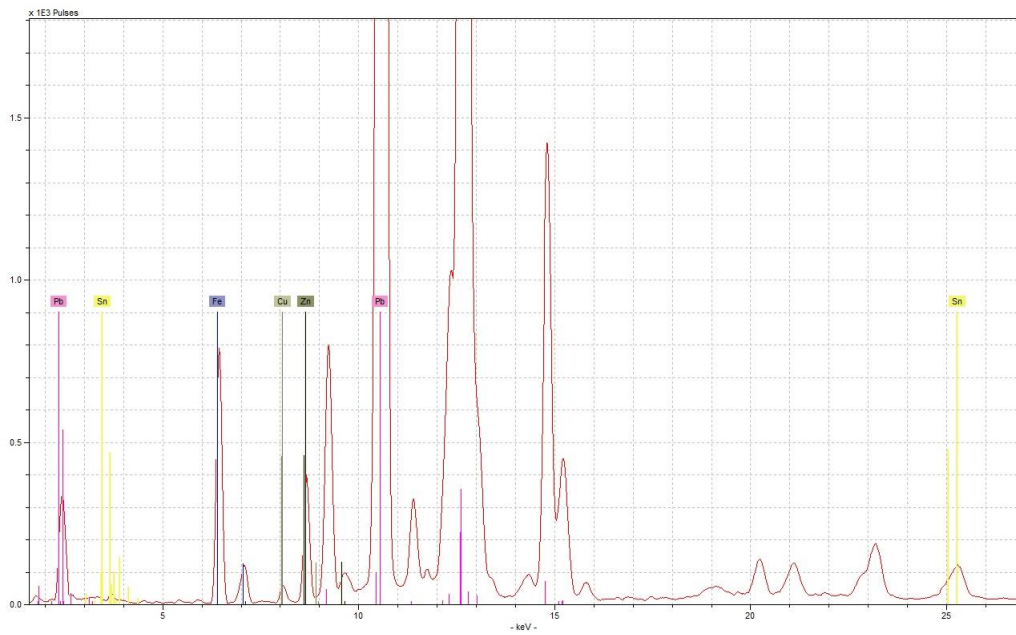
Appendix Figure 69 - example spectrum for red enamel type 2 from 620, obtained under low voltage condition (upper), and high voltage condition (lower)



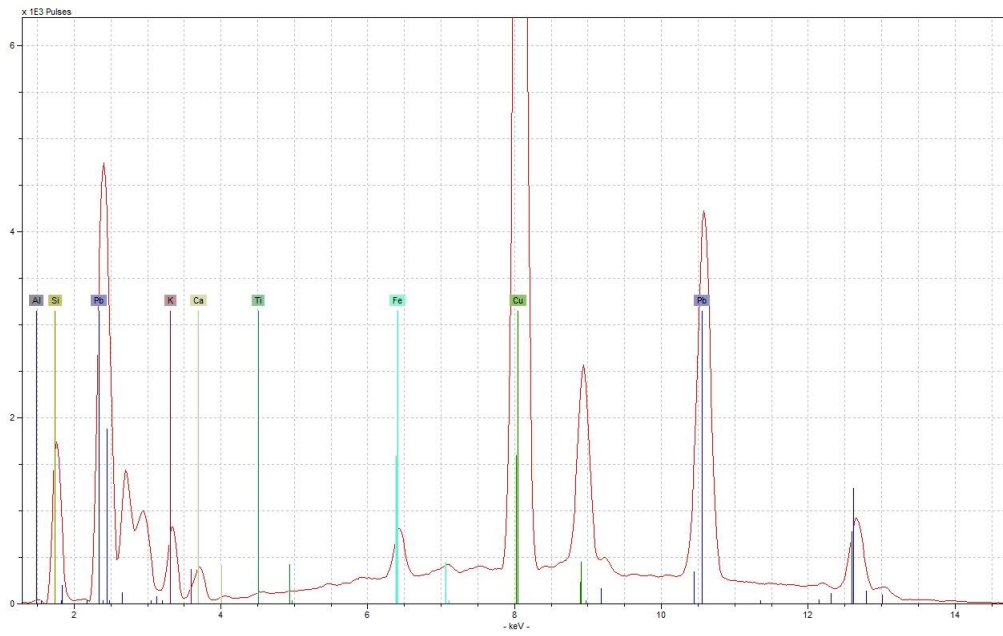
Appendix 7: Hand-Held XRF data



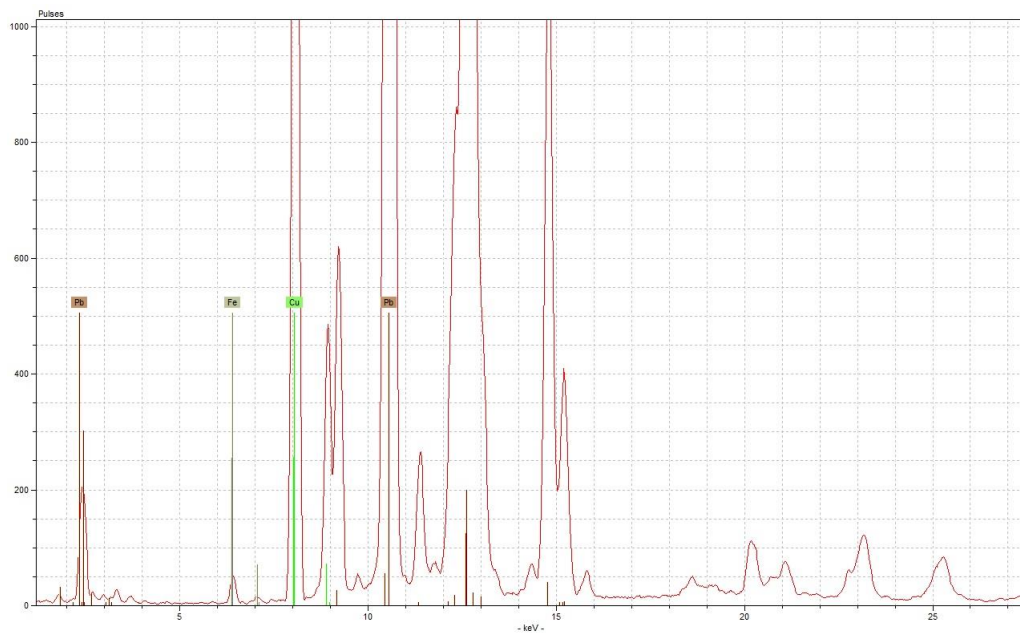
Appendix Figure 70 - example spectrum for red enamel type 3 from 705, obtained under low voltage condition (upper), and high voltage condition (lower)



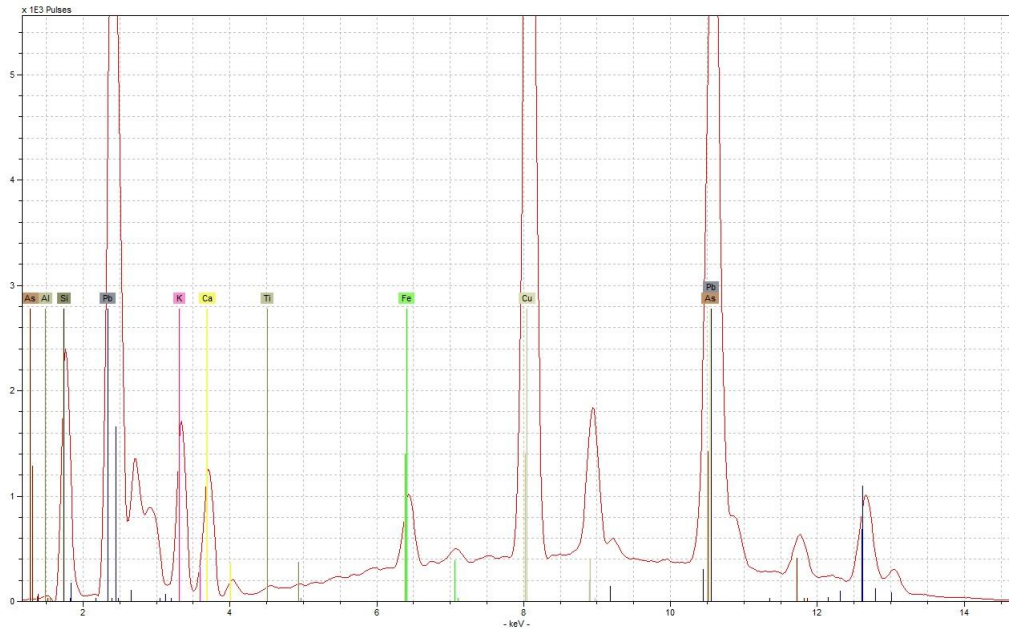
Appendix 7: Hand-Held XRF data



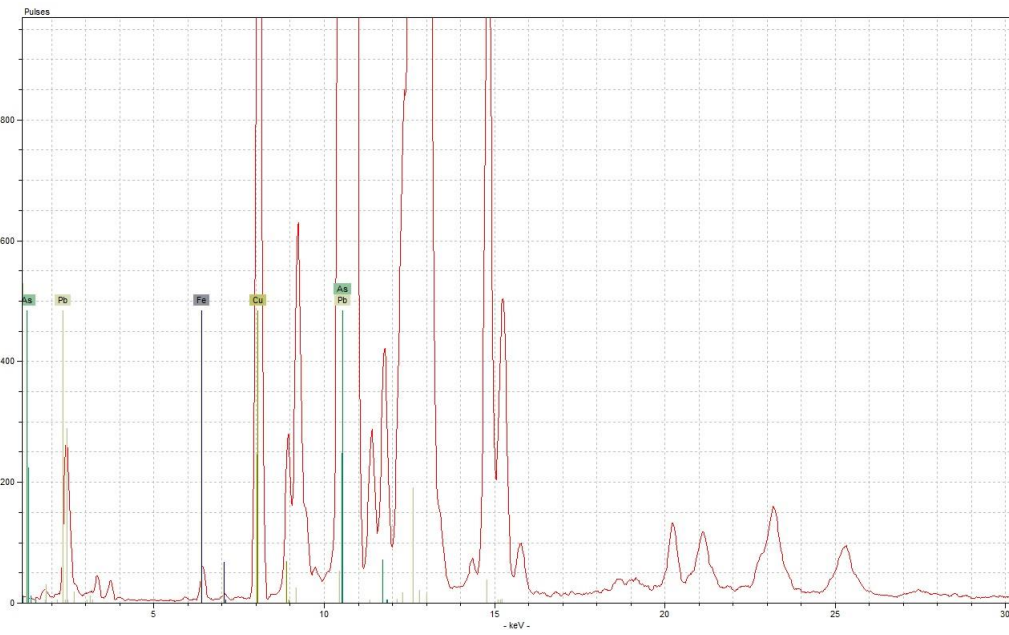
Appendix Figure 71 - example spectrum for turquoise enamel type 1 from 577, obtained under low voltage condition (upper), and high voltage condition (lower)



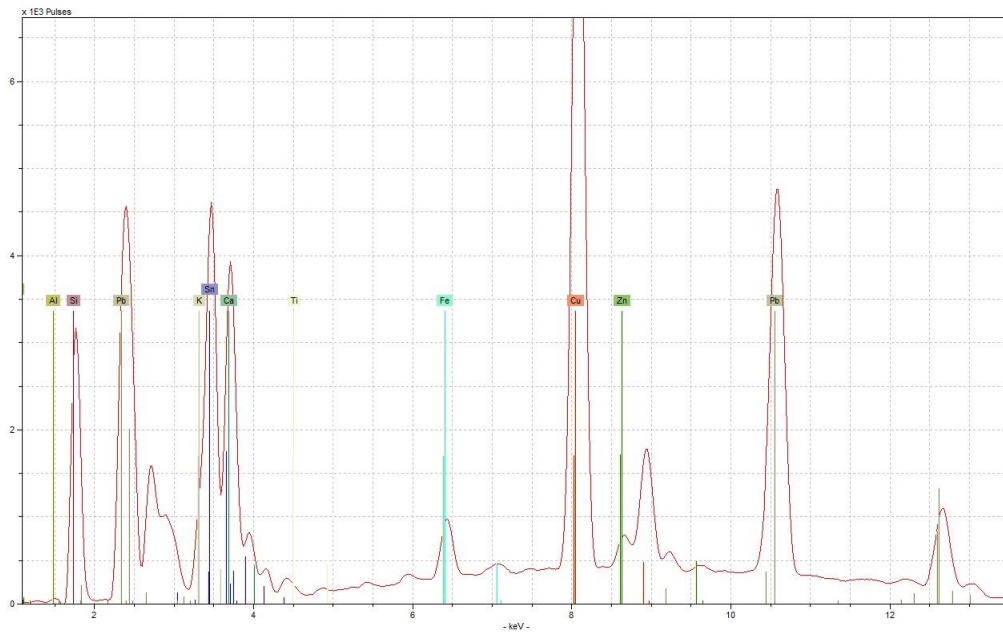
Appendix 7: Hand-Held XRF data



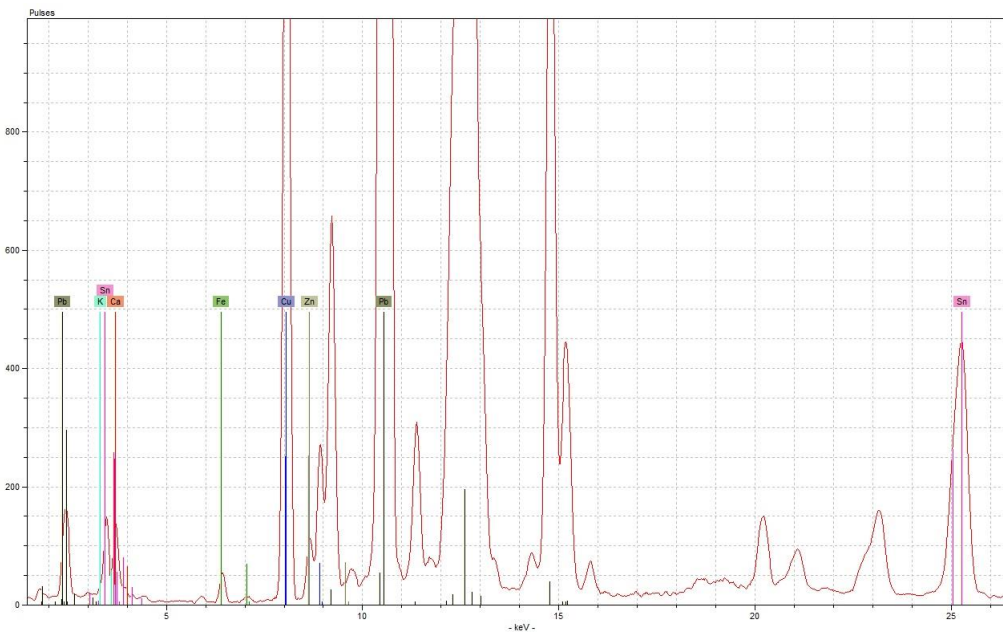
Appendix Figure 72 - example spectrum for turquoise enamel type 2 from 698, obtained under low voltage condition (upper), and high voltage condition (lower)



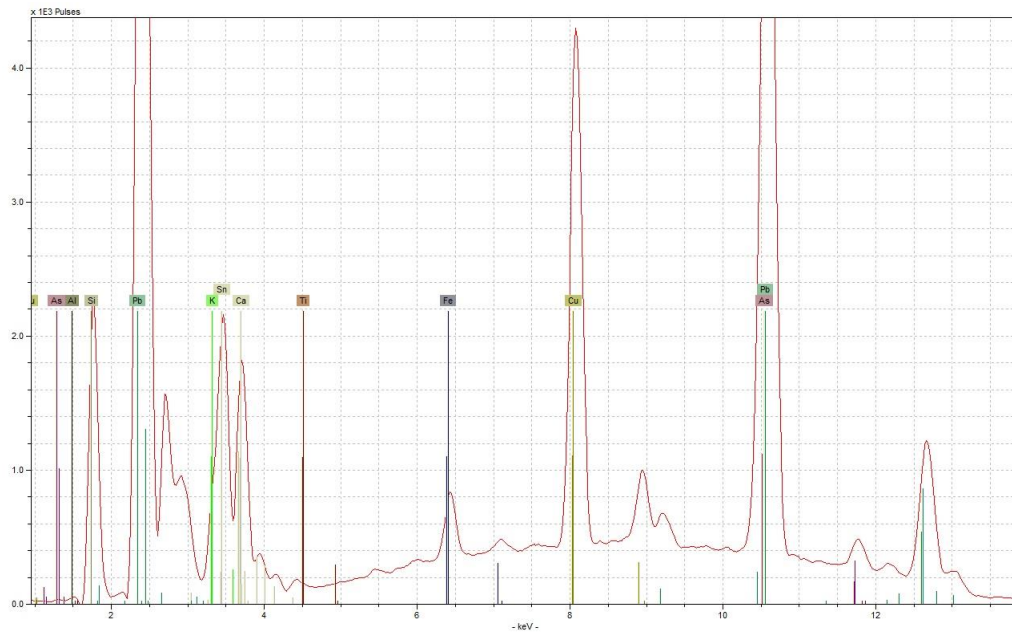
Appendix 7: Hand-Held XRF data



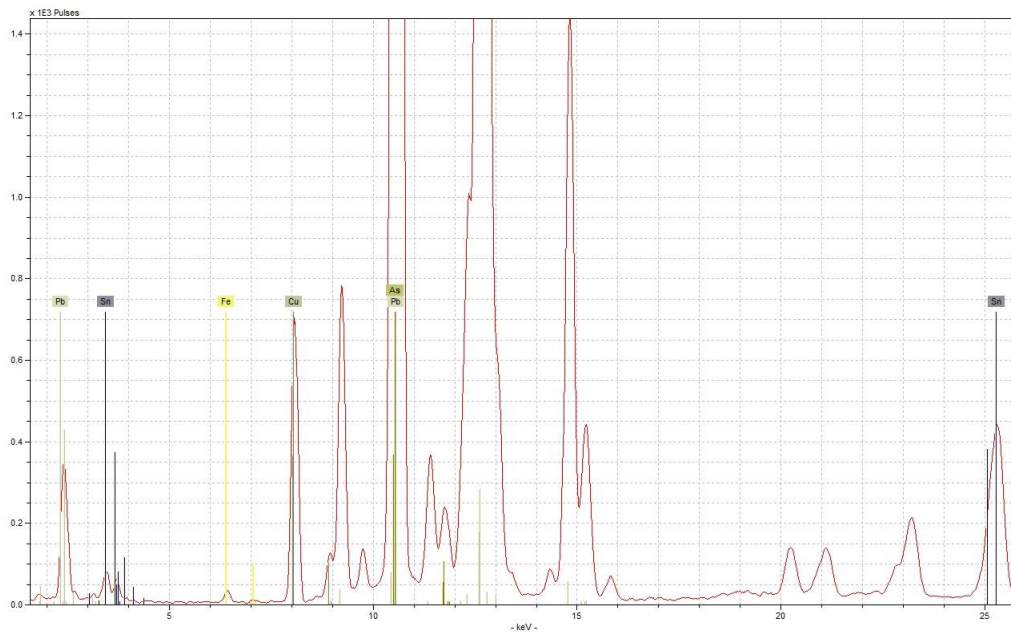
Appendix Figure 73 - example spectrum for turquoise enamel type 3 from 700, obtained under low voltage condition (upper), and high voltage condition (lower)



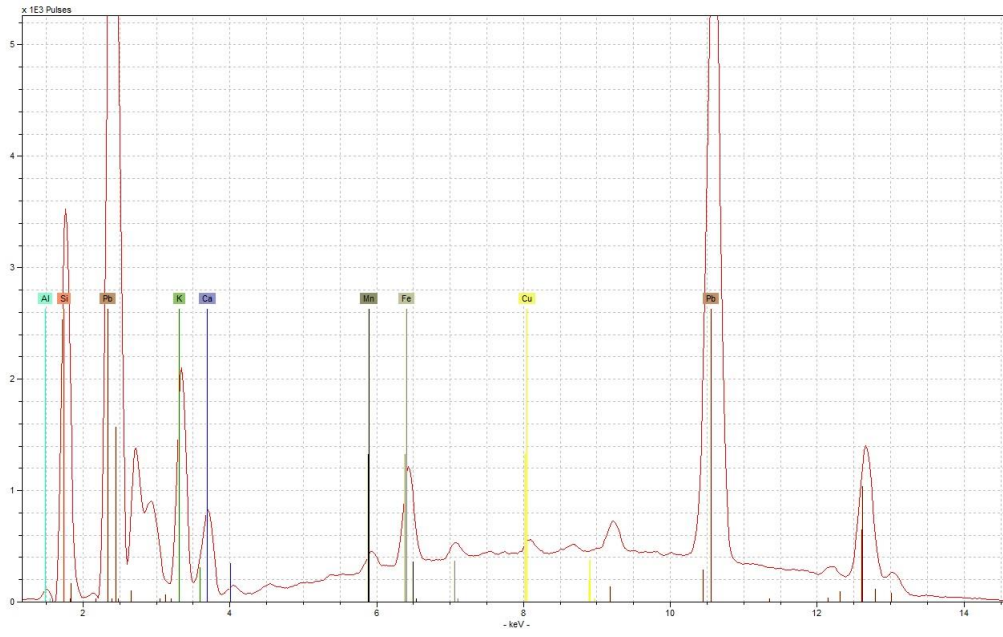
Appendix 7: Hand-Held XRF data



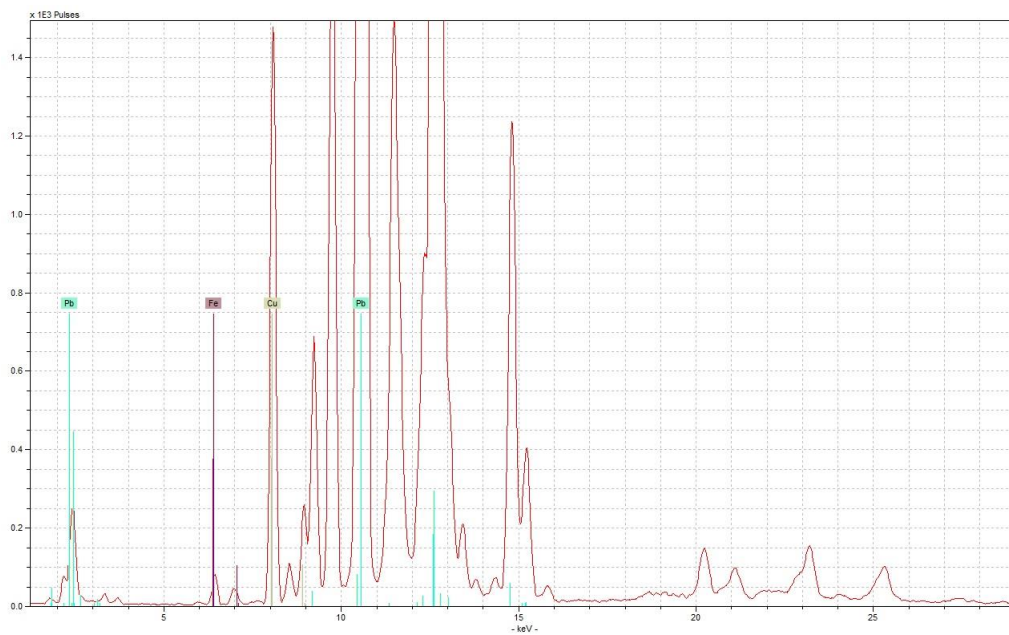
Appendix Figure 74 - example spectrum for turquoise enamel type 4 from 705, obtained under low voltage condition (upper), and high voltage condition (lower)



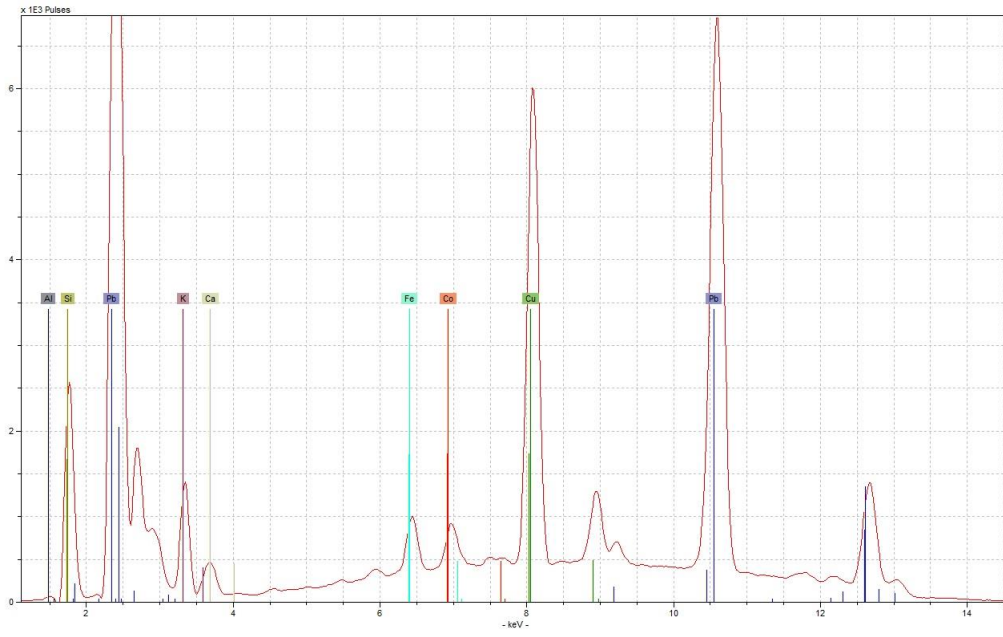
Appendix 7: Hand-Held XRF data



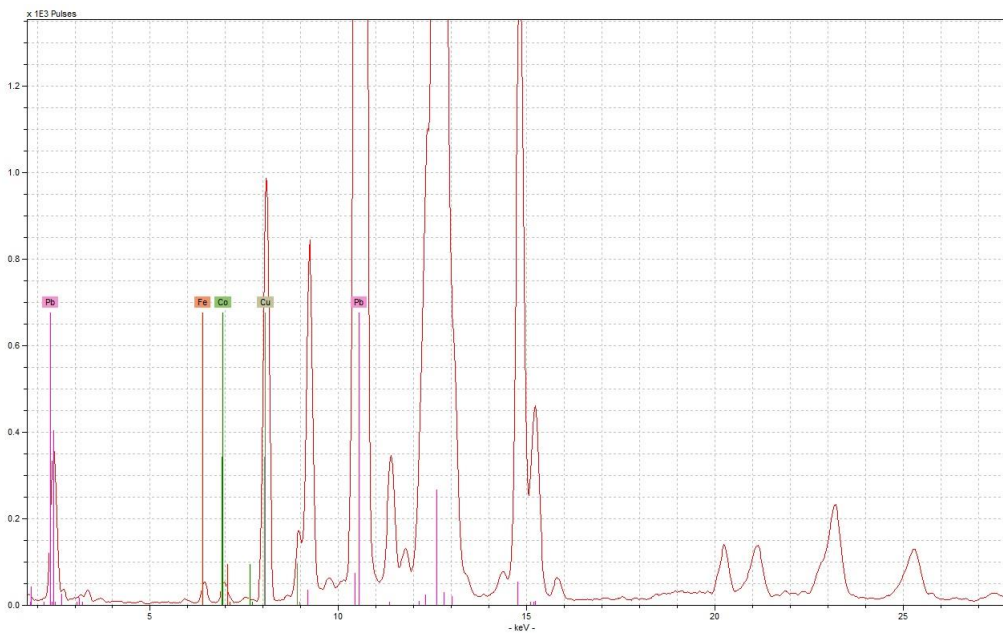
Appendix Figure 75 - example spectrum for turquoise enamel type 5 from 702, obtained under low voltage condition (upper), and high voltage condition (lower)



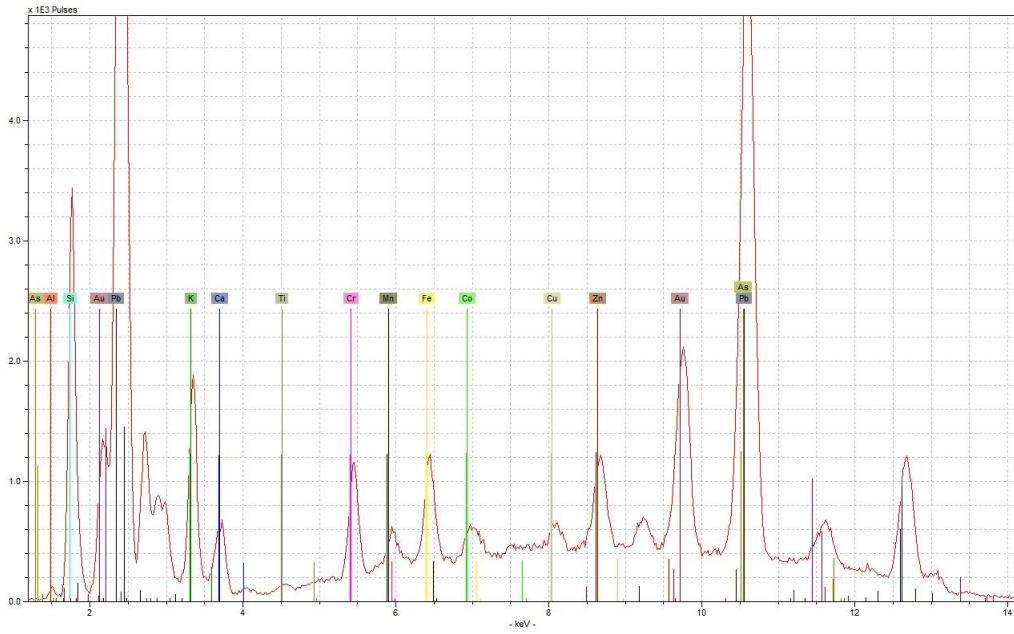
Appendix 7: Hand-Held XRF data



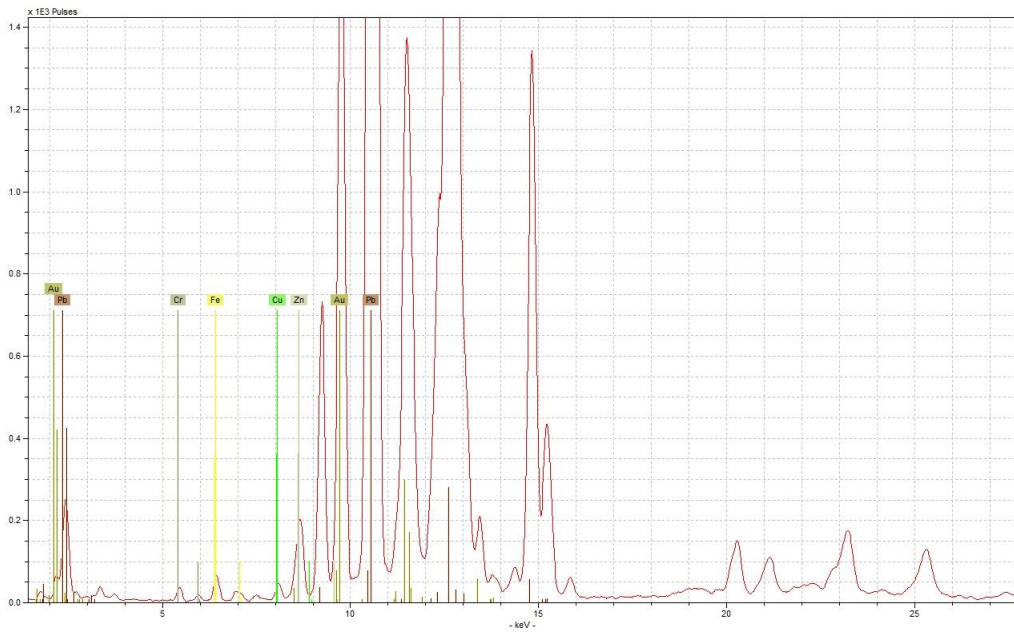
Appendix Figure 76 - example spectrum for turquoise enamel type 6 from 65, obtained under low voltage condition (upper), and high voltage condition (lower)



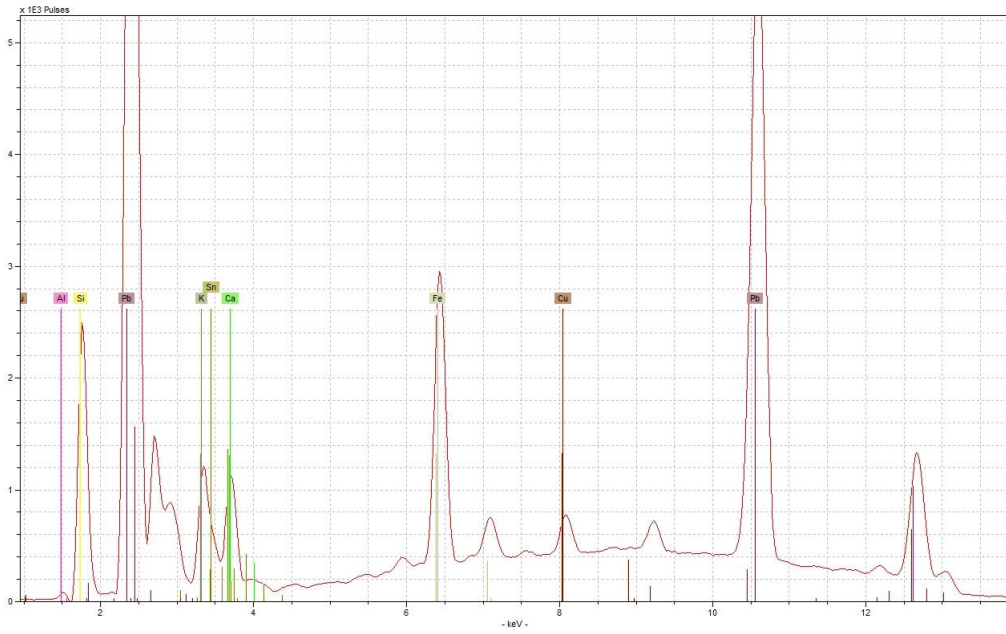
Appendix 7: Hand-Held XRF data



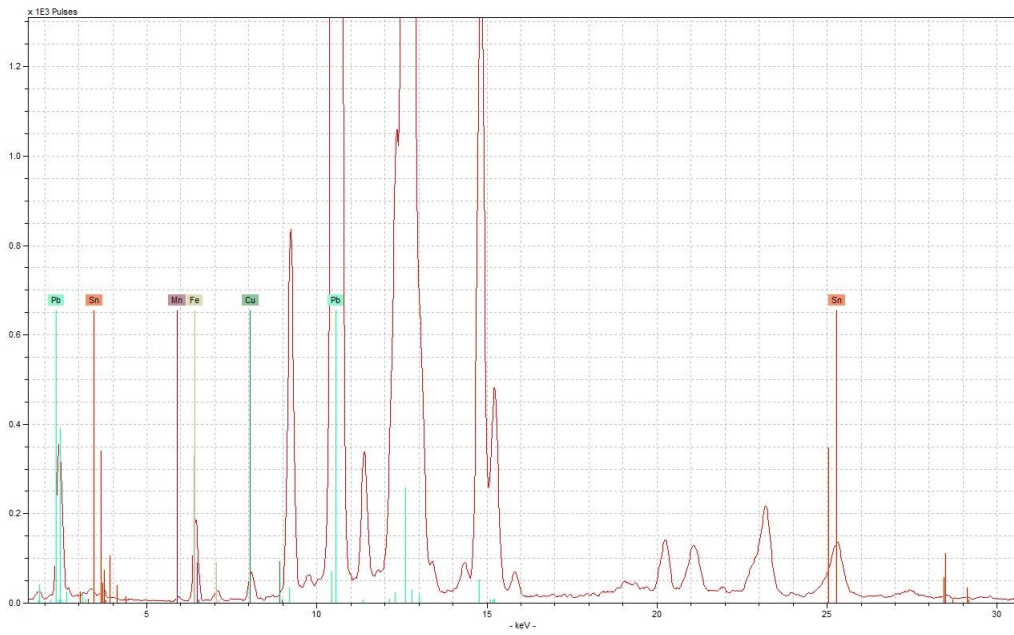
Appendix Figure 77 - example spectrum for turquoise enamel type 7 from 914, obtained under low voltage condition (upper), and high voltage condition (lower)



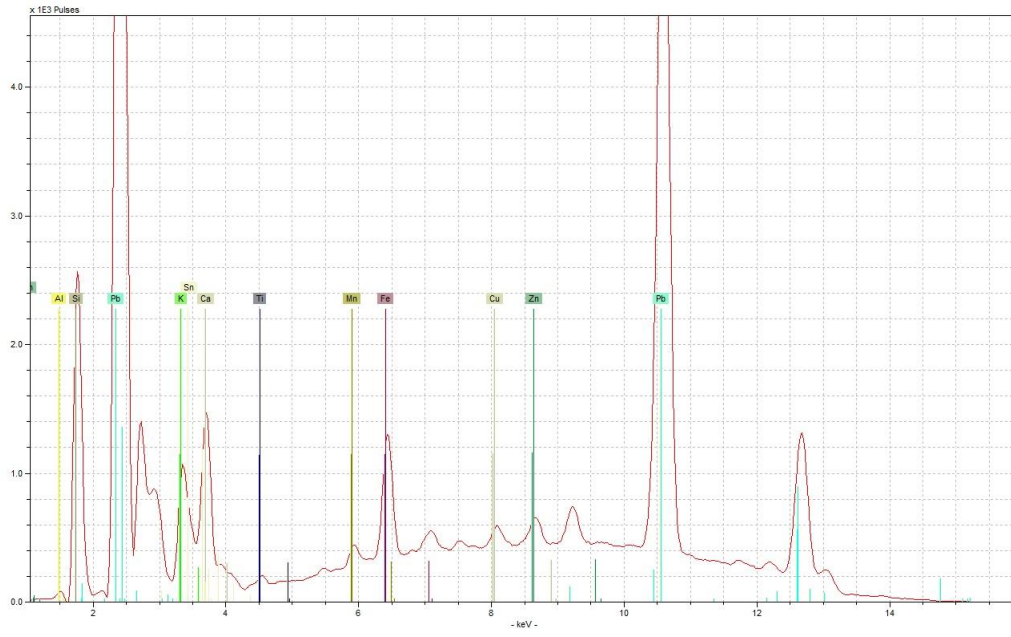
Appendix 7: Hand-Held XRF data



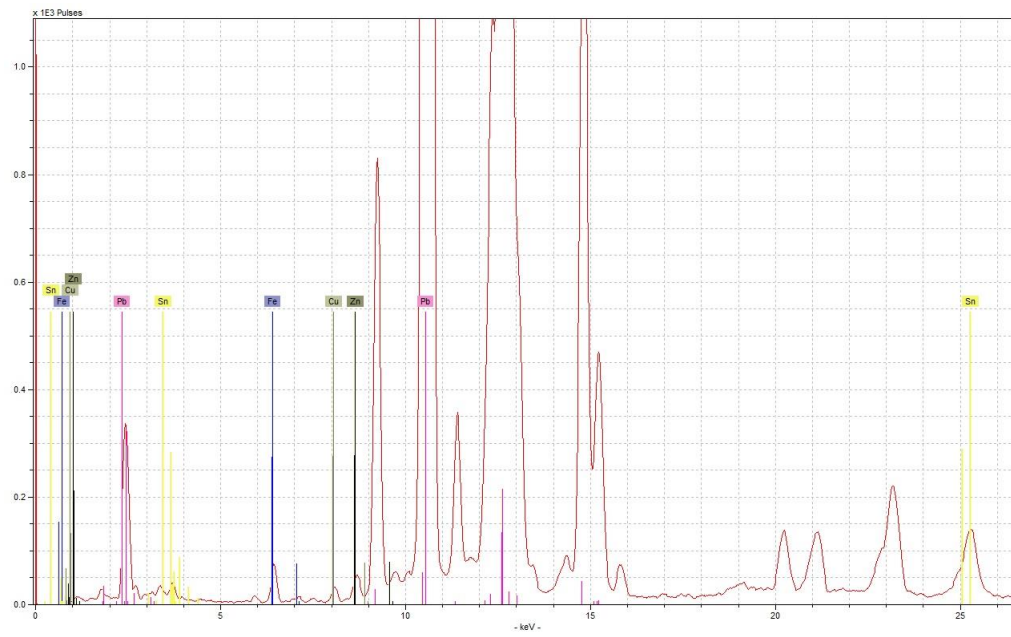
Appendix Figure 78 - example spectrum for yellow enamel type 1 from 65, obtained under low voltage condition (upper), and high voltage condition (lower)



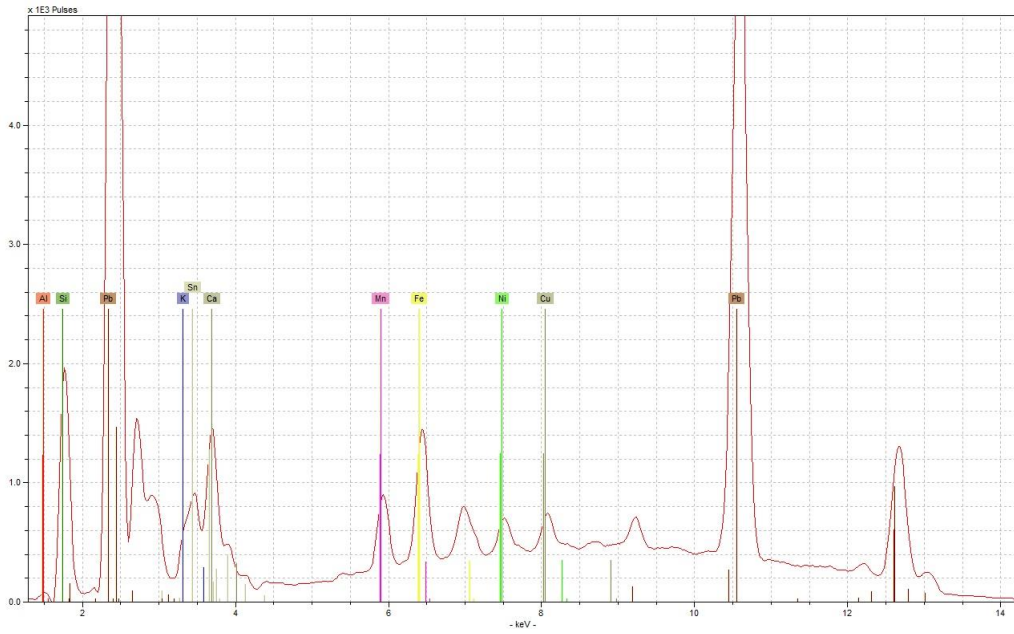
Appendix 7: Hand-Held XRF data



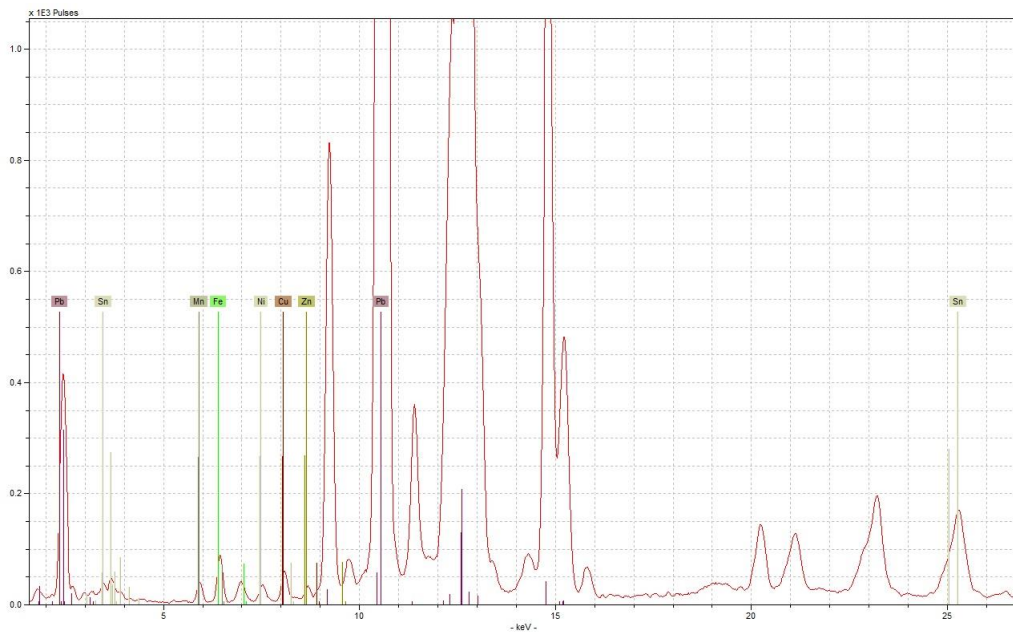
Appendix Figure 79 - example spectrum for yellow enamel type 2 from 480, obtained under low voltage condition (upper), and high voltage condition (lower)



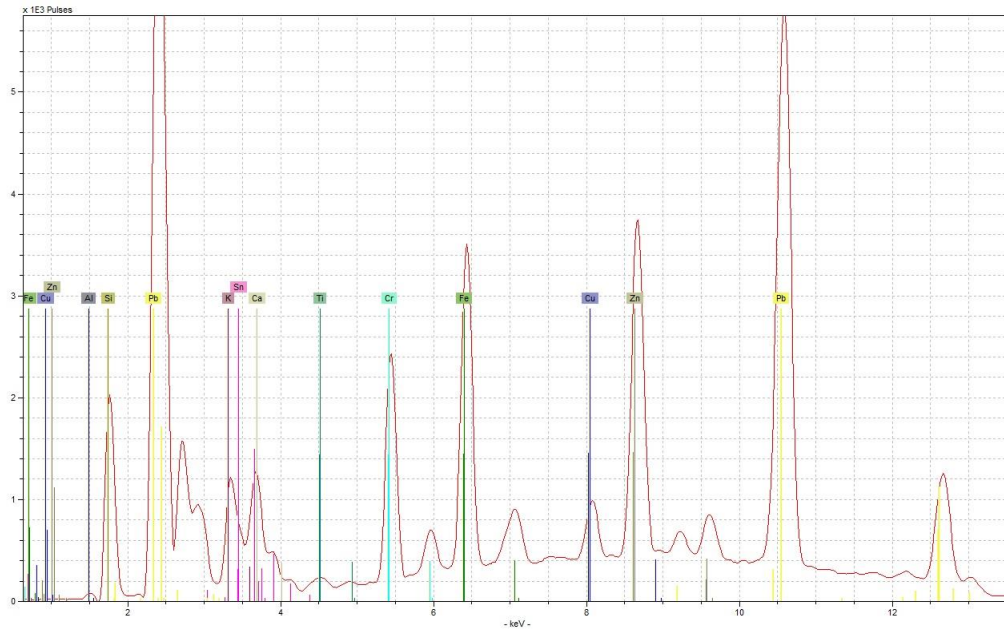
Appendix 7: Hand-Held XRF data



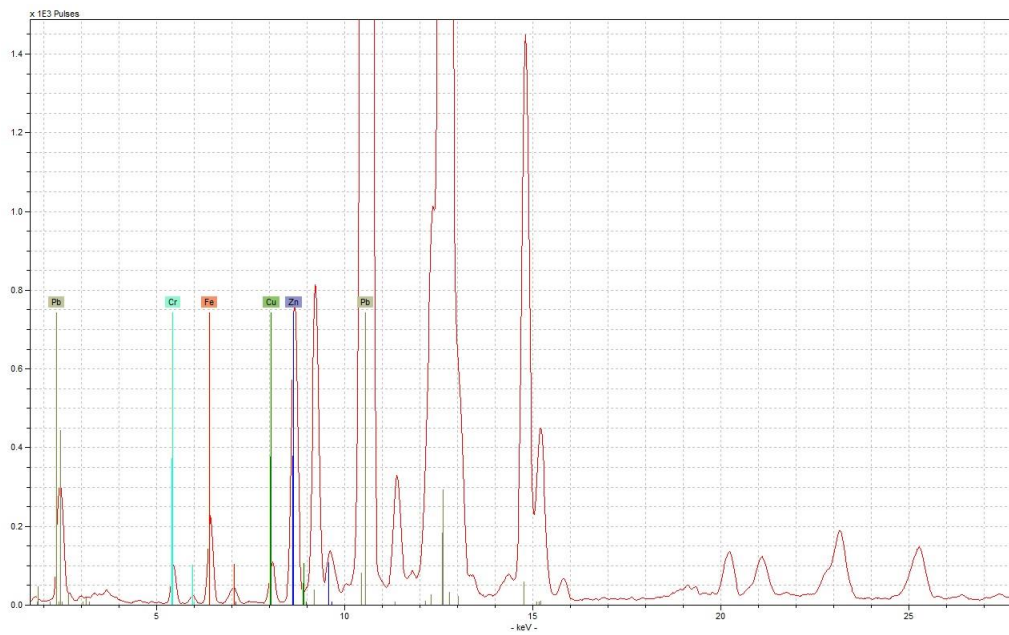
Appendix Figure 80 - example spectrum for yellow enamel type 3 from WWR5, obtained under low voltage condition (upper), and high voltage condition (lower)



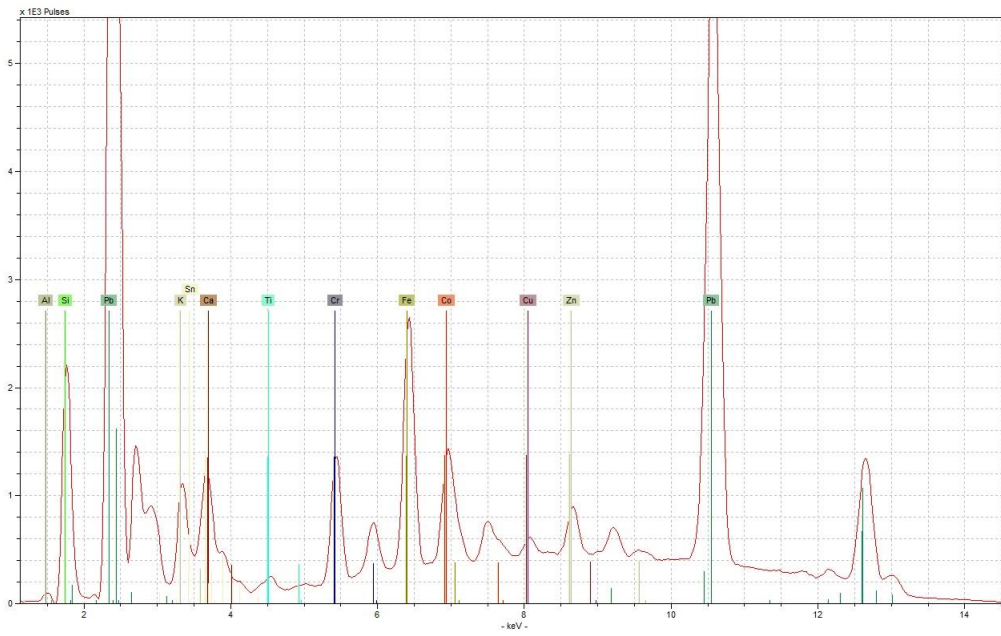
Appendix 7: Hand-Held XRF data



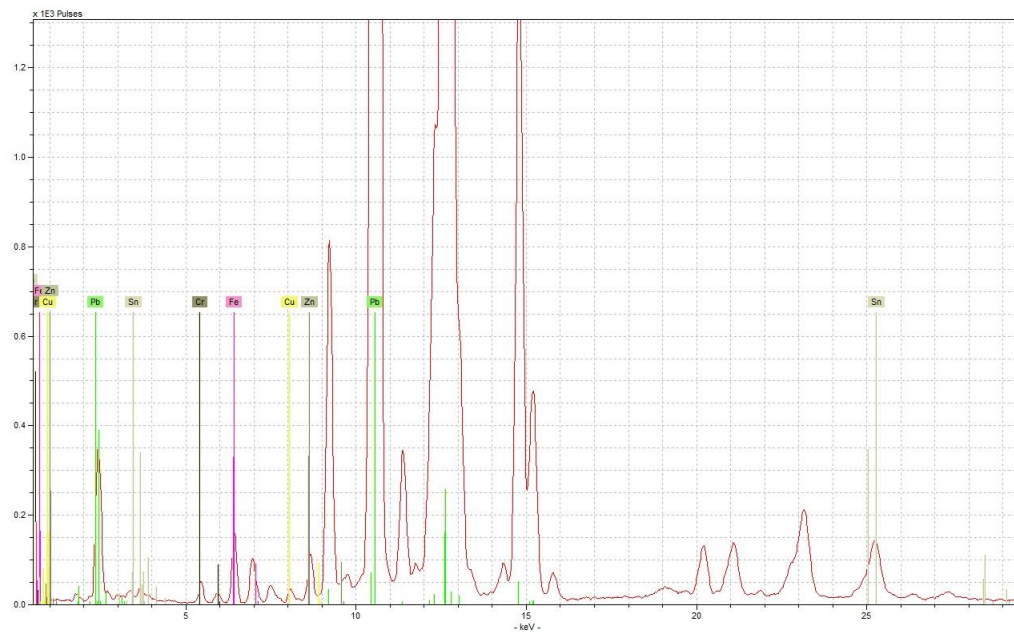
Appendix Figure 81 - example spectrum for yellow enamel type 4 from 696, obtained under low voltage condition (upper), and high voltage condition (lower)



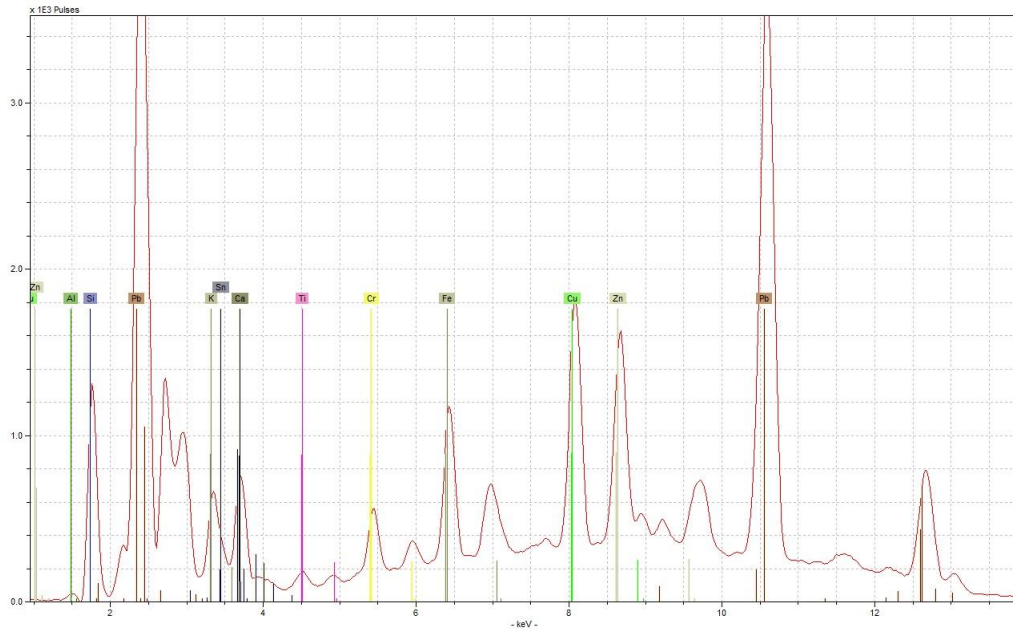
Appendix 7: Hand-Held XRF data



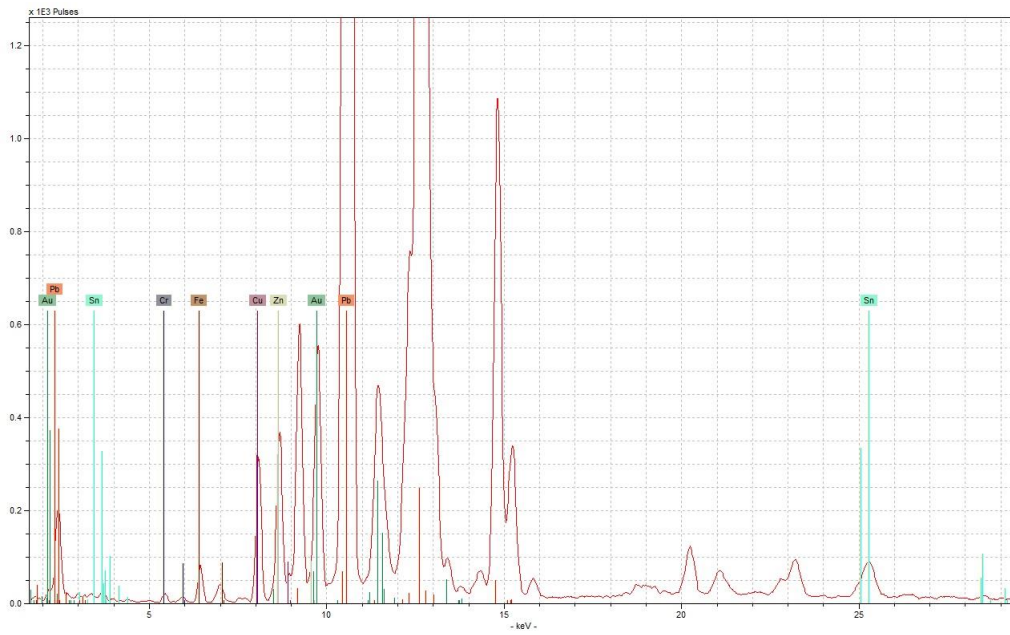
Appendix Figure 82 - example spectrum for yellow enamel type 5 from 292, obtained under low voltage condition (upper), and high voltage condition (lower)



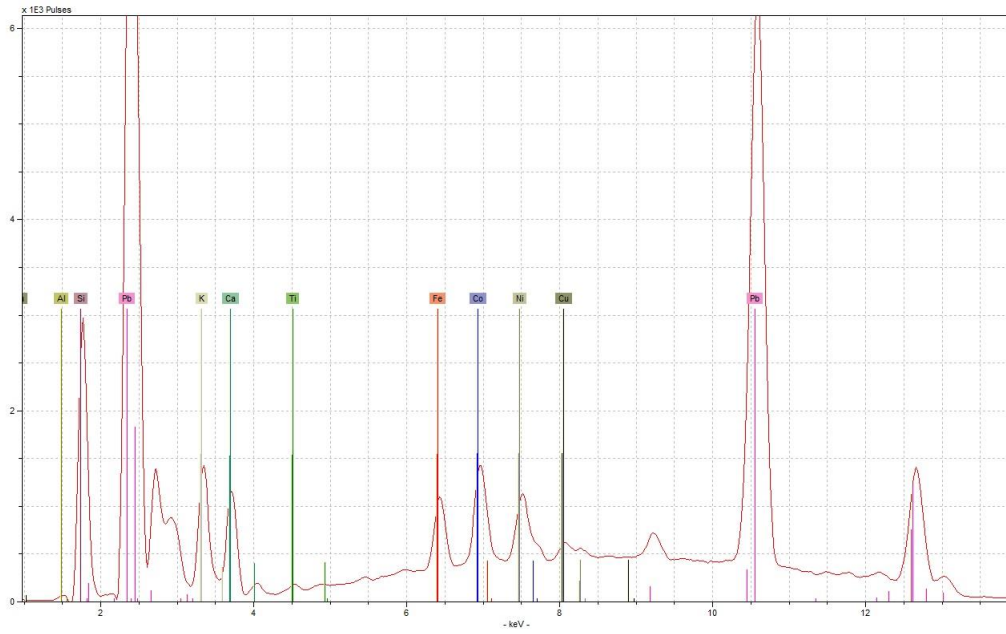
Appendix 7: Hand-Held XRF data



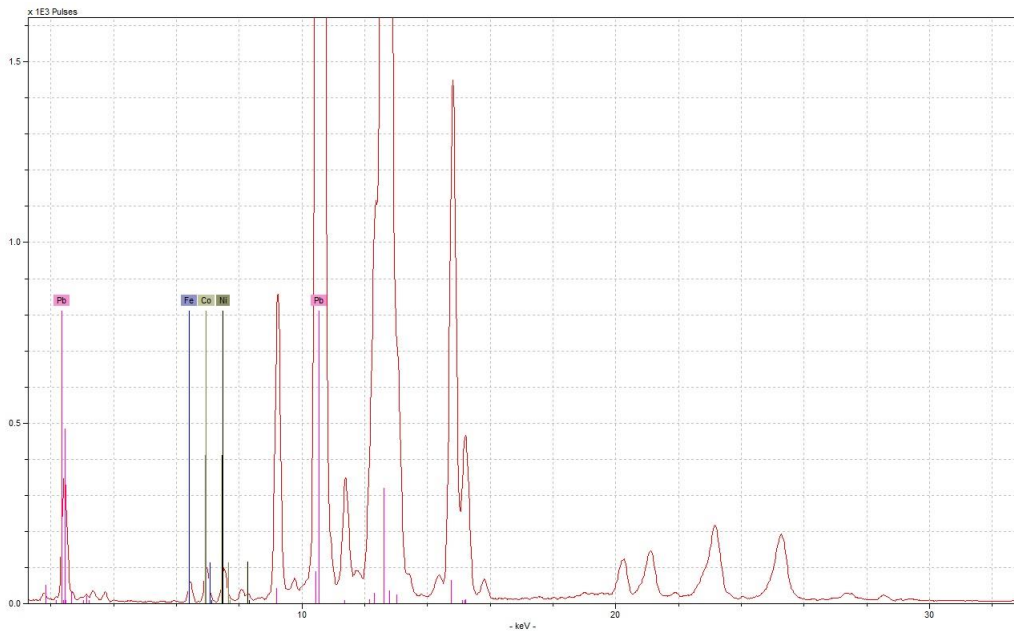
Appendix Figure 83 - example spectrum for yellow enamel type 6 from 705, obtained under low voltage condition (upper), and high voltage condition (lower)



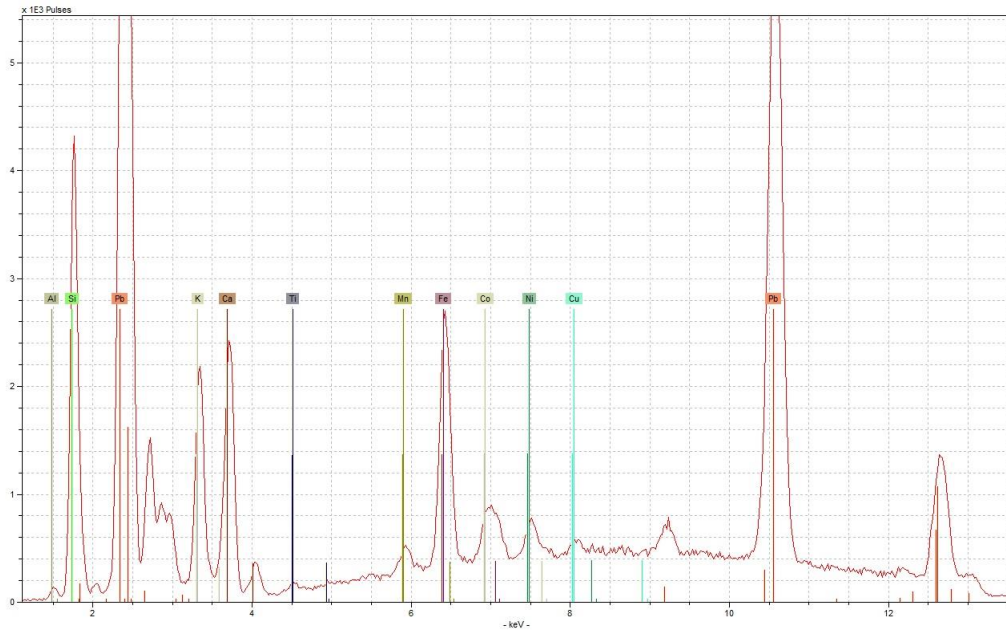
Appendix 7: Hand-Held XRF data



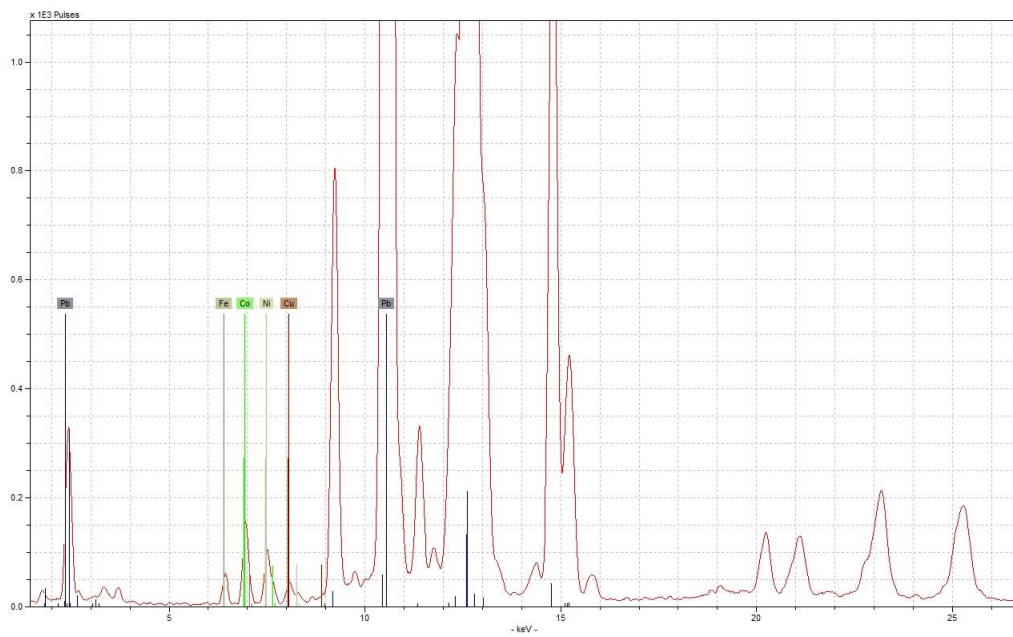
Appendix Figure 84 - example spectrum for underglaze blue type 1 from Bow pl3, obtained under low voltage condition (upper), and high voltage condition (lower)



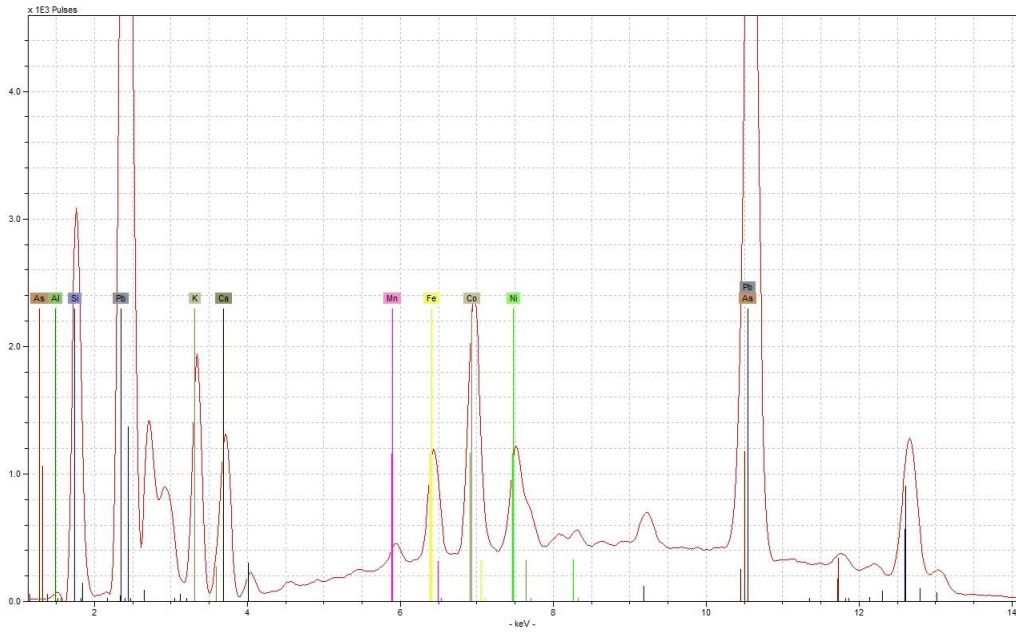
Appendix 7: Hand-Held XRF data



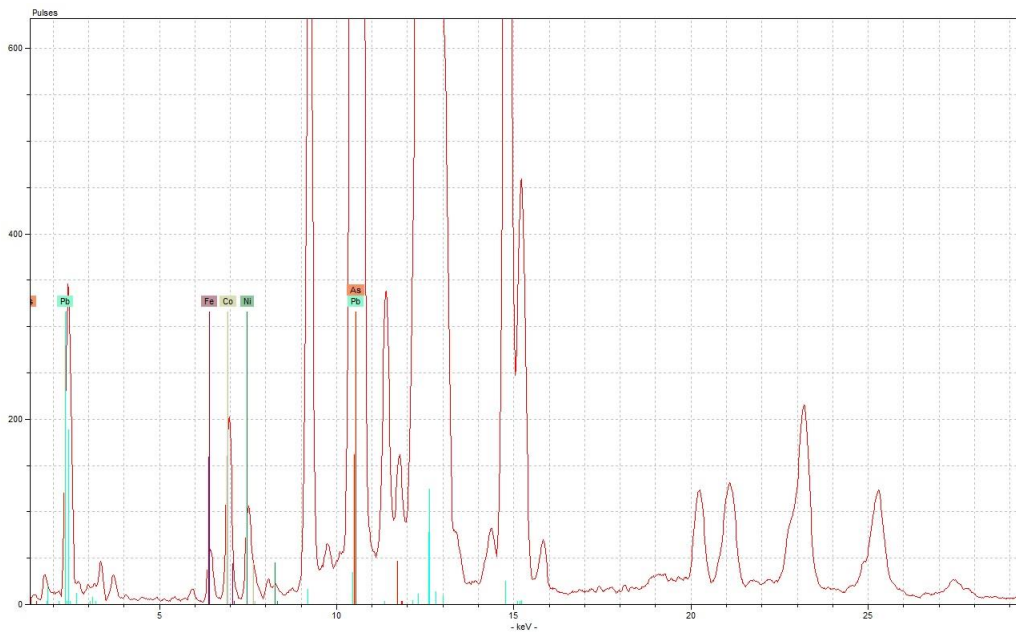
Appendix Figure 85 - example spectrum for underglaze blue type 2 from GAH sherd1, obtained under low voltage condition (upper), and high voltage condition (lower)



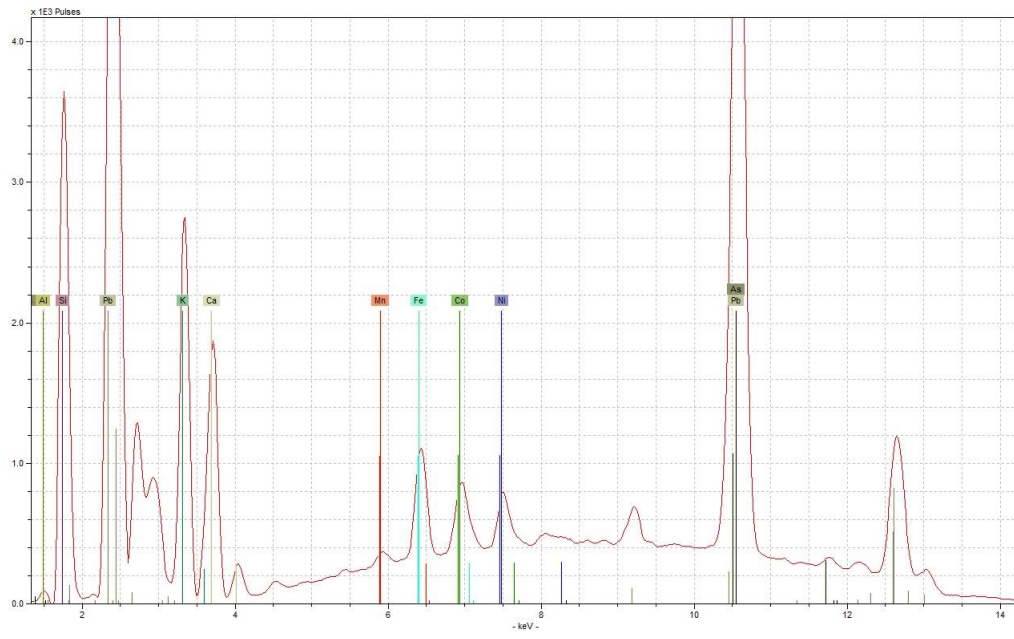
Appendix 7: Hand-Held XRF data



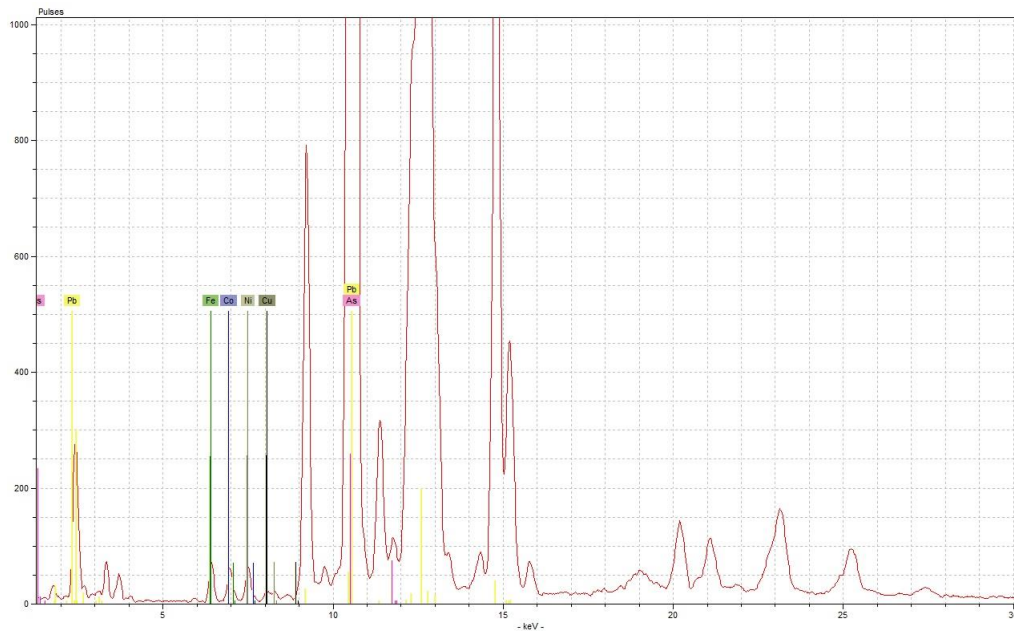
Appendix Figure 86 - example spectrum for underglaze blue type 3 from dby vase1, obtained under low voltage condition (upper), and high voltage condition (lower)



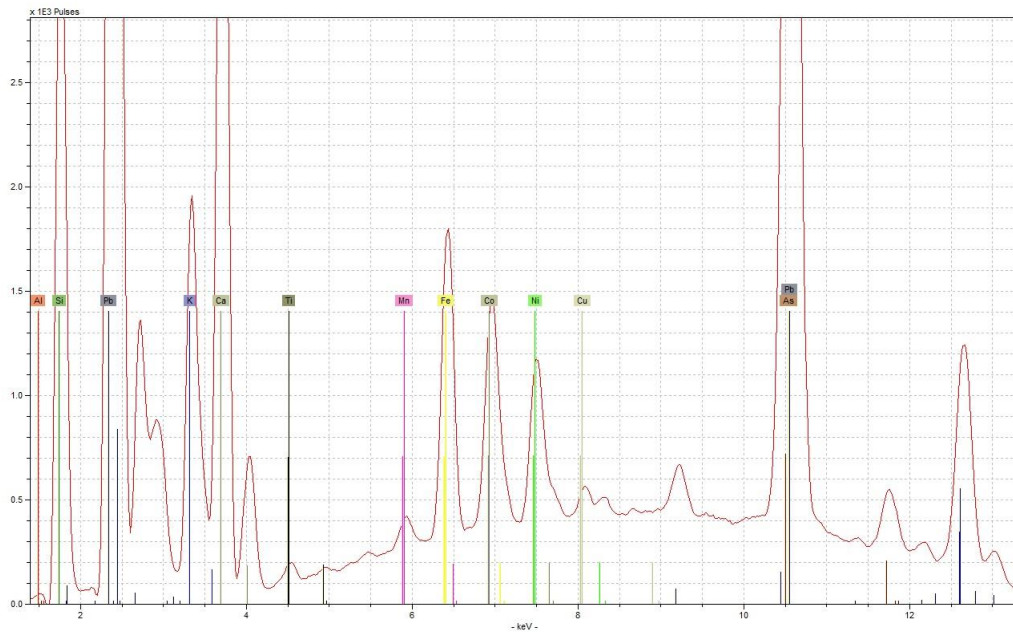
Appendix 7: Hand-Held XRF data



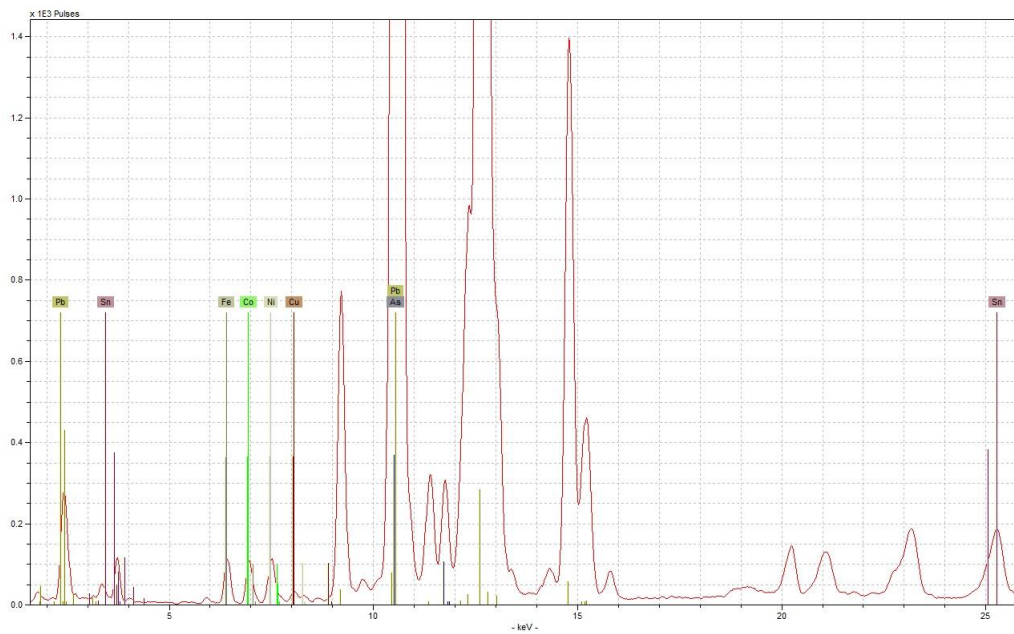
Appendix Figure 87 - example spectrum for underglaze blue type 4 from dby bskt, obtained under low voltage condition (upper), and high voltage condition (lower)



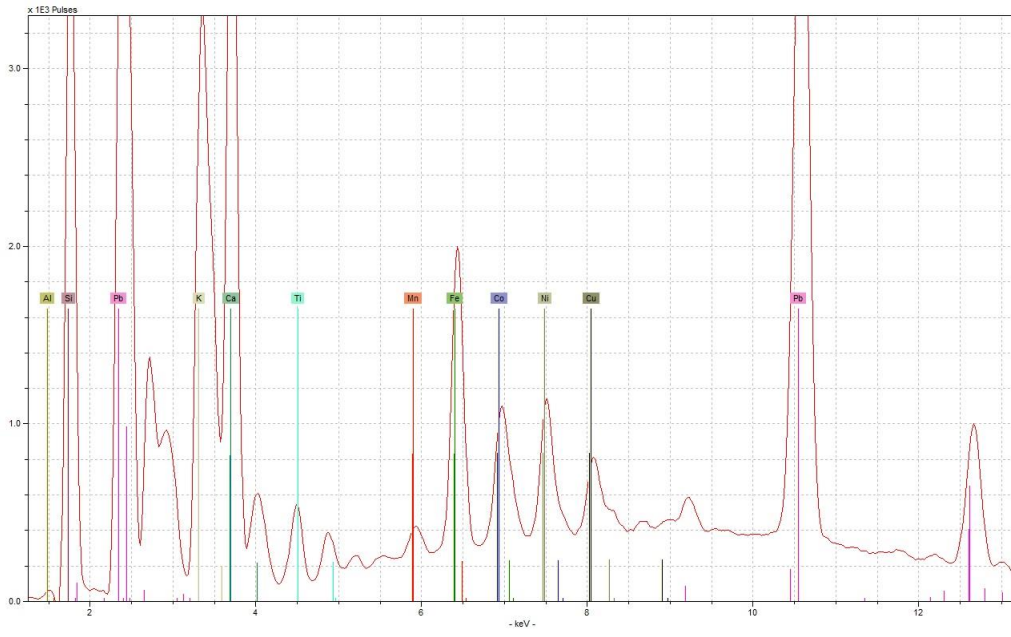
Appendix 7: Hand-Held XRF data



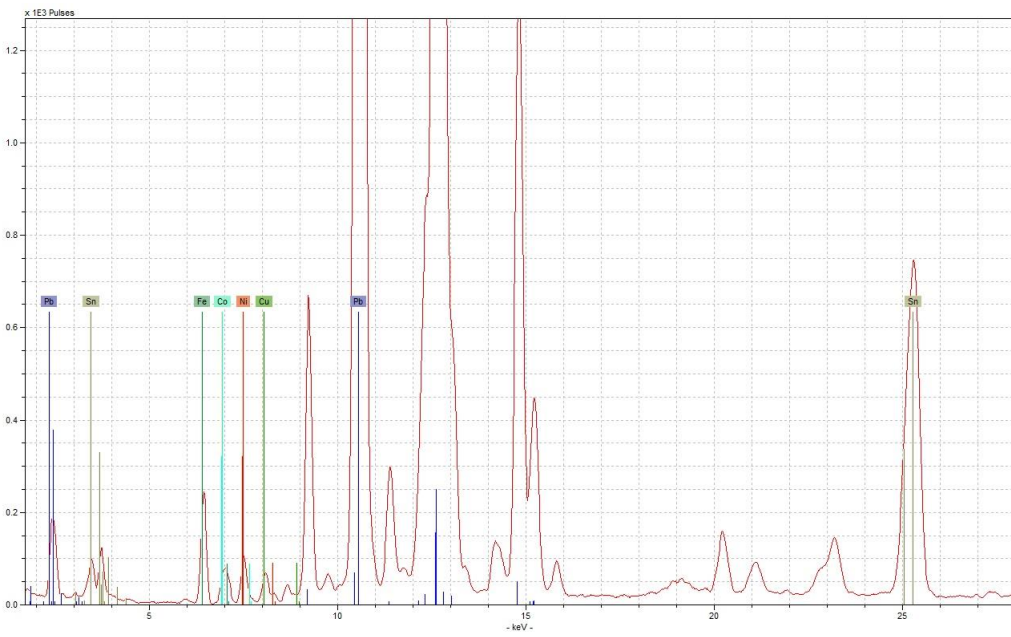
Appendix Figure 88 - example spectrum for underglaze blue type 5 from LH sb1, obtained under low voltage condition (upper), and high voltage condition (lower)



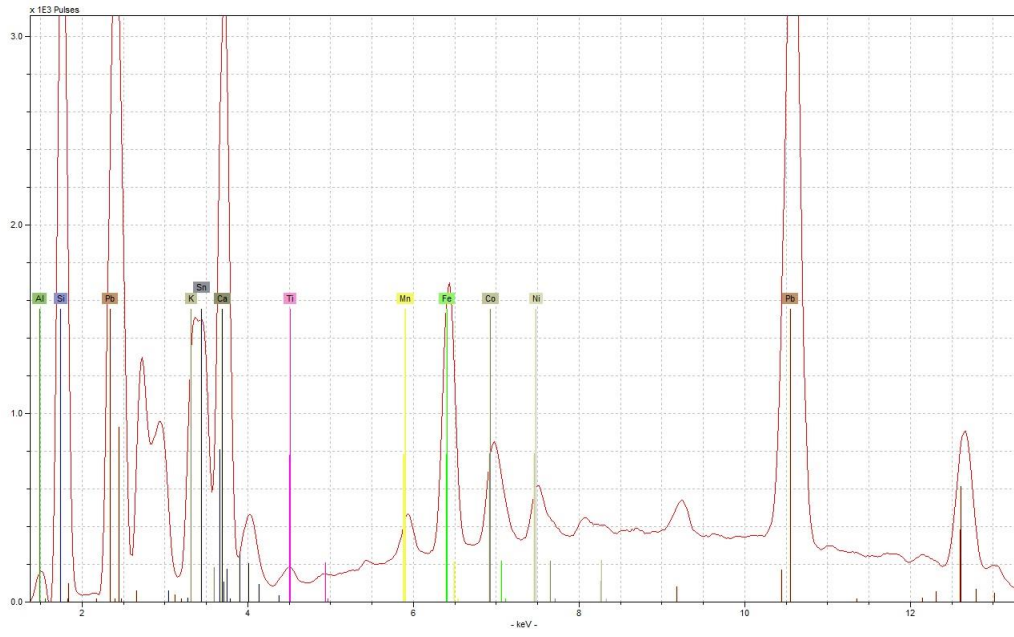
Appendix 7: Hand-Held XRF data



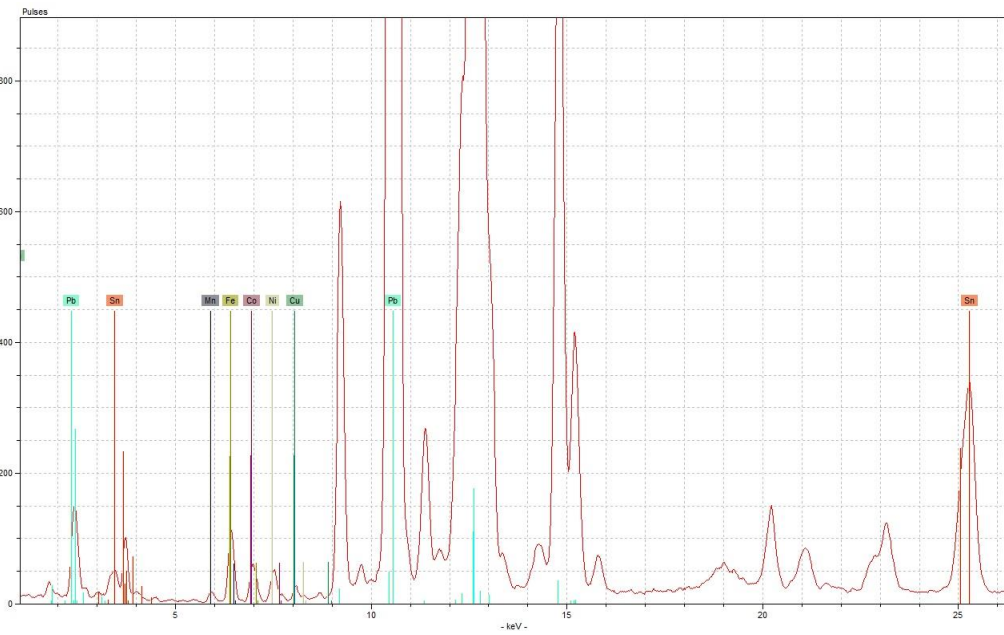
Appendix Figure 89 - example spectrum for underglaze blue type 6 from Vx sb1, obtained under low voltage condition (upper), and high voltage condition (lower)



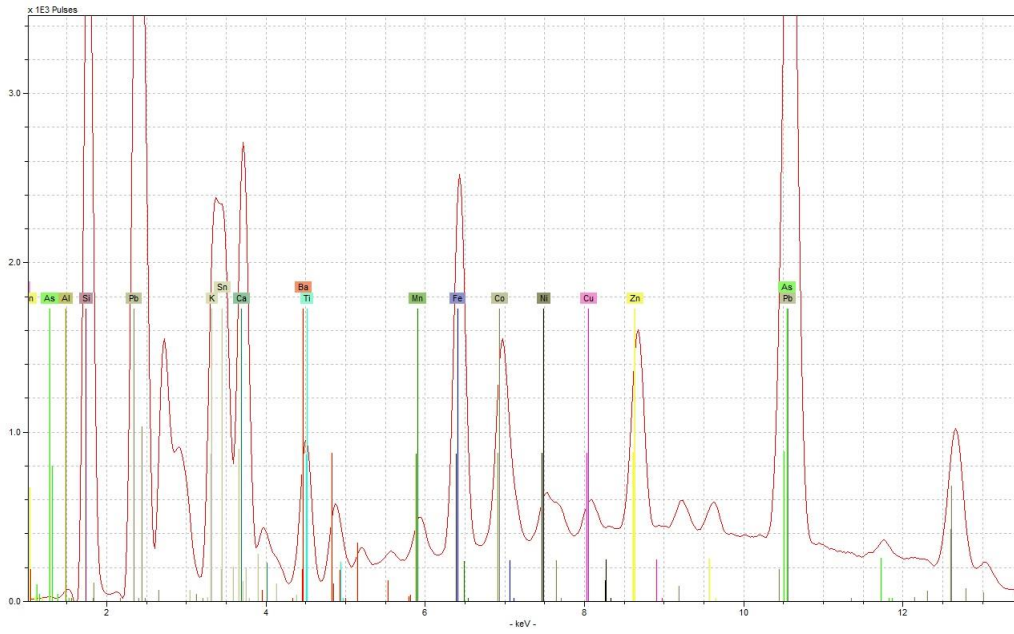
Appendix 7: Hand-Held XRF data



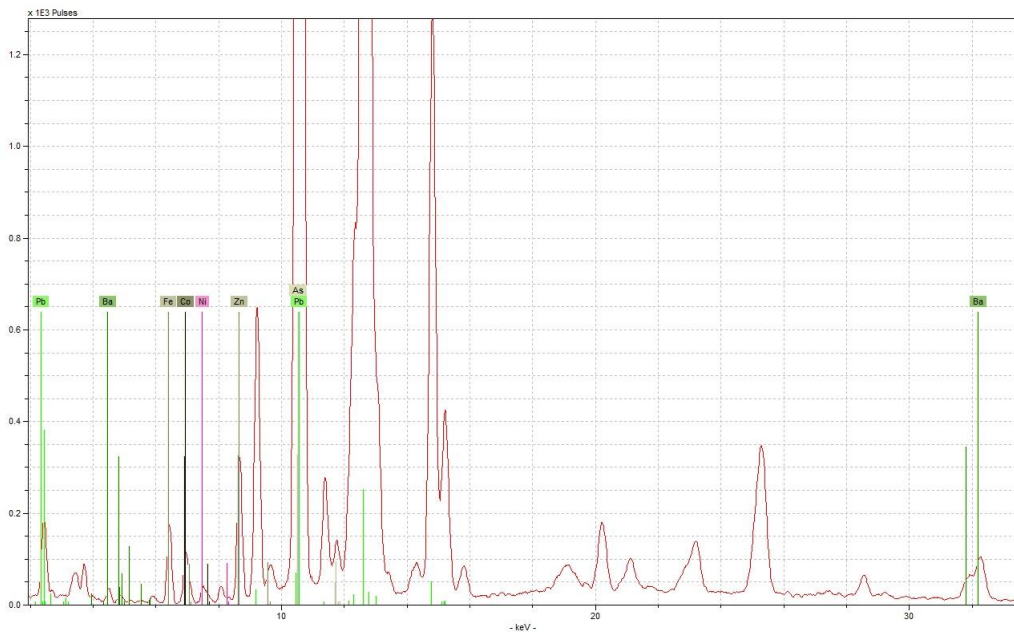
Appendix Figure 91 - example spectrum for underglaze blue type 8 from LLK sherd 4, obtained under low voltage condition (upper), and high voltage condition (lower)



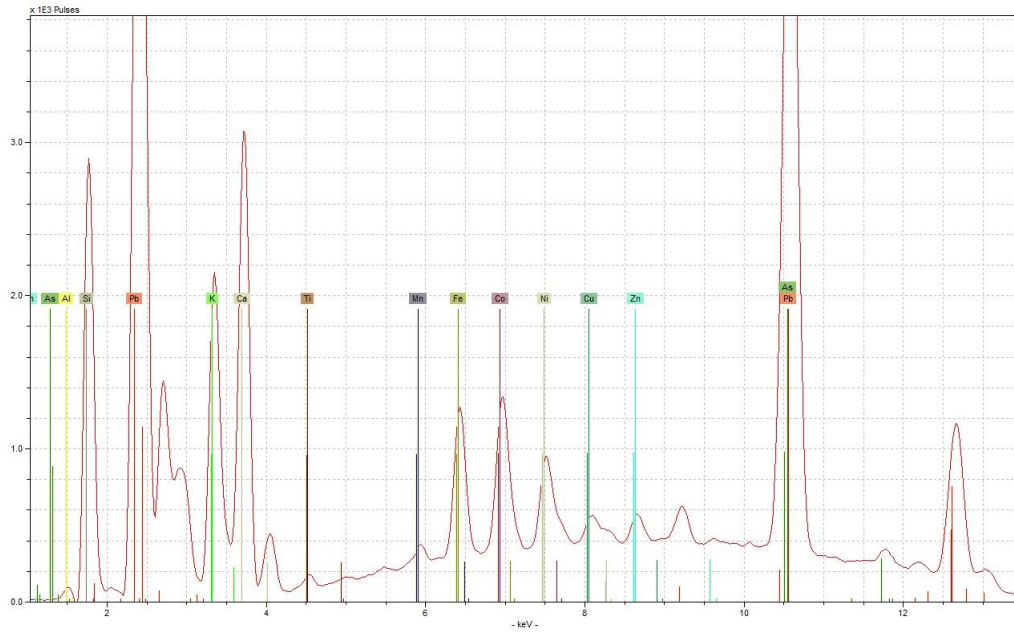
Appendix 7: Hand-Held XRF data



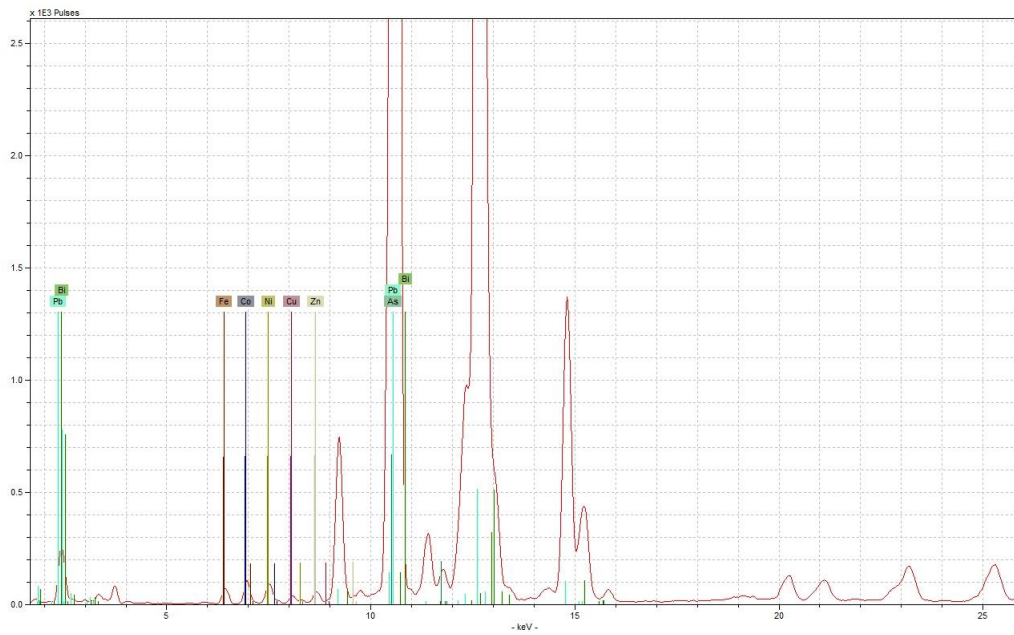
Appendix Figure 92 - example spectrum for underglaze blue type 9 from BTr sb1, obtained under low voltage condition (upper), and high voltage condition (lower)



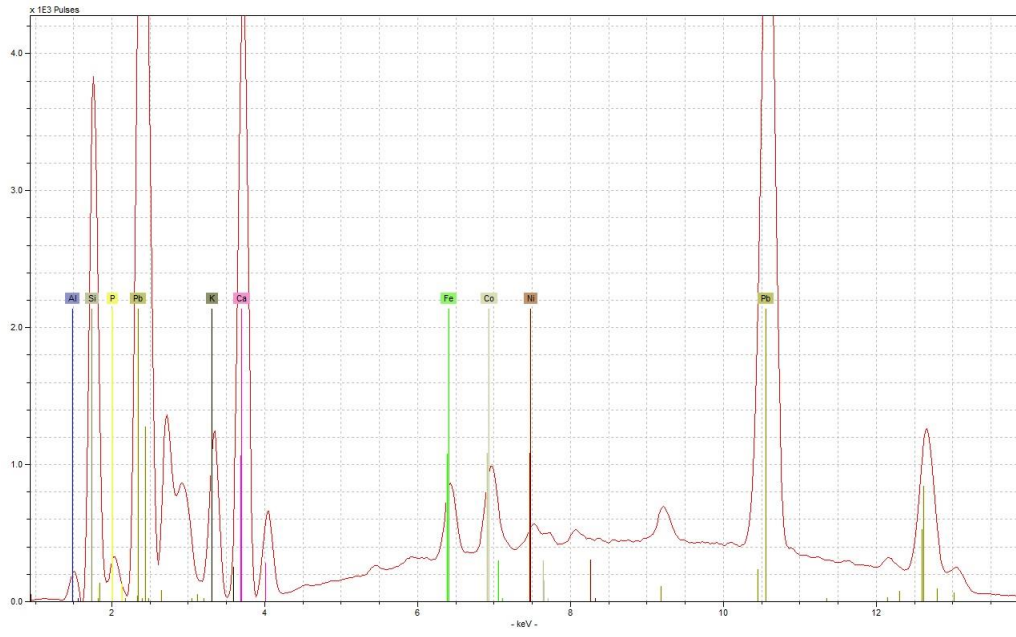
Appendix 7: Hand-Held XRF data



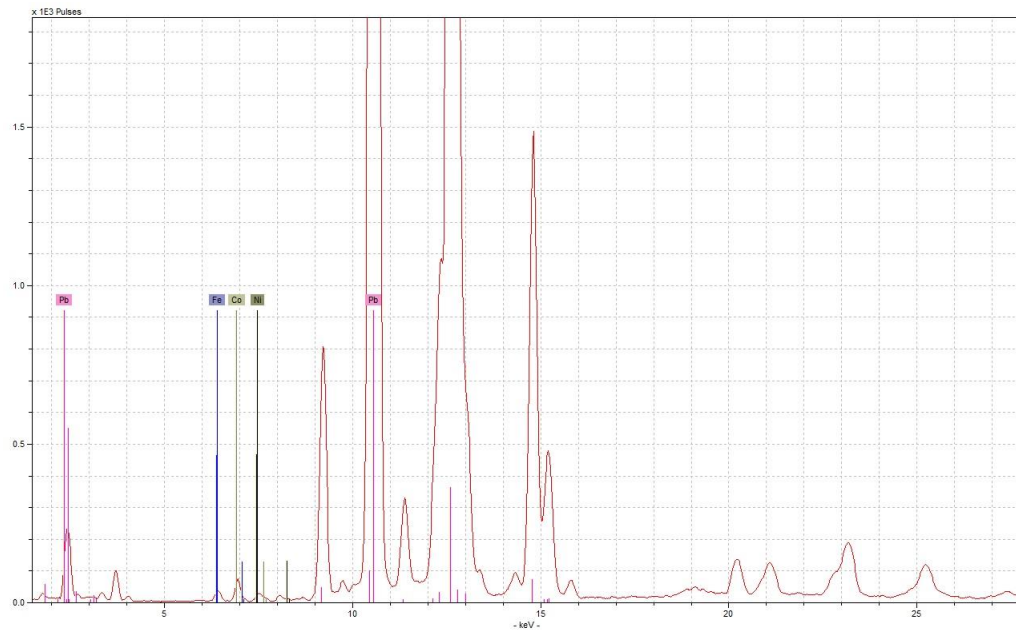
Appendix Figure 93 - example spectrum for underglaze blue type 10 from WP sherd 1, obtained under low voltage condition (upper), and high voltage condition (lower)



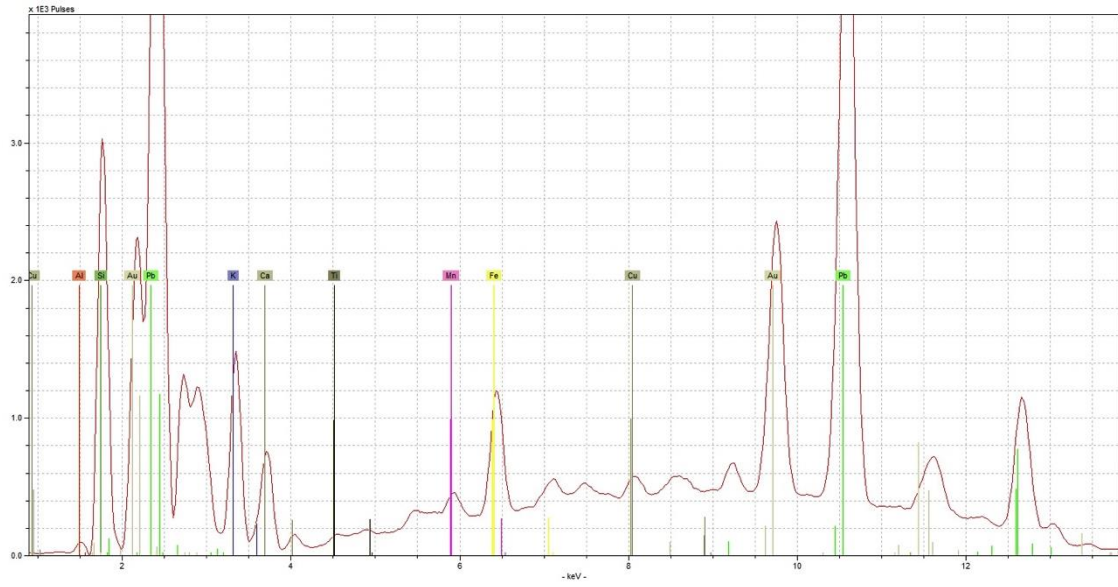
Appendix 7: Hand-Held XRF data



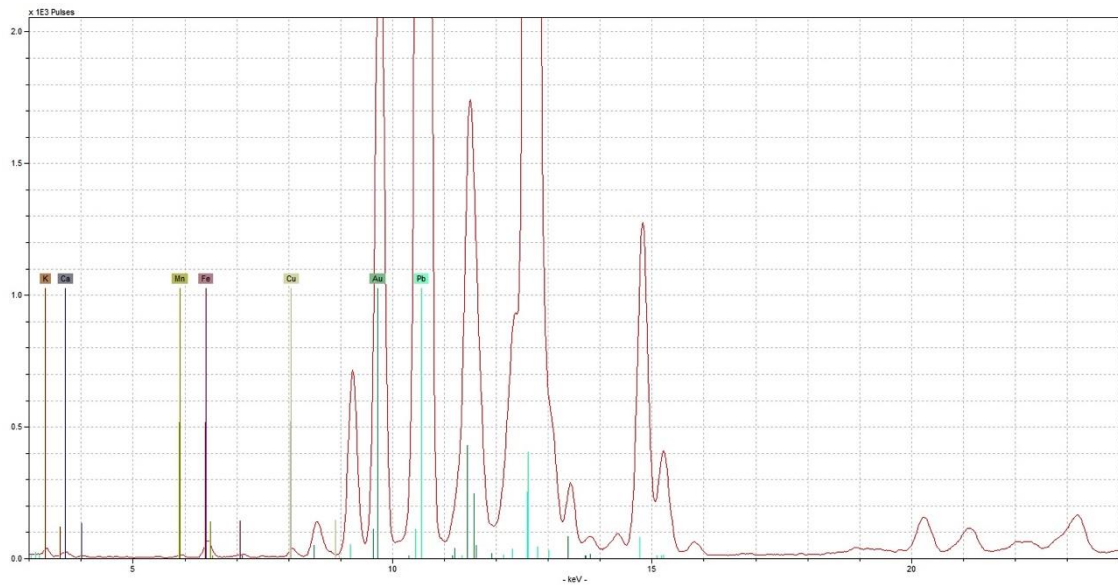
Appendix Figure 94 - example spectrum for underglaze blue type 11 from NH sc1, obtained under low voltage condition (upper), and high voltage condition (lower)



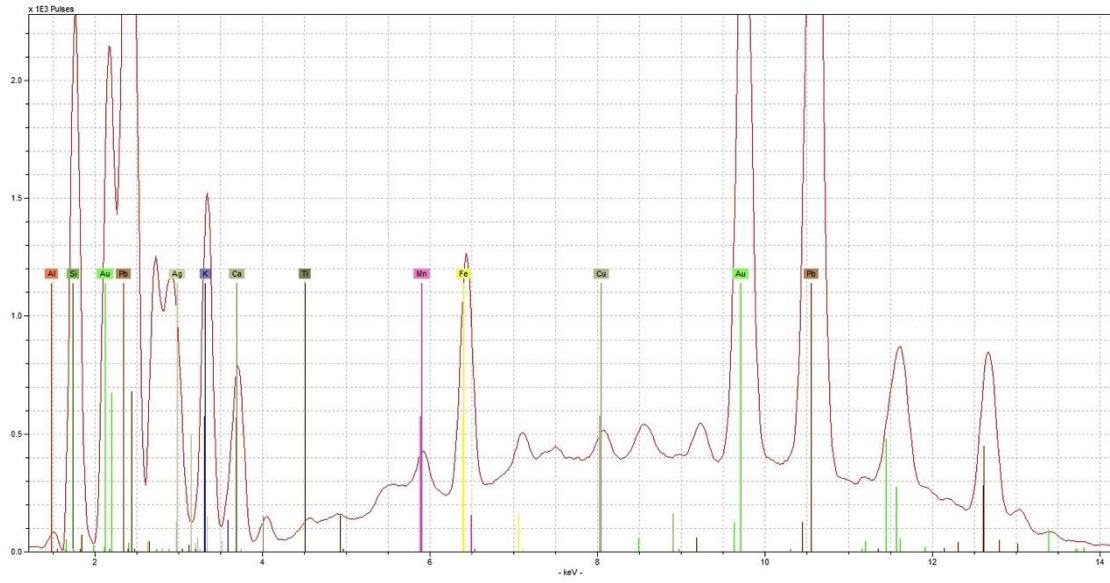
Appendix 7: Hand-Held XRF data



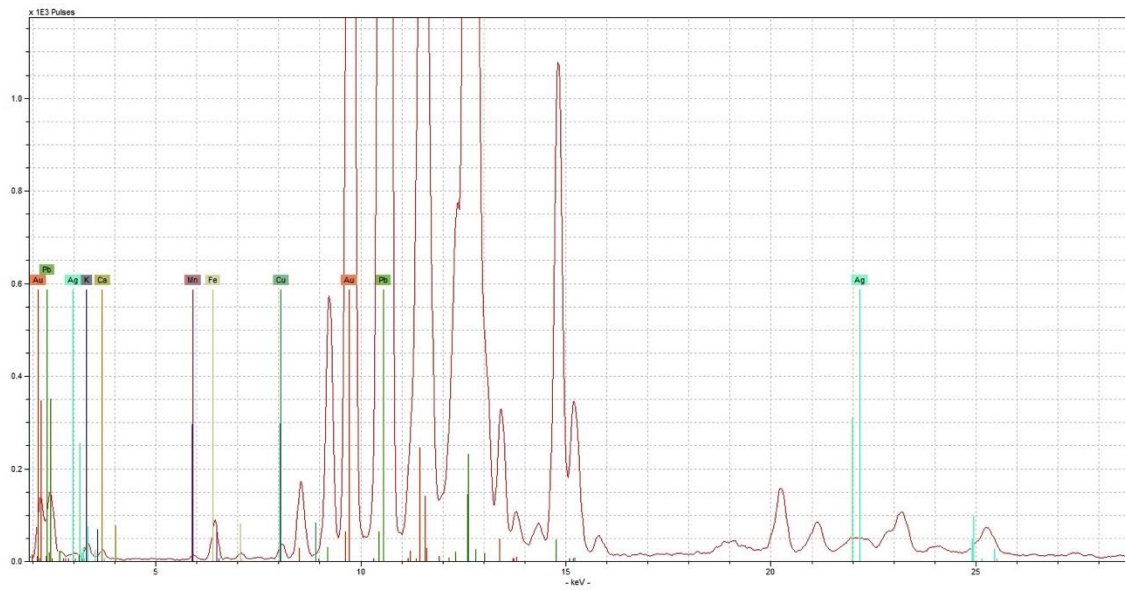
Appendix Figure 95 - example spectrum for gilding type 1 from object number 480, obtained under low voltage condition (upper), and high voltage condition (lower)



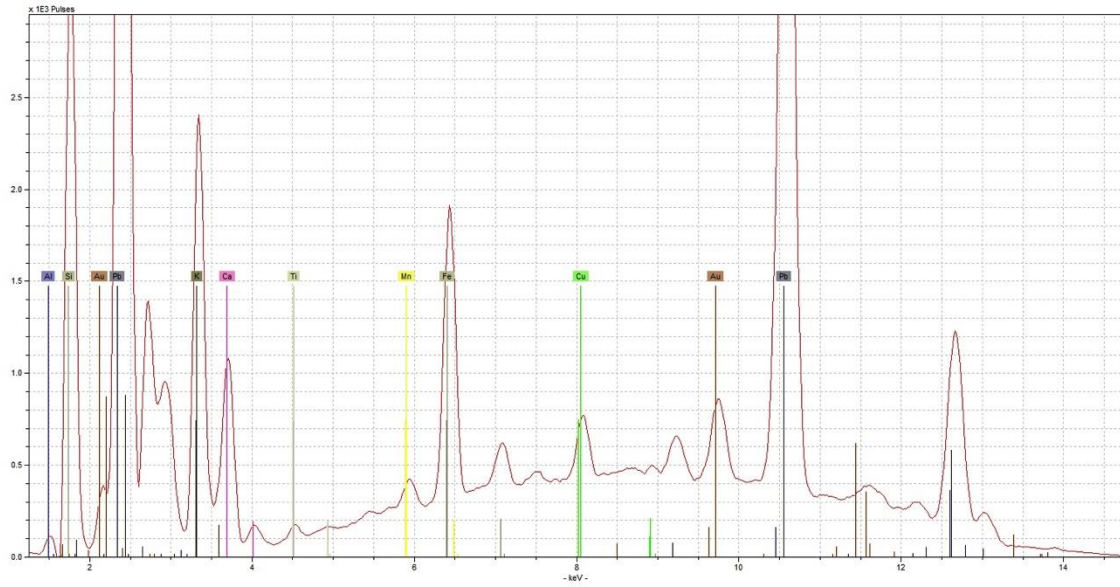
Appendix 7: Hand-Held XRF data



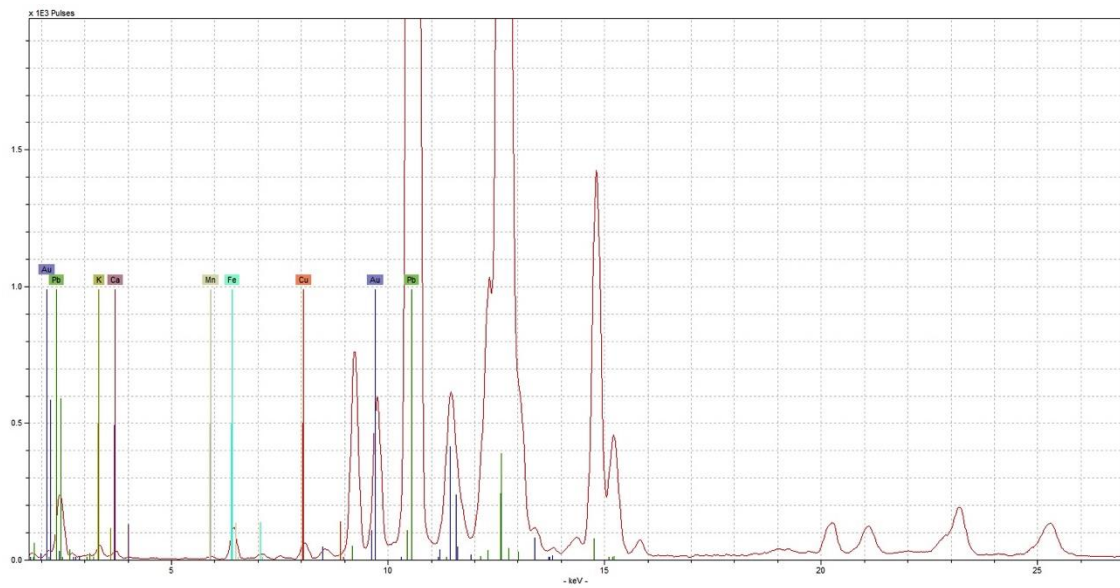
Appendix Figure 96 - example spectrum for gilding type 2 from object number 703, obtained under low voltage condition (upper) and high voltage condition (lower)



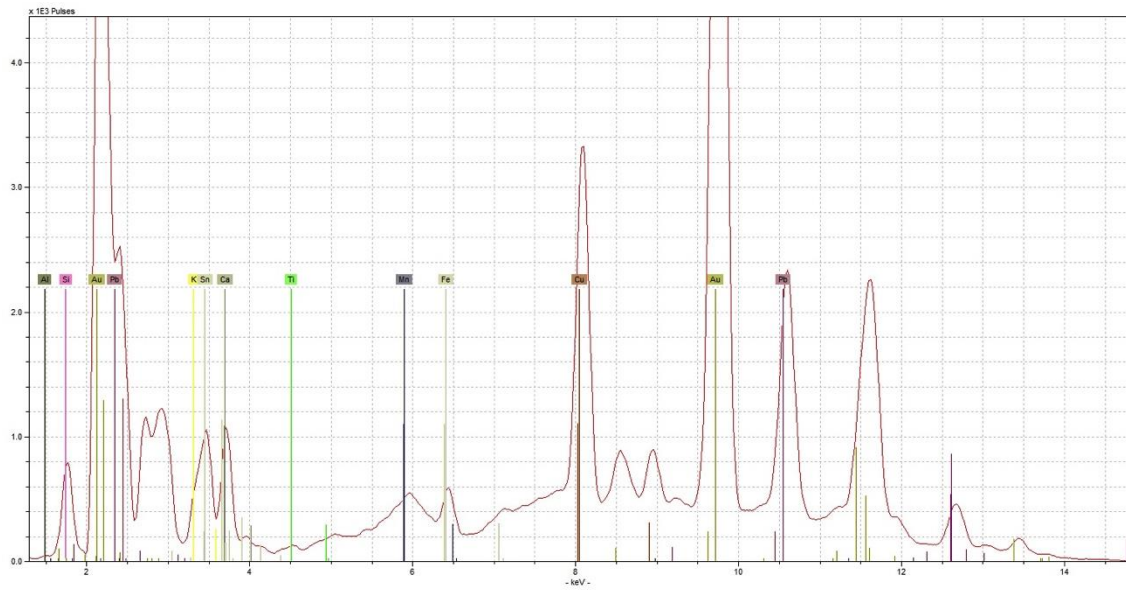
Appendix 7: Hand-Held XRF data



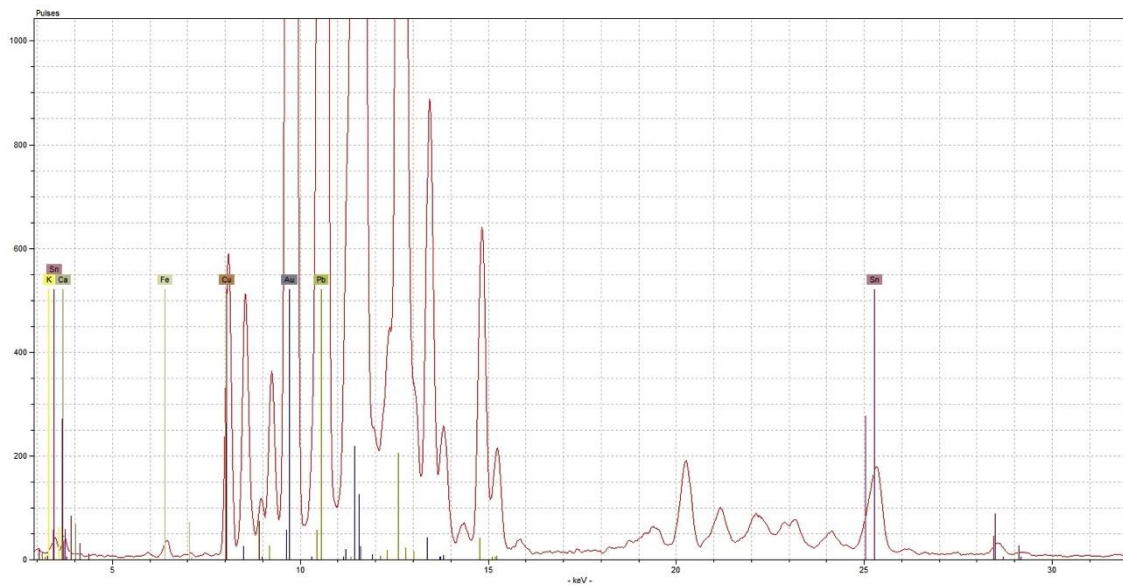
Appendix Figure 97 - example spectrum for gilding type 3 from object number 699, obtained under low voltage condition (upper), and high voltage condition (lower)



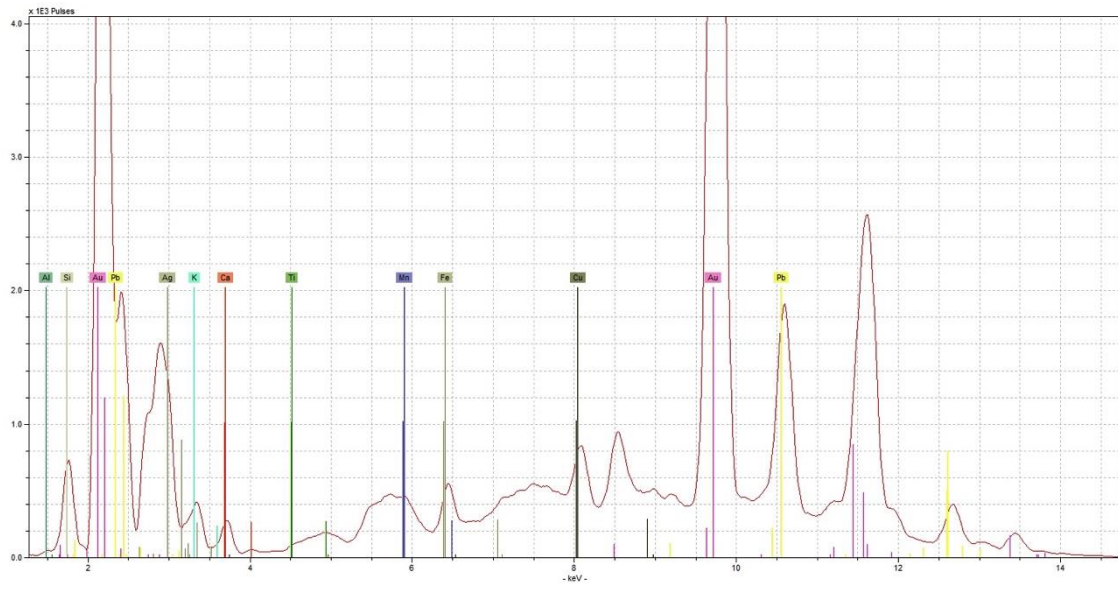
Appendix 7: Hand-Held XRF data



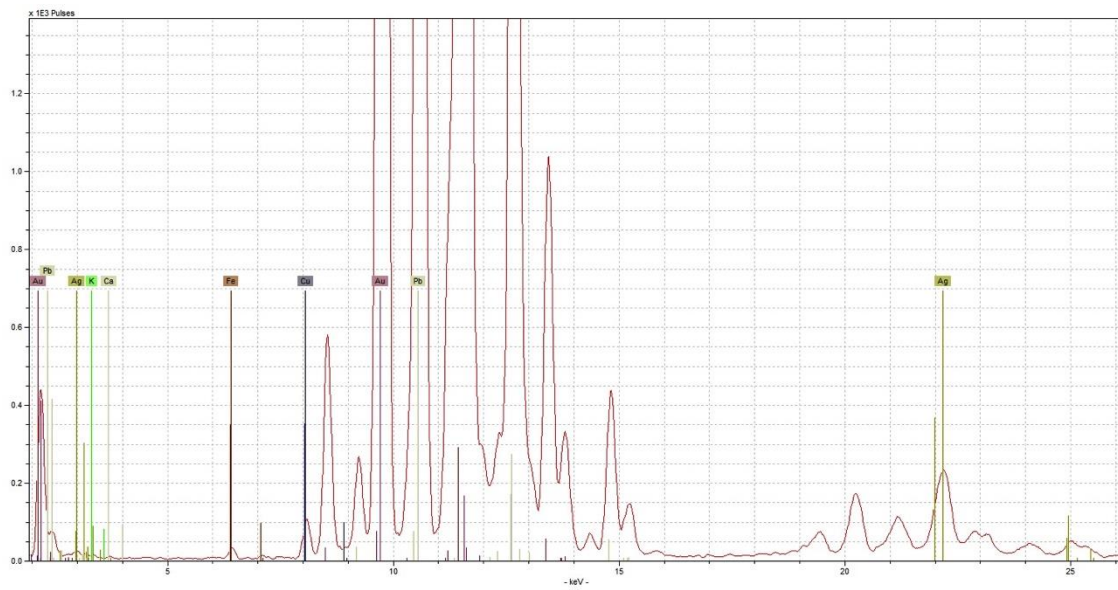
Appendix Figure 98 - example spectrum for gilding type 4 from object number 914, obtained under low voltage condition (upper), and high voltage condition (lower)



Appendix 7: Hand-Held XRF data



Appendix Figure 99 - example spectrum for gilding type 5 from object 804, obtained under low voltage condition (upper), and high voltage condition (lower)



A.8 Spectrophotometry data

Sample	Factory	Period	L*	a*	b*	
WA1967.28.151	Chelsea	1	88.10	-0.86	2.83	
		2	85.82	-0.92	2.86	
		3	85.40	-0.88	2.85	
		μ	μ	86.96	-0.89	2.85
		σ	σ	1.61	0.04	0.02
		$\% \sigma$	$\% \sigma$	1.85	-4.77	0.75
		WA1971.351	Chelsea	1	88.89	-0.50
		2	87.45	-0.60	5.16	
		3	87.65	-0.60	5.09	
μ		μ	88.17	-0.55	5.11	
σ		σ	1.02	0.07	0.07	
$\% \sigma$		$\% \sigma$	1.15	-12.86	1.38	
LI186.12	Chelsea	1	87.33	-0.51	3.43	
		2	85.90	-0.63	3.26	
		3	86.20	-0.58	3.33	
		μ	μ	86.62	-0.57	3.35
		σ	σ	1.01	0.08	0.12
		$\% \sigma$	$\% \sigma$	1.17	-14.89	3.59
		LI186.14	Chelsea	1	89.62	-0.91
2	87.88			-1.02	2.81	
3	88.92			-0.97	2.96	
μ	μ			88.75	-0.97	2.92
σ	σ			1.23	0.08	0.16
$\% \sigma$	$\% \sigma$			1.39	-8.06	5.33
LI1092.5	Bow			1	87.40	-0.91
		2	85.46	-0.60	6.70	
		3	85.44	-0.73	6.22	
		μ	μ	86.43	-0.76	6.30
		σ	σ	1.37	0.22	0.57
		$\% \sigma$	$\% \sigma$	1.59	-29.03	8.98
		LI1092.3	Bow	1	83.77	-1.04
2	82.65			-1.07	8.84	
3	83.01			-1.05	8.77	
μ	μ			83.21	-1.06	8.76
σ	σ			0.79	0.02	0.11
$\% \sigma$	$\% \sigma$			0.95	-2.01	1.29
LI1092.4	Bow			1	85.37	-0.82
		2	83.37	-0.88	10.45	
		3	84.12	-0.85	10.32	
		μ	μ	84.37	-0.85	10.29
		σ	σ	1.41	0.04	0.23
		$\% \sigma$	$\% \sigma$	1.68	-4.99	2.27

Appendix 8: Spectrophotometer data

Sample	Factory	Period	L*	a*	b*	
LI1092.1	Bow	1	85.92	-1.92	5.19	
		2	84.49	-1.97	5.30	
		3	85.58	-1.94	5.22	
		μ	μ	85.21	-1.95	5.25
		σ	σ	1.01	0.04	0.08
		$\% \sigma$	$\% \sigma$	1.19	-1.82	1.48
		<hr/>				
WA1971.375	Derby	1	85.68	-2.51	5.64	
		2	83.93	-2.67	5.58	
		3	84.72	-2.43	5.59	
		μ	μ	84.81	-2.59	5.61
		σ	σ	1.24	0.11	0.04
		$\% \sigma$	$\% \sigma$	1.46	-4.37	0.76
		<hr/>				
WA1957.24.1.58	Derby	1	87.36	-1.24	2.66	
		2	86.65	-1.27	2.69	
		3	86.99	-1.23	2.67	
		μ	μ	87.01	-1.26	2.68
		σ	σ	0.50	0.02	0.02
		$\% \sigma$	$\% \sigma$	0.58	-1.69	0.79
		<hr/>				
WA1957.24.1.59	Derby	1	88.26	-0.12	5.10	
		2	86.91	-0.08	5.37	
		3	87.01	-0.10	5.24	
		μ	μ	87.59	-0.10	5.24
		σ	σ	0.95	0.03	0.19
		$\% \sigma$	$\% \sigma$	1.09	-28.28	3.65
		<hr/>				
WA1957.24.1.704	Worcester	1	86.80	-1.20	6.64	
		2	84.17	-1.25	6.97	
		3	85.52	-1.23	6.49	
		μ	μ	85.49	-1.23	6.81
		σ	σ	1.86	0.04	0.23
		$\% \sigma$	$\% \sigma$	2.18	-2.89	3.43
		<hr/>				
WA1957.24.1.397	Worcester	1	61.98	4.28	1.02	
		2	59.14	4.55	0.74	
		3	60.62	4.34	0.92	
		μ	μ	60.56	4.42	0.88
		σ	σ	2.01	0.19	0.20
		$\% \sigma$	$\% \sigma$	3.32	4.32	22.50
		<hr/>				
WA1957.24.1.681	Worcester	1	84.21	-1.02	4.49	
		2	82.46	-1.10	4.58	
		3	83.04	-1.09	4.52	
		μ	μ	83.34	-1.06	4.54
		σ	σ	1.24	0.06	0.06
		$\% \sigma$	$\% \sigma$	1.48	-5.34	1.40

Appendix 8: Spectrophotometer data

Sample	Factory	Period	L*	a*	b*	
WA1957.24.1.706	Worcester	1	85.00	-1.57	7.53	
		2	82.11	-1.64	8.04	
		3	84.94	-1.61	8.10	
	μ		μ	83.56	-1.61	7.79
	σ		σ	2.04	0.05	0.36
	$\% \sigma$		$\% \sigma$	2.45	-3.08	4.63
	WA1957.24.1.599	Worcester (scratch- cross)	1	83.52	-1.17	4.27
2			81.17	-1.22	4.47	
3			82.29	-1.23	4.32	
μ			μ	82.35	-1.20	4.37
σ			σ	1.66	0.04	0.14
$\% \sigma$			$\% \sigma$	2.02	-2.96	3.24
1968.34		Worcester (scratch- cross)	1	85.42	-0.71	0.99
	2		83.54	-0.74	1.07	
	3		84.42	-0.72	1.01	
	μ		μ	84.48	-0.73	1.03
	σ		σ	1.33	0.02	0.06
	$\% \sigma$		$\% \sigma$	1.57	-2.93	5.49
	WA1957.24.1.773	Worcester (Dr Wall)	1	87.51	-2.05	4.99
2			86.34	-2.07	5.09	
3			88.01	-2.05	5.04	
μ			μ	86.93	-2.06	5.04
σ			σ	0.83	0.01	0.07
$\% \sigma$			$\% \sigma$	0.95	-0.69	1.40

A.9 Laser Ablation Inductively Coupled Plasma Mass Spectroscopy data

Appendix Table 24 - LA-ICPMS data (parts per million) for 53 British porcelain pastes, major and minor elements

Sample	Na	Mg	Al	Si	P	K	Ca	Fe	Pb
'A'-marked									
47122R	30935	8612	120088	287418	1458	27457	38128	2098	3767
Bow									
32703X	6173	3192	31606	221335	36359	7583	253194	938	18
29105Q	5736	4195	43807	194525	81024	9810	196136	3941	596
29100P	2738	2331	29878	231252	72493	6089	183892	2996	299
29104S	4005	2173	31949	224737	72487	5444	191706	2462	254
Caughley									
1069 E39	5283	51902	29769	342773	316	34442	7459	10662	42681
Chaffers									
32704V	12739	52963	23454	367269	36	21964	17438	1548	1130
Chelsea									
32699W	3306	1519	24749	333860	469	20255	96915	2878	50303
29103U	4307	1683	21877	316714	730	34305	142875	1984	19409
29106Z	4439	3099	51520	194670	93048	2363	177594	1615	287
66983 Y1	4260	1602	33481	321003	412	23195	120217	1421	34208
1055 E6	2529	1498	21671	325339	256	18523	157263	1002	6910
Coalport									
1072 E44	10228	3202	62383	171835	111341	12283	157953	1817	37
Crown Derby									
1057 E18	4614	3986	49861	177327	99109	6333	188555	5294	399
1056 E17	4896	4014	47916	177215	106451	6968	178029	5000	1652
Limehouse									
40419P	18808	4900	63980	346251	2416	15919	39727	2887	7560
Limehouse (continued)									
40150S	3138	1194	89938	372191	11	6516	2828	3865	55
40012W	19607	5359	68940	341120	1827	15715	39903	3342	11538
40011Y	17470	4744	59569	349400	2038	15749	44178	2756	9240
40010P	18511	5963	60258	349829	2543	13610	37085	3909	11753
40009X	3749	1035	101235	361433	114	8357	3905	1670	248
40008Z	19289	3730	52992	354344	523	20299	46710	1259	6127
40007Q	17790	5499	69454	341531	3441	10433	46143	3309	6439
40006S	20234	5757	67045	347099	2843	12472	37744	3549	5013
40000S	18144	5279	54983	347247	570	16502	32808	3588	34685
40004W	18379	5468	63171	334266	643	15533	47441	2985	27182
40003Y	16166	4675	60514	334415	580	16468	31778	3017	56504
40002P	17958	5149	57681	343938	424	15813	33348	3579	36642

Appendix 9: LA-ICPMS data

Appendix Table 24 - LA-ICPMS data (parts per million) for 53 British porcelain pastes, major and minor elements (continued)

Sample	Na	Mg	Al	Si	P	K	Ca	Fe	Pb
Liverpool (Ball)									
32705T	5803	59752	15205	315920	0	77857	53968	2127	1660
32706R	15990	46981	20406	361703	4984	9567	33650	1146	9210
Longton Hall									
29101Y	4401	1457	14396	350648	187	37756	62454	1125	56985
29098V	11745	1947	13746	358631	0	58572	34831	833	51152
Lowestoft									
32707P	3304	2089	32727	244704	53453	1586	197024	416	375
Nantgarw									
1059 E22	7588	2217	65494	141303	125399	15341	179536	1045	63
New Hall									
1054 E4	7839	902	102656	344443	293	8123	29914	1398	713
1053 E3	13728	913	132055	327044	860	13845	5064	1188	1119
Pinxton									
1058 E19	3748	3793	46594	161117	129962	6620	172750	2691	196
Plymouth									
32701Q	4044	1591	116727	346224	861	13153	1661	5351	26
Pomona									
32702Z	5191	60388	15930	345928	755	16622	10047	3036	71969
Swansea									
36554Q	3510	1310	100979	361898	0	6716	2115	4415	42
1060 E23	9270	2147	107606	192892	80854	19666	110249	1912	104
1070 E40	8491	15864	38231	399836	554	19547	3267	1017	1347
Worcester									
32700S	6024	52803	17452	345439	242	26460	11938	826	70904
29099T	5350	69078	22195	339208	1238	27694	11104	4186	41729
29263P	5288	65235	17502	330236	665	32279	7761	5879	74587
1065 E34	7995	73134	16538	323436	1480	31167	12006	5688	64355
1064 E32	8078	66956	15078	316278	1458	35300	16353	4155	86756
1063 E31	6436	71294	17819	322214	920	33710	6783	3853	82045
1062 E27	4044	67184	14800	356478	824	19248	8733	3632	41628
1068 E37	6054	34392	32901	362742	289	16012	10909	865	52926
1067 E36	5178	52195	16154	355915	651	10424	11557	1646	67507
1066 E35	3513	50558	14962	351690	188	12720	14373	1728	78698

Appendix 9: LA-ICPMS data

Appendix Table 25 - LA-ICPMS data (parts per million) for 53 British porcelain pastes, trace elements minus REEs (see Appendix Table 26)

Sample	Li	B	Ti	V	Cr	Mn	Co	Ni	Cu	Zn	As	Rb	Sr	Y	Zr	Nb	Mo	Ag	Sn	Sb	Cs	Ba	Hf	Bi	Th	U	
'A'-marked																											
47122R	94	39	325	6	1	364	45	41	51	66	148	29	364	4	29	2	2	2	1880	13	1	257	1	8	1	1	
Bow																											
32703X	28	18	1387	34	20	20	269	79	69	51	890	41	146	6	32	6	3	0	7	1	13	196	1	81	3	3	
29105Q	31	30	2393	42	29	25	415	130	23	60	1091	50	178	8	48	12	2	0	10	2	18	843	1	102	4	2	
29100P	20	26	1303	28	22	26	199	81	17	69	803	32	267	24	675	6	2	2	11	1	11	381	16	33	4	2	
29104S	26	13	1502	29	20	19	167	52	15	57	841	29	257	6	32	6	1	0	14	0	10	305	1	47	3	2	
Caughley																											
1069 E39	49	82	397	7	13	274	74	82	48	128	107	365	178	4	17	16	1	2	20	20	4	55	1	7	2	5	
Chaffers																											
32704V	73	13	341	8	13	669	237	297	1049	561	474	16	123	5	26	3	0	1	3994	7	2	88	1	144	2	2	
Chelsea																											
32699W	12	72	1849	23	14	539	17	17	42	55	342	54	278	6	54	5	1	2	5606	64	3	134	1	18	3	1	
29103U	1	27	1754	29	8	573	12	9	10	33	654	42	366	8	66	7	0	1	40	171	3	128	2	1	3	1	
29106Z	27	26	2982	52	39	21	250	72	27	77	856	27	142	10	75	10	2	1	6	6	5	183	2	105	7	2	
66983 Y1	29	80	940	29	0	490	1	220	58	30	1206	87	256	7	46	5	9	2	116	95	11	169	1	1	3	1	
1055 E6	22	51	753	25	17	600	3	133	41	23	214	36	367	6	49	4	9	1	59	1377	3	95	2	0	3	1	
Coalport																											
1072 E44	48	35	322	6	6	31	1	2	15	103	4	188	167	3	13	14	0	3	9	0	9	154	1	4	3	3	
Crown Derby																											
1057	26	17	2326	53	42	27	141	82	37	116	850	22	152	35	324	9	2	0	8	2	5	194	6	45	6	3	
1056	40	15	2518	51	42	23	135	133	94	110	543	28	147	11	72	9	1	1	14	3	7	201	2	68	6	2	
Limehouse																											
40419P	39	35	4407	71	47	301	333	55	43	43	1061	45	320	14	115	16	1	3	75	9	6	999	3	4	9	2	
40150S	5	25	5209	69	67	14	3	25	3	31	12	43	78	17	154	18	0	0	8	2	9	231	4	0	9	2	
40012W	41	33	3046	69	51	222	219	80	36	35	831	38	256	11	85	11	2	2	44	8	6	200	2	73	7	5	

Appendix 9: LA-ICPMS data

Appendix Table 25 - LA-ICPMS data (parts per million) for 53 British porcelain pastes, trace elements minus REEs (see Appendix Table 26) (continued)

Sample	Li	B	Ti	V	Cr	Mn	Co	Ni	Cu	Zn	As	Rb	Sr	Y	Zr	Nb	Mo	Ag	Sn	Sb	Cs	Ba	Hf	Bi	Th	U	
Limehouse (continued)																											
40011Y	30	35	2879	70	42	186	245	53	66	45	897	40	314	11	118	10	2	2	189	17	6	853	3	2	6	2	
40010P	51	62	3869	60	50	203	236	60	37	39	680	66	285	13	89	11	1	2	54	21	5	870	3	31	8	3	
40009X	17	29	5163	99	78	24	4	20	4	30	16	60	85	15	106	26	0	0	43	2	10	229	2	0	9	2	
40008Z	46	43	3092	58	41	163	254	58	37	39	1339	58	304	22	192	13	1	1	68	8	6	936	4	16	6	2	
40007Q	51	73	3224	59	44	229	112	33	57	31	300	43	288	77	98	10	3	2	0	12	5	351	3	48	9	3	
40006S	45	75	3183	62	41	231	226	98	40	30	890	38	253	10	83	10	6	2	56	63	4	217	2	114	8	8	
40000S	40	78	3834	56	36	160	279	59	37	36	652	56	304	13	98	13	1	1	4	10	6	941	3	12	8	2	
40004W	36	89	4209	64	41	225	305	50	35	35	899	41	311	20	111	13	2	1	0	9	5	929	3	7	9	2	
40003Y	32	89	3388	62	46	128	284	45	25	30	855	44	323	10	89	11	1	2	4	11	5	919	2	1	8	2	
40002P	41	102	4326	62	48	127	214	41	7	38	688	56	293	13	93	14	2	1	85	0	6	834	3	15	8	2	
Liverpool (Ball)																											
32705T	394	0	2628	2	808	1326	97	5	101	1005	1093	298	145	3	17	11	130	20	173	1151	0	89	17	78	0	1	
32706R	116	157	381	14	5	393	228	247	282	577	1101	31	957	3	23	3	2	2	11	19	1	86	1	111	2	6	
Longton Hall																											
29101Y	21	21	811	18	8	423	9	7	184	53	939	78	158	6	37	3	1	3	10823	112	6	115	1	6	2	1	
29098V	32	23	563	14	54	290	7	0	635	0	181	63	153	0	19	4	21	24	6980	158	6	87	0	20	1	0	
Lowestoft																											
32707P	19	39	1448	30	16	29	200	87	5	67	865	40	301	9	90	6	2	0	10	7	12	534	2	39	4	2	
Nantgarw																											
1059	84	33	167	2	7	24	1	1	19	46	9	134	178	2	13	10	0	2	9	2	4	116	0	2	3	1	
New Hall																											
1054	31	104	167	0	25	53	79	79	17	14	26	289	118	3	11	28	7	1	10	6	14	75	1	18	3	8	
1053	36	81	133	0	0	44	48	152	5	15	35	451	102	2	10	26	1	2	15	14	25	79	1	12	4	7	
Pinxton																											
1058 E19	27	15	1804	32	32	16	2	6	21	77	127	55	160	10	77	10	1	1	8	0	5	191	3	4	5	2	
Plymouth																											
32701Q	212	136	161	1	3	91	1	3	31	14	8	654	167	2	18	30	0	0	37	2	24	114	1	2	5	5	

Appendix 9: LA-ICPMS data

Appendix Table 25 - LA-ICPMS data (parts per million) for 53 British porcelain pastes, trace elements minus REEs (see Appendix Table 26) (continued)

Sample	Li	B	Ti	V	Cr	Mn	Co	Ni	Cu	Zn	As	Rb	Sr	Y	Zr	Nb	Mo	Ag	Sn	Sb	Cs	Ba	Hf	Bi	Th	U	
Pomona																											
32702Z	97	57	317	7	6	357	94	187	60	178	1693	39	255	2	16	3	1	5	30	60	1	119	1	70	1	3	
Swansea																											
36554Q	17	40	5386	103	76	14	3	23	7	29	4	61	88	19	108	19	0	0	5	1	10	251	3	0	10	2	
1060	34	53	164	0	9	44	1	1	16	28	16	319	182	3	65	57	1	3	16	1	11	115	3	4	5	5	
1070	58	48	268	3	6	33	10	20	30	23	17	506	34	1	12	22	0	1	9	2	6	48	0	0	2	3	
Worcester																											
32700S	125	41	296	6	9	299	119	233	68	144	2188	36	268	5	22	3	1	4	18	62	1	112	1	63	1	3	
29099T	167	43	385	8	7	492	217	226	114	267	2635	30	818	4	37	3	2	3	54	46	1	274	1	66	3	3	
29263P	154	32	356	8	12	297	105	195	76	228	1582	47	261	4	27	3	2	5	1	81	1	178	1	67	1	3	
1065	116	65	440	9	12	320	137	249	66	434	4240	30	489	5	72	3	2	4	37	62	1	130	2	149	2	8	
1064	413	78	249	9	10	401	74	179	172	248	448	45	708	3	22	2	1	6	25	111	1	82	1	47	1	3	
1063	116	45	263	9	20	378	203	217	85	223	490	33	342	2	19	3	1	3	32	142	2	303	0	7	1	1	
1062	38	126	296	6	12	286	225	243	68	303	912	77	315	3	38	3	1	2	58	30	1	117	1	174	1	7	
1068	59	53	234	4	0	149	212	391	59	46	557	203	34	3	76	15	6	2	10	16	5	31	2	74	2	5	
1067	88	67	354	8	5	351	261	919	74	203	3570	29	336	5	32	3	1	5	27	40	1	433	2	96	1	4	
1066	87	61	539	8	18	192	143	791	124	184	1824	58	139	7	1055	3	8	7	81	70	1	69	23	88	3	5	

Appendix 9: LA-ICPMS data

Appendix Table 26 - LA-ICPMS data (parts per million) for 53 British porcelain pastes, uncorrected REEs

Sample	La	Ce	Pr	Nd	Sm	Eu	Gd	Tb	Dy	Ho	Er	Tm	Yb	Lu
'A'-marked														
47122R	17.48	20.64	2.52	7.40	1.22	0.69	0.89	0.14	0.77	0.15	0.42	0.05	0.41	0.05
Bow														
32703X	13.78	25.45	3.74	11.61	1.92	0.43	1.56	0.20	1.03	0.23	0.59	0.09	0.41	0.09
29105Q	16.99	29.66	4.48	14.85	2.63	0.51	2.12	0.27	1.72	0.31	0.78	0.13	0.81	0.10
29100P	13.82	25.20	3.65	12.10	2.14	0.45	3.27	0.67	4.58	0.86	2.24	0.32	1.89	0.32
29104S	14.13	24.82	3.56	11.44	1.89	0.39	1.40	0.17	1.12	0.20	0.51	0.05	0.56	0.10
Caughley														
1069 E39	2.42	5.01	0.57	2.11	0.43	0.13	0.57	0.09	0.69	0.12	0.37	0.08	0.32	0.07
Chaffers														
32704V	4.30	10.29	1.41	4.38	1.29	0.02	0.90	0.11	0.76	0.17	0.50	0.08	0.48	0.10
Chelsea														
32699W	11.32	20.39	2.30	8.25	1.36	0.30	1.01	0.14	0.94	0.19	0.57	0.08	0.60	0.10
29103U	16.75	23.50	3.69	11.84	1.67	0.38	1.58	0.19	1.19	0.25	0.67	0.10	0.62	0.11
29106Z	24.53	42.68	5.77	19.41	3.01	0.67	1.93	0.26	1.72	0.32	1.05	0.15	1.10	0.19
66983 Y1	12.11	21.81	3.24	10.91	1.83	0.26	1.61	0.36	1.18	0.21	0.79	0.16	0.71	0.00
1055 E6	14.32	21.77	2.90	9.46	2.56	0.37	1.77	0.25	1.10	0.36	0.58	0.09	0.93	0.12
Coalport														
1072 E44	9.24	17.82	2.22	8.10	1.56	0.26	1.01	0.12	0.71	0.12	0.34	0.03	0.42	0.03
Crown Derby														
1057 E18	22.80	41.06	5.42	17.95	3.01	0.60	3.35	0.66	5.48	1.18	3.59	0.55	3.62	0.54
1056 E17	22.05	39.30	5.21	17.09	2.98	0.57	1.88	0.30	1.96	0.36	1.14	0.18	1.17	0.17
Limehouse														
40419P	33.04	57.83	7.62	24.08	3.79	0.97	2.45	0.29	2.19	0.43	1.37	0.17	1.63	0.22
40150S	41.17	72.68	9.15	28.94	4.86	1.02	3.23	0.41	2.54	0.46	1.57	0.22	1.84	0.31
40012W	23.67	40.91	5.46	17.28	2.72	0.56	2.06	0.25	1.59	0.25	0.96	0.22	1.18	0.18
40011Y	22.94	38.95	5.33	17.38	2.74	0.56	1.70	0.27	1.88	0.32	0.94	0.16	1.35	0.17
40010P	27.59	54.27	5.72	19.81	3.42	0.46	3.43	0.36	2.35	0.47	1.58	0.23	1.12	0.13
40009X	35.48	67.21	8.66	28.08	4.59	1.05	2.74	0.44	2.59	0.49	1.38	0.21	1.58	0.27
40008Z	35.66	49.67	8.03	26.54	4.68	1.06	3.02	0.53	3.10	0.54	1.69	0.21	1.59	0.18
40007Q	26.69	50.56	5.47	19.03	4.06	1.11	7.33	1.99	14.46	2.89	7.71	1.01	6.08	0.74
40006S	26.13	49.11	5.19	18.54	3.21	0.65	2.08	0.34	2.01	0.39	1.12	0.17	1.55	0.23
40000S	29.92	52.72	7.08	23.38	3.61	0.70	2.28	0.35	2.24	0.47	1.22	0.20	1.50	0.21
40004W	32.84	57.29	7.76	25.91	3.98	0.73	3.15	0.47	2.98	0.66	1.86	0.30	2.08	0.31
40003Y	25.34	45.11	6.13	19.94	3.33	0.75	2.33	0.26	1.84	0.33	0.97	0.21	1.40	0.20
40002P	29.26	53.17	7.05	23.62	3.88	0.61	2.76	0.63	2.12	0.35	1.29	0.24	1.61	0.38
Liverpool (Ball)														
32705T	0.19	13.33	8.72	25.64	0.00	0.22	0.00	2.05	0.00	0.07	19.06	0.00	0.76	0.00
32706R	3.03	6.79	0.75	2.80	0.62	0.11	0.68	0.09	0.58	0.11	0.31	0.05	0.30	0.04
Longton Hall														
29101Y	8.30	13.99	1.98	6.50	1.32	0.19	1.22	0.15	1.12	0.19	0.64	0.08	0.53	0.08
29098V	2.76	11.19	0.00	1.57	0.09	0.06	8.03	0.00	3.64	0.03	0.00	0.00	1.50	0.68

Appendix 9: LA-ICPMS data

Appendix Table 27 - normalisation values used for Rare Earth Elements (REEs) in British porcelain pastes.

Sample	La	Ce	Pr	Nd	Sm	Eu	Gd	Tb	Dy	Ho	Er	Tm	Yb	Lu
Lowestoft														
32707P	14.97	30.60	3.50	12.27	2.31	0.62	2.00	0.30	1.87	0.34	0.91	0.13	0.85	0.14
Nantgarw														
1059 E22	3.56	8.07	0.95	3.78	0.77	0.13	0.64	0.08	0.46	0.05	0.19	0.02	0.19	0.04
New Hall														
1054 E4	4.66	12.65	1.40	5.45	2.20	0.12	0.79	0.10	0.98	0.05	0.37	0.02	0.25	0.03
1053 E3	10.54	23.20	2.39	5.88	1.26	0.12	1.08	0.18	0.58	0.07	0.12	0.04	0.00	0.00
Pinxton														
1058 E19	18.29	35.48	3.88	13.81	2.28	0.44	1.77	0.24	1.44	0.29	1.15	0.19	1.40	0.21
Plymouth														
32701Q	2.61	7.45	0.81	3.14	0.79	0.15	0.72	0.10	0.46	0.07	0.21	0.03	0.20	0.03
Pomona														
32702Z	2.55	6.24	0.62	2.32	0.57	0.07	0.69	0.09	0.44	0.08	0.25	0.05	0.27	0.03
Swansea														
36554Q	41.94	77.63	10.03	32.05	5.25	1.06	3.52	0.43	2.98	0.58	1.85	0.28	1.84	0.27
1060 E23	4.38	9.91	1.09	4.48	1.10	0.25	0.74	0.11	0.62	0.13	0.32	0.07	0.68	0.10
1070 E40	2.94	7.68	0.80	2.98	0.39	0.17	0.58	0.04	0.39	0.08	0.08	0.03	0.06	0.02
Worcester														
32700S	2.46	5.37	0.70	2.28	0.69	0.31	1.02	0.10	0.80	0.13	0.49	0.08	0.40	0.07
29099T	3.42	7.60	0.89	3.03	0.69	0.13	0.71	0.10	0.62	0.14	0.45	0.05	0.49	0.07
29263P	2.96	6.89	0.88	2.74	0.68	0.05	0.54	0.09	0.64	0.12	0.47	0.05	0.39	0.08
1065 E34	3.94	8.54	1.01	3.26	0.74	0.17	0.69	0.14	0.87	0.15	0.52	0.08	0.56	0.09
1064 E32	2.76	5.48	0.72	2.48	0.49	0.12	0.46	0.08	0.57	0.09	0.26	0.05	0.34	0.04
1063 E31	2.28	5.21	0.67	2.26	0.38	0.18	0.36	0.08	0.31	0.07	0.16	0.03	0.34	0.06
1062 E27	2.35	5.93	0.58	1.96	0.27	0.09	0.42	0.09	0.60	0.13	0.33	0.04	0.47	0.07
1068 E37	1.34	4.67	0.44	1.31	0.67	0.11	0.79	0.09	0.79	0.10	0.41	0.05	0.57	0.06
1067 E36	3.55	7.77	0.80	2.77	0.53	0.18	0.37	0.16	1.06	0.10	0.41	0.06	0.50	0.05
1066 E35	2.30	8.91	0.84	2.15	0.66	0.09	0.63	0.15	0.77	0.19	0.83	0.12	0.64	0.20

Chondrite values are from Evensen et al (1978), and MUQ from Kamber et al (2005).

Label	La	Ce	Pr	Nd	Sm	Eu	Gd	Tb	Dy	Ho	Er	Tm	Yb	Lu
chondrite	0.24	0.61	0.09	0.46	0.15	0.06	0.20	0.04	0.25	0.05	0.16	0.02	0.16	0.02
MUQ	32.51	71.09	8.46	32.91	6.88	1.57	6.36	0.99	5.89	1.22	3.37	0.51	3.25	0.49

Appendix 9: LA-ICPMS data

Appendix Table 28 - LA-ICPMS data (parts per million) for 36 British porcelain glazes, major and minor elements

Label	Na	Mg	Al	Si	P	K	Ca	Ti	Fe	Sn	Pb
Bow											
32703X	5077	557	6533	174506	471	18071	11379	347	190	12	519633
29100P	2745	726	10413	189693	16723	32916	42133	459	3075	13288	378916
Caughley											
1069 E39	9366	8343	22331	224317	223	32999	4256	237	4842	691	363988
Chaffers											
32704V	42334	15873	5523	275060	816	32404	31708	314	1109	34856	166777
Chelsea											
32699W	7241	1001	7609	277226	11	16266	74402	836	569	4411	228294
29106Z	8993	252	2415	343282	2015	25663	26422	160	3079	193	157093
Coalport											
1072 E44	10447	956	38508	242014	3534	17126	41134	207	1377	17	250867
Crown Derby											
1057 E18	5299	352	3367	201742	716	86195	7678	132	2643	21	329553
1056 E17	6419	4111	45861	155621	108038	26631	168652	2121	5220	12	33108
Limehouse											
40419P	15818	3106	34127	237141	710	11632	29008	1330	2111	33247	270934
40012W	20098	7187	32893	239946	7925	12450	48838	427	1778	19127	234344
40010P	18887	5318	35187	238960	2238	11763	32798	584	2922	7836	281663
40008Z	25677	6133	38237	263689	472	20303	48579	773	1356	14146	185240
40007Q	17592	6083	35738	244330	2979	8651	36573	586	3307	15148	257216
40006S	33404	4899	68807	337273	2399	16792	26363	3254	3453	107	17256
40000S	10262	3597	18881	134552	343	7529	18235	352	1665	6758	564046
40004W	9509	4222	15135	133761	364	6509	22719	329	1566	10327	563469
40003Y	4932	590	7921	79762	75	3843	3893	74	641	14915	717807
40002P	12183	4016	20252	134195	306	7966	19472	289	1649	6925	557405
Liverpool Ball											
32706R	22698	12777	28697	246156	1107	8851	10749	242	473	24	308271
Longton Hall											
29101Y	9396	1679	13688	316548	398	55262	49203	724	1622	11084	115753
Lowestoft											
32707P	3321	118	5747	200479	389	14957	5366	258	100	16229	468690
Nantgarw											
1059 E22	5755	863	47589	238839	1630	14285	58555	200	1375	23	241529
New Hall											
1054 E4	6475	910	92597	260834	656	6913	73405	356	514	7	129454
1053 E3	8346	727	58879	161146	539	5206	22086	260	418	49	454425
Pinxton											
1058 E19	1849	664	24068	168660	12679	17724	32620	469	1031	11	454275

Appendix 9: LA-ICPMS data

Appendix Table 28 - LA-ICPMS data (parts per million) for 36 British porcelain glazes, major and minor elements (continued)

Label	Na	Mg	Al	Si	P	K	Ca	Ti	Fe	Sn	Pb
Plymouth											
32701Q	5614	14602	70896	360960	2112	16428	21099	177	3287	32	97
Pomona											
32702Z	6340	16243	31732	235548	336	16322	8573	303	2626	2501	331089
Swansea											
1060 E23	7723	1244	56129	234972	5099	22172	54087	191	2421	26	225801
1071 E41	108994	3651	7235	151281	19133	51356	31992	997	14147	1979	258570
Worcester											
32700S	8089	9783	21605	220175	135	29838	7628	240	808	2751	374384
29099T	8968	11650	21033	240206	1050	30555	11696	244	3288	2474	311487
29263P	9094	25196	21162	248839	472	40611	7547	282	2410	4266	277494
1062 E27	10569	9753	24219	213506	219	31856	4910	217	2234	1892	377794
1068 E37	6293	7474	24718	295892	341	7603	42579	142	651	37	209730
1067 E36	5740	10476	31058	301920	29	9331	20091	105	1857	3260	194116

Appendix 9: LA-ICPMS data

Appendix Table 29 - LA-ICPMS data (parts per million) for 36 British porcelain glazes, trace elements minus REEs

Sample	Li	B	V	Cr	Mn	Co	Ni	Cu	Zn	As	Rb	Sr	Y	Zr	Nb	Mo	Ag	Sb	Cs	Ba	Hf	Bi	Th	U	
Bow																									
32703X	66	23	8	8	151	45	18	193	21	4497	32	24	3	19	2	2	18	179	2	54	0	28	1	0	
29100P	71	201	15	7	46	50	26	154	40	290	69	66	4	334	2	2	13	21	3	122	9	11	1	1	
Caughley																									
1069 E39	246	152	6	83	416	48	50	329	87	994	289	82	4	22	10	5	20	159	4	98	1	64	2	2	
Chaffers																									
32704V	602	78	15	9	245	72	88	2417	330	162	44	200	3	31	2	1	12	104	2	94	1	45	1	0	
Chelsea																									
32699W	37	49	15	1137	242	22	39	189	263	188	42	111	1	12	2	0	18	207	2	41	1	12	1	1	
29106Z	239	129	14	74	32	20	11	242	59	50	110	33	2	4	0	0	34	11	3	59	0	5	0	0	
Coalport																									
1072 E44	158	10173	4	25	64	4	7	403	375	42	185	114	3	17	22	0	6	45	6	94	1	2	2	2	
Crown Derby																									
1057 E18	225	118	4	8	167	17469	701	18803	113	23056	69	28	2	12	1	6	72	117	1	268	0	88	0	0	
1056 E17	54	15	49	46	54	106	125	27	89	741	57	138	9	72	8	1	8	7	7	141	2	56	6	1	
Limehouse																									
40419P	77	23	26	83	410	225	55	248	46	2354	40	219	7	45	7	0	7	207	6	549	1	18	4	2	
40012W	125	27	11	22	515	133	56	340	64	883	29	289	3	32	2	2	3	243	3	153	1	44	1	2	
40010P	219	51	10	14	645	119	31	218	56	722	70	236	7	36	6	1	4	209	7	446	1	5	3	3	
40008Z	116	48	18	18	629	177	35	175	66	833	67	337	9	146	7	1	3	106	9	579	4	18	3	3	
40007Q	123	71	15	20	593	735	344	297	64	877	39	245	7	37	6	3	4	141	6	201	1	263	3	5	
40006S	86	71	60	45	215	181	77	67	24	837	48	197	10	90	11	7	4	89	4	165	2	98	8	9	
40000S	49	24	9	13	289	96	16	123	35	246	28	163	4	22	4	0	1	67	4	347	1	79	2	1	
40004W	51	40	10	11	289	72	15	113	34	328	22	182	4	21	3	1	2	78	3	237	1	5	1	1	

Appendix 9: LA-ICPMS data

Appendix Table 29 - LA-ICPMS data (parts per million) for 36 British porcelain glazes, trace elements minus REEs (continued)

Sample	Li	B	V	Cr	Mn	Co	Ni	Cu	Zn	As	Rb	Sr	Y	Zr	Nb	Mo	Ag	Sb	Cs	Ba	Hf	Bi	Th	U
Limehouse (continued)																								
40003Y	27	20	2	2	160	27	7	92	12	1899	12	41	2	7	2	0	3	86	2	73	0	4	1	1
40002P	61	47	6	6	303	66	13	69	33	243	33	173	4	19	3	1	2	23	4	256	1	21	1	2
Liverpool (Ball)																								
32706R	233	65	6	8	578	123	59	381	223	1670	100	368	6	29	4	2	9	270	22	81	1	122	3	3
Longton Hall																								
29101Y	61	27	16	10	332	5	8	373	93	672	83	160	13	42	3	1	8	116	6	110	1	11	1	1
Lowestoft																								
32707P	55	644	5	3	52	29	16	116	10	232	93	16	1	7	1	2	23	40	1	59	0	18	1	1
Nantgarw																								
1059 E22	191	6723	5	132	317	4	7	543	268	37	144	119	2	19	16	0	189	18	4	78	1	1	2	3
New Hall																								
1054 E4	40	185	9	378	76	66	120	211	52	25	218	120	3	16	106	14	4	536	10	29	1	12	5	3
1053 E3	86	92	0	125	164	8	270	276	32	142	136	78	3	41	31	2	9	98	5	62	1	5	2	2
Pinxton																								
1058 E19	131	39	9	17	225	2	6	232	75	486	71	53	2	33	4	3	133	115	3	97	1	5	2	1
Plymouth																								
32701Q	415	59	7	4	150	3	4	75	18	18	700	195	1	9	23	0	2	1	15	63	1	1	3	6
Pomona																								
32702Z	126	57	7	9	477	44	44	114	122	1322	51	162	7	52	5	2	12	226	3	97	2	46	3	3
Swansea																								
1060 E23	86	4911	4	27	84	4	3	300	76	99	271	153	3	33	35	1	6	27	8	96	1	4	2	4
1071 E41	2761	2773	138	1	1847	255	932	10747	6913	2440	0	109	0	2	18	0	236	6641	92	1191	6	468	5	12

Appendix 9: LA-ICPMS data

Appendix Table 29 - LA-ICPMS data (parts per million) for 36 British porcelain glazes, trace elements minus REEs (continued)

Sample	Li	B	V	Cr	Mn	Co	Ni	Cu	Zn	As	Rb	Sr	Y	Zr	Nb	Mo	Ag	Sb	Cs	Ba	Hf	Bi	Th	U
Worcester																								
32700S	186	45	7	8	443	53	69	136	117	2502	54	119	5	32	4	3	13	294	5	73	1	57	2	2
29099T	312	50	9	90	326	2342	957	223	386	3422	41	350	5	31	4	8	13	248	4	137	1	3290	1	5
29263P	290	50	8	13	333	61	80	135	176	1551	60	218	6	35	4	4	12	239	5	101	1	63	2	2
1064 E32	415	70	4	331	599	177	77	342	169	931	57	276	5	30	4	5	7	315	9	77	0	203	2	2
1062 E27	176	76	8	24	389	805	524	283	317	2452	167	106	5	24	4	4	18	177	4	67	1	404	2	5
1068 E37	144	104	7	370	137	185	0	279	54	176	86	35	2	18	8	9	15	42	2	153	0	16	0	1
1067 E36	125	43	14	382	382	1300	2432	236	64	1033	47	94	7	39	2	0	4716	113	3	145	2	1042	3	3

Appendix 9: LA-ICPMS data

Appendix Table 30 - LA-ICPMS data (parts per million) for 36 British porcelain glazes, uncorrected REEs

Sample	La	Ce	Pr	Nd	Sm	Eu	Gd	Tb	Dy	Ho	Er	Tm	Yb	Lu
Bow														
32703X	3.28	5.40	0.84	2.83	0.54	0.06	0.56	0.08	0.51	0.11	0.31	0.04	0.19	0.05
29100P	4.80	9.15	1.28	4.31	0.79	0.18	0.67	0.10	0.71	0.14	0.43	0.08	0.67	0.14
Caughley														
1069 E39	3.18	6.05	0.69	2.83	0.68	0.11	0.70	0.11	0.77	0.11	0.38	0.07	0.23	0.08
Chaffers														
32704V	3.95	6.91	1.06	3.30	0.76	0.09	0.68	0.07	0.51	0.10	0.32	0.05	0.26	0.06
Chelsea														
32699W	3.29	8.82	0.80	2.51	0.42	0.99	2.81	0.02	0.43	0.06	0.33	0.04	0.00	0.26
29106Z	2.04	2.26	0.24	1.41	0.27	0.23	0.18	0.03	0.22	0.04	0.17	0.00	0.00	0.10
Coalport														
1072 E44	3.76	5.82	0.76	3.09	0.69	0.13	0.53	0.07	0.47	0.10	0.29	0.04	0.42	0.02
Crown Derby														
1057 E18	1.88	2.71	0.43	1.48	0.33	0.06	0.32	0.04	0.28	0.05	0.12	0.02	0.13	0.02
1056 E17	22.27	40.17	5.29	16.99	2.83	0.57	1.71	0.26	1.54	0.31	0.93	0.16	1.02	0.16
Limehouse														
40419P	11.90	20.60	2.69	8.90	1.62	0.43	1.13	0.14	1.10	0.19	0.55	0.07	0.65	0.10
40012W	7.78	9.61	1.44	4.13	0.62	0.20	0.65	0.07	0.42	0.05	0.21	0.07	0.25	0.04
40010P	6.84	14.34	1.52	5.57	1.48	0.10	1.61	0.22	1.22	0.21	0.70	0.08	0.47	0.06
40008Z glaze	8.45	16.58	2.11	6.85	1.62	0.33	1.28	0.24	1.53	0.23	0.66	0.09	0.69	0.06
40007Q	6.34	13.02	1.45	5.24	1.32	0.25	1.23	0.25	1.48	0.23	0.59	0.10	0.69	0.07
40006S	25.23	46.01	4.78	18.24	3.30	0.74	1.87	0.33	2.01	0.38	1.04	0.14	1.42	0.21
40000S	3.89	7.26	0.92	3.12	0.61	0.13	0.56	0.12	0.73	0.14	0.30	0.03	0.35	0.03

Appendix 9: LA-ICPMS data

Appendix Table 30 - LA-ICPMS data (parts per million) for 36 British porcelain glazes, uncorrected REEs (continued)

Sample	La	Ce	Pr	Nd	Sm	Eu	Gd	Tb	Dy	Ho	Er	Tm	Yb	Lu
Limehouse (continued)														
40004W	3.82	7.11	0.93	3.15	0.59	0.07	0.68	0.09	0.61	0.10	0.30	0.05	0.28	0.04
40003Y	0.92	2.20	0.24	0.91	0.25	0.05	0.29	0.04	0.26	0.04	0.12	0.02	0.15	0.02
40002P	3.66	7.28	0.89	2.99	0.57	0.01	0.86	0.27	0.72	0.08	0.31	0.05	0.37	0.16
Liverpool (Ball)														
32706R	3.75	6.52	0.82	3.68	1.02	0.16	1.20	0.20	1.21	0.21	0.61	0.08	0.50	0.08
Longton Hall														
29101Y	6.95	10.65	1.59	5.41	1.02	0.18	0.96	0.12	1.32	0.36	1.41	0.23	1.63	0.23
Lowestoft														
32707P	2.55	5.78	0.61	2.31	0.46	0.15	0.41	0.05	0.27	0.05	0.14	0.03	0.14	0.02
Nantgarw														
1059 E22	2.66	4.45	0.60	2.33	0.33	0.02	0.72	0.04	0.40	0.03	0.54	0.01	0.25	0.13
New Hall														
1054 E4	2.74	3.09	0.32	4.43	1.08	0.19	1.18	0.21	0.17	0.00	0.34	0.13	0.92	0.11
1053 E3	4.21	6.29	0.32	2.74	0.18	0.07	0.40	0.07	0.35	0.00	0.06	0.00	0.50	0.04
Pinxton														
1058 E19	3.83	7.41	0.82	3.16	0.40	0.09	0.61	0.08	0.38	0.06	0.26	0.05	0.24	0.03
Plymouth														
32701Q	2.61	5.30	0.60	2.13	0.47	0.05	0.30	0.05	0.24	0.04	0.13	0.02	0.17	0.02
Pomona														
32702Z	3.76	6.82	0.78	3.35	1.04	0.10	1.24	0.21	1.27	0.22	0.65	0.10	0.65	0.09
Swansea														
1060 E23	4.19	6.61	0.86	3.62	0.72	0.16	0.53	0.08	0.47	0.08	0.23	0.03	0.30	0.05
1071 E41	46.16	31.21	30.37	51.16	0.00	26.43	119.15	7.09	65.07	48.93	6.99	1.11	0.12	14.99

Appendix 9: LA-ICPMS data

Appendix Table 30 - LA-ICPMS data (parts per million) for 36 British porcelain glazes, uncorrected REEs (continued)

Sample	La	Ce	Pr	Nd	Sm	Eu	Gd	Tb	Dy	Ho	Er	Tm	Yb	Lu
Worcester														
32700S	2.97	6.03	0.78	2.71	0.82	0.26	1.02	0.14	0.88	0.14	0.43	0.06	0.31	0.05
29099T	3.15	6.24	0.68	2.29	0.89	0.10	1.38	0.14	0.75	0.26	0.81	0.03	0.65	0.09
29263P	3.17	6.44	0.87	2.97	0.79	0.09	0.89	0.16	1.06	0.16	0.52	0.07	0.46	0.08
1064 E32	3.99	6.90	0.75	2.89	0.14	1.48	0.78	0.04	0.38	0.11	0.05	0.07	2.69	0.37
1062 E27	2.98	6.78	0.71	2.61	0.60	0.14	0.85	0.17	0.95	0.19	0.47	0.05	0.48	0.06
1068 E37	2.14	2.68	0.30	0.56	0.53	0.10	0.00	0.00	0.67	0.00	0.00	0.00	0.00	0.08
1067 E36	4.82	5.15	0.92	1.89	0.58	0.79	0.83	0.12	1.21	0.17	0.36	0.26	1.06	0.18

